UNIVERSITY OF SOUTHAMPTON

FACULTY OF ENGINEERING, SCIENCE & MATHEMATICS

School of Chemistry

An exploration of the solid-state architectures formed by 1,8-naphthyridine-2,7-dicarbonyl derivatives

by

Andrew James Bailey

Supervisor: Dr. M. C. Grossel

Thesis for the degree of Doctor of Philosophy

UNIVERSITY OF SOUTHAMPTON

ABSTRACT

FACULTY OF ENGINEERING, SCIENCE & MATHEMATICS

SCHOOL OF CHEMISTRY

Doctor of Philosophy

AN EXPLORATION OF THE SOLID-STATE ARCHITECTURES FORMED BY 1,8-NAPHTHYRIDINE-2,7-DICARBONYL DERIVATIVES

By Andrew James Bailey

Building on previous studies of tape formation by dicarbonyl substituted pyridine derivatives in the solid state, it was proposed that expansion of the hydrogen bonding array from three donor-acceptor pairs to four should increase the strength of the hydrogen-bonded array. Accordingly an investigation into the 1,8-naphthyridine-2,7-dicarbonyl derivatives has now been undertaken.

Following the synthesis of 1,8-naphthyridine-2,7-dicarboxylic acid, during which the solid-state structures of three key intermediates were obtained, thirty-five novel 1,8-naphthyridine-2,7-dicarboxylates and fourteen novel 1,8-naphthyridine-2,7-dicarboxamides have been synthesised. Solid-state structures have been obtained for thirty-two of these derivatives confirming that the hydrogen bonding motifs observed for the dicarbonyl-substituted pyridines are also adopted by their naphthyridine analogues. In the diesters the familiar one-dimensional taping motif was observed, with additional secondary interactions, caused by the substitution on the pendent arm, influencing the packing of these structural units. For the corresponding diamides, intramolecular hydrogen bonding was found to organise the molecules into a cleft arrangement. Additionally an initial investigation into the solid-state motifs observed upon co-ordination to a metal centre has been carried out.

A number of novel pyridine-2,6-dicarbonyl derivatives have also been synthesised and their solid-state behaviour has been studied. One of these structures is thought to be only the second known non-tape-forming pyridine-2,6-dicarboxylate. Finally the successful synthesis of 4,4’-linked pyridine-2,6-dicarboxamides has been achieved, the latter offering the potential for forming extended networks through co-ordination around metal centres.

Contents

DECLARATION OF AUTHORSHIP

I, Andrew Bailey

declare that the thesis entitled

An exploration of the solid-state architectures formed by 1,8-naphthyridine-2,7-dicarbonyl derivatives

and the work presented in the thesis are both my own, and have been generated by me as the result of my own original research. I confirm that:

- this work was done wholly or mainly while in candidature for a research degree at this University;
- where any part of this thesis has previously been submitted for a degree or any other qualification at this University or any other institution, this has been clearly stated;
- where I have consulted the published work of others, this is always clearly attributed;
- where I have quoted from the work of others, the source is always given. With the exception of such quotations, this thesis is entirely my own work;
- I have acknowledged all main sources of help;
- where the thesis is based on work done by myself jointly with others, I have made clear exactly what was done by others and what I have contributed myself;
- At the time of writing part of this work is in the process of being published as:

A. J. Bailey, P. N. Horton and M. C. Grossel, "Self-assembly into infinite tapes by 2,7-disubstituted-1,8-naphthyridines in the solid state", CrystEngComm, 2010, **12**, 4321-4327

Signed: ……..

Date:……..

Acknowledgements

First and foremost I would like to thank Martin for offering me the opportunity to study for a PhD. That simple statement covers much more than just the time I have been doing my PhD, thank you for all your help and support over the past 8 years that I have been in Southampton, from the first organic teaching lab to the writing of this thesis, you have been a constant source of encouragement and wisdom.

I would also like to thank all the members of the Grossel group, both past and present, a list of whom would easily use most of the space that I have so I shall say only this: Each and every one of you has made my experience of university life a truly remarkable one and I thank you for that.

I would also like to thank the different people around the department who have made life that little bit better. To Karl, Graham, Tony and Clive in stores; to the ladies in the offices, in particular to Sally, Jan, Bevy and Mary, thank you for all your help with sorting out my administrative woes; to Neil and Joan thank you for all your help regarding NMR in particular for your suggestions of other solvents that might be of use with my particularly insoluble products; to John and Julie, you truly run one of the best mass spectrometry services possible! Without Mark Light and Peter Horton and all those in the national crystallography service this thesis would be rather devoid of content, thank you for your patience with all my questions. Finally I would like to thank John Mellor for the financial support that he provided, without which I would not have been able to study for my PhD

Alex, Dave, Alan, Jon, Louise and Richard, thank you all so much for you support and friendship through my time at university, I am very lucky to have met such kind and caring people.

Lauren, I'm not sure why you put up with me sometimes, I just know that I am very glad that you do! Thank you so much for all your help and support while going through the dreaded write-up, job hunting, moving and everything else.

I would like to thank my Mum and my sister Katherine. I know that the past 4 years have been as stressful for the both of you as they have for me. Thank you for your love and support throughout.

Finally I would like to dedicate this thesis to my Dad; I hope that I have made you proud.

Abbreviations

The following abbreviations have been used in this report.

Abbreviation	Meaning
Boc	*tert*-Butyloxycarbonyl
Cbz	Carbobenzyloxy
CCDC	Cambridge Crystallographic Database
$CDCl_3$	Deuterated chloroform
Conc.	Concentrated
DCM	Dichloromethane
DMA	Dimethylacetamide
DMF	Dimethylformamide
DMSO	Dimethylsulphoxide
DSC	Differential scanning calorimetry.
EA	Ethyl acetate
EDTA	Ethylenediamine tetra-acetate
EI	Electron ionisation
ES^+	Electrospray positive
ES^-	Electrospray negative
FTIR	Fourier transform infrared
MeCN	Acetonitrile
MP	Melting point
MS	Mass spectrometry
NCS	N-Chlorosuccinimide
NMR	Nuclear magnetic resonance
PPA	Polyphosphoric acid
TLC	Thin layer chromatography
UV – Vis	Ultraviolet – visible light (spectrometry)

1 Introduction

1.1 Supramolecular Chemistry

The origins of Supramolecular Chemistry lie in work by Cram,[1] Lehn[2] and Pedersen,[3] for which they shared the Nobel Prize for chemistry in 1987.

After Pedersen's serendipitous discovery of the crown ethers,[4] Lehn went on to create complex 3D architectures and more complicated multi-component structures,[5] discussed later. Cram investigated furthering of the shape selectivity by creating a series of 3D structures that could interact with selected guest molecules because of their complementary shape, an example of which is the carcerand family.[6] Their work inspired many chemists in the field, which has now broadened to encompass the exploration of novel polymeric systems,[7] functional molecular assemblies and machines,[7-10] enzyme mimics,[11-14] anion recognition[15-18] and the application of such systems to the control of solid state architectures and crystal engineering.[19-22]

Unlike traditional organic synthesis, supramolecular chemistry involves chemistry beyond the covalent bond.[2] This simple statement covers a diverse area of research from static self-assembled systems, where molecules arrange themselves based on a variety of recognition features, [23-27] to highly functional dynamic systems in which recognition is only one aspect of the process.[28-30] Nature provides a plethora of elegant examples of these functions such as: structural recognition in DNA;[31] ion transport in haemoglobin[32] and selective ion channels;[33] reaction catalysis in enzymatic systems and molecular motors in systems such as ATP synthase[34] and kinesin.[35, 36] Indeed, a great deal of supramolecular chemistry focuses on the exploration of synthetic systems which can mimic the functions seen in nature: crown ether like materials showing ion transport capabilities;[37-39] rotaxanes and catenanes forming molecular motors,[40-44] and self assembled systems forming a key constituent of a catalytic systems, either as nano-scaled reaction vessels [45] or undergoing autocatalysis.[28-30]

Supramolecular chemistry often relies on host-guest interactions. In order to capture a certain target molecule (the guest) it is necessary to design a suitable

receptor (the host). To achieve this it is important to utilise the principle known as complementarity, which can be visualised using Emil Fischer's[46] "Lock and Key" concept (Figure 1).[2, 46, 47] In order for a key to be able to open a lock it must have the correct shape and size. Continuing the analogy supramolecular chemistry often works the other way around; the key is known but the lock must be designed.

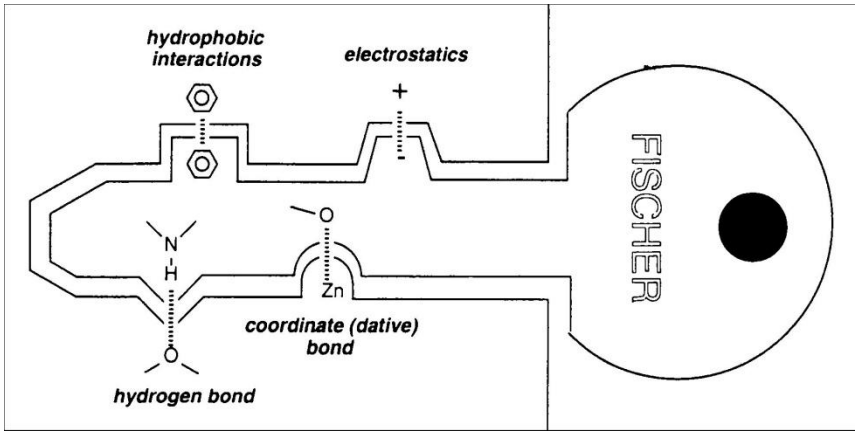

Figure 1 - A depiction of Fischer's "Lock & Key" principle.[47]

As supramolecular chemistry relies on an understanding of weaker intermolecular interactions it has prompted a great deal of investigation into non-covalent interactions.

Interaction	Typical Range of Strengths / kJ mol^{-1}
Ion – Ion	400 - 4000
Hydrogen bonding	3 – 150
Ion - Dipole	40 - 600
Dipole – Dipole interaction	5 - 25
van der Waals	2

Table 1 - The comparative strengths of the non covalent interactions.

In some cases this investigation has managed to spark controversy particularly in the case of very weak interactions which are often overpowered in traditional chemical environments. However, as the field of supramolecular chemistry has developed the understanding of the role that multiple weak interactions play in the assembly of molecules has developed greatly.

1.2 Crystal Engineering

One area of supramolecular chemistry that has seen a massive growth is that of crystal engineering,[48] due in part to the increasing ease and reducing cost of obtaining X-ray crystal structures. While the study of crystals is becoming more available, an understanding of their formation "more readily destroyed than built [cleanly],"[49] is a research field in itself.

Crystal engineering combines the study of solid-state structure of known compounds with a desire to be able to predict the solid-state behaviour of pre-designed compounds. However, total prediction of a crystal structure from first principles is not facile. Indeed in 1988 Maddox proclaimed that "One of the continuing scandals in the physical sciences is that it remains, in general, impossible to predict the structure of even the simplest crystalline solids from a knowledge of their chemical composition."[50] He does acknowledge work by others on prediction of molecular clusters but states that "a demonstration of success [in the prediction of a crystal structure] can rank, psychologically, with the example set by those who first climbed Everest".[50] Six year later Gavezzotti answered his own question of "Are crystal structures predictable" with a simple answer "No" stating that organic solid state chemistry at that time suffered because those studying it were utilising different methodologies and were interested in the compounds for different purposes.[49] He also commented that, while the understanding of intramolecular valence was satisfactory, the understanding of intermolecular forces were rudimentary. In 2003 Dunitz provided an updated perspective on this commenting that, while progress had been made in the prediction by clustering lowest energy structures from all possible close packed crystal structures, this method is a brute force technique rather than one borne out of understanding and predicting the formation of a crystal structure.[51] At around the same time Desiraju pointed out that, unlike most supramolecular reactions, crystallisation is a kinetically controlled process and states that the method described by Dunitz does not account for the experimental variables of the crystallisation procedure, a key factor in the formation of local minimum crystal structures.[52] Desiraju suggests that given the kinetic control, it is impossible to model the events of crystallisation however,

utilising a fingerprinting technique of synthons, like those used in code ciphers, on a database of examples it should be possible to identify structural trends to impart chemical knowledge as to preferred structures.[52] Desiraju and Dunitz both draw parallels between the field of crystal structure prediction and that of protein folding and suggest that polymorphism, the ability of one molecule to form more than one stable crystal structure, is a key property. Indeed polymorphism proves to be a major issue in the prediction of molecular solid state structures from first principles. Since 1999 the CCDC has hosted the Crystal Structure Prediction Blind Tests,[53] in the hope that this would encourage research in the area as well as highlighting progress made. In the most recent blind test a group comprising of Frank Leusen and John Kendrick of the University of Bradford, UK, and Marcus Neumann of Avant-garde Materials Simulation in Saint-Germain-en-Laye, France, correctly predicted the structure of all four molecules,[54] the first time this had been achieved.[53] This is not however, the end of work in this area; indeed the results of the next CCDC blind test are due in August 2010. Furthermore a review of the area in 2008 suggested that, while modelling has become a routine procedure, total prediction is still a developing area as the techniques used to date are not suitable for all cases and further work is required to make them universally applicable.[55]

It is in the pursuit of drug-like molecules that crystal engineering receives most exposure to a general scientific audience, due to the effects of polymorphism in the pharmaceutical industry. Polymorphism is an extremely important issue in the pharmaceutical industry as it is estimated that 30 -50 % of pharmaceutically important compounds exhibit polymorphism. This rises to 90 % when solvates are considered.[56, 57] Indeed in recent years there has been an annual review of patents and papers from the pharmaceutical sector reporting polymorphic systems.[58-61] A polymorph, though chemically identical, may exhibit different physical properties; the best known example being the case of Ritonavir (**1**), manufactured by Abbott Laboratories.[62]

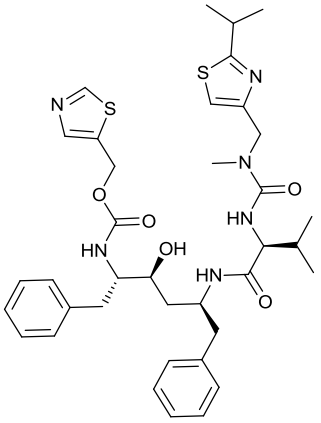

Ritonavir - 1

Despite successful synthesis, formulation, and manufacture of Norvir capsules (the trade name for Ritonavir) containing only one polymorph (I) it was discovered in mid 1998 that a number of the semi-solid capsules had formed a precipitate. This precipitate was identified as a new polymorph (II) which had greatly reduced solubility. This caused Abbott to remove the drug from the market and undertake a thorough investigation and reformulation. They discovered that a trace impurity and high concentrations of Ritonavir in solutions led to the initial formation of polymorph II. However, once formed, contamination of their manufacturing facilities led to the preferential formation of form II in most newly manufactured batches. This was despite the thermodynamic favourability of form I which was counteracted by the low solubility of form II which led to earlier super-saturation. Their investigation led to an academic publication highlighting the importance of polymorphism in drug-like molecules even when supplied in solution. [62] It is not only new drugs that yield new polymorphs; many established drugs are the subject of investigation for polymorphism as a method of "patent busting". [56, 63]

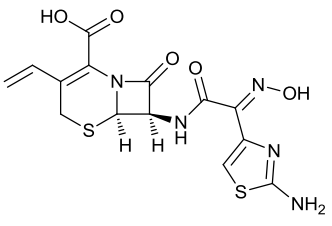

Cefdinir - 2

A recent case study focusing on the polymorphic forms of Cefdinir (**2**) has highlighted the complexities that the issue of polymorphism can cause, with 8 companies filing 11 patents relating to 5 different crystalline forms. This is by no

means a unique case.[63] There has recently been great debate following the report of a new polymorph of asprin,[64] with an initial investigation by Bond, Boese and Desiraju claiming that it was, in fact, an incorrectly reported structure of the known polymorph.[65] A further discussion was published in which it was concluded that the structure was in fact a mixed polymorph structure.[66]

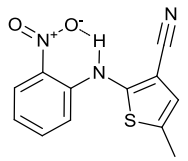

5-Methyl-2-[(2-nitrophenyl)amino]-3-thiophenecarbonitrile
(ROY) - **3**

However, it is not only industry that is interested in the study of crystal engineering; there are many academic groups working on the subject. In a survey in 2000 Yu identified 5-methyl-2-[(2-nitrophenyl)amino]-3-thiophenecarbonitrile (**3)** which, with the possibility of 6 polymorphic forms formed from solution crystallisation coexisting at room temperature, is the compound with the most known polymorphs in the CCDC.[67] Further research has shown that this structure and its derivatives are capable of creating a large number of other polymorphs.[68, 69]

In order to understand more about crystal engineering, and supramolecular chemistry as a whole, it is important to understand the interactions being exploited.

1.2.1 Contact Types

1.2.1.1 The Covalent Bond

Chemistry relies on the interactions of individual particles. At the simplest chemical level this is the interaction of atoms which, from an organic chemist's point of view, are normally connected by covalent bonds. Covalent bonds are formed through the interaction of each atom's molecular orbitals to form bonding orbitals in which the atoms can share electrons to ensure a full outer shell.

Bond Type	Strength	Bond Type	Strength	Bond Type	Strength
C-H	411	C-C	346	N-N	167
N-H	386	C=C	602	N=N	418
O-H	459	C≡C	839	N≡N	942
S-H	363	C-O	358	C=O	799

Table 2 - A selection of covalent bond enthalpies.[70, 71]

Covalent bonds vary in strength from extremely strong C≡C and N≡N to the weak N-N. It is important to note that although covalent bonds share their electrons, when two atoms of different electronegativity share electrons the bond is polarised towards the atom with higher electronegativity.

Our understanding of the nature of a covalent bond has developed greatly in the last 100 years starting with Lewis[72] and Pauling's[73, 74] individual contributions at the beginning of the twentieth century, through to the increased development of quantum mechanics in the latter half of the century. The advent of molecular orbital theory has allowed physical chemists to advance their calculations to describe far more complex structures yet, due to the computational complexities of very large structures, limits remain. Supramolecular chemistry aims to study the non-covalent intermolecular interactions between molecules and it is therefore important to understand the comparative strength of these interactions used in comparison to a covalent bond.

1.2.1.2 Interactions between charged species

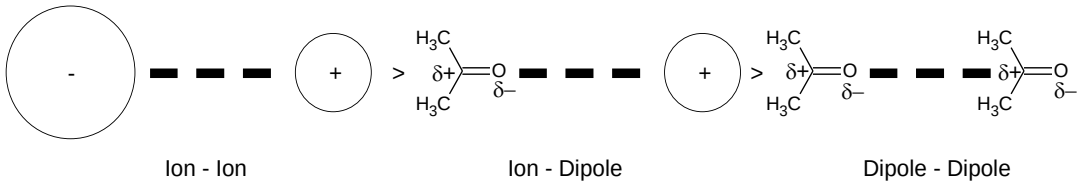

Figure 2 - An illustration of the different types of electrostatic interactions.

Interactions between charged species are, when present, normally the strongest intermolecular interactions. Supramolecular chemistry involving these interactions is often based around design of receptors for cations,[3, 4] a more traditional interest, or anions, a more recent area of interest.[15-17, 75] It is however, also possible for interactions to occur between molecules which, while not exhibiting a formal

charge, are polarised in such a way that the molecules exhibit dipoles, such as that seen in acetone (Figure 2). Interactions involving dipoles are not only much weaker than those between two formally charged species; they are also much more difficult to incorporate into a designed supramolecular system. Receptor design must take into account the purpose for which the complex will be utilised. Techniques such as catch and release allow for the transport of ions through membranes by encapsulating the charged species within a protective medium from which it can later be released.[75] While for selective recognition, detection and quantification purposes, shape and size selectivity are crucial for differentiating between similar species.[76, 77]

1.2.1.3 Van der Waals

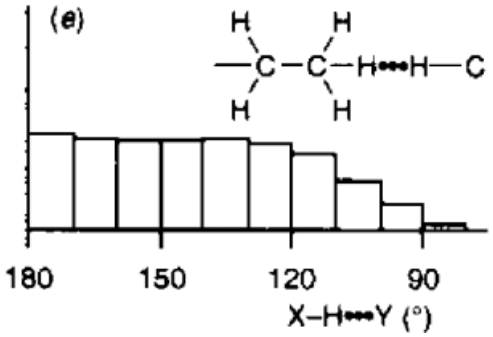

Figure 3 - Illustration to show the directional distribution of van der Waal C-H...H-C interaction observed in the CCDC.[78]

Van der Waals contacts, also referred to as dispersion or London interactions, are weak interactions present in all molecular systems and are always attractive forces. They arise from induced dipole – dipole interactions, where spontaneous alignment of induced dipoles give an attractive interaction which has no preferred directional orientation.[78] The spontaneous nature of these interactions makes it very difficult to design a molecule which takes advantage of these interactions, yet in nature these interactions can play a key role.[79] This fact alone means that any work towards the understanding and utilisation of these interactions is of great interest.

1.2.1.4 Hydrogen Bonding

1.2.1.4.1 Introduction

The effects of hydrogen bonding had been identified long before the formal discovery of the principle in the early 20th century. In some cases, such as Faraday's chlorine gas hydrates from 1823, the presence of hydrogen bonding was only recognised over 100 years later when X-ray crystal structures were carried out.[80] There were terms in use in both England and Germany for the effects of the hydrogen bond in the years preceding the formal discovery.[81] Pauling claims that credit for this should be given, independently, to Huggins and a pair of collaborators called Latimer and Rodebush, though Huggins claimed to have been the first.[82] Pauling's paper in 1931 on the nature of the chemical bond[73] (the precursor to his book on the subject[74]) used the term hydrogen bond for possibly the first time.[80] Huggins seems to have taken issue with the word bond[83, 84] and preferred the term hydrogen bridge, an expression that, Desiraju has since argued could be reinstated in order to alleviate some of the preconceptions of details necessary for an interaction to be considered a bond.[19] In the years following Pauling's book there was a great deal of work into the area of hydrogen bonding but it wasn't until 27 years later that the first formalised international conference on the subject took place.[80] This was followed in 1960 by the first book devoted to the topic by Pimentel and McClellan.[85] This book was instrumental in giving a more generalised definition of a hydrogen bond which allowed work on many weaker interactions to take place. In 1971 the definition was updated by Vinogradov and Linnell[86] and in the following years a number of books and reviews were published. Jeffery estimated[80] that between 1977 and 1991 a paper containing the concept of hydrogen bonding was published every 15 minutes. Without the numerical proof this might be seen as an overestimation but during 2006 - 2008 the CAS Scifinder system showed an increase of over 31000 papers containing the term hydrogen bond, a figure equating to approximately 1 paper an hour.[87] In 1997 Jeffery published his introduction to hydrogen bonding which updated the previous literature while offering a more accessible guide for those entering the area.[80]

Much of the early work in the area was carried out without the aid of spectroscopic and analytical tools that we have come to expect today and instead relied on infrared experiments as its key spectroscopic tool. However, the development of NMR spectroscopy and both X-ray and neutron diffraction led to an explosion of interest in weak interactions.[80] The limitations of the developing field of X-ray diffraction, especially the inability to determine the location of hydrogen atoms, led to the publication by Hamilton and Ibers of a qualitative definition of a hydrogen bond. They suggested that "a heavy atom distance less than the van der Waals distance is perhaps sufficient, but not necessarily a condition for the presence of hydrogen bonding".[88] Although only a proposal, it has subsequently become the *de facto* crystallographic definition for a hydrogen bonding interaction.[80] This definition has however been the subject of much discussion over the past decade as work on weak hydrogen bonds has gained greater recognition.[81, 89, 90] Huggins predicted that one of the most fruitful applications of the hydrogen-bridge theory would be the better understanding of the nature and behaviour of complicated organic structures[83] which, 24 years later, Pimentel and McClellan pronounced as prophetic.[85] Indeed almost 75 years on not even Huggins could have foreseen the extent to which this would be true.

Hydrogen bonds span a very large range of strengths from being, in a few cases, almost as strong as a weak covalent bond to associations that are only of energy comparable to that of van der Waals interactions. This variation is due, in part, to the complex balance of many different interactions that make up a hydrogen bond. Some of the common misconceptions about hydrogen bonding arise from a lack of distinction between different types of hydrogen bond. In 2004 IUPAC set up a committee to produce an updated definition of the hydrogen bond, in order that the definition should take into account more recent findings. [87]

The proposed definition is:

The hydrogen bond is an attractive interaction between a hydrogen atom from a fragment or molecule X–H in which X is more electronegative than H, and an atom or a group of atoms, in the same or a different molecule, in which there is evidence of bond formation.

The committee also highlight current thinking that indicates that: hydrogen bonds are a mixture of electrostatic, charge transfer (partial covalent nature) and dispersion forces; that the strength of the hydrogen bond depends on the polarisation of the donor hydrogen bond; and that hydrogen bonds are directional with strength increasing as the bond tends towards 180 °. The committee also reinforce Jeffrey's assertion that the use of the sum of van der Waal radii as an indicator of hydrogen bonding is not a reliable method for determining the presence of a hydrogen bond. [87]

1.2.1.4.2 Terms to Describe Hydrogen Bonding

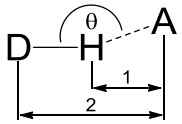

Figure 4 - Measurements required to describe a Hydrogen Bond.

In order to define any hydrogen bond, reference must be made to three measurements (Figure 4). The distance between the hydrogen and acceptor (**1** in Figure 4), the distance between the donor and acceptor (**2** in Figure 4) and the angle of the donor to acceptor along the hydrogen bond (**θ** in Figure 4). In strong bonds the angle is ~180 °, however, in most other systems bent bonds are favoured due to the geometry of the donor atom. This has led to the development of the *"conic correction"* a mathematical descriptor which normalises the angle of the hydrogen to 180 °.[91]

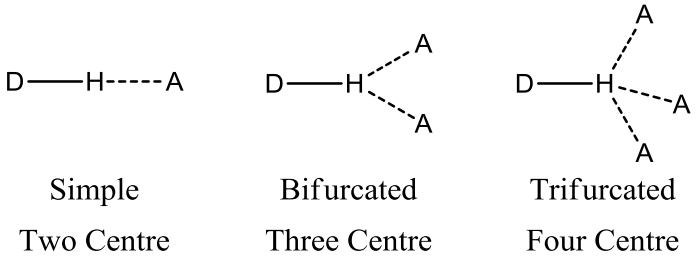

Figure 5 - An illustration showing examples of multi acceptor hydrogen bonding and the nomenclature associated.[80]

In addition to this it is also necessary to describe the multiplicity of the hydrogen bond as there are cases of multiple donors or multiple acceptors; Figure 5 shows the classification of these multicentre hydrogen bonds. Three- and four-centre

bonds are less common than simple, two-centre hydrogen bonds; in biological systems they account for approximately 25 % and < 5 % of examples respectively.[80] In four-centre hydrogen bonds all the hydrogen bond angles must be greater than 90° and the hydrogen bond length is typically longer than in the other systems; indeed in some cases they are regarded by some to be non-bonding interactions.[80]

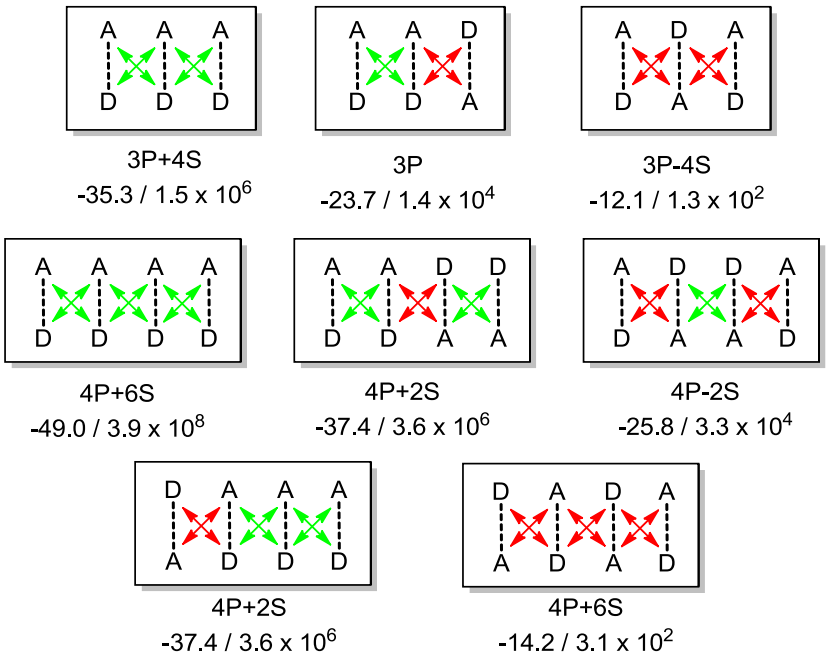

Figure 6 - Possible arrangements of triple and quadruple hydrogen bonding arrays, along with Sartorius' calculated ΔG (kJ mol^{-1}) and K (mol^{-1}) in chloroform. P: Primary interaction, S: Secondary interaction.[92]

Within systems in which hydrogen bonds form in arrays, such as in the base pairs in DNA, it has been observed that the array exhibits additive effects, affected not only by the primary interactions but also by weaker secondary interactions between neighbouring hydrogen bond pairs.[26] The effect of these secondary interactions can be either attractive of repulsive depending on the alignment of neighbouring hydrogen bond pairs. Following on from seminal work by Jorgensen,[93, 94] Sartorius[92] investigated the effect of secondary interactions on the association strength of a number of hydrogen bond arrays. Figure 6 shows Sartorius' predicted strengths of different three and four hydrogen bond arrays. It clearly shows the effect that secondary interactions have on both the Gibbs free energy and the association constant.[92]

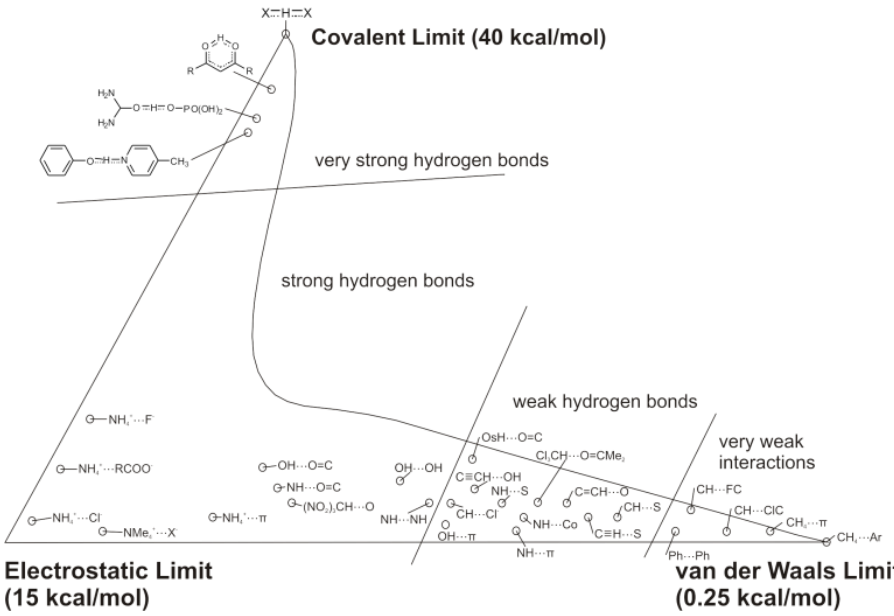

Figure 7 – Desiraju's schematic depicting the classification of hydrogen bond strengths according to the strength observed. This schematic also gives some insight to the potential balance of interactions in the hydrogen bonds.[19]

A recent study by Desiraju[19] produced the schematics above (Figure 7) which shows the segregation of hydrogen bonds into a number of categories depending on their strengths. More recently Seddon has published an evaluation of C-H···X hydrogen bonding in which he investigates the utility of the van der Waals distance as a method of proving or disproving hydrogen bonding.[90] In this work he details the use of a new technique: isotropic density correction. This work demonstrates that many of the weak interactions thought by some to be hydrogen bonds do indeed have a strong directional component, a key aspect of a hydrogen bond. However the contact distances are in some cases longer than would be acceptable when making use of the van der Waal radii definition.

	Strong	Moderate	Weak
Dominant interaction type	Mostly covalent	Mostly electrostatic	Electrostatic
Bond Lengths	A-H ≈ H···B	A-H < H···B	A-H << H···B
H···B	~1.2-1.5	~1.5-2.2	2.2-3.2
A···B	2.2-2.5	2.5-3.2	3.2-4.0
Bond Angles (°)	175-180	130-180	90-150
Bond Energies (kcal/mol)	14-40	4-15	<4

Table 3 - A table containing the classification of strength of hydrogen bonds and the properties associated with them as reported by Jeffrey.[78]

Table 3 shows the classification of hydrogen bonds proposed by Jeffrey and the properties associated with each classification. While the classifications do leave some hydrogen bond interactions, such as carboxylic acid pairs, exhibiting properties of two categories it is generally accepted as a useful guide.

1.2.1.4.2.1 Strong Hydrogen Bonds

Strong hydrogen bonds are classed as those that have an energy of between 15 – 40 kcal/mol. They are normally formed by groups with deficient or excess electron density, often charged species. They have been referred to as ionic hydrogen bonds,[80] which is indicative of the nature of the system as well as their strength. It is common for strong hydrogen bonds to have very significant lengthening of the D-H bond length, sometimes with the hydrogen appearing to take a symmetrical position in the neutron diffraction crystal structure though, taking thermal parameters into consideration, it is difficult to determine if it is exactly in the centre.[80]

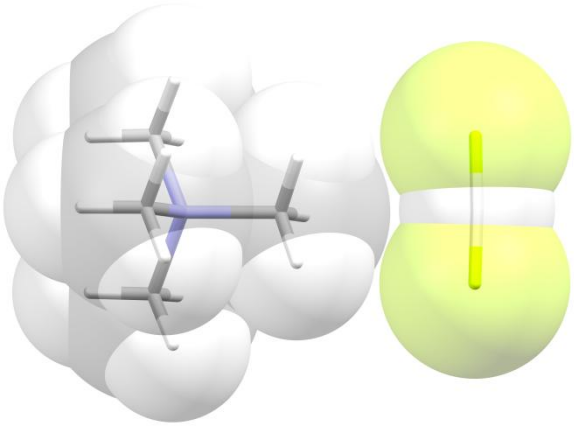

Figure 8 - One of the best known examples of very strong hydrogen bonding is the $[H\text{-}F\text{-}H]^-$ system.[95]

One of the first examined examples is that of $[H\text{-}F\text{-}H]^-$ (Figure 8) which has a very short F-F distance of 2.25 Å.[95] A range of values have been proposed for its bond strength however 39.0 ± 1 kcal has been agreed to be the most reasonable, a figure that is in the order of a weak covalent bond.

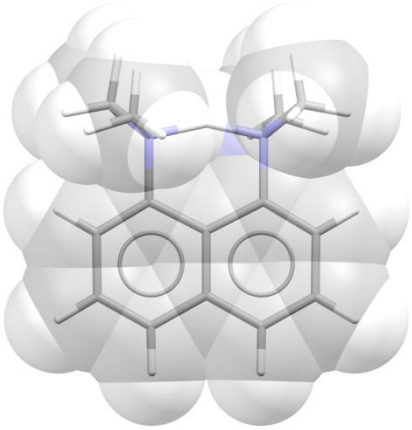

Figure 9 - More recently strong hydrogen bonds have been of interest as proton sponges such as this 1,8-*bis*-*(*dimethylamine) naphthalene.[96]

More recently interest in strong hydrogen bonds has been shown through materials referred to as proton sponges an example of which is 1,8-*bis*-(dimethylamine) naphthalene (Figure 9). Proton sponges have a very strong, basic character due to the close proximity of the basic centres, which when unprotonated causes a distortion of the naphthalene ring system. When protonated the hydrogen appears to sit almost symmetrically between the two nitrogen centres, the exact position of the proton has been found to vary depending on the counter ion present in the crystal structure.

1.2.1.4.2.2 Moderate Hydrogen Bonds

These are hydrogen bonds of an intermediate strength which typically have energies of 4-15 kcal/mol. This classification includes the hydrogen bonds most commonly referred to in both organic chemistry and biological systems, typically involving O-H and N-H donors and nitrogen and oxygen acceptors.

O-H···O contacts are amongst the most studied hydrogen bonds. This is not only because of the interest in the study of water's crystal structure,[80, 97, 98] but also due to the propensity for crystal structures to form hydrated forms and the presence of oxygen species in many of the simple building blocks of biological systems e.g. carbohydrates and peptides.

Hydrogen bonds in carboxylic acids show some of the properties of strong hydrogen bonds however, it is included in the moderate category as it relies on moderate bonds which are strengthened by resonance assistance. As this category of

hydrogen bond is an area of such interest it is not surprising that there have been, and continue to be, a large number of database surveys of the properties of these hydrogen bonds, with 27 of these surveys highlighted by Jeffery in 1997.[80]

1.2.1.4.2.3 Weak Hydrogen Bonds

These hydrogen bonds, with energy comparable to that of van der Waal interactions, were initially identified by spectroscopists studying gas phase interactions. Acetylene was recognised as a weak hydrogen bond donor and weak acceptor by Green[99] in 1974. Work in the 1980's focused on gas phase adducts of HF, HCl, HBr and HCN with N_2, CO, OCS, CO_2 and acetylene,[100] while in the 1990's attention had shifted to the adducts formed with chloromethanes.[101, 102]

While weak hydrogen bonding interactions had been identified by spectroscopists, their conclusions provided great controversy from a crystallographic perspective. When C-H···O hydrogen bonds were initially suggested by Sutor[103, 104] the findings were very firmly rebutted by Donoghue,[105] acknowledged to be the leading expert in the field at the time.[80, 106] This led to a period during which the idea of weak hydrogen bond interactions were shunned. Much of this controversy appears to stem from Hamilton's proposed threshold hydrogen bonding,[88] something which ruled out many of the proposed weak hydrogen bonds.[88] However, in the past 30 years many people have carried out work to further understand the interaction. Steiner and Saenger carried out a survey of neutron diffraction data for carbohydrates which showed, of the 395 potential C-H donors, 61% were to OH groups while only 2% where to O=C groups.[107] Interestingly they also observed some very short contact distances at low angle which, they suggested, could be forced contacts possibly repulsive in nature. However the other contact distances produced an even distribution around the van der Waals interaction distance.[107]

Despite the controversy surrounding the C-H···O contact, in recent years Desiraju has been a strong advocate for its existance.[89] Desiraju has continued to carry out research into the area of weak hydrogen bonds and has commented that the strong early objections in the 1960's have been diluted to oral objections that can be best described as stationary.[108] That said those objections still exist[109] and the topic of weak hydrogen bonding is still a field which incites strong opinions.

1.2.1.5 Interactions with π-electron systems

These interactions rely on the fact that areas of electron density, such as lone pairs and π-delocalised electrons, can act as a weak/soft hydrogen acceptor however the energy of these interactions is typically assumed to be less than 1 kcal/mol. While the idea of weak hydrogen bonds is becoming far more accepted, interactions of this type are viewed by some as an over interpretation of data,[110] but those who argue in favour of their existence point to their apparent presence in many biological systems[81, 111-114] and the implications that they have in general organic chemistry. [113-118]

1.2.1.5.1 X-H ···π

It has been argued that if it is possible for a weak hydrogen donor to form an interaction with a strong acceptor, the opposite might be true with a π-electron system performing the weak acceptor role.[113] As such O-H···π and N-H···π interactions appear to have been accepted quite reasonably by those who have been pushing for weak hydrogen bonding interactions to be recognised. [19, 114] Indeed for many examples there is both crystallographic and spectroscopic evidence for the presence of the interaction.[81]

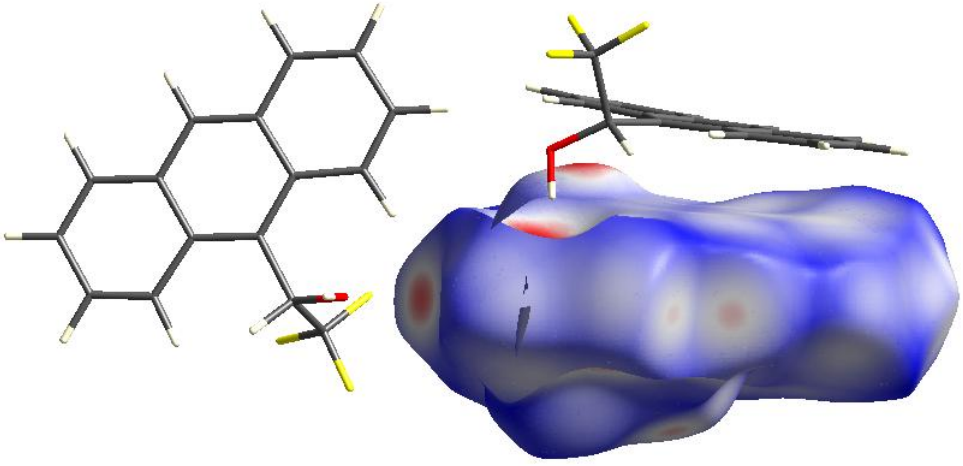

Figure 10 – CrystalExplorer image showing the O-H···π interaction in (S)-2,2,2-trifluoro-1-(9-anthryl)ethanol.[119]

Tamres[120] is thought to have been the first to recognise that C-H groups interact favourably with aromatic compounds, having described in 1952 an exothermic mixing of chloroform and benzene. Furthermore by altering the aromatic

compound, a difference in heat of mixing was noticed. This was correlated with a differing shift of the C-H bond at an IR frequency,[120] behaviour similar to that seen in hydrogen bonded systems by IR spectroscopy.[85]

The C-H···π interaction, also sometimes referred to as a "phenyl" interaction or "hybrid" interaction, has had greater difficulty in gaining widespread acceptance due to the combination of a weak donor and a weak acceptor.[116, 121, 122] It currently evokes much the same opinion as weak hydrogen bonds did in the 1960's although again this objection appears to be easing. [19, 114] Such contacts are thought by some to be purely a feature of molecular packing, yet it has been observed that activation of either the acceptor or the donor leads to a shortening of the contact distance, behaviour in line with a hydrogen bond-like interaction.[19]

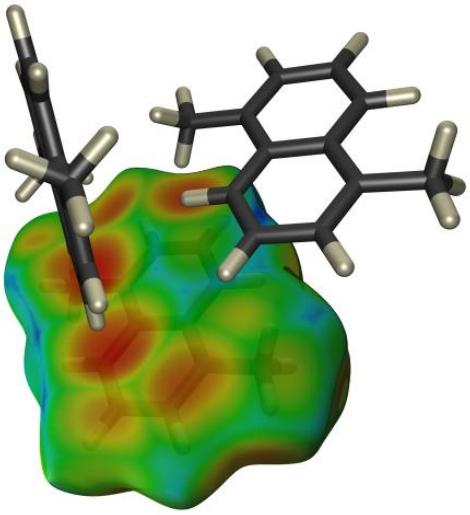

Figure 11 – A CrystalExplorer image showing the Hirshfeld surface of 1,5-dimethylnaphthalene which can be seen to show a number of different C-H···π interactions.

1,5-Dimethylnaphthalene (Figure 11) has also been of interest as it exhibited C-H···π interactions which appears to lock the conformation of the methyl group in the solid-state. It has been the subject of both X-ray[123] and neutron diffraction studies[124, 125] as well as being subjected to computational studies of these interactions in order to gain an insight into the strength of these weak interactions. While C-H···π interactions are not completely understood, it is believed by some that they have crucial implications for organic chemistry as a whole.[118]

1.2.1.5.2 π ⋯π interactions

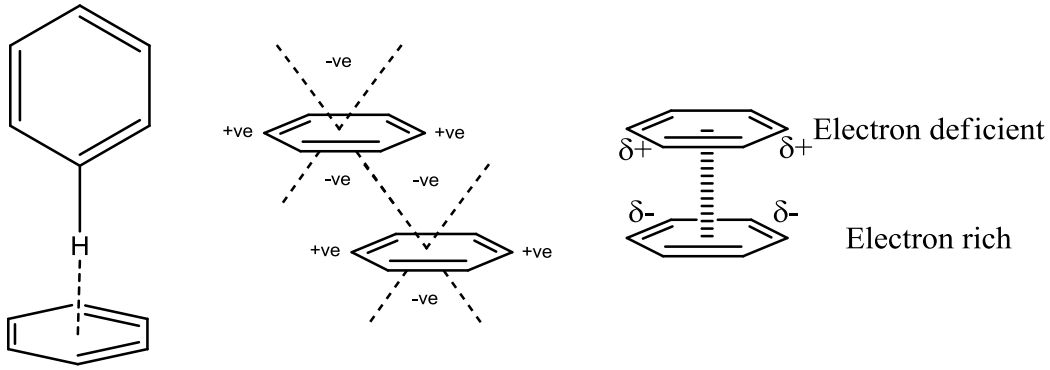

Figure 12 - There are 3 recognised motifs that two interacting aromatic systems could form. On the left is the herringbone motif, in the centre is the slip-stacked motif, and on the right is the face to face motif.

π⋯π interactions were identified as a key component of protein structure stabilisation by Burley and Petsko in 1985 and have been the subject of intense research in the three decades following.[111] Aromatic rings are usually observed in one of three motifs when in the solid-state: herringbone; slip stacked or π⋯π stacked. Herringbone stacking can be explained by looking at the C-H⋯π interaction, while slip stacking appears to be due to the interaction of the quadrapoles ensuring that the positive and negative sections overlap.

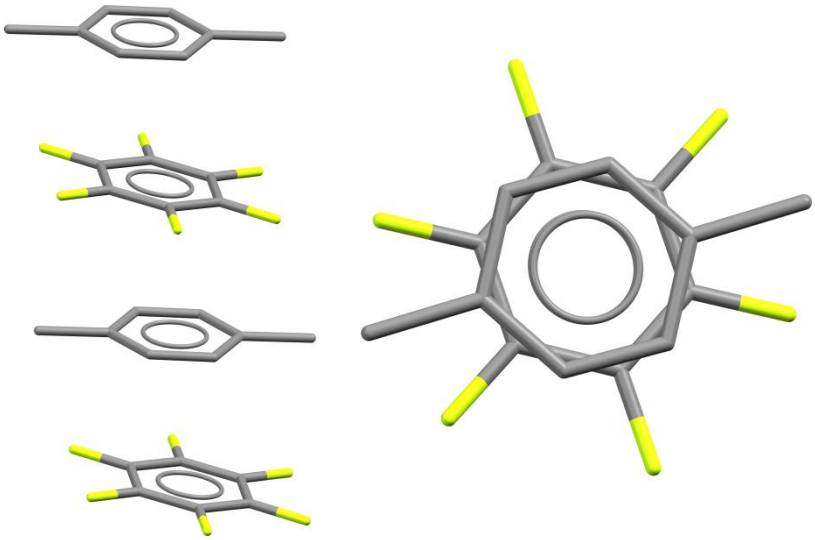

Figure 13 - The face to face π⋯π exhibited by hexafluorobenzene and *p*-xylene is brought about by the difference in π electron density bringing about a favourable overlap.[126]

However, it has been observed that in some instances two substituted benzene rings will align one on top of the other (Figure 12 right). This appears to occur between two benzene rings in which the substitution alters the electron density of the π cloud so that one is electron rich, while the other is electron deficient. This

alteration of electron density ensures that a favourable overlap may occur as seen in the packing of hexafluorobenzene and *p*-xylene (Figure 13).[126] It is believed that interactions of this type have an influence on the hydrogen bonding capabilities of DNA base pairs.[127]

Hunter has carried out a great deal of work, both practically and theoretically, investigating the fundamental interactions between molecules[128-134] as well as the importance of solvent effects on these molecular interactions.[135, 136]

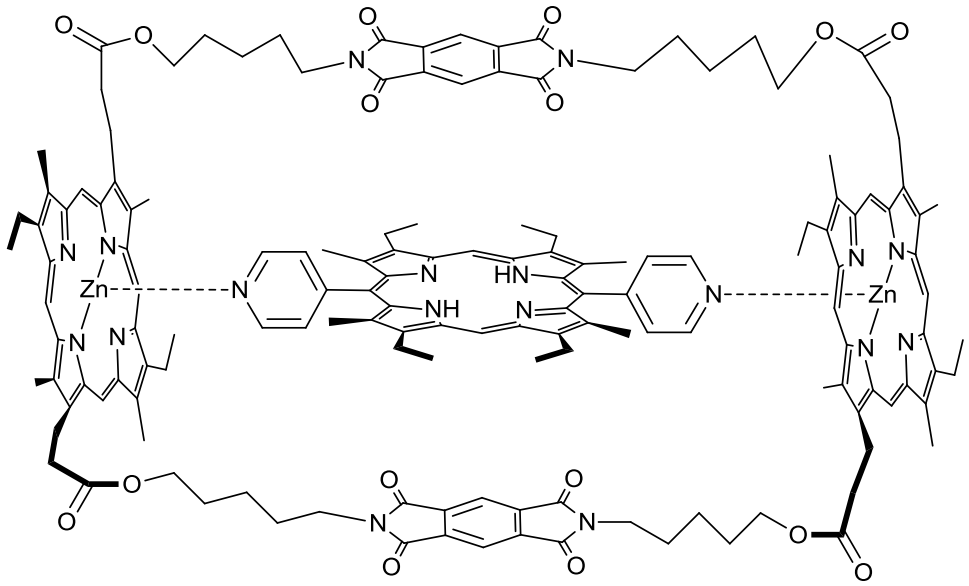

4·5

Figure 14 – Hunter's initial work in Sanders group involved the synthesis and characterisation of this porphyrin complex (4·5) **in which π···π interactions were found to provide stabilisation of the bound central porphyrin (**4**).[137]**

Hunter's initial work in this area followed on from his work on porphyrins while a student in Sanders' group. While the complex (**4·5**)shown in Figure 14 appeared to primarily form because of coordination of the pyridine nitrogen to the porphyrins co-ordinated zinc, further studies indicated that there was a substantial π···π interaction.[137]

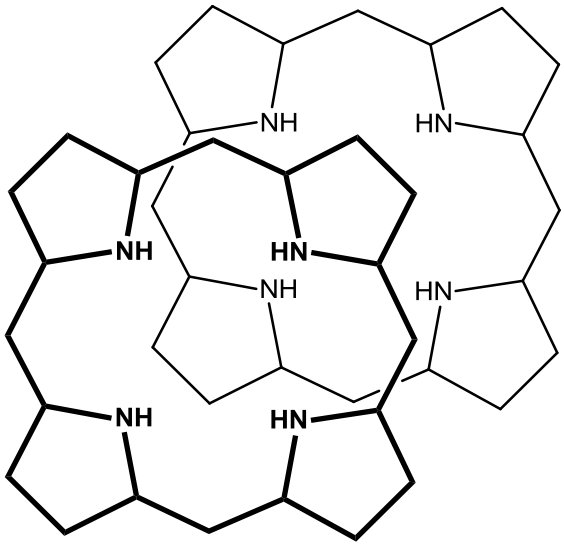

Figure 15 – This is the alignment that Sanders published in 1990 as the optimum overlap for π···π interactions between porphyrins. (The system is aromatic however the double bonds have been omitted for the sake of clarity).[128]

The paper he co-authored with Sanders in 1990 described the nature of the π···π interaction, which they believed was controlled by electrostatic effects. However they believed that the main stabilising energy came from elsewhere and outweighed the destabilising repulsion between neighbouring π clouds.[128] Hunter proposed, with theoretical backing, that π···π interactions showed a preference to both offset and angular rotation verified by examining the different benzene crystal structures which favour slip-stacked over T-shaped.[128]

Further work by Hunter has reported methods for investigating the energies of the π···π interactions and more recently has gone further by looking at tools for quantifying intermolecular interactions. This work included a detailed list of the many factors that must be considered in order to fully understand a molecular interaction,[131] which was followed by a more detailed investigation into the effect of solvent on an intermolecular association.[135, 136]

In 1978 after synthesising a number of caffeine-based derivatives, in which two caffeine analogues were linked together by a carbon chain containing a dicarbyne unit (**6**) (Figure 16), Chen and Whitlock reported that their compounds had formed "sandwich-like π-system hydrophobic complexes" which they referred to as "molecular tweezers".[138]

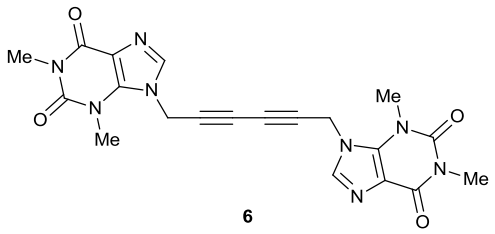

6

Figure 16 - Chen and Whitlock's caffeine based molecular pincer.

They reported a list of properties which they believed would enhance the complexation properties of such molecules:

- There should be a rigid unit as the core of the molecule
- The caffeine units need to be in a syn conformation ≈ 7 Å apart
- The side arms need to be held rigidly

It was this last property that their own compounds lacked, however they also concluded that the pendant arms did not necessarily have to maintain a parallel orientation relative to one another.[138]

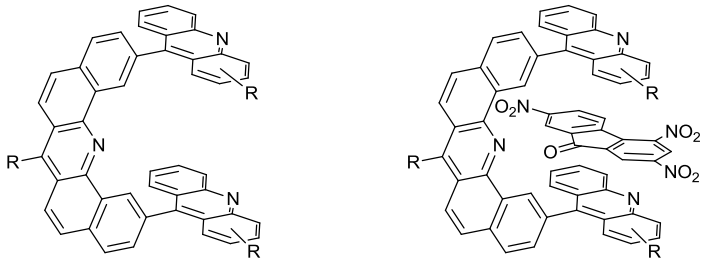

7 7·8

Figure 17 – Zimmerman's molecular tweezers shown with no guest (left) and with 2,4,7-trinitrofluorenone (right).

Subsequently, Zimmerman also developed the concept of molecular tweezers.[139] This work aimed to design a molecular tweezer (**7**) (Figure 17) which obeys all of the Chen and Whitlock rules, utilising a very rigid core that would hold the side arms at the correct distance apart. Molecules that have all these features benefit from a phenomenon called pre-organisation which brings with it a huge advantage for the binding of a guest molecule. Zimmerman's system exhibits binding of 2,4,7-trinitrofluorenone (**8**) with binding constants of between 149 M^{-1} and 697 M^{-1} in chloroform, depending on the R group. While π···π interactions generally appear to be weak they, like many of the other interactions discussed previously, can have a

defining influence on the arrangement of molecules in both the solid and solution state.

Despite the ever growing body of work demonstrating the presence of weak π···π interactions there are still those who doubt the existence of π···π interactions. A recent publication by Grimme reported a computational study which appeared to show no evidence of π···π stabilisation until much larger aromatic systems were involved.[110]

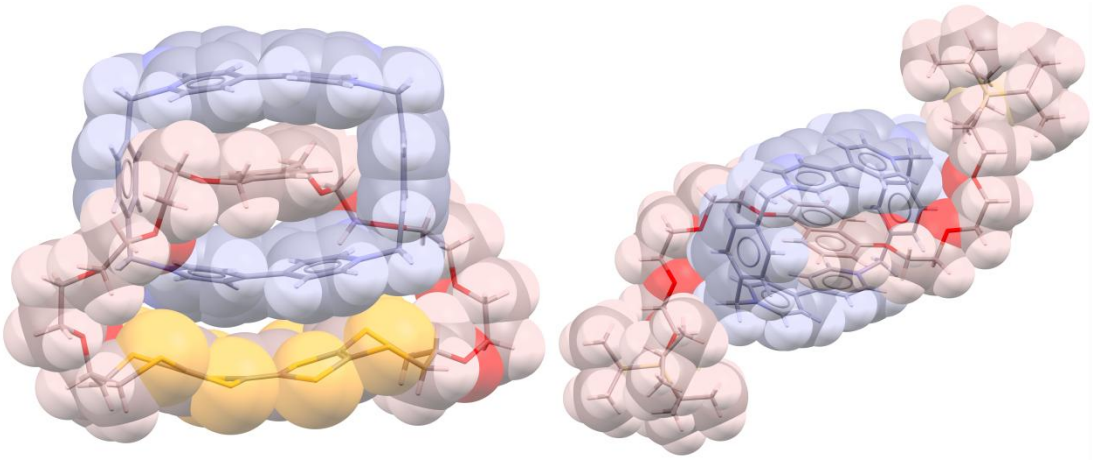

Figure 18 – Examples of Stoddart's catenane (left) and rotaxane (right).

Stoddart has carried out a great deal of work utilising π···π interactions in the field that he refers to as "Mechanostereochemistry", an area which examines the science of mechanically interlocked species.[20] Stoddart has utilised π···π interactions to a large degree in the design of his rotaxanes and catenanes (Figure 18).[140] It important to note that the π ··· π interactions that Stoddart makes use of are markedly different to the interactions that Hunter reports. Stoddart's systems involve the highly charged paraquat box which, in turn, leads to the observation of charge transfer bands within the UV/visible spectra suggesting an element of electrostatic donor-acceptor interaction.

There are many different approaches to the synthesis of these interlocked species but central to them all is the association of the two separate molecules forming a pseudorotaxane. This undergoes a synthetic modification, a capping or cross-linking, to form either the rotaxane or catenane. In order for this pre-organisation to occur there needs to be a driving force, in some cases this is the coordination of metal centres but Stoddart's examples rely on the charge transfer π···π interactions.

1.2.1.6 Key work utilising intermolecular interactions in Crystal Engineering

1.2.1.6.1 Hydrogen Bonded Assemblies

Whitesides has been a key exponent of molecular self-assembly, through intermolecular interactions such as hydrogen bonding, as a methodology for the formation of nanostructures. In his review[141] he discusses the precedent that nature sets for molecular self-assembly, as well as highlighting the complexity of examples seen in nature compared to synthetic attempts. Furthermore he concludes that molecular self assembly is vital to a "bottom up" engineering of new nano-materials for applications varying from high density data storage devices in molecular electronics to micro sensors or catalysts.[141, 142]

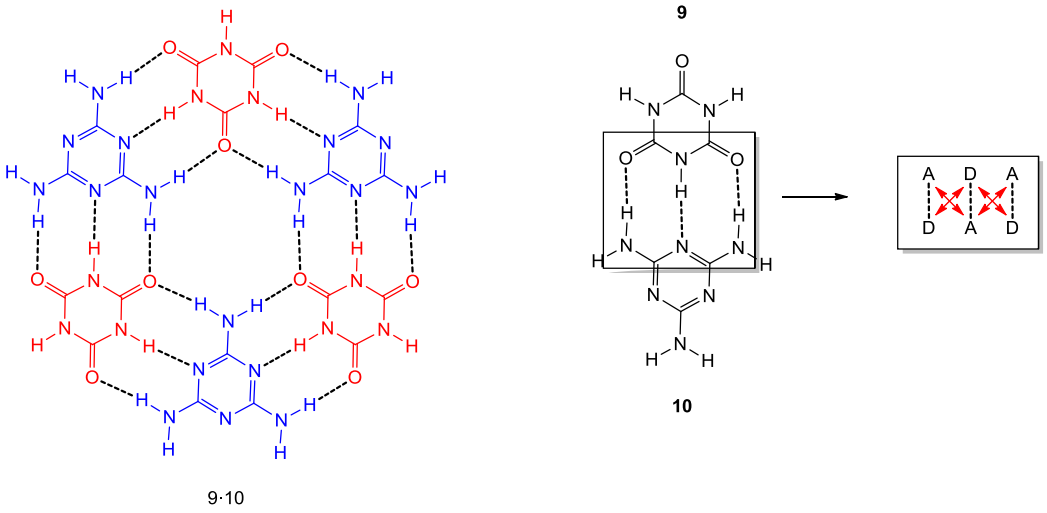

9·10

Figure 19 – Initial work carried out by Whitesides focussed understanding the solid state structure of the hydrogen bonded complex formed by mixing cyanuric acid and melamine.

Whitesides started with a series of studies aimed at proving the solid state structure of the insoluble product formed by mixing cyanuric acid (**9**) and melamine (**10**) together (Figure 19).[143] While Whitesides, amongst others, believed he understood how the two molecules interacted, proving it was a different matter.

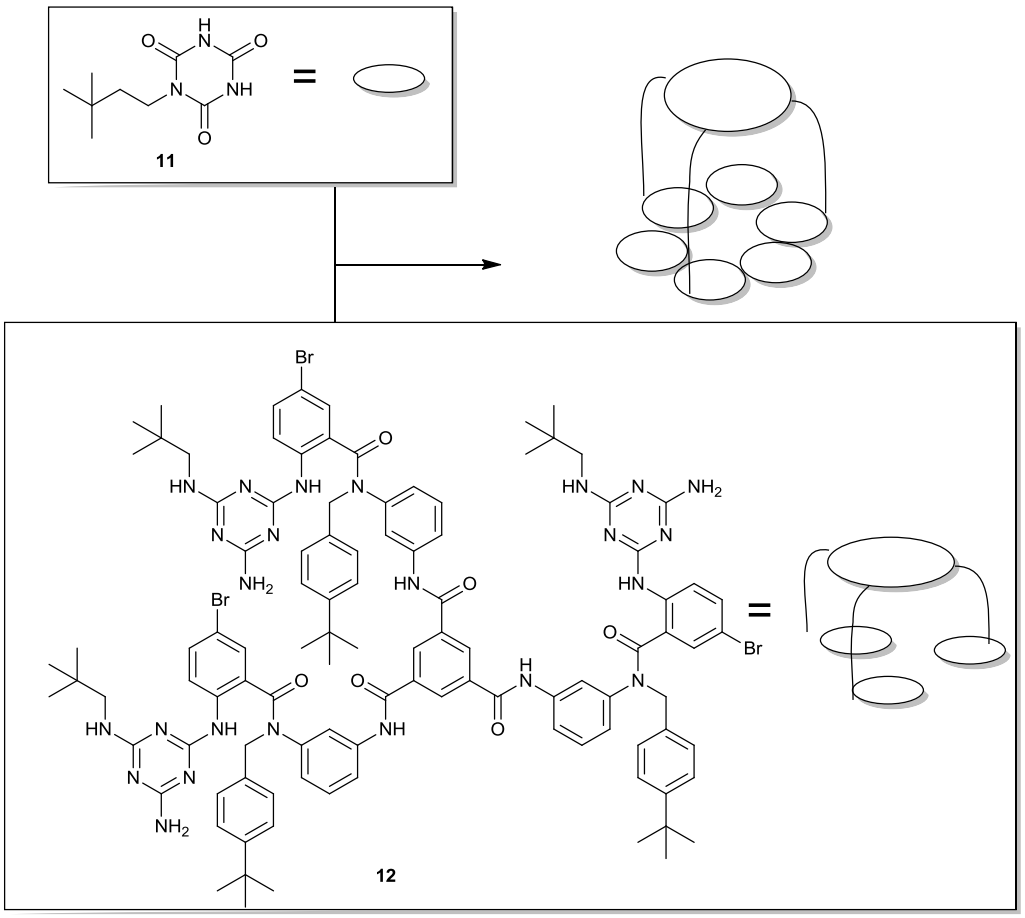

Figure 20 - Schematic diagram showing the tripodal melamine derivative synthesised by Whitesides and the cyanuric acid derivative he titrated against in order to form the complex illustrated.[143, 144]

Whitesides described the synthesis of a linked tris-melamine unit (**12**) which could be used in NMR titrations against a modified cyanuric acid (**11**), yielding data which enabled Whitesides to add weight to the proposed motif for the normal melamine cyanuric acid adduct (Figure 20).[143, 144] Given that this work led to a large body of further work, Whitesides conclusions were only confirmed nine years later when Rao managed to obtain the X-ray crystal structure of the melamine:cyanuric acid adduct.[145]

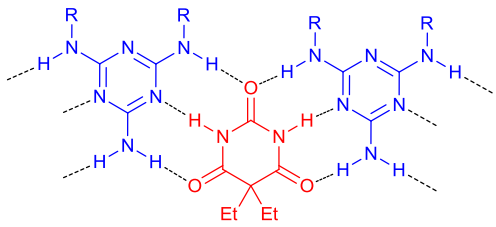

13·14

Figure 21 - By substitution at the positions indicated (R) Whitesides aimed to limit the directionality of the self-assembly prompting the formation of one-dimensional tapes.

Whitesides identified that by modifying the molecules involved in this highly directional self-assembly, it was possible to constrain the large number of orientations usually possible in the solid-state.[146] This would aid any study of the relationship between molecular structure and solid-state structure. Whitesides therefore went on to characterise a series of structures formed between barbituric acid derivatives and melamine derivatives (**13·14**) (Figure 21).[147]

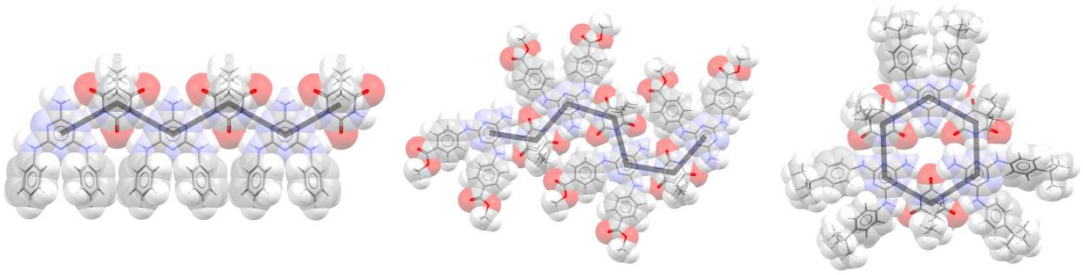

Figure 22 - Some of the different motifs found by variation of pendent substituent of the molecules in Figure 21. On the left is the predicted two molecule repeating unit tape, in the centre is a four molecule repeat unit "crinkled tape" and on the right is a molecular rosette.

Figure 22 shows a few examples of structures reported by Whitesides and highlight some of the more common motifs that he found. These include a simple, alternating tape which gives a very symmetrical 2 molecule repeat unit. The central structure is a case where the barbiturate unit sits in a different arrangement. This forces the next melamine unit into a different alignment and causes the repeat unit to become 4 units long. In the right hand example it is possible to see that the two units form a molecular rosette. The variation in solid-state structure appears to result from the alteration of the substituent R group. This is a stark example of the importance of interactions beyond the hydrogen bonding array being investigated, determining the secondary and tertiary structure of any self-assembled material.

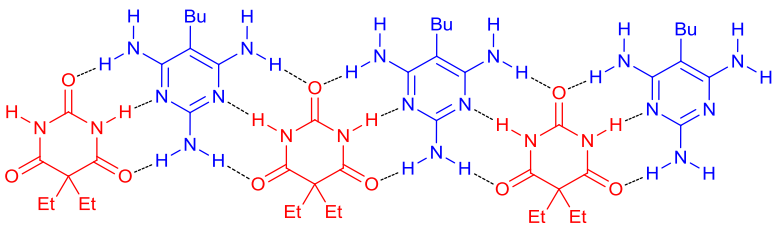

15·16

Figure 23 – In similar work to that carried out by Whitesides, Lehn was investigating melamine barbituric acid derivatives.

At around the same time as Whitesides was carrying out his work on these compounds Lehn also explored the self-assembly of barbituric acid and melamine derivatives (**15·16**)(Figure 23).[24] Lehn developed this work further by examining the ability of molecules to form different shaped arrays based on the components present.[148]

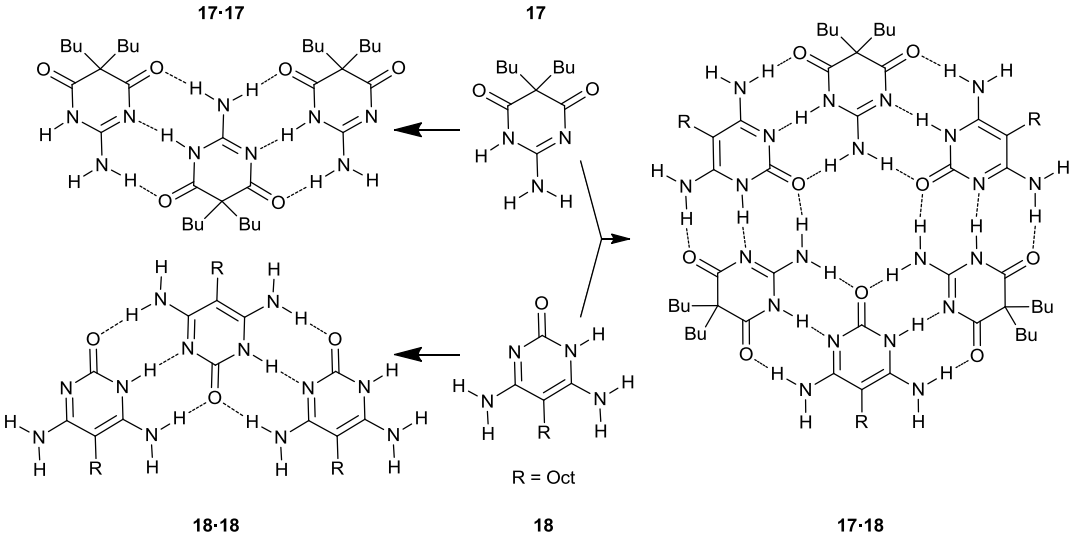

Figure 24 - Following initial work show in Figure 19 Lehn devised a system in which two self complimentary materials could be mixed forming a different structural motif.

Lehn synthesised two molecules that were both complementary (**17·18**) and self-complimentary (17·17 and 18·18) (Figure 24) meaning that they would form tapes as individual materials but upon mixing they would form a different more complex structure. While he was able to confirm the taping of one component, the lack of solubility of the other appeared to hamper the determination of the other component or indeed the multi-component array.

1.2.1.6.2 Foldamers

One of the driving factors of supramolecular chemistry is the study of assemblies inspired by nature. The process of folding and unfolding of proteins in nature has prompted investigation into molecules that can undergo a similar process.[149] Synthetic "foldamers" have been investigated for a number of reasons, initially for the control of conformation that could be imparted. However, this work has subsequently developed from exploring the control of the folding/unfolding process as a result of different stimuli, through to the development of foldamers with

cavities for guest recognition. There are, as yet, only a handful of "good folders." This appears to stem from our lack of understanding in the utilisation of van der Waals interactions and solvophobic interactions in the stabilisation of foldamer molecules.[150]

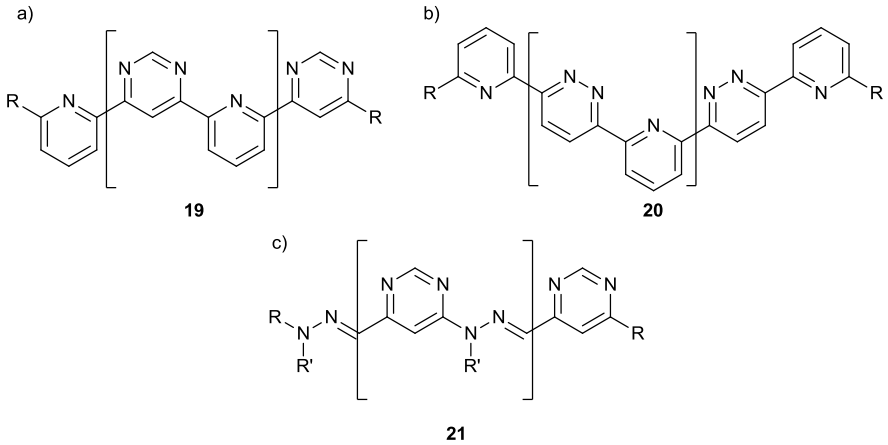

Figure 25 – Lehn's first foldamers a) pyridine-pyrimidine[151] b) pyridine-pyridazine[151] c)pyrimidine-hydrazone.[152]

Lehn has carried out a great deal of work studying heterocyclic oligomeric systems which form helical foldamers. His work originally started by looking at pyridine – pyrimidine/pyridazine[151] systems (**19**) and has more recently moved on to naphthyridine – pyrimidine[153] systems (**20**). Variation of the heterocycles used is an attempt to fine tune the properties of the helix formed, including the pitch and the cavity formed in the centre. Lehn has also reported systems with a hydrazone link between the pyrimidine molecules (**21**).[152] Lehn reports that hydrazone linked materials were discovered in an attempt to produce foldamers which were simpler to synthesise; they also offered the ability to increase solubility through the introduction of a solubilising chain at the additional substitution point.

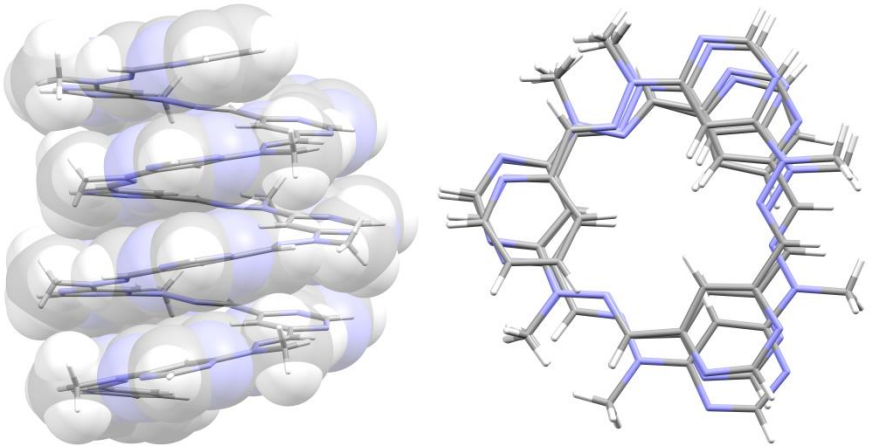

Figure 26 – X-ray crystal structure of the longest hydrazone –pyrimidine oligomer (21), the view on the left shows how the foldamer packs in the vertical plane while the view on the left shows the overlapping nature of the foldamer when viewed from above.[152]

Figure 26 shows the most extended of Lehn's hydrazone – pyrimidine oligomeric foldamers (with n = 9). As can be seen, the molecule is arranged in a helical manner caused by the intramolecular hydrogen bonding between the hydrazone nitrogen and the aromatic C-H groups on the pyrimidine. It appears that the helix might also be stabilised by a π···π interaction between the pyrimidine rings as each ring is slightly offset from its neighbouring ring in an arrangement that Hunter describes as favourable.[128]

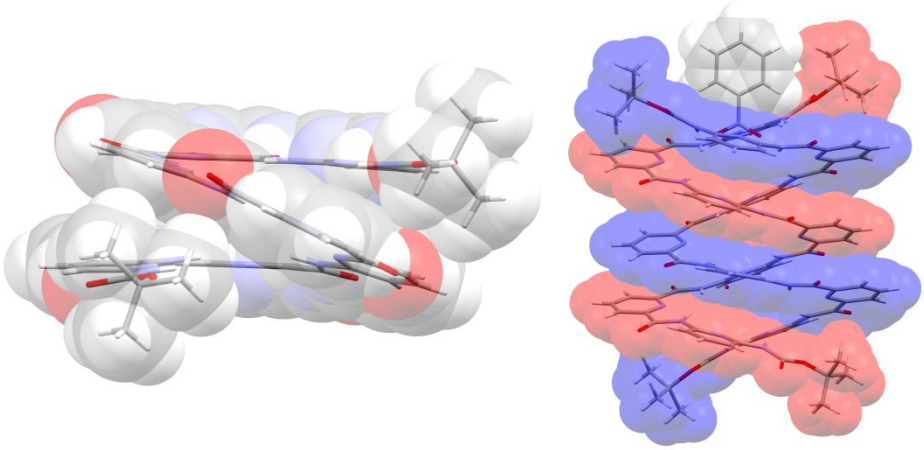

Figure 27 – The crystallisation of the heptameric pyridine carboxamide oligomer is solvent dependent. The structure on the left is a single stranded helix formed during the crystallisation from DMSO/acetonitrile whereas the structure on the right is the material crystallised from nitrobenzene/heptane.[154-156]

While there are examples of ligands forming helical structures upon co-ordination to a metal centre, [157] there are very few examples of non-templated, synthetic self-assembled double helix structures.[155, 156] In the metal based systems the helical

nature is driven by the co-ordination environment of the metal centres rather than through recognition of a complementary strand such as seen in DNA. Lehn reported that foldamers based on a family of oligomeric amides formed by the reaction of 2,6-diaminopyridine and pyridine-2,6-dicarboxylic acid formed not only a single stranded helical conformation of some of the oligomers,[154] but that the pentamer and heptamer could interchange between the single and double helix structures due to the reversible nature of the helix formation.[154-156]

1.2.1.6.3 Supramolecular polymers

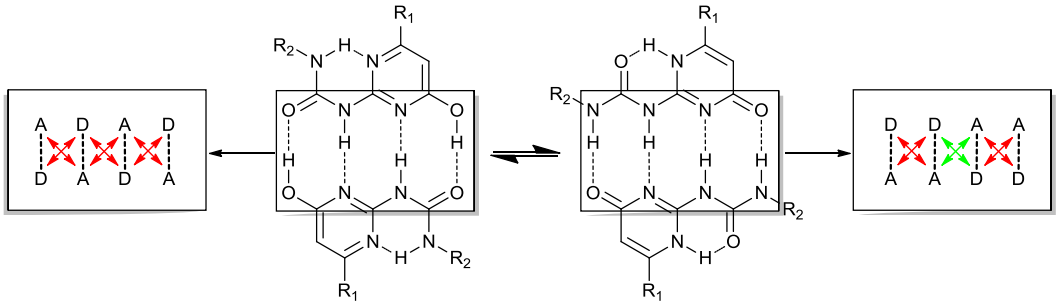

Figure 28 –Meijer's work focused on the ureidopyrimidinone molecules, which can form more than one self-associating dimer pair due to the molecules ability to tautomerise.[158]

Meijer's work has focused on utilising self-assembled systems to create polymeric materials that assemble through highly directional hydrogen bonding arrays. [159] The ureidopyrimidinones (Figure 29) can exist in three tautomeric forms two of which form self-complimentary dimers (**22a** and **22b)**.[158] Meijer reported one of these compounds (R_1= CH_3 R_2= C_4H_{10}) which has an association constant of $>10^6$ M^{-1} in chloroform and provided a stable scaffold from which it was possible for Meijer to produce a great amount of work on polymeric materials.[160-168] While this molecule shows great potential as a building block due to its high binding constant, it is slightly complicated by the aforementioned presence of alternate tautomers which form weaker dimer pairs.[158]

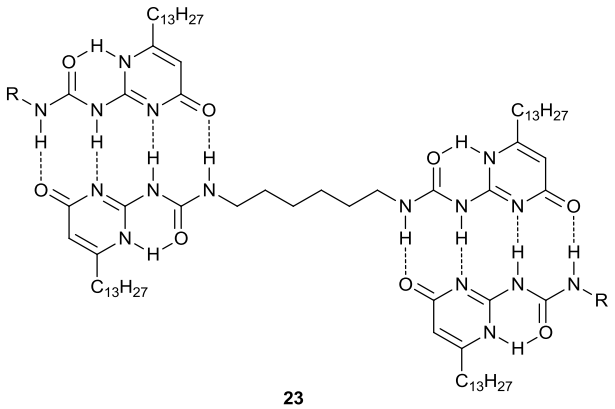

23

Figure 29 –Meijer linked two ureidopyrimidinone units together (23**) in one of the earliest examples of a supramolecular polymer.**

One early example of utilisation of this dimer unit for supramolecular polymer formation involved a simple substitution of the methyl group for a tridecyl chain with two units linked together (**23**).[159] This material formed viscous solutions, consistent with polymer formation, in chloroform down to concentrations of 5 $gmol^{-1}$. Addition of an unlinked monomer unit, which acts as a stopper, to this viscous solution caused a dramatic drop in viscosity suggesting the breaking up of the polymeric system. [159] This observation led Meijer to study the solution phase behaviour of both poly-ureidopyrimidinone oligomers and similar materials.

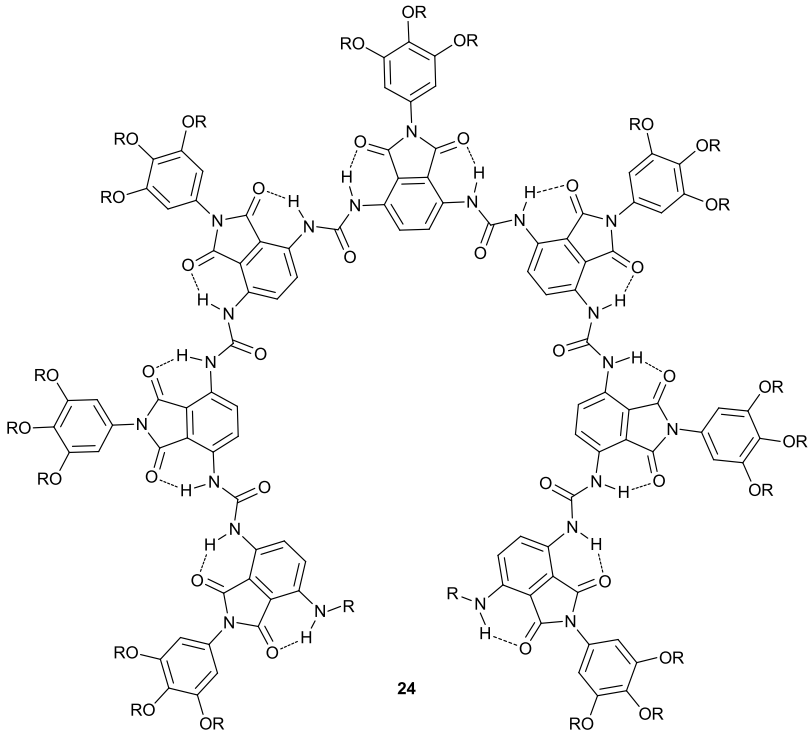

24

Figure 30 – Following on from the work on ureidopyrimidinones (22**) Meijer identified that the poly-ureidophthalamides (**24**) could also form a helical structure thanks to the intramolecular hydrogen bonding.**

More recently he has extended his systems to include an oligo ureidophthalamide system (**24**), in the hope that it would adopt a helical arrangement arising from the turn that the intramolecular hydrogen bonding imparts.[169] Meijer synthesised a range of molecular weight fractions (30, 7 and 3.5 average molecule units respectively) as well as defined oligomeric fractions up to 8 units.[169] He observed that compounds with low molecular weight show no sign of helicity, the medium molecular weight show some signs while the higher molecular weight material shows strong ordering. This led to the suggestion that this shows that the poly-ureidophthalamide (**24**) forms a helicate with a pitch somewhere in the region of 6-8 units. The poly-ureidophthalamide (**24**) system is very sensitive to solvent, with the helicity being observed in THF and not at all in chloroform. [170, 171] When tested for degradation by the addition of chloroform to a THF solution of the high molecular weight it was noted that a sharp reversal of the chiral nature of the material occurred at 50% chloroform in THF.[169]

1.3 Previous Work on Disubstituted Pyridines

Within the Grossel research group there is over a decade of research into the solid state behaviour of disubstituted pyridine derivatives. Work was originally started with a view to utilising some of the materials for applications such as molecular delivery systems however, it led to investigations into the detailed behaviour of the synthesised materials and self association.

1.3.1 Pyridine-2,6-dicarboxamides

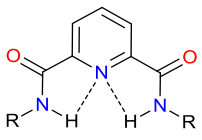

25

Figure 31 – Pyridine-2,6-dicarboxamides adopt a syn – syn conformation with the amide N-H bonds pointing inwards creating a conformation in which they can form an intramolecular hydrogen bond to the pyridine nitrogen.

Initial work was carried out by Parker[172] who was investigating the use of pyridine-2,6-dicarboxamides (**25**) as "molecular tweezers" due in part to predicted internal preorganisation involving the amide hydrogen and the pyridine core (Figure 31).

This behaviour is reported by Hunter,[173, 174] Vögtle[175-177] and Leigh[178-180] who utilised this behaviour in catenane synthesis. Parker was aiming to create a molecular pincer that could be attached to a dendritic surface to provide a large number of binding sites on a single molecule. His work required examination of a number of different factors including the mechanism of attachment to the dendrimer, the functionalisation of the "tweezer" to provide selectivity and, if possible, a mechanism to control the binding. Parker's preliminary work on molecular delivery systems was continued by Golden[181] who studied the attachment of chelidamate dicarboxamides to polymer resins.

1.3.1.1 Solid-state behaviour

Before synthesis was started on the pyridine-2,6-dicarboxamides no analogous solid-state structures had been reported, although Hunter[173] had reported a computational study of the difference in conformation between pyridine-2,6-dicarboxamides and the analogous isophthalamides. This led Gomm[182] to investigate the solid-state architectures of the pyridine-2,6-dicarboxamides in which he identified three packing motifs: molecule chains. where: the carbonyl from a neighbouring molecule sat within the amide cleft (Figure 32a); self-complimentary dimers, where the pendent arm of one molecule sat within the cleft of its neighbour (Figure 32b) and host – water complexes (Figure 32c).

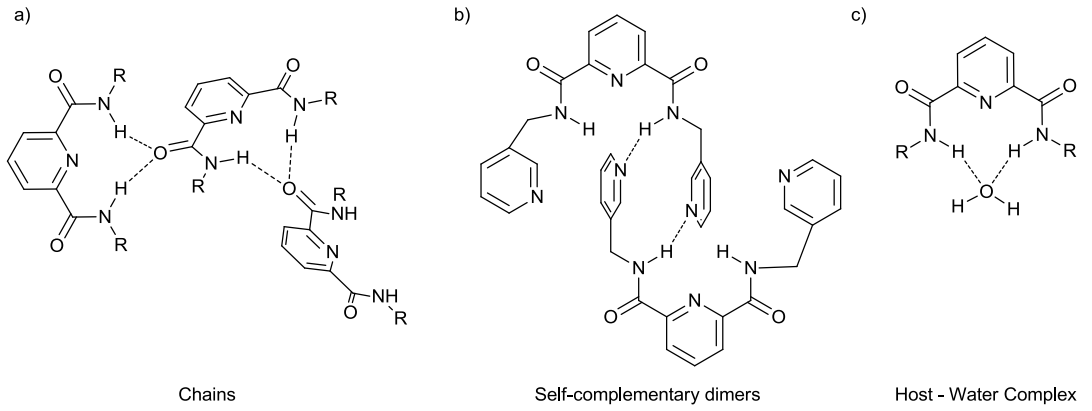

Figure 32 - Three different packing motifs observed in the solid-state packing of pyridine-2,6-dicaroxamides.

More recently Dwyer[183, 184] continued the work on pyridine-2,6-dicarboxyamides, only this time looking at utilising enantiomeric pendent side arms to make the

"chiral molecular tweezers" in the hope that this would yield a material which could be utilised for chiral separation or chiral catalysis.

1.3.1.2 Metal binding properties

Following the detailed study of the solid-state architecture of some of the pyridine-2,6-dicarboxamides and given the literature precedence for metal co-ordination by pyridine-2,6-dicarboxamides and analogous motifs,[185-192] attempts were made to investigate the metal co-ordination of some of the novel derivatives reported by Gomm[182] and Dwyer.[183, 184] Looking at only one compound, *N,N'-bis*[pyridine-2-ylmethyl]pyridine-2,6-dicarboxamide (**26**), Gomm and Dwyer found that three different metal centres gave very different solid-state architectures.

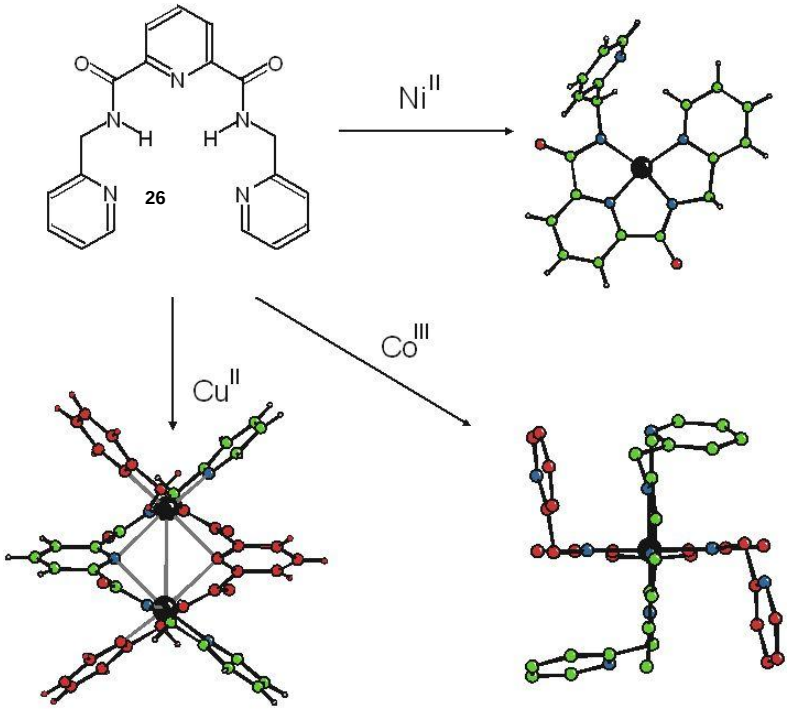

Figure 33 – *N,N'-bis*-2(pyridylmethyl)pyridine-2,6-dicarboxamide (26**) forms three very different motifs when co-ordinated to nickel, cobalt and copper.[193]**

Dwyer[184] went further with this work examining the metal binding capabilities of his chiral pyridine-2,6-dicarboxamides with metals such as palladium, a useful catalytic metal centre, and found them capable of forming chiral metal complexes with some potential for enantiomeric selective catalysis.

1.3.2 Pyridine-2,6-dicarboxylates

As part of the investigation into the pyridine-2,6-dicarboxamides Oszer[194] made a preliminary investigation into the solid state properties of pyridine-2,6-dicarboxylates which were predicted to form an extended anti-anti conformation. In this study Oszer synthesised a number of compounds analogous to Parker's dicarboxamides.

1.3.2.1 Solid State Behaviour

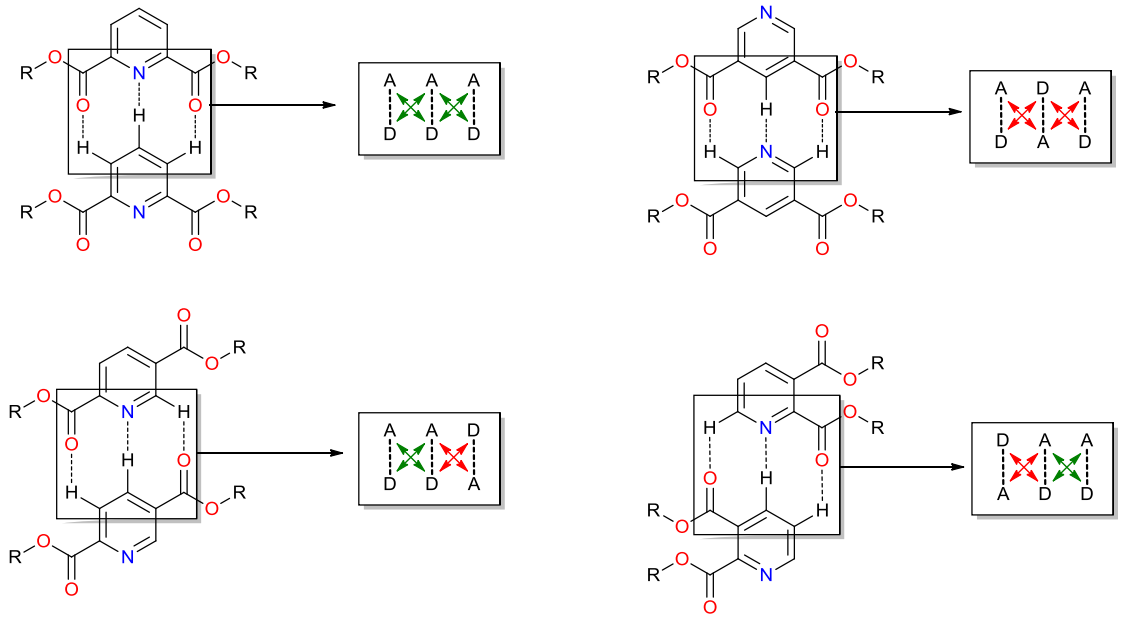

Figure 34 – The different structural isomers of pyridine dicarboxylate give rise to different hydrogen bonding arrays which have been studied by Oszer,[194] Parker,[172] Gomm,[182] Orton[195] and Cheesewright.[196]

Oszer's initial study[197] showed the first examples of solid-state structural information for simple pyridine-2,6-dicarboxylates without any metal complexation and led to a detailed study of more derivatives. Oszer's work was then developed by Gomm[182] who synthesised a larger library of dialkyl pyridine-2,6-dicarboxylates as well as beginning to examine the effect of altering the core substitution pattern by exploring the behaviour of the 3,5; 2,3 and 2,5 disubstituted analogues in an attempt to compare interaction strength with varying secondary interactions as shown in Figure 34. This gave a good opportunity to directly compare the effect that secondary interactions have on the hydrogen bonding arrays. Further work was carried out by Orton[195] who completed a more detailed analysis by attempting to

complete the library of analogues for each pyridine core whilst carrying out a more detailed examination of the crystallographic structural similarities and differences. More recently, Cheesewright[196] has investigated a further series of compounds looking at the effect of halogen substitution on the benzyl ester. In addition the differences and similarities observed in analogous methyl and chloro substituted compounds, which are of similar van der Waals radii, were compared. Cheesewright has also synthesised compounds with larger conjugated ring systems to investigate the impact of potential π···π and charge transfer interactions on the hydrogen bonded taping motif.

1.3.2.2 Secondary structure

One of the key observations initially made by Gomm, and further substantiated by Orton, was that the secondary packing structure of the pyridine-2,6-dicarboxylate derivatives was through the packing of the one dimensional tapes formed, not through the packing of individual molecules.[182, 195]

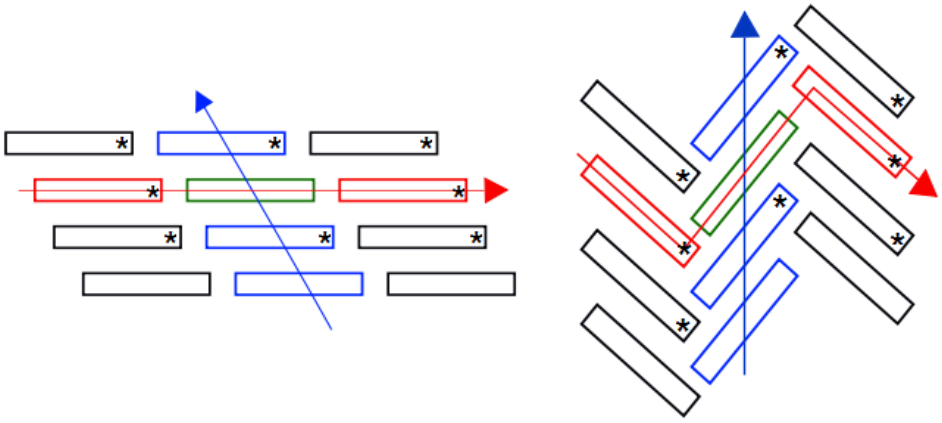

Figure 35 – The infinite one-dimensional tapes formed by pyridine-2,6-dicarboxylates arrange themselves into either a co-planar motif (left) or a herringbone motif (right).

It was found that there were two major packing motifs for the tapes. In many cases the tapes would align in flat sheets which would then assemble into stacks of sheets (Figure 35). The alignment of the individual tapes into sheets in either planar parallel sheet structure (P) (Figure 35 left) or a herringboned structure (H) (Figure 35 right) appeared to be dependent on the peripheral substituents as was the orientation of the sheets relative to one another. Orton[195] then added further detail to this by strictly defining the terms layer and stack:

"A layer is formed by the extension from the side of the tape, parallel to the core to the nearest neighbouring tape; a stack is defined as the two tape arrays above and below the reference tape which exhibit 50% overlap."[195]

It is very important to note that this stacking ***is not*** an indication of intermolecular stacking analogous to the π···π stacking discussed earlier. That said, in many cases there do appear to be interactions between the layers in a stack but in this work the description of stacking tapes refers to purely geometric organisation. Gomm, Orton and Cheesewright have developed a set of numerical descriptors which describe the nature of the assemblies formed and this will be utilised in the current work.[182, 195, 196]

1.3.2.2.1 Descriptors for pyridine-2,6-dicarboxylate tapes

In order to accurately describe the solid-state architecture, a detailed system of measurements and descriptors has been developed.

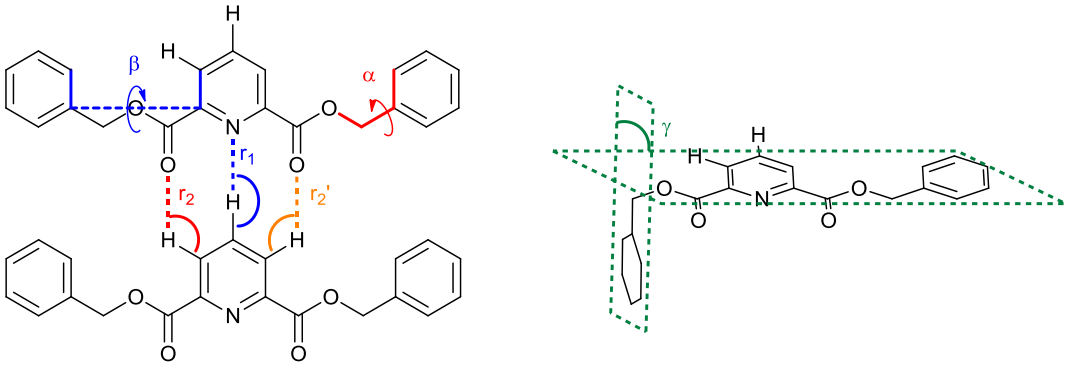

Figure 36 – The pyridine-2,6-dicarboxylate tapes have been parameterised in order to ease the description of the taping contact lengths and the twist and bend of the pendent ring side arm.

Figure 36 shows the parameters used by Orton and Cheesewright to describe the pyridine-2,6-dicarboxylate structures they had reported, as well as one additional parameter which has been added to help better describe the bent geometry observed in sheet formations which will be reported later.

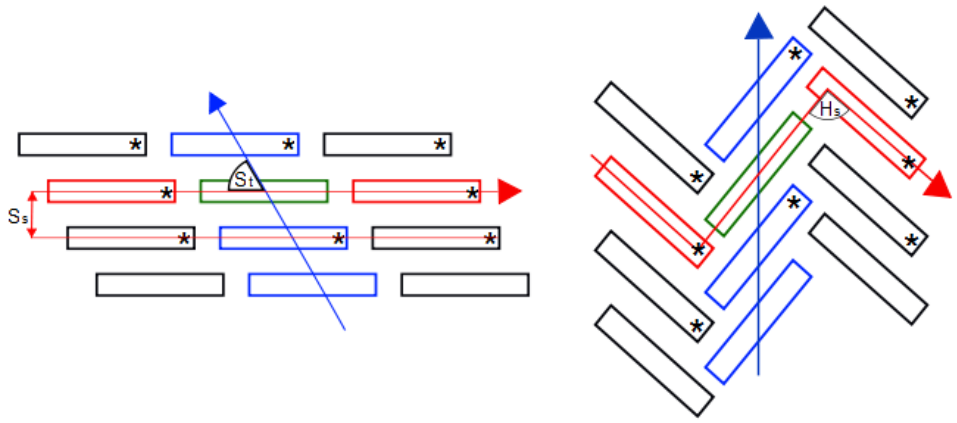

Figure 37 – The description of the secondary packing of the hydrogen bonded tapes can be enhanced by the addition of descriptive terms for interstack distance (S_s), long axis shift (S_t) and Herringbone angle (H_s).

As discussed previously, Gomm[182] initially suggested that structures which exhibited taping formed one of two architectures; either a planar parallel sheet structure (P) or a herringboned structure (H). Orton and Cheesewright added numerical descriptors for interstack distance (S_s), long axis stack shift (S_t) and herringbone angle (H_s) in order to allow a simple, none visual description of the packing arrangement.

This basic set of descriptors can be further added to it by detailing the core directionality within the sheets and the stacks. This is denoted by a pair of arrows pointing in the same direction in the case of parallel packing, or in opposite directions in the case of anti-parallel packing. Thus a descriptor $HL_{\uparrow\uparrow}S_{\uparrow\downarrow}$ would denote a herringbone structure with parallel layers and anti-parallel stacks.

1.4 1,8-Naphthyridine

1.4.1 Background

Whilst the pyridine-cored systems have been heavily investigated over the previous decade it was thought that it would also be of interest to look at the possibility of extending the hydrogen bonded array using a 1,8-naphthyridine core. 1,8-Naphthyridines have been shown to have a number of interesting applications but little is known at present about the solid state behaviour of 2,7-dicarbonyl-1,8-naphthyridine derivatives.

1.4.1.1 Medicinal uses

To date 1,8-naphthyridine chemistry has mainly been driven by the pharmacological and medicinal applications that its derivatives have shown.[198] A brief look at medicinal chemistry literature shows that a number of 1,8-naphthyridine-cored compounds are commercially available drugs and a far greater number have been synthesised and tested for potential activity.[199-204]

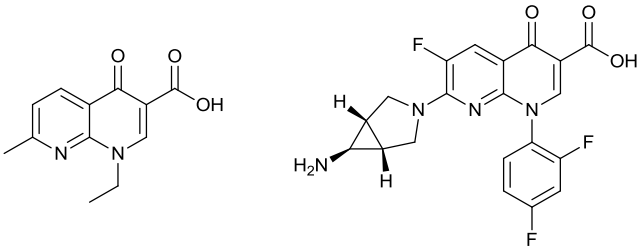

Naldixic acid - **27** trovafloacin - **28**

One of the most common classes of compounds that 1,8-naphthyridine derivatives have been found in are the quinolone antibiotics, indeed Nalidixic acid (**27**) is generally acknowledged as being the first drug in the class when introduced to clinical use in 1967.[205] Since this time many thousands of analogues have been synthesised, though only a few, such as Trovafloxacin (**28**),[206] made it to clinical use.[205] However in more recent times, use has been discouraged as the quinolone antibiotics have been found to have serious, adverse effects with Nalidixic acid being shown to induce convulsions[207] and Trovafloxacin being shown to cause acute liver failure.[208]

1.4.1.2 Metal binding

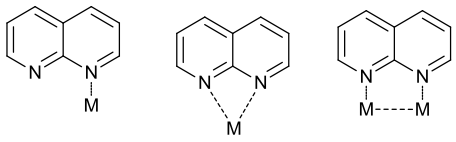

Figure 38 – 1,8-Naphthyridine has been shown to be able to co-ordinate to metal centres in more than one motif.

Since 1970 1,8-naphthyridine has been a commonly used ligand in co-ordination chemistry.[198] This is due in part to its ability to co-ordinate in 3 distinct motifs, one of which offers interesting multidentate co-ordination possibilities,[209-212 213, 214] as well as the constrained bite angle of 2.2°.[198] However, the topology of the co-ordination complex depends on more factors than just the main ligand. These

include: the nature of the ancillary ligands; the metal ion size/charge and the solvent system utilised in the crystallisation.[198]

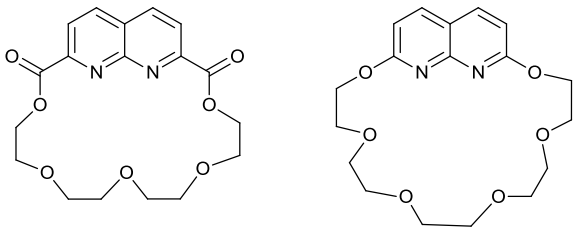

29 30

Figure 39 – Work by Deady and Newkome focused on synthesising 1,8-naphthyridine in order to synthesise 1,8-naphthyridine containing macrocycles.

There has also been interest in the incorporation of the 1,8-naphthyridine unit into macrocyclic structures. In particular a number of 1,8-naphthyridine containing crown ethers (Figure 39) have been synthesised by Deady[215] and Newkome.[216, 217] The synthetic routes employed will be discussed in chapter 2 however, there is as yet little information on the metal binding properties of such structures.

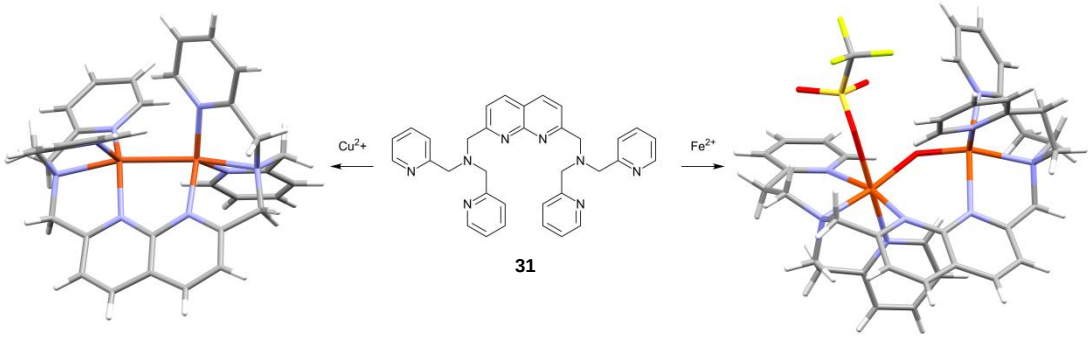

31

Figure 40 – Lippard's 1,8-naphthyridine cored ligands were designed to act as "masked carboxylate" units.

In 2000 Lippard designed a series of 1,8-naphthyridine-cored ligands[213] in order to investigate the biomimetic behaviour of dinuclear molecules (one example (**31**) is shown in Figure 40). Work had been carried out previously on utilising carboxylic acid-based ligands to produce the dinuclear structures however, in aqueous conditions it was found that the latter tended to dissociate into the mononuclear species. Lippard's ligands were designed using a 1,8-naphthyridine core unit as it offered a "masked carboxylate."

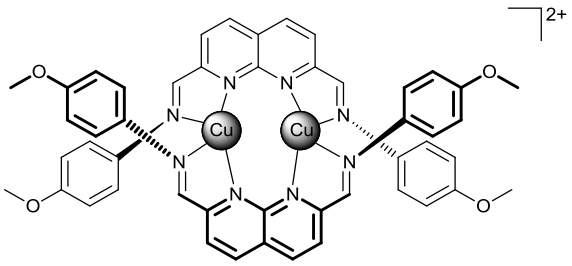

2:2: **32**·Cu complex

Figure 41 - A reported naphthyridine-based co-ordination helix.[218]

At around the same time Zeissel[218] reported the structure shown in Figure 41, which he claims is one of the first reported naphthyridine complexes to show a helical architecture. One of the reasons that there has been such interest in these bimetallic metal complexes is that they are viewed as potentially good catalytic materials.[198, 219, 220]

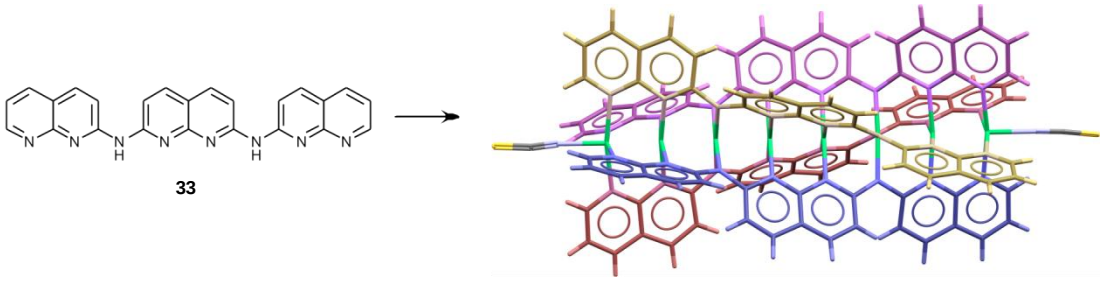

33

Figure 42 – Oligo-1,8-naphthyridine molecules such as 33 **have been shown to form molecular strings when co-ordinated with metal ions.[221]**

More recently oligo-1,8-naphthyridine and analogous materials have been utilised to form "metal strings" (Figure 42). [221] These compounds offer extended arrays of metal chelation sites allowing the formation of extended metal arrays, which are of interest for quantum electronics.[222-224] Metal strings have also been made with nickel, cobalt, copper and chromium, with each centre giving rise to different conductivity. While the nickel complexes often give lower conductivity values, the apparent ease of synthesis and comparatively high yields mean that they are still of interest. This has led to Peng suggesting that introducing multivalent nickel centres could improve the conductivity.[222, 223]

1.4.1.3 Molecular self-assembly

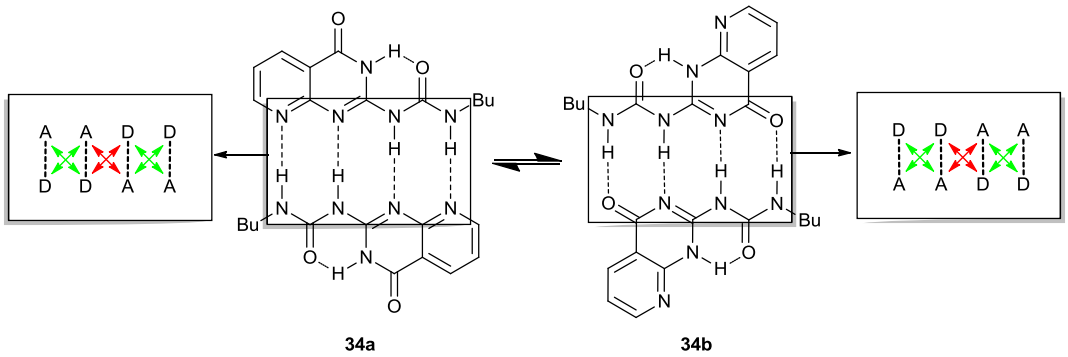

Figure 43 – Zimmerman's self assembling systems focussed on the use of deazapterin, which can exist in two different conformers, both of which are self-complementary.

The 1,8-naphthyridine core offers the potential for creating extended hydrogen bonding arrays. Zimmerman, Meijer and Lehn have each been instrumental in the development of supramolecular polymers.[166] Much of Zimmerman's work has utilised deazapterin (**34**) (Figure 43) a versatile heterocycle which, like Meijer's ureidopyrimidinone, can exist in a variety of tautomeric forms (**34a** and **34b**).[225] On its own it forms self complimentary dimers exploiting the AADD hydrogen bonding array that both conformers exhibit (Figure 43).

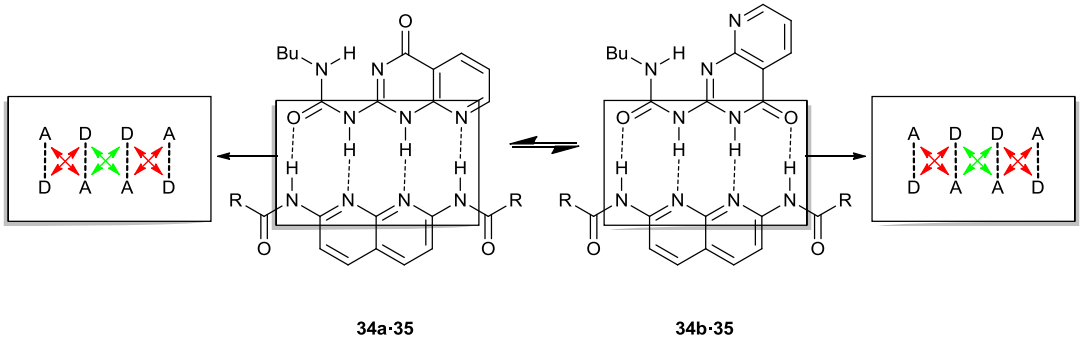

Figure 44 – When deazapterin is combined with a 2,7-diamido-1,8-naphthyridine derivative (35) it forms an equilibrium in which a complex is formed with each conformer of deazapterin (34).

Interestingly, when combined with 2,7-amido-1,8-naphthyridine the deazapterin undergoes a further tautomeric arrangement so that it provides a complimentary hydrogen bonding arrangement and then forms dimer pairs (Figure 44).[225] Zimmerman has utilised the 1,8-naphthyridine core for molecular recognition of urea as well as a monomer unit in supramolecular polymerisation.

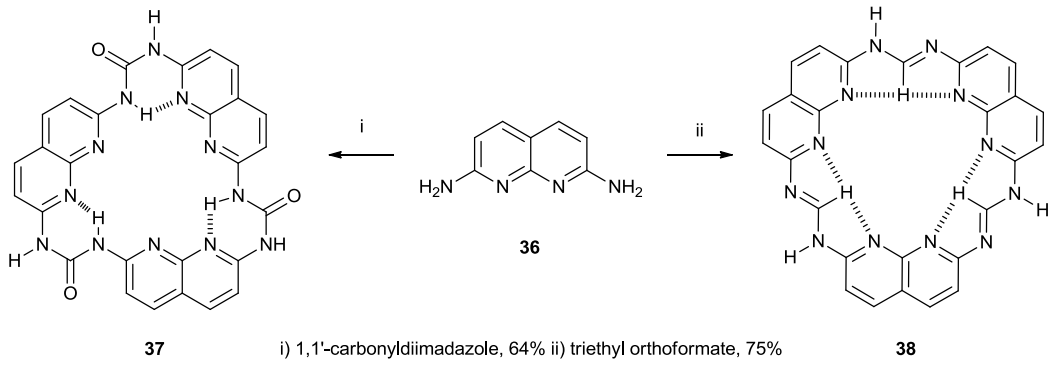

Scheme 1- Sutherlands synthesis of two 1,8-naphthyridine macrocycles was completed in high yield without the use of high-dilution techniques.

In 2005 Sutherland[226] reported a facile synthesis of two 1,8-naphthyridine containing macrocycles (Scheme 1) analogous to those which Böhme had synthesised from 2,6-diaminopyridine.[227, 228] What was of particular interest was the high yield obtained without the need for high dilution techniques so commonly required for macrocycle synthesis.

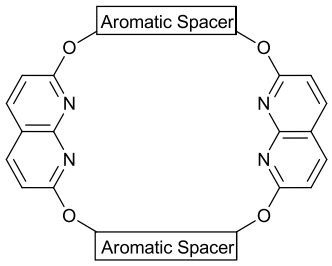

Figure 45 – Katz demonstrated the formation of calixarene-like molecules with 1,8-naphthyridine units which formed a 1,3-alternate conformation.

Following this it was shown by Katz[229] that it was possible to form calixarene-like molecules with 1,8-naphthyridine cores (Figure 45). These molecules were seen to adopt a 1,3 alternate conformation giving a pincer-like molecule with a cavity of approximately 7.0 Å, fulfilling the three principles originally set out by Chen and Whitlock.[138] Katz has subsequently investigated the effect of varying the aromatic spacer on the solid-state structure having noted that weak binding of guests was observed in the preliminary study.[229]

1.4.2 Previous Synthetic Work in the Research Group

The structural similarities of Zeissel's helix(Figure 41) to the pyridine-2,6-dicarboxamide complexes reported by Gomm[182] and Dwyer[184] have given encouragement that 1,8-naphthyridine-2,7-dicarboxamide complexes could yield an

interesting series of co-ordination complexes. Furthermore the potential for forming extended hydrogen bonding arrays based on 1,8-naphthyridine-2,7-dicarboxylates is also of interest in light of the work carried out by Meijer.[159]

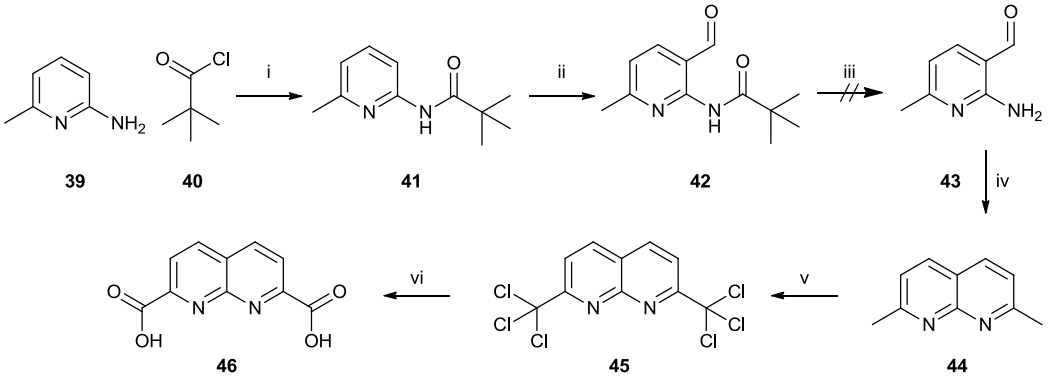

i) DCM/TEA/0 °C ii) a) BuLi/THF b)morpholine-4-carbaldehyde iii) 10% KOH, reflux iv)acetone, NaOH/EtOH v)NCS vi)P_2O_5

Scheme 2 – Gomm attempted synthesis of 1,8-naphthyridine-2,7-dicarboxylic acid by following the proposed synthesis shown above.[230]

As part of his work investigating alternate cores, Gomm[182] attempted to synthesise 1,8-naphthyridine-2,7-dicaboxylic acid (**46**), by the literature route shown in Scheme 2,[230] in order to explore the behaviour of both amide and ester derivatives. Unfortunately he came across problems during the amine deprotection to give **43** (Scheme 2 step iii) and work on this route was abandoned.

1.5 Descriptors for 1,8-Naphthyridine-2,7-dicarboxylate Tapes

In order to enable a simple comparison between pyridine-2,6-dicarboxamides and 1,8-naphthyridine-2,7-dicarboxylates, a similar level of parameterisation is required.

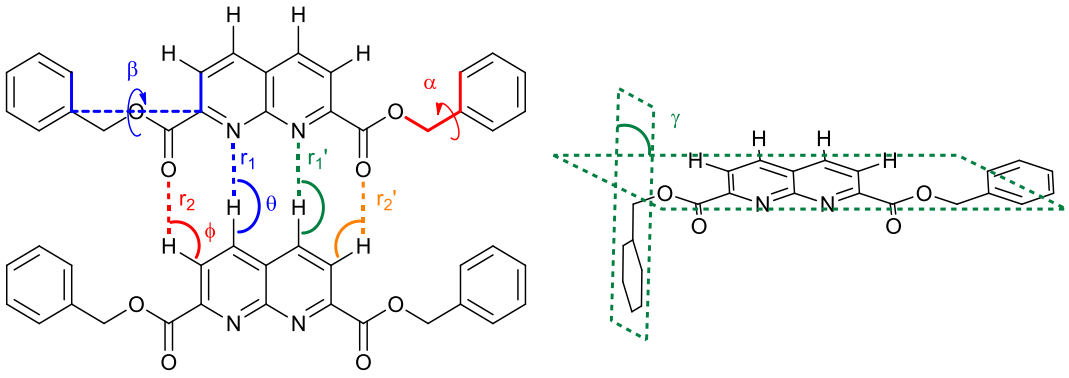

Figure 46 – 1,8-naphthyridine-2,7-dicarboxylate molecules have been assigned parameters very similar in nature to those used to describe the pyridine-2,6-dicarboxylate systems.

Figure 46 illustrates the parameters which will be used to describe the 1,8-naphthyridine-2,7-dicarboxylate structures reported in this study. It is worth noting

that in cases where the molecule is present in a space group which contains a symmetry element across the centre of the naphthyridine ring that $r_1 = r_1'$.

1.6 Hirshfeld Surfaces (CrystalExplorer)

Single crystal X-ray diffraction offers a detailed insight into the structural and spatial arrangement of individual molecules within a crystal. However it gives no definitive answer about molecular contacts and much of this information is therefore based on inference. As previously mentioned crystallographers have, rightly or wrongly, adopted Hamilton and Ibers' suggestion that the sum of the molecule's van der Waals radii could be used as a guide to the presence of an interaction. Even this approximation leaves the average viewer of a crystal structure no more able to clearly establish between what is a contact and what is simply a close packing.

Mark Spackman has been interested in the analysis and modelling of hydrogen bonding for some time, initially proposing a mathematical model for hydrogen bonding in 1986.[231] This study appears to have prompted much of his following work. In 1998 he published a description of the use of Hirshfeld surfaces as a visualisation technique for establishing the molecular domain in a crystal.[232, 233]

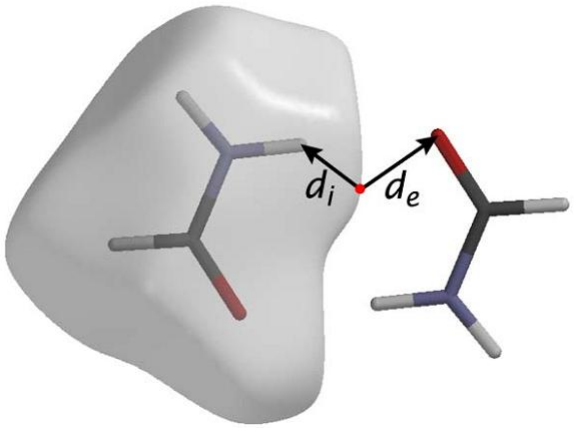

Figure 47 – The Hirshfeld surface of formamide is shown with the d_e and d_i distance illustrated.[234]

Hirshfeld surfaces have been compared to surfaces previously used in the analysis of molecular crystals e.g. fused Van der Waal surface[235, 236] and solvent excluded/accessible surfaces.[237, 238] They appear to have a larger overall volume, while still leaving voids within the molecular crystal which are areas of lower electron density. Hirshfeld surfaces have the advantage of being specific to the

crystal structure being analysed, meaning that polymorphic crystals will have different Hirshfeld surfaces and can be analysed for differences.[239]

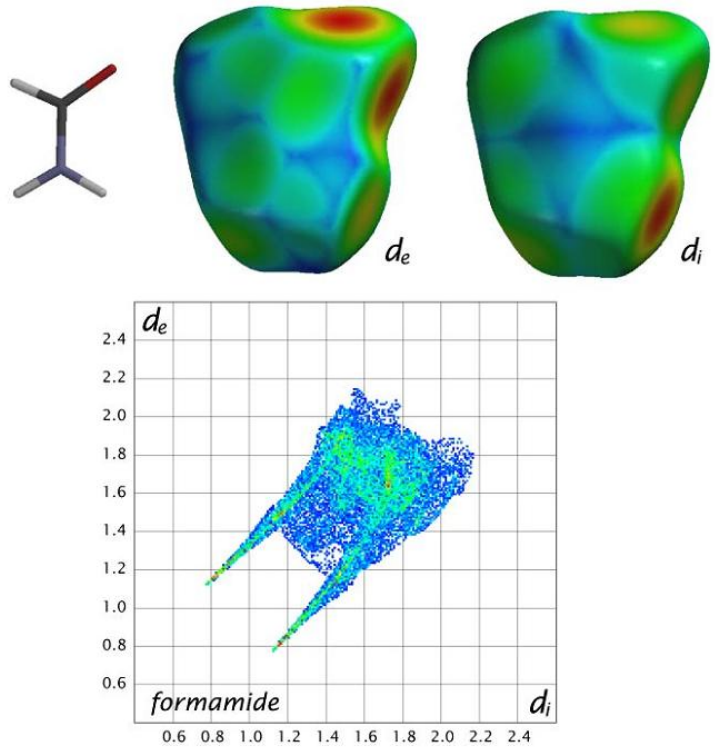

Figure 48 – Mapping the d_e and d_i lengths onto the Hirshfeld surface as a function of colour allows for visualisation of areas of close contact to the surface either internally or externally. It is also possible to plot this information on a scatter graph to produce a "fingerprint plot."[234]

The Hirshfeld surface, as initially reported, gave no further information about the molecule however Spackman realised that by analysing distances from the molecule to the surface (d_i) or the distance from the surface to nearest neighbouring molecule (d_e), the surface could be used to display a greater level of information. As such, by colouring the Hirshfeld surface according to the distance (red = short blue = long), Spackman has enabled the visualisation of close contacts between molecules within a packing arrangement. This information can also be displayed as a scatter graph producing a fingerprint plot for the molecule from which intermolecular interactions can be examined.[234]

Spackman and McKinnon have since released CrystalExplorer[240] a program which allows this type of analysis to be carried out on any X-ray crystal structure. Since the first release of CrystalExplorer there have been a couple of refinements to the software including the introduction of a normalised surface colour (d_{norm}) which takes into account the difference in size of constituent atoms. In addition to this it is

now also possible to selectively colour the surface (and fingerprint plot) to highlight the contact types.[241]

In the present study CrystalExplorer has been used to analyse in detail the various intermolecular contacts present in the crystal structures reported.

1.7 Aim

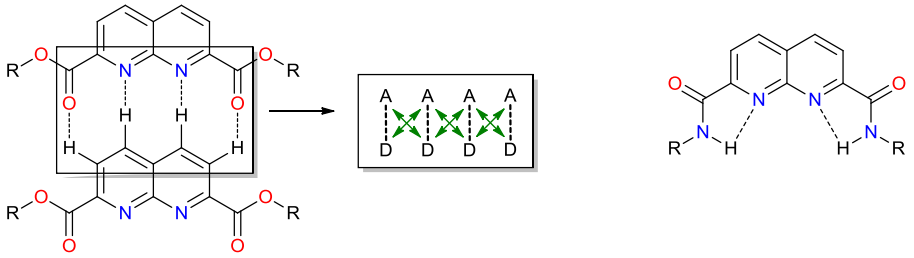

Figure 49 – This project focussed on the formation of 2,7- diester and diamide 1,8-naphthyridine derivatives which are predicted to offer two distinct sets of solid-state behaviour.

In this study it is envisaged that the starting material 1,8-naphthyridine-2,7-dicarboxylic acid will be synthesised in order that a library of novel 2,7-dicarbonyl substituted 1,8-naphthyridine may be created, focussing specifically on the diester (**47**) and diamide (**48**) derivatives. These derivatives offer the potential to study the effect of extending the hydrogen bond array from an AAA-DDD system in the analogous pyridine system to an AAAA-DDDD array in the 1,8-naphthyridine analogues.

A study of the solid-state structure of these 2,7-dicarbonyl substituted 1,8-naphthyridine derivatives will be carried out with the aim of identifying structural trends within the library of compounds, as well as allowing a direct comparison with the properties found in the corresponding pyridine derivatives previously studied.

As such chapter 2 details the different synthetic routes attempted for the synthesis of 1,8-naphthyridine-2,7-dicarboxylic acid, a key starting material for the synthesis of 1,8-naphthyridine-2,7-dicarbonyl derivatives. It also reports the attempted application of the synthetic methodology learnt during the synthesis of 1,8-naphthyridine-2,7-dicarboxylic acid to the synthesis of 1,9,10-anthyridine-2,8-dicarboxylic acid.

The results of solid-state structural studies of 1,8-naphthyridine-2,7-dicarboxylate analogues (**47**) are reported in chapter 3 and the effects of different substituents and substituent position are investigated.

Similarly the solid-state structures of the 1,8-naphthyridine-2,7-dicarboxamide derivatives (**48**) are reported in chapter 4. Attempts to undertake metal complexation with (2-pyridylmethyl)-1,8-naphthyridine-2,7-dicarboxamide yielded a metal complex which is also reported.

Finally chapter 5 details the synthesis of a number of 2,6-dicarbonyl substituted pyridine compound. In the case of the halogen substituted benzyl diesters this was carried out in order to study the solid-state structure, which could then be compared to that reported for the analogous 1,8-naphthyridne compounds.

Details of work carried out towards the linking of two functionalised pyridine units, with the hope that this will produce functional novel materials, is also reported within this chapter.

2 Synthesis of 1,8-naphthyridine Derivatives

In order to explore the solid state behaviour of 1,8-naphthyridine-2,7-dicarbonyl derivatives (**47** and **48**) it was first necessary to obtain a suitable starting material. While pyridine-2,6-dicarboxylic acid is readily available, 1,8-naphthyridine-2,7-dicarboxylic acid (**46**) is not commercially available and so must be synthesised from readily available starting materials. There is a reasonable amount of literature concerning the synthesis of 1,8-naphthyridines, given the medicinal properties highlighted in the introduction, though much of this literature appears to be low yielding. While this is not a problem for applications that require small quantities of materials, it is less satisfactory when a further functionalisation and/or relatively large amounts of material are required.

Examination of the literature highlights three potential routes to the desired 1,8-naphthyridine-2,7-dicarboxylic acid. They are discussed here in the order in which they were investigated.

2.1 Skraup Synthesis

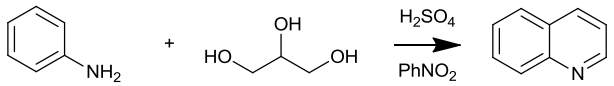

49 **50** **51**

Scheme 3 – The Skraup synthesis between aniline and glycerol carried out under strongly acidic conditions.

The Skraup synthesis is a well known methodology for the synthesis of quinolines (Scheme 3).[242, 243] It can however, give rise to a large range of side products and the reaction is known to be particularly violent. In 1943 Utermohlen[244] published an improved methodology utilising a nitrobenzene sulphonic acid solution in sulphuric acid (sulpho-mix) instead of nitrobenzene itself. While the Skraup synthesis has long been utilised for the synthesis of quinolines, use of this route to the analogous naphthyridines proved more testing. During a study of analogous naphthyridine isomers (1,5- and 1,6-) Paudler and Kress[245] reported the first successful use of the Skraup synthesis in a one step formation of 1,8-naphthyridine with a yield of 30% (replacing a 5-step synthesis from 2-aminonicotinate with a 28% yield). This was yield was later improved to 70% by Hamada[246, 247] by the addition of a ferrous

sulphate/boric acid catalyst. Hamada also reports improvement in yields for a number of Paudler and Kress's compounds, including 2-methyl-1,8-naphthyridine with an increase in yield from 10%, reported by Paudler[245], to 50% following his synthetic alterations.[246, 247]

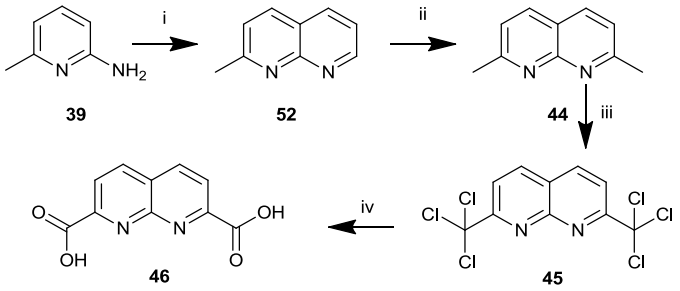

i) glycerol, H_2SO_4, sodium m-nitrobenzenesulphonate, H_3BO_3, $FeSO_4$ ii) 3eq MeLi, then $KMnO_4$, then Me_2CO iii) 8eq NCS, CCl_4 iv) H_3PO_4, 170 °C

Scheme 4 - Proposed synthesis of 1,8-naphthyridine via Skraup synthesis.[217]

More recent work by Newkome[217] investigated the further functionalisation of Hamada's 2-methyl-1,8-naphthyridine (**52**) to yield 1,8-naphthyridine-2,7-dicarboxylic acid (**46**) (Scheme 4). Newkome's work involved further functionalisation of the 2 and 7 positions avoiding the only previously reported method involving a selenium oxide oxidation of which Newkome states: "despite reports, this oxidation was not easily reproduced".[217] With this is mind Newkome's methodology was the first route to be investigated.

Unfortunately we immediately ran into problems recreating the initial formation of 2-methyl-1,8-naphthyridine (**52**), with our yields being closer to those reported by Paudler and Kress.[245] This poor yield is probably due, in part, to the dependence on dehydration of glycerol to produce acrolein. Interestingly, theoretical work into the dehydration of glycerol (**50**) by Nimlos[248] suggests that there could be a number of different intermediates and products with low barriers of inter-conversion which, added to the use of elevated temperatures, increases the likelihood of self-polymerisation; it is therefore unsurprising that the reaction gives a poor yield. As 2-methyl-1,8-naphthyridine is a key starting material for further functionalisation to form 1,8-napthyridine-2,7-dicarboxylic acid it was decided that this was not the most efficient of paths to be following and so it would be desirable to find an alternative.

2.2 Newkome's Synthesis of 2,7-Dichloro-1,8-naphthyridine

Looking at Newkome's previous work in the area of 1,8-naphthyridines his report of the first 1,8-naphthyridine containing macrocycle contained a potentially useful material, 2,7-dichloronaphthyridine, which was obtained in 67% yield over three steps (Scheme 5).[216]

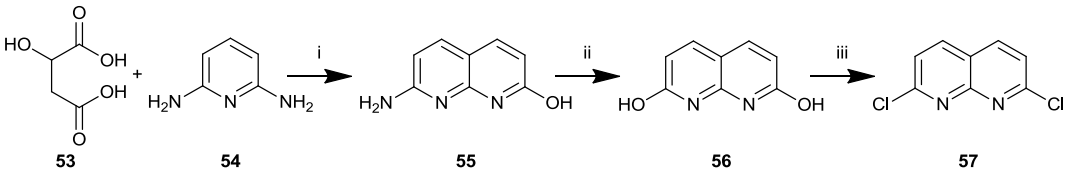

i) H_2SO_4, H_2O, Ammonium Hydroxide ii) H_2SO_4, Sodium Nitrite then ice and Na_2CO_3 then Glacial Acetic Acid iii) PCl_5 and $POCl_3$

Scheme 5 - Synthesis of 2,7-dichloro-1,8-naphthyridine.[216]

This material offers a number of potential options for further functionalisation to yield the desired 1,8-naphthyridine-2,7-dicarboxylic acid (**46**). It is worth noting that this material is commercially available from rare chemical libraries but at a cost of £144 per 100 mg.[249] Purification and characterisation of the products from the first two steps were restricted by a lack of solubility; the product (**56**) was isolated following precipitation from water and extensive drying. Crude 2,7-dichloro-1,8-naphthyridine (**57**) was successfully obtained and despite literature precedence for purification by re-crystallisation from acetone to give a white solid, this was not as simple as expected. While it was possible to remove insoluble material through filtration, concentration of the filtrate *in vacuo* yielded a pale brown solid which, while appearing to contain the desired material, was by no means pure. It is believed that the impurities may have been inherited from previous steps. As 2,7-dichloro-1,8-naphthyridine is more soluble in organic solvents suitable for column chromatography, attempts were then taken to purify this compound however it has not been possible to purify this material to a satisfactory level.

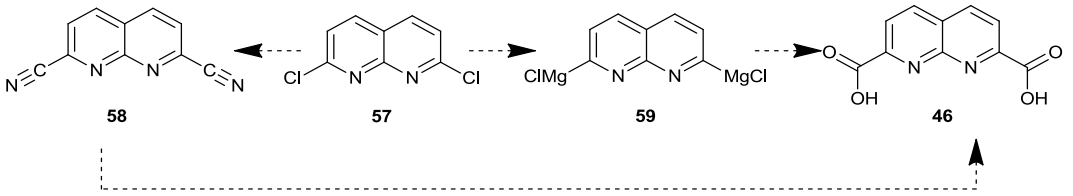

Scheme 6 - Potential Routes to 1,8-naphthyridine-2,7-dicarboxylic acid.

Following the synthesis of 2,7-dichloro-1,8-naphthyridine it was hoped that further functionalisation could continue along one of two routes as shown in Scheme 6, either by formation of a Grignard reagent before reaction with carbon dioxide, or by substitution with cyanide before oxidation to give the desired product. Small amounts of 2,7-dichloro-1,8-napthyridine (**57**) were used to attempt a Rosenmund von Braun [250] procedure to produce 2,7-dicyano-1,8-napthyridine (**58**) using copper cyanide as the source of the cyanide nucleophile. Initial experiments indicated that this had yielded a number of products which were very difficult to separate. One such product was isolated and identified as 2,7-*bis*-*N,N'*-dimethylamino-1,8-napthyridine. It is believed that, as a result of the high temperatures necessary to force the reaction to completion, there was some degradation of the DMF solvent. This resulted in the production of dimethyl amine, which then appears to have attacked some of the starting material. Preliminary attempts to investigate the use of a different solvent (DMA) were abandoned due to progress via a different route.

2.3 Successful Synthesis

Successful synthesis was achieved following a route devised by Deady.[215] This approach includes a selenium oxidation of the type described by Newkome as difficult to repeat.

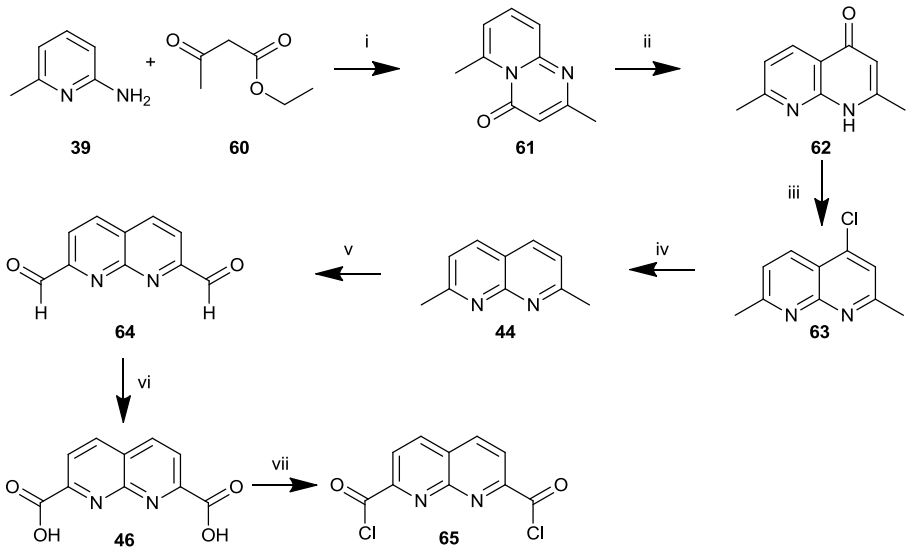

i) a) PPA, 100 °C 1.25 h b) 4M NaOH ii) Δ 350 °C 30 mins iii) a)$POCl_3$, 100 °C for 30 mins b) 4M NaOH c) filter through silica with DCM:EA eluent iv) Ammonium Formate, Pd/C, MeOH v) SeO_2 1,4-dioxane vi) a) HNO_3, reflux 30 min b) 4M NaOH to pH 5 vii) $SOCl_2$, DCM reflux

Scheme 7 - Third Synthetic route attempted towards 1,8-naphthyridine-2,7-dicarboxylic acid based on work by Deady.[215]

2-Amino-6-methyl-pyridine (**39**) was condensed with ethyl acetoacetate (**60**) in PPA to give a kinetic product (Scheme 7, step i). The literature describes the precipitation of a solid upon neutralisation of the PPA, which is then combined with the organic extracts. Upon analysis of this precipitate we identified it as the desired product. Purification was achieved by dissolving in DCM, washing with water and drying with magnesium sulphate to yield the desired product (**61**). Solvent extraction of the filtrate was also carried out but the extra material this afforded required additional purification before it could be used further. Given previous experience with naphthyridine compounds it seemed desirable to remove any impurities since solubility was good. The following step involved a thermal rearrangement of the heterocycle in liquid paraffin to give the ketone **62** (Scheme 7, step ii). This was then reacted with phosphorus oxychloride to aromatise the saturated ring (Scheme 7, step iii) giving 4-chloro-2,7-methyl-1,8-naphthyridine (**63**). The next step involved the removal of the chlorine substituent from the 5 position (Scheme 7, step iv). Deady[215] reports the use of a procedure involving reaction of hydrogen/palladium on carbon with the 4-chloro-2,7-dimethyl-1,8-naphthyridine (**63**) which is dissolved in basic methanol. While, in our hands, this worked on a small scale, on scale up it yielded an impurity which was identified to be 5-methoxy-2,7-dimethyl-1,8-naphthyridine. Literature precedence for the removal of chlorine from aromatic ring systems was found[251] utilising ammonium formate as the hydrogen source in methanol. This was attempted and gave a clean product in high yield. While the impurity could possibly been avoided by removing the base from the reaction, the ammonium formate method removed the need for the use of gaseous hydrogen. Initially 2,7-dimethyl-1,8-naphthyridine (**44**) was then reacted with selenium dioxide for 3 hours in refluxing 1,4-dioxane which successfully produced 1,8-naphthyridine-2,7-dialdehyde (**64**) albeit in poor yield (Scheme 7, step v). A further literature search revealed examples where the selenium oxide oxidation was carried out at only slightly elevated temperatures for extended periods of time. Accordingly subsequent reactions were carried out at 40 °C overnight, and this appeared to increase the yield achieved. Soxhlet extraction of the solid filtered off before workup also resulted in the recovery of additional material. The final step is the oxidation of the dialdehyde **64** to the dicarboxylic acid

46 using concentrated nitric acid (Scheme 7, step vi) which was carried out successfully with the desired product readily precipitating from the reaction mixture as the pH was increased (approx pH 5) during the workup.

Following the successful synthesis of 1,8-naphthyridine-2,7-dicarboxylic acid (**46**) this was converted into 1,8-naphthyridine-2,7-dicarbonyl dichloride using thionyl chloride in the presence of DMF. 1,8-Naphthyridine-2,7-dicarbonyl dichloride appears to be much less stable than its pyridine analogue and it was therefore prepared for immediate use and reacted in its crude form to minimise degradation.

2.3.1 Crystal Structures of Synthetic Intermediates

During the synthesis of 1,8-naphthyridine-2,7-dicarboxylic acid it was possible to obtain crystal structures of three of the key intermediates which has allowed comparison with their pyridine analogues.

2.3.1.1 2-Methyl-1,8-naphthyridine (52)

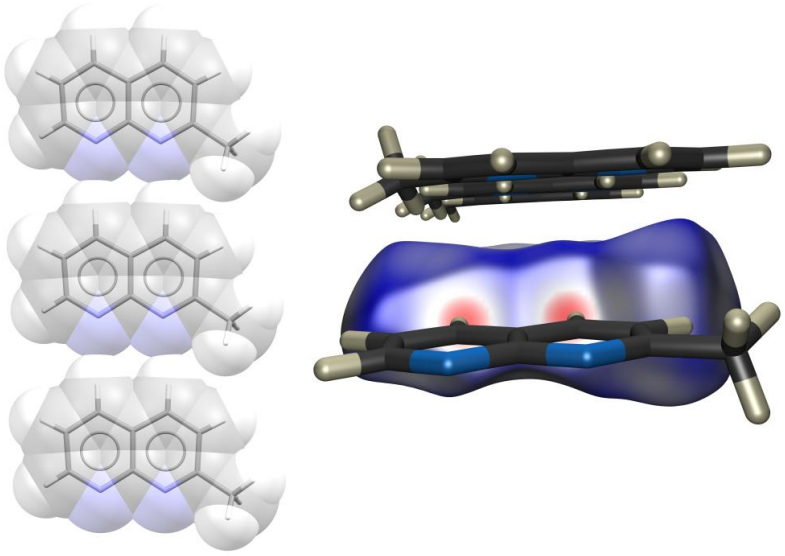

Figure 50 -2-Methyl-1,8-naphthyridine (52) forms infinite one dimensional tapes with the methyl functionality on the same side of the tape. The Hirshfeld surface visualises quite clearly the main taping interactions.

Upon first inspection 2-methyl-1,8-naphthyridine (**52**) appears to form the predicted one-dimensional taping arrays. It is apparent from the examination of the Hirschfield surface that there appear to be contacts between the pyridyl nitrogen and the aromatic C-H at distances of C-**H**···**N** 2.52 Å , **C**-H···**N** 3.47 Å (174.2 °) and C-

H···**N** 2.53 Å, **C**-H···**N** 3.47 Å (171.4 °) (Figure 50). Examining the Hirshfeld surfaces shows that these are the primary contacts within the solid state architecture.

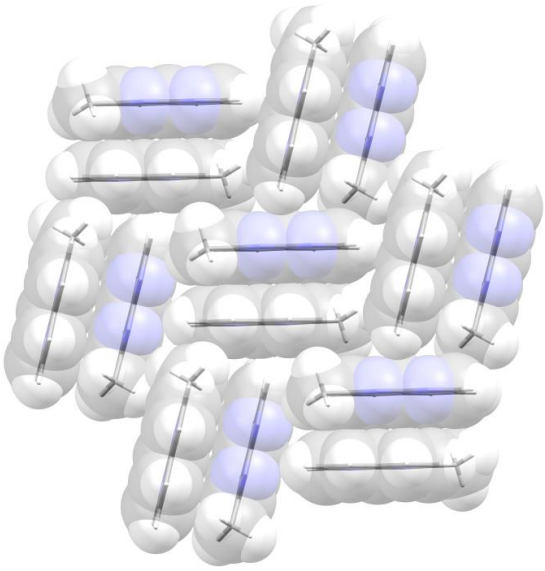

Figure 51 – The tapes of 52 pack with two tapes stacked on top of one another, aligned in opposite directions to one another. The neighbouring pairs of tapes align in a pattern that resembles a parquet floor.

In the 2,6-disubstituted pyridine esters the formation of parallel stacks of tapes has been observed however, despite the obvious formation of a pair of stacked tapes in the 2-methyl-1,8-naphthyridine, it quickly becomes apparent on further expansion that the parallel tapes are then organised in a perpendicular manner to their neighbours creating a parquet-like packing motif (Figure 51).

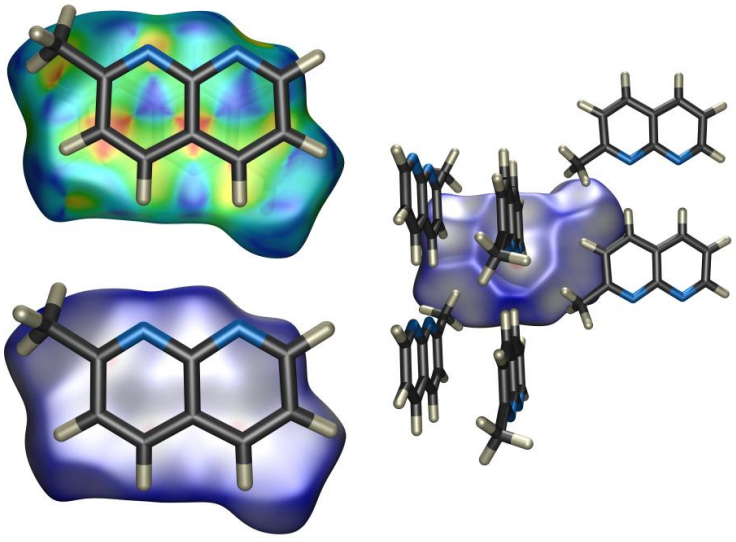

Figure 52 – Examination of the Hirshfeld surfaces from either side of the molecule enables the identification of potential π···π stacking between the pair of tapes (left), and a potential C-H··· π interaction to a neighbouring tape in the parquet packing.

In the hope of gaining a greater understanding of this interaction the Hirschfield surface has been examined on both sides of the molecule. It appears that between the two parallel tapes there are no strong interactions. However, an examination of the surface coloured with the shape index, an indication of subtle variation on flat surfaces, indicates that the pattern observed is similar to that observed in simple aromatic systems which are thought to experience π···π interactions. In this case the two rings are held at a distance of 3.32 Å apart. It also appears that there is a C-H···π interaction between the C(7)-H and the neighbouring ring in the parquet packing (C-**H**···**π** 2.77 Å, **C**-H···**π** 3.53 Å).

2.3.1.2 2,7-dimethyl-1,8-naphthyridine (44)

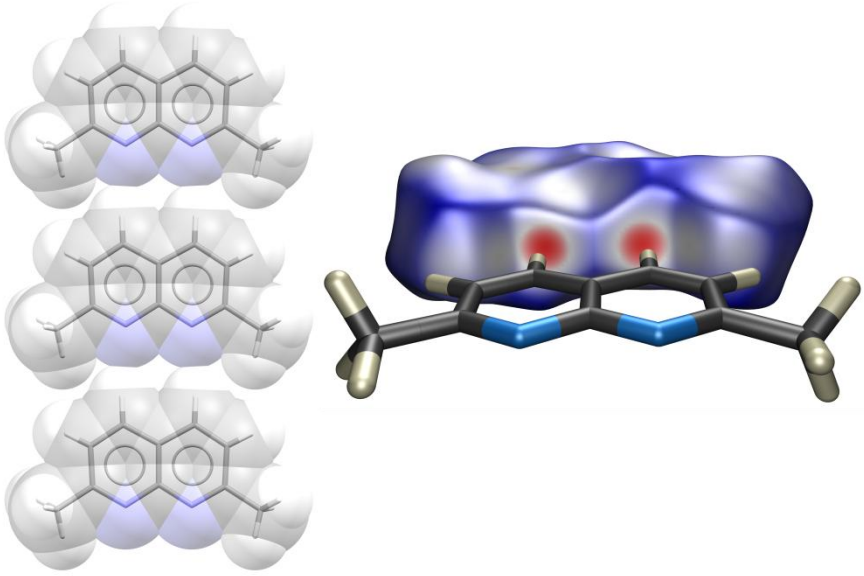

Figure 53 – 2,7-Dimethyl-1,8-naphthyridine (44) forms the expected one dimensional tapes through the main interactions clearly highlighted on the Hirshfeld surface.

The structure for 2,7-dimethyl-1,8-naphthyridine (**44**) was also obtained during the successful synthetic route detailed above, and has since been confirmed by a structural report by Goswami.[252] The structure again shows the expected hydrogen bond interactions forming one-dimensional tapes (Figure 53) involving two C-H···N hydrogen bonding contacts between the pyridyl nitrogen atoms and the aromatic C-H which are identical thanks to the symmetric nature of the molecule (C-**H**···**N** 2.57 Å, **C**-H···**N** 3.50 Å (174.5 °)). The structure shows the desired on-dimensional

taping motif that we have predicted for the diester derivatives that are the aim of this project.

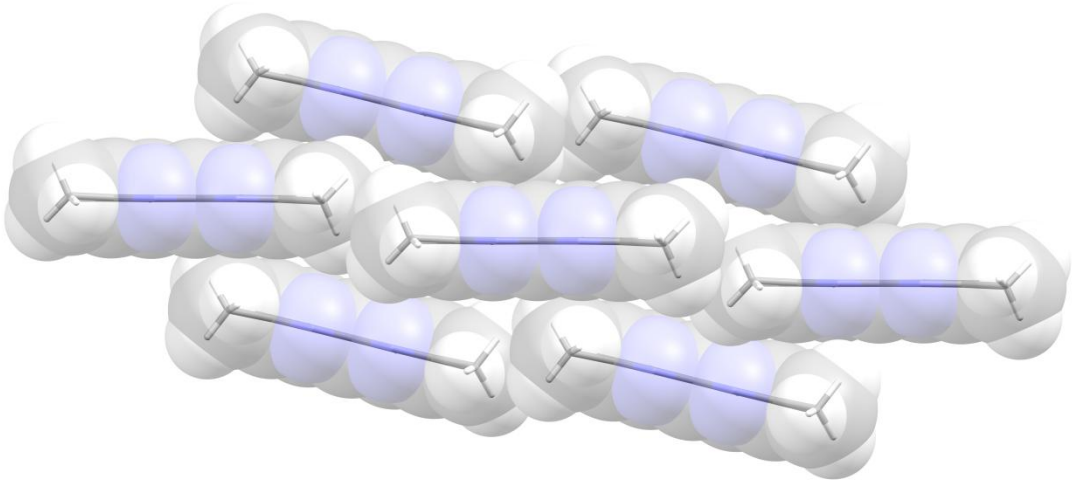

Figure 54 – Examining the packing motif for 44 shows the neighbouring tapes all aligning in the same direction with the sheets of tapes aligning at an angle to one another.

Further expansion of the structure reveals that the packing is more akin to that expected in the dicarboxylate derivatives which will be discussed in the next chapter. Each tape arranges itself into parallel stacks, in which the angle between neighbouring sheets is 13.6 ° with respect to the sheet plane (Figure 54). In neighbouring sheets all the molecules are oriented in the same direction but with the tilt angle inverted. Interestingly the structure reported[253] for 2,6-dimethylpyridine shows similar behaviour though the contacts in the case of 1,8-naphthyridine are slightly shorter.

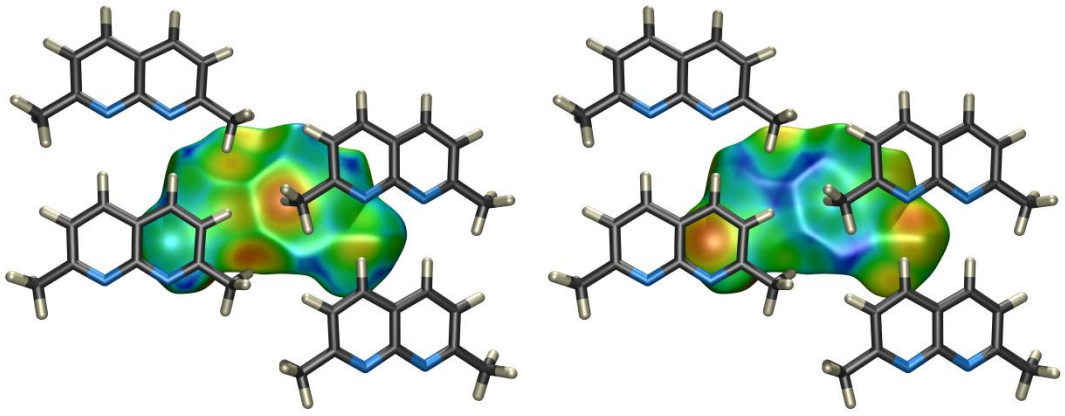

Figure 55 – Goswami's report of this structure made suggestions about the presence of a C-H···π interaction between molecules in neighbouring layers. The d_i and d_e surfaces clearly show close contacts which would suggest the presence of this type of contact.

In his report of this structure, Goswami[252] makes a suggestion that the peripheral methyl groups make a C-H···π contact with an adjacent naphthyridine ring; this is supported by the Hirshfeld surface obtained using "Crystal Explorer"[240, 241] for this structure (Figure 55). In this case the contact distances are C-**H**···**π** 2.79 Å and **C**-H···**π** 3.55 Å.

2.3.1.3 2,7-(Trichloromethyl)-1,8-naphthyridine (45)

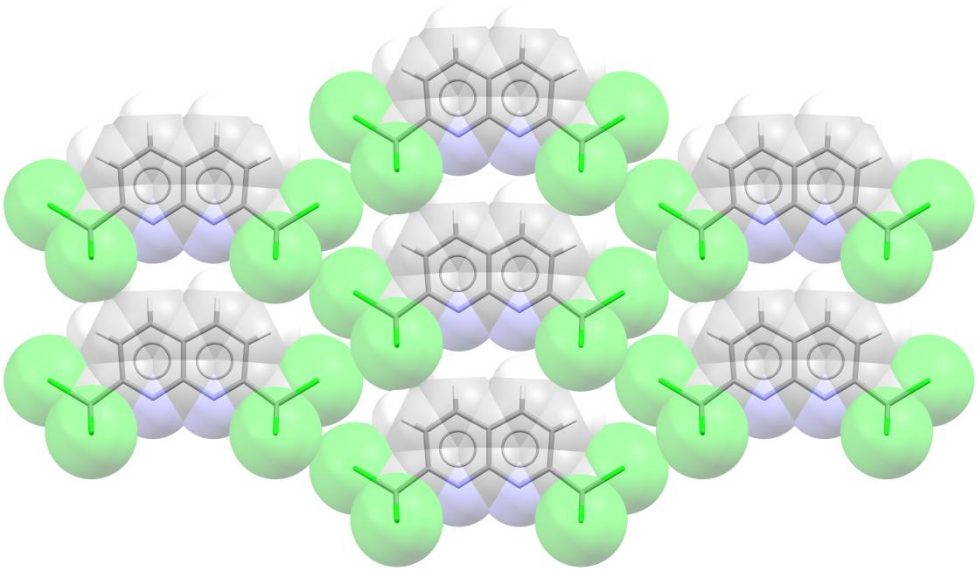

Figure 56 - 2,7-(Trichloromethyl)1,8-naphthyridine appears at first glance to form the expected infinite one dimensional tapes. However it quickly becomes apparent that this is not the case.

2,7-(Trichloromethyl)1,8-naphthyridine (**45**) was obtained as an intermediate in the potential synthesis of 1,8-naphthyridine-2,7-dicarboxylic acid. Although this route was not utilised in the eventual production of the dicarboxylic acid, it proved possible to crystallise a small sample of 2,7-(trichloromethyl)1,8-naphthyridine. This structure has also been reported by Goswami during the course of this work.[254] At first glance 2,7-(trichloromethyl)-1,8-naphthyridine appears to experience the same two C-H···N hydrogen bonding contacts between the pyridyl nitrogen atoms and the aromatic C-H (Figure 56), but further examination of the structure shows that the two molecules are further apart than the previous two examples (**44** and **52**), with a contact distance of C-**H**···**N** 2.88 Å, **C**-H···**N** 3.81 Å, (174.9 °). These distances are longer than would be expected for a hydrogen bond contact of this type. It is

apparent that the spatial requirement for the chlorine atoms is partly responsible for the packing arrangement observed because of the steric bulk of these atoms.

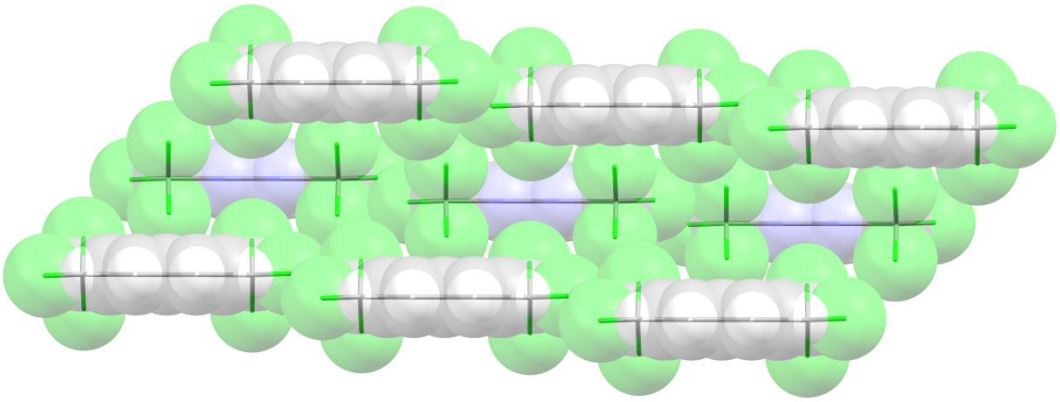

Figure 57 – It is apparent that one of the substituent chlorine groups from a neighbouring molecule sits over the top of the naphthyridine nitrogen atoms forcing the next molecule in the pseudo tape further away.

The packing motif of the pseudo-tape structure remains surprisingly similar to that seen in the 2,7-dimethyl-1,8-naphthyridine. Pseudo tape-like arrays form which then align into sheets in which all tapes point in the same direction while the sheets above and below are oriented in the opposite direction (Figure 57).

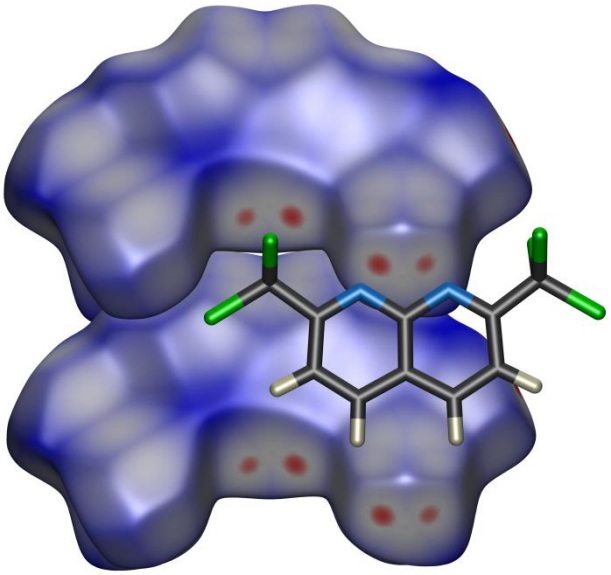

Figure 58 – This Hirshfeld surface shows no evidence of the taping contacts that are expected in the 1,8-naphthyridine-2,7-dicarboxylate derivatives. The only interactions observed on the surface are between the naphthyridine nitrogen atoms and the substituent chlorine atoms, which is most likely a close packing artefact.

Figure 58 shows that the packing of the layers appears to occur in such a way that the bulky trichloromethyl group can sit over less bulky areas of neighbouring

sheets. Despite the increased length of the intermolecular taping contacts it is curious that the solid-state architecture does not change entirely, leaving the possibility of a stabilising effect from the C-H···N interactions between the pyridyl nitrogen atoms and the aromatic C-H despite the increased internuclear distance.

2.4 Attempts to Synthesise 1,9,10-Anthyridine-2,8-dicarboxylic Acid

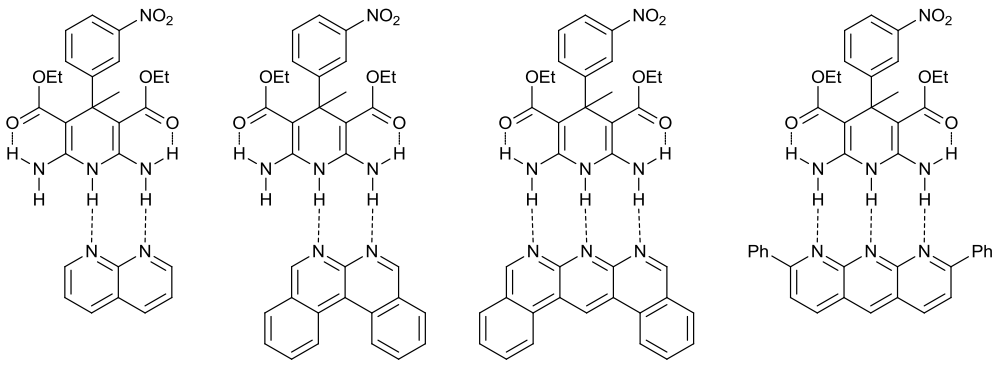

Figure 59 – Zimmerman and Leigh have both synthesised species capable of forming hydrogen bonded complexes with the dihydropyridine 67.

Zimmerman[255] and, more recently, Leigh[256, 257] have reported syntheses of compounds containing a 1,9,10-anthyridine unit which have exhibited extremely high dimerisation constants in the pairings, shown in Figure 59. This work suggests an obvious extension of the work that has been discussed thus far; the exploration of the behaviour of 2,8-dicarbonyl-1,9,10-anthyridine derivatives. An examination of the literature was carried out in order to investigate the possibility of synthesising 1,9,10-anthyrdine-2,8-dicarboxylic acid. It is immediately obvious that there has been some work on the synthesis of 1,9,10-anthyridines[258-261] and while there are reports of 2,8-disubstituted derivatives these derivatives do not offer any simple routes for conversion to 1,9,10-anthyrdine-2,8-dicarboxylic acid. However, it was thought that an attempt should be made to exploit the insights gained from the synthesis of 1,8-naphthyridine in an attempt to synthesise 1,9,10-anthyrdine-2,8-dicarboxylic acid (Scheme 7 and Scheme 8).

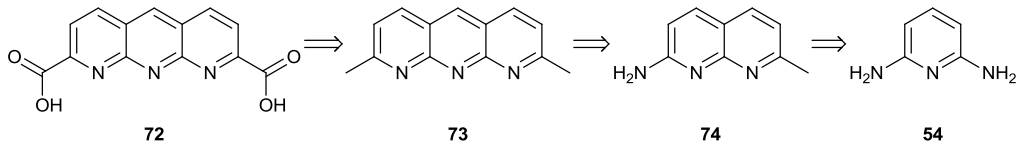

Scheme 8 – Retrosynthetic analysis of a potential synthetic route to 1,9,10-anthyridine-2,8-dicarboxylic acid.

Following the number of routes attempted before successfully making 1,8-naphthyridine it was hoped that it would be possible to utilise the same, successful approach towards 1,9,10-anthyridine-2,8-dicarboxylic acid.

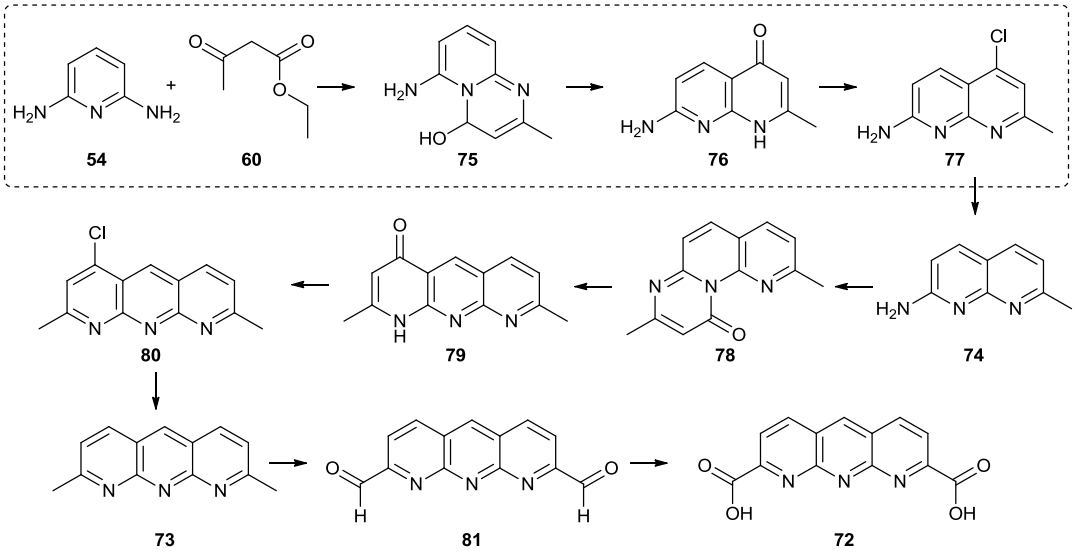

Scheme 9 - Proposed synthesis of 1,9,10-anthyridine-2,8-dicarboxylic acid.

The first step was attempted using the same condensation as used to make 2,6-dimethylpyrido[1,2-α]pyrimin-4-one (**61**) except for the use of 2,6-diaminopyridine (**54**) instead of 2-amino-6-methylpyridine (**39**). However, this reaction yielded two different crude materials.

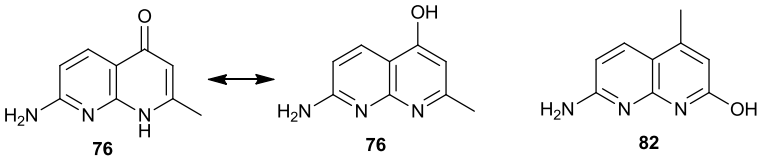

Figure 60 – Hauser and Brown disagreed over which structural isomer was produced from the reaction of 54 and 60.

Upon reference to the literature there seemed to be some disagreement about the product of this condensation, albeit involving procedures carried out under different reaction conditions. Hauser[262, 263] claimed the production of 2-methyl-4-hydroxy-7-amino-1,8-naphthyridine (**76**) in low yield, whereas Brown[264] claimed

this to be untrue and that he had only managed to produce 2-hydroxy-4-methyl-7-amino-1,8-naphthryidine (**82**), both by his own method and by recreating that of Hauser.

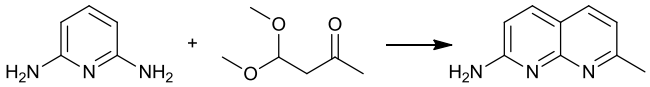

54 **83** **74**

Scheme 10 – Brown reported the synthesis of 74 which allowed for the removal of the boxed section of Scheme 9.

However, in the same paper, Brown did report a synthesis of 2-amino-7-methyl-1,8-naphthyridine (**74**) in one step by the reaction of 2,6-diaminopyridine (**54**) with 3-ketobutanal dimethyl acetal (**83**) which significantly simplified the proposed synthesis. This method was utilised to prepare the desired intermediate which was then used in attempted reactions to form the third fused cycle either by condensation with ethyl acetoacetate (**60**) in polyphosphoric acid, or via the same procedure used to obtain the 2-amino-7-methyl-1,8-naphthyridine (**82**). However these reactions have shown little sign of success, normally only yielding recovered 2-amino-7-methyl-1,8-naphthyridine (**74**) and degraded starting material.

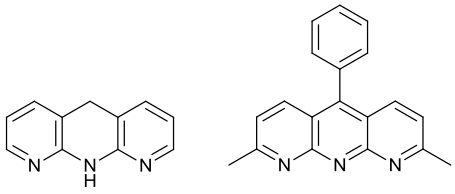

84 **85**

Further investigation into 1,9,10-anthyridine derivatives reported by others has offered a couple of possible explanations. Firstly, Caluwe[258] observes that while he was able to affect the formation of the 1,9,10-anythridine ring system he did so by utilising a double Friedländer reaction. However, he does state that this methodology did in fact afford the reduced product anthyridan (**84**), which he then oxidised back to the anthyridine. Zimmerman[265] has reported the synthesis of a compound analogous to our desired anthyridine (**85**) in which the phenyl ring was used to inhibit the reduction of the central ring, an approach which would be undesirable in our case as this would interfere with the hydrogen bonding system that we are interested in investigating. If this is to be continued then it would seem best achieved using the Friedländer method, either blocking the reducible position

with something that could be removed or by allowing the reduction to occur and carrying out the functional group interchanges required before finally re-oxidising to give the desired product.

3 1,8-Naphthyridine-2,7-dicarboxylates

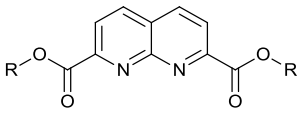

47

Following on from the previous work within the Grossel group[172, 181, 182, 184, 194-197] it was envisaged that a library of compounds based on the 1,8-naphthyridine core (**47**) would be synthesised that could be studied in order to gain greater insight into the solid-state architectural trends caused by slight structural changes. In general the compounds discussed here are directly analogous to pyridine derivatives previously studied however, in the case of the mono halogen-substituted benzyl esters, there has been no previous investigation into the effect of varying the substitution position on the observed solid-state structure.

3.1 Geometric Differences between Pyridine-2,6-dicarboxylates and 1,8-Naphthyridine-2,7-dicarboxylates

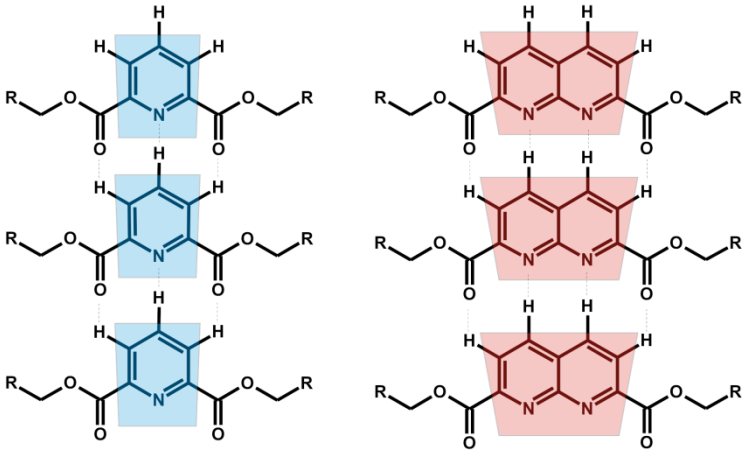

Figure 61 - The major difference between the pyridine-2,6-dicarboxylates and 1,8-naphthyridine-2,7-dicarboxylates comes about because of the difference in length between C-C and C-N bonds which causes the puckering of the heterocyclic cores.

When considering the interaction of molecules within a solid-state structure it is important to consider any geometric restraints that may affect the packing of the molecules being studied.

A pyridine ring is not totally symmetrical, as the length of a C-C bond differs from that of a C-N bond the ring is puckered at the front of the molecule. The

implications on the alignment of the hydrogen bonding array are only minor but may be of significance when accommodating the neighbouring molecule. In diethyl pyridine-2,6-dicarboxylate the sides of the pyridine ring are held at an angle of 3.3 ° to one another, while the carbonyl groups are splayed at an angle of 6.2 °. By comparison, in diethyl-1,8-naphthyridine-2,7-dicarboxylate, the sides of the naphthyridine ring are held at a greater angle of 8.7 ° to one another, while the carbonyl groups experience a reduced splay with an angle of 1.5 °. These changes mean that in the ethyl pyridine derivative the carbonyl oxygen atoms are held 4.90 Å apart with the H3 and H5 atoms 4.00 Å apart, while in the ethyl naphthyridine derivative the carbonyl oxygen atoms are held 7.13 Å apart with the H3 and H5 atoms 6.54 Å apart. In crystallography the contact distance has often been used as an indicator of relative strength of the contact being examined. As such, it was expected that the 1,8-naphthyridine derivatives would experience shorter contacts within the hydrogen bonding array thanks to the introduction of an additional hydrogen bond. However it has been found that this is not the case and it is believed that this could be due in part to the geometric constraint.

3.2 Aliphatic Esters

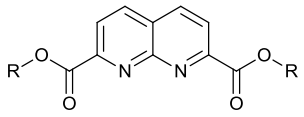

47

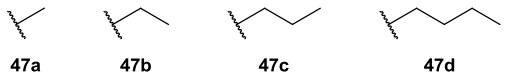

47a **47b** **47c** **47d**

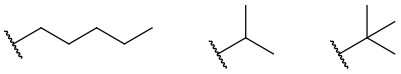

47e **47f** **47g**

With the exception of the *t*-butyl ester (**47g**), each of the desired aliphatic 1,8-naphthyridine dicarboxylate derivatives, outlined above, were successfully synthesised. It was hoped that the simple nature of the pendent arms would allow an examination of the interactions of the 1,8-naphthyridine core without competing interactions. The t-butyl ester (**47g**) proved problematic due to its sensitivity to water, which meant that each time its synthesis was attempted a crude NMR showed the product to be present but any attempted to purify the product led to

decomposition. Crystal structures of three aliphatic esters (**47a**, **47b** and **47d**) have been obtained and are discussed below.

3.2.1 Dimethyl 1,8-naphthyridine-2,7-dicarboxylate (47a)

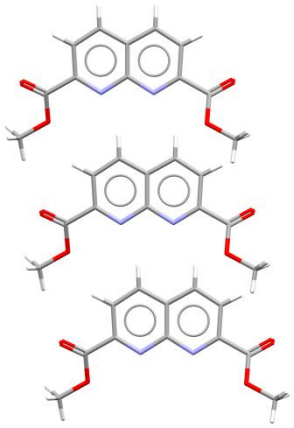

Figure 62 –First impressions would suggest that 47a forms an infinite one-dimensional tape similar to that observed in the majority of pyridine-2,6-dicarboxylate derivatives.

At first glance (Figure 62) the methyl ester (**47a**) exhibits taping contacts, but on further examination it becomes apparent that this is not the case. This behaviour is not unexpected as dimethyl pyridine-2,6-dicarboxylate also displays anomalous behaviour, however the two analogous materials adopt different solid-state architectures. In the 1,8-naphthyridine case the first thing to note is the rotation of the two esters to the syn – syn conformation, pushing the methyl groups towards the next molecule in the expected tape. This rotation is important for two reasons: firstly the steric requirements of the methyl group force the contact distances to be extended; while secondly the rotation changes the orientation of the hydrogen bonding array, with the carbonyl groups oriented out to the side of the molecule, introducing the possibility of external interactions with other molecules.

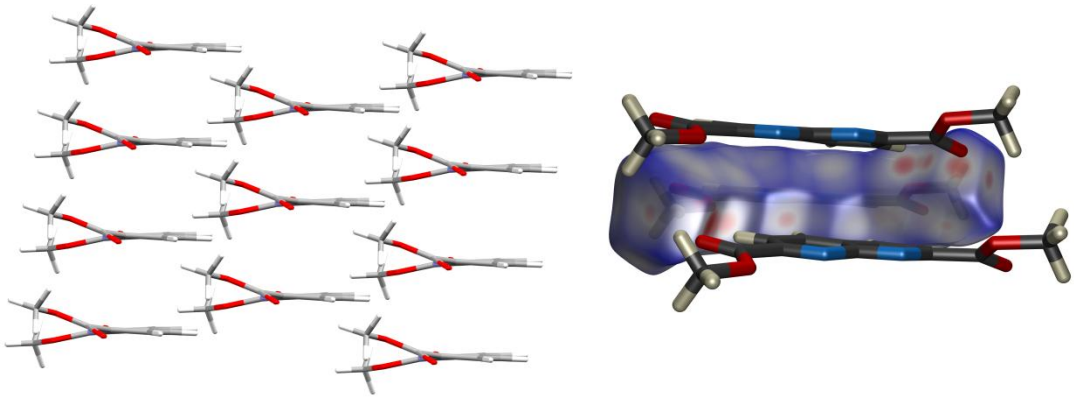

Figure 63 –Looking along the side of the packing seen in Figure 62 shows that the molecules do not sit in the same plane as one another. This is highlighted on the Hirshfeld surface which shows the major contacts between neighbouring molecules.

The picture in Figure 62 is deceptive as the molecules are not in the same plane, as Figure 63 reveals. Looking at a perpendicular angle to the apparent tape (Figure 63 left) shows that for each molecule there are two molecules directly in front, one slightly above the plane of the molecule, offset to the left, and one below the plane, offset to the right. Looking at the Hirshfeld surface (Figure 63 right) this offset is caused by interactions between: (a) the ether oxygen of the ester and one of the methyl protons and (b) the carbonyl oxygen and the *meta*-hydrogen on a neighbouring ring system.

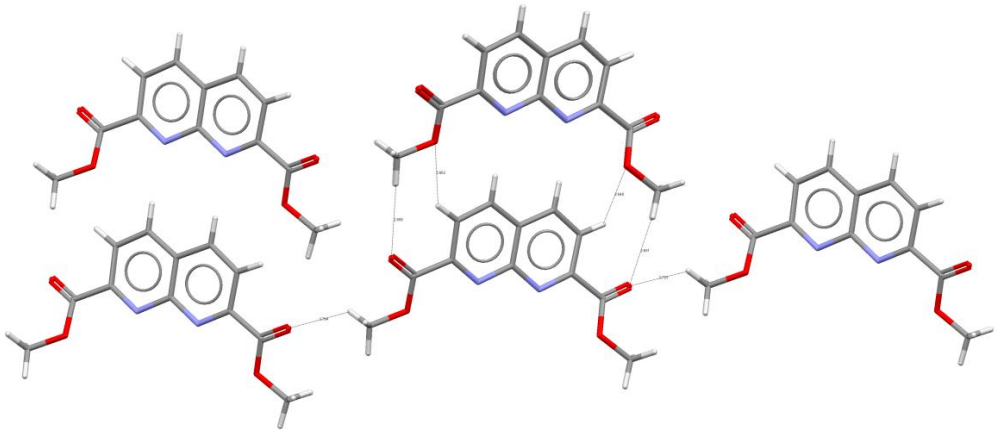

Figure 64 – The packing of 47a appears to be due to the interactions shown in this figure.

There is a further interaction between a methyl hydrogen atom and the carbonyl of a molecule in the neighbouring pseudo tape-like array which causes the structure to form columns of corrugated stacked chains. The next column is then arranged in a

herringbone fashion to accommodate contacts between the carbonyl group and pendent methyl hydrogen atoms.

3.2.2 Diethyl 1,8-naphthyridine-2,7-dicarboxylate (47b)

Fortunately the solid-state structure of the ethyl ester (**47b**) reveals that, in this case, the desired tape formation is indeed observed. This result is analogous to that previously seen in the pyridine-2,6-dicarboxylates.[172, 195]

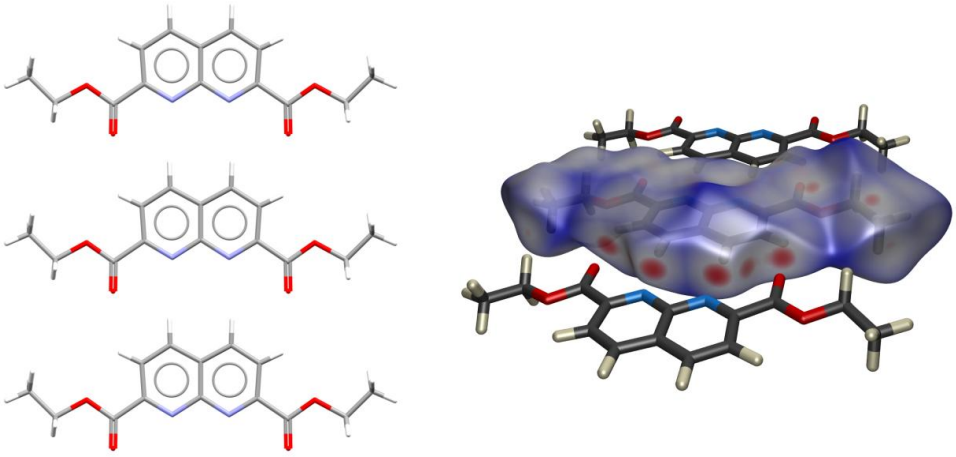

Figure 65 – The ethyl ester (47b) can be clearly seen to form the expected one-dimensional tapes seen previously in the pyridine-2,6-dicarboxylate systems. The Hirshfeld surface shows that the primary interactions involved are indeed the C-H···N and C-H···O in the hydrogen bond forming array.

Almost immediately it is obvious that this structure exhibits the formation of infinite 1D tapes as shown in Figure 65. Examining the Hirshfeld surface clearly suggest that there are strong contacts between both carbonyl oxygen and pyridyl nitrogen acceptors and pyridyl hydrogen donors (H_3, H_4 H_5, and H_6). The Hirshfeld surface shows no other obvious strong interactions, though it does suggest the presence of some potential weak interactions between: (a) the terminal CH_3 group of the ester and the ether oxygen of a neighbouring molecule and (b) an interaction between the ester CH_2 group and one of the ring systems of the naphthyridine. While no further evidence has been obtained to confirm the presence of these interactions they are typical of the very weak interactions discussed in the introduction.

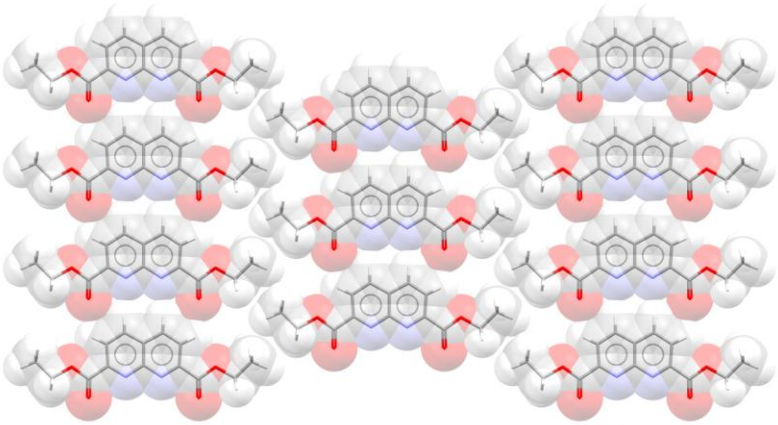

Figure 66 – The tapes formed by the ethyl ester 47b can be clearly seen to form into sheets in which all neighbouring sheets align in the same orientation, with the ethyl groups interdigitating between gaps in the neighbouring tapes.

Beyond the primary taping interaction Figure 66 illustrates the organisation of the tapes into sheets. The tapes lie parallel to one another and are slip-stacked in order to accommodate the ethyl pendent groups. From the view seen in Figure 66 there appear to be slight gaps in the packing, however these accommodate the CH_2 groups from neighbouring sheets.

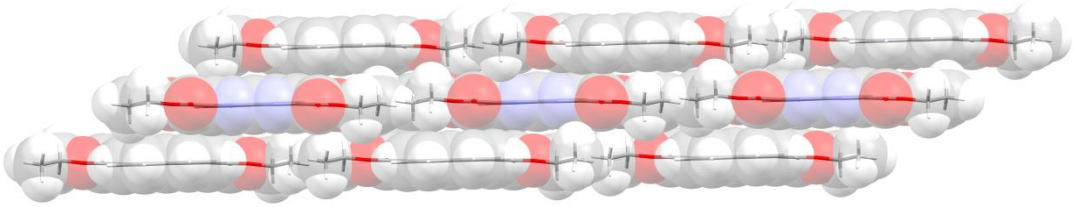

Figure 67 – The sheets of tapes formed by 47b then stack upon one another with alternating alignments.

As Figure 67 shows the sheets of tapes stack so that each sheet runs in the opposite direction with respect to its neighbour and with neighbouring individual tapes appearing to form offset stacks. The factors that influence the secondary structure of the tapes are of as much interest as the primary taping contact but the present structure provides insight into the basic taping structure unimpaired by any strong external competing interactions.

3.2.3 Dibutyl 1,8-naphthyridine-2,7-dicarboxylate (47d)

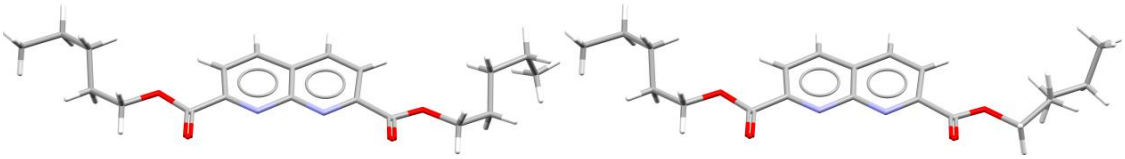

Figure 68 – Dibutyl 1,8-naphthyridine-2,7-dicarboxylate (47d) displays disorder for pendent side arms (right hand side of the molecules above); the two different conformations are shown above.

The dibutyl ester (**47d)** exists in two forms within the crystal examined. This shows up as disorder in the molecule with one butyl arm being split in a 50:50 ratio between two conformations (Figure 68). The exact cause for this disorder is unclear but it would appear that each conformer is able to form different interactions of similar strength and the disorder shows the inter-changeability of these conformations. For the sake of simplicity the packing of only one conformer is examined.

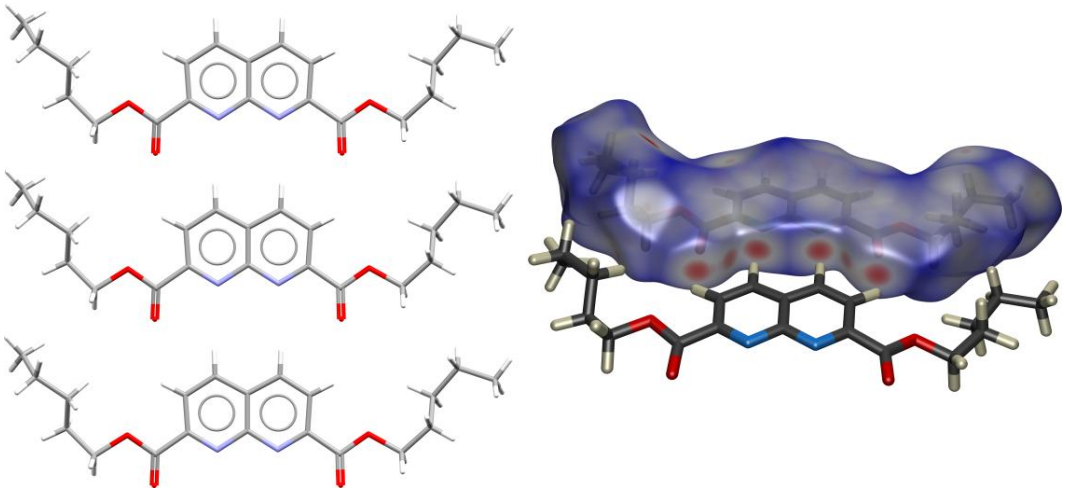

Figure 69 - Dibutyl 1,8-naphthyridine-2,7-dicarboxylate (47d) forms the expected hydrogen bond array and aligns into infinite one-dimensional tapes.

The butyl derivative forms the expected one-dimensional hydrogen bond array however there is little sign of any additional interactions on the Hirshfeld surface. This should mean that the packing displayed here is the consequence of close packing rather than being influenced by other interactions.

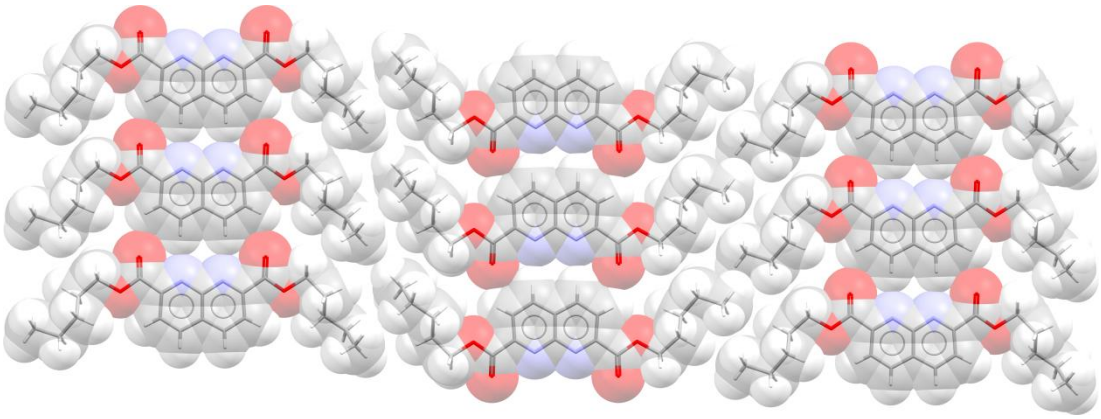

Figure 70 – The infinite one-dimensional tapes arrange into anti-parallel sheets with the butyl side arm interdigitated between the neighbouring chains.

The tapes pack into sheets which arrange in an anti-parallel fashion, with the butyl pendent arms interdigitating between neighbouring pendent chains. The disorder of one side of the molecule may be due to the low energy of interconversion for the conformation of the butyl chain given the lack of secondary directing interactions.

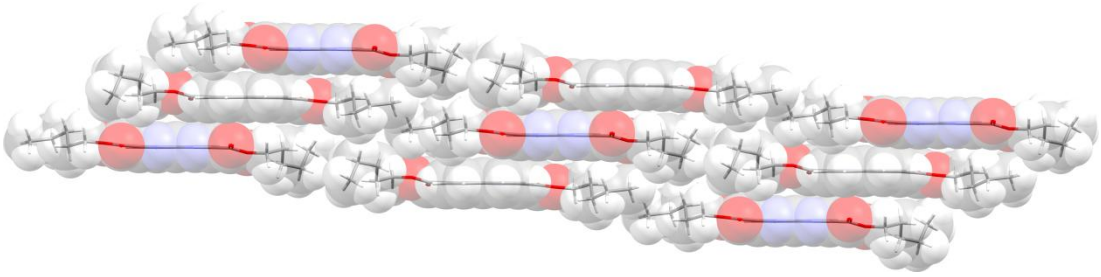

Figure 71 –The sheets pack into stacks which are also anti-parallel in arrangement.

When the sheets pack upon one another to give stacks they do so in an anti-parallel fashion with a small long axis shift. It would appear the packing is aligned in order to minimise steric clashes in a close packed arrangement.

3.3 Dibenzyl 1,8-naphtyridine dicarboxylate derivatives

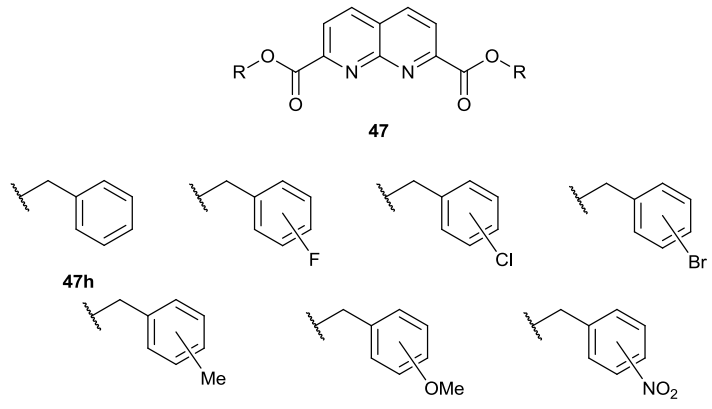

Figure 72 - The dibenzyl 1,8-naphthyridine derivatives shown above will be studied in this section

Following the synthesis of simple aliphatic esters (**47a-g**) it was hoped a systematic study of the substituted benzyl derivatives shown in Figure 72 would allow a comparison of the effect of different functional groups and substitution position. Synthetic work for many of the halogen substituted species was carried out by Emily Markham while she undertook a 3rd year undergraduate research project under my supervision however, spectroscopic characterisation and X-ray structural studies were carried out by the author.

3.3.1 Dibenzyl 1,8-naphthyridine-2,7-dicarbonyl (47h)

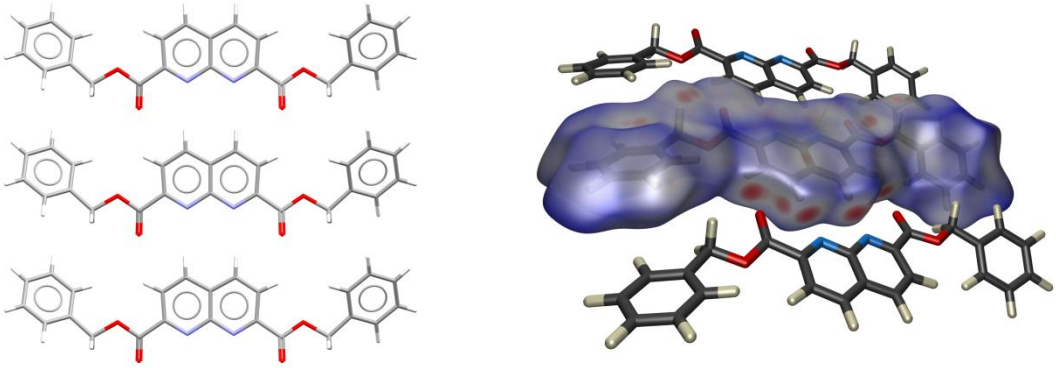

Figure 73 – The benzyl derivative 47h forms the predicted infinite one-dimensional tape through the interaction of the contacts highlighted on the Hirshfeld surface.

Having investigated some of the simplest pendent arms this study moved onto investigating more complex systems. The benzyl ester offers a wide scope for the introduction of other functionalities whilst not in itself contributing multiple strong interactions. Figure 73 shows the solid-state behaviour of the dibenzyl ester. As with the ethyl ester it is immediately possible to identify the formation of the expected one-dimensional tapes. The Hirshfeld surface indicates that, other than the primary taping contact, there appears to only be one other significant interaction in the centre of the benzylic pendent arm. This interaction will be discussed further below.

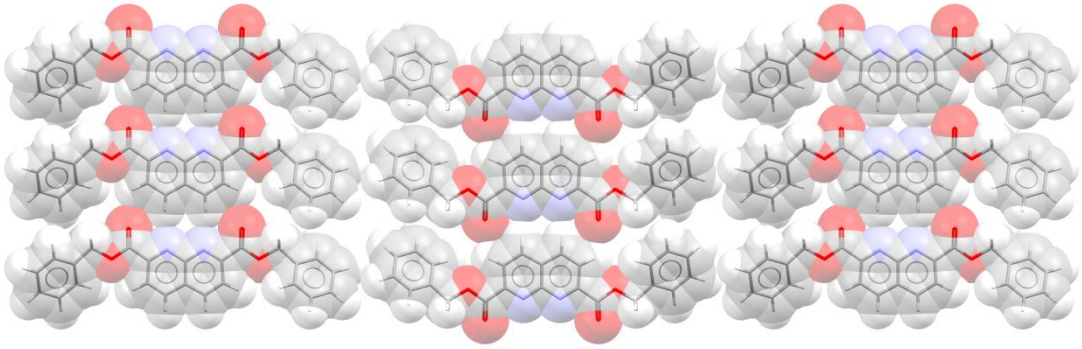

Figure 74 – The tapes formed by the benzyl derivative 47h arrange themselves so that they are anti-parallel in alignment to their neighbouring tape.

The one-dimensional tapes pack into sheets in which the naphthyridine cores are in the same plane (Figure 74). The first obvious difference in comparison with the aliphatic esters above is the orientation of the neighbouring tapes; each tape is orientated in the opposite direction to its immediate neighbour. This may be due to the additional bulk of the benzyl group.

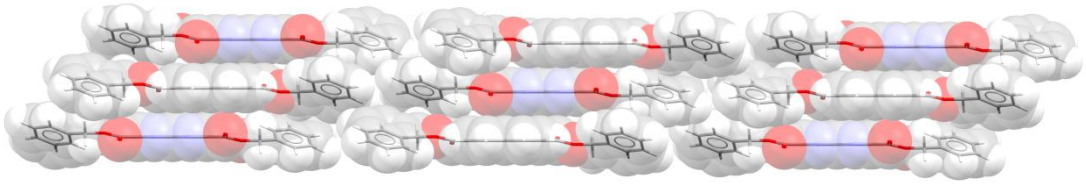

Figure 75 – The sheets shown in Figure 74 then pack on top of one another so that neighbouring tapes are once again in an anti-parallel arrangement to its nearest neighbour.

The sheets then stack upon one another, with the neighbouring tapes in a stack (either above or below) running in the opposite direction (Figure 75).

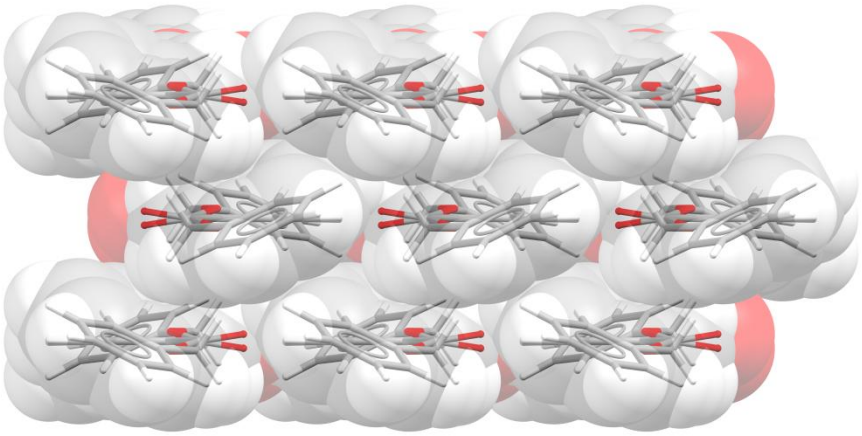

Figure 76 – The packing of the tapes means that the pendent benzyl ring must twist slightly out of the plane of the 1,8-naphthyridine core in order to optimise the packing of the molecules.

Looking perpendicular to the z axis of this packing arrangement, it is also noticeable that the benzyl pendent group is slightly twisted with respect to the naphthyridine core (25.4 ° Figure 76). This twist, along with a slight staggering of the sheets, facilitates the accommodation of the benzyl ring within the structure; in this case interdigitating to the sheet above rather than to the neighbouring tape within its sheet, as seen in the ethyl derivative (**47b)**.

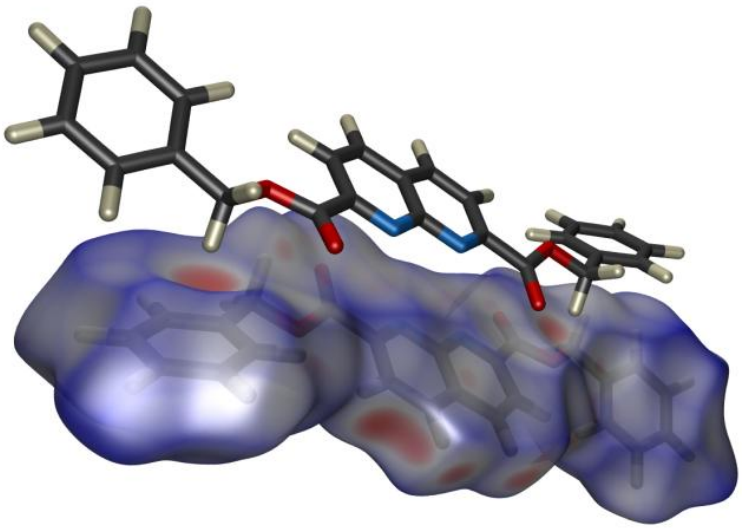

Figure 77 – The Hirshfeld surface does however, indicate the presence of another interaction in the packing of the molecules. In this case a C-H···π interaction from methylene C-H to the centre of one of the pendent rings in the sheet below.

As mentioned previously, the Hirshfeld surface indicates that there is only one strong interaction in addition to the hydrogen bonding array. It appears that the methylene CH_2 interacts with the benzyl ring of the molecule in the sheet above (Figure 77). This appears to be a C-H···π interaction of length C-**H**···**π** 2.62 Å and **C**-H···**π** 3.59 Å (163.9 °). As mentioned in the introduction these interactions are very weak which brings with it two questions: firstly is this a 'real' interaction, and secondly does this interaction play a part in defining the packing of this molecule or is it simply a packing artefact.

3.3.2 Methyl Substituent

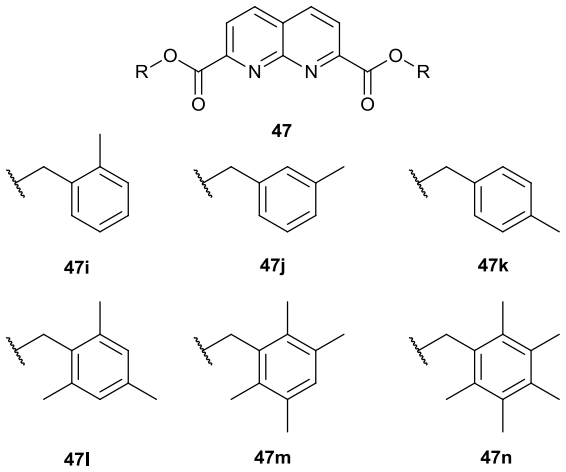

There are a number of commercially available isomers of methyl-substituted benzyl alcohols which has allowed a detailed study of the effect the crystallographically bulky methyl groups have on the packing of the infinite one-dimensional tapes.

3.3.2.1 (2-Methylbenzyl) 1,8-naphthyridine-2,7-dicarboxylate (47i)

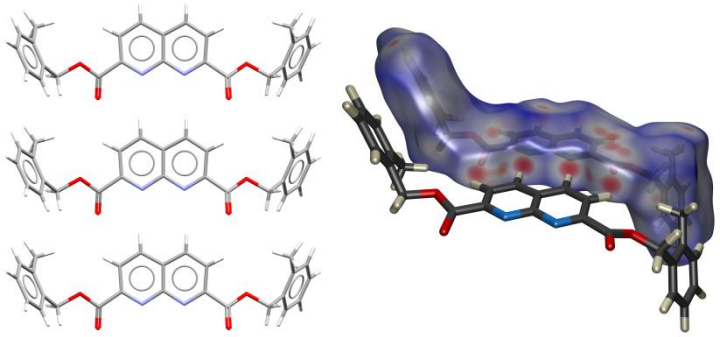

Figure 78 – *bis*-(2-Methylbenzyl) 1,8-naphthyridine-2,7-dicarboxylate 47i forms infinite one-dimensional tapes through the contacts highlighted on the Hirshfeld surface. It is also notable that the pendent rings are twisted out of the plane of the naphthyridine core.

The introduction of an *ortho*-methyl substituent onto the pendent benzyl arm appears to have a stark effect on the orientation of the pendent rings. Figure 78 shows the arrangement of the molecules within the one-dimensional tapes, however the key feature to note is the significant twisting of the benzyl ring out of the plane of the molecule. From a geometric point of view it would appear that this would be caused by the steric bulk of the methyl group. If the molecule retained the same structure as seen in the unsubstituted benzyl derivative then the packing of the structure would be compromised.

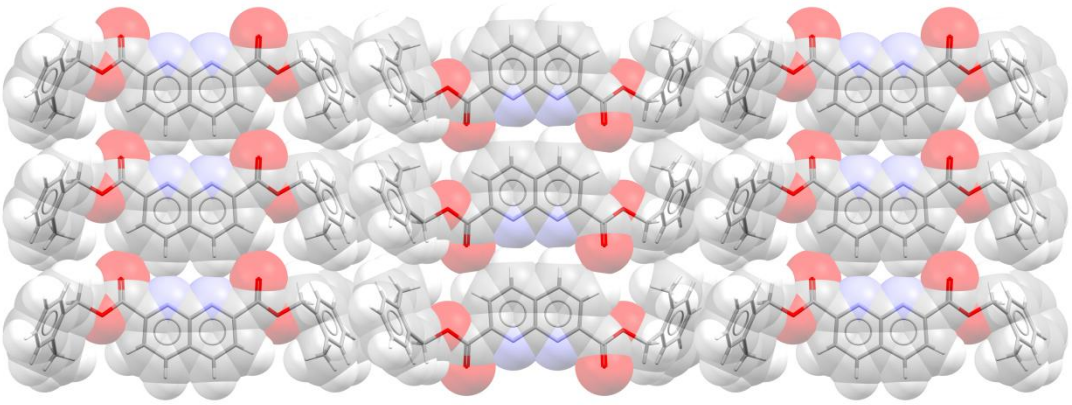

Figure 79 – The tape-like arrays align themselves into stepped sheets in which the neighbouring molecules appear to experience a face to face interaction between the pendent rings. Neighbouring tapes are aligned in an anti-parallel fashion.

Neighbouring tapes align themselves into sheets in which their nearest neighbour tapes in an anti parallel fashion (Figure 79). The pendent benzyl groups of each neighbouring tape appear to stack in an offset face to face arrangement with a perpendicular interfacial distance of 3.73 Å.

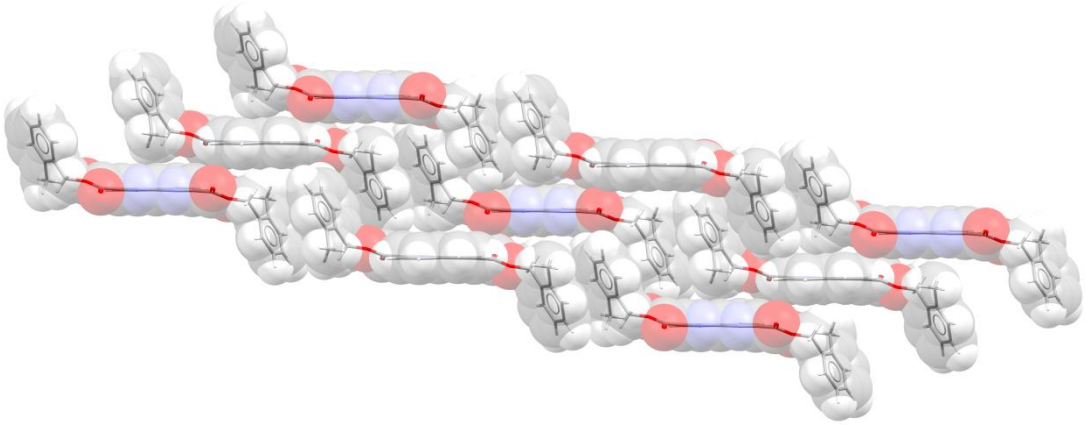

Figure 80 – Viewing the packing of sheets from a perpendicular view point to that of Figure 79 shows that the sheets stack so that neighbouring tapes are aligned in opposite directions to one another.

When examining the arrangement of the sheets of tapes it becomes obvious that the introduction of this 2-methylsubstituent onto the pendent benzyl group has a greater effect than simply causing the ring to twist out of the plane of the naphthyridine core (Figure 80). The twist causes the sheets of tapes to adopt a stepping arrangement which in turn causes the stacking of the sheets to be significantly different to that observed previously.

3.3.2.2 (3-Methylbenzyl) 1,8-naphthyridine-2,7-dicarboxylate (47j)

The 3-methyl benzyl derivative behaves rather differently in the solid-state. Once again individual molecules assemble into tapes which then form sheets. However, in this case, the orientation of the pendent aromatic groups is rather different.

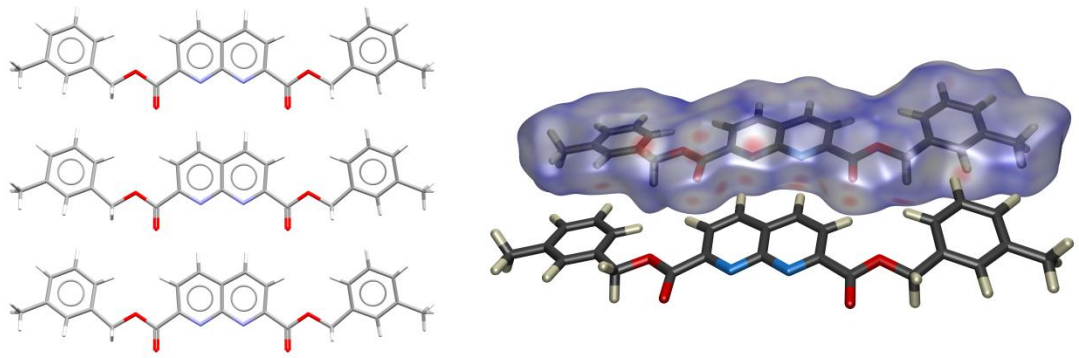

Figure 81 – *bis*-(3-Methylbenzyl) 1,8-naphthyridine-2,7-dicarboxylate (47j) forms the expected infinite one-dimensional tapes through the contacts highlighted on the Hirshfeld surface.

Interestingly, in contrast to the 2-methyl substituted benzyl derivative the pendent ring is still more or less in the plane of the naphthyridine core. There is only a slight twist of the benzyl ring (12.4 °) with respect to the naphthyridine core which is much smaller than that observed for the unsubstituted benzyl ester (47). As well as the expected taping contacts *bis*-(3-methyl benzyl) 1,8-naphthyridine-2,7-dicarboxylate shows other potential contacts on the Hirshfeld surface. While there appears to be a simple steric clash between two hydrogen atoms on neighbouring benzyl rings, the contact observed to the methylene and the naphthyridine nitrogen is explored further below.

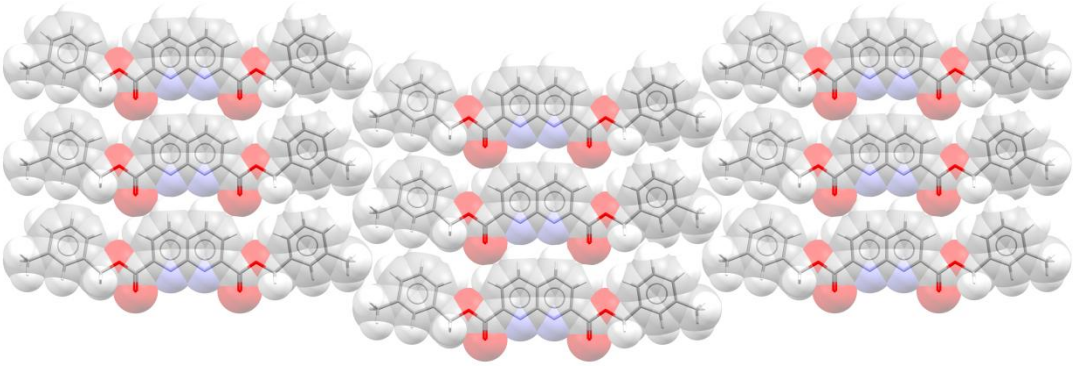

Figure 82 – The packing of tapes show that the tapes arrange themselves in such a way that the methyl substituent is sat within a void left in the packing of the neighbouring tape. The tapes are all aligned in the same direction within a sheet.

The individual tapes align in a parallel fashion in which the tapes pack with the interdigitation of the peripheral methyl groups. The methyl groups sit within a void created on the edge of the pendent ring of the neighbouring tape. It is worth noting that all the tapes within a single sheet are oriented in the same direction; most likely to accommodate the interdigitation of the methyl groups and thereby minimise voids within the structure.

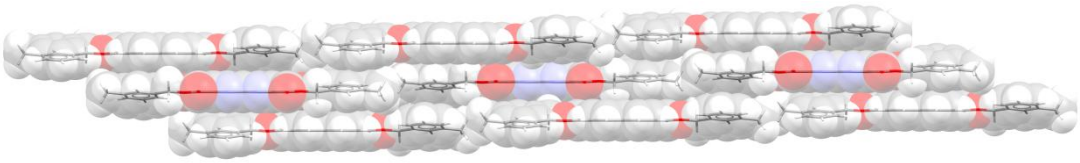

Figure 83 – The sheets of tapes stack upon one another in an anti-parallel arrangement to one another with a slight long axis shift.

The sheets arrange themselves in an offset manner such that the columns of stacks are long axis slipped. The sheets are aligned in an anti parallel nature to the neighbouring sheets above and below in the stacks.

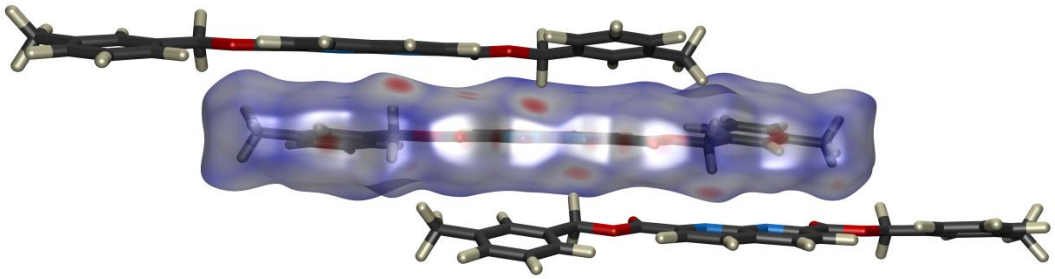

Figure 84 – The Hirshfeld surface shown in Figure 81 showed the presence of additional contacts besides the hydrogen bonding array expected. As can be seen here these additional contacts are to molecules in the stacks above and below.

As can be seen in Figure 84 the molecules in the neighbouring sheets appear to interact with one another via a contact involving the methylene CH_2 of one molecule and the naphthyridine nitrogen of the neighbouring molecule with a contact distance of C-**H**···**N** 2.57 Å, **C**-H···**N** 3.52 Å (166.2 °). It would appear that this is a co-operative arrangement with two molecules interacting on each face of the molecule, one above the plane and one below.

3.3.2.3 *bis*-(4-Methylbenzyl) 1,8-naphthyridine-2,7-dicarboxylate (47k)

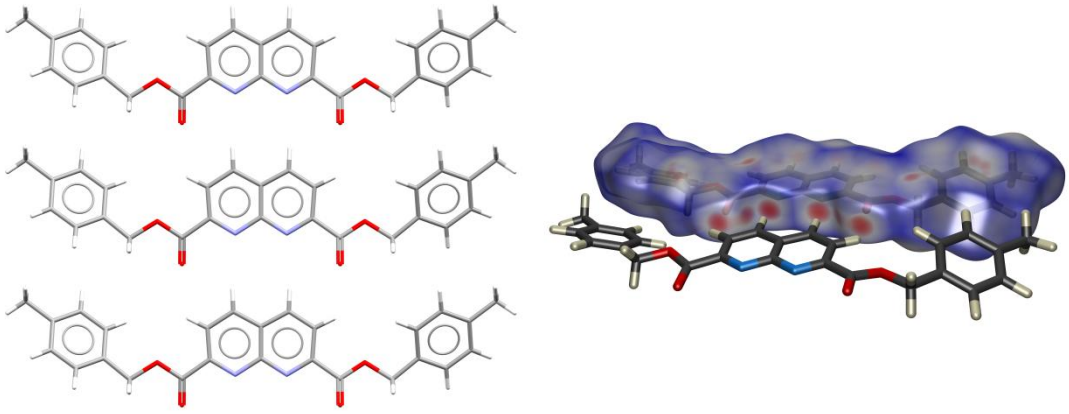

Figure 85 – *bis*-(4-Methylbenzyl) 1,8-naphthyridine-2,7-dicarboxylate (47k) can be seen to form the expected one-dimensional tapes. The pendent side arms are, like its 3-methylbenzyl analogue, held almost parallel to the plane of the naphthyridine core.

When the methyl substituent is moved to the 4-position (**47k**) the molecule adopts a motif very similar to that seen in the 3-methylbenzyl substituted isomer **47i** (Figure 85). Using the $d_{(norm)}$ Hirschfield surface the expected contacts are present within the sheets of tapes, but the interlayer interactions observed for the 3-methylbenzyl derivative (**47i**) are not present; instead it appears that there is an interaction between one methylene group and the centre of a neighbouring benzene ring.

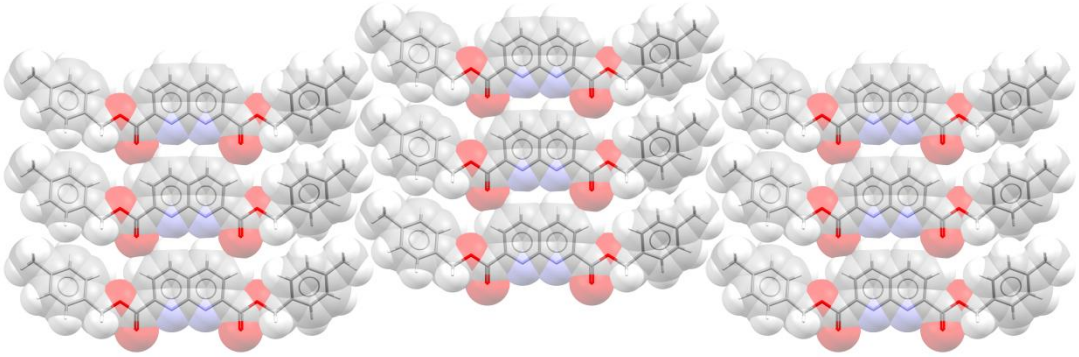

Figure 86 – Interestingly despite the change in substitution position the sheet packing structure is very similar to that seen in the 3-methylbenzyl derivative (47i). The methyl group once again interdigitates between neighbouring tapes.

As we saw in the 3-methyl substituted benzyl derivative (**47i**) the neighbouring tapes in the sheet are stacked in a parallel arrangement to one another. Despite the position of substitution being altered (Figure 86), the packing motif is remarkably similar. The methyl group sat to the rear of the molecule, rather than to the front, is

interdigitated with the neighbouring tapes with the only significant difference being the relative order of the interaction.

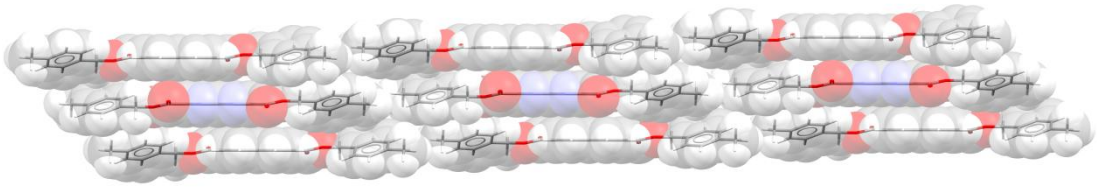

Figure 87 - The neighbouring sheets are seen to stack in an anti-parallel arrangement to one another.

Neighbouring sheets are again mutually inverted (Figure 87), but the columns of tapes appear to experience a smaller long axis shift that in the 3-methylbenzyl derivative (**47i**).

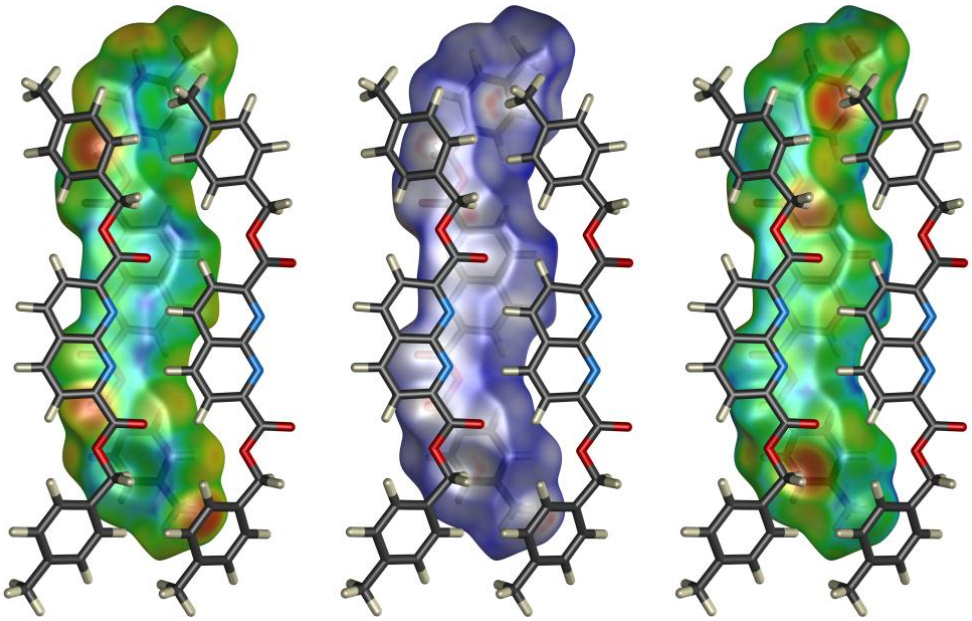

Figure 88 – Unlike the 3-methylbenzyl derivative (47i) there does not appear to be any strong intermolecular interactions between neighbouring stacks in the 4-methylbenzyl derivative (47h). In this case there appear to weak C-H···π interactions between neighbouring sheets. This is highlighted on the Hirshfeld surfaces (left d_i, centre $d_{(norm)}$, right d_e)

It would appear that the reduction in the long axis slip angle could be due, in part, to the weak C-H···π interaction that was indicated by the Hirschfield surface. Figure 88 shows these interactions via a top down view of the molecular stacks using different surface colourings to highlight the contacts. As previously mentioned it appears that one of the methyl group C-H bonds interacts with a neighbouring benzyl ring in the sheet above while a methylene group appears to interact with a neighbouring benzyl ring through a C-H··· π contact. In both cases the contact

distance is 2.61 Å. These interactions do not show up particularly well in the d(norm) colouring but when looking at the d_i and the d_e surfaces it becomes more obvious.

3.3.2.4 *bis*-(2,4,6-Trimethylbenzyl) 1,8-naphthyridine-2,7-dicarboxylate (47l)

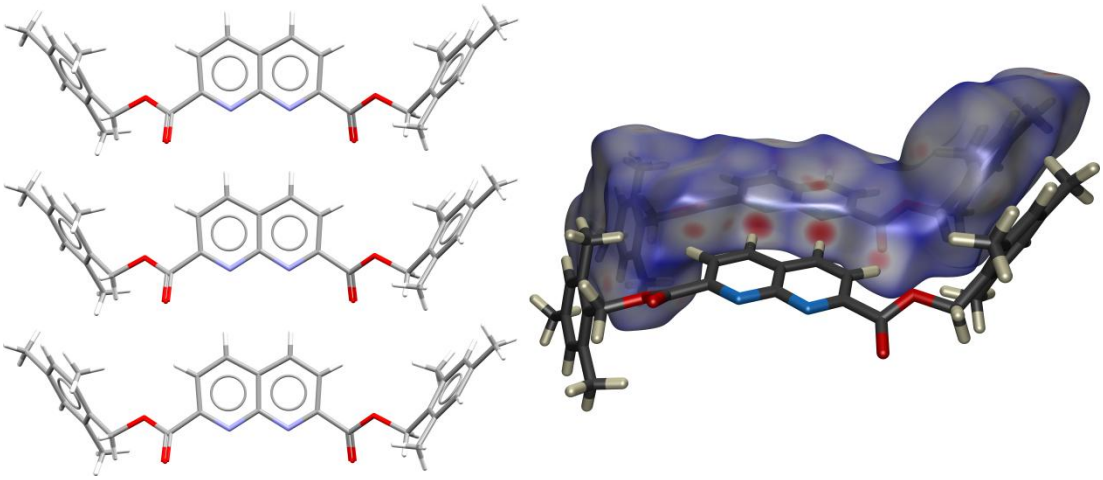

Figure 89 – *bis*-(2,4,6-Trimethylbenzyl) 1,8-naphthyridine-2,7-dicarboxylate (47l) is seen to form the expected hydrogen bonding array. However, like the 2-methylbenzyl derivative (47i) it can be seen that the pendent ring is twisted out of the plane of the naphthyridine core.

Multiple methyl substitution of the benzyl ring appears to force the pendent ring to be strongly twisted out of the plane of the naphthyridine core. In the case of 2,4,6-trimethylbenzyl ester the pendent rings sits at an angle of 73.9 ° from the plane of the naphthyridine core with a torsion angle of -32.7 °.

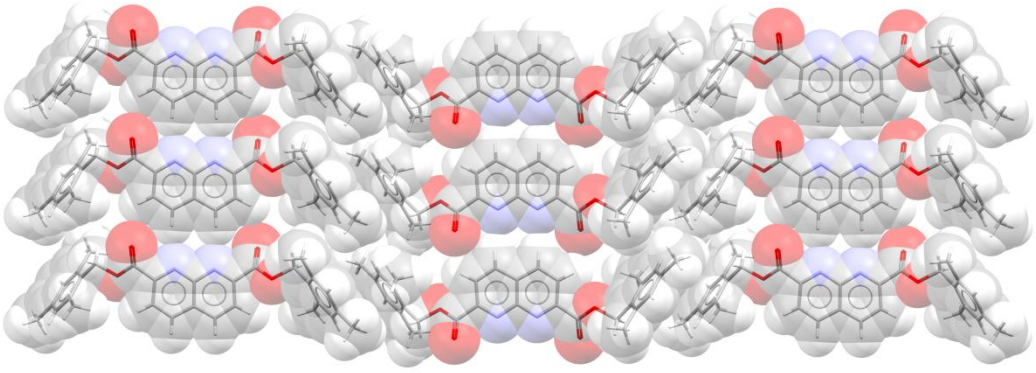

Figure 90 – The tapes form into sheets in which neighbouring tapes are in the opposite alignment to one another. The tapes appear to pack with a face to face arrangement of the pendent benzyl rings in a step-like sheet formation.

Once again the tapes organise into sheets (Figure 90) and the packing appears to be dominated by the need to accommodate the very bulky benzyl groups. Immediate long axis neighbours are inverted and the substituted benzyl pendent rings are aligned in a face-to-face manner however the face-to-face separation of 4.01 Å is too large for there to be any significant π···π interaction. It is worth noting that neighbouring rings are twisted into a staggered conformation in order to minimise steric clashes.

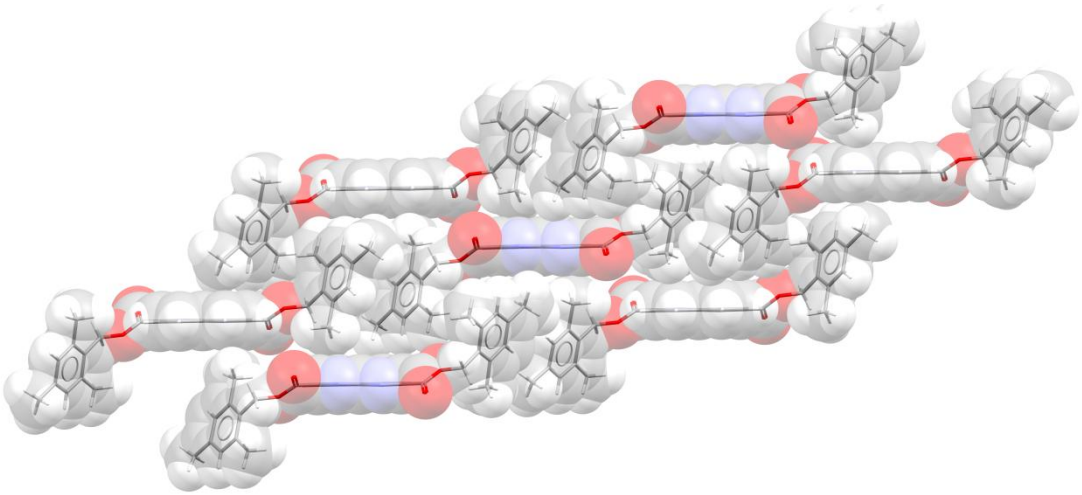

Figure 91 –The sheets pack so that neighbouring tapes in a stack are in opposite alignment to one another.

Figure 91 shows the organisation of neighbouring sheets with the sheet illustrated in Figure 90 as the middle layer. It appears that the structure accommodates the sterically bulky benzyl rings in channels with the naphthyridine core of the molecule from the sheet above and below sitting around it.

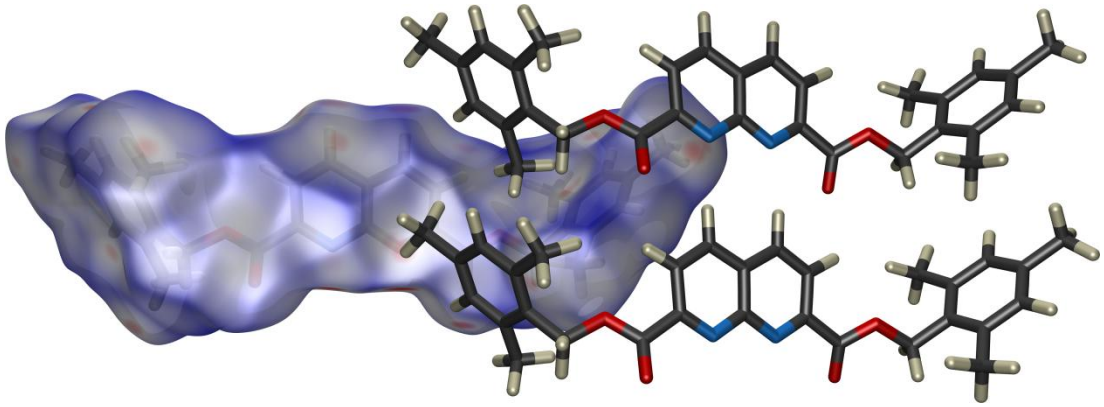

Figure 92 - Examining the Hirshfeld surface higlights a number of weaker C-H···π interactions originating from the methyl groups on the pendent benzyl ring.

Within a stack of tapes the molecules are stacked diagonally in the opposite direction to their nearest neighbour. The columns are sufficiently long-axis slipped

(angle) that there is not significant overlap between neighbouring naphthyridine cores.

3.3.2.5 *bis*-(2,3,5,6-Tetramethylbenzyl) 1,8-naphthyridine-2,7-dicarboxylate (47m)

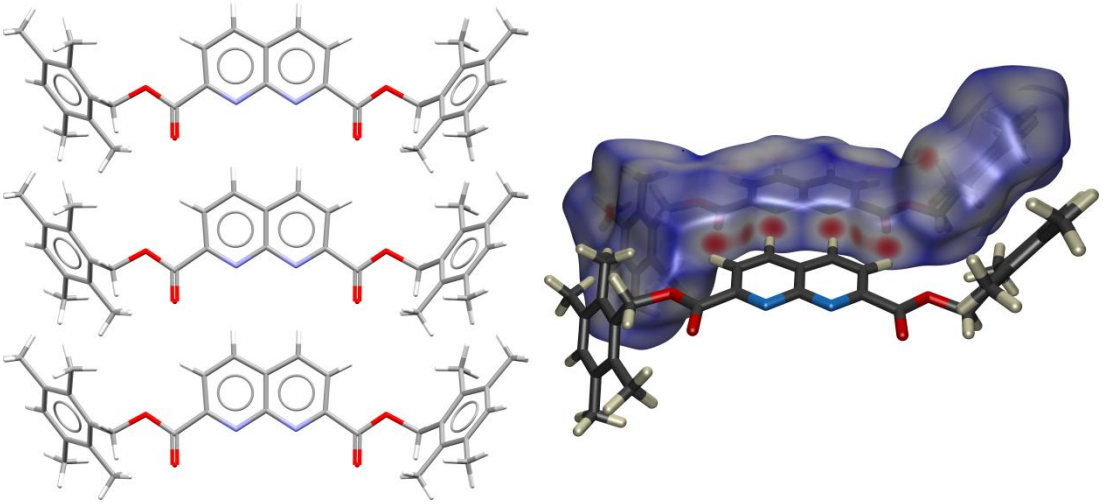

Figure 93 – *bis*-(2,3,5,6-Tetramethylbenzyl) 1,8-naphthyridine-2,7-dicarboxylate (47m) forms the expected infinite one-dimensional tapes with the key interactions highlighted on the Hirshfeld surface. The pendent benzyl rings are once again twisted out of the plane of the naphthyridine core.

Moving to the 2,3,5,6-tetramethylbenzyl ester it is found that the bend of the ring out of the plane of the naphthyridine core has been reduced to 62.0 ° with a torsion angle of 10.3 °.

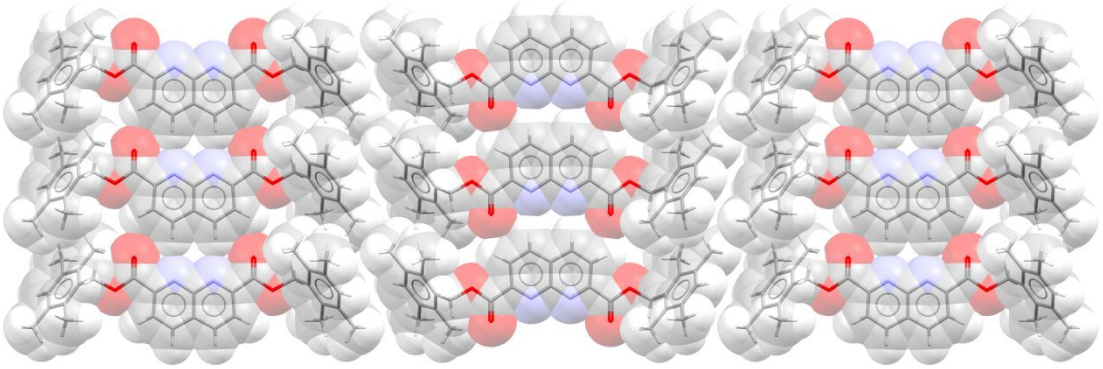

Figure 94 – The infinite one-dimensional tapes assemble into step-like sheets which have an anti-parallel alignment with one another.

Once again the tapes organise into sheets (Figure 94) and the packing appears to be dominated by the need to accommodate the very bulky benzyl groups. Unlike the 2,4,6-trimethyl benzyl derivative (**47l**) the pendent benzyl rings do not appear to

form π···π face to face interactions, instead they form a herringbone arrangement which will be discussed later.

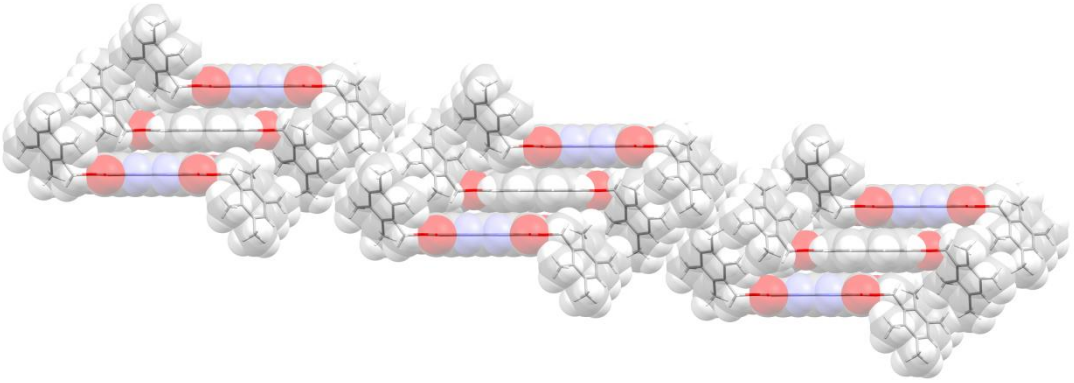

Figure 95 –The sheets of tapes stack on one another in an anti-parallel arrangement.

It becomes immediately apparent when looking at the secondary structure that this is because the introduction of the additional methyl group has blocked the staggered interdigitated packing arrangement of the neighbouring benzyl rings. To accommodate the even bulkier pendent ring it has become necessary to stack the tapes in such a way that they form discreet channels of core stacks and pendent arms.

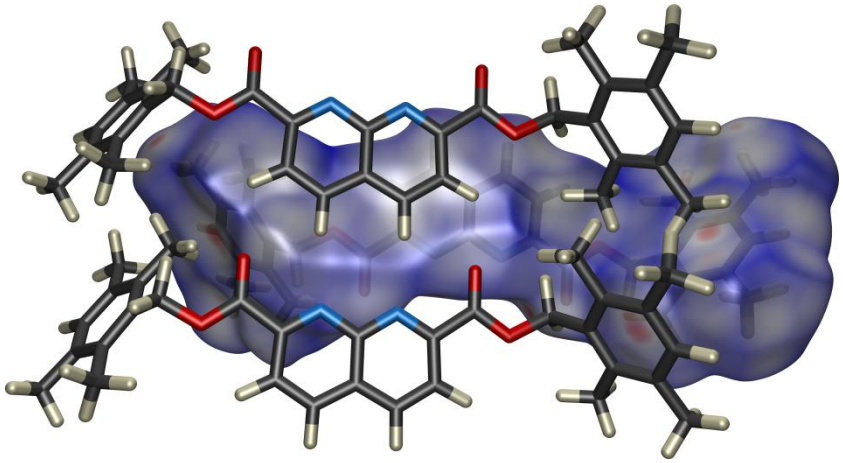

Figure 96 – The Hirshfeld surface shows weak C-H···π interactions which may act as a stabilisation for the herringbone arrangment.

The Hirshfeld surface indicates that within the stacks of tapes there are close contacts indicative of two weak C-H···π interactions from the methyl substituents on the benzyl ring to the pendent benzyl rings on neighbouring molecules (C-H···π 2.98 Å and C-H···π 3.08 Å respectively) (Figure 96). Unfortunately it is not possible

to identify whether these contacts come about because of the packing arrangement or whether they aid in the formation of the packing arrangement.

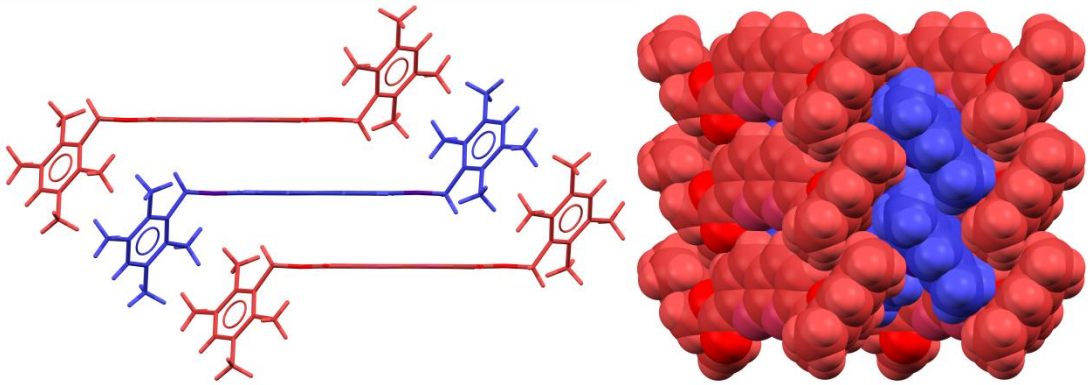

Figure 97 – The packing of 47m appears to centre around the stacking of molecules. The tessellation of the pendent side arms is of interest as the extremely bulky tetramethyl benzyl ring appears to be easily accommodated by arrangement of the rings into a herringbone pattern.

The packing of the pendent arms is examined in Figure 97, where the molecules in the stacks are differently coloured to differentiate them. Looking at the stack side on then allows us to see that by stacking neighbours in opposite direction, the substituted benzyl can easily tessellate.

3.3.2.6 Comparison of methyl substituted benzyl derivatives (47i-n)

Structure	$r_{1\ C?N}$	θ	$r_1'_{H?N}$	$r_1'_{C?N}$	θ'	$r_{1\ H?N}$	$r_{2\ C?O}$	ϕ	$r_{2\ H?O}$	$r_{2\ C?O}$	ϕ	$r_{2\ H?O}$
Benzyl	3.48	174.6	2.50	n/a	n/a	n/a	3.10	121.9	2.47	n/a	n/a	n/a
2 Me Bn	3.49	173.4	2.54	n/a	n/a	n/a	3.12	124.7	2.48	n/a	n/a	n/a
3 Me Bn	3.70	173.8	2.72	n/a	n/a	n/a	3.25	121.2	2.64	n/a	n/a	n/a
4 Me Bn	3.50	175.0	2.56	n/a	n/a	n/a	3.09	123.3	2.47	n/a	n/a	n/a
246 tri Me Bn *	3.46	172.9	2.53	3.45	176.4	2.53	3.24	123.9	2.60	3.22	127.1	2.59
2356 tetra Me Bn	3.49	175.2	2.55	n/a	n/a	n/a	3.07	123.2	2.44	n/a	n/a	n/a

Table 4 - Primary hydrogen bonding array contact distances for the methyl substituted benzyl 1,8-napthyridine derivatives

Throughout the descriptions above no details of the contact distances for the central hydrogen bonding array were given, but they are contained in Table 4.

It is obvious that, with the exception of the 3-methylbenzyl derivative **47j**, there is little variation in the r_1 or r_2 contact distances, suggesting that the contact is relatively unaffected by these variations on the pendent benzyl ring. The cause of the elongation of r_1 in **47j** is unclear but may be due to the introduction of the inter-sheet contacts illustrated in Figure 84.

Unfortunately it has not proved possible to obtain an X-ray structure for *bis*-(2,3,4,5,6-pentamethylbenzyl) 1,8-naphthyridine-2,7-dicarboxylate due to its almost complete insolubility. Ideally it would be desirable to investigate some alternate substitution patterns, preferably without a methyl group in the 2-position, to investigate the orientation of the side arms without the sterics clash that substitution in the 2 position brings.

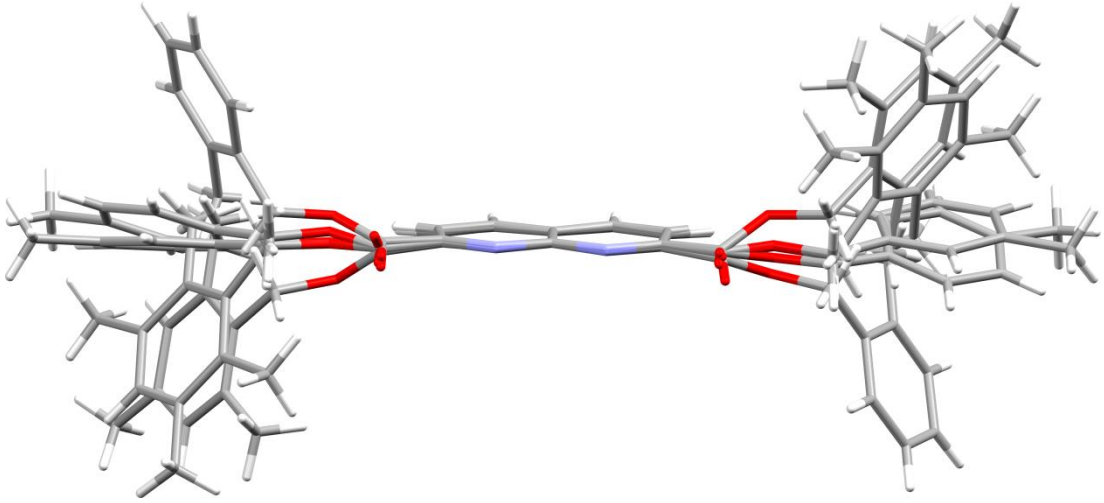

Figure 98 - Shows the overlay of the 5 methyl substituted benzyl derivatives studied.

Figure 98 illustrates the differences seen between the different methyl-substituted benzyl ester derivatives. Introduction of a sole methyl group in the 3- and 4-positions results in the pendent arms remaining almost in the plane of the naphthyridine core. However substitution at the 2- position causes the benzyl ring to be bent out of the plane of the naphthyridine core, presumably to minimise the steric clashes that this substitution causes. Addition of further methyl groups shows that this trend continues as the pendent benzyl ring gets more and more bulky, however to date no poly-methyl substituted benzyl derivative has been prepared that does not have a methyl group in the 2- position. It would be desirable, therefore, to do so in an attempt to understand the extent to which the behaviour of the multi-substituted benzyl derivatives are being dominated by this interaction.

3.3.3 Halogen Substituent

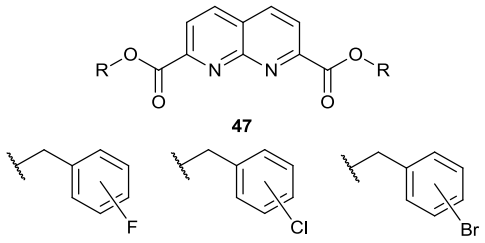

47

Cheesewright[196] investigated the effects of changing a methyl group for a chlorine atom in the pyridine-2,6-dicarboxylates because of their similar van der Waal radii.[266, 267] As such, attempts were made to synthesise analogues of the previously reported *bis*-(4-halogenbenzyl) pyridine-2,6-dicarboxylates. Interestingly while the 4-fluorobenzyl naphthyridine derivative was soluble in chloroform the 4-chloro and 4-bromo derivatives were at best sparingly soluble in boiling DMSO. This vast difference in solubility prompted the synthesis of the other regioisomers for further study.

3.3.3.1 Fluorine substitution

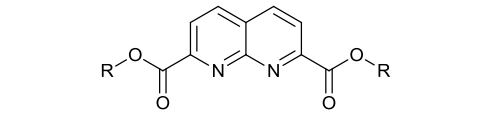

47

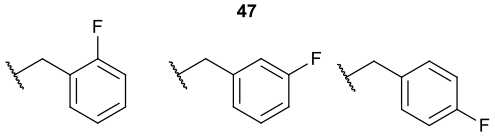

47o 47p 47q

As fluorine is so electronegative it creates highly polarised bonds; because of this is has been implicated as a potential hydrogen bond acceptor[268-271] however, there is much debate to the extent of this.[272, 273] There has been an investigation into this and although these appear to be weak interactions it is commonly believed that the interaction is real. The effect that this might have on the secondary and tertiary structure of our molecules might provide marked changes arising from these additional interactions.

3.3.3.1.1 bis-(2-Fluorobenzyl) 1,8-naphthyridine-2,7-dicarboxylate(47o)

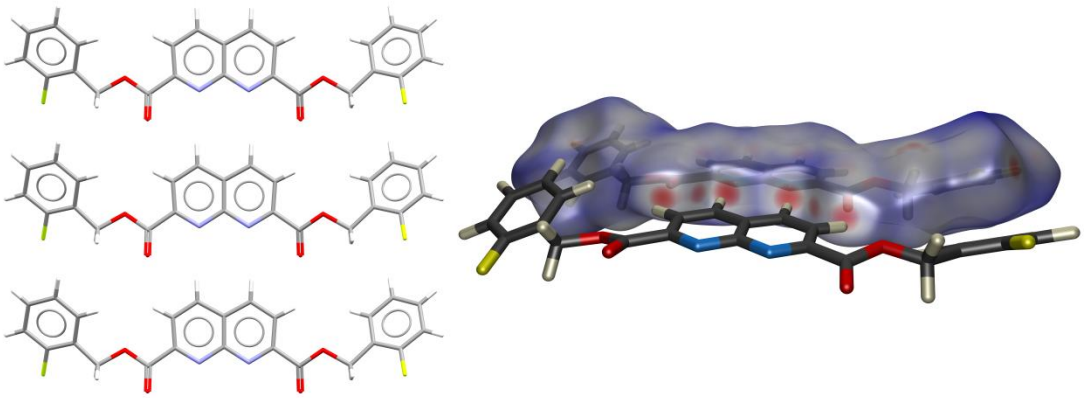

Figure 99 – *bis*-(2-Fluorobenzyl) 1,8-naphthyridine-2,7-dicarboxylate(47o) forms the expected hydrogen bonding array which leads to the formation of infinite one-dimensional tapes.

The solid-state structure of the 2-fluoro substituted benzyl derivative shows that the molecules continue to form the expected one-dimensional tapes, however the Hirshfeld surface would appear to indicate that the fluorine atoms are indeed providing secondary interactions. It is interesting that in contrast to the methyl substituted benzyl derivative, the pendent ring is only slightly twisted out of the plane of the naphthyridine core (Figure 99).

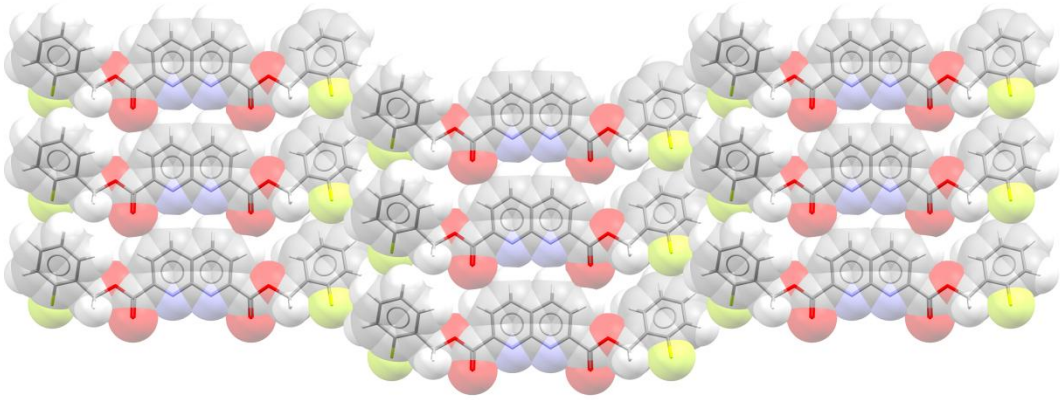

Figure 100 – The tapes of 47o form slightly stepped sheets in which all the tapes are aligned in the same direction.

Within a sheet, neighbouring tapes pack in parallel alignment (Figure 100), but closer inspection would suggest that this could be in part due to the interactions of the fluorine substituents and the acidic C-H groups on neighbouring tapes. In order that these interactions may occur the benzyl rings are twisted out of the plane of the naphthyridine core. The pendent side arms are interdigitated which, because of

the twist of the benzyl ring, creates a herringbone-like pattern between neighbouring molecules.

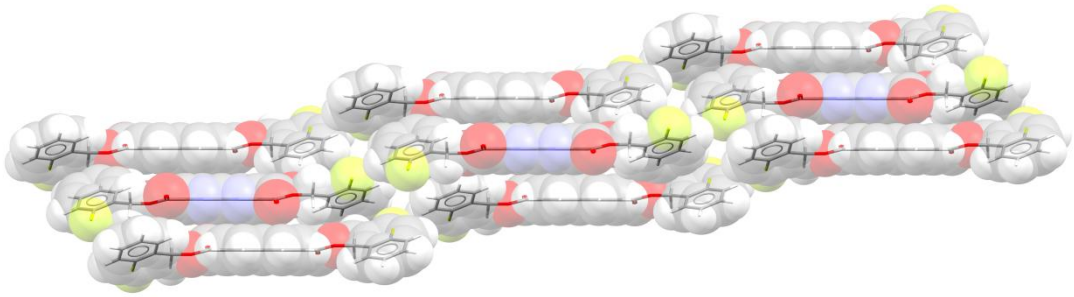

Figure 101 – The sheets form stacks in which each sheet is aligned in the opposite direction to the neighbouring sheets.

The sheets of tapes stack in anti-parallel arrangement most likely in order to accommodate the close packing of the sheets which have the benzyl groups twisted out of the plane creating a pocket.

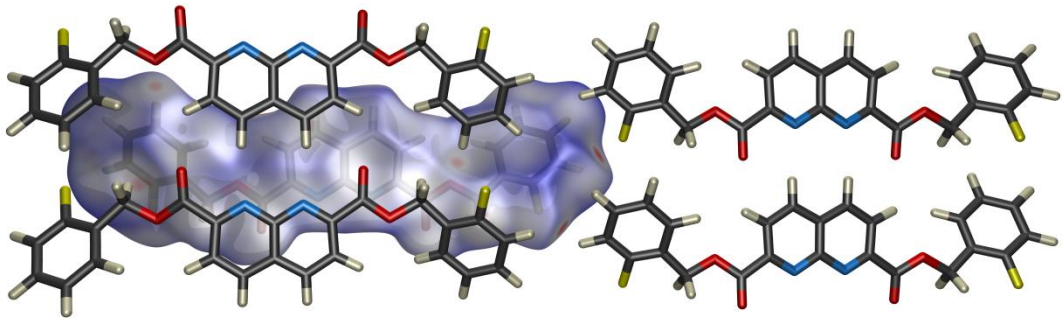

Figure 102 – An illustration of the interactions with the immediate neighbouring molecules around a d(norm) Hirshfeld surface. There appears to be evidence of a weak C-H···F interaction.

Examining the interactions around one such pocket shows that the two molecules to the right of Figure 102 are in the same sheet as the molecule enclosed in the Hirshfeld surface. This shows quite clearly the two reciprocal interactions, of distance C-**H**···**F** 2.55 Å **C**-H···**F** 3.27 Å (133.6 °), between the neighbouring sheet molecules. The two molecules that are sat above the surface appear to be subject to an interaction between one of the benzyl groups C-H and the ether oxygen of the ester bond; this interaction would be very weak but is enhanced by the resonance effect of the fluorine substituent in the ring which increases the acidity of the benzyl C-H group involved.

3.3.3.1.2 bis-(3-Fluorobenzyl) 1,8-naphthyridine-2,7-dicarboxylate (47p)

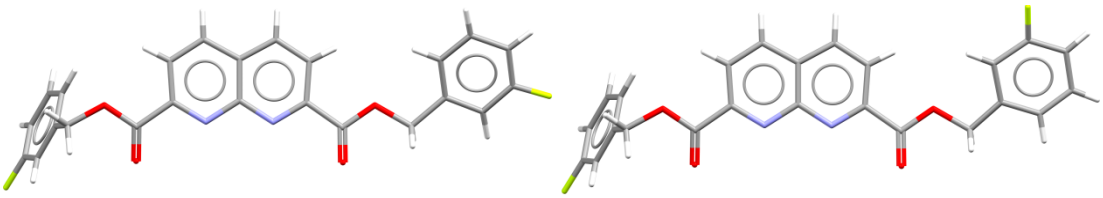

Figure 103 - The structure of 3-fluorobenzyl 1,8-naphthyridine-2,7-dicarboxylate is disordered on one ring in a ratio of 61:39.

There are two interesting features of the structure obtained for *bis*-(3-fluorobenzyl) diester: Firstly in this structure one aromatic pendent ring is bent out of the plane of the naphthyridine core while the other remains within in the plane; secondly the ring that remains within the plane of the naphthyridine core is disordered around the central axis of the benzyl ring, allowing the fluorine group to exist in both possible orientations (Figure 103). Interestingly the disorder is shifted away from the 50:50 distribution that would be expected, to a 61:39 ratio.

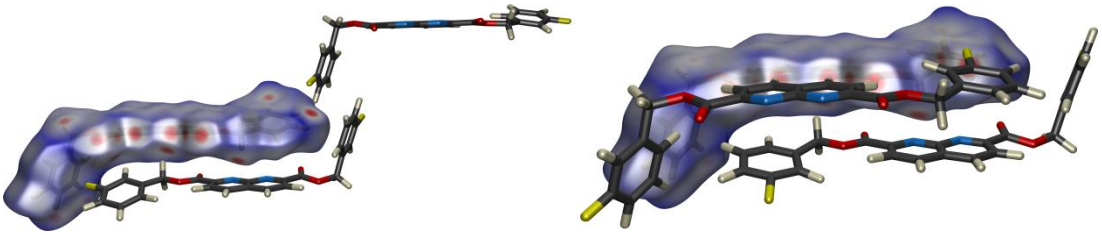

Figure 104 – Examination of the Hirshfeld surface of the two different conformers could perhaps give some information as to the cause of the disorder.

A study of the Hirshfeld surfaces of the two different conformers (Figure 104) appears to give an indication of why the disorder occurs. It would appear that in the secondary packing of the molecules there is the potential for more than one interaction to occur. It would appear that the side arm can adopt the conformation required for either interaction due to the similarity in shape and size of the two conformers. The refinement of the free variable to a 61:39 ratio would tend to suggest that the conformer in which the fluorine substituent points out away from the naphthyridine core is the preferred conformer in the crystal examined.

For analysis of the remaining packing architecture the preferred conformer is used.

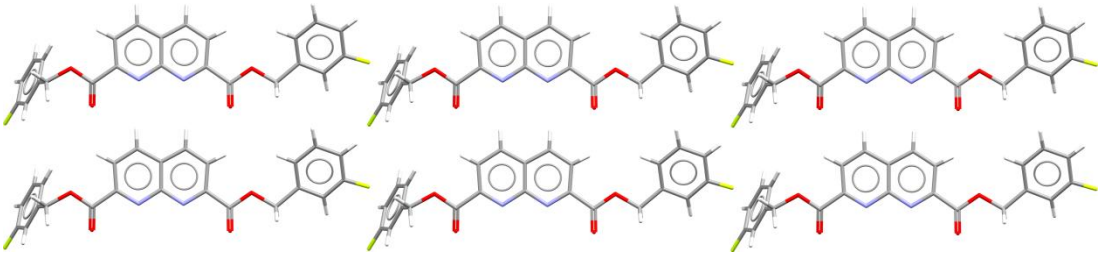

Figure 105 – With the pendent arms in opposite conformations (one in the plane of the core, one twisted out) the molecule appears to form sheets of molecules all aligned in one direction.

The structure forms sheets in which the neighbouring tapes sit in a parallel arrangement. This leads to the pendent arm twisted out of the plane all pointing in the same direction It appears that the sheet forming contact in the preferred conformer is the result of an interaction between fluorine and hydrogen in the neighbouring flat and bent rings (Figure 105) (**F**···**H**-C 2.53 Å, **F**···H-**C** 3.41 Å (154.7 °) and F···**H**-C 2.62 Å, **F**···H-**C** 3.28 Å (127.1 °)).

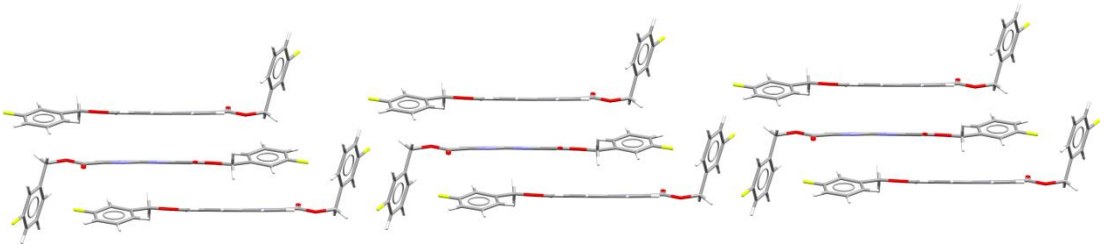

Figure 106 – The stacking of the sheets into anti-parallel alignment leads the complimentary packing of the pendent benzyl ring which is twisted out of the plane of the core.

The formation of stacks is more interesting as formation of layers introduces a step-stacked arrangement but there are also interactions between the tapes immediately above and below one another, thanks to the short contacts highlighted in Figure 104. These occur between the naphthyridine nitrogen and the methylene C-H as well as the carbonyl oxygen and one of the hydrogen atoms from the flat pendent rings similar to that seen in the *bis*-(3-methylbenzyl) derivative (C=O···C-H 2.58 Å, C=O···C-H 3.17 Å (120.5 °) and N···C-H 2.54 Å, N···C-H 3.50 Å (161.2 °). Description of the behaviour of this material is complicated by the disorder in the system as well as the different conformations of the two pendent side arms.

3.3.3.1.3 bis-(4-Fluorobenzyl) 1,8-naphthyridine-2,7-dicarboxylate (47q)

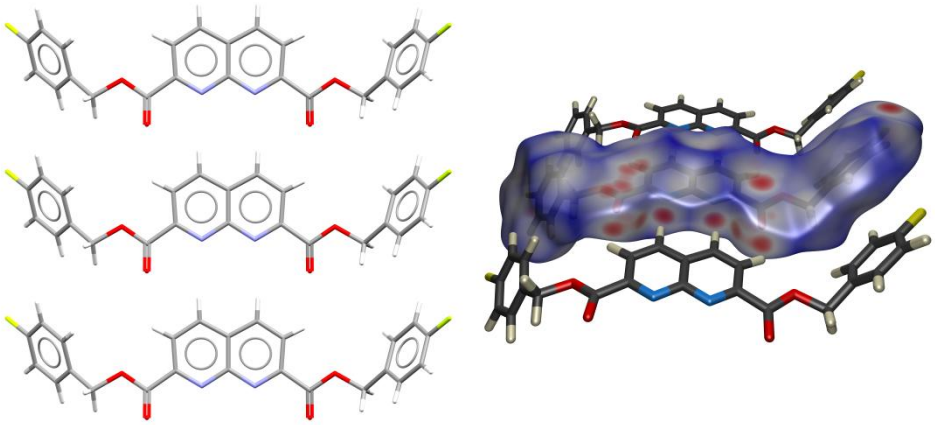

Figure 107 – *bis*-(4-Fluorobenzyl) 1,8-naphthyridine-2,7-dicarboxylate (47q) forms the expected hydrogen bonded array leading to the formation of infinite one-dimensional tapes. The pendent arms are twisted slightly out of the plane of the naphthyridine core.

bis-(4-Fluorobenzyl) 1,8-naphthyridine-2,7-dicarboxylate exhibits the expected formation of infinite one-dimensional tapes, and again in contrast to the *bis*-(4-methyl)benzyl analogue the benzyl ring is twisted out of the plane of the naphthyridine core at an angle of 56.4 ° with a torsion angle of 19.7 °.

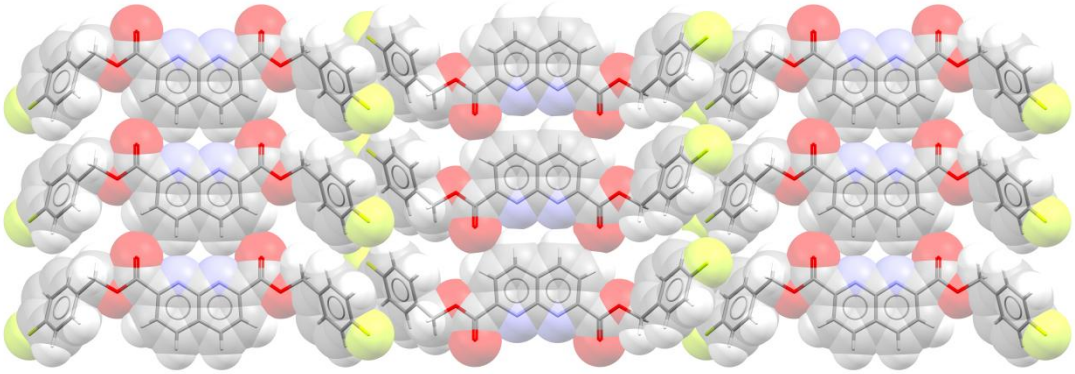

Figure 108 – The formation of anti-parallel sheets appears to occur through the formation of face to face interactions of the benzyl pendent arms leading to the formation of a step –like sheet.

Within a sheet, individual tapes are then aligned in an anti-parallel arrangement relative to their nearest neighbour. The pendent rings are arranged so that they adopt a face to face conformation, with a perpendicular inter-face distance of 3.82 Å, and the fluorine substituent sitting in opposite directions to one another. It is possible to imagine that this could enable the two rings to align such that any dipole that the rings experience is arranged to pack in an attractive conformation.

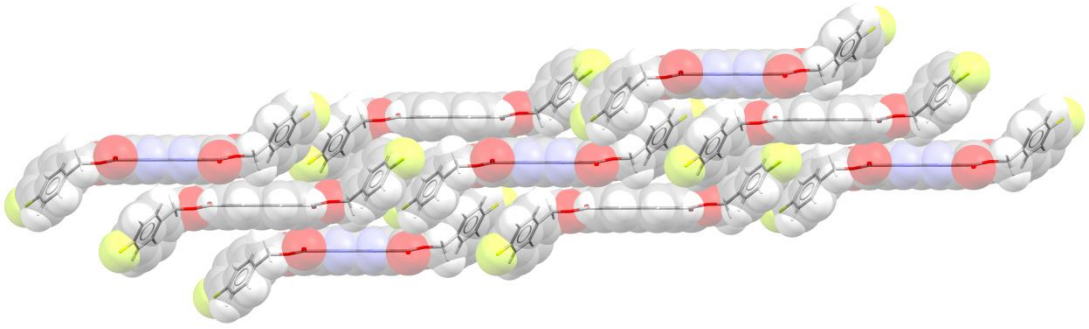

Figure 109 –The sheets stack upon one another in an anti-parallel arrangement.

The sheets pack on top of one another in an anti-parallel arrangement which is affected by the stepwise structure of the individual sheets meaning that the tape stacks appear to be offset from one another.

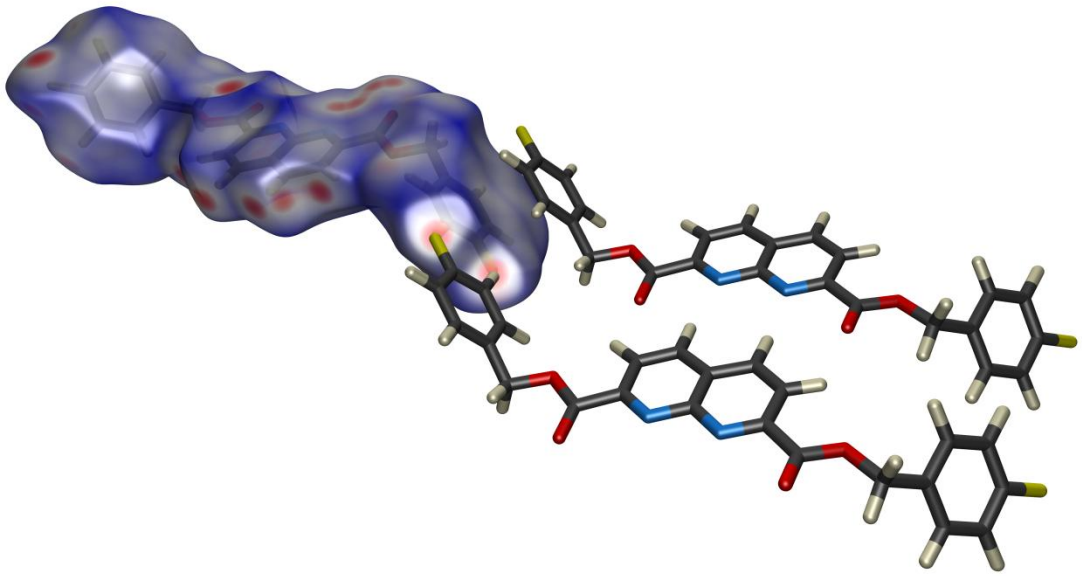

Figure 110 –The Hirshfeld surface indicates that, although the sheets appear to form through the face to face arrangement with its neighbour, there are interactions with the molecule in front of that neighbour.

Closer examination of the interactions involving the pendent arms of the molecules shows that, as well as the potential face-to-face interaction of the benzylic rings, there is a potential C-F···H-C contact between two molecules in neighbouring tapes; this is highlighted on the Hirshfeld surface. The contact between the fluorine and the hydrogen is (**C**-H···**F** =3.36 Å C-**H**···**F** = 2.49 Å (155.5 °)).

3.3.3.1.4 Comparison of the fluorine substituted benzyl derivatives

Structure	$r_{1\ C?N}$	θ	$r_{1}'_{\ H?\ N}$	$r_{1}'_{\ C?N}$	θ'	$r_{1\ H?\ N}$	$r_{2\ C?O}$	ϕ	$r_{2\ H?O}$	$r_{2\ C?O}$	ϕ	$r_{2\ H?O}$
Benzyl	3.48	174.6	2.50	n/a	n/a	n/a	3.10	121.9	2.47	n/a	n/a	n/a
2 F Bn	3.52	175.1	2.57	n/a	n/a	n/a	3.14	124.0	2.51	n/a	n/a	n/a
3 F Bn†	3.56	172.8	2.61	3.56	171.3	2.62	3.13	123.5	2.51	3.20	122.4	2.59
4 F Bn	3.54	174.6	2.51	n/a	n/a	n/a	3.12	123.6	2.51	n/a	n/a	n/a

Table 5 - The hydrogen bonding array contact distances for the fluorine substituted benzyl derivatives.

The contacts observed for the core hydrogen bonding array for the fluorine substituted benzyl derivatives are all very similar to one another (Table 5), in spite of the obvious difference in the structure of the 3-fluorobenzyl derivative (**47p**). The overall contact distances are slightly elongated from the base benzyl derivative (**47h**).

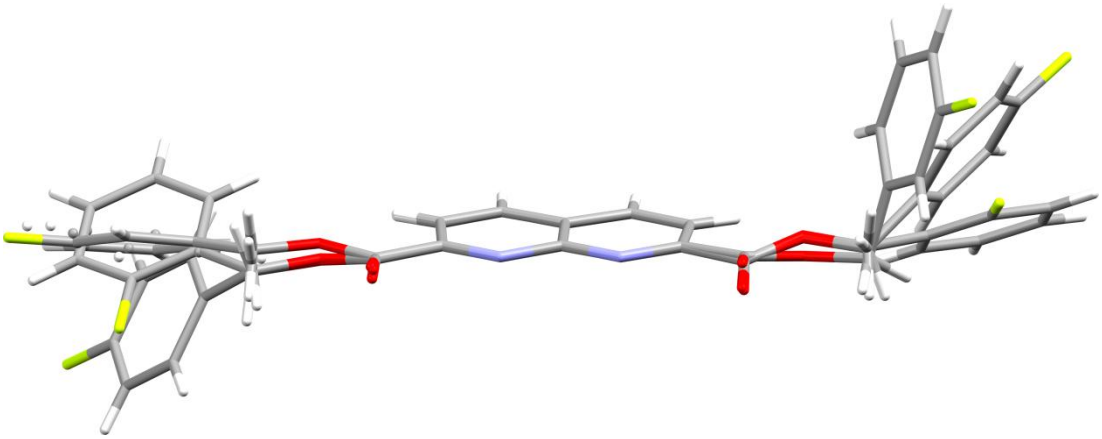

Figure 111 –This is the overlay of the fluoro substituted benzyl derivatives studied.

By overlaying the three structures upon one another it is possible to see that the fluorine-substituted benzyl derivatives adopt three distinct structures: One in which both of the pendent rings are in the plane of the naphthyridine core; one in which they are both bent out of the plane, and one in which one is bent out of the plane and one ring is parallel to the naphthyridine core. This series is particularly interesting as it is only in the fluorine system that this mixed conformation is observed, the reason for which is not understood.

3.3.3.2 Chlorine substitution

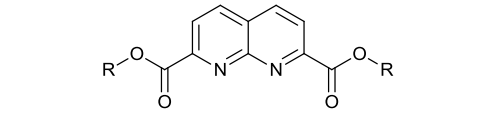

47

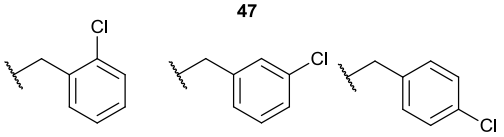

47r 47s 47t

With a chlorine substituent the electron density of the benzyl ring should be less polarised. Somewhat surprisingly it is more accepted that the chlorine substituent, rather than the fluorine substituent, can participate in hydrogen bonds as the acceptor.[81, 114] As such it is interesting to examine how the presence of chlorine affects the solid-state structure. These structures will also be compared with those observed for the mono-methyl substituted benzyl derivatives as chlorine has a similar van der Waal radius to that observed for a methyl group.[266, 267]

3.3.3.2.1 bis-(2-Chlorobenzyl) 1,8-naphthyridine-2,7-dicarboxylate (47r)

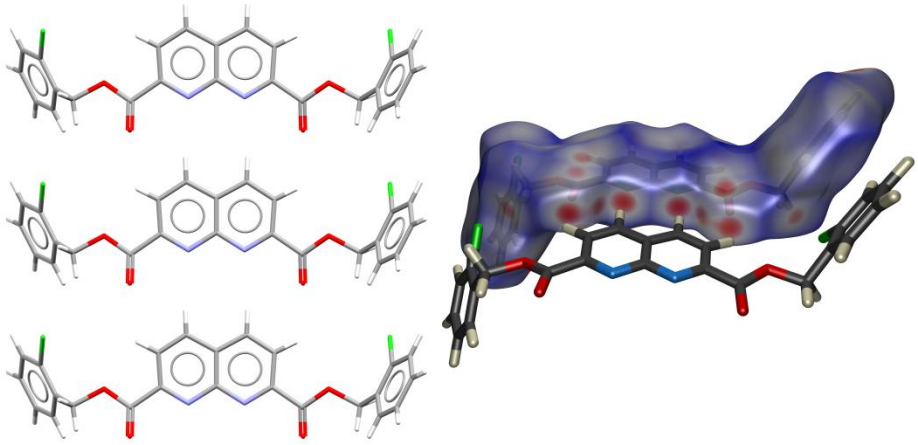

Figure 112 – *bis*-(2-Chlorobenzyl) 1,8-naphthyridine-2,7-dicarboxylate (47r) forms the expected hydrogen bond array at the core, which causes the formation of infinite one-dimensional tapes.

The 2-chlorobenzyl diester (**47r**), like its 2-methylbenzyl analogue (**47i**), shows the benzyl sidearm twisted out of the plane of the naphthyridine core at an angle of 66.3 °. Additional close contacts are highlighted between the left hand chlorine group and the methylene C-H on the molecule behind (C-**H**···**Cl** 2.87 Å, **C**-H···**Cl** 3.72 Å (143.7°)). There is also a contact between the C(4)-H on the right hand ring and a carbonyl group of a molecule in the sheet above (C-**H**···**O**=C 2.58 Å, **C**-H···**O**=C 3.30 Å (133.0°).

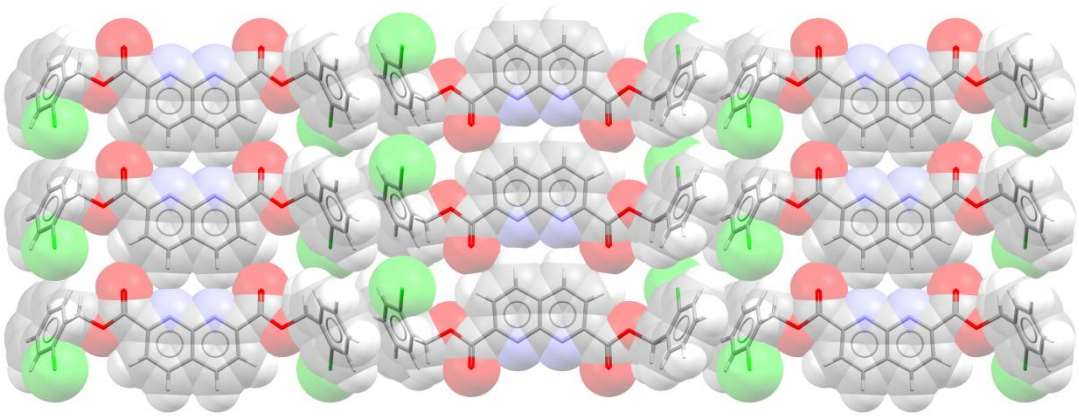

Figure 113 – The tapes align into step-like anti-parallel sheets which have a face to face alignment of the pendent benzyl groups.

Once again the tapes pack in an anti-parallel orientation with the benzyl rings from neighbouring tapes sat in a face to face arrangement, this time with a inter-centroid distance of 3.65 Å. As has been seen in previous examples of substituted benzyl derivatives, the rings sit so that the chloro-substituents are aligned in opposite directions.

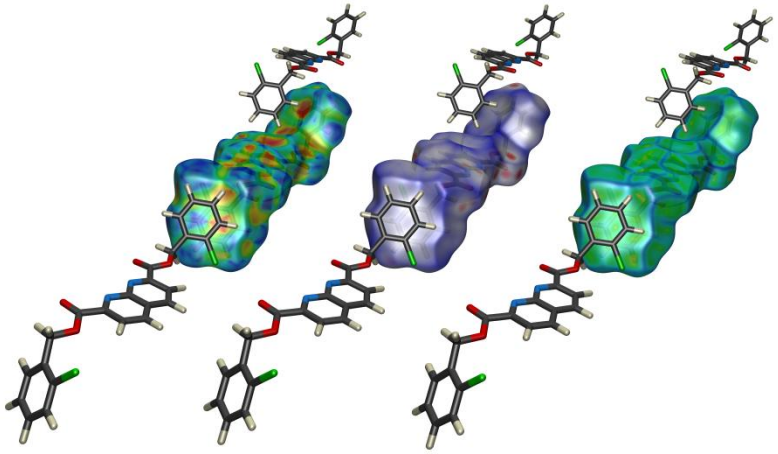

Figure 114 –Examining different surface colourings of the Hirshfeld surface leads to the suggestion that these pendent benzyl rings maybe subject to a π···π interaction. (left = shape index, centre = $d_{(norm)}$ and right =curvedness).

Figure 114 serves to illustrate the interactions between the pendent rings. On one side the rings overlap in a slip stacked face-to-face fashion with the chloro substituents aligned in opposite directions. While the $d_{(norm)}$ and curvedness surface colouring show no interesting features, the shape index surface colouring pattern is similar to that seen in systems thought to exhibit π ··· π interactions. On the other side of the pendent benzyl group it appears that there may be some type of interaction with one of the benzylic hydrogens from a molecule in the sheet above

pressing into the face of the benzyl ring and another pointing towards the ether oxygen atom in the ester.

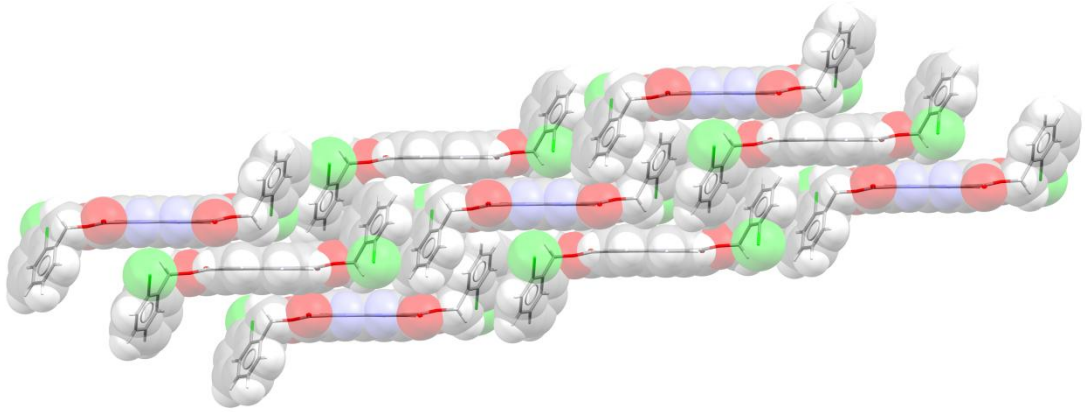

Figure 115 – The sheets stack in an anti-parallel manner with a slight long axis shift.

In this molecule it can seen that the sheets pack into stacks in an anti-parallel manner. The stacks are long axis slipped from one another, most likely to accommodate the bend of the pendent arms out of the plane of the naphthyridine core.

3.3.3.2.2 bis-(3-Chlorobenzyl) 1,8-naphthyridine-2,7-dicarboxylate (47s)

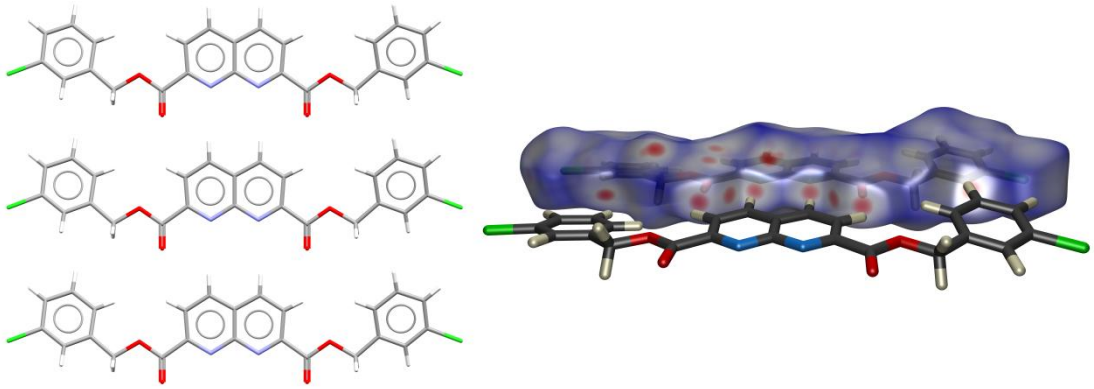

Figure 116 – *bis*-(3-Chlorobenzyl) 1,8-naphthyridine-2,7-dicarboxylate (47s) forms the expected hydrogen bond array at the core, which causes the formation of infinite one-dimensional tapes.

For the 3-chlorobenzyl derivative (**47s**), like its 3-methylbenzyl analogue (**47j**), the pendent arm is once again almost coplanar with the naphthyridine core. The Hirshfeld surface highlights the expected taping contacts but also appears to suggest a couple of additional interactions.

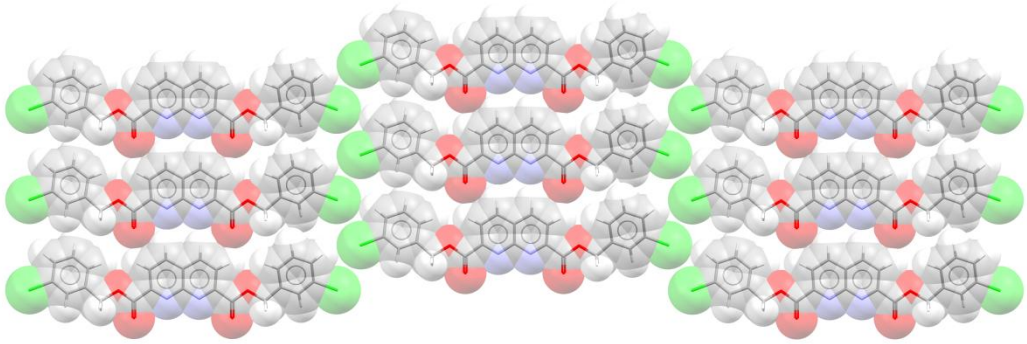

Figure 117 – The packing of the infinite tapes into parallel sheets bares a marked resemblance to the packing observed in the 3-methylbenzyl derivative (74j).

As with the 3-methylbenzyl derivative, the 3-chlorobenzyl derivative forms sheets of tapes where all tapes are aligned parallel to one another. Individual tapes are slightly offset from one another within the plane of the sheet in order to accommodate the chlorine atom which is protruding from the edge of the tape; this interdigitation gives the edges where the tapes meet an appearance of a zip-like interplay.

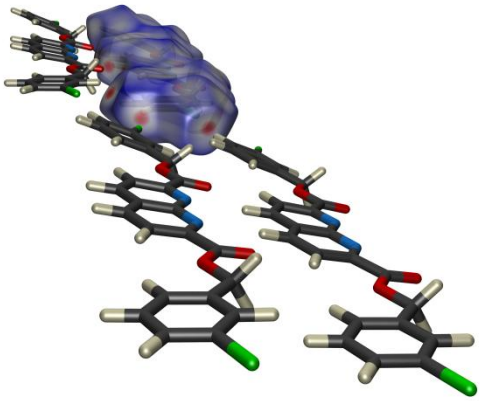

Figure 118 – Examining the Hirshfeld surface highlights a potential inter-sheet C-H···Cl contact.

In Figure 118 the colouring of the Hirshfeld surface suggests that, in this zipper junction between the tapes in a sheet, there is evidence of a C-H···Cl contact which alternates up the tape. This could explain the formation of the motif (C-**H**···**Cl** 2.91Å, **C**-H···**Cl** 3.79 Å (155.0 °)). The Hirshfeld surface does however also suggest a contact which on further investigation appears to be a close contact of two hydrogen atoms, more likely an artefact of the packing. It does however, highlight the importance of applying a degree of chemical common sense to the information visualised on a Hirshfeld surface.

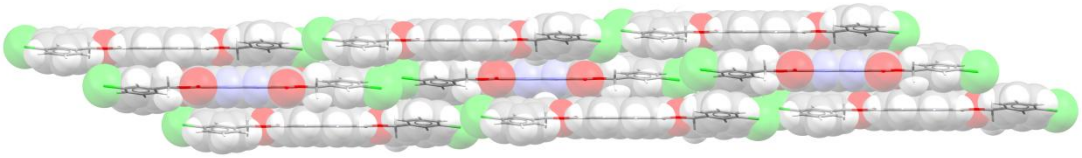

Figure 119 – The sheets pack on top of one another in an anti-parallel arrangement.

The sheets pack on top of one another in alternating anti-parallel arrangement (Figure 119), the cause of which could be the apparent interactions that are seen on the top of the Hirshfeld surface (Figure 120). An inter-sheet contact of this type was observed in the solid-state structure of the 3-methylbenzyl analogue.

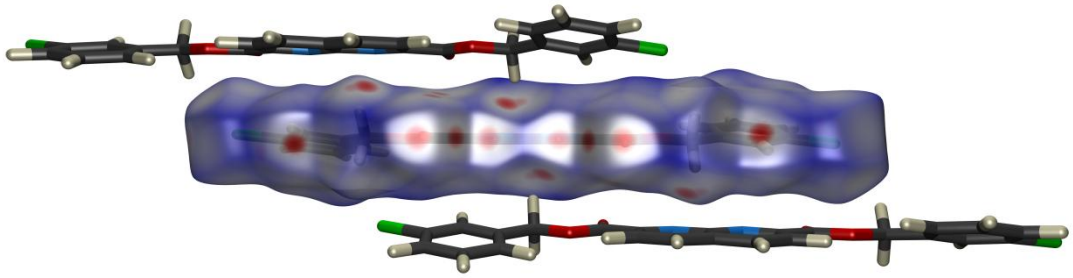

Figure 120 – The Hirshfeld surface highlights additional contacts between molecules in neighbouring stacks similar to those observed in the 3-methylbenzyl derivative.

The contacts are clarified by examining the Hirshfeld surface in Figure 120 which allows identification of this as a contact between the methylene hydrogen atom and one of the naphthyridine nitrogen atoms (C-**H**···**N** 2.67Å, **C**-H···**N** 3.60 Å (157.6 °)). It appears that the molecule in the neighbouring layer is shifted so that it can form a pair of such interactions. This means that, through symmetry, on the opposite face the same interaction appears on the other side of the molecule.

3.3.3.2.3 bis-(4-Chlorobenzyl) 1,8-naphthyridine-2,7-dicarboxylate (47t)

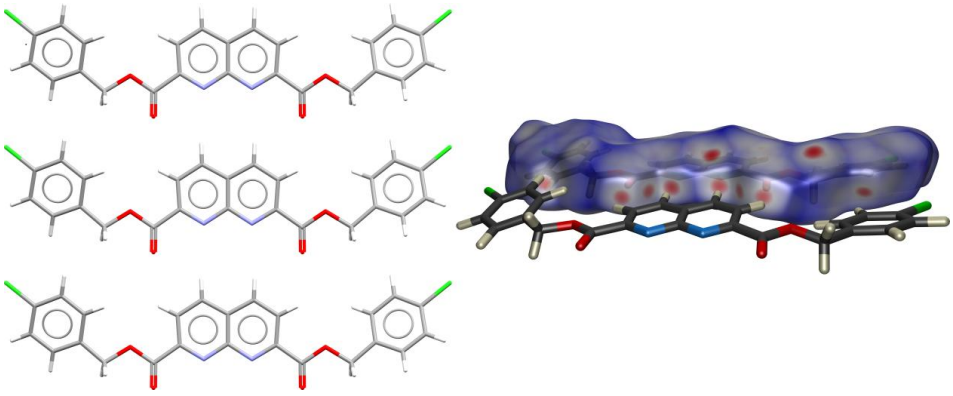

Figure 121 – *bis*-(4-Chlorobenzyl) 1,8-naphthyridine-2,7-dicarboxylate (47t) forms the expected hydrogen bond array at the core, which causes the formation of infinite one-dimensional tapes.

The structure of the 4-chlorobenzyl derivative (**47t**) is of particular interest given the stark change in solubility observed between this and the other regioisomers. In the 4-chloro derivative (**47t**) the benzyl rings lie in the plane of the naphthyridine core although with a twist of 17.6 °. The Hirshfeld surface (Figure 121) shows quite clearly that the hydrogen bonded interactions are the primary interactions, however it highlights the presence of additional inter-stack interactions.

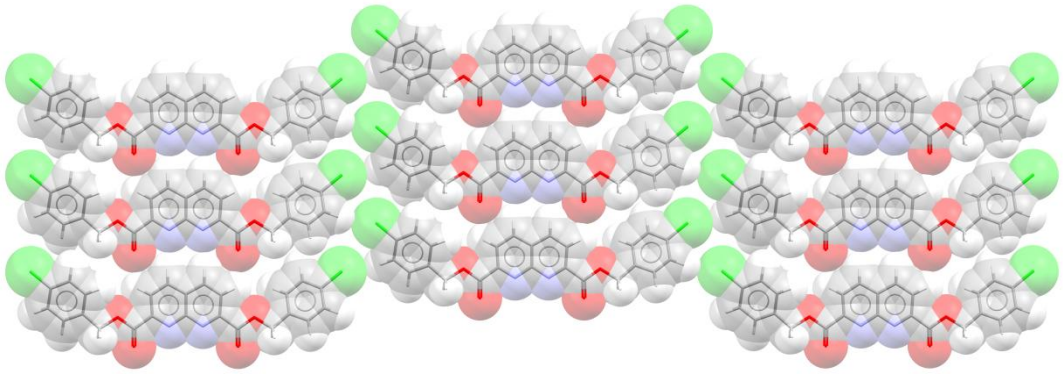

Figure 122 – The 4-chlorobenzyl derivative (47t) forms sheets in which the tapes align in the same direction and, like the methyl group in the 4-methylbenzyl analogue, the pendent chlorine sits interdigitated between the neighbouring molecules.

The tapes form sheets in which neighbouring tapes are aligned in the same direction, with the chlorine substituents interleaving between the gaps in the sheet. Each chlorine atom has a short contact to a hydrogen atom in the 3 position of a neighbouring benzylic ring with length of C-**H**···**Cl** 2.87 Å, **C**-H···**Cl** 3.73 Å (149.8 °).

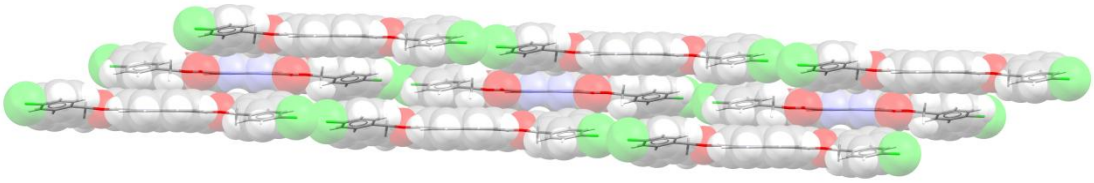

Figure 123 – The sheets stack upon one another in an anti-parallel alignment.

The sheets then stack one upon another with neighbouring sheets sitting in the opposite direction to one another (Figure 123). The sheets have a short inter-layer distance which could be the result of the interaction highlighted in the Hirshfeld surface (Figure 121).

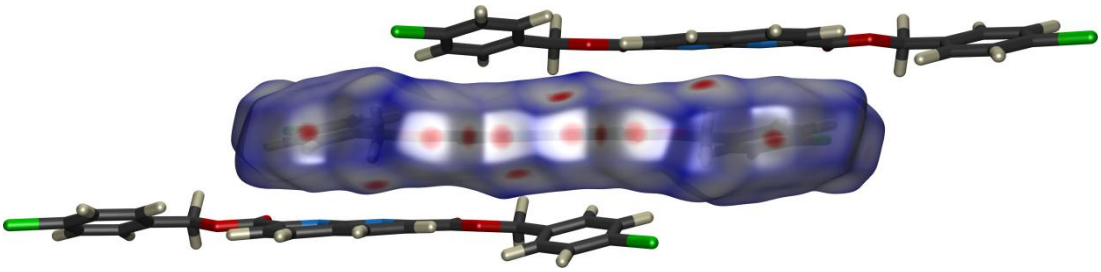

Figure 124 – The Hirshfeld surface highlights the C-H···N contacts that appear to form between the sheets.

This interaction is between the methylene CH_2 and the naphthyridine nitrogen, analogous to that seen in the 3-methyl (**47j**) and 3-chloro-benzyl derivatives (**47t**) (C-**H**···**N** 2.88 Å **C**-H···**N** 3.73 Å (149.8°)). Interestingly a contact of this type was not observed for the analogous 4-methybenzyl derivative (**47k**).

3.3.3.2.4 Comparison of the chlorine substituted benzyl derivatives

Structure	r_1 C?N	θ	r_1' H? N	r_1' C?N	θ'	r_1 H? N	r_2 C?O	ϕ	r_2 H?O	r_2 C?O	ϕ	r_2 H?O
Benzyl	3.48	174.6	2.50	n/a	n/a	n/a	3.10	121.9	2.47	n/a	n/a	n/a
2 Cl Bn	3.50	174.5	2.55	n/a	n/a	n/a	3.10	124.1	2.46	n/a	n/a	n/a
3 Cl Bn	3.68	175.4	2.73	n/a	n/a	n/a	3.22	122.6	2.60	n/a	n/a	n/a
4 Cl Bn	3.65	175.0	2.70	n/a	n/a	n/a	3.24	122.9	2.62	n/a	n/a	n/a
2 Me Bn	3.49	173.4	2.54	n/a	n/a	n/a	3.12	124.7	2.48	n/a	n/a	n/a
3 Me Bn	3.70	173.8	2.72	n/a	n/a	n/a	3.25	121.2	2.64	n/a	n/a	n/a
4 Me Bn	3.50	175.0	2.56	n/a	n/a	n/a	3.09	123.3	2.47	n/a	n/a	n/a

Table 6 - The hydrogen bonding array contact distances for the chlorine substituted benzyl derivatives.

The chlorine substituted benzyl derivatives all form the expected hydrogen bonding arrays, the contact distances for which are shown in Table 6. When compared to the basic benzyl derivative (**47h**) only the 2-chlorobenzyl derivative has a comparable set of contact distances. The contact distances for the 3-chlorobenzyl (**47s**) and 4-chlorobenzyl (**47t**) derivatives are elongated. As mentioned previously there has been a body of work on the similarity of chloro and methyl substituents, in a phenomenon known as chloro-methyl exchange. When comparing the contact distances for chlorine and methyl substituted benzyl 1,8-naphthyridne dicarboxylate analogues it is seen that the contact distances and the structures are very similar except in the 4-substituted examples. In this case the 4-chlorobenzyl derivative (**47t**) is seen to have an elongated set of hydrogen bond array contact distances, as well as additional inter-sheet contacts.

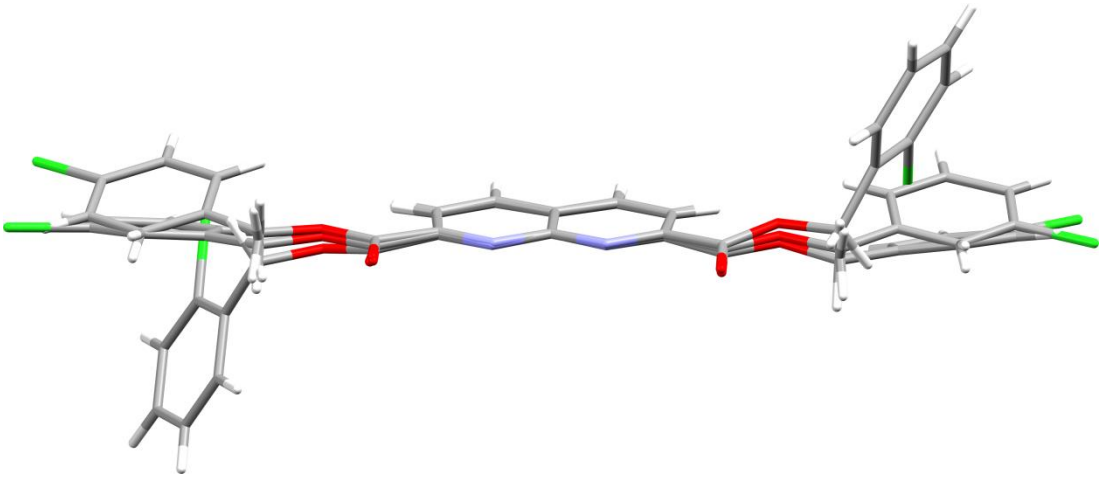

Figure 125 - Shows the structures of the chlorobenzyl derivative overlaid.

By studying the structural overlay of the 3-chlorobenzyl derivatives it is possible to see that only the 2-chlorobenzyl derivative is bent significantly out of the plane of the naphthyridine core. Once again it is assumed that this is due to the steric clashes that the chlorine atoms would otherwise undergo. The chlorine substituted benzyl derivatives behave more like their methylbenzyl analogues than the corresponding fluorobenzyl analogues.

3.3.3.3 Bromine substitution

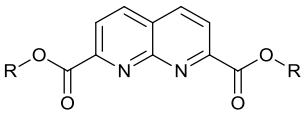

47

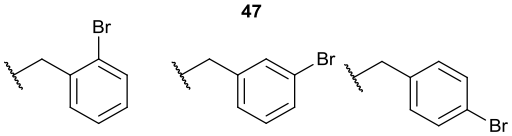

47u **47v** **47w**

All three regioisomers of the bromine-substituted benzyl ester have yielded crystals of suitable quality for single crystal X-ray diffraction. Given the increase in van der Waal radius from chlorine to bromine it was of interest to determine how this would affect the solid-state structure.

3.3.3.3.1 bis-(2-Bromobenzyl) 1,8-naphthyridine-2,7-dicarboxylate (47u)

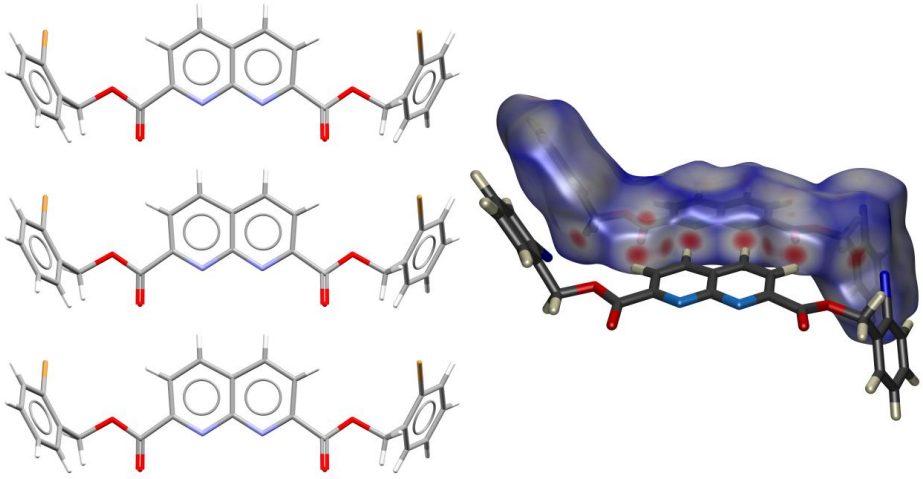

Figure 126 – *bis*-(2-Bromobenzyl) 1,8-naphthyridine-2,7-dicarboxylate (47u) forms the expected hydrogen bond array at the core, which causes the formation of infinite one-dimensional tapes.

The 2-bromobenzyl derivative (**47u**), like its chlorine (**47r**) and methyl substituted (**47i**) analogues, has the pendent substituent bent out of the plane of the naphthyridine core. The expected taping interaction is present and the Hirshfeld surface (Figure 126) indicates additional potential contacts.

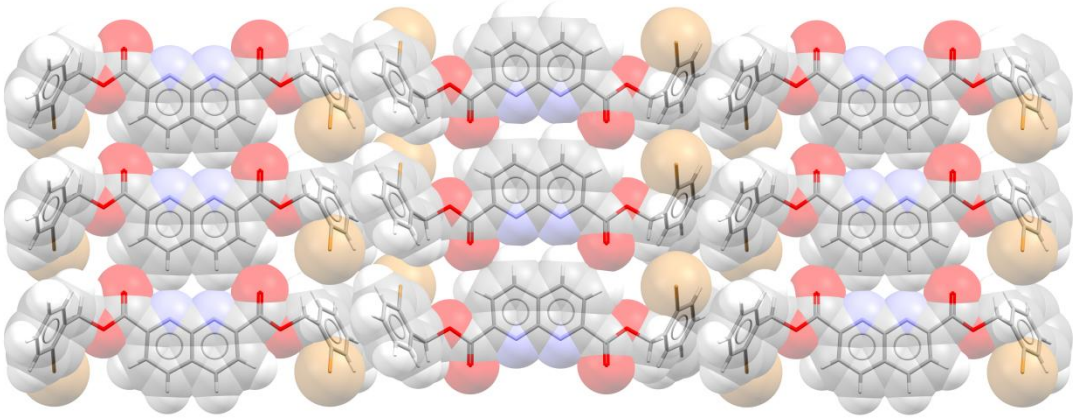

Figure 127 – The tapes align into step-like anti-parallel sheets which have a face to face alignment of the pendent benzyl groups.

The arrangement of the tapes into sheets (Figure 127) is again influenced by the benzyl pendent ring being twisted out of the plane of the naphthyridine core. The tapes adopt an anti-parallel arrangement and, as has been observed for both the methyl and chloro analogues, it appears that the pendent rings arrange themselves in such a way that they might be involved in a face-to-face interaction with one of the molecules in the neighbouring tapes.

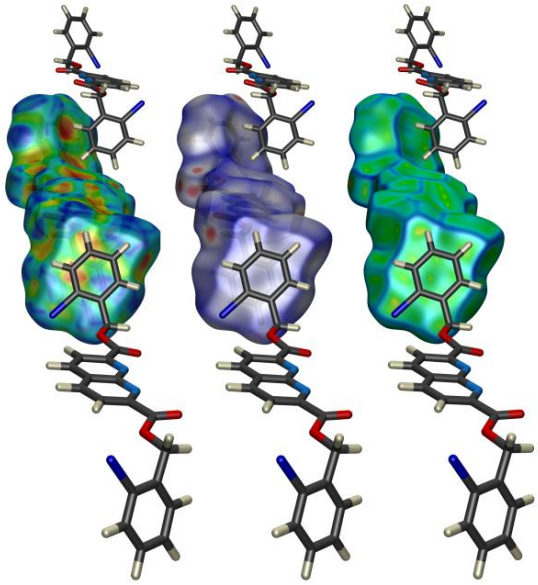

Figure 128 – Examining different surface colourings of the Hirshfeld surface leads to the suggestion that these pendent benzyl rings maybe subject to a π···π interaction. (left = shape index, centre = $d_{(norm)}$ and right =curvedness).

Viewing the Hirshfeld surface of the face-to-face arrangement (Figure 128) again produces little in terms of colouring on the $d_{(norm)}$ surface, however it does yield some potentially useful information in the shape index colouring system, the pattern of which is not unlike that seen for systems that undergo face to face π···π interactions when analysed with Hirshfeld surfaces. The two ring systems are held at a distance of 3.45 Å from one another. It is also worth noting the apparent close contact, between one of the hydrogen atoms *meta* to the bromine and a pendent ring, on the sheet below.

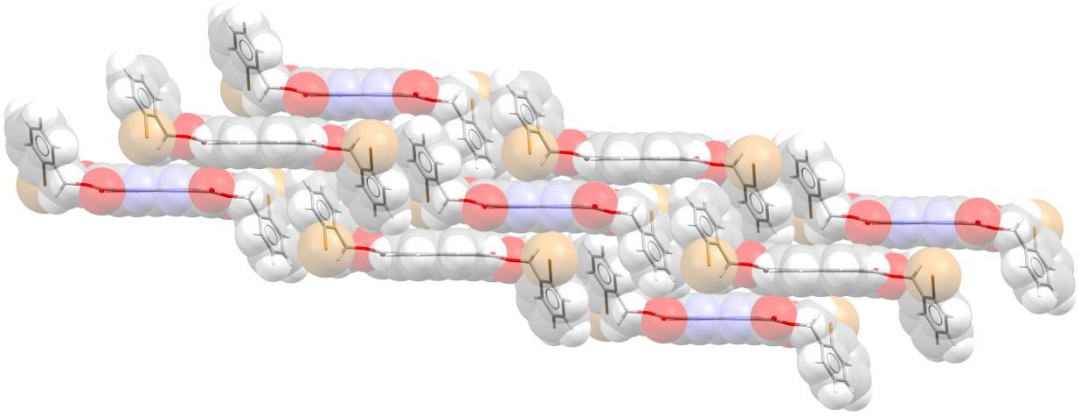

Figure 129 – The sheets pack in an anti-parallel fashion like that observed in the 2-chlorobenzyl derivative (47r).

When the sheets stack together they align in anti-parallel arrays with the step like sheets forming overlapping edges (Figure 129).

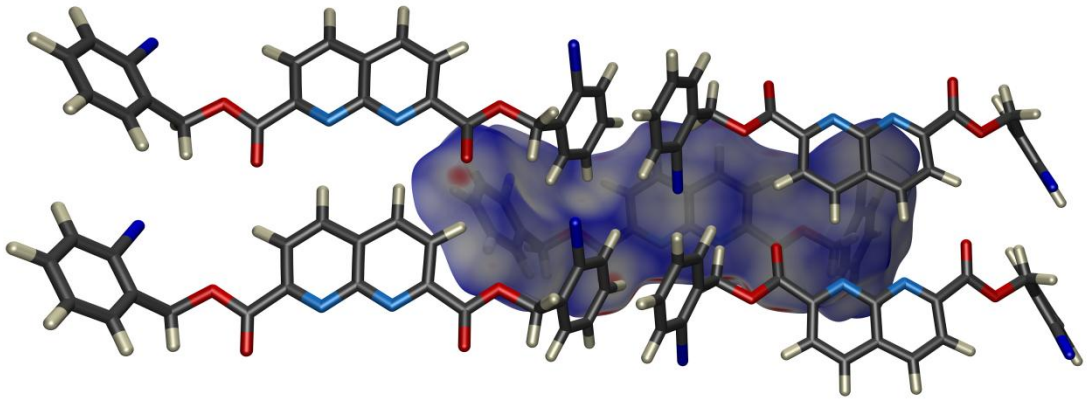

Figure 130 – The Hirshfeld surface highlights two close contacts indicative of an intermolecular interaction, one C-H···π and one C-H···O=C.

As noted above it appears that one of the hydrogen atoms *meta* to the bromine substituent on the pendent ring seems to be pressing into the back of a neighbouring benzyl ring from the sheet below. This has a contact distance of (C-**H**···**π** 2.84 Å, **C**-H···**π** 3.57 Å (133.3 °). In addition to this contact (which only shows on the shape index Hirshfeld surface) there is another contact which shows up more clearly on the $d_{(norm)}$ surface. This contact appears to be between the carbonyl oxygen and the other hydrogen atom *meta* to the bromine substituent. While this contact seems odd it has a contact distance well within the limits of a weak hydrogen bond (C-**H**···**O**=C 2.62 Å, **C**-H···**O**=C 3.34 Å (132.3°)).

3.3.3.3.2 bis-(3-Bromobenzyl) 1,8-naphthyridine-2,7-dicarboxylate (47v)

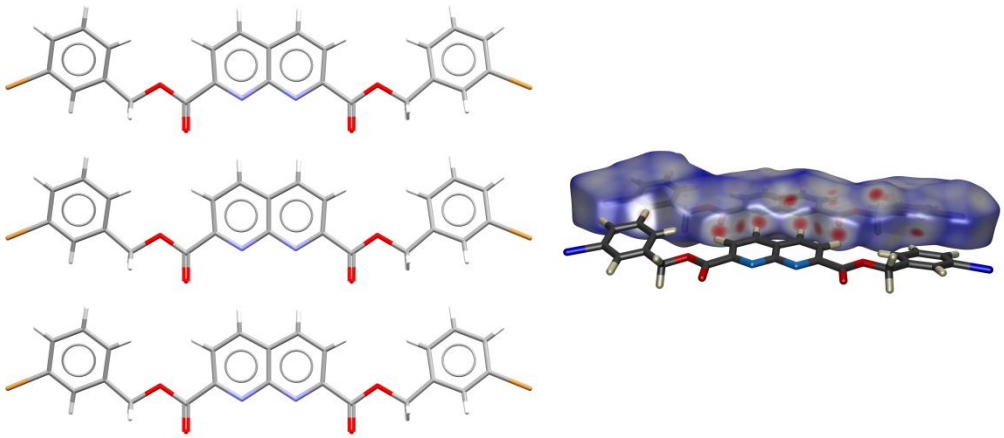

Figure 131 – *bis*-(3-Bromobenzyl) 1,8-naphthyridine-2,7-dicarboxylate (47v) forms the expected hydrogen bond array at the core, which causes the formation of infinite one-dimensional tapes.

For the 3-bromobenzyl derivative (**47v**) the pendent benzyl ring is once again in the plane of the naphthyridine core in a manner similar to that seen for its chlorine (**47s**) and methyl analogues (**47j**) (Figure 131).

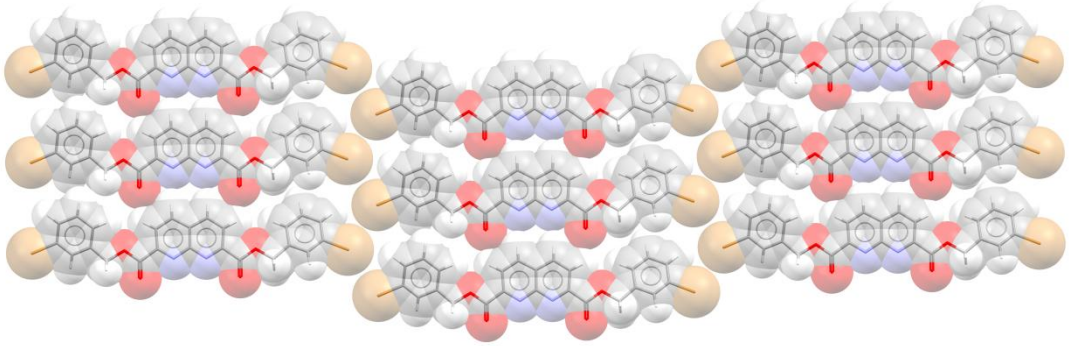

Figure 132 – Like the 3-chlorobenzyl (47s) and 3-methyl benzyl (47j) derivatives the 3-bromobenzyl derivative (47v) forms sheets of tapes aligned in a parallel arrangement. Similarly the bromine group is interleaved between neighbouring tapes.

Within a sheet neighbouring tapes adopt a parallel arrangement with respect to one another and the taping motif accommodates the bulky bromine substituent by offsetting and interleaving the neighbouring tapes (Figure 132).

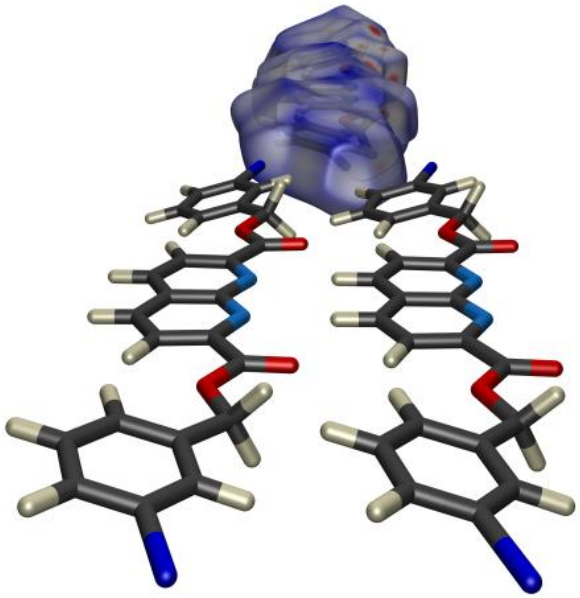

Figure 133 – Unlike the 3-chlorobenzyl derivative (47s) in this case there is no evidence shown on the Hirshfeld surface of intermolecular interactions between neighbouring tapes.

In contrast with the chlorobenzyl analogue (**47s**), the Hirshfeld surface shows no sign of any form of interaction between the bromine atom and the hydrogen atoms on the pendent benzyl group from the neighbouring tapes (Figure 133).

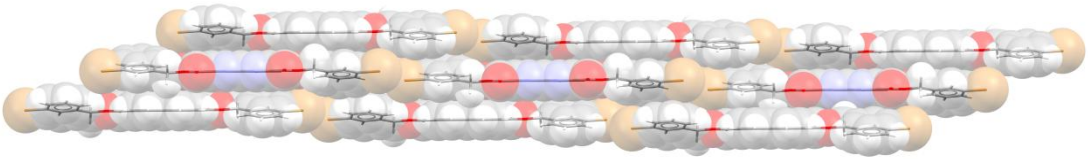

Figure 134 – The sheets pack on top of one another in an anti-parallel arrangement.

The packing of the sheets of tapes occurs so that the sheets are offset and in an anti-parallel arrangement (Figure 134). It is noticeable that the inter-sheet distance of 3.10 Å is quite short.

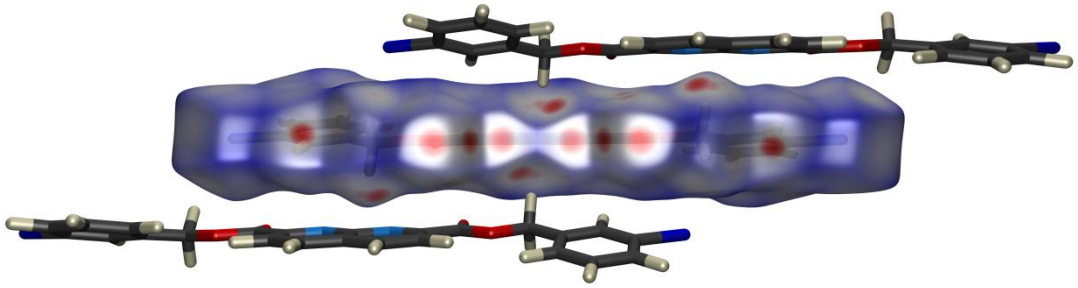

Figure 135 - The Hirshfeld surface highlights additional contacts between molecules in neighbouring stacks similar to those observed in the 3-chlorobenzyl derivative (47s).

Figure 135 illustrates that the close packing of the neighbouring sheets may be the result of interactions between neighbouring tapes. The colouring of the Hirshfeld surface suggests that there may be dimeric interactions between the methylene C-H and naphthyridine nitrogen atoms (C-**H**···**N** 2.65 Å, **C**-H···**N** 3.55 Å (154.7 °)). It is very difficult to confirm the presence of these interactions in solution and the effect they have on crystallisation but it is an interesting feature of a number of compounds in which the molecules adopt an almost completely planar conformation.

3.3.3.3.3 bis-(4-Bromobenzyl) 1,8-naphthyridine-2,7-dicarboxylate (47w)

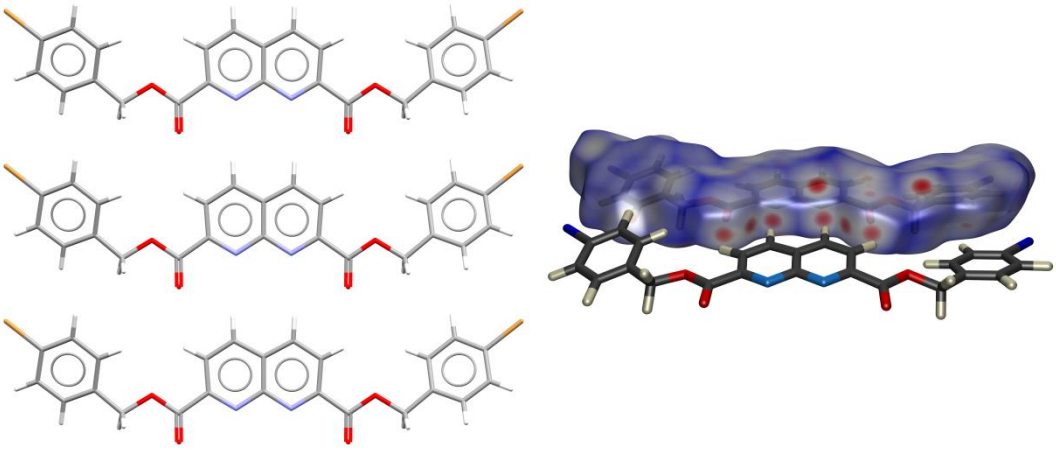

Figure 136 –*bis*-(4-Bromobenzyl) 1,8-naphthyridine-2,7-dicarboxylate (47w) forms the expected hydrogen bond array at the core, which causes the formation of infinite one-dimensional tapes. The Hirshfeld surface like its chlorobenzyl analogue (47t) shows additional inter-sheet contacts.

The 4-bromobenzyl derivative adopts a structure that appears to be isostructural to that observed in the 4-chlorobenzyl derivative (47k). As expected the molecules form infinite one-dimensional tapes with the expected C=O···H-C and N···H-C contacts being observed on the Hirshfeld surface, along with some additional contacts being inferred on the top surface of the molecule (Figure 136).

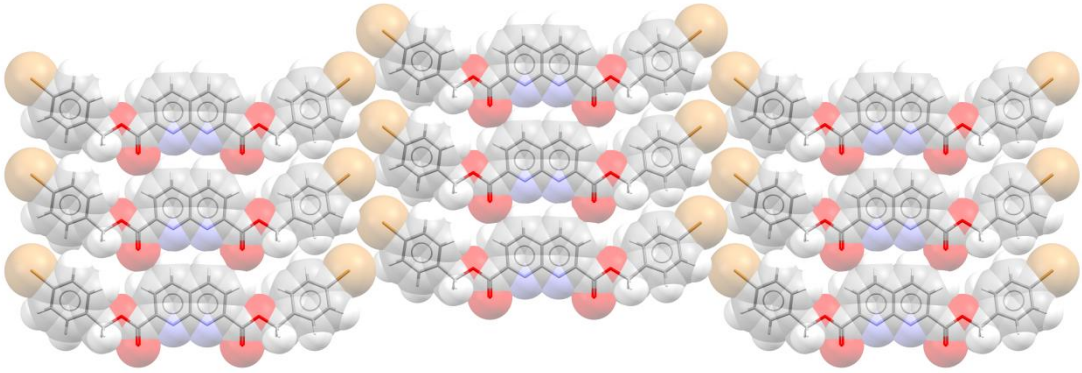

Figure 137 –The 4-bromobenzyl derivative (47w) forms sheets in which the tapes align in the same direction and, like methyl group in the 4-chlorobenzyl analogue, the pendent bromine sits interdigitated between the neighbouring molecules.

The tape assemblies then arrange themselves into offset parallel sheets (Figure 137), with the bulky bromine substituent being placed so it may interdigitate within the gap on the edge of the neighbouring tape.

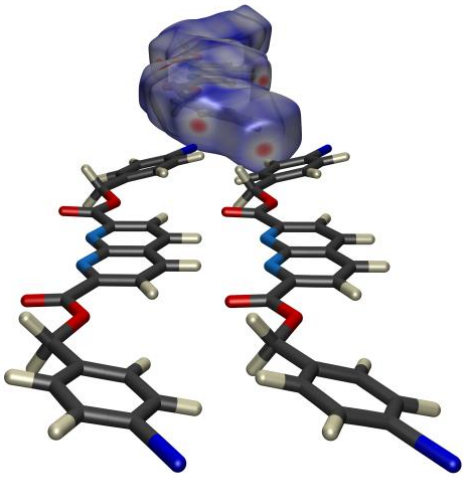

Figure 138 – The 4-bromobenzyl derivative shows some evidence of inter-sheet interactions, unlike its 3-bromobenzyl derivative (47v).

Examining the Hirshfeld surface (Figure 138) shows that, in contrast to the 3-bromobenzyl derivative, there does appear to be a close contact between the bromine and the hydrogen in the *ortho*-position to the bromine of one of the molecules in the neighbouring tape (C-**H**···**Br** 2.98 Å, **C**-H···**Br** 3.82 Å (147.5 °)).

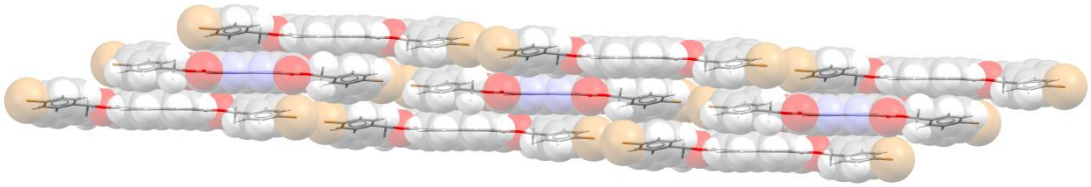

Figure 139 – The sheets pack on one another in an anti-parallel arrangement.

The sheets of tapes then stack upon one another in an anti-parallel fashion (Figure 139) with the tapes sat in an offset alignment relative to one another.

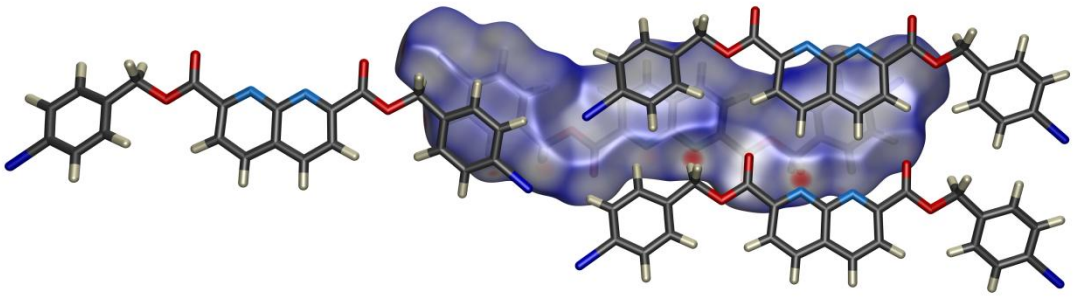

Figure 140 – The Hirshfeld surface shows that the pendent side arms align over one another and also highlights the inter-sheet interaction seen in the 4-chlorobenzyl derivative (47t).

Figure 140 shows the molecules sat in the layer above the Hirshfeld surface with the most obvious features of the surface, the red spots, discussed below. It is however, also worth noting that the pendent arm on the left of the picture overlaps with the neighbouring molecules pendent arm in an arrangement which places the bromine in a top-and-tail alignment. The third molecule in Figure 140 illustrates the location of the pendent ring which sits over the naphthyridine core of the molecule in the sheet below. However, with an inter-ring distance of 3.98 Å it is not clear whether this involves a π ⋯ π interaction or is simply a close-packing arrangement.

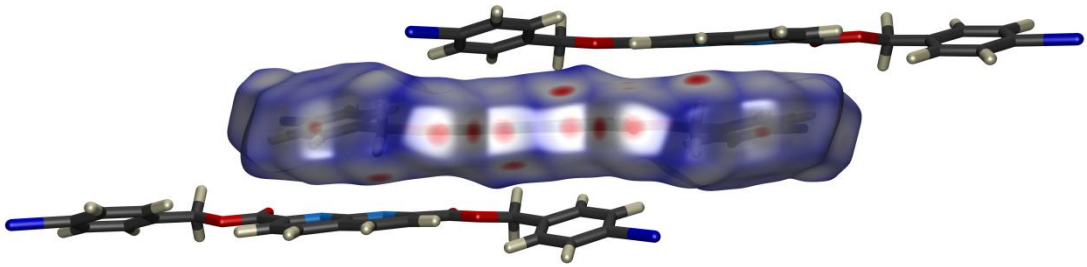

Figure 141 – In analogy to the 4-chlorobenzyl derivative (47t) the Hirshfeld surface for 4-bromobenzyl derivative (47w) appears to indicate inter-sheet C-H⋯N interactions.

The very obvious red spots highlighted in Figure 140 are examined in Figure 141. Again, as for the 4-chlorobenzyl derivative, the interactions appear to involve the methylene C-H and the naphthyridine nitrogen atoms (C-**H**⋯**N** 2.61 Å, **C**-H⋯**N** 3.55 Å (158.9 °)).

3.3.3.3.4 Comparison of the bromine substituted benzyl derivatives

Structure	r_1 C?N	θ	r_1' H? N	r_1' C?N	θ'	r_1 H? N	r_2 C?O	ϕ	r_2 H?O	r_2 C?O	ϕ	r_2 H?O
Benzyl	3.48	174.6	2.50	n/a	n/a	n/a	3.10	121.9	2.47	n/a	n/a	n/a
2 Cl Bn	3.50	174.5	2.55	n/a	n/a	n/a	3.10	124.1	2.46	n/a	n/a	n/a
3 Cl Bn	3.68	175.4	2.73	n/a	n/a	n/a	3.22	122.6	2.60	n/a	n/a	n/a
4 Cl Bn	3.65	175.0	2.70	n/a	n/a	n/a	3.24	122.9	2.62	n/a	n/a	n/a
2 Br Bn	3.54	174.1	2.59	n/a	n/a	n/a	3.12	123.5	2.49	n/a	n/a	n/a
3 Br Bn	3.61	174.7	2.68	n/a	n/a	n/a	3.16	123.9	2.55	n/a	n/a	n/a
4 Br Bn	3.64	174.4	2.70	n/a	n/a	n/a	3.20	122.2	2.59	n/a	n/a	n/a

Table 7 - The hydrogen bonding array contact distances for the bromine substituted benzyl derivatives.

The bromobenzyl derivatives appear to assume isostructural solid-state architectures to those seen in the chlorobenzyl derivatives.

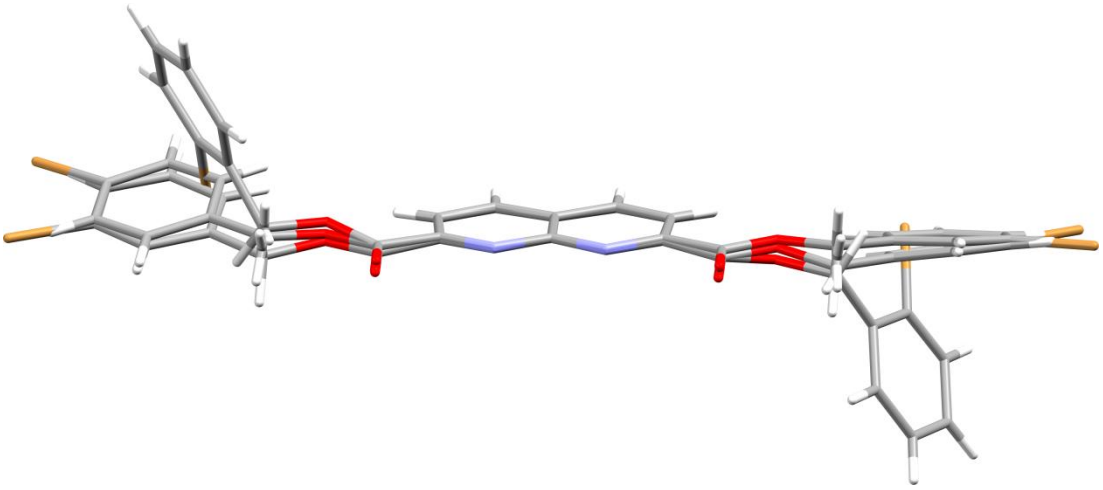

Figure 142 – Shows the structures of the bromobenzyl derivatives overlaid.

By studying the structural overlay of the 3 bromobenzyl derivatives it is possible to see that they behave more like the methyl and chlorobenzyl derivatives than the fluorobenzyl derivative. Indeed it would appear that the bromobenzyl derivatives are isostructural to the chlorobenzyl derivatives. As in the methyl and chloro substituted case the pendent benzyl ring for the 2-bromobenzyl derivative is bent significantly out of the plane of the naphthyridine core. Once again it is assumed that this is due to the steric clashes that the bromine would otherwise undergo.

3.3.3.4 Overall comparison of the halogen substituted benzyl derivatives

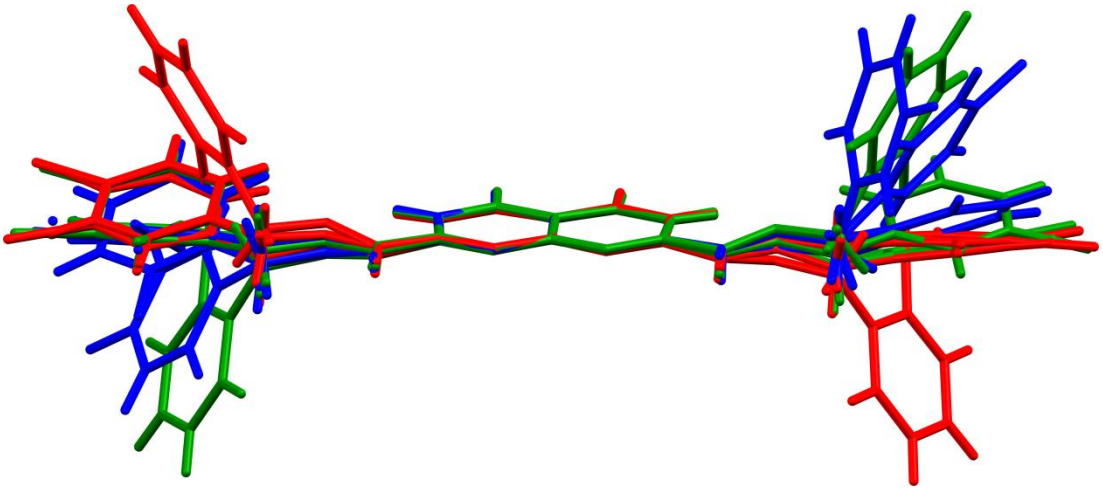

Figure 143 – With all the halogen substituted benzyl derivative overlaid the structural similarities and differences are highlighted quite starkly (F=blue, Cl=green and Br= red).

The overlay of the different halogen substituted benzyl derivatives shows, quite starkly, the differences in structure adopted by the different derivatives studied. It

is interesting to note that the chloro- and bromo- derivatives are very similar in structure, with the exception of the 2-substitued derivative in which the structures appear to be in different absolute conformations. The fluoro-substituted derivatives appear to be anomalous in the structures they form but the reasoning behind this is ambiguous. It would be of interest to study further multi halogen substitution patterns, in analogy to Orton[195] and Cheesewright's[196] work in the pyridine-2,6-dicarboxylates, in order to gain further insight into the effect that the different halogen species have on the packing of these molecules.

3.3.4 *bis*-(4-Methoxybenzyl)-1,8-naphthyridine-2,7-dicarboxylate (47x)

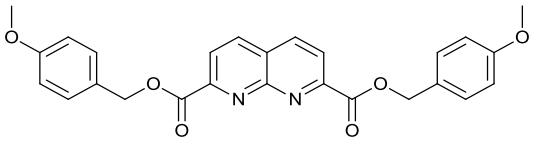

47x

In previous work on the pyridine-2,6-dicarboxylates and dicarboxamides, the *N*-alkoxybenzyl derivatives showed solid-state behaviour which was influenced by C-H···O interactions involving the methoxy- substituent. *bis*-(4-Methoxybenzyl) 1,8-naphthyridine-2,7-dicarboxylate (**47x**) was synthesised in order to study if it adopted a similar solid-state architecture to its pyridine analogue.

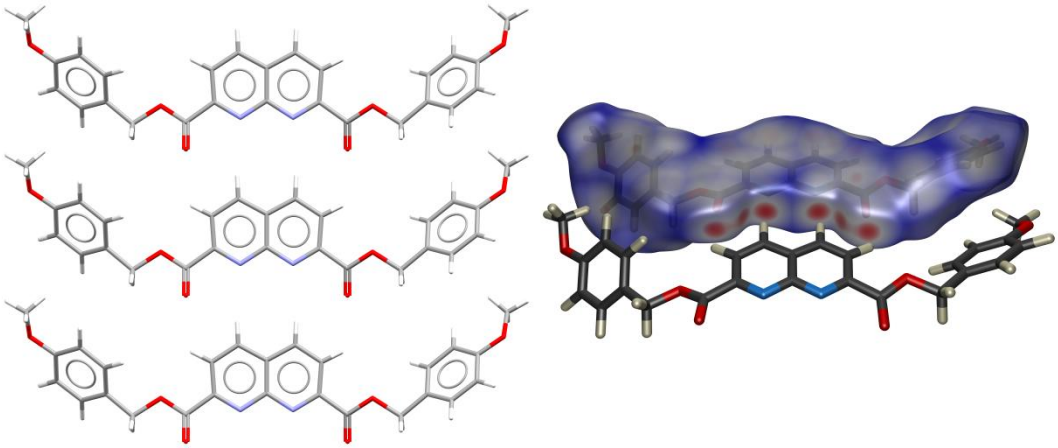

Figure 144 – *bis*-(4-Methoxybenzyl)-1,8-naphthyridine-2,7-dicarboxylate (47x) forms the expect hydrogen bonding array giving rise to infinite one-dimensional tapes.

The 4-methoxybenzyl derivative forms the expected taping array with the taping contacts shown to be clearly present (Figure 144). The pendent side arms sit in the plane of the naphthyridine core with the ring twisted slightly out of the axis of the

central core, and with the methoxy substituent pointing towards the nearest neighbouring molecule within the one-dimensional tape.

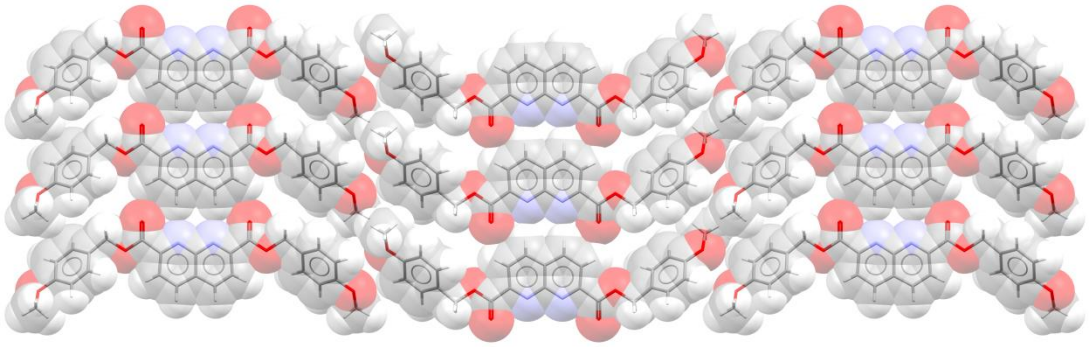

Figure 145 – The tapes form into sheets aligned in an anti-parallel fashion.

The infinite one-dimensional tapes arrange in an anti-parallel fashion, with a slight step in the sheet when viewed from a perpendicular angle.

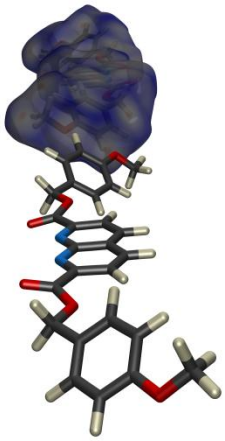

Figure 146 – Weak interactions between the methoxy oxygen and the hydrogen *ortho* to the substituent group in the neighbouring molecule.

The Hirshfeld surface shows very few major intermolecular interactions within this structure (Figure 146). However, there does appear to be evidence for a weak interaction between the methoxy oxygen and the hydrogen *ortho* to the substituent group in the lateral neighbouring molecule within a sheet of tapes (**O**···**H**-C 2.74 Å, **O**···H-**C** 3.49 Å (136.7 °)).

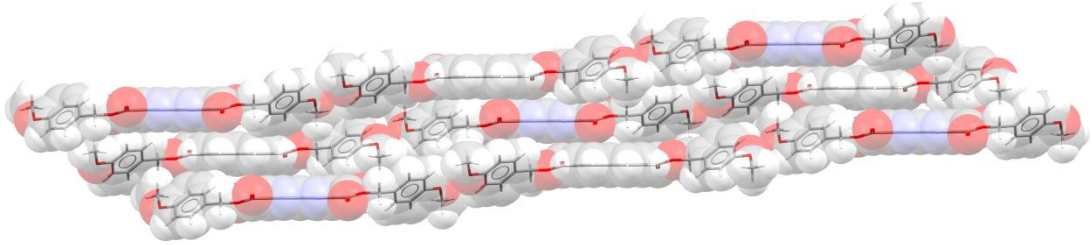

Figure 147 – The sheets stack upon one another to form stacks which are aligned in an anti-parallel fashion.

The sheets of infinite one-dimensional tapes arrange themselves into anti-parallel stacks, which appear to have little interaction between the sheets. The lack of additional interactions beyond the hydrogen bonding array is somewhat surprising in this example; it may be that the weak interaction exerted by the methoxy oxygen is sufficient to lock the conformation in such a way that close packing is the key packing factor.

3.3.5 *bis*-4-(Nitrobenzyl) 1,8-naphthyridine-2,7-dicarboxylate (47y)

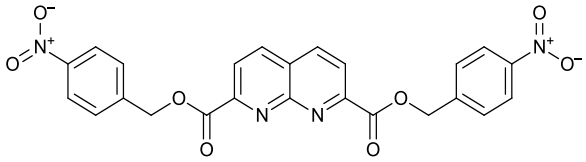

47y

4-Nitrobenzyl prydine-2,6-dicarboxylate was originally synthesised in order to be reduced to the amine however, while attempts to synthesise the amine derivative were unsuccessful the structure of the 4-nitrobenzyl derivative proved to be quite interesting. Accordingly the 1,8-naphthyridine analogue was synthesised in the present study.

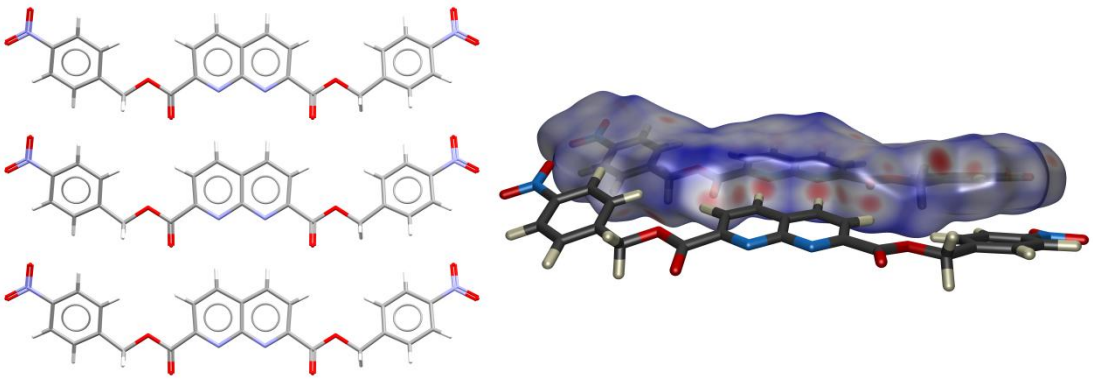

Figure 148 – *bis*-4-(Nitrobenzyl) 1,8-naphthyridine-2,7-dicarboxylate (47y) forms the expected hydrogen bonding array. It also shows evidence of other interactions on the Hirshfeld surface.

Once again the expected hydrogen bonding array was formed with the pendent rings sitting in the plane to the naphthyridine core (Figure 148). However, unlike the methoxybenzyl derivative (**47x**) there is evidence of additional interactions which are likely to influence the packing arrangement of the tapes.

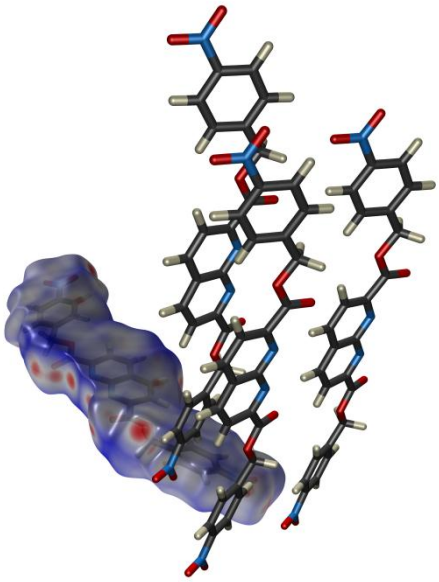

Figure 149 – The Hirshfeld surface shows weak interactions at the periphery of the molecule which may be responsible for the formation of the herringbone motif observed.

Looking at the Hirshfeld surface of the molecule around the pendent arm it is clear to see that there appears to be a close contact between one of the nitro oxygen atoms and the nitrogen atom of a neighbouring nitro group (Figure 149). This behaviour should come as no surprise given the dipolar nature of the nitro group which, given the strength of electrostatic interactions, could play a significant role in controlling the packing of this structure.

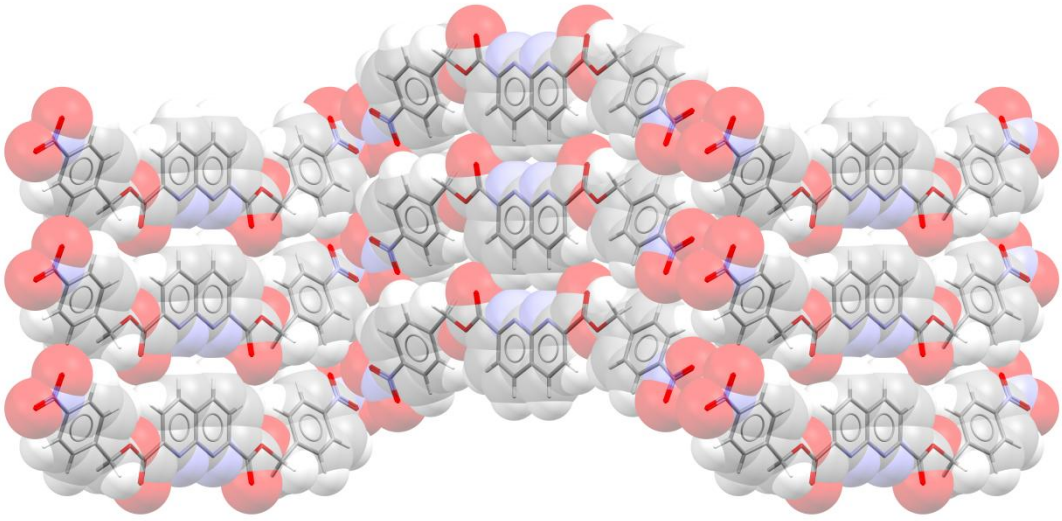

Figure 150 – The formation of tapes into sheets occurs with the sheet exhibiting a herringbone motif.

This close contact would appear to be the factor that causes this system to adopt a herringbone conformation when forming sheets of tapes (Figure 150).

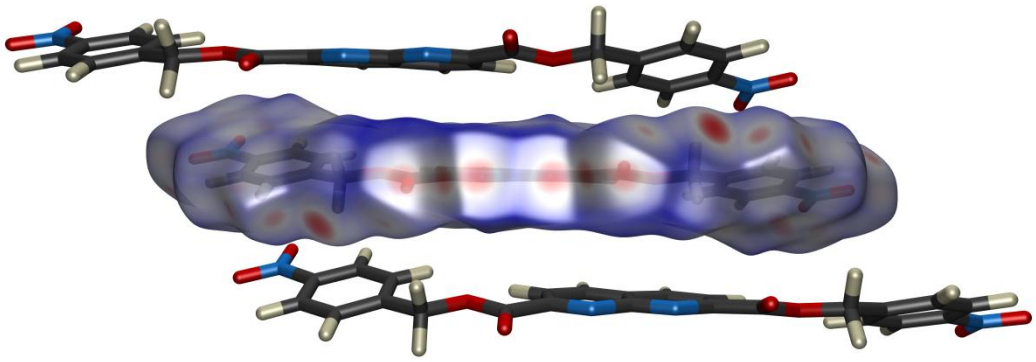

Figure 151 – This Hirshfeld surface shows the formation of inter-sheet contacts involving the nitro group's oxygen atom and both the methylene C-H and one of the benzyl hydrogen atoms.

The Hirshfeld surface shown in Figure 151 suggests that the nitro group is also involved in a contact with the methylene C-H group of a neighbouring molecule (C-**H**···**O**=N 2.40 Å, **C**-H···**O**=N 3.25 Å, (142.9 °)) as well as a contact to one of the benzyl hydrogen atoms (C-**H**···**O**=N 2.67 Å, **C**-H···**O**=N 3.43 Å, (137.6 °)).These interactions seem to be the dominating interactions in the stacking of the tapes.

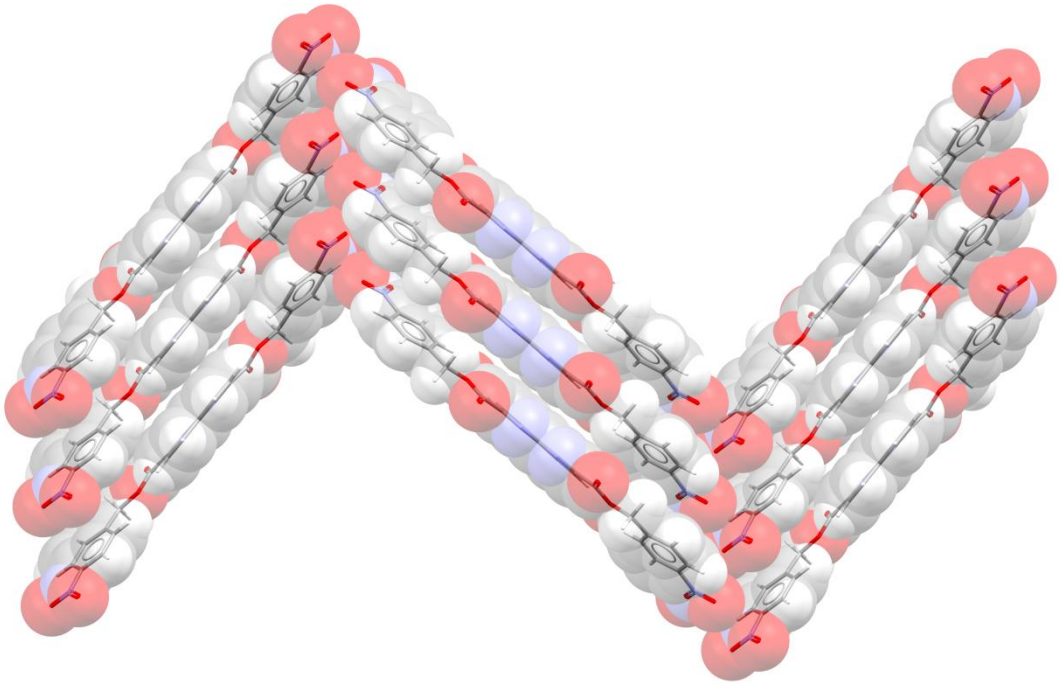

Figure 152 – The sheets pack into stacks in which neighbouring molecules are in a parallel arrangement.

The combination of the herringbone interaction and the stacking interaction leads us to the packing shown in Figure 152. Given the interactions observed in the 4-nitrobenzyl derivative it would clearly be of interest to explore the behaviour of the 3- and 4-nitrobenzyl derivatives.

3.4 Investigation of the Effects of Introducing Alternate Pendent Side Arms

3.4.1 *bis*-(Pyridylmethyl)-1,8-naphthyridine-2,7-dicarboxylates

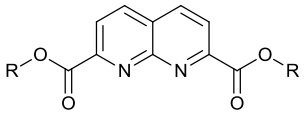

47

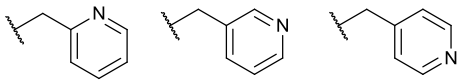

47z 47aa 47bb

Molecules with pendent pyridyl groups have shown interesting solid-state behaviour in the pyridine dicarboxylates and dicarboxamides. This is the result of the introduction of a strong hydrogen bond acceptor on the pendent ring. Although all three structural isomers were synthesised, a structural study of only one isomer has been completed. In all cases the materials formed extremely fine needles during crystallisation which proved to be very weakly diffracting.

3.4.1.1 *bis*-(2-Pyridylmethyl)-1,8-naphthyridine-2,7-dicarboxylate (47z)

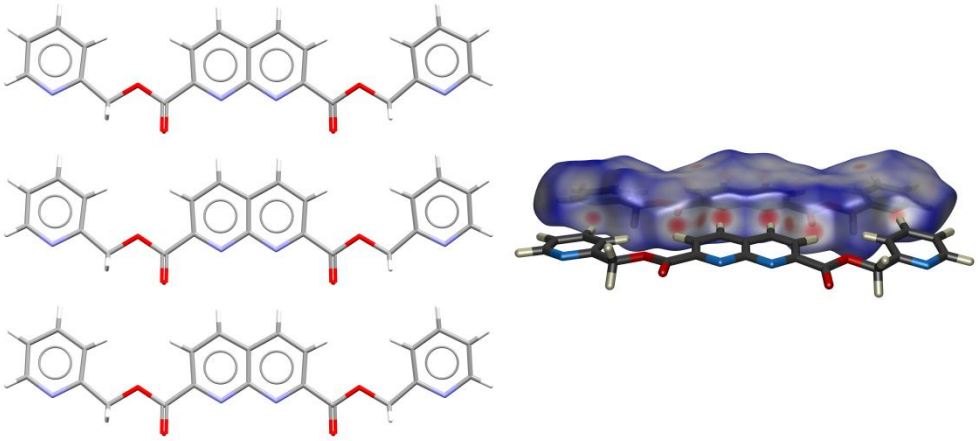

Figure 153 – Illustrates the taping behaviour of *bis*-(2-pyridyl)-1,8-naphthyridine-2,7-dicarboxylate. The Hirshfeld surface shows the normal hydrogen bonding array but also highlights an additional interaction from the pendent pyridine nitrogen to the hydrogen *gamma* to the pendent pyridine nitrogen.

The packing of the (2-pyridyl) 1,8-naphthyridine-2,7-dicarboxylate, (Figure 153) reveals that this compound adopts the usual taping motif, with the hydrogen bonding interactions quite clearly indicated on the Hirshfeld surface. There is however, another interaction that is highlighted, between the pendent pyridine

nitrogen and the *beta* hydrogen on the pendent pyridine nitrogen from the neighbouring molecule within a tape (Figure 153).

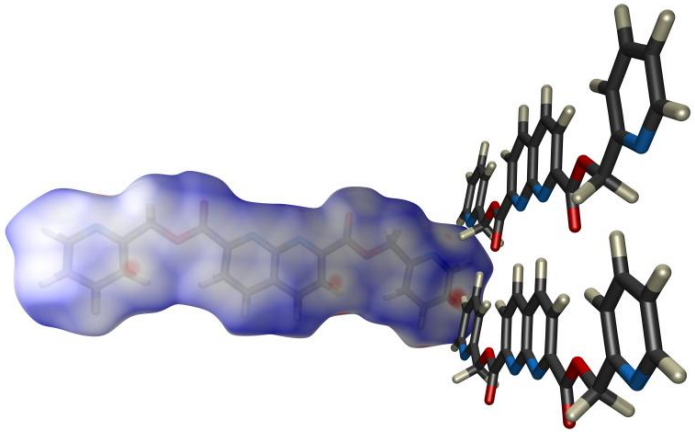

Figure 154 – Examination of the Hirshfeld surface shows that there appears to be an interaction from the hydrogen *ortho* to the pendent pyridine nitrogen atom to the π-face of the pyridine ring in a neighbouring tape.

The Hirshfeld surface also indicates a close interaction from the *alpha* hydrogen atom on the pendent pyridine ring to the top of the pyridine ring of a molecule in a neighbouring tape, although it appears to align over one of the carbon atoms in the ring, rather than directly over the centre of the ring system.

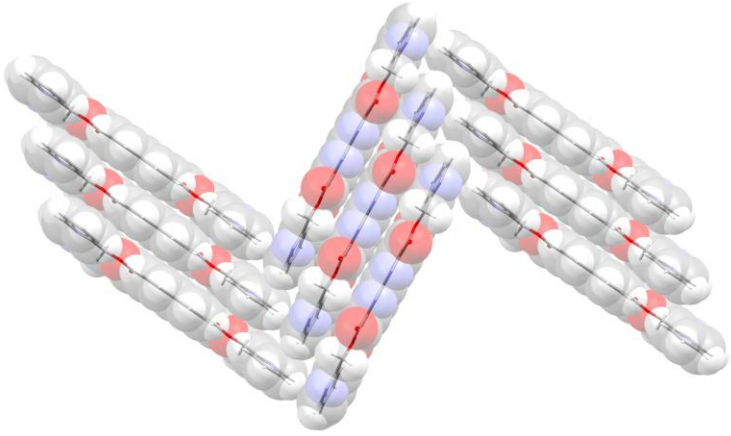

Figure 155 – The interaction shown in Figure 154 leads to the herringboned packing of tape shown.

The contact suggested by the Hirshfeld surface and discussed above would appear to have a profound effect on the packing of the taped molecules. Instead of the neat flat parallel sheets this architecture arranges itself into a herringbone array. Similar behaviour is seen for the pyridine analogues.

3.4.2 *bis*-(Thiophenylmethyl) 1,8-naphthyridine-2,7-dicarboxylates

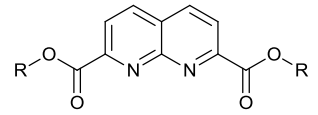

47

47cc 47dd

Although both of these materials have been synthesised it has not proved possible to obtain crystals suitable for X-ray structural studies. This might be due in part to competing interactions ensuring that there is no particularly stable conformation for these systems as highlighted in work by Orton.[195] Orton described the disorder of the thiophene pendent rings in the pyridine analogues.

3.4.3 Cyclic Non-Aromatic Esters

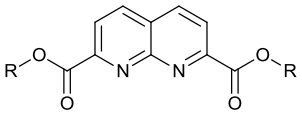

47

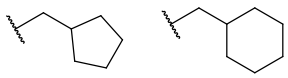

47ff 47gg

Cyclic non aromatic compounds were synthesised in the hope that it might cast some light on the effect that aromaticity has on the solid-state packing of the molecules studied thus far. The non aromatic ring does however present a different set of problems in that they are by nature far more bulky with the additional hydrogens present due to the sp^3 hybridisation of the rings.

3.4.3.1 *bis*-(Cyclopentylmethyl) 1,8-naphthyridine-2,7-dicarboxylate (47ff)

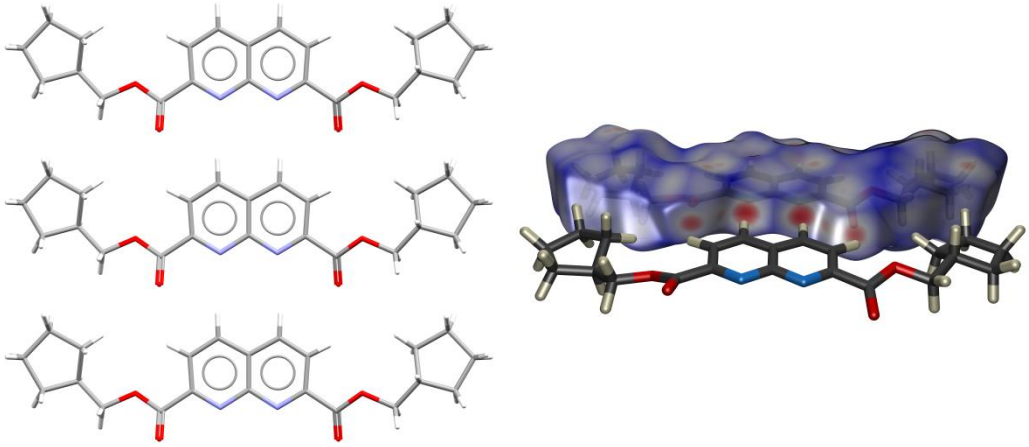

Figure 156 – *bis*-(Cyclopentylmethyl) 1,8-naphthyridine-2,7-dicarboxylate (47ff) forms the expected hydrogen bond array but shows little evidence of significant additional interactions.

The cyclopentylmethyl diester forms the expected taped structure (Figure 156). Interestingly the structure of the individual molecule resembles that of some of the benzyl derivatives, with the pendent rings held out parallel to the naphthyridine core and the ring system swept slightly back. This is particularly interesting when the additional bulk of the saturated ring system is considered.

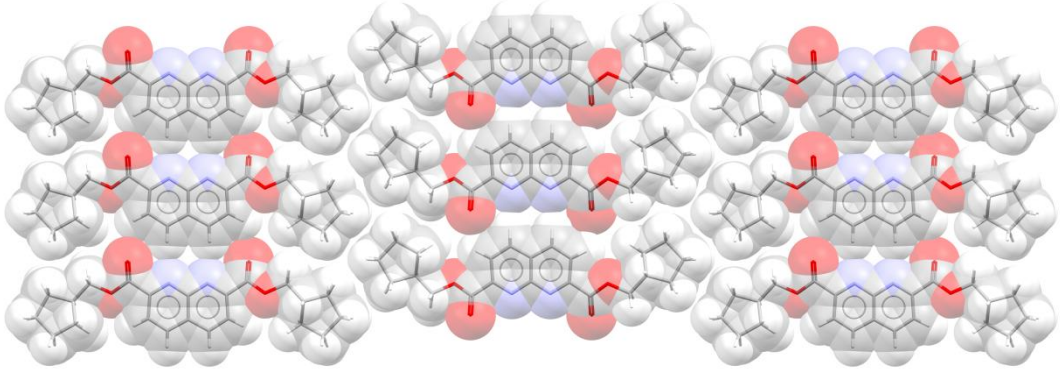

Figure 157 – The tapes form sheets which appear to be assembled through simple close packing.

In the cyclopentyl system the packing of the tapes into sheets is accomplished with very little free space due, in part, to the optimal shape of the pendent arm which creates a very clean zipper like edge (Figure 157). Within a sheet there is the common anti-parallel tape alignment.

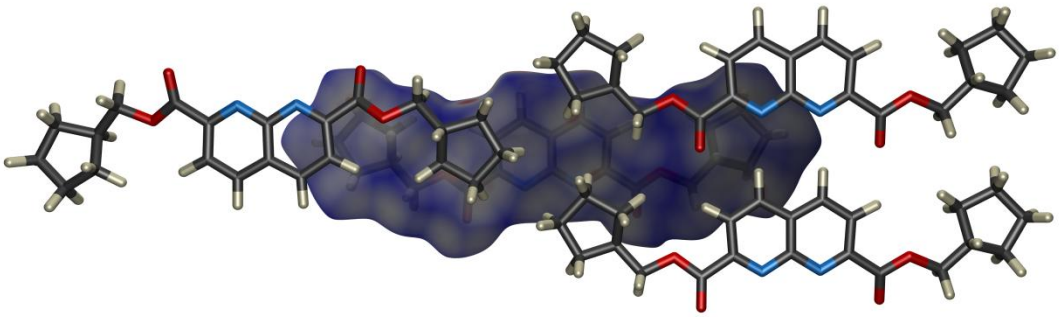

Figure 158 – Viewing the Hirshfeld surface from above there is little evidence of any secondary interactions between the stacked sheets.

Examining the Hirshfeld surface (Figure 158) from a top down view it is clear that, in this example, there appear to be no additional close contact interactions. This observation would lead us to expect that the secondary packing arrangement would therefore be governed by steric effects leading to a close packed architecture.

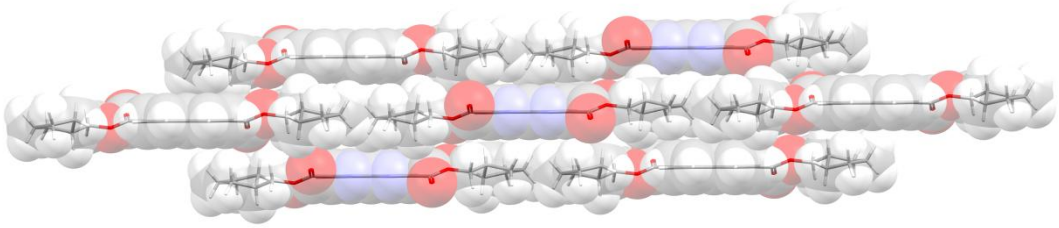

Figure 159 – Viewing the stacked sheet from a perpendicular angle allows large long axis shift to be observed. It appears that this might be in order that the bulky saturated cyclopentane can sit in the relatively non-bulky naphthyridine core.

A side-on view of several sheets stacked upon one another reveals that the non aromatic cyclopentane is located directly above a naphthyridine core from the layer below (Figure 159). This would appear to be the result of the need to accommodate the additional bulk of the saturated ring. It can be noted that this location appears to lead to very close packing by optimising the arrangement of the tapes in the layer above and below.

3.4.3.2 *bis*-(Cyclohexylmethyl) 1,8-naphthyridine-2,7-dicarboxylate (47gg)

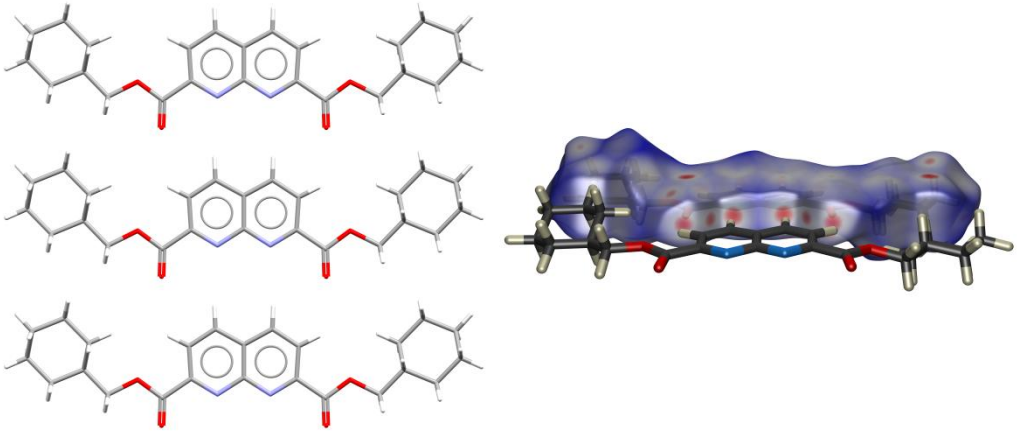

Figure 160 – *bis*-(Cyclohexylmethyl) 1,8-naphthyridine-2,7-dicarboxylate (47gg) forms the expected hydrogen bonded array and the Hirshfeld surface shows a few potential secondary interactions.

The cyclohexyl pendent group offers a yet more bulky side arm, because its non-aromatic structure forces the ring into a chair conformation, yet once again the taping array persists (Figure 160).

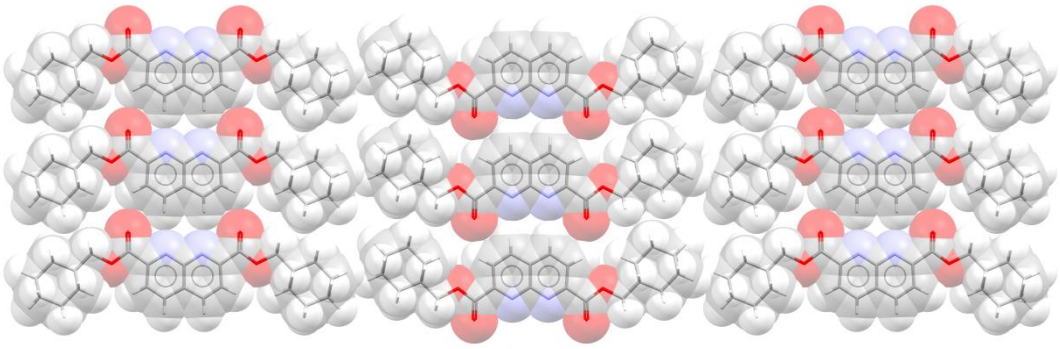

Figure 161 – The tapes form sheets with neighbouring tapes in an anti parallel arrangement. The packing at the periphery of the tapes appears to be less efficient than that observed in the cyclopentyl derivative (47ff).

The cyclohexane diester behaves in a similar manner to that seen in the cyclopentyl diester (Figure 161) although the slightly more bulky pendent arm seems to result in a less efficient packing in order to accommodate the chair conformation of the cyclohexane ring.

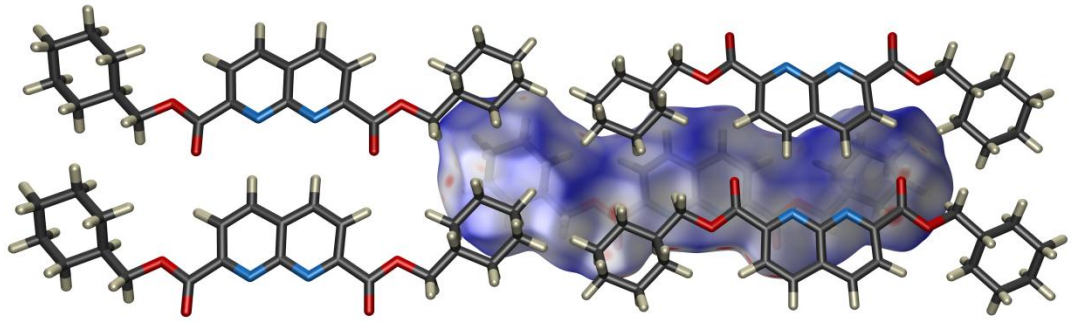

Figure 162 – Viewing the Hirshfeld surface from the top highlights only one C-H···O=C interaction.

Examination of the structure from the top-down view of the Hirshfeld surface (Figure 162) suggests that there may be an interaction between one of the carbonyl oxygen atoms and a hydrogen atom on the cyclohexyl ring (C-**H**···**O**=C 2.70 Å, **C**-H···**O**=C 3.47 Å (135.1 °)). Beyond this interaction the other contacts appear to be simple, close contacts caused by the close packing.

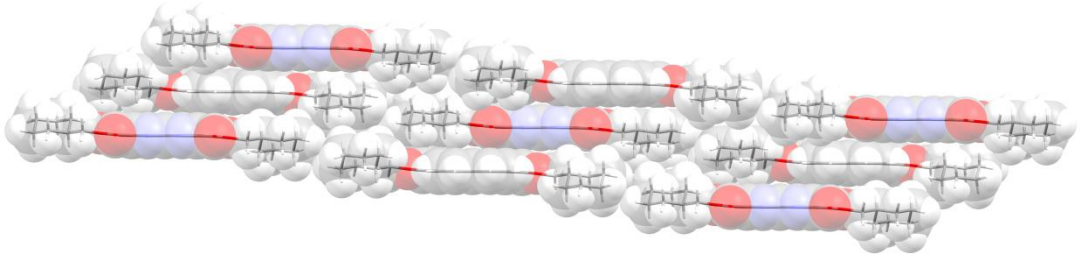

Figure 163 – The sheets of tapes pack upon one another in an anti-parallel arrangement with a far shorter long axis shift than is observed in the cyclopentyl derivative.

The tapes pack into sheets with a downward long axis shift (Figure 163). This would appear to be a characteristic of the difficulty in interleaving the bulky, cyclohexyl pendent arms between one another.

3.4.4 Polyaromatic Derivatives

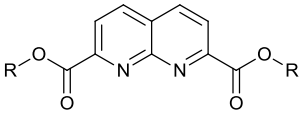

47

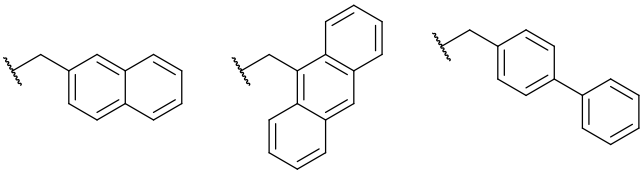

47hh 47ii 47jj

Having explored the solid-state behaviour of a number of substituted benzyl ring systems and the successful characterisation by Cheesewright[196] of a number of polyaromatic pyridine-2,6-dicarboxylate species it was hoped that the synthesis of some polyaromatic 1,8-naphthyridine-2,7-dicarboxylate systems would allow us to investigate the effect of changing the aromatic ring in the structure. It had been observed that the pyridine species were quite insoluble,[196] so it came as no surprise that the 1,8-naphthyridine analogues produced were extremely insoluble.

3.4.4.1 *bis*-(9-Anthrylmethyl) 1,8-naphthyidine-2,7-dicarboxylate (47ii)

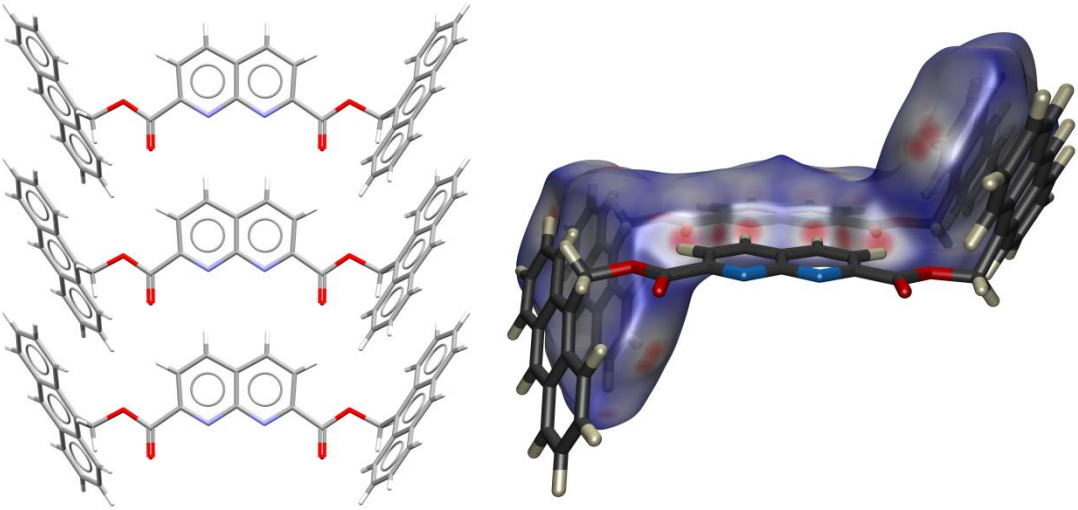

Figure 164 - *bis*-(9-Anthrylmethyl) 1,8-naphthyidine-2,7-dicarboxylate(47ii) forms the expected hydrogen bond array. The anthryl pendent arm is far bulkier than any of the previous pendent arms and is seen to be twisted out of the plane of the naphthyridine core.

Fortunately we were able to obtain X-ray structural data for *bis*-(9-anthrylmethyl) 1,8-naphthyridine-2,7-dicarboxylate which exhibited some very interesting structural properties.

First and foremost the expected hydrogen bonding array was retained (Figure 164) despite the large increase in bulk of the pendent side arm. In order for the large pendent group to be accommodated in the overall architecture it was necessary for the rings to bend out of the plane of the naphthyridine core and rotate to an almost perpendicular angle to the naphthyridine core.

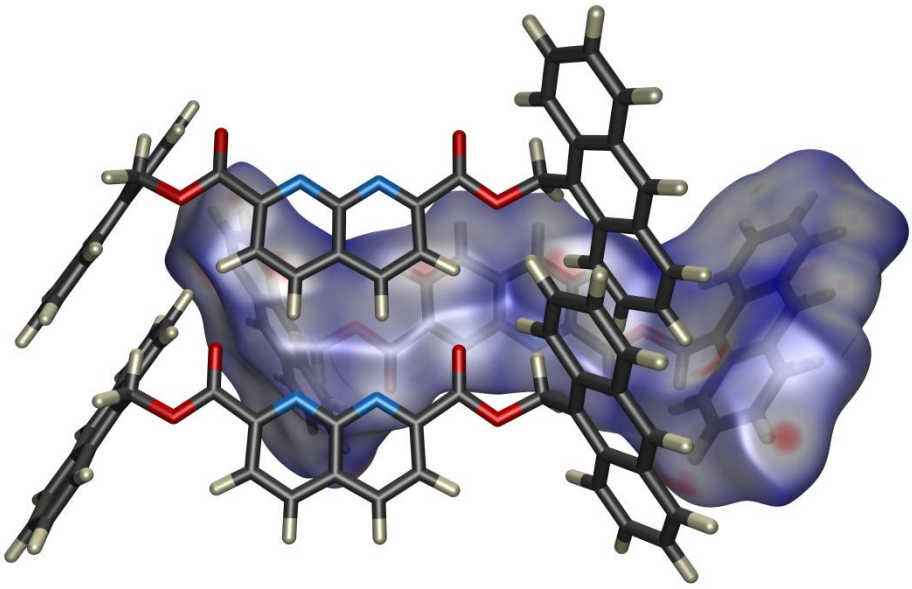

Figure 165 – Viewing the Hirshfeld surface from above allows the C-H···π interaction between the pendent anthryl arms to be identified.

The bend and twist of the anthryl pendent arm appears to allow the tapes to pack together in a manner which enables the large aromatic pendent groups in the molecule to overlap in a face-to-face manner with the molecules in front and behind the tape (Figure 165). There also appear to be two C-H···π interactions from the pendent anthryl ring to the molecule in the sheet below, one to the neighbouring molecule's pendent anthryl ring (C-**H**···**π** 2.67 Å, **C**-H···**π** 3.48 Å) and the other to the naphthyridine core (C-**H**···**π** 3.00 Å, **C**-H···**π** 3.81 Å).

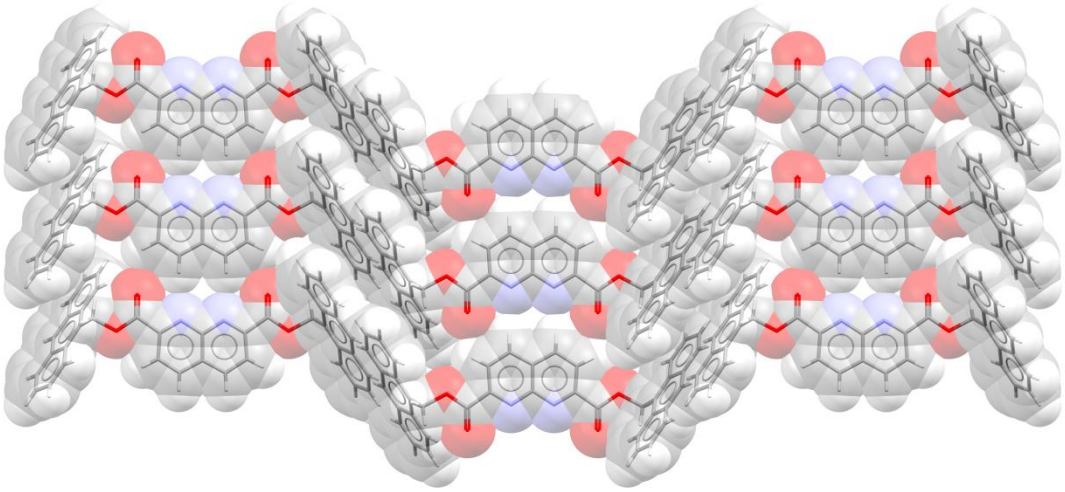

Figure 166 – The tapes pack into sheets in an anti-parallel fashion. It appears that the sheet experiences little in the way of inter-tape interactions.

The tapes then arrange into sheets (Figure 166) in which the pendent rings are not overlapping but are simply packed in a close arrangement to one another. This arrangement gives the sheets a step-stacked appearance.

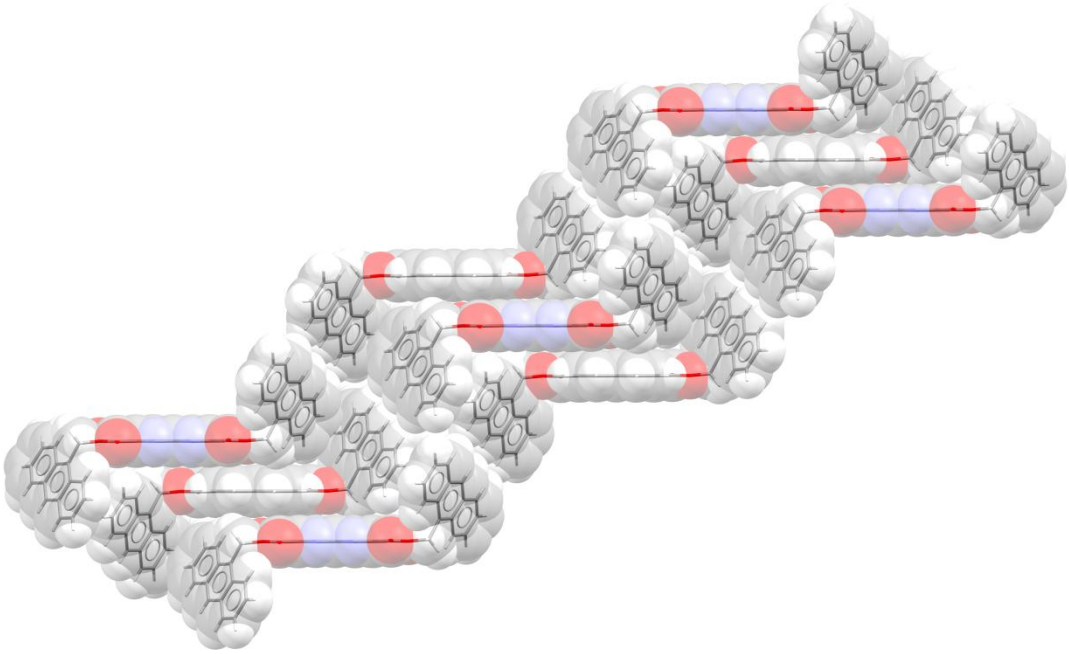

Figure 167 – The sheets pack upon one another to give an anti-parallel arrangement. It appears that the dominant interactions in the stack formation are the C-H···π interactions described above and a π···π interaction between overlapping anthryl rings.

The Hirshfeld surface shown in Figure 165 would appear to indicate that the pendent aromatic group also experiences a C-H···π interaction to the tape above and below (described above) and a π··· π interaction between overlapping pendent

anthryl groups (inter-centroid distance of 3.67 Å). Given the apparent lack of inter-tape contacts it could be imagined that it was this contact that influences the packing arrangement of the sheets into stacks (Figure 167). There appear to be few interactions between stacks of tapes and it could be suggested that the packing is therefore the closest packing that can be managed.

Structure	$r_{1\ C\ N}$	θ	$r_1'_{H\ N}$	$r_1'_{C\ N}$	θ'	$r_{1\ H\ N}$	$r_{2\ C\ O}$	ϕ	$r_{2\ H\ O}$	$r_{2\ C\ O}$	ϕ	$r_{2\ H\ O}$	α	β	γ	α'	β'	γ'	=	II	SS	Motif	Sheet	Stack
Ethyl	3.56	175.2	2.57	n/a	n/a	n/a	3.16	121.7	2.54	n/a	n/a	n/a	n/a	n/a	n/a	n/a	n/a	n/a	34.1	65.2	3.30	S	↑↑	↓↑
Butyl	3.54	174.5	2.61	3.55	175.2	2.62	3.15	124.2	2.51	3.15	125.4	2.51	n/a	n/a	n/a	n/a	n/a	n/a	39.7	45.1	3.70	S	↓↑	↓↑
Benzyl	3.48	174.6	2.50	n/a	n/a	n/a	3.10	121.9	2.47	n/a	n/a	n/a	29.4	25.4	28.3	n/a	n/a	n/a	52.5	43.5	3.33	S	↓↑	↓↑
2 Me Bn	3.49	173.4	2.54	n/a	n/a	n/a	3.12	124.7	2.48	n/a	n/a	n/a	69.9	9.1	67.5	n/a	n/a	n/a	56.5	52.8	2.99	S	↓↑	↓↑
3 Me Bn	3.70	173.8	2.72	n/a	n/a	n/a	3.25	121.2	2.64	n/a	n/a	n/a	4.9	12.4	11.8	n/a	n/a	n/a	24.9	57.8	3.05	S	↑↑	↓↑
4 Me Bn	3.50	175.0	2.56	n/a	n/a	n/a	3.09	123.3	2.47	n/a	n/a	n/a	26.0	22.0	24.5	n/a	n/a	n/a	49.4	49.3	3.30	S	↑↑	↓↑
246 tri Me Bn *	3.46	172.9	2.53	3.45	176.4	2.53	3.24	123.9	2.60	3.22	127.1	2.59	-76.8	-30.9	74.8	-76.6	-32.7	73.6	21.6	46.9	3.33	S	↓↑	↓↑
2356 tetra Me Bn	3.49	175.2	2.55	n/a	n/a	n/a	3.07	123.2	2.44	n/a	n/a	n/a	-87.0	-10.3	62.0	n/a	n/a	n/a	40.0	67.0	3.34	S	↑↑	↓↑
2 F Bn	3.52	175.1	2.57	n/a	n/a	n/a	3.14	124.0	2.51	n/a	n/a	n/a	-29.0	-26.5	29.4	n/a	n/a	n/a	50.8	49.1	3.28	S	↑↑	↓↑
2 Cl Bn	3.50	174.5	2.55	n/a	n/a	n/a	3.10	124.1	2.46	n/a	n/a	n/a	-75.7	-1.7	66.3	n/a	n/a	n/a	24.6	60.8	3.00	S	↓↑	↓↑
2 Br Bn	3.54	174.1	2.59	n/a	n/a	n/a	3.12	123.5	2.49	n/a	n/a	n/a	75.8	3.4	65.9	n/a	n/a	n/a	25.1	64.7	3.06	S	↓↑	↓↑
3 F Bn†	3.56	172.8	2.61	3.56	171.3	2.62	3.13	123.5	2.51	3.20	122.4	2.59	-40.0	38.9	73.1	14.3	20.5	21.8	25.8	64.2	3.00	S	↓↑	↑↑
3 Cl Bn	3.68	175.4	2.73	n/a	n/a	n/a	3.22	122.6	2.60	n/a	n/a	n/a	8.0	13.0	12.6	n/a	n/a	n/a	26.1	63.8	3.09	S	↑↑	↓↑
3 Br Bn	3.61	174.7	2.68	n/a	n/a	n/a	3.16	123.9	2.55	n/a	n/a	n/a	-4.9	-13.4	14.2	n/a	n/a	n/a	26.7	60.0	3.10	S	↑↑	↓↑
4 F Bn	3.54	174.6	2.51	n/a	n/a	n/a	3.12	123.6	2.51	n/a	n/a	n/a	-60.8	-19.7	56.4	n/a	n/a	n/a	25.8	53.2	3.09	S	↓↑	↓↑
4 Cl Bn	3.65	175.0	2.70	n/a	n/a	n/a	3.24	122.9	2.62	n/a	n/a	n/a	-20.2	-17.6	15.4	n/a	n/a	n/a	23.9	55.9	2.93	S	↑↑	↓↑
4 Br Bn	3.64	174.4	2.70	n/a	n/a	n/a	3.20	122.2	2.59	n/a	n/a	n/a	-22.0	-18.5	16.5	n/a	n/a	n/a	22.8	56.0	2.89	S	↑↑	↓↑
4 Ome	3.52	174.3	2.57	n/a	n/a	n/a	3.11	122.8	2.49	n/a	n/a	n/a	-44.8	-33.0	42.7	n/a	n/a	n/a	35.5	39.2	3.29	S	↓↑	↓↑
2 Py	3.50	174.5	2.57	n/a	n/a	n/a	3.12	123.9	2.51	n/a	n/a	n/a	0.7	6.1	7.5	n/a	n/a	n/a	42.0	90.0	3.38	H	↓↑	↑↑
Cyclo Pentyl	3.46	175.3	2.52	n/a	n/a	n/a	3.19	124.6	2.55	n/a	n/a	n/a	-55.0	-28.0	n/a	n/a	n/a	n/a	21.7	50.2	3.88	S	↓↑	↑↑
Cyclo Hexyl	3.63	174.9	2.69	n/a	n/a	n/a	3.24	124.1	2.61	n/a	n/a	n/a	-56.5	-10.2	n/a	n/a	n/a	n/a	32.9	43.7	3.15	S	↓↑	↓↑
Anthryl	3.53	174.9	2.60	n/a	n/a	n/a	3.10	123.3	2.49	n/a	n/a	n/a	-84.6	-7.4	71.0	n/a	n/a	n/a	31.9	60.9	3.19	S	↓↑	↓↑
4 Nitro	3.51	174.2	2.62	n/a	n/a	n/a	3.13	121.4	2.53	n/a	n/a	n/a	-10.3	-16.7	20.5	n/a	n/a	n/a	44.4	90.0	3.43	H	↓↑	↑↑

The methyl ester derivative is excluded from this table as it does not form the expected one dimensional taping array. † Due to disorder of one of the pendent rings the 3-F Bn derivative has an additional α' = 1.8, β' = 17.0, γ' = 13.9

Table 8 – Structural summary for the 1,8-naphthyridine-2,7-dicarboxylates.

3.5 Conclusion

This study has reported the solid-state structures of a great number of 1,8-naphthyridine-2,7-dicarboxylates. The behaviour observed in these structures is very similar to that observed in the pyridine-2,6-dicarboxylate systems reported by Parker,[172] Gomm,[182] Orton[195] and Cheesewright.[196]

While examining the structures of the methyl and chlorine substituted benzyl derivatives it has been noted that the structures are extremely similar, with the exception of the derivatives where the substitution is in the 4-position. It was also noted that further to the structural similarities observed between the methyl and chlorine substituted benzyl derivatives, the bromine substituted derivatives appear to be isostructural to the chloro substituted benzyl derivatives.

It has also been possible to examine the effect of having alternate cores as the pendent rings, with the solid-state structure of the pyridylmethyl, cyclopentylmethyl, cyclohexylmethyl and anthrylmethyl derivatives reported. While other examples have been synthesised, the lack of solubility and formation of extremely small crystals has hampered the collection of data for all of the compounds synthesised.

Initial attempts have been made to carry out physical measurements such as DSC on these compounds however most of the compounds appear to decompose on melting.

4 1,8-Naphthyridine-2,7-dicarboxamides

As discussed in the introduction Parker,[172] Gomm,[182] Horton[274] and Dwyer[184] each studied the solid-state behaviour of a number of pyridine-2,6-dicarboxamides discovering that the molecules synthesised, in general, formed one of three architectures. Given the work illustrated in the previous chapter studying the 1,8-naphthyridine-2,7-dicarboxylate derivatives and in light of the Grossel group's previous work concerning the pyridine-2,6-dicarboxamides, it was an obvious extension of our study to look at the solid-state behaviour of some 1,8-naphthyridine-2,7-dicarboxamides.

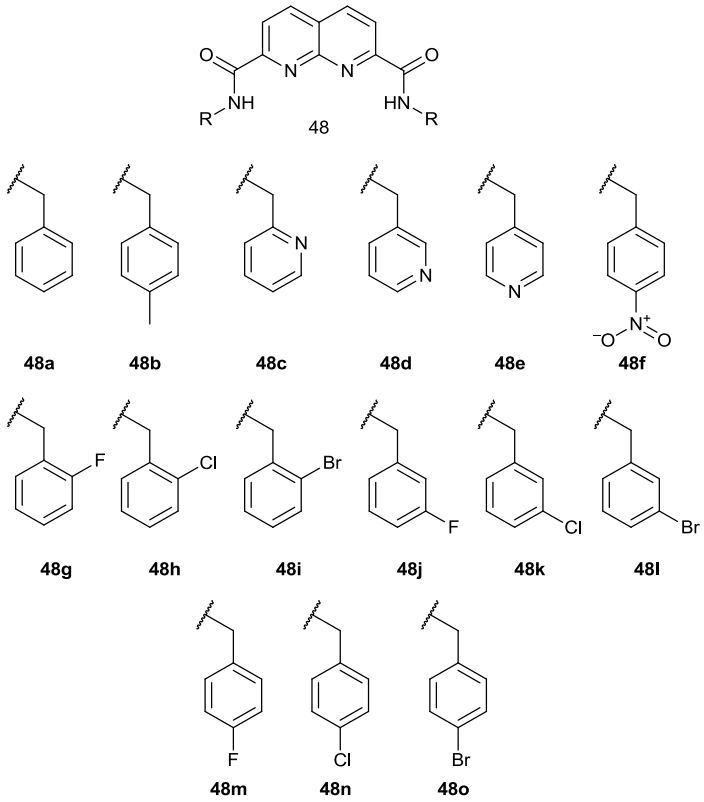

The different derivatives that were successfully synthesised are shown above. The synthesis occurred through the reaction of the corresponding amine with 1,8-naphthyrdidine-2,7-dicarbonyl dichloride in the presence of triethylamine. This chapter details the solid-state behaviour of those materials which yielded crystals of sufficient quality to undertake X-ray structural studies.

4.1 *N,N'-bis-(Benzyl)-1,8-naphthyridine-2,7-dicarboxamide (48a)*

N,N'-bis-(benzyl)-1,8-naphthyridine-2,7-dicarboxamide (48a) was the first compound synthesised and yielded good crystals suitable for a study of key interactions and the packing motif favoured.

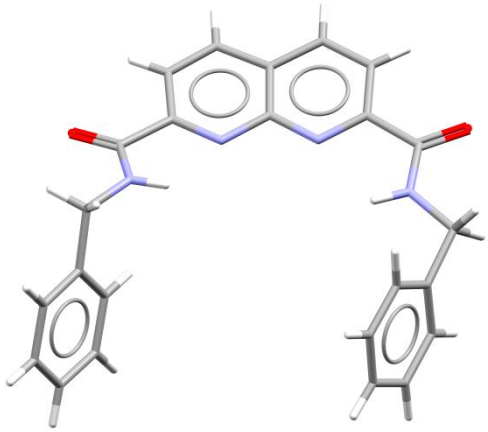

Figure 168 –The basic structure of N,N'-*bis*-(benzyl)-1,8-naphthyridine-2,7-dicarboxamide.

In the solid-state the carbonyl groups adopt a syn – syn conformation, as previously observed in the pyridine analogues.[172] The benzyl side arms are then twisted down out of the plane of the naphthyridine core and are rotated so they are almost perpendicular to the plane of the core (Figure 168).

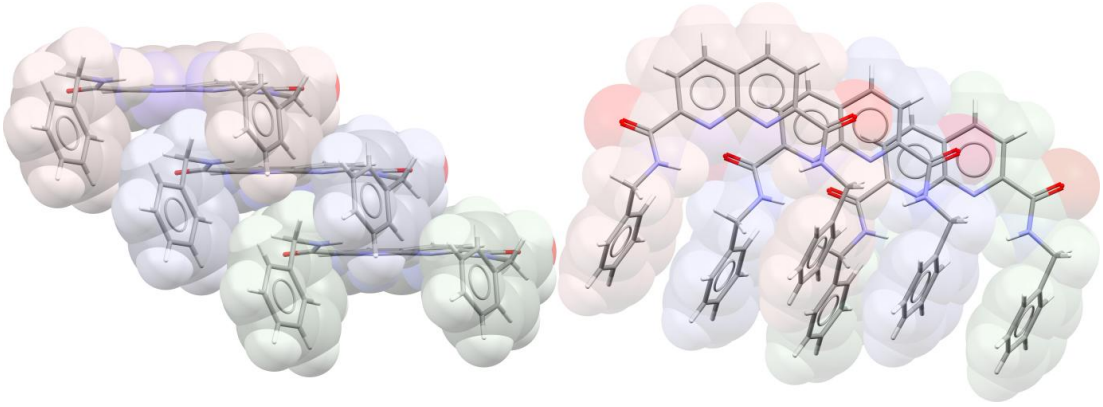

Figure 169 – A side on and top down view of the stacked molecules, coloured to aid differentiation of the position in stack of the molecule. (Red is at the top, Green is at the bottom)

Once the packing of the individual molecules is examined (Figure 169) it becomes apparent that the positioning of the pendent rings is such that the pendent ring from the neighbouring molecules directly above and below both sit half in the cleft its neighbouring molecule. This packing behaviour means that the molecules

arrangement themselves into packed columns, contrasting with the pyridine analogue[172] which shows no sign of chain formation.

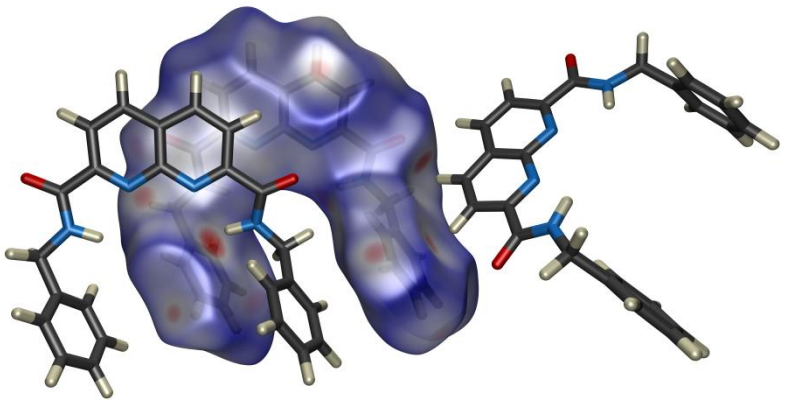

Figure 170 - The Hirshfeld surface of this molecule allows visualisation of close contacts, and potential intermolecular interactions present.

Examining the Hirshfeld surface of these molecules (Figure 170) shows that there does not appear to be many particularly strong interactions between interdigitated molecules within the column. The one close contact highlighted comes from the interaction of the amide hydrogen with one of the pendent rings in the plane below (N-**H**···**π** 3.10 Å, **N**-H···**π** 3.72 Å (129.4 °)).

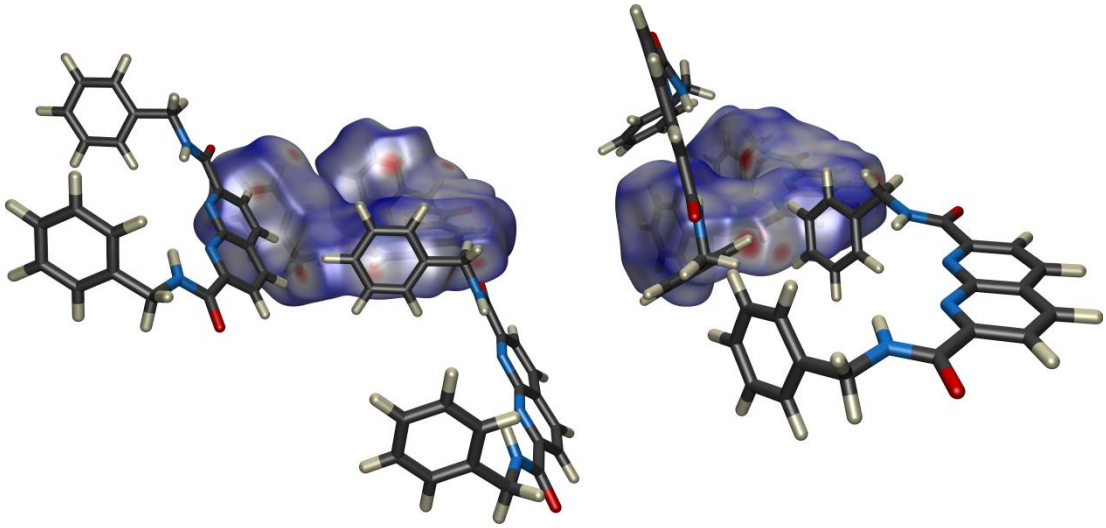

Figure 171 - Views from both sides of the Hirshfeld surface showing how the surrounding molecules interact their carbonyl groups

Indeed it appears that the main interactions present in the benzyl derivative are between the two carbonyl groups and the surrounding molecules in the sheet. In Figure 171 it is possible to see that the main interactions involving these carbonyl groups are C-H···O=C interactions. The contact is between the carbonyl oxygen

(O(3)) and the naphthyridine hydrogens (H(4) and H(5)) with a contact distances of C=**O**···**H**-C of 2.60 Å and 2.51 Å and C=**O**···H-**C** of 3.38 Å (139.4 °) and 3.30 Å (140.9 °) respectively. In Figure 171 (right) it appears that both molecules interacting with the Hirshfeld surface are undergoing a similar interaction, however, in this case it is the pendent benzyl rings that are providing the hydrogen bond donors and the contact is between O(1) and hydrogen atoms H(14) (C=**O**···**H**-C 2.41 Å, C=**O**···H-**C** 3.34 Å (170.7 °)) from one neighbouring molecule, and H(23) and H(24) (C=**O**···**H**-C of 2.54 Å and 2.72 Å and C=**O**···H-**C** of 3.20 Å (126.7°) and 3.29 Å (119.6 °) respectively) from the other.

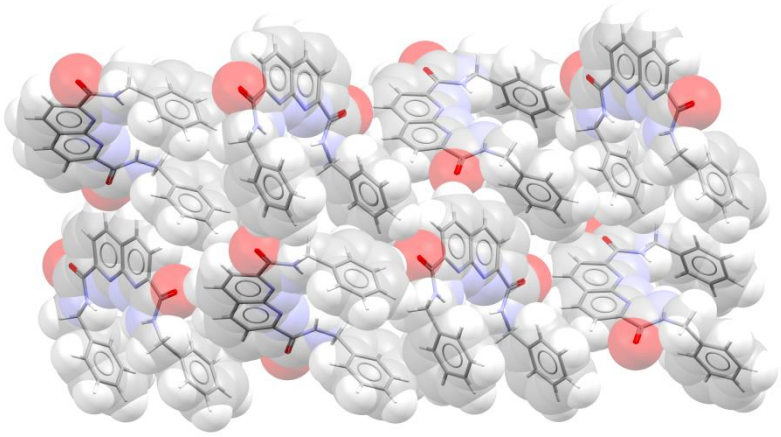

Figure 172 - The secondary interlayer packing brought about by the C=O···H-C contacts described above

The interactions illustrated in Figure 171 lead to the formation of the complex secondary packing that can be seen in Figure 172. The molecules form stacks with one another and the stacks arrange themselves so that, within a layer of molecules, it is possible for the additional secondary interactions to occur.

4.2 N,N'-bis-(Pyridylmethyl) 1,8-naphthyridine-2,7-dicarboxamides (48c-e)

N,N'-Pyridylmethyl-2,6-pyridine dicarboxamide derivatives have been studied in detail within the group because they offer not only interesting solid-state properties but, as discussed in the introduction, they also provide a potent metal-binding ligand system.

4.2.1 *N,N'-bis*-(2-Pyridylmethyl) 1,8-naphthyridine-2,7-dicarboxamide (48c)

Unfortunately it has not been possible to produce high quality crystals of *N,N'-bis*-(2-pyridylmethyl)-1,8-naphthyridine-2,7-dicarboxamide. Very small crystals have been examined from which data collection was attempted, however this afforded very poor diffraction patterns. However, during the attempted formation of a metal complexes with this ligand crystals were isolated which did give better diffraction patterns and it has been possible to collect data which solved as the *bis*-hydrochloride salt structure (**48c·2HCl**) as shown in Figure 173.

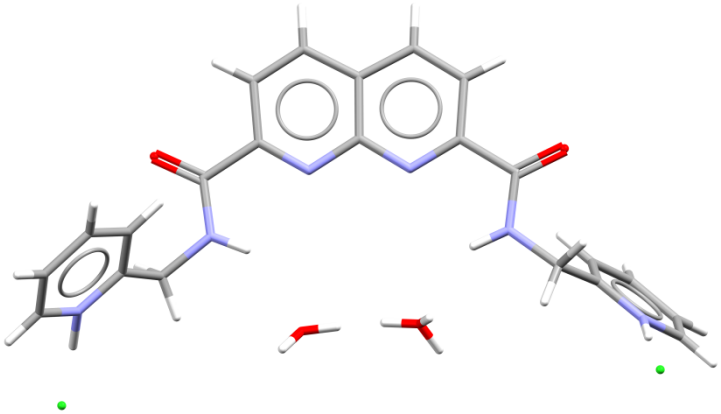

Figure 173 – A view of *N,N'-bis*-(2-pyridyl)-1,8-naphthyridine-2,7-dicarboxamide hydrochloride salt (48c·2HCl), which also contains two water molecules both of which are disordered.

The asymmetric unit is, in fact, half of the figure shown as the molecule, like many of the dicarboxylates reported in the previous chapter it is symmetric. It is interesting to note that it is the pendent pyridine nitrogen are protonated and that, in the cleft of the dicarboxamide which through packing forms a cavity, there is a chain of disordered water molecules.

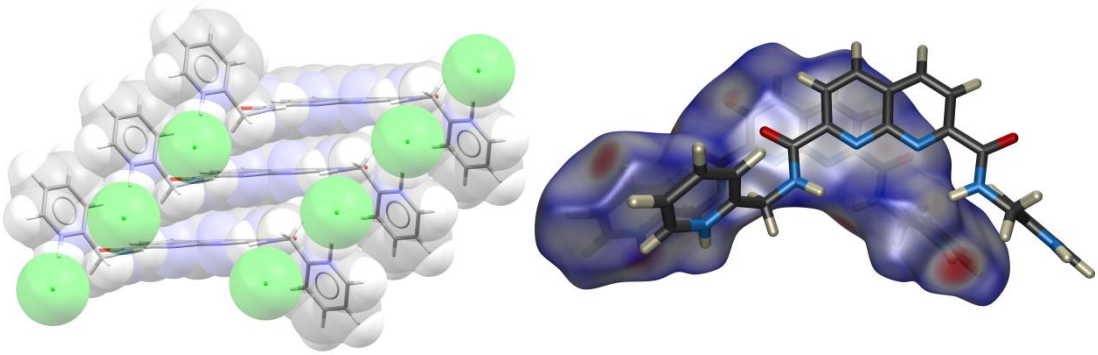

Figure 174 - Primary packing of N,N'-*bis*-(2-pyridyl)-1,8-naphthyridine-2,7-dicarboxamide hydrochloride (48c·2HCl).

Ignoring the water chain it is possible to see that the main packing motif present is a stack assembly which leads to the cavity containing the water chains (Figure 174). It is however quite obvious when examining the Hirshfeld surface that there are no significant interactions between adjacent stacking molecules, the mains contacts that are present are between the chloride ion and the protonated site on the pendent pyridyl group, and from the amide N-H groups to the water chain.

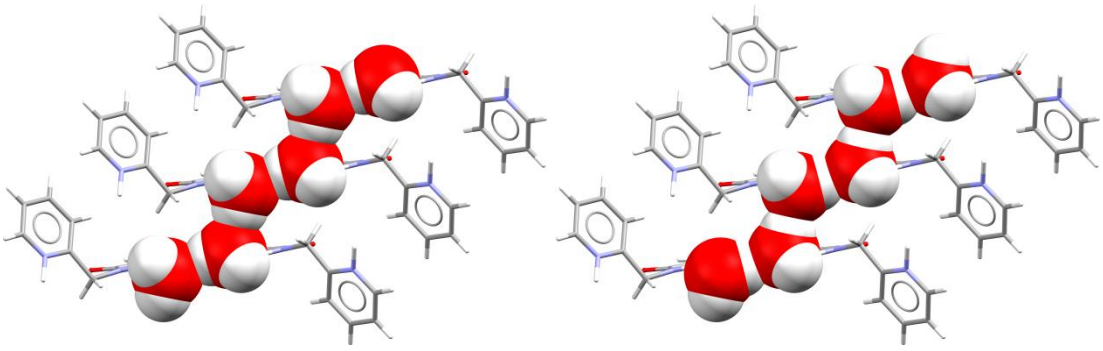

Figure 175 - A view of the two different occupancies of the disordered water molecules.

A more detailed examination of the disordered water chain (Figure 175) shows how the disorder of the water molecule is most likely due to the possibility of two differing water chains filling the cavity. When occupancy was freely refined it tended towards a 50:50 distribution so the occupancy was then fixed at this ratio. It would appear that this disorder is most likely due to the presence of the two amide N-H groups with which the water chain can form a hydrogen bond. This would suggest that the disorder is not present within single cavities and it is more likely that in different stacks one conformation was adopted and this continued throughout the cavity.

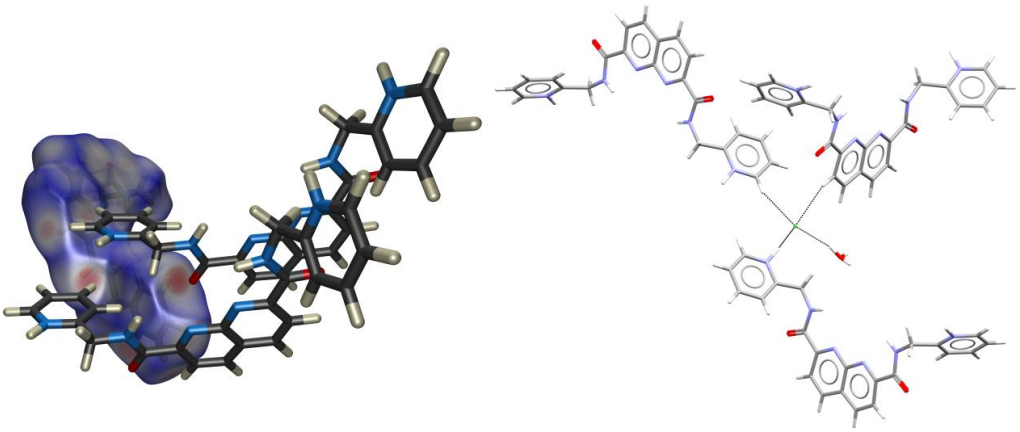

Figure 176 - Key secondary interactions from the carbonyl oxygen (left) and from the chloride (right)

Obviously whilst the basic structure of packed columns appears to be centred around the water chains the overall structure appears to be heavily influenced by the interaction of the carbonyl oxygen (O(1)) and the hydrogen in the *γ* position relative to the protonated pyridine nitrogen on the pendent pyridyl ring H(12) (C=**O**···**H**-C 2.27 Å C=**O**···H-**C** 3.05 Å (138.6 °)). These contacts appear to be the guiding interaction for the secondary structure here. Finally, although the chloride is very closely bound to the protonated pyridine nitrogen of the pendent ring (**Cl**$^-$···**H**-N$^+$ 1.88 Å, **Cl**$^-$···H-**N**$^+$ 3.00 Å (177.0 °), it appears to interact with a number of other surrounding molecules in slightly longer, weaker interactions. One such interaction is to the water molecule involving the fully occupied hydrogen(H(1w)) (**Cl**$^-$···**H**-O 2.35 Å, **Cl**$^-$···H-**O** 3.14 Å (163.2 °) while the other two contacts are with the neighbouring molecules H(9) (**Cl**$^-$···**H**-C 2.81 Å, **Cl**$^-$···H-**C** 3.69 Å (153.9 °) and H(10) (**Cl**$^-$···**H**-C 2.71 Å, **Cl**$^-$···H-**C** 3.60 Å (157.9 °).

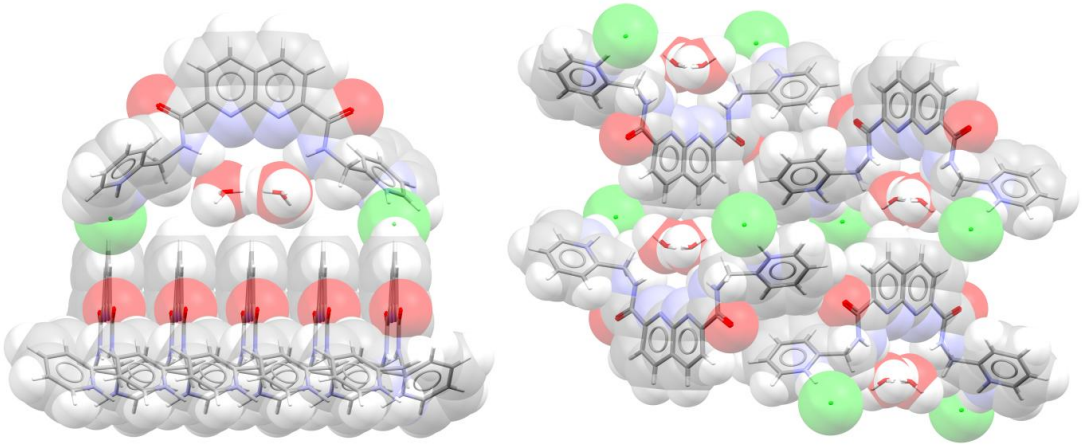

Figure 177 – Secondary packing of the stacks: each molecule sits perpendicular to the neighbouring stack due in part to the secondary contacts with the chloride anions (left); stacks assemble into rows of stacks which all point in the same direction with the neighbouring row sitting anti parallel to its neighbour (right).

With this in mind it is possible to examine the secondary images (Figure 177) to gain a better understanding of the overall solid-state architecture of the molecules. Figure 177 (right) gives a clear view of the assembly of the stacked molecules. The individual stacks assemble into rows with each alternating stack sit at 90 ° to one another, which then sit in an anti-parallel direction to the neighbouring row.

4.2.2 Metal Complexation of *N,N'-bis*-(2-Pyridylmethyl) 1,8-naphthyridine-2,7-dicarboxamide (48c·2Cu^{2+})

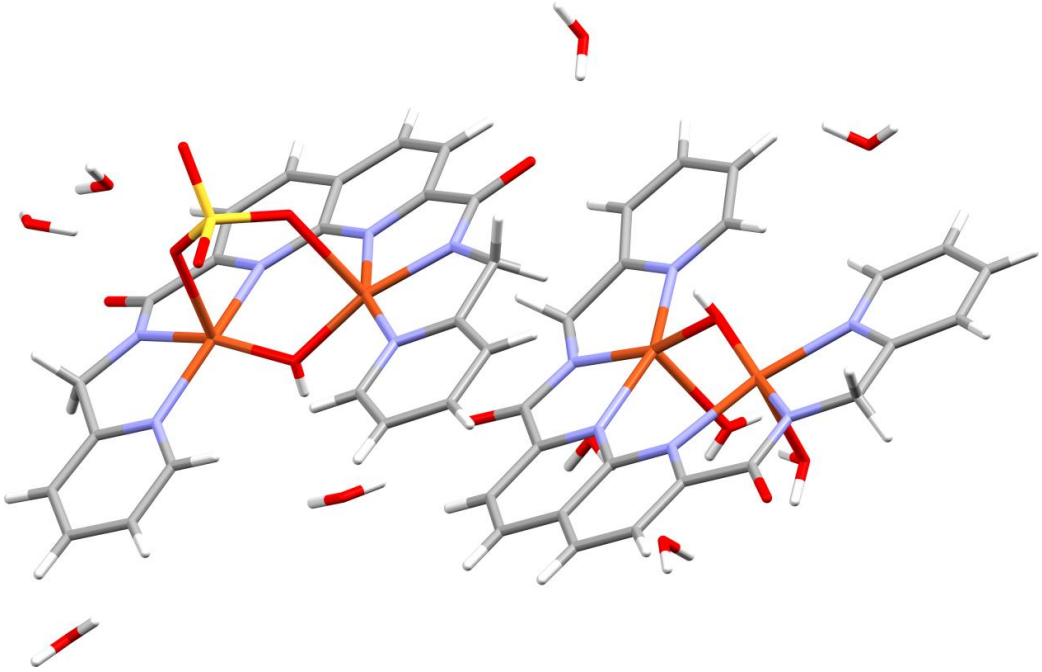

Figure 178 - The asymmetric unit of the copper complex of N,N'-*bis*-(2-pyridyl)-1,8-naphthyridine-2,7-dicarboxamide (48c·2Cu^{2+}) contains two metal complexes species and 8 solvent waters

As discussed in the introduction *N,N'-bis*-(2-pyridyl)pyridine-2,6-dicarboxamide (**26**) has been shown to readily complex transition metal ions to produce a number of different architectures by simple variation of the metal centre. This together with the history of 1,8-naphthyridines being utilised as metal complexing ligands, led us to carry out some initial metal complexation experiments with a limited range of metal ions. Fortunately it was possible to isolate crystals of sufficient quality to obtain solid-state characterisation of the copper (II) complex (Figure 178).

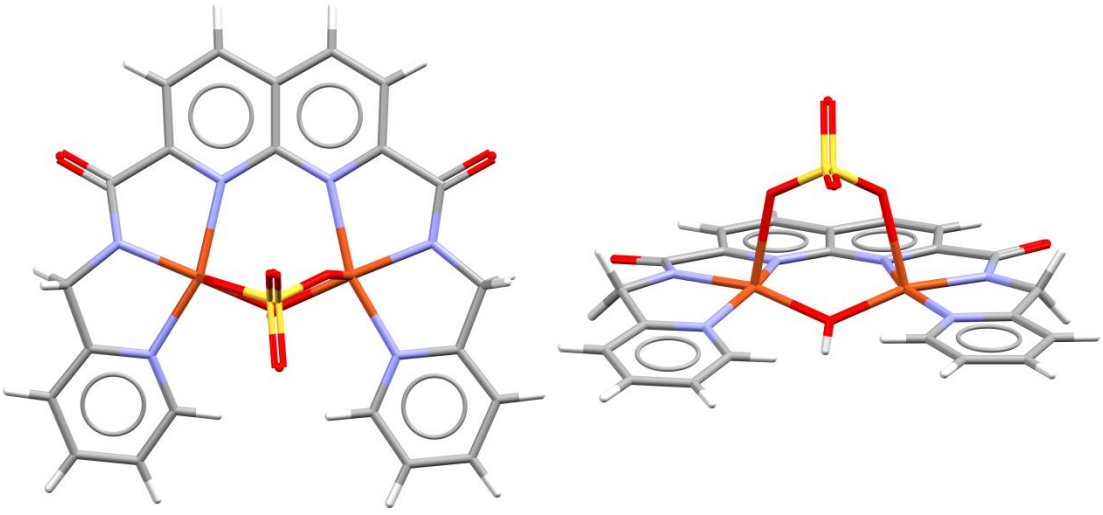

Figure 179 – Anionic metal complex in the asymmetric unit with bridging sulphate and hydroxide

Within the asymmetric unit there are two metal complex units; Figure 179 illustrates one of these. *N,N'-bis*-(2-Pyridyl)pyridine-2,6-dicarboxamide forms a 1:2 complex with the copper (II) ions (**48c·2Cu^{2+}**), in which each copper centre appears to be co-ordinated in a slightly distorted square pyramidal arrangement. This distortion appears to arise from the presence of a bridging hydroxyl group located in an approximately symmetrical position between the two copper centres (Cu(1) 1.87 Å, Cu(4) 1.88 Å) which are 3.30 Å apart. Apart from the bridging hydroxide each copper ion is co-ordinated to a naphthyridine nitrogen (Cu(1) 2.14 Å, Cu(4) 2.16 Å), a deprotonated amide nitrogen (Cu(1) 1.92 Å, Cu(4) 1.91 Å) and one of the nitrogen atoms on the pendent pyridyl group (Cu(1) 2.02 Å, Cu(4) 2.03 Å) as well as the sulphate counter ion in the axial position (Cu(1) 2.24 Å, Cu(4) 2.22 Å).

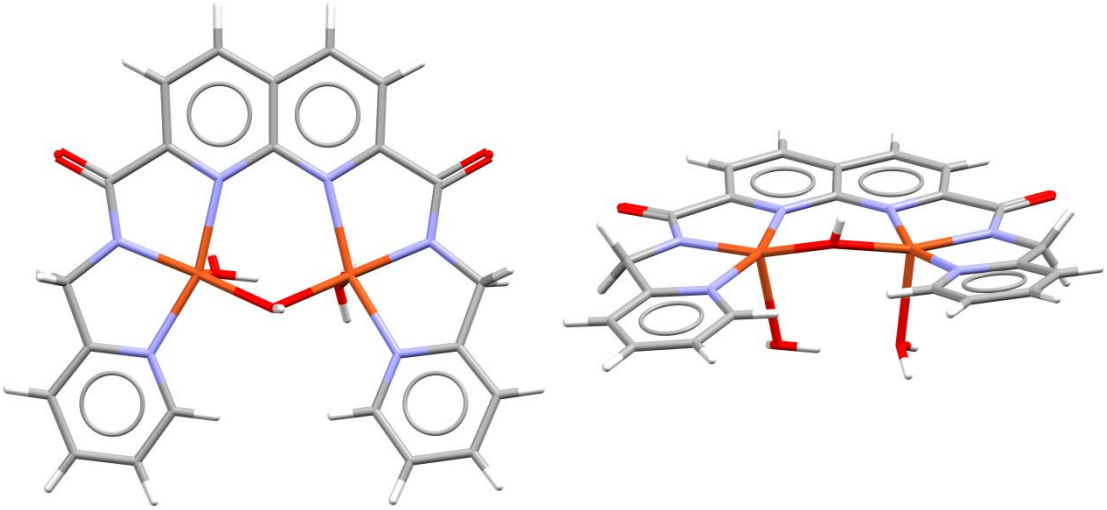

Figure 180 – Cationic metal complex unit in the asymmetric unit with axial water molecules

The other metal complex in the asymmetric unit can only be differentiated by the lack of a sulphate group bridging the two copper ions. In this case it is replaced by two axial water molecules with one at each copper centre (Cu(2) 2.14 Å, Cu(3) 2.16 Å). The copper ions are once again bridged by a hydroxyl group (Cu(2) 1.90 Å, Cu(3) 1.90 Å) and are 3.33 Å apart. They are also coordinated in the same motif by the organic ligand: naphthyridine nitrogen (Cu(2) 2.16 Å, Cu(3) 2.14 Å), a deprotonated amide nitrogen (Cu(1) 1.90 Å, Cu(4) 1.91 Å) and one of the pendent pyridyl group nitrogen atoms (Cu(1) 2.04 Å, Cu(4) 2.04 Å). Overall it is believed that the material reported is a neutral species with 4 copper (II) species balanced by 4 deprotonated amide nitrogen atoms, one sulphate and two bridging hydroxide units.

Despite considerable effort no other characterisable metal complexes have as yet been obtained for this ligand.

4.2.3 *N,N'-bis*-(3-Pyridylmethyl) 1,8-naphthyridine-2,7-dicarboxamides (48d)

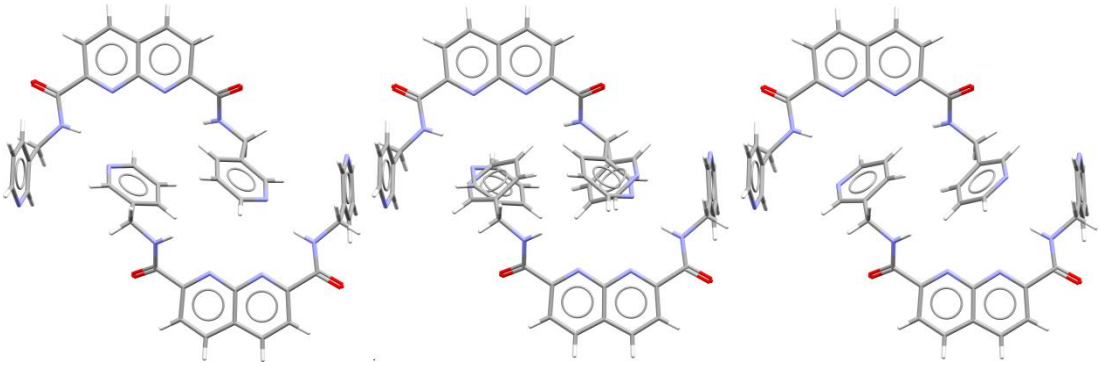

Figure 181 – An X-ray structure of *N,N'-bis*-(3-pyridylmethyl)-1,8-naphthyridine-2,7-dicarboxamide shows that the ring sitting in the cleft of its self-complimentary dimer is disordered (centre). The two partially occupied conformers are shown (left and right)

The structure of *N,N'-bis*-(3-pyridylmethyl)-1,8-naphthyridine-2,7-dicarboxamide (**48d**) that was obtained is interesting as although it forms a self-complimentary dimer like those reported in the N,N'-*bis*-(pyridylmethyl)pyridine-2,6-dicarboxamides, the increased size of the cleft means that it is not possible for the pendent pyridine ring to interact with both amide hydrogen atoms in a bifurcated manner. Instead the pendent arm in the cleft is disordered as shown in Figure 181.

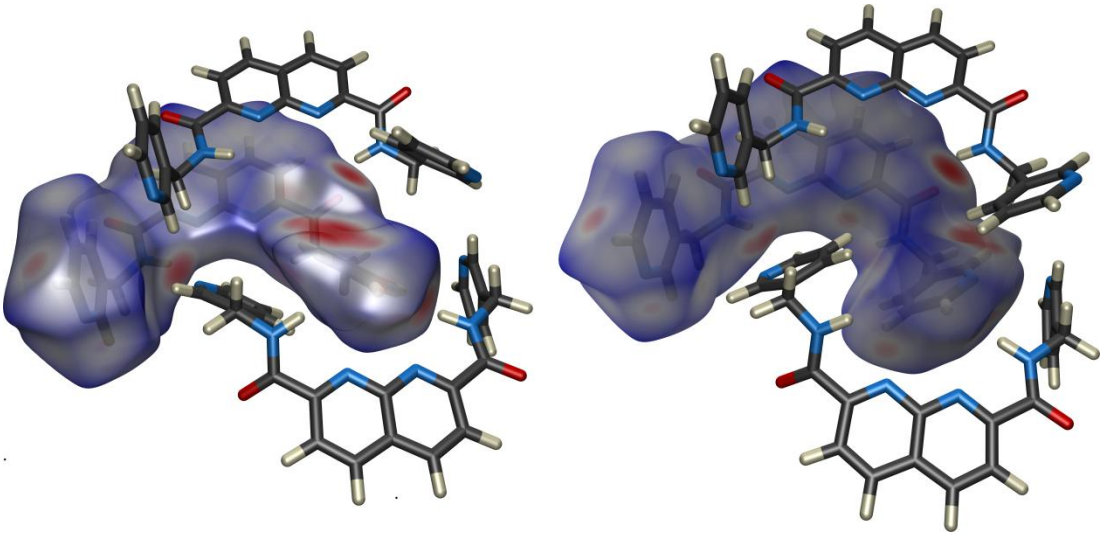

Figure 182 - The Hirshfeld surfaces for the two different conformers. These show that although the conformers are only subtly different, the close packing contacts are quite distinct. The image on the left is missing the connecting bond to the pendent arm because of difficulties the visualization package has displaying disorder.

Figure 182 shows that the slight difference in the orientation of the pendent ring leads to a quite distinct set of close contacts. In particular the degree to which the pendent pyridine nitrogen atoms interact with the amide hydrogens is noticeably different as is the very obvious close contact on the surface in the left hand illustration. This contact appears to arise from steric clashes between neighbouring pendent rings which could be a contributing factor to the disorder seen in this system.

The conformation illustrated on the left shows contacts from the pyridine nitrogen atoms in the cleft to the amide hydrogens (**N**(6B)···**H**(9B)-N(9) 2.19 Å, **N**(6B)···H(9B)-**N**(9) 2.93 Å (149.4 °) and **N**(11A)···**H**(3N)-N(3) 2.09 Å, **N**(11A)···H(3N)-**N**(3) 2.97 Å (155.3 °)). In addition there are contacts between the carbonyl oxygen group and the other amide hydrogen in the neighbouring stacked molecule (C=**O**(4)···**H**(10N)-N(10) 2.08 Å, C=**O**(4)···H(10N)-**N**(10) 2.82 Å (151.0 °) and C=**O**(2)···**H**(4N)-N(4) 2.10 Å, C=**O**(2)···H(4N)-**N**(4) 2.80 Å (142.5 °)). The second conformation shows a slightly different contact motif involving the contact from the pyridine nitrogen atoms in the cleft to the amide hydrogen atoms with contact distances longer than those in the previous conformer. (**N**(6A)···**H**(9N)-N(9) 2.60 Å, **N**(6A)···H(9N)-**N**(9) 3.26 Å (137.2 °) and **N**(11B)···**H**(3N)-N(3) 2.60 Å, **N**(11B)···H(3N)-**N**(3) 3.40 Å (144.3 °)). In one case, the nitrogen (N(11)) is bifurcated to another hydrogen bond donor. (**N**(11B)···**H**(42B)-C(42B) 2.27 Å, **N**(11B)···H(42B)-**C**(42B) 2.75 Å (110.9 °)). Finally there are additional contacts from the naphthyridine nitrogen atom to the hydrogen atom α to the pendent pyridine's nitrogen (**N**(7)···**H**(21A)-C(21A) 2.64 Å, **N**(7)···H(21A)-**C**(21A) 3.34 Å (130.4 °) and **N**(1)···**H**(43B)-C(43B) 2.65 Å, **N**(1)···H(43B)-**C**(43B) 3.38 Å (133.4 °)).

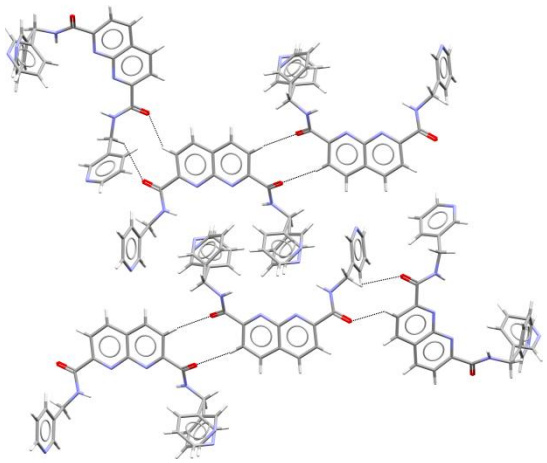

Figure 183 – The secondary interactions involving the carbonyl oxygen are shown above.

Having looked at the interactions within the cleft it is possible to examine the interactions which cause the secondary arrangement of the self-complimentary dimers (Figure 183). In this case as the interactions occur from ordered arms and between the molecules in the asymmetric unit, there are only two pairs of contacts to report. One of these involves the neighbouring molecule sat in the same plane as the naphthyridine core (C=O(2)···H(27)-C(27) 2.53 Å, C=O(2)···H(27)-C(27) 3.33 Å (141.4 °) and C=O(4)···H(2)-C(2) 2.51 Å, C=O(4)···H(2)-C(2) 3.30 Å (140.7 °)) while the other involves the herringboned neighbouring molecule (C=O(1)···H(24)-C(24) 2.40 Å, C=O(1)···H(24)-C(24) 3.17 Å (138.3 °) and C=O(3)···H(10A)-C(10) 2.79 Å, C=O(3)···H(10A)-C(10) 3.49 Å (128.5 °)).

4.2.4 *N,N'-bis*-(4-Pyridylmethyl) 1,8-naphthyridine-2,7-dicarboxamide (48e)

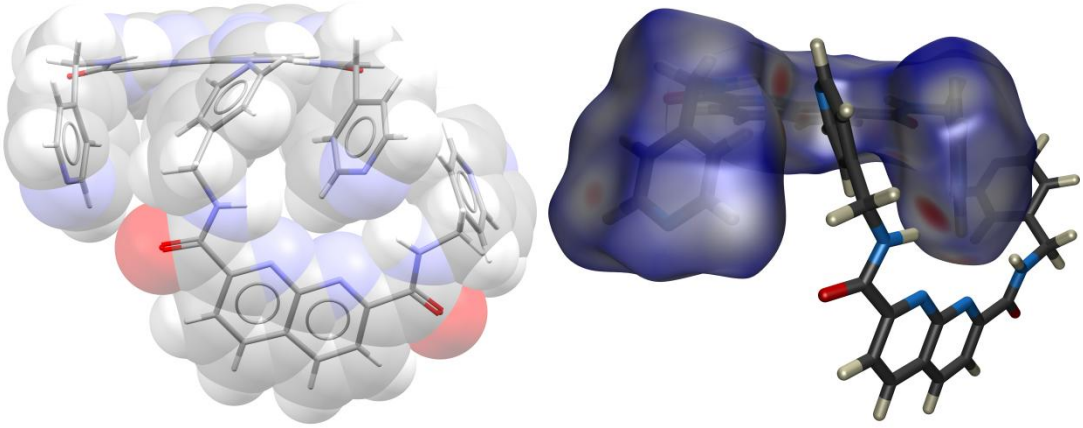

Figure 184 – The self-complimentary dimer formed by N,N'-*bis*-(4-pyridylmethyl)-1,8-naphthyridine-2,7-dicarboxamide (48e) in the solid-state.

Figure 184 shows quite clearly that *N,N'-bis*-(4-pyridylmethyl)-1,8-naphthyridine-2,7-dicarboxamide (**48e**) forms a self-complimentary dimer in the solid-state. This pairing appears to be brought about by the interaction of the amide hydrogen with the pendent pyridine's nitrogen within the cleft of its dimer molecule (**N(11)**···**H(8)**-N(8) 2.51 Å, **N(11)**···H(8)-**N(8)** 3.29 Å (147.3 °) and **N(1)**···**H(10)**-N(10) 2.36 Å, **N(1)**···H(10)-**N(10)** 3.15 Å (149.0). It appears that in this case, unlike that of the 3-pyridyl derivative, only one arrangement of the pendent group can exist with the result being that the pendent rings are not disordered in the present case.

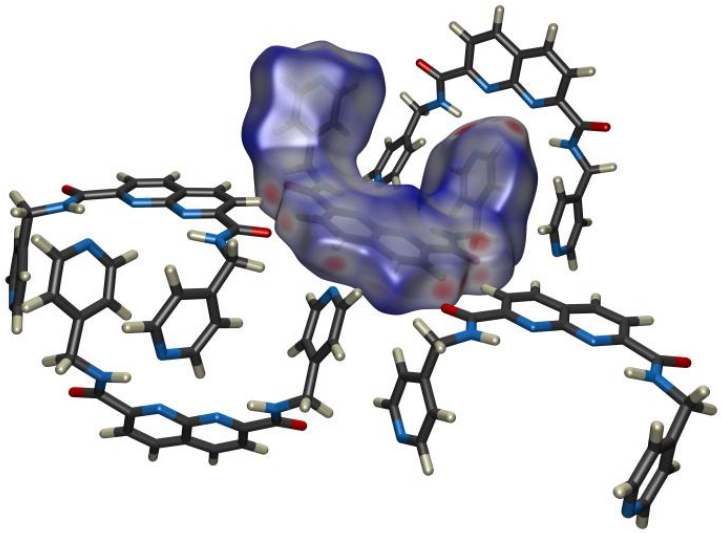

Figure 185 – A Hirshfeld surface highlighting the secondary interactions around the self-complimentary dimer formed by the 4-(pyridylmethyl) derivative (48e).

As Figure 185 shows there are some significant secondary interactions which are key factors in the secondary structure present in this crystal. As there are two non-equivalent molecules these contacts are slightly different in each case.

4.3 Halogen Substituted Benzyl 1,8-naphthyridine-2,7-dicarboxamides (48g-o)

Following on from the success investigating the effects of changing halogen substituents and the substituent position on a benzyl ring, it was hoped that a similar study would be possible with the halogen substituted benzyl amides. However, to date only two compounds have yielded crystals of sufficient quality to run X-ray diffraction studies. The details of these structures are given below.

4.3.1 *N,N'-bis-(*2-Bromobenzyl) 1,8-naphthyridine-2,7-dicarboxamide (48i)

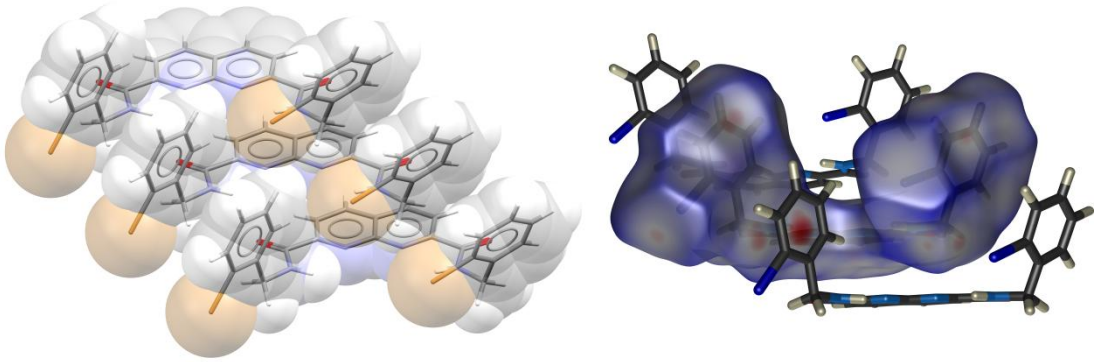

Figure 186 – The basic structure formed by N,N'-*bis*-(2-bromobenzyl)-1,8-naphthyridine-2,7-dicarboxamide. This shows the packing of one molecule on top of the other (left) with the Hirshfeld surface (right) seeming to indicate only one major interaction.

N,N'-bis-(2-Bromobenzyl)-1,8-naphthyridine-2,7-dicarboxamide (**48i**) like the other structures examined so far, adopts the syn-syn conformation. The pendent benzyl groups are bent up out of the plane of the naphthyridine core and are both then twisted away, by differing amounts, from the perpendicular plane to the ring. There appear to be few major interactions in the cleft of the molecule, with the only significant example appearing to be a C-H···π interaction between the amide hydrogen with the pendent benzyl ring. (N-**H**···**π** (centroid) 2.97 Å, **N**-H··· **π** (centroid) 3.54 Å (124.63 °).

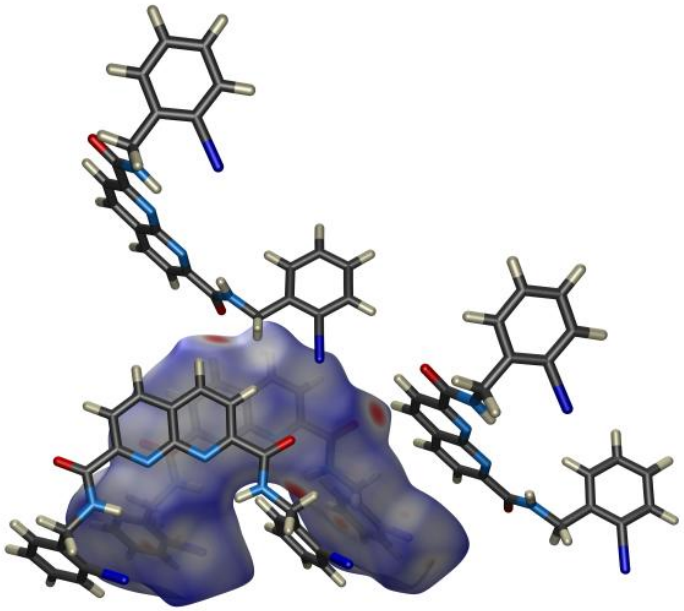

Figure 187 - This top down view on the Hirshfeld surface of the molecule highlights not only the primary packing interaction but also the secondary interactions experienced by the molecule

Figure 187 shows the other interactions experienced by the molecule in the solid state. Other than the interactions involved in the stacking of the molecules it is possible to see that the carbonyl oxygen (O(1)) is once again involved in the secondary interactions forming a contact with one of the naphthyridine hydrogens (H(6)) (C=**O**···**H**-C 2.41 Å C=**O**···H-**C** 3.24 Å (145.2 °)). Further examination of the structure shows that, although the carbonyl group on the other side of the molecule is in close proximity to the neighbouring benzyl ring, the twist of the ring causes the hydrogen that it might otherwise interact with to turn out of its immediate proximity. This interaction may influence the packing of close neighbours into a herringbone motif as can be seen in Figure 187

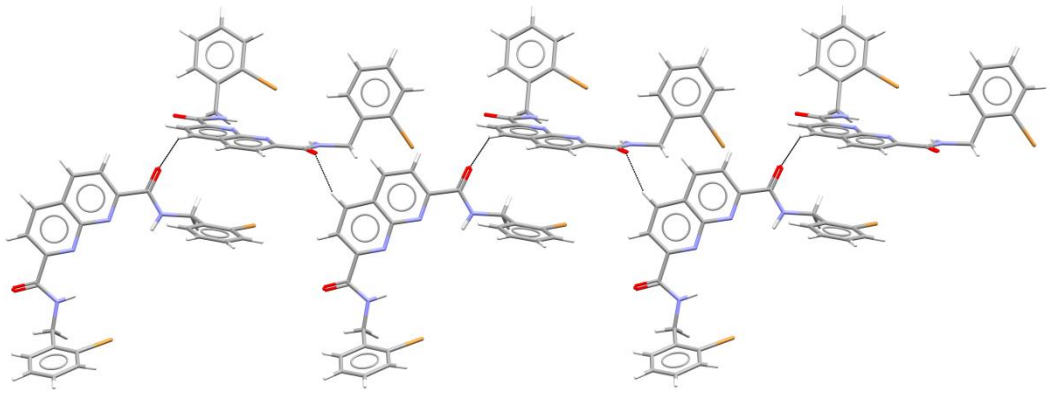

Figure 188 - Illustration of the taping motif resulting from the interaction of the amide carbonyl oxygen and the naphthyridine hydrogen (H-4) on the neighbouring molecule which arrange in a herringbone fashion.

This leads to a rather haphazard secondary packing in which there are obviously defined tapes formed with alternating molecules arranged in a herringboned fashion (Figure 188). However, it is unclear what causes the neighbouring tapes to interact with one another. The Hirshfeld surface suggests that there are some additional close contacts on the periphery of the benzyl ring, perhaps involving C-H ···π interactions.

4.3.2 *N,N'-bis*-(4-Chlorobenzyl)-1,8-naphthyridine-2,7-dicarboxamide (48n)

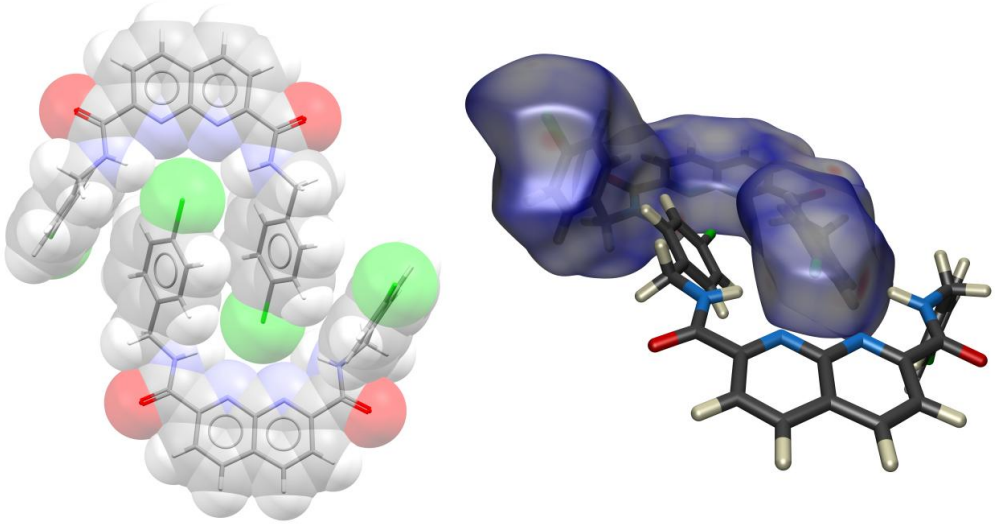

Figure 189 - N,N'-*bis*-(4-chlorobenzyl)-1,8-naphthyridine-2,7-dicarboxamide (48n) forms self-complimentary dimers

N,N'-bis-(4-Chlorobenzyl)-1,8-naphthyridine-2,7-dicarboxamide (**48n**) forms self-complimentary dimers similar to those seen for the 3-pyridyl and 4-pyridyl analogues. It is however, much less clear why the 4-chloro derivative forms this architecture. Careful examination of the Hirshfeld surface (Figure 189) suggests that there is a close contact between the two amide hydrogen atoms and the chloro-substituent although one is significantly shorter. ((**Cl(2)**···**H(12)**-N(12) 2.77 Å, **Cl(2)**···H(12)-**N(12)** 3.60 Å (157.8 °) (**Cl(2)**···**H(21)**-N(21) 3.03 Å, **Cl(2)**···H(21)-**N(21)** 3.90 Å (172.7 °). While one of these could be comfortably called a hydrogen bond-like contact the other is perhaps a little too long.

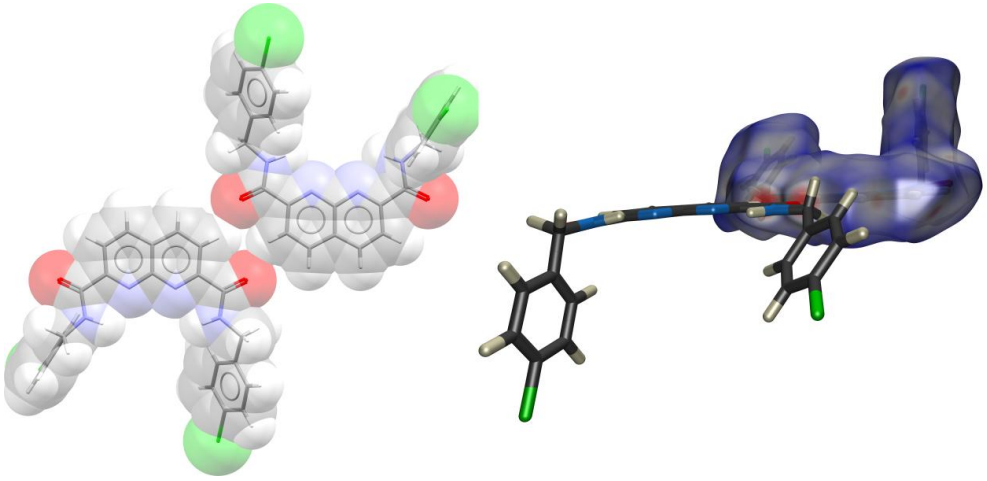

Figure 190 – The carbonyl oxygen atom in the 4-chloro derivative (48n) is once again involved in the formation of the secondary packing architecture.

Once again the carbonyl oxygen atom is heavily involved in the secondary packing architecture. In the present example it is involved in an interaction with one of the naphthyridine hydrogen atoms in a dimeric arrangement which is shown very clearly on the Hirshfeld surface (Figure 190) (C=**O(2)**···**H(3)**-C(3) 2.27 Å C=**O(2)**···H(3)-**C(3)** 3.11 Å (146.9 °)).

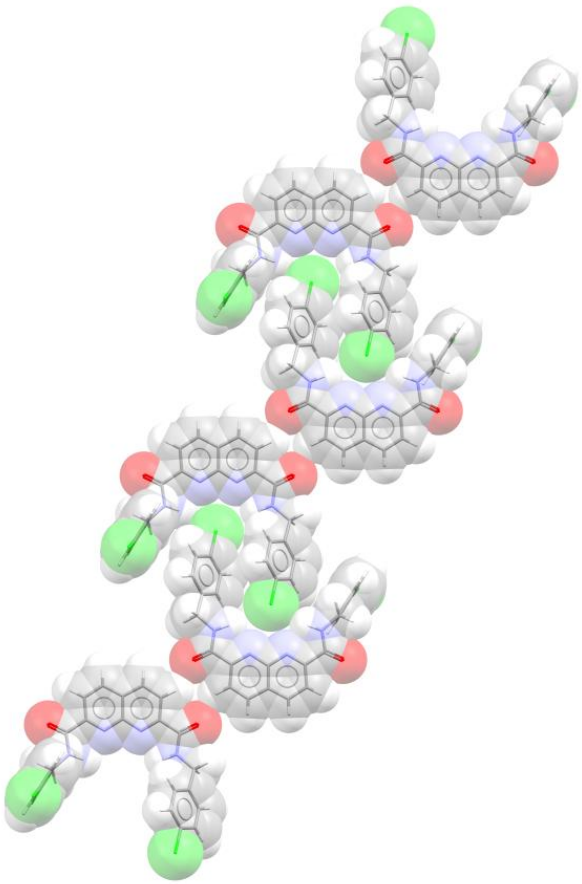

Figure 191 - The combination of the self-complimentary dimer and the carbonyl dimer pair gives rise to the tape like array formed by the 4-chloro derivative (48n).

Figure 191 shows how these two architectural units combine to form a tape-like array. This arrangement appears to be the main structural feature in the secondary packing of these molecules but there are further interactions involved in the packing of these chains.

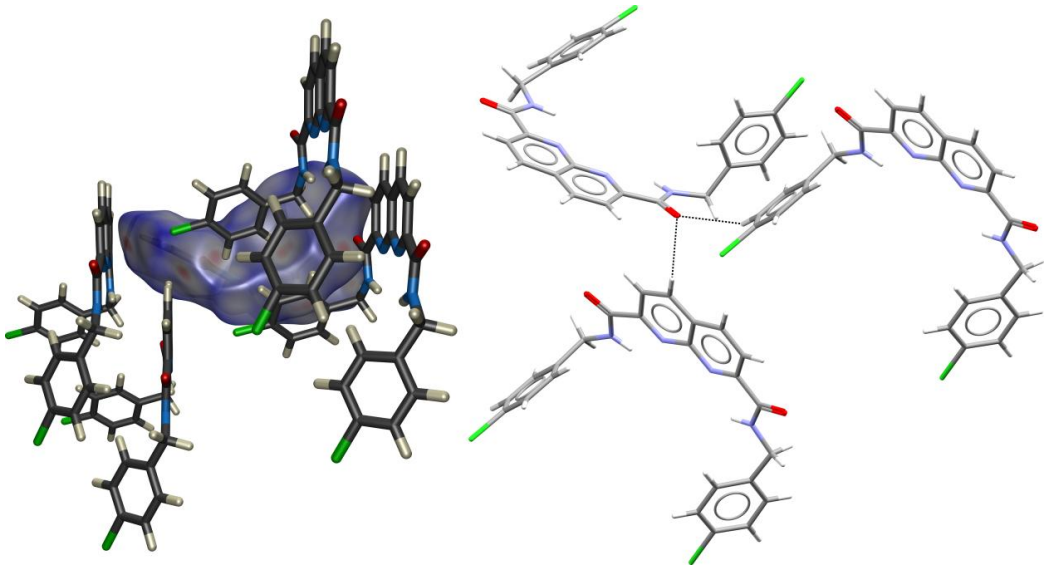

Figure 192 - Investigation of the Hirshfeld surface (left) shows that the carbonyl oxygen interactions aid in the secondary packing motif (right)

As might be expected, the other carbonyl oxygen (O(1)) is involved in the packing of the chains, with two contacts highlighted on the Hirshfeld surface (Figure 192). While they show up on the Hirshfeld surface, these contacts are less intensely coloured than those for O(2), indicating that they are longer contacts, and therefore presumably weaker. These contacts involve two molecules in neighbouring chains which are perpendicular each other; in one case to one of the naphthyridine hydrogen atom (C=**O(1)**···**H(5)**-C(5) 2.51 Å C=**O(1)**···H(3)-**C(3)** 3.14 Å (124.2 °)) and in the other case to one of the hydrogen atom *ortho*- to the chloro- substituent on the pendent ring (C=**O(1)**···**H(27)**-C(27) 2.62 Å C=**O(1)**···H(27)-**C(27)** 3.34 Å (132.7 °)).

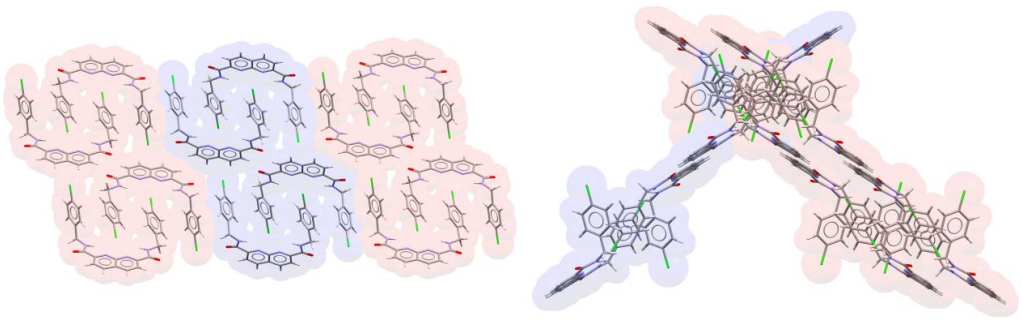

Figure 193 - With all the interactions taken into account it is possible to look at the overall packing which shows the chains packing together with the colouring reflecting the groups at perpendicular alignment to one another.

The overall packing structure of N,N'-*bis*-(4-chlorobenzyl)-1,8-naphthyridine-2,7-dicarboxamide (**48n**) comes about thanks to a number of separate interactions giving a very elegant example of self-assembly. As with all the structures reported thus far, the order that the interactions organise within the structure during crystallisation, poses an interesting dilemma, does the self-complimentary dimer form initially leading to the arrangement of the dimers into tapes, or does the carbonyl dimer form first with the interlinking coming later as a method of close packing.

4.4 N,N'-bis-(4-Nitrobenzyl) 1,8-naphthyidine-2,7-dicarboxamide (48f)

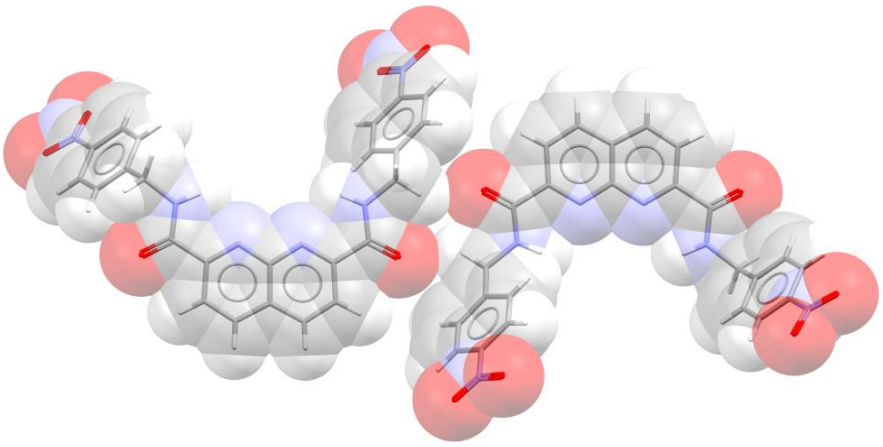

Figure 194 -The structure of *N,N'-bis*-(4-nitrobenzyl)-1,8-naphthyridine-2,7-dicarboxamide (48f) after SQUEEZE has been used to remove the disordered water molecules from the cavity.

N,N'-bis-(4-Nitrobenzyl)-1,8-naphthyridine-2,7-dicarboxamide (**48f**) forms as a particularly insoluble solid which is soluble only in boiling DMSO from which it crashes out very quickly on cooling, Crystals of this compound were grown by controlled cooling of a DMSO solution from near to boiling point. Figure 194 shows the solid-state structure of *N,N'-bis*-(4-nitrobenzyl)-1,8-naphthyridine-2,7-dicarboxamide which has been obtained.

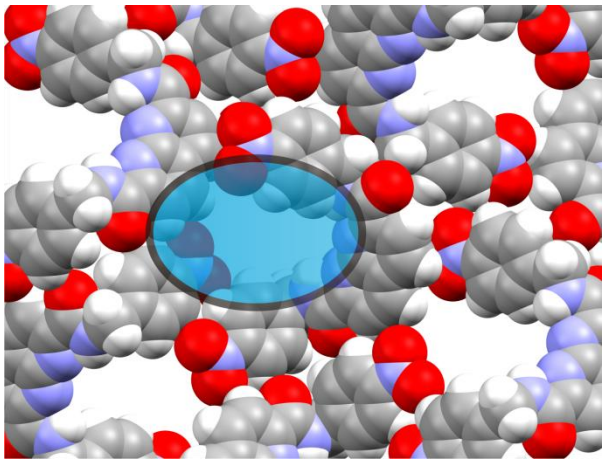

Figure 195 –A representative packing diagram of the structure with the area of excluded solvent density highlighted in blue.

During the structure solution of this molecule it became apparent that there was some form of solvent in the molecular cleft that was proving difficult to satisfactorily model, in order to obtain a crystal structure with satisfactory R-factor, the program SQUEEZE was used to remove the reflections due to this cavity solvent and allowing the refinement to be carried out without these data points.

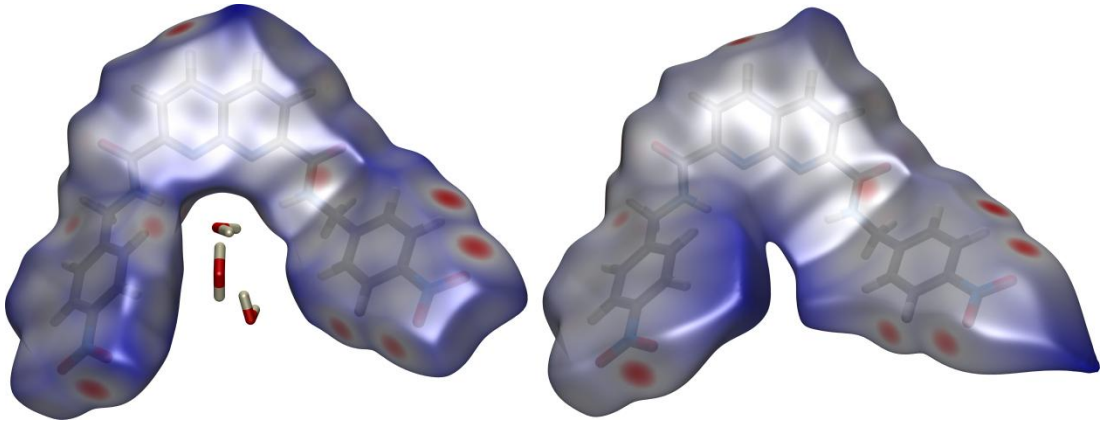

Figure 196 - The effect that the use of SQUEEZE to remove the disordered water molecules has on the Hirshfeld surface is quite marked. However the contacts that are illustrated on the two surfaces are the same. (Structure with poorly modelled solvent in (left) structure after use of SQUEEZE (right)

It is important for the sake of this structural analysis to make note of the presence of this solvent, thought to be water which seemed to exist in some form of extended chain in the area highlighted in Figure 195. The lack of the solvent water molecules also means that the Hirshfeld surface is distorted in the molecular cleft as the surface calculation does not have any ability to deal with voids within the crystal. (Figure 196)

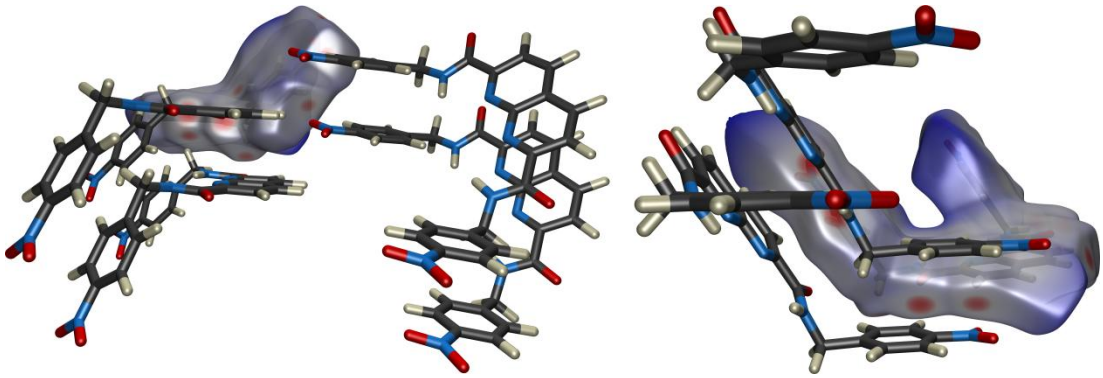

Figure 197 - Looking from both sides of the Hirshfeld surface enables the secondary contacts to be identified which are responsible for the packing of the molecules

The packing architecture for this derivative centres around the dimer contact shown in Figure 194 (C=O(1)···H(10A)-C(10) 2.37 Å, C=O(1)···H(10A)-C(10) 3.23 Å (144.4 °)) (Figure 197), and a pair of contacts on the other amide carbonyl to one of the pendent benzylic hydrogen atom C=**O**(2)···**H**(23)-C(23) 2.37 Å, C=**O**(2)···H(23)-**C**(23) 3.23 Å (144.4 °)).

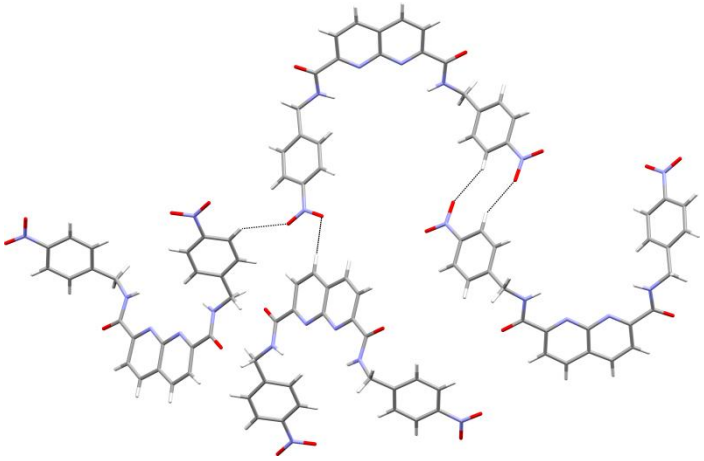

Figure 198 - Additional contacts can be observed from the nitro oxygen atoms leading to the packing arrangement that we observe

The nitro substituents participate in a number of interactions, including a contact between one of the nitro group oxygen atoms to naphthyridine hydrogen atoms (**O**(6)···**H**(5)-C(5) 2.48 Å, **O**(6)···H(5)-**C**(5) 3.28 Å (141.7 °) as well as a contact from nitro O(3) to a neighbouring molecule **O**(3)···**H**(13)-C(13) 2.62 Å, **O**(4)···H(3)-**C**(3) 3.38 Å (136.8 °). Finally the remaining nitro oxygen atoms form interactions with molecules in front of the core which give rise to the formation of the cavity that the disordered waters sit within **O**(4)···**H**(3)-C(3) 2.48 Å, **O**(4)···H(3)-**C**(3) 3.36 Å (153.5 °) and **O**(5)···**H**(21)-C(21) 2.56 Å, **O**(5)···H(21)-**C**(21) 3.43 Å (151.5 °)).

4.5 Conclusion

In this chapter the synthesis of 15 novel 1,8-naphthyridine-2,7-dicarboxamide derivatives are reported. It has been possible to obtain X-ray diffraction solid-state structures of 6 of these derivatives. In addition it has also been possible to obtain the solid-state structures of *N,N'-bis*-(2-pyridyl)-1,8-naphthyridine-2,7-dicarboxamide dihydrochloride (**48c·2HCl)** and a *N,N'-bis*-(2-pyridyl)-1,8-naphthyridine-2,7-dicarboxamide copper complex (**48c·2Cu**). The structures reported in this chapter have demonstrated primary packing behaviour similar to that observed in the pyridine-2,6-dicarboxamide systems. By examination of the Hirshfeld surface of these structures it has become apparent that, while the interactions within the cleft of the dicarboxamide are important for the primary packing motif, the interactions formed by the carbonyl oxygen atoms appear to be crucial to the formation of secondary packing motif. The metal complex reported, along with the literature precedent discussed in the introduction, show that the 1,8-naphthyridine-2,7-dicarboxamides may be used as metal complexation ligands. It is hoped that further work would allow the collection of X-ray structural information for the remaining 1,8-napthyridine derivatives reported, as well as a more complete examination of the metal binding properties of these materials.

5 2,6-Dicarbonyl Substituted Pyridine Derivatives.

5.1 Halogen Substituted bis-benzyl pyridine-2,6-dicarboxylate derivatives

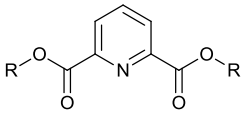

25

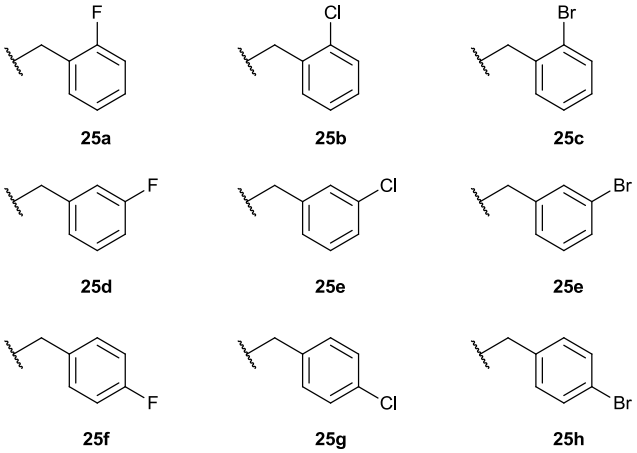

25a **25b** **25c**

25d **25e** **25e**

25f **25g** **25h**

Given the previous work in the group on 4-substituted benzyl pyridine-2,6-dicarboxylates (**25f-h**) and the interesting structural changes observed in the 2- and 3-halogen substituted *bis*-benzyl 1,8-naphthyridine-2,7-dicarboxylates, it was hoped that synthesis of the analogous pyridine-2,6-dicarboxylates (**25a-e**) would provide further insight into the effects of halogen substitution on the secondary structure; not only between structural analogues but also between systems with three and four hydrogen bond arrays respectively. The structures of the 4-halogen-substituted benzyl derivatives (**25f-h**) shown here are those previously reported in the literature by the group.[197] The 2- and 3-halogenated *bis*-benzyl 1,8-naphthyridine-2,7-dicarboxylates (**25a-e**) were prepared by the reaction of the corresponding alcohol with pyridine-2,6-dicarbonyl dichloride in the presence of triethylamine, and the samples were then crystallised in order to undertake X-ray structural studies.

5.1.1 *bis*-(2-Fluorobenzyl) pyridine-2,6-dicarboxylate (25a)

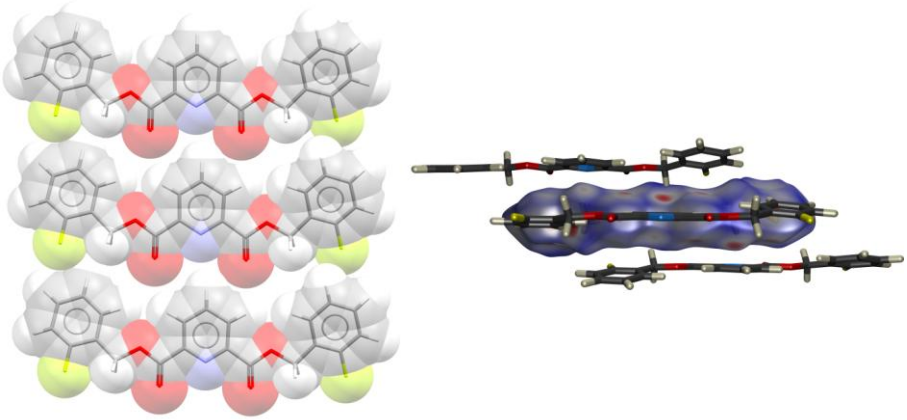

Figure 199 - At first glance (2-fluorobenzyl) pyridine-2,6-dicarboxylate (25a) forms the expected infinite 1D tapes (left) however the Hirshfeld surface (right) shows no sign of the expected hydrogen bonding contacts.

As discussed in the introduction, there are very few examples of pyridine-2,6-dicarboxylates for which the expected one-dimensional tapes do not form. On first inspection (2-fluorobenzyl) pyridine-2,6-dicarboxylate (**25a**) appears to follow the expected behaviour however, on closer examination of the Hirshfeld surface and by measuring the contact distances present it becomes apparent that while this compound adopts the expected packing arrangement, it might not be due to the expected hydrogen bonding array

The contact distances for the expected hydrogen bond array contacts are **N**···**H**-C 3.05 Å, **N**···H-**C** 4.00 Å (170.7 °) for the pyridine nitrogen to C(4)-H contacts while the two carbonyl oxygen contacts are C=**O**···**H**-C 2.88 Å, C=**O**···H-**C** 3.44 Å (119.0 °) and C=**O**···**H**-C 3.01 Å, C=**O**···H-**C** 3.72 Å (133.1 °) respectively. It is clear from this data that, in the present case, either these contacts are not present or that they are significantly weaker than expected. The Hirshfeld surface does highlight one contact in the expected array which is usually considered to be a secondary interaction from the carbonyl oxygen O(2) to the hydrogen in the *γ* position from the pyridine nitrogen (C=**O**···**H**-C 2.67 Å, C=**O**···H-**C** 3.39 Å (128.4 °)).

The Hirshfeld surface (Figure 199 right) does however suggest the presence of other interactions to the molecules in the neighbouring layer. The most obvious of these involves contacts between the methylene C-H and the pyridine nitrogen, in a manner analogous to that seen in the 3- and 4- bromo- and chloro- *bis*-benzyl 1,8-naphthyridine derivatives (**N**···**H(7A)**-C(7) 2.53 Å, **N**···H(7A)-**C(7)** 3.48 Å (162.3 °),

N···**H(15A)**-C(15) 2.78 Å, **N**···H(15A)-**C(15)** 3.72 Å (158.2 °)). It would appear when looking at the spatial location of the atoms involved that the methylene C-H bonds sit at just the right orientation to interact between layers. There are a few further contacts which are focused around the fluorine atom on the pendent ring. However the nature of these interactions is hard to determine; are they simply a steric clash resulting from close packing or are they an interaction which contributes to the association of the molecular array?

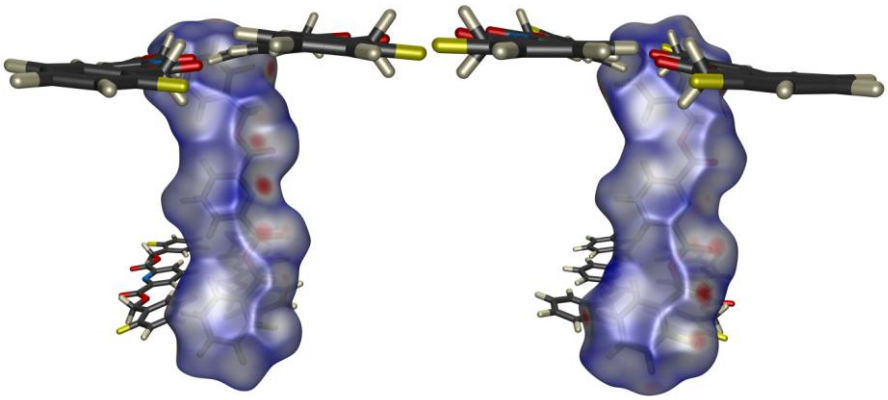

Figure 200 – The Hirshfeld surface identifies close contacts to the pendent rings which would appear to influence the secondary packing of (2-fluorobenzyl) pyridine-2,6-dicarboxylate.

Examination of the Hirshfeld surface shows that there are two contacts on the periphery of the molecule which might influence the secondary packing of the pseudo-tapes. One such interaction is between C(19)-H(19) and one of the pendent benzyl rings (C-H···π(centroid) 2.85 Å) while the other interaction appears to be between C(2)-H(2) and the carbon to which the fluorine is attached (C-**H**···**C**-F) 2.77 Å), though it is unclear if this is an attractive interaction or simply a steric clash.

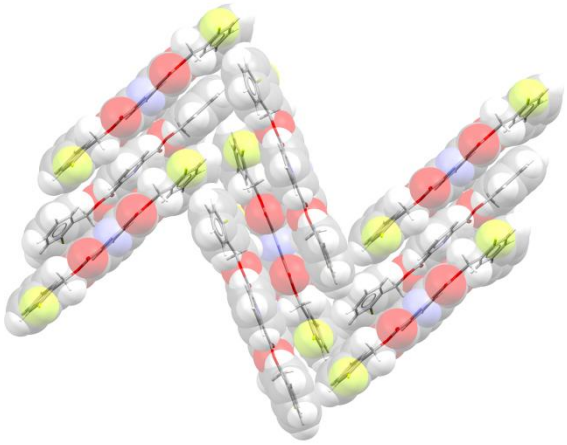

Figure 201 – Secondary interactions lead the pseudo tapes of (2-fluorobenzyl) pyridine-2,6-dicarboxylate to adopt a herringbone packing motif.

Whether these are true interactions or not, it is very obvious that in (2-fluorobenzyl) pyridine-2,6-dicarboxylate there is something which causes the molecules to pack in a herringbone motif (Figure 202).

5.1.2 *bis*-(2-Chlorobenzyl) pyridine-2,6-dicarboxylate (25b)

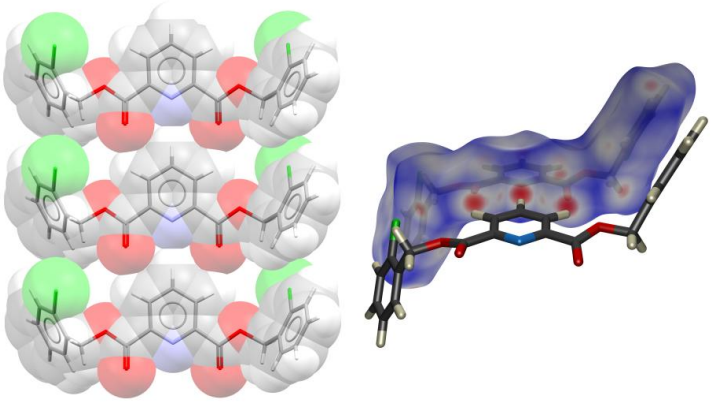

Figure 202 - (2-Chlorobenzyl) pyridine-2,6-dicarboxylate can be seen to arrange itself into "true" infinite one dimensional tapes thanks to the expected hydrogen bonding array.

Having seen such unexpected behaviour from the 2-fluoro derivative (**25a**) it is somewhat reassuring to observe that this behaviour is most likely an anomaly as the (2-chlorobenzyl) analogue (**25b**) forms the expected one dimensional tapes with the normal contacts being observed on the Hirshfeld surface (**N**···**H**-C 2.53 Å, **N**···H-**C** 3.49 Å (180 °) and C=**O**···**H**-C 2.47 Å, C=**O**···H-**C** 3.12 Å (126.0 °)) (Figure 202). The Hirshfeld surface also infers some form of interaction between the pendent chlorine substituent and the methylene hydrogen (**Cl**···**H**-C 2.93 Å, **Cl**···H-**C** 3.72 Å (140.5 °)).

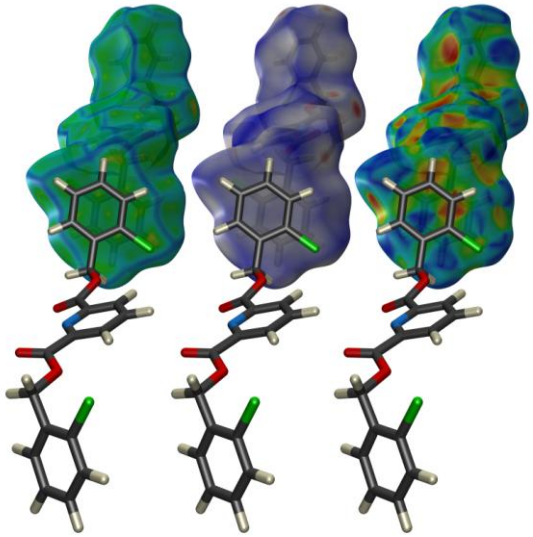

Figure 203 – Examination of Hirshfeld surfaces with colouring of curvedness (left) d(norm) (centre) shape index (right) indicates the presence of a π···π contact between neighbouring tapes.

The pendent ring is bent out of the plane of the pyridine core and examination of the various colourings of the Hirshfeld surface (Figure 203) gives an indication that this may be in order that the rings can interact with the pendent ring of neighbouring tape assemblies (inter-centroid distance 3.63 Å). It is also worth noting that the rings align so that the chlorine substituents are oppositely aligned which could infer that this interaction could be a combination of a π···π interaction and a dipole-dipole interaction.

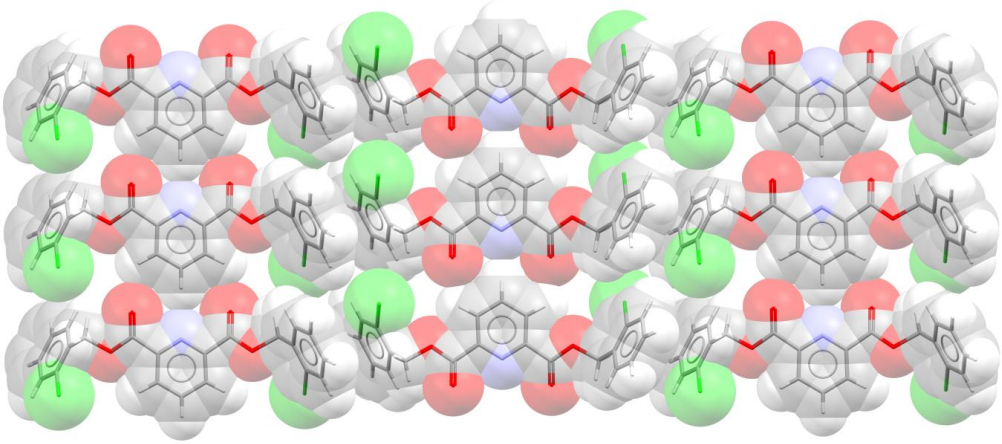

Figure 204 - The interaction between the pendent rings means that the tapes align into sheets in which the neighbouring tape has an anti-parallel alignment.

This interaction ensures that the tapes align into stepped sheets in which neighbours are aligned in an anti-parallel manner (Figure 204).

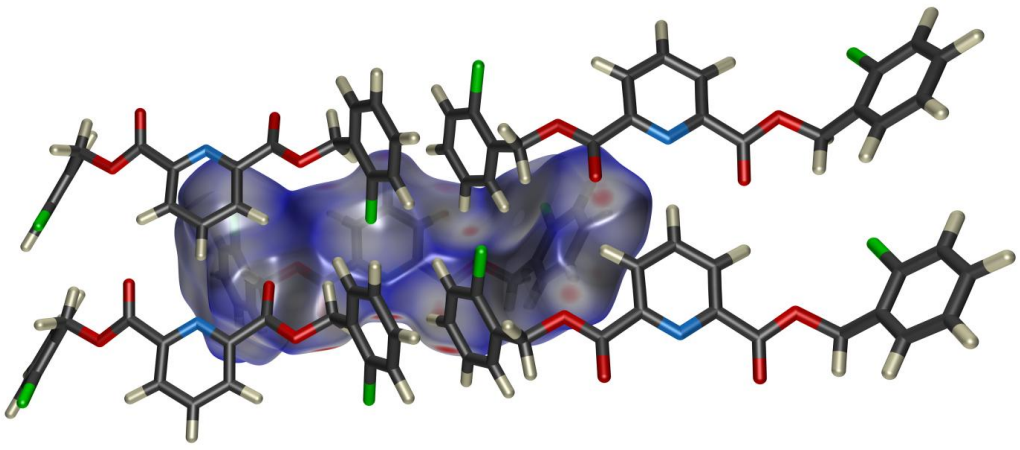

Figure 205 – This Hirshfeld surface explores inter-sheet contacts in the secondary structure of (2-chlorobenzyl) pyridine-2,6-dicarboxylate.

The Hirshfeld surface in Figure 205 suggests the presence of two inter-sheet interactions are highlighted, one being between the carbonyl oxygen atom and the hydrogen *meta* to the chlorine substituent (C=**O**···**H**-C 2.68 Å, C=**O**···H-**C** 3.39 Å

(133.0 °)) while the other is from the ether oxygen to the hydrogen *para* to the chlorine substituent (**O**···**H**-C 2.76 Å, C=**O**···H-**C** 3.66 Å (164.5 °)).

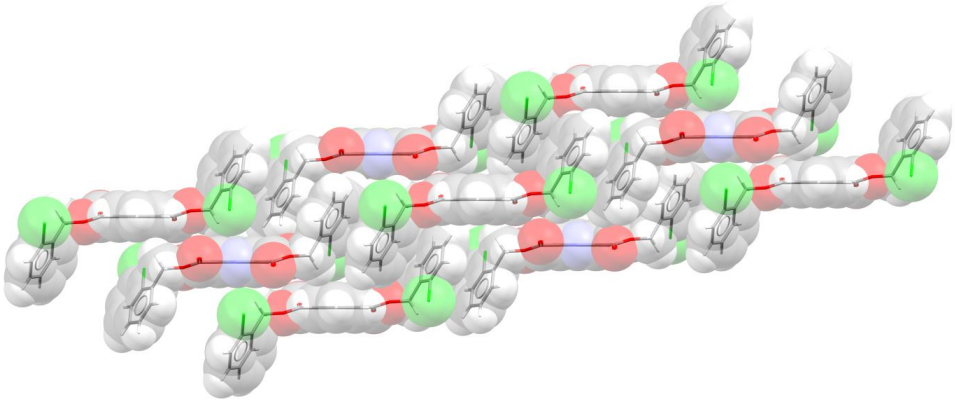

Figure 206 - The interactions highlighted in Figure 205 are involved in the formation of the packing of the sheets into the secondary structure observed.

The sheets of molecules then pack into stacks in which the corrugated sheets are slightly offset relative to each other and with the neighbouring tapes sitting in an anti-parallel arrangement (Figure 206). However, it is difficult to be sure if the interactions shown in Figure 205 are involved in the formation of this packing arrangement or if they are simply a consequence of it.

5.1.3 *bis*-(2-Bromobenzyl) pyridine-2,6-dicarboxylate (25c)

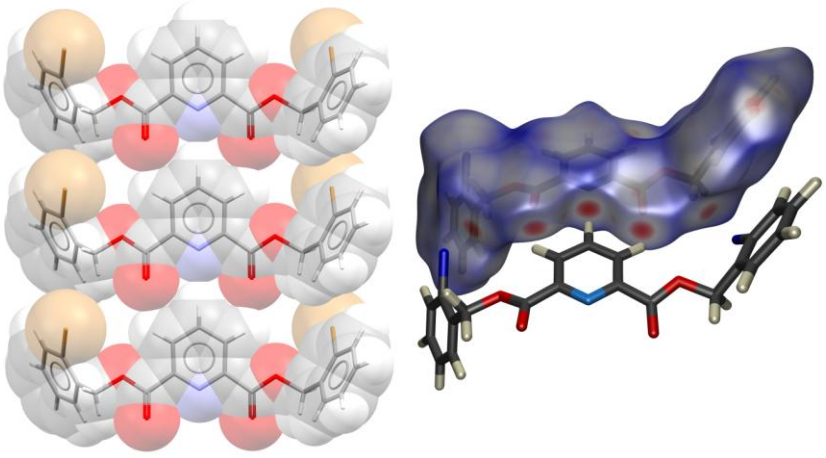

Figure 207 – The solid state structure of (2-bromobenzyl) pyridine-2,6-dicarboxylate bear great similarity to that observed in the 2-chlorobenzyl derivative.

From initial examination of the solid-state behaviour of (2-bromobenzyl) pyridine-2,6-dicarboxylate (**25c**) (Figure 207) it appears that the molecule adopts a stucture which is isostructural to that seen for the 2-chlorobenzyl derivative. Given the

behaviour of the chloro- and bromo- benzyl 1,8-naphthyridine derivatives this is unsurprising. The expected hydrogen bonding array contacts form (**N**···**H**-C 2.61 Å, **N**···H-**C** 3.54 Å (180 °) and C=**O**···**H**-C 2.52 Å, C=**O**···H-**C** 3.17 Å (127.2 °)) and align the molecules into the expected infinite one dimensional tapes. There also appears to be a weak interaction between the pendent halogen substituent and the methylene hydrogen (**Br**···**H**-C 2.92 Å, **Br**···H-**C** 3.70 Å (138.8 °). The increased size of the halogen substituent in this case could be partly responsible for the slight increase in length of the pyridine core's hydrogen bonded array interaction distances.

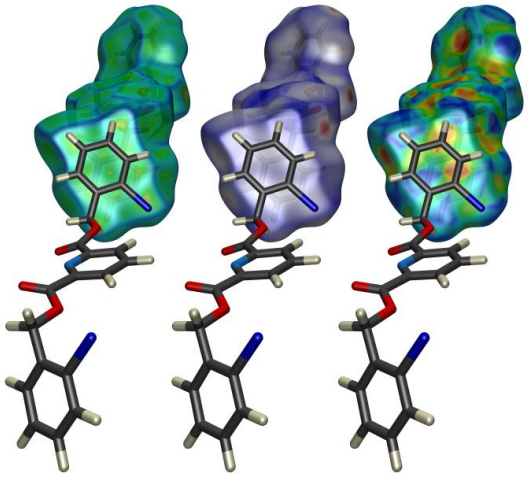

Figure 208 - As with the 2-chloro derivative the Hirshfeld surface for the 2-bromo derivative gives an indication that there is a π···π interaction between the two pendent benzyl rings.

As with the 2-chloro derivative the Hirshfeld surfaces (Figure 208) seem to suggest that the pendent benzyl rings undergo some form of interaction (inter-centroid distance 3.71 Å)

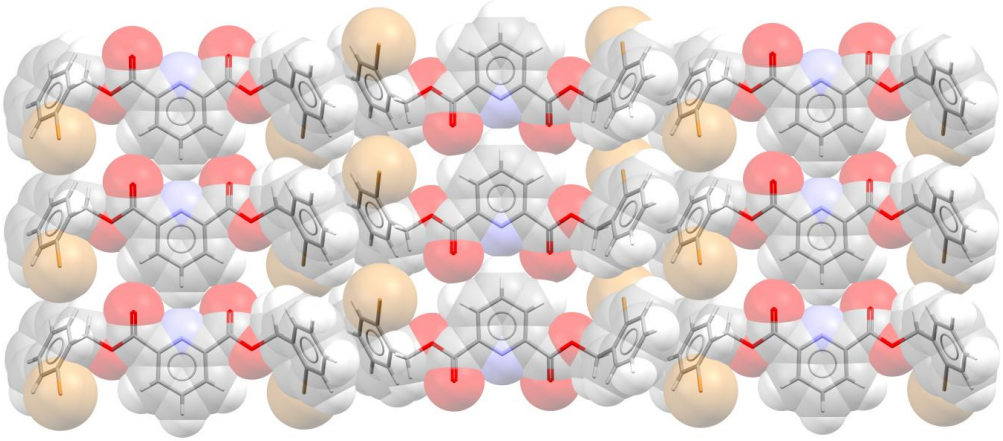

Figure 209 - The interaction between the pendent rings means that the tapes align into sheets in which the neighbouring tape is anti-parallel in alignment.

This interaction leads to the formation of the sheet-like structure shown in Figure 209. The architecture is step-packed which gives the sheet the appearance of being corrugated.

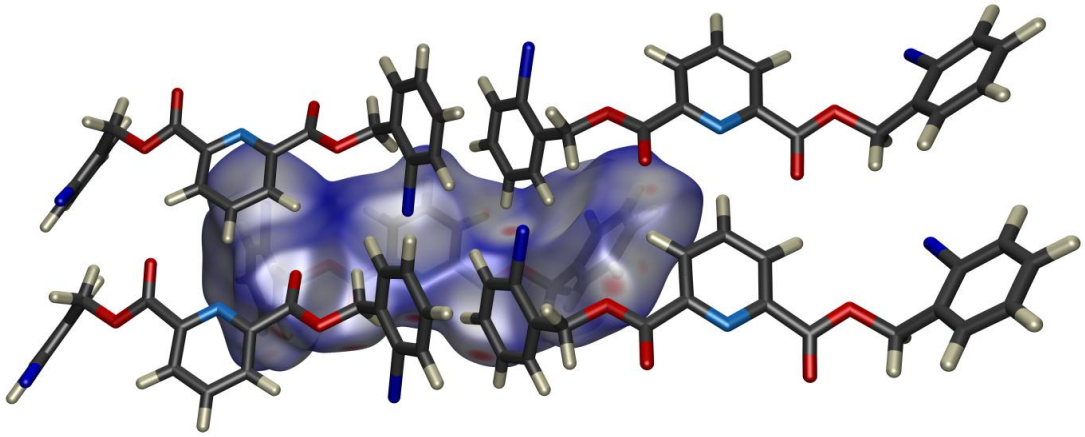

Figure 210 - This Hirshfeld surface diagram shows that the inter-sheet interactions that were observed in the 2-chloro derivative are present in this isostructural compound

Figure 210 highlights that the contacts observed for the 2-chloro derivative remain present for its bromo- analogue namely those between the carbonyl oxygen and the hydrogen *meta* to the bromine substituent (C=**O**···**H**-C 2.77 Å, C=**O**···H-**C** 3.48 Å (133.3 °)) and from the ether oxygen to the hydrogen *para*- to the chlorine substituent (**O**···**H**-C 2.73 Å, C=**O**···H-**C** 3.63 Å (164.2 °)).

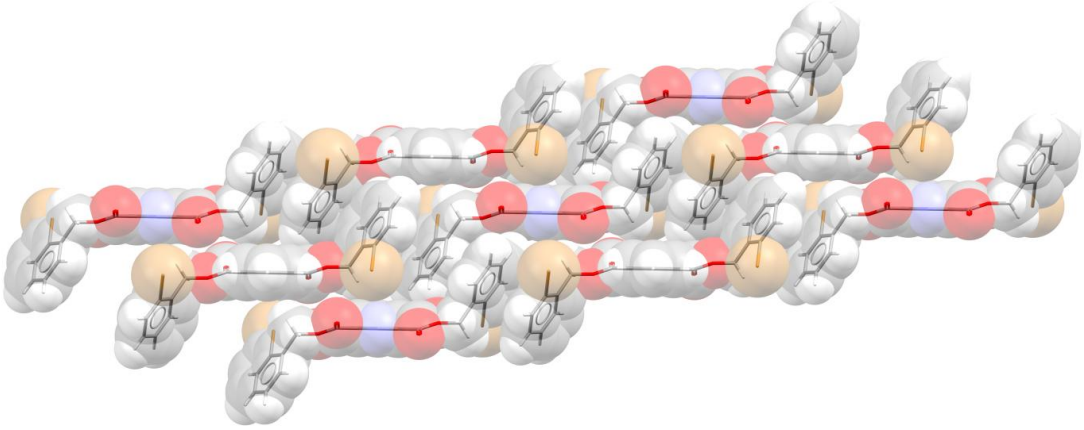

Figure 211 - Packing of the corrugated sheets leads to the secondary architecture shown above.

These interactions give rise to the secondary packing architecture shown in Figure 211, identical to that seen in the 2-chloro derivative.

5.1.4 *bis*-(3-Chlorobenzyl) pyridine-2,6-dicarboxylate (25e)

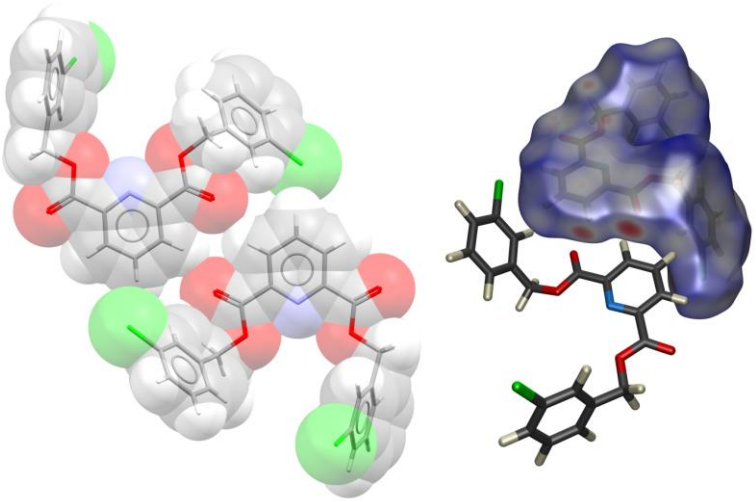

Figure 212 - In the case of (3-chloro) pyridine-2,6-dicarboxylate it appears that the main contact is the dimer formation through the carbonyl oxygen

Having shown that the (2-fluorobenzyl) pyridine-2,6-dicarboxylate (**25a**) was anomolous in its solid-state architecture, forming a psuedo tape-like array with extended contact distances, we find that (3-chlorobenzyl) pyridine-2,6-dicarboxylate (**25e**) is another anomolous example. Within the asymetric unit there are two separate molecules which are mirror images of one another, most interestingly within these two molecules the carbonyl groups adopt an anti – anti orientation. This behaviour means that the main contacts appear to be a dimer pairing from the the carbonyl oxygen to the pyridine hydrogen (C=**O(6)**···**H(2)**-C(2) 2.34 Å, C=**O(6)**···H(2)-**C(2)** 3.19 Å (151.9 °) and (C=**O(2)**···**H(24)**-C(24) 2.49 Å, C=**O(2)**···H(24)-**C(24)** 3.36 Å (155.8 °)) (Figure 212).

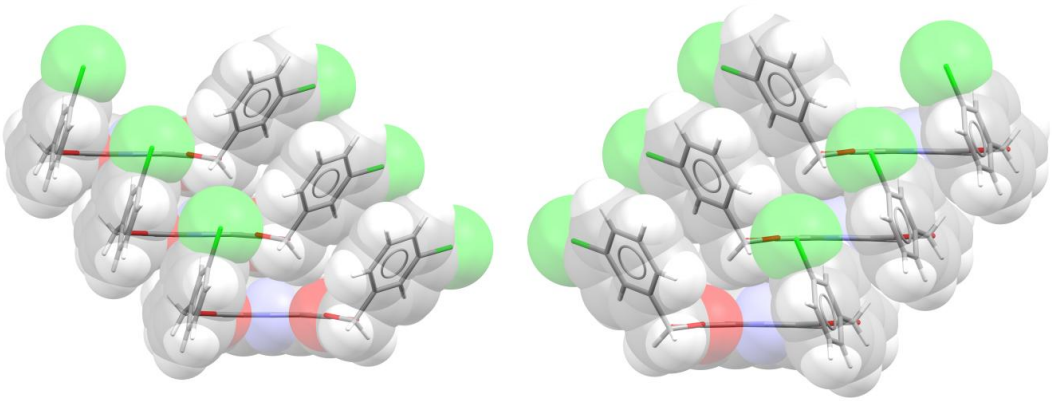

Figure 213 - In both conformers one pendent ring is almost perpendicular to the pyridine core while the other is turned out of the plane.

Contacts of this type are more typical in the pyridine-2,6-dicarboxamides than in the pyridine-2,6-dicarboxylates which, considering the structural arrangement of this derivative (Figure 213) is unsurprising. It is the only known example of this behaviour in a pyridine-2,6-diester derivative.

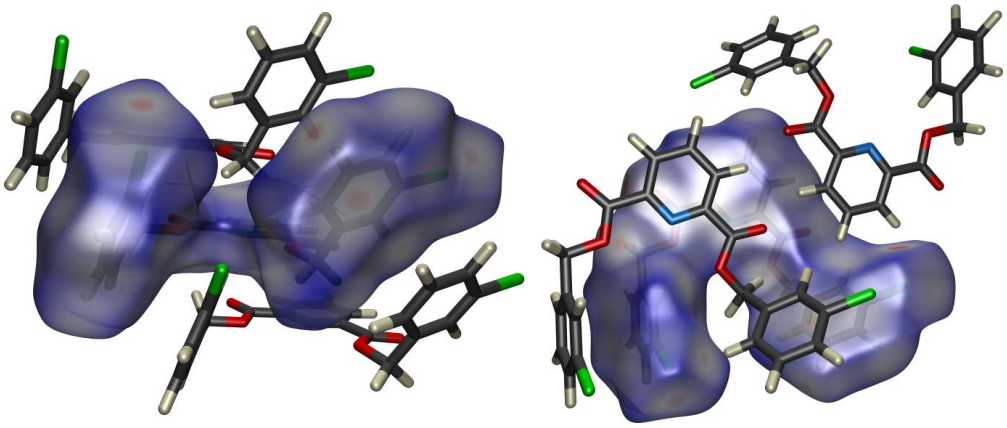

Figure 214 –The Hirshfeld surfaces allow the examination of secondary interactions between packed molecules which may be responsible for the packing arrangement observed.

While the interactions that direct the formation of the dimer pair are simple to visualise the contacts which cause the secondary packing are more complicated. Examining the Hirshfeld surfaces (Figure 214) of one of the molecules shows that there are no clear interactions within the molecular cleft, instead that there are a number of weak interactions on the periphery.

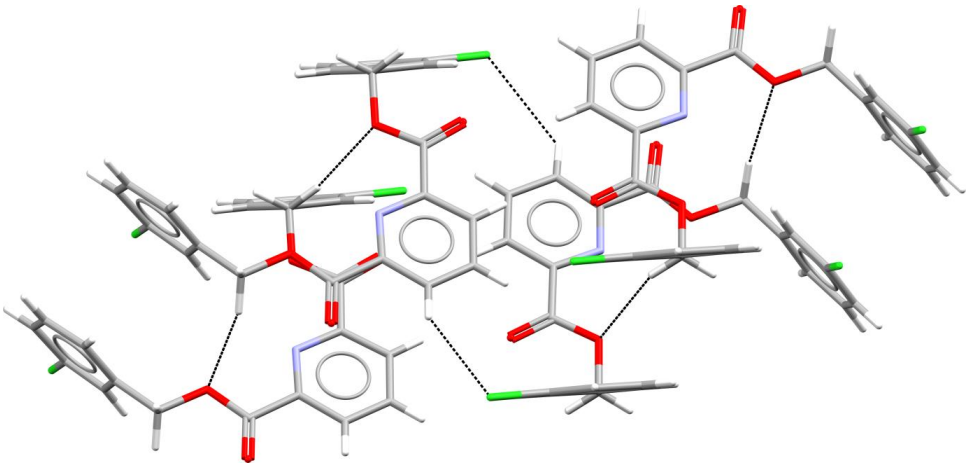

Figure 215 –The weaker interactions on the periphery are shown complicated slightly by the fact that there are two units in the asymmetric unit.

Figure 215 shows the interactions which are highlighted on the Hirshfeld surface, with each contact being duplicated as there are two inequivalent molecules in the

asymmetric unit. It appears that these are the interactions that are responsible for the packing of the molecules into the stacks show in Figure 213.

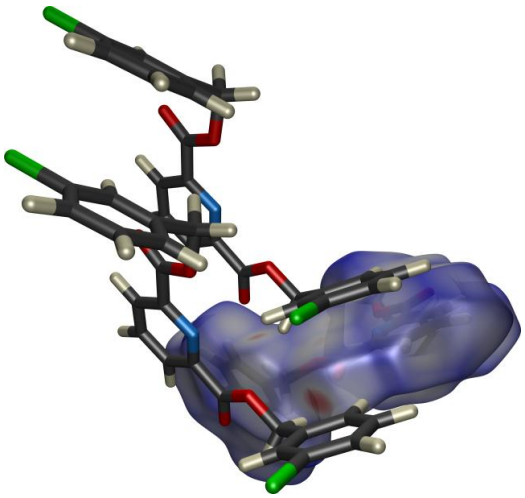

Figure 216 - The Hirshfeld surface of the non-dimer forming carbonyl shows that it does take part in another interaction aiding the formation of the herringbone formation.

Having looked at the interactions that cause the stacking of the molecules, it only remains to attempt to understand which interactions are involved in the packing of the stacks into the complete architecture. The Hirshfeld surface shown in Figure 216 highlights that the carbonyl atom not involved in the main dimer pairing undergoes a pair of weaker interactions: (C=**O(5)**···**H(16A)**-C(16 2.41 Å, C=**O(5)**···H(16A)-**C(16)** 3.37 Å (150.0 °) and (C=**O(1)**···**H(29A)**-C(29) 2.67 Å, C=**O(1)**···H(29A)-**C(29)** 3.51 Å (144.4 °)). These could be responsible for the secondary packing of the stacks.

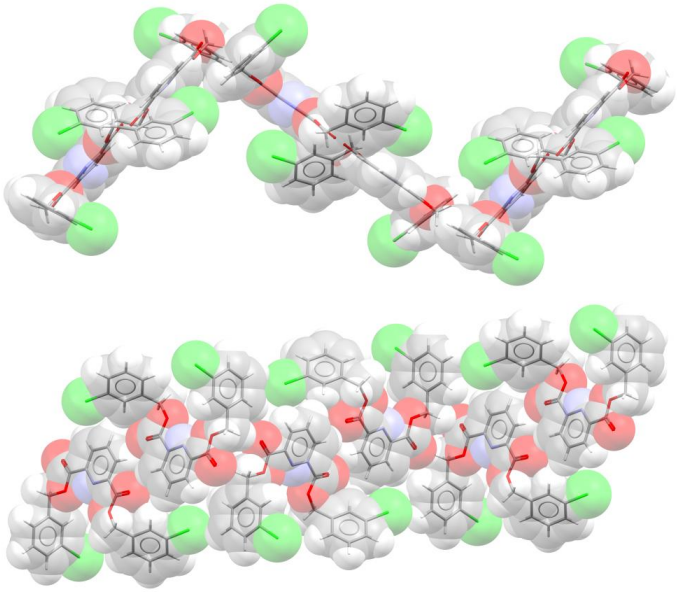

Figure 217 – The combination of these interactions leads to a packing arrangement in which the stacks of tapes align themselves in a herringbone fashion.

The pair of interactions depicted in Figure 216 would appear to ensure that each dimer pair of molecules associates with its neighbour to form a herringbone arrangement in which stacks of tapes are almost at right angles to one another.

5.1.5 Comparison of Halogen Substituted Benzyl Pyridine-2,6-dicarboxylates

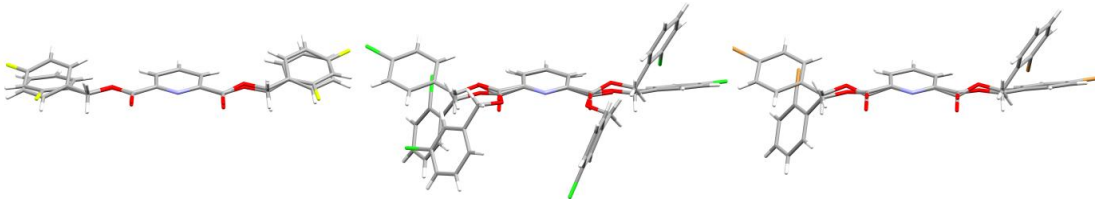

Figure 218 – The crystal structures for each series of halogen substituted benzyl pyridine-2,6-dicarboxylate structural isomers are overlaid. (fluoro- derivatives on the left, chloro derivatives in the middle, and the bromo derivatives on the right).

Although it has not been possible to obtain structures for 3-fluoro and 3-bromo benzyl derivatives (**25d** and **25f**) it is useful to compare the different conformations that the mono halogen substituted benzyl derivatives adopt. What is immediately obvious is that the two fluorine substituted benzyl derivatives have quite a similar positioning of the pendent arms, although that for the 2-fluorobenzyl derivative is deceptive because of the extended contacts within the taping motif. While in both the chlorine and bromine substituted systems there appears to be great variety of positioning of the pendent side arms, especially for the 3-chlorobenzyl derivative which adopt a structure and packing motif more reminiscent of a pyridine-2,6-dicarboxamide system.

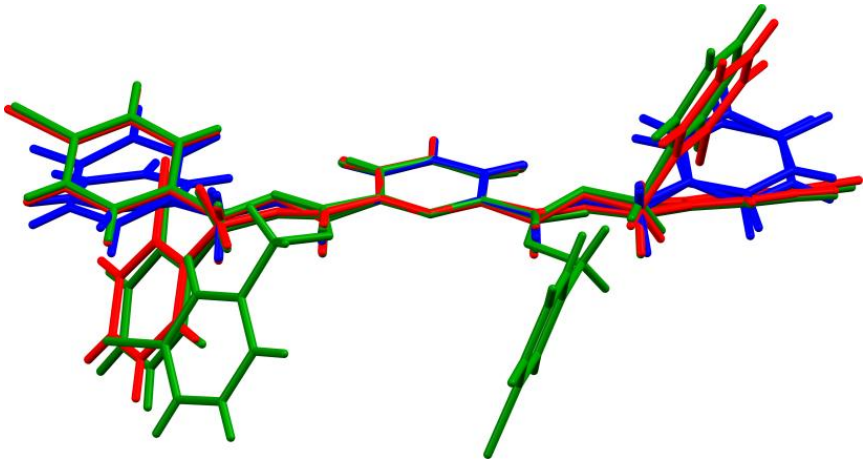

Figure 219 – With all the halogen substituted benzyl derivatives overlaid the structural changes are clear to see (F = Blue Cl= Green Br = Red)

By overlaying all the structures available (Figure 219) it is possible to see two things: Firstly the structures of the chlorine and bromine substituted benzyl derivatives are extremely similar for each substitution position while the fluorine derivatives are starkly different; Secondly the chloro- substituted benzyl derivatives serve to illustrate the low energy of interconversion for the orientation of the pendent side arms, with the 2-chloro derivative displaying one pendent group in the plane of the pyridine core and one bent out of the plane of the ring, the 4-chloro derivative has both pendent arms in the plane of the pyridine core and the 3-chloro derivative displays the dicarboxamide-like orientation. Interestingly it appears that there is little evidence of halogen – halogen contact between the derivatives reported in this work.

5.2 Chelidamic Acid Derivatives

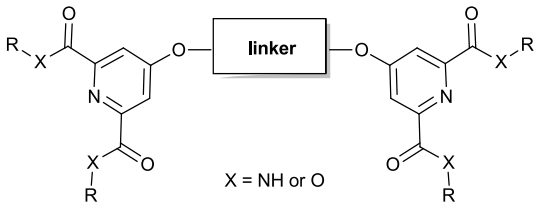

Figure 220 – It was envisaged that by linking two pyridine-2,6-dicarbonyl functionalised units together it would be possible to produce materials that offered interesting solid-state architectures and had potential utility as supramolecular polymers

Following on from previous work in the group[181] it was envisaged that linking two pyridine-2,6-dicarbonyl functionalised units together via a simple spacer (Figure 220) could yield materials with potential application for forming supramolecular polymers when co-ordinated to metal ions. In the intervening years Yin[275] has published a synthetic route to tetraethyl-4,4`-[butane-1,4-diyl*bis*-(oxy)]dipyridine-2,6-dicarboxylate (

Scheme 11).

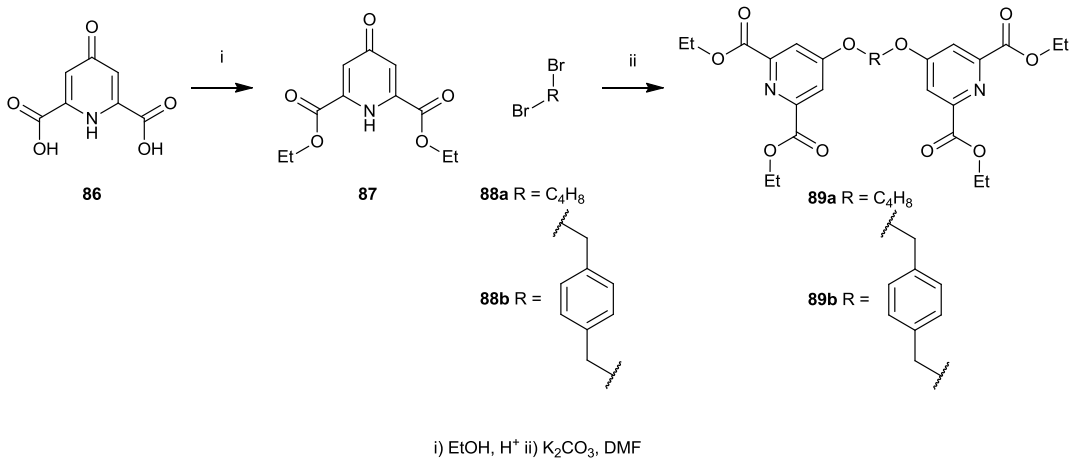

Scheme 11 – Yin's synthetic route to linked chelidamic acid units.[181]

This was seen as a useful synthetic methodology for the synthesis of linked chelidamic acid units which could then be further functionalised to yield materials analogous to the simple pyridine-2,6- diester and diamide derivatives. Given the ability of *N,N'-bis*-(2-pyridyl) pyridine-2,6-dicarboxamide to form a self-assembled molecular structure as well as acting as a ligand to a number of metal centres. It was selected as a suitable target to test this concept.

5.2.1 Synthesis of Chelidamic Acid

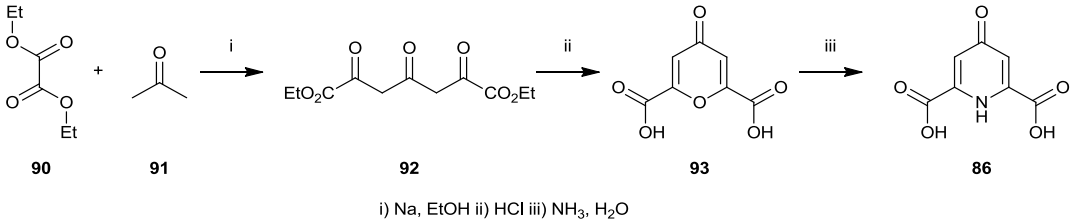

Scheme 12 - Literature synthesis of chelidamic acid.[181]

A key component for this work was chelidamic acid and while chelidamic acid is available from commercial sources it is not only expensive but it has been found in previous work in the group that the quality is, at best, poor. As a consequence of this the majority of chelidamic acid used in the Grossel group has been synthesised in house, using the synthetic route in Scheme 12, as this gives a known level of purity.[181] Fortunately large quantities of chelidonic acid remained from previous preparations so this was the starting point for the present work. The reaction with ammonium hydroxide to form **86** yielded a crude material which was then recrystallised in batches from very large volumes of water.

5.2.2 Linking Two Chelidamic Units Together

The synthetic procedure reported by Yin[275] was followed (

Scheme 11). This yielded the desired tetraethyl-4,4`-[butane-1,4-diyl*bis*-(oxy)]dipyridine-2,6-dicarboxylate. From this point attempts were made to convert the tetraester into a tetraamide (Scheme 13).

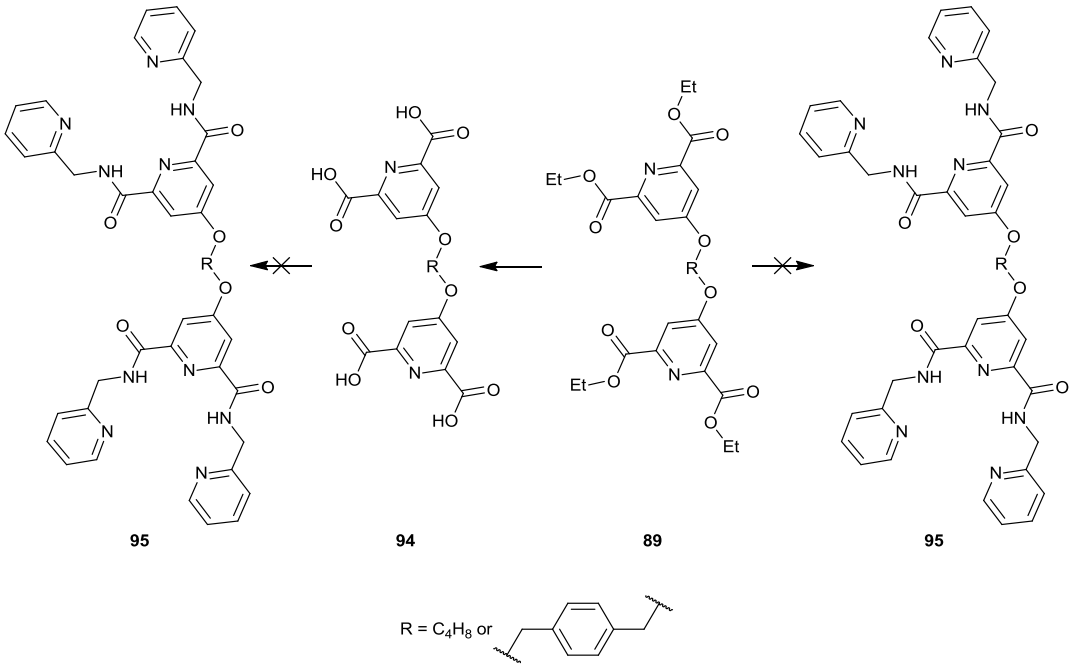

Scheme 13 - Attempted synthesis of tetraamide (91)

While synthesis of the tetra ester (**89**) proved successful further functionalisation of this system proved to be difficult. Literature precident[276] was found for a simple transformation of the ester (**89**) to an amide (**95**). However, this conversion was attempted several times using both zinc chloride and anhydrous tin (IV) chloride as the Lewis acid catalyst, but on each occasion a white precipitate was formed when the 2-(aminomethyl) pyridine was added. It would appear that the white precipitate formed was, in fact, a co-ordination complex with the metal centre meaning that neither material was available to effect the reaction. This theory is backed up by the number of co-ordination complexes involving 2-(aminomethyl)pyridine and a metal centre that can be found in the CCDC.[277] Following the lack of success with the Lewis acid method it was envisaged that using an organic base such as triethylamine might be more successful. Accordingly 2-(aminomethyl) pyridine was mixed with the tetra ethyl ester in the presence of triethylamine and the mixture was stirred at reflux. This method did not appear to yield any sign of reaction. Following this

attempts were made to transform tetraethyl-4,4`-[butane-1,4-diyl*bis*-(oxy)]dipyridine-2,6-dicarboxylate (**89**) into the tetracarboxylic acid (**94**) before creating the acid chloride *in situ* which could then be coupled to 2-(aminomethyl) pyridine. This method did appear to yield the tetracarboxylic acid (**94**) as a white solid on neutralisation. However this proved to be a particularly insoluble and unreactive solid.

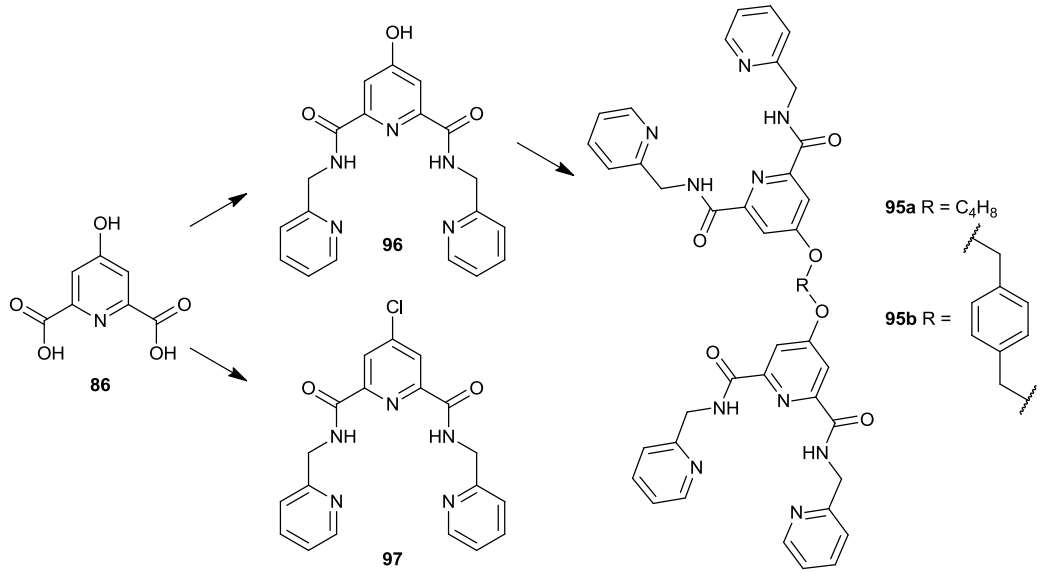

Scheme 14 – Synthesis of the linked tetra-amide via preformation of the amide followed by linking.

Finally it was decided to attempt the formation of the desired chelidamic acid based pincer (**96**) first and then carry out the linking procedure. Reacting chelidamic acid with oxalyl chloride until gas evolution ceased was deemed to be the best route to the desired diacid chloride avoiding chlorine substitution at the 4 position (**97**). The acid chloride was used crude and the resulting solid was then recrystallised yielding the desired product. Removal of solvent from the mother liquor and analysis of the resulting material showed that it contained a mixture of 4-chloro substituted product (**97**) as well as some by product of the reaction between oxalyl chloride and 2-(aminomethyl)pyridine. Finally the diamide (**96**) was then reacted with either 1,4-dibromobutane or 1,4-*bis*-(bromomethyl)benzene to yield the desired cross linked products **95a** and **95b** respectively. Attempts have been made to obtain crystals of suitable quality for X-ray structural study for each compound but only the butyl-linked derivative has yielded a crystalline material.

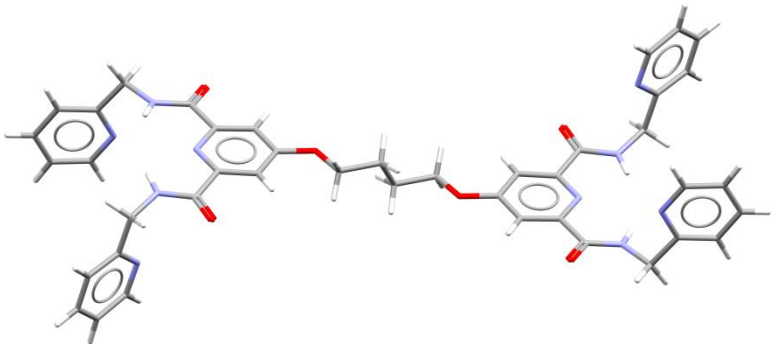

Figure 221 - The crystal structure of 4,4'-[1,4-butanediyl*bis*-(oxy)]*bis*-(N,N'-*bis*-(2-pyridylmethyl)-2,6-pyridine dicarboxamide) (95a) crystallised by slow evaporation of methanol.

The structure of 4,4'-[1,4-butanediyl*bis*-(oxy)]*bis*-(N,N'-*bis*-(2-pyridylmethyl)-2,6-pyridine dicarboxamide) (**95a**) is shown in Figure 221. The material formed extremely fine crystals which required synchrotron radiation to create diffraction patterns suitable for structure solution and refinement. The structure obtained has a plane of symmetry across the central bond of the butyl linker.

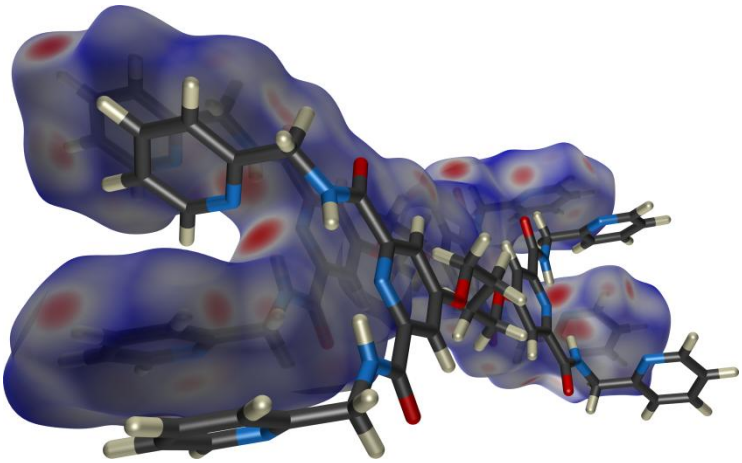

Figure 222 – The Hirshfeld surface shows quite clearly the interactions that appear to direct the packing of molecules into stacks.

The packing of the linked pyridine-2,6-dicarboxamide units appear to occur primarily through the interactions between molecules which result in the formation of stacks (Figure 222). The main contact appears to involve two hydrogen bonds from the pyridine amide core to the pendent pyridine nitrogen of the neighbouring molecule (**N(5)**···**H(3)**-N(3) 2.34 Å, **N(5)**···H(3)-**N(3)** 3.12 Å (146.9 °), **N(5)**···**H(2)**-N(2) 2.54 Å, **N(5)**···H(2)-**N(2)** 3.33 Å (150.3 °) (Figure 222). This behaviour seems to mirror that observed in the monomeric structures reported by Gomm[182] and Parker.[172]

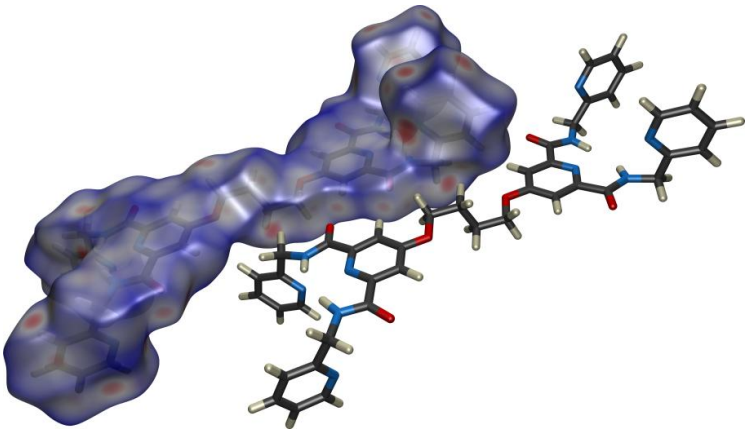

Figure 223 - Packing of the linked pyridine-2,6-dicarboxamide shows the molecules packing into sheets.

The molecules also appear to align into sheets with two interactions highlighted on the Hirshfeld surface (Figure 223) from the carbonyl oxygen to (a) one of the hydrogens on the neighbouring molecule (C=**O(1)**···**H(4)**-C(4) 2.73 Å C=**O(1)**···H(4)-**C(4)** 3.67 Å (171.8 °)) and (b) one of the methylene group hydrogen atoms (C=**O(1)**···**H(21A)**-C(21) 2.67 Å C=**O(1)**···H(21A)-**C(21)** 3.20 Å (113.0 °)). However, it does appear that there may be some form of steric clash between the methylene hydrogen atoms attached to C(15) and C(24).

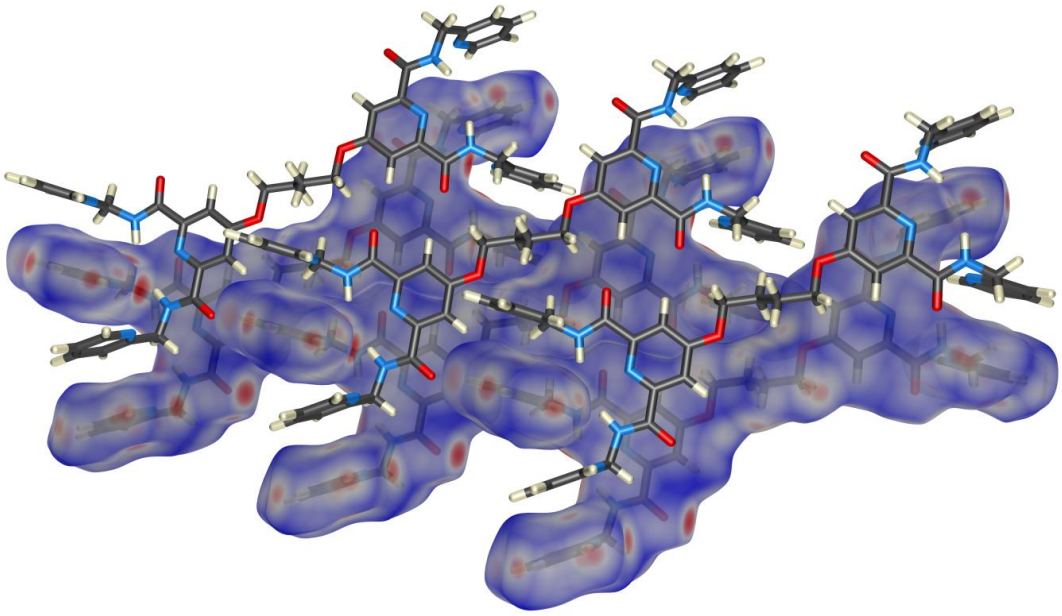

Figure 224 – The combination of the stacking and sheet forming interactions rise to stacked sheets as shown here.

The combination of the two interaction types gives rise to the packing motif shown in Figure 224 however it is important to examine the secondary interactions to understand how these molecules interact with one another.

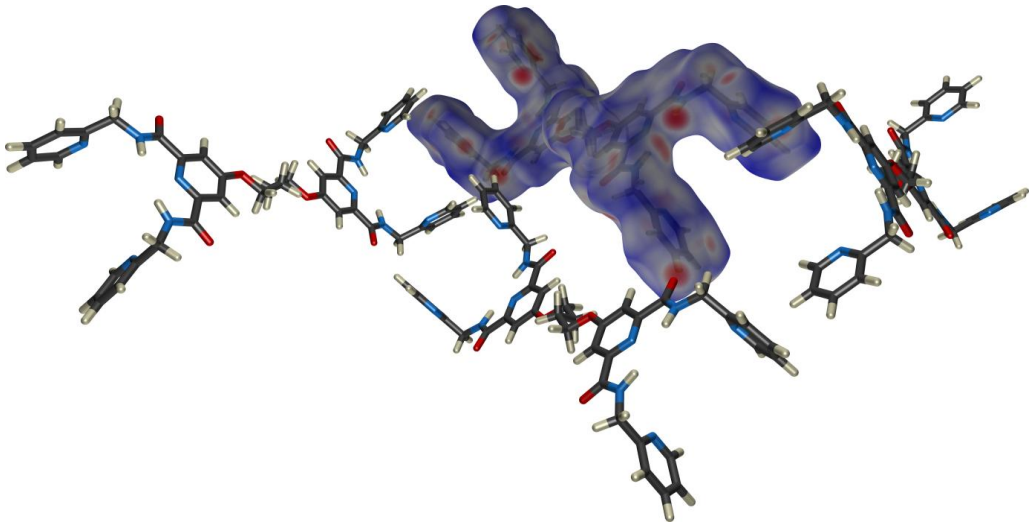

Figure 225 – Hirshfeld surface showing the secondary interactions which govern the packing of the stacked sheets.

Examining the Hirshfeld surface (Figure 225) shows that there appear to be some very strong interactions involved in the secondary packing of the molecules. The most obvious is from the carbonyl oxygen atom O(2) to the pendent pyridine hydrogen H(19) ((C=**O(2)**···**H(19)**-C(19) 2.37 Å C=**O(2)**···H(19)-**C(19)** 3.14 Å (138.6 °)). There is also an interaction from the pendent pyridine nitrogen atom N(4) to one of the other pendent pyridine hydrogens H(13) (**N(4)**···**H(13)**-C(13) 2.56 Å **N(4)**···H(13)-**C(13)** 3.41 Å (150.0 °)). Finally there also appears to be a weaker interaction from O(2) to H(13) ((C=**O(2)**···**H(12)**-C(19) 2.67 Å C=**O(2)**···H(12)-**C(12)** 3.60 Å (166.1 °). The large number of secondary interactions, two of which could be quite strong may explain the steric clash between the methylene C-H and the linking chain observed in the sheet formation.

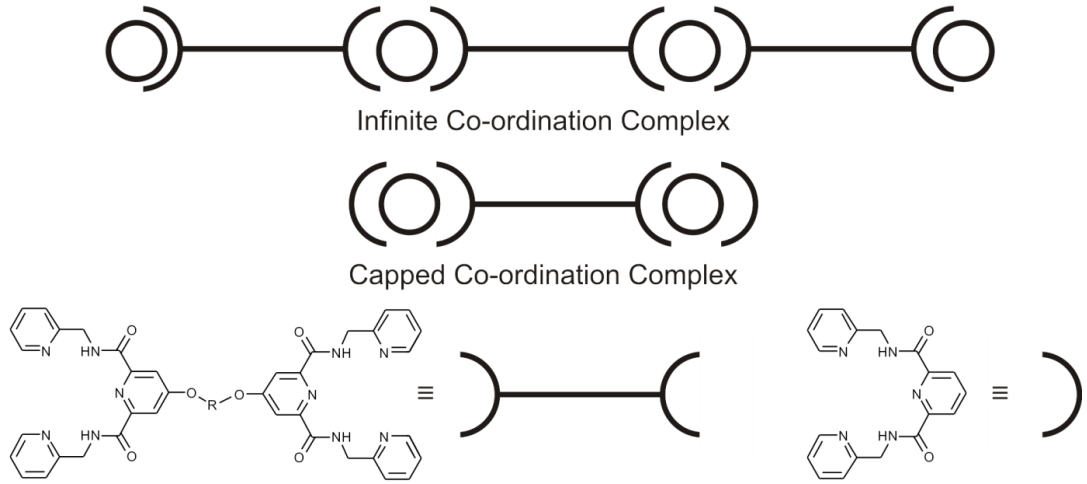

Figure 226 - Illustration to show planned metal complexation with and without a capping molecule.

Having successfully formed two compounds with linked chelidamic units, and examined the solid-state structure of one of the compounds it was hoped that it would be possible to demonstrate the complexation of metal centres in order to form supramolecular polymers. Attempts have therefore been made to form metal co-ordination complexes utilising metal centres such as cobalt, copper and iron with and without capping molecules (Figure 226). However, despite observing colour changes though to be caused by complexation, it has not been possible to isolate any material which could be characterised to confirm the success of the complexation. In the case of the capped co-ordination attempts, only the capping molecule was isolated. This initial investigation has shown that it is possible to carry out the desired linking of two chelidamic dicarboxamide units and it is hoped that further work would demonstrate the use of these materials to form supramolecular polymers.

5.2.3 A Potential Liquid Crystal?

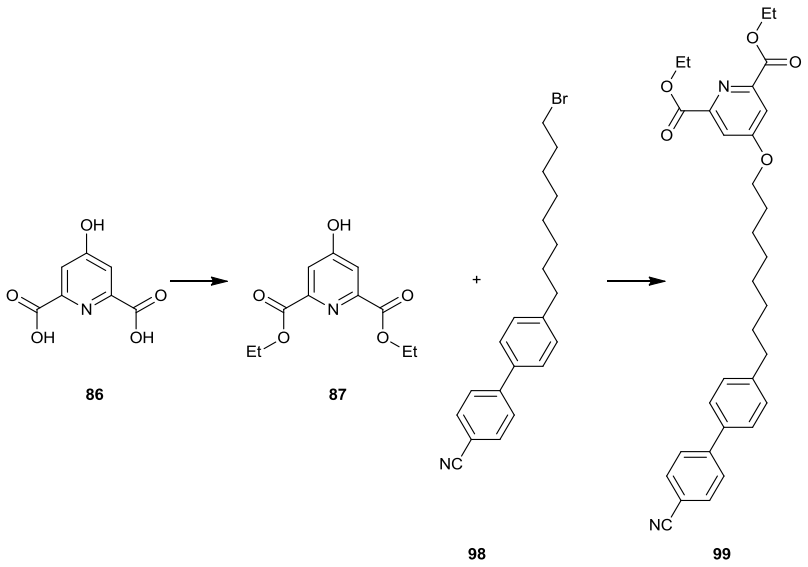

Figure 227 – The crosslinking methodology was used to connect the chelidamic ester (87).

In view of the success of this coupling route, it was hoped that introduction of a longer aliphatic chain spacer, such as those often found in liquid crystal materials might yield materials with liquid crystalline properties.[278] Accordingly chelidamic acid was coupled to 1-bromo-8-(cyanobiphenyl)octane (**98**).[278] This gave a material (**99**) with a tendency to remain liquid once melted. Examination under a cross polarising microscope through the melting process did not appear to show any of the markers seen in typical liquid crystalline samples.

5.3 Other Pyridine-2,6-dicarboxamides

During the course of this project attempts were made to synthesise a number of amines which could be used to create novel pyridine-2,6-dicarboxamides. It was hoped that it would be possible to study the solid-state behaviour of these compounds. However, to date, it has not been possible to obtain crystals of suitable quality for study by X-ray diffraction from several of the samples. This has normally been a result of poor solubility.

5.3.1 *N,N'-bis*-(7-Methyl-1,8-naphthyridine)-2,6-pyridine dicarboxamide

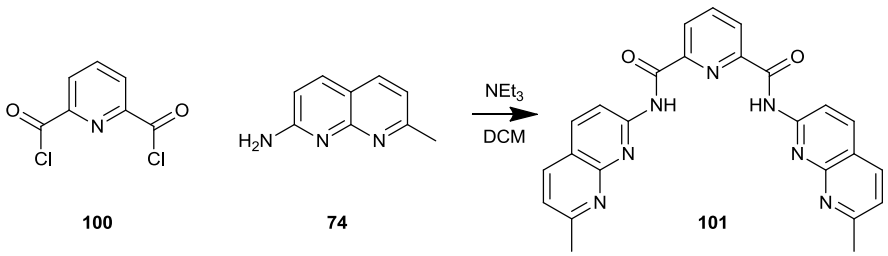

Scheme 15 – The attempted synthesis of *N,N'-bis*-(7-methyl-1,8-naphthyridine)-2,6-pyridine dicarboxamide

Having synthesised 2-amino-7-methyl-1,8-naphthyridine (**74**) in attempts to create 1,9,10-anthyridine-2,8-anthyridine (**72**), it was envisaged that this might be an useful side arm for the pyridine amide-based system. Especially given the interesting binding properties exhibited by the analogous compounds which use an isophthaloyl core.[27, 279-281] This material was synthesised using standard amide bond forming conditions, to yield a highly insoluble brown solid. It seems unlikely that it will be possible to crystallise this material due to its insoluble nature in common laboratory solvents. However it might be possible to create co-ordination complexes which are slightly more soluble.

5.3.2 *N,N'-bis*-(Cbz-4-Aminobenzyl)-2,6-pyridine dicarboxamide

During the course of this project efforts have been made to synthesise two other amines in order to examine the properties of the associated pyridine-2,6-carboxamides and the 1,8-naphthyridine-2,7-dicarboxamides.

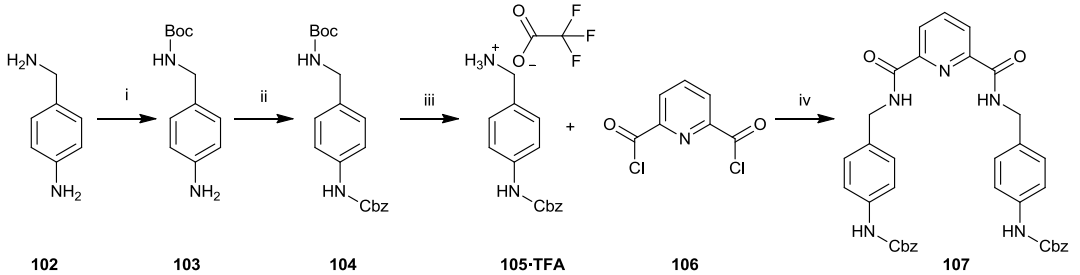

i) di-t-butyl dicarbonate, THF ii) Benzyl chloroformate, THF iii) 50% TFA in DCM iv) NEt_3, DCM

Scheme 16 - Synthetic route to *N,N'-bis*-(CBz-4-aminobenzyl)-2,6-pyridine dicarboxamide

Previous attempts to synthesise *N,N'-bis*-(4-aminobenzyl)pyridine-2,6-dicarboxamide directly had been problematic[172] and so a route exploiting the N-protected derivatives(**107**) was explored. Scheme 16 was followed to synthesise the

N-protected *N,N'-bis*-(4-aminobenzyl)pyridine-2,6-dicarboxamide (**107**). It was hoped that high quality crystals would be obtained, before deprotection of the amine to give the 4-aminobenzyl diamide. While it has been possible to synthesise both the protected amine (**105**) and the coupled diamide (**107**) it has not been possible to obtain a crystal structure of either, nor has the deprotection been attempted due to the small quantity of the diamide (**107**) prepared. It is interesting to note that, whilst obtaining the melting point of the diamide, the material appeared to melt, solidify and then re-melt. As the material appeared clean by spectroscopic methods it is believed that this could be an indication of either solvent loss, polymorphism or even thermally induced deprotection of the amine.

5.3.3 *N,N'-bis*-(terphenyl)-2,6-pyridine dicarboxamide

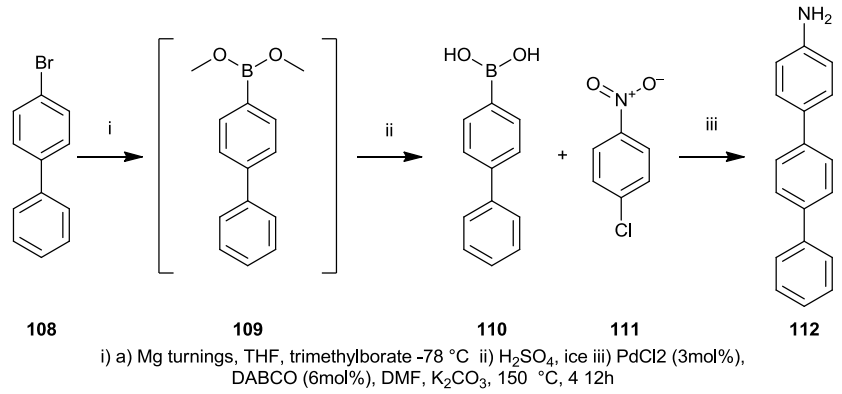

108 **109** **110** **111** **112**

i) a) Mg turnings, THF, trimethylborate -78 °C ii) H_2SO_4, ice iii) PdCl2 (3mol%), DABCO (6mol%), DMF, K_2CO_3, 150 °C, 4 12h

Scheme 17 - Synthetic work towards the formation of *N,N'-bis*-(terphenyl)-2,6-pyridine dicarboxamide.

The synthesis of the amide (**113**) derived from 4-aminoterphenyl (**112**) has also been explored (Scheme 17) in light of the work of Azumaya on the effect of aromatic - aromatic interactions in the formation of benzene dicarboxamide macrocycles.[282] 4-Aminoterphenyl (**112**) was prepared from biphenyl-4-boronic acid (**110**)[283] using a Suzuki coupling reaction in a DMF/H_2O mixed solvent system, which has been reported to reduce the nitro group to an amine *in situ*.[284] However, in the present study some of the nitro compound was also isolated explaining the lower than expected yield. If this synthesis was required on a larger scale it would be desirable to use a 4-bromonitrobenzene as the literature reports this to be higher yielding,[284] but the present work shows proof of reaction viability.

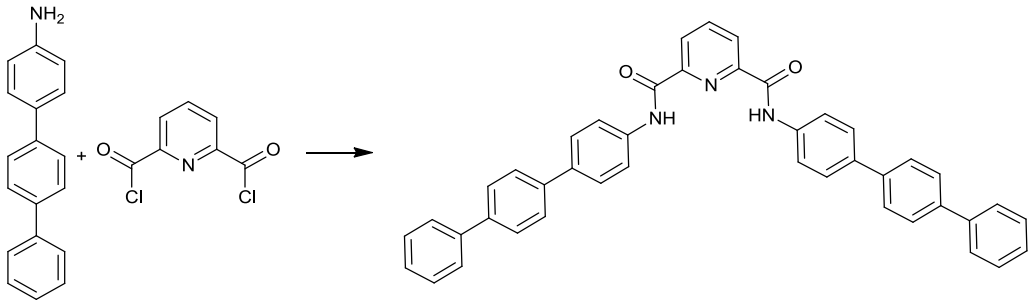

112 106 113

Scheme 18 - The trial amide couple reaction carried out with 112

A trial amide coupling reaction to give **113** was carried out with the 4-aminoterphenyl however the crude material proved to be very insoluble with characterisation and purification proving impossible.

5.4 Conclusion

Dicarbonyl substituted pyridine systems are a family of compounds which have received a large amount of interest due to their interesting solid-state architectures and, in the case of the diamide systems, useful metal complexation properties. Work on the pyridine-2,6-dicarboxylates, reported in this chapter, has been carried out in order to examine the differences in solid-state structure seen between different structural isomers of halogen substituted benzyl pyridine-2,6-dicarboxylates, in analogy to the work reported on the 1,8-naphthyridine-2,7-dicarboxylates. Attempts have been made to synthesise three novel pyridine-2,6-dicarboxamides all of which offer the opportunity to examine the effects of competing interactions from the pendent side arms on the overall packing motif. Finally work has been carried out to realise the ambition of creating linked disubstituted pyridine-2,6-dicarboxamide systems. The success of this initial work opens a new avenue of investigation for subsequent researchers.

6 Conclusion and Further Work

Following the successful synthesis of 1,8-naphthyridine-2,7-dicarboxylic acid, a number of 1,8-naphthyridine-2,7-dicarboxylates and 1,8-naphthyridine-2,7-dicarboxamides have been synthesised. A number of these molecules yielded crystals of sufficient quality to obtain X-ray solid-state structures.

It has been found that the 1,8-naphthyridine-2,7-dicarboxylate derivatives display very similar behaviour to that observed in the pyridine-2,6-dicarboxylate systems reported by Parker,[172] Gomm,[182] Orton[195] and Cheesewright.[196]

Examination of the methyl and chloro substituted benzyl derivatives have revealed structural similarities except when the substitution is in the 4-position. In addition to this it has been observed that the bromine substituted derivatives appear to be isostructural to the chlorine substituted benzyl derivatives. During this study efforts have been made to investigate the effect of having alternate ring systems as the pendent rings, with the solid-state structure of the pyridylmethyl, cyclopentylmethyl, cyclohexylmethyl and anthrylmethyl derivatives reported. Unfortunately there have been a number of the 1,8-naphthyridine-2,7-dicarboxylate derivatives that have proved extremely insoluble with the consequence that no structural data could be obtained. Initial attempts have been made to carry out physical measurements such as DSC on these compounds however most of the compounds appear to decompose on melting.

In addition to this fifteen novel 1,8-naphthyridine-2,7-dicarboxamide derivatives were synthesised with the solid-state structures reported for 6 of these derivatives. These derivatives demonstrated similar behaviour to that observed in the pyridine-2,6-dicarboxamides previously reported. In addition it has also been possible to obtain the solid-state structure of *N,N'-bis*-(2-pyridyl)-1,8-naphthyridine-2,7-dicarboxamide dihydrochloride (**48c·2HCl)** as well as a *N,N'-bis*-(2-pyridyl)-1,8-naphthyridine-2,7-dicarboxamide copper complex (**48c·2Cu**).

Work on the pyridine-2,6-dicarboxylates reported in this study has been carried out in order to examine the differences in solid-state structure seen between different structural isomers of halogen substituted benzyl pyridine-2,6-dicarboxylates, by analogy to the work reported on the 1,8-naphthyridine-2,7-dicarboxylates.

Additional work has been attempted to synthesise three novel pyridine-2,6-dicarboxamides, all of which offer the opportunity to examine the effects of competing interactions from the pendent side arms on the overall packing motif. Finally work has been carried out to realise the ambition of creating linked disubstituted pyridine-2,6-dicarboxamide systems.

It is suggested that there are two areas which would benefit from further work: Firstly it is envisaged that the synthesis of the missing pyridine and 1,8-naphthyridine dicarboxylate derivatives, along with further attempts to form crystals of suitable quality for X-ray structural studies, would allow the completion of the study of the effects of pendent rings on the secondary packing of these systems. It is also believed that given the number of compounds identified that more concerted efforts should be made to investigate the physical properties of these materials, making use of techniques such as NMR and IR dilution studies;

Secondly, given the success of initial work linking two functionalised pyridine derivatives, it is hoped that further investigation may allow the development of materials that can form polymers either through the use of hydrogen bonding arrays or through the complexation of metal centres.

7 Experimental

7.1 General Experimental

1,8-Naphthyrdine-2,7-dicarbonyl dichloride was prepared by literature methods from 1,8-naphthyridine-2,7-dicarboxylic acid.[215]

Commercially available compounds were obtained from Sigma Aldrich or Fisher and, unless specified, all reagents and solvents were reagent grade or better and were used as supplied without further purification.

Melting points (MP) were measured using a Gallenkamp melting point apparatus and are uncorrected.

Electrospray (ES) mass spectra were recorded using a Micromass Platform II single quadrapole mass spectrometer using either methanol or acetonitrile. High resolution spectra were collected by the Mass Spectrometry Service, School of Chemistry, University of Southampton using a Bruker Apex III FT-ICR mass spectrometer fitted with an Apollo electrospray ionisation source.

Nuclear magnetic resonance (NMR) spectra were collected using either a Bruker AV300 spectrometer, or a Bruker DPX400 spectrometer; operating at 300 or 400 MHz respectively for ^{1}H NMR experiments and at 75 MHz or 100 MHz respectively for ^{13}C and Dept-135 NMR experiments. ^{13}C spectra were collected fully decoupled. ACD Labs software was used to process and analyse the spectral data. Chemical Shifts are given in ppm. Multiplicities are denoted as follows: s, singlet; d, doublet; dd, double doublet; t, triplet; q, quartet; m, multiplet.

Infrared (IR) spectra were collected on a Nicolet 380 FT-IR spectrometer with a SmartOrbit Golden Gate Attenuated Total Reflection (ATR) attachment.

UV-visible spectra were collected using a Shimadzu UV-1601 UV-visible spectrophotometer running UVPC version 3.5.

Single crystal X-ray diffraction data was collected using either a Bruker-Nonius Kappa CCD or Bruker-Nonius Apex II CCD detector. X-rays were generated using a Bruker-Nonius FR591 rotating anode X-ray generator using a molybdenum target Data was processed using COLLECT,[285] Denzo,[286] DirAX,[287, 288] HKL,[286] SADABS[289, 290] and XPREP[291] software applications. The data was also collected at Station 9.8 at

Daresbury SRS and Diamond Light source, Didcot, using a Bruker SMART APEX2[292]detector at a wavelength λ = 0.6939Å and was processed using SAINT.[293] The structures were solved and refined using the SHELX-97[294, 295] and WinGX[296] software packages, including PLATON.[297] The Crystallographic Information Files (CIFs) were edited in EnCIFer[298] and graphical visualisation was carried out in Mercury[299, 300] and CrystalExplorer.[239, 301]

7.2 1,8-Naphthyridine Synthesis

7.2.1 2-Methyl-1,8-napthyridine[246] (52)

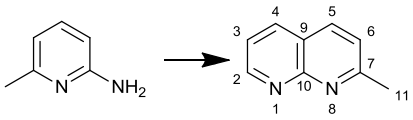

Sodium m-nitrobenzenesulphonate (17.5 g, 77.8 mmol) was added to conc. H_2SO_4 (41 g), followed by H_3BO_3 (2.4 g, 38.8 mmol) and $FeSO_4$ (1.4 g, 9.21 mmol) the solution was then cooled to 0-5 °C. Glycerol (12.5 mL, 0.11 mol) was then added followed by 2-amino-6-methyl pyridine (4.33 g, 0.04 mol) and warm water (22.5 mL). Following this the reaction was heated at 135 °C for 4 hours. The reaction mixture was allowed to cool before being basified using NaOH (50 % in water) to approx pH 10 and then extracted with $CHCl_3$ (3 x 150ml), dried with $MgSO_4$, and the solvent was removed *in vacuo* yielding a yellow oil. This oil was then purified by flash column chromatography (5:95 MeOH:DCM eluent) which yielded a yellow solid (0.88 g, 15 %) Attempts to crystallise this from methanol yielded a purple crystalline solid.

MP: 90 °C (lit.[245] 99 - 100 °C).

UV λ_{max}(MeOH)/nm 264.5 (ε/dm^3 mol^{-1} cm^{-1} 20589).

ν/cm^{-1} 3058 (w, C-H), 3023 (w, aromatic C-H), 1596 (s, aromatic C-C), 1496 (s, aromatic C-C).

δ_H (300 MHz, $CDCl_3$) 2.81 (3 H, s, H-11), 7.37 (1H, d, *J*=8.4 Hz, H-3), 7.41 (1H, dd, *J*=8.1, 4.4 Hz, H-6), 8.06 (1H, d, *J*=8.4 Hz, H-4), 8.13 (1H, dd, *J*=8.1, 1.9 Hz, H-5), 9.06 (1H, dd, *J*=4.2, 2.0 Hz, H-7).

δ_C (75 MHz, $CDCl_3$) 25.6 (C-11), 120.7 (C-9), 121.3 (C-6), 122.9 (C-3), 136.6 (C-5), 136.8 (C-4), 153.3 (C-7), 156.0 (C-2), 163.0 (C-10).

M/S: (ES $^{+}$) 145 (76 %, $[M+H]^{+}$), 156 (13, $[2M+Na]^{2+}$), 167 (100, $[M+Na]^{+}$), 289 (1, $[2M+H]^{+}$), 311 (31, $[2M+Na]^{2+}$).

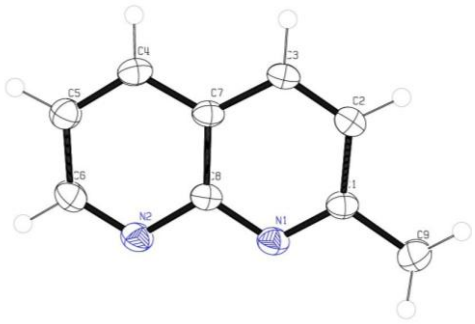

$C_9H_8N_2$	a = 6.2852 (3) Å	T = 120 K
P2(1)/n	b = 8.3977 (6) Å	λ = 0.71073 Å
V = 737.88 (8) Å	c = 14.2217 (8) Å	D_c = 1.298 g cm^{-3}
Z = 4	α = 90.00 (0) °	μ = 0.080 mm^{-1}
R_1 =8.44 %	β = 100.577 (4) °	0.4 x 0.1 x 0.08 mm^3
$wR_2(F^2)$ = 16.56 %	γ = 90.00 (0) °	Colourless prism

Crystallised from a methanol solution

7.2.2 2-Amino-7-hydroxy-1,8-napthyridine[216] (55)

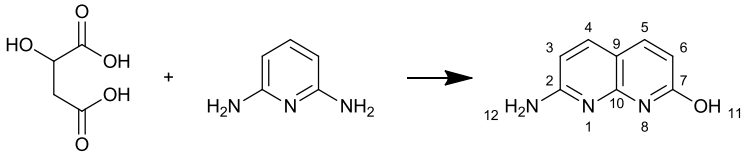

Malic acid (6.0 g, 44 mmol) and 2,6-diaminopyridine (4.4 g, 40 mmol) were ground into an intimate powder and cooled in an ice bath before the addition of concentrated sulphuric acid (20 mL). The solution was then heated to 110 °C for 3 hours. After cooling the solution was poured over ice (200 mL) and the solution was then made alkaline with ammonium hydroxide solution.

As the solution became alkaline a very fine particulate precipitate appeared to form. This was filtered off and then dried under high vacuum over silica gel for 2 days to give a brown solid (3.66 g, 58 %)

MP: > 305 °C (lit.[216] >350 °C).

UV λ_{max}(DMSO)/nm 344.5 (ε/dm^3 mol^{-1} cm^{-1} 7023), 360.5 (ε/dm^3 mol^{-1} cm^{-1} 6685).

ν/cm^{-1} 3399 (m, N-H), 3163 (s, O-H), 3000 (s, H-Bonded O-H), 1622 (s, N-H), 1604 (m, aromatic C-C), 1545 (m, aromatic C-N), 1506 (m, aromatic C-C).

δ_H (300 MHz, DMSO-d_6) 6.09 (1 H, d, J=9.1 Hz, H-3), 6.33 (1 H, d, J=8.6 Hz, H-6), 6.78 (2 H, br. s. H-11), 7.62 (2 H, d, J=9.0 Hz, H-4 + H-5), 11.59 (1 H, br. s, H-12.).

δ_C (75 MHz, DMSO-d_6) 105.1 (C-9), 105.4 (C-3), 114.8 (C-6), 137.4 (C-5), 140.0 (C-4), 150.4 (C-10), 160.7 (C-2), 163.9 (C-7).

M/S: (ES $^-$) 160 (100 %, $[M-H]^-$).

(ES $^+$) 162 (39 %, $[M+H]^+$), 184 (100, $[M+Na]^+$), 216 (31, $[M+Na+MeOH]^+$), 345 (67, $[2M+Na]^+$), 506 (7, $[3M+Na]^+$).

7.2.3 2,7-Dihydroxy-1,8-naphthyridine[216] (56)

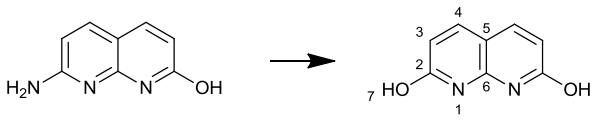

2-Amino-7-hydroxy-1,8-naphthyridine (2.00 g, 12.5 mmol) was ground into a fine powder before being added to concentrated sulphuric acid (20 mL). Sodium nitrite (1.02 g, 15.6 mmol) was then added and the mixture was allowed to stand for 5 minutes while until gas evolution ceased. The reaction was then poured over crushed ice, and allowed to stand for a further 10 minutes. The solution was then slowly neutralised with sodium carbonate (approx 100 g), before being re-acidified with glacial acetic acid. During the re-acidification a fine brown precipitate was formed which was filtered off and dried *in vacuo* (1.31 g, 64 %).

MP: > 305 °C (lit.[216] >321 - 323 °C).

UV λ_{max}(DMSO)/nm 331 (ε/dm^3 mol^{-1} cm^{-1} 7242), 345 (ε/dm^3 mol^{-1} cm^{-1} 7920).

ν/cm^{-1} 2992 (m, C-H), 2908 (m, C-H), 2900 (m, broad O-H), 2805 (w, C-O), 1629 (s, aromatic C-C), 1556 (m, aromatic C-N), 1508 (m, aromatic C-C).

δ_H (300 MHz, DMSO-d_6) 6.34 (2 H, d, J=9.0 Hz, H-3), 7.81 (2 H, d, J=9.0 Hz, H-4), 11.63 (2 H, br. s., H-11).

δ_C (75 MHz, DMSO-d_6) 106.3 (C-5), 112.1 (C-3), 139.5 (C-4), 148.3 (C-6), 163.4 (C-2).

M/S: (ES $^-$) 161 (100 %, $[M-H]^-$).

(ES$^+$) 163 (11 %, $[M+H]^+$), 185 (100, $[M+Na]^+$), 217 ($[M+Na+MeOH]^+$), 347 (33, $[2M+Na]^+$).

7.2.4 2,7-Dichloro-1,8-naphthyridine[216] (57)

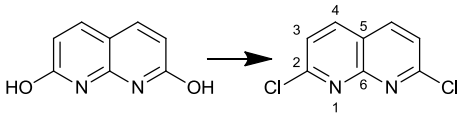

To a mixture of phosphorus oxychloride (1.12 g, 7 mmol) and phosphorus pentachloride (1.25 g, 6 mmol) 2,7-dihydroxy-1,8-naphthyridine (500 mg, 3.1 mmol) was slowly added. The resulting solution was slowly heated and was refluxed for 3 hours. After cooling the solution was chilled in an ice bath and very carefully ice was added to the reaction vessel. Following the completion of gas evolution the now aqueous solution was made alkaline with sodium carbonate, during which the solution changed from being black to opaque brown. When passed though a filter paper a brown precipitate was collected. (0.56 g)

The literature[216] states that the brown precipitate is then recrystallised from acetone to give a white solid. However in this case the brown precipitate was washed with acetone, leaving an insoluble brown material, which appeared to be an inorganic residue. The acetone solution was reduced *in vacuo* to yield a pale yellow solid (125 mg, 20 %) an impure sample of the desired product (approx 75 % purity).

Impure Product:

MP: evidence of sublimation (not the whole sample) at 255 ºC (lit.[216] sublimation @ 259 ºC).

ν/cm^{-1} 3092 (w, C-H), 3046 (m, C-H), 2986 (w, C-H), 1584 (s, aromatic C-C), 1538 (s, aromatic C-N), 1470 (s, aromatic C-C).

δ_H (300 MHz, $CDCl_3$) 7.54 (2H, d, *J*=8.6 Hz, H-3 + H-6), 8.16 (2H, d, *J*=8.4 Hz, H-4 +H-5).

δ_C (75 MHz, DMSO-d_6) 120.7 (C-9), 123.9 (C-3 + C-6), 140.8 (C-4 + C-5), 151.4 (C-10), 153.7 (C-2 + C-7).

M/S: (ES $^+$) 199 (16 %, $[M+H]^+$), 201 (13, $[M+H]^+$), 203 (3, $[M+H]^+$), 221 (100, $[M+Na]^+$), 223 (65, $[M+Na]^+$), 225 (12, $[M+Na]^+$), 253 (24, $[M+Na+MeOH]^+$), 255 (18, $[M+Na+MeOH]^+$), 257 (6, $[M+Na+MeOH]^+$), 421 (15, $[2M+Na]^+$), 423 (20, $[2M+Na]^+$), 425 (11, $[2M+Na]^+$).

7.2.5 Attempted Synthesis of 2,7-dicyano-1,8-naphthyridine (58)

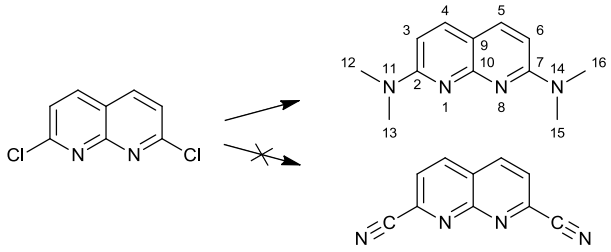

For the attempted synthesis of 2,7-dicyano-1,8-naphthyridine Rosenmund von Braun conditions were utilised.[250] 2,7-Dichloro-1,8-napthyridine (50 mg , 0.25 mmol) was added to a stirred solution of cuprous cyanide (90 mg, 1 mmol) in dimethylformamide (4 mL). The reaction mixture was then heated to reflux and the reaction was monitored by TLC (10 % MeOH:DCM). After about 6 h this suggested that the starting material had all been consumed, and the reaction was worked up.

The reaction was cooled to room temperature before addition of ferric chloride (1 mL, 60 % aq solution) and ethanol (1 mL). The resulting mixture was then heated to reflux once again for two minutes. Once cooled the reaction was poured into rapidly stirred iced hydrochloric acid (10 mL, 20 mL conc HCl in 80 mL water).

The solution was then extracted with DCM (50 mL, then 4 x 20 mL) and the combined organic extracts were then washed with sodium EDTA solution and the dried with sodium sulphate. The solvent was removed *in vacuo* to give an yellow oil (52.8 mg)

Purification was attempted by column chromatography (using varying mixtures of methanol in DCM, between 1 % MeOH:DCM and 10 % MeOH:DCM, to slowly increase the polarity). This yielded a number of mixed fractions including a small amounts of starting material and one separated compound which was not the desired product but 2,7-di(dimethylamino)-1,8-naphthyridine as a yellow oil (6.8 mg, 12.5 %).

ν/cm^{-1} 2935 (m, N-H), 2923 (m, C-H), 2853 (m, CH_3), 2359 (w, C-N), 2342 (w, C-N), 1619 (s, aromatic C-C), 1529 (w, aromatic C-C).

δ_H (300 MHz, $CDCl_3$) 3.27 (12 H, s, H-12 + H-13 + H-15 + H16), 6.56 (2 H, d, J = 8.9 Hz, H-3 + H-6), 7.64 (2 H, d, J=8.9, H-4 + H-5).

M/S (ES +) 217 (100 % $[M+H]^+$).

HRMS 217.1447 ($C_{12}H_{17}N_4$).

7.2.6 Formation of 2,6-dimethylpyrido[1,2-α]pyrimidin-4-one[215] (61)

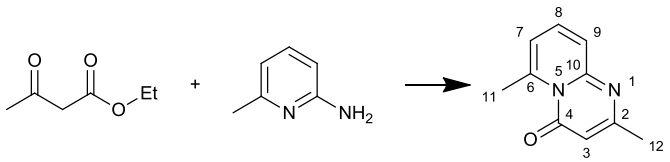

Polyphosphoric acid (65 g) was added to a mixture of 2-amino-6-methyl-pyridine (10.8 g, 0.1 mol) and ethyl acetoacetate (14.5 g, 0.11 mol). The resulting mixture was heated with stirring for 1.25 h at 100 °C, during which time the reaction went from yellow to deep red. The viscous mixture was cooled and neutralised with 4M NaOH solution. Upon cooling a yellow solid formed which separated was filtered off. The isolated solid was identified as the desired product. It appeared to be wet so was dissolved in DCM (100 mL) and the solution was dried with $MgSO_4$ and concentrated *in vacuo* to give a dry product. The filtrate was also extracted with DCM (3 x 150 mL) the organic washings were then dried with $MgSO_4$ and concentrated *in vacuo* to yield a further crop of the desired material (6.224 g, 36 %)
MP 85-92 °C (lit.[215] 105 °C).
UV λ_{max}(MeOH)/nm 250 (ε/dm^3 mol^{-1} cm^{-1} 13719), 320.5 (ε/dm^3 mol^{-1} cm^{-1} 8554), 355 (ε/dm^3 mol^{-1} cm^{-1} 11289).
ν/cm^{-1} 3073 (w, C-H), 2988 (w, C-H), 2973 (w, C-H), 1696 (s, tertiary amide), 1636 (s, C=O), 1581 (m, aromatic C-C), 1551 (m, aromatic C-N), 1498 (m, aromatic C-C).
δ_H (300 MHz, $CDCl_3$) 2.36 (3H, s, H-11), 3.04 (3H, s, H-12), 6.16 (1H, s, H-3), 6.62 (1H, d, J= 6Hz, H-7), 7.30-7.40 (2H, m, H-8 + H-9).
δ_C (75 MHz, $CDCl_3$) 23.8 (C-11), 24.7 (C-12), 105.7 (C-3), 117.9 (C-7), 124.8 (C-9), 135.1 (C-8), 143.9 (C-6), 153.3 (C-10), 162.1 (C-4), 163.4 (C-2).
M/S (ES $^+$) 175 (100 %, $[M+H]^+$), 197 (75, $[M+Na]^+$), 229 (57, $[M+Na+MeOH]^+$), 371 (21, $[2M+Na]^+$)

7.2.7 2,7-Dimethyl-1,8-naphthyridin-5(1H)-one[215] (62)

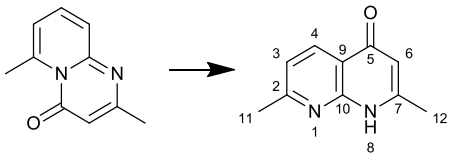

Liquid paraffin (50 mL) in a RB flask was heated to 350 °C in a heating mantle. The solid 2,6-dimethylpyrido[1,2-α]pyrimidin-4-one (2.5 g, 14.3 mmol) was added in small portions and the oil was maintained at 350 °C for 30 mins after the addition was complete. Light petroleum (40-60 °C) (50 mL) was then added to the cooled reaction mixture. A brown solid precipitated which was filtered off and washed with toluene (2.037 g, 80 %).

MP: >300 °C (lit.[215] 320 °C).

UV λ_{max}(DMSO)/nm 333.5 (ε/dm^3 mol^{-1} cm^{-1} 6115).

ν/cm^{-1} 3050 (w, N-H), 2921 (m, C-H), 2852 (m, C-H), 2725 (w, C-H), 1640 (s, C=O), 1603 (s, aromatic C-C), 1551 (s, aromatic C-N), 1519 (s, aromatic C-C).

δ_H (300 MHz, DMSO-d_6) 2.31 (3H, s, H-12), 2.56 (3H, s, H-11), 5.92 (1H, s, H-6), 7.21 (1H, d, *J*=8.1 Hz, H-3), 8.26 (1H, d, *J*=8.1 Hz, H-4), 11.98 (1H, br. s., H-8).

δc (75 MHz, DMSO-d_6) 19.3 (C-12), 24.2 (C-11), 109.1 (C-6), 116.7 (C-9), 119.5 (C-3), 134.6 (C-4), 150.4 (C-7), 150.6 (C-10), 161.9 (C-2), 177.0 (C-5).

M/S: It has not been possible to obtain M/S data due to the insolubility of the product.

7.2.8 5-Chloro-2,7-dimethyl-1,8-naphthyridine[215] (63)

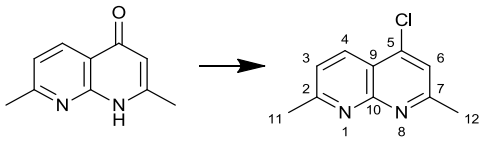

2,7-Dimethyl-1,8-naphthyridin-4(1H)-one (2.45 g, 14.1 mmol) was mixed with phosphorus oxychloride (16 mL, 0.17 mmol) and the mixture was then heated for 30 mins at between 90-130 °C. The solution was then cooled and poured onto ice. The resulting solution was then made slightly basic (pH 9) with 30 % sodium hydroxide before extraction with chloroform (3 x 100 mL).

The organic extracts were dried with magnesium sulphate before the solvent was removed *in vacuo*. The brown residue was then filtered through a silica pad (15 g) using 1:1 DCM:EA as the eluent. This yielded a light brown solid (2.27 g, 84 %)

MP: 80 °C (lit.[215] 83 °C).

UV λ_{max}(MeOH)/nm 217 (ε/dm^3 mol^{-1} cm^{-1} 21787), 305.5 (ε/dm^3 mol^{-1} cm^{-1} 3271), 318 (ε/dm^3 mol^{-1} cm^{-1} 3854).

ν/cm^{-1} 3077 (w, C-H), 3054 (w, C-H), 2915 (w, C-H), 2847 (w, C-H), 1596 (s, aromatic C-C), 1536 (s, aromatic C-N), 1499 (s, aromatic C-C), 832 (s, C-Cl).

δ_H (300 MHz, $CDCl_3$) 2.76 (3H, s, H-11), 2.80 (3H, s, H-12), 7.39 (1H, d, *J*=8.4, H-3), 7.39 (1H, s, H-6), 8.39 (1H, d, J=8.4 Hz, H-4).

δc (75 MHz, $CDCl_3$) 25.4 (C-11 + C-12), 117.6 (C-9), 121.9 (C-3), 122.8 (C-6), 133.2 (C-4), 142.4 (C-9), 156.0 (C-5), 162.5 (C-2), 163.7 (C-7).

M/S (ES $^+$) 215 (54 %, $[M+Na]^+$), 216 (6, $[M+Na]^+$), 217 (18, $[M+Na]^+$), 247 (6, $[M+Na+MeOH]^+$), 407 (100, $[2M+Na]^+$), 408 (21, $[2M+Na]^+$), 409 (67, $[2M+Na]^+$), 410 (15, $[2M+Na]^+$), 411 (11, $[2M+Na]^+$).

There were some doubts that both C-11 and C-12 could be assigned to very similar chemical shift, especially given that the protons are visible at two slightly different chemical shifts. However an HMQC indicates that both of the proton signals do in-fact correlate to the carbon peak at 25.4 ppm.

7.2.9 2,7-Dimethyl-1,8-naphthyridine[215] (44)

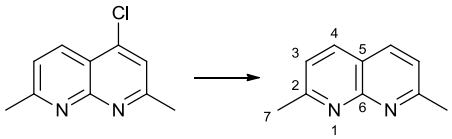

5-Chloro-2,7-dimethyl-1,8-naphthyridine (1.695 g, 8.80 mmol) was dissolved in methanol and ammonium formate (1.714 g, 27.1 mmol) was then added. The mixture was left under a nitrogen gas flow for 15 mins to purge the reaction prior to the addition of Pd on carbon (0.7g). Progress of the reaction was monitored by TLC and appeared to have gone to completion after ca. 4 hours. The catalyst was then filtered off and the filtrate was concentrated *in vacuo*. The residues were taken up in DCM (100 mL) and the solution was then washed with water (3 x 50 mL), dried

with magnesium sulphate. The solvent was removed *in vacuo* yielding a pale yellow solid (1.056 g, 97 %).

MP: 186-187 °C (lit.[215] 193 – 194 ºC).

UV λ_{max}(MeOH)/nm 210 (ε/dm^3 mol^{-1} cm^{-1} 10443), 268 (ε/dm^3 mol^{-1} cm^{-1} 6549), 315.5 (ε/dm^3 mol^{-1} cm^{-1} 5011).

ν/cm^{-1} 3053 (w, C-H), 3001 (w, C-H), 2918 (w, C-H), 2853 (w, C-H), 1603 (s, aromatic C-C), 1538 (s, aromatic C-N), 1508 (s, aromatic C-C).

δ_H (300 MHz, $CDCl_3$) 2.78 (6H, s, H-7), 7.30 (2H, d, J=8.3 Hz, H-3), 8.01 (2H, d, J=8.3 Hz, H-4).

δc (75 MHz, $CDCl_3$) 25.5 (C-7), 118.6 (C-5), 122.0 (C-3), 136.4 (C-4), 155.6 (C-6), 162.6 (C-2).

M/S (ES $^+$) 159 (37 %, $[M+H]^+$), 181 (62, $[M+Na]^+$), 213 (4, $[M+Na+MeOH]^+$), 339 (100, $[2M+Na]^+$).

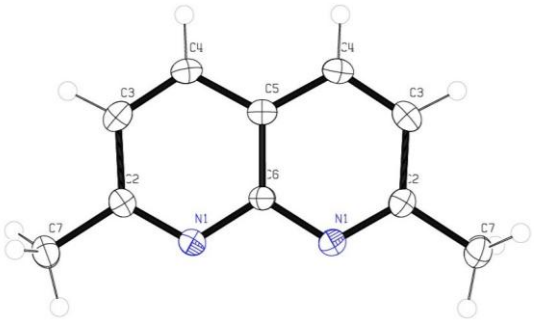

$C_{10}H_{10}N_2$	a = 13.4667 (6) Å	T = 120 K
Fdd2	b = 19.3913 (10) Å	λ = 0.71073 Å
V = 1649.47 (14) Å	c = 6.3165 (3) Å	D_c = 1.274 g cm^{-3}
Z = 8	α = 90.00 (0) °	μ = 0.078 mm^{-1}
R_1 =5.74 %	β = 90.00 (0) °	0.1 x 0.06 x 0.04 mm^3
$wR_2(F^2)$ = 12.15 %	γ = 90.00 (0) °	Colourless split plate

Crystallised from a chloroform solution

7.2.10 2,7-Di(trichloromethyl)-1,8-naphthyridine[217] (44)

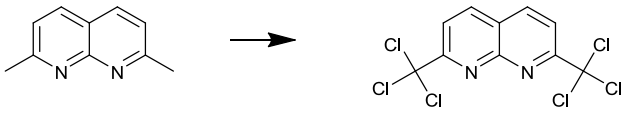

Following the literature procedure[217] A suspension of 2,7-dimethyl-1,8-naphthyridine (500 mg, 3.16 mmol), N-chlorosuccinimide (3.38 g, 26.0 mmol) and benzoyl peroxide (100 mg) in carbon tetrachloride was refluxed for 2 h, before being cooled. The solution was filtered (2.0779 g, this appeared to be excess NCS and succinimide) and the solution was reduced *in vacuo* to give a slightly yellow crystalline solid (1.13 g).However this material contained more than one spot by TLC so column chromatography was carried out (DCM eluent) which yielded a white crystalline solid (522.5 mg, 44%).

The material still appeared to be a mixture of 2,7-di(trichloromethyl)-1,8-naphthyridine and 2,7-di(dichloromethyl)-1,8-naphthyridine, which was difficult to separate but on crystallisation from DCM a crystal was picked that yielded the structure shown below.

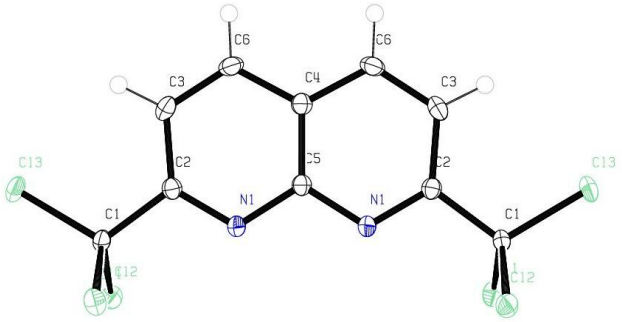

$C_{10}H_4N_2Cl_6$	a = 19.9501 (11) Å	T = 120 K
C2/c	b = 6.6190 (2) Å	λ = 0.71073 Å
V = 1305.05 (11) Å	c = 10.6239 (6) Å	D_c = 1.857 g cm^{-3}
Z = 4	α = 90 (0) °	μ = 1.295 mm^{-1}
R_1 = 3.05 %	β = 111.524 (2) °	0.8 x 0.4 x 0.04 mm^3
$wR_2(F^2)$ = 8.17 %	γ = 90 (0) °	Colourless plate
	Crystallisation from DCM	

7.2.11 1,8-Naphthyridine-2,7-dicarboxaldehyde[215] (64)

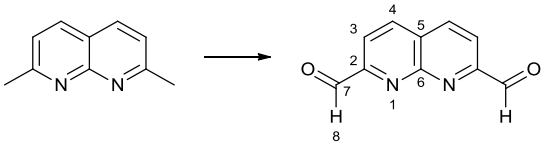

The 2,7-dimethyl-1,8-naphthyridine (106.4 mg, 0.67 mmol) was added in one portion to mixture of selenium dioxide (215.3 mg, 1.94 mmol) and 1,4-dioxane (7.5 mL) warmed to 40 °C. This reaction mixture was warmed for 12 h. The mixture was filtered while hot and the filtrate was concentrated to a third of the volume *in vacuo*. DCM (100 mL) was added to this concentrated mixture and the aqueous mixture was then extracted against water (3 x 100 mL). The aqueous extracts were further washed with DCM (3 x 50 mL) which was combined with the other organics extracts. The resulting solution was dried over magnesium sulphate and the reduced to dryness *in vacuo* yielding a light brown solid (52.3 mg, 47 %).

The filtered solid was placed within a soxhlet extraction thimble and the solid was extracted with DCM for 24 hours. This yielded an additional crop of material.

MP: decomposed at 180 °C (lit.[215] 225 – 227 °C).

ν/cm^{-1} 3117 (w, C-H), 3065 (w, C-H), 3003 (w, C-H), 2923 (w, C-H), 2864 (w, C-H), 1710 (s, C=O), 1601 (s, aromatic C-C), 1538 (s, aromatic C-N).

δ_H (300 MHz, DMSO-d_6) 8.21 (2H, d, J=8.5 Hz, H-3), 8.84 (2H, d, J=8.5Hz, H-4), 10.20 (2H, s, H-8).

δc (75 MHz, DMSO-d_6) 119.9 (C-3), 127.2 (C-5), 140.2 (C-4), 155.8 (C-2), 193.5 (C-7).

7.2.12 1,8-Naphthyridine-2,7-dicarboxylic acid[215] (46)

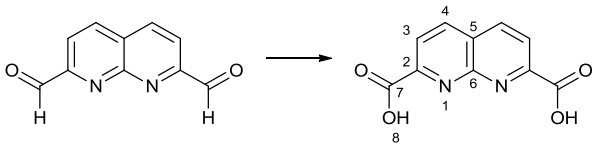

2,7-dialdehyde-1,8-naphthyridine (1.355 g, 6.2 mmol) was added to concentrated nitric acid (50 mL). This mixture was then heated to reflux for 3 h.

After this the reaction was allowed to cool, after which the reaction vessel was placed in an ice bath and 4M sodium hydroxide was added until a off white precipitate was seen to be forming (approx. pH 5). This precipitate was collected and dried in a desiccator for 2 days giving an yellow solid (1.270 g, 93 %).

MP: 236-240 °C dec. (lit.[215] 242 °C dec)

ν/cm^{-1} 3317 (w, C-H), 3206 (w, C-H), 3079 (w, C-H), 1756 (m, C=O), 1699 (m, C=O), 1603 (w, aromatic C-C), 1552 (w, aromatic C-N), 1502 (w, aromatic C-C).

δ_H (300 MHz; DMSO) 8.29 (2H, d, *J* = 8.3 Hz, H-3), 8.74 (2H, d, *J* = 8.3 Hz, H-4).

δ_c (75 MHz; DMSO) 123.0 (C-3), 124.9 (C-5), 139.4 (C-4), 153.2 (C-2), 166.1 (C-7)

7.2.13 1,8-Naphthyridine-2,7-dicarbonyl dichloride[215] (65)

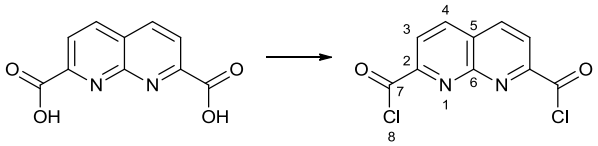

Thionyl chloride (18mL) was added to 1,8-naphthyridine-2,7-dicarboxylic acid (1.034 g, 4.8 mmol) followed by DMF (3 drops). The reaction mixture was then heated to reflux for 6 hours. After which the reaction mixture was allowed to cool the thionyl chloride was removed *in vacuo* to yield a brown solid (1.2743 g, 5.0 mmol, assumed to be quantitative). This material was used crude in the following reactions due to sensitivity to water.

δ_H (300 MHz; DMSO) 8.29 (2H, d, *J* = 8.4 Hz), 8.76 (2H, d, *J* = 8.4 Hz).

δ_c (75 MHz; DMSO) 123.0 (C-3), 125.0 (C-5), 139.4 (C-4), 152.6 (C-2), 153.6 (C-6), 166.0 (C-7).

7.3 1,8-Naphthyridine-2,7-dicarboxylates (47)

7.3.1 2,7-Dimethyl 1,8-naphthyridine-2,7-dicarboxylate[217] (47a)

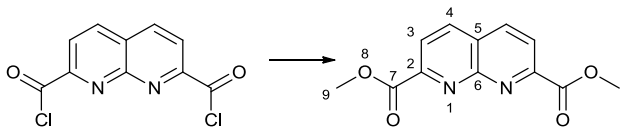

1,8-naphthyridine-2,7-dicarbonyl dichloride (200 mg, 0.78 mmol) was dissolved in methanol (10 mL). This was stirred for 5 minutes before the addition of triethylamine (0.17 mL. 1.64 mmol) resulted in the solution turning purple with a small amount of off white precipitate. The reaction mixture was left for a further 24 h, during which time the purple colour had disappeared, before the solvent was removed *in vacuo* to give an off white solid (114.6 mg). Recrystallisation by vapour

diffusion of diethyl ether into DCM yielded crystals of X-ray crystallography quality (66 mg, 34 %).

Mp: 214 – 215 °C (lit[217] 215 – 217 °C).

ν/cm^{-1} 3019 (w, C-H), 2963 (w, C-H), 2847 (w, C-H), 1704 (s, C=O), 1604 (m, aromatic C-C), 1556 (m, aromatic C-N), 1537 (m, aromatic C-C).

δ_H (300 MHz; $CDCl_3$) 4.05 (6H, s, H-9), 8.34 (2H, d, *J* = 8.5 Hz, H-3), 8.43 (2H, d, *J* = 8.5 Hz, H-4).

δ_c (75 MHz; $CDCl_3$) 53.1 (C-9), 123.2 (C-3), 125.3 (C-5), 138.3 (C-4), 152.0 (C-2), 154.2 (C-6), 165.3 (C-7).

MS (ES $^+$): *m/z* 247 (31 %, $[M+H]^+$), 269 (10, $[M+Na]^+$), 301 (23, $[M+Na+MeOH]^+$), 515 (100, $[2M+Na]^+$).

HR-M/S: Found 269.0536, Expected 269.0533 ($C_{12}H_{10}N_2O_4Na_1$)

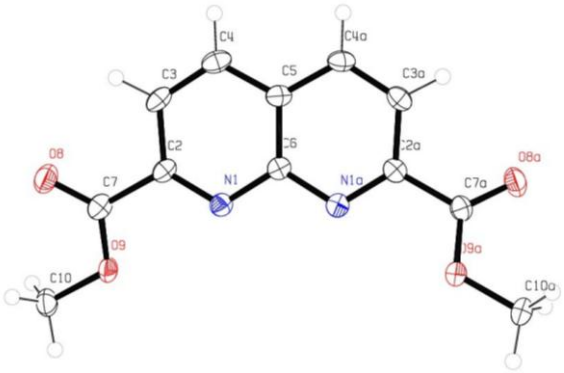

$C_{12}H_{10}N_2O_4$	a = 3.7854 (3) Å	T = 120 K
Cc	b = 46.326 (5) Å	λ = 0.71073 Å
V = 1048.68 (17) Å	c = 6.1728 (6) Å	D_c = 1.560 g cm^{-3}
Z = 4	α = 90 (0) °	μ = 0.120 mm^{-1}
R_1 4.65= %	β = 104.357 (6) °	0.4 x 0.4 x 0.1 mm^3
$wR_2(F^2)$ = 12.98 %	γ = 90 (0) °	Colourless block

Crystallised from DCM solution

7.3.2 Diethyl 1,8-naphthyridine-2,7-dicarboxylate (47b)

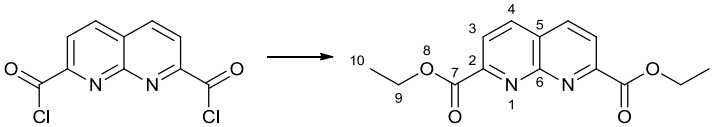

1,8-naphthyridine-2,7-dicarbonyl dichloride (200 mg, 0.78 mmol) was dissolved in ethanol (20 mL). This was stirred for 5 minutes before the addition of triethylamine

(0.17 mL, 1.64 mmol) gave a red solution which turned slowly purple. The reaction mixture was left for a further 24 h, during which time the purple colour disappeared, before the solvent was removed *in vacuo* to give an off white solid (161.8 mg). Recrystallisation by vapour diffusion of diethyl ether into DCM yielded crystals of X-ray crystallography quality (78.1 mg, 36 %).

MP: 149 -150 °C.

ν/cm^{-1} 3048 (w, C-H), 2991 (w, C-H), 2961 (w, C-H), 2945 (w, C-H), 2904 (w, C-H), 1736 (s, C=O), 1598 (m, aromatic C-C), 1556 (m, aromatic C-C), 1532 (m, aromatic C-N), 1477 (m, aromatic C-C).

δ_H (300 MHz; $CDCl_3$) 1.50 (6H, t, *J* = 7.2 Hz, H-10), 4.56 (4H, q, *J* = 7.2 Hz, H-9), 8.36 (2H, d, *J* = 8.4 Hz, H-3), 8.43 (2H, d, *J* = 8.4 Hz, H-4).

δ_c (75 MHz; $CDCl_3$) 14.3 (C-10), 62.4 (C-9), 123.3 (C-3), 125.3 (C-5), 138.2 (C-4), 152.4 (C-2), 154.3 (C-6), 164.9 (C-7).

MS (ES $^+$): *m/z* 275 (24 %, $[M+H]^+$), 297 (4, $[M+Na]^+$), 329 (20, $[M+Na+MeOH]^+$), 549 (14, $[2M+H]^+$), 571 (100, $[2M+Na]^+$).

HR-M/S: Found 297.0847, Expected 297.0846 ($C_{14}H_{14}N_2O_4Na_1$)

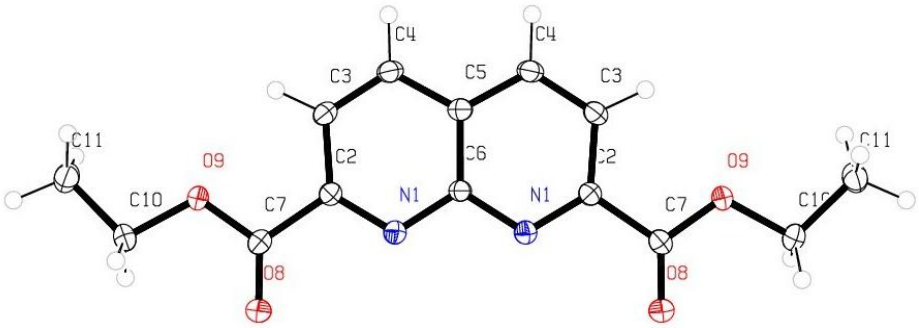

$C_{14}H_{14}N_2O_4$	a = 17.7099 (6) Å	T = 120 K
C2/c	b = 6.3908 (2) Å	λ = 0.71073 Å
V = 1314.73 (8) Å	c = 11.7770 (5) Å	D_c = 1.386 g cm^{-3}
Z = 4	α = 90.0 (0) °	μ = 0.103 mm^{-1}
R_1 = 5.75 %	β = 99.479 (2) °	0.42 x 0.1 x 0.06 mm^3
$wR_2(F^2)$ = 14.41 %	γ = 90 (0) °	Colourless block

Crystallisation by vapour diffusion of diethyl ether into DCM

7.3.3 Dipropyl 1,8-naphthyridine-2,7-dicarboxylate (47c)

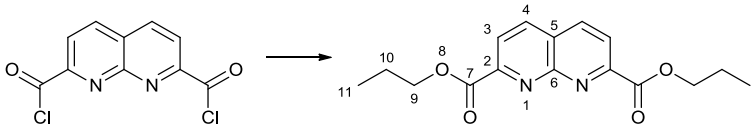

1,8-Naphthyridine-2,7-dicarbonyl dichloride (211 mg, 0.83 mmol) was stirred in DCM (30 ml). Propan-1-ol (0.13 mL, 2.16 mmol, 2.2 equiv) was added followed by triethylamine (0.3 ml, 2.16 mmol). DCM (15 ml) was added to the reaction mixture, which was then washed with water (3 × 50 ml). The organic phase was dried over $MgSO_4$ and the solvent removed *in vacuo* to yield the product (0.1921 g, 76 %).The product was columned in 1 % NEt_3/DCM solvent to give a yellow solid (128.6 mg, 51 %).

MP: 115 – 117 °C.

IR (υ_{max}/cm^{-1}) 3051 (C-H), 3008 (C-H), 2969 (C-H), 2938 (C-H), 2879 (C-H), 1736 (C=O), 1708 (C=O), 1601 (C=C), 1537 (C=N), 1501 (C=C).

δ_H (400 MHz, $CDCl_3$) 1.06 (6H, t, J=7.5 Hz, H-11), 1.90 (4H, sxt, J=7.2 Hz, H-10), 4.45 (4H, t, J=6.9 Hz, H-9), 8.35 (2H, d, J=8.5 Hz), 8.42 (2H, d, J=8.5 Hz).

δ_C (100 MHz, $CDCl_3$) 10.4 (C-11), 22.0 (C-10), 68.0 (C-9), 123.4 (C-3), 125.3 (C-5), 138.2 (C-4), 152.5 (C-2), 154.4 (C-6), 165.0 (C-7).

HR-M/S: Found 325.1153, Expected 325.1159 ($C_{16}H_{18}N_2O_4Na$)

7.3.4 Dibutyl 1,8-naphthyridine-2,7-dicarboxylate (47d)

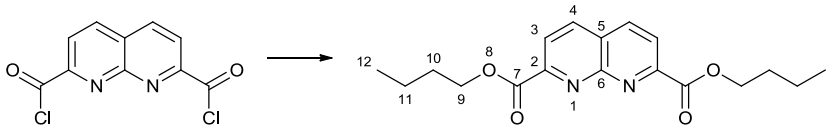

1,8-Naphthyridine-2,7-dicarbonyl dichloride (245.4 mg, 0.83 mmol) was stirred in DCM (30 ml). Butan-1-ol (168 mg , 2.16 mmol, 2.2 equiv) was added followed by triethylamine (0.3 ml, 2.16 mmol). DCM (15 ml) was added to the reaction mixture, which was then washed with water (3 × 50 ml). The organic phase was dried over $MgSO_4$ and the solvent removed *in vacuo* to yield the an off white solid (385.4 mg).The product was columned in 1 % NEt_3/DCM solvent and then recrystallised from DCM/Petrol mixed solvent to give a solid (105.8 mg, 32 %).

MP: 101 – 104 °C.

IR (υ_{max}/cm^{-1}) 3051 (C-H), 3008 (C-H), 2956 (C-H), 2870 (C-H), 1736 (C=O), 1599 (C=C), 1535 (C=N), 1464 (C=C).

δ_H (400 MHz, $CDCl_3$) 0.99 (6H, t, J=7.4 Hz, H-12), 1.51 (4H, sxt, J=7.5 Hz, H-11), 1.85 (4H, quin, J=7.3 Hz, H-10), 4.49 (4H, t, J=6.8, H-9), 8.35 (2H, d, J=8.3, H-3), 8.42 (2H, d, J=8.5, H-4).

δ_C (100 MHz, $CDCl_3$) 13.7 (C-12), 19.1 (C-11), 30.7 (C-10), 66.4 (C-9), 123.4 (C-3), 125.3 (C-5), 138.2 (C-C-4), 152.5 (C-2), 154.4 (C-6), 165.0 (C-7).

M/S (ESI) m/z 331 (10 %, $[M+H]^+$), 394 (100 %, $[M+Na+MeCN]^+$), 683 (38 %, $[2M+Na]^+$).

HR-M/S: 331.1658 Found, 331.1652 Expected ($C_{18}H_{23}N_2O_4$)

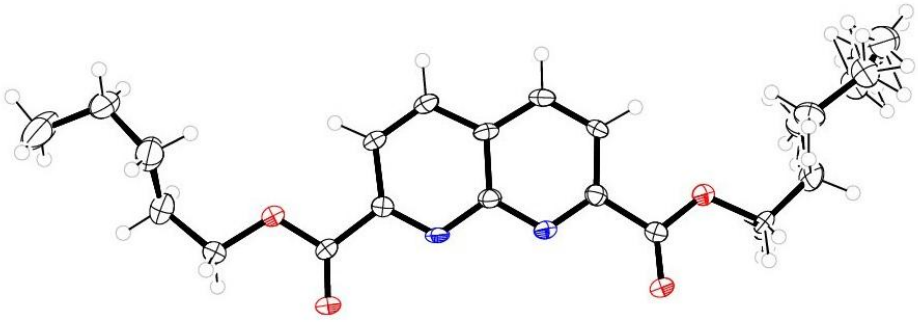

$C_{20}H_{26}N_2O_4$	a = 6.3600 (4) Å	T = 120 K
P-1	b = 11.2540 (8) Å	λ = 0.71073 Å
V = 953.82 (12) Å	c = 13.6090 (11) Å	D_c = 1.248 g cm^{-3}
Z = 2	α = 97.291 (4) °	μ = 0.087 mm^{-1}
R_1 = 11.29 %	β = 99.067 (4) °	0.26 x 0.14 x 0.02 mm^3
$wR_2(F^2)$ = 23.52 %	γ = 90.267 (5) °	Colourless fragment

Crystallisation by vapour diffusion of diethyl ether into chloroform

7.3.5 Di(*iso*-propyl) 1,8-naphthyridine-2,7-dicarboxylate (47f)

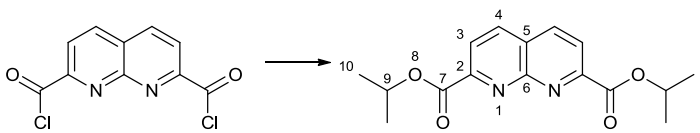

1,8-Naphthyridine-2,7-dicarbonyl dichloride (245.5 mg, 0.98 mmol) was stirred in DCM (30 ml). Propan-2-ol (130 mg, 2.16 mmol, 2.2 equiv) was added followed by triethylamine (0.3 ml, 2.16 mmol). DCM (15 ml) was added to the reaction mixture, which was then washed with water (3 × 50 ml). The organic phase was dried over

$MgSO_4$ and the solvent removed *in vacuo* to yield the product (144 mg).The product was columned in 1 % NEt_3/DCM solvent and then recrystallised from DCM/Petrol mixed solvent to give a solid (85.1 mg, 29 %).

MP: 181 – 185 °C (decomposes).

IR (υ_{max}/cm^{-1}) 3051 (C-H), 2988 (C-H), 2980 (C-H), 2940 (C-H), 1731 (C=O), 1600 (C=C), 1538 (C=N).

δ_H (400 MHz, $CDCl_3$) 1.48 (12H, d, *J* =6.3 Hz, H-10), 5.40 (2H, spt, *J*=6.3, H-9), 8.34 (2H, d, J=8.3 Hz, H-3), 8.41 (2H, d, J=8.8 Hz, H-4).

δ_C (100 MHz, $CDCl_3$) 22.3 (C-10), 70.9 (C-9), 123.8 (C-3), 125.6 (C-5), 138.5 (C-4), 153.3 (C-2), 154.9 (C-6), 165.0 (C-7).

M/S (ESI) m/z 366 (100 %, $[M+Na+MeCN]^+$), 627 (43 %, $[2M+Na]^+$).

HR-M/S: Found 303.1344, Expected 303.1339 ($C_{16}H_{19}N_2O_4$)

7.3.6 Di(*tert*-butyl) 1,8-naphthyridine-2,7-dicarboxylate (47g)

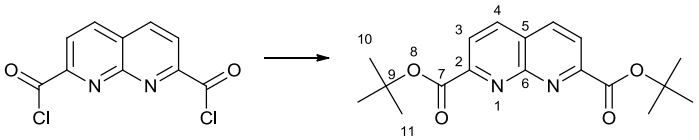

1,8-Naphthyridine-2,7-dicarbonyl dichloride (250 mg, 0.98 mmol) was stirred in DCM (30 ml). *tert*-Butanol (193 mg, 2.16 mmol, 2.2 equiv) was added followed by triethylamine (0.3 ml, 2.16 mmol). DCM (15 ml) was added to the reaction mixture. Having been left to stir overnight the solvent removed *in vacuo* to yield the product (144 mg). The product was columned in 2 % NEt_3/DCM solvent and then recrystallised from DCM/Petrol mixed solvent to give a solid (58.6 mg, 18 %).

ν/cm^{-1} 2960 (C-H), 3051 (C-H), 2916 (C-H), 2848 (C-H), 1704 (C=O), 1634 (aromatic C-C), 1602 (aromatic C-C), 1538 (aromatic C-N), 1437 (aromatic C-C).

7.3.7 Dipentyl 1,8-naphthyridine-2,7-dicarboxylate (47e)

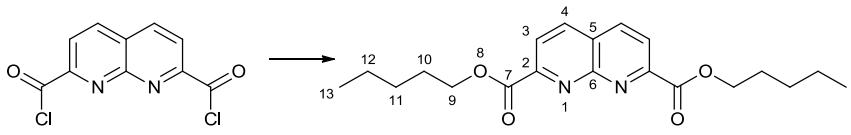

1,8-Naphthyridine-2,7-dicarbonyl dichloride (220.4 mg, 0.86 mmol) was stirred in DCM (30 ml). Pentan-1-ol (190 mg, 2.16 mmol, 2.2 equiv) was added followed by

triethylamine (0.3 ml, 2.16 mmol). DCM (15 ml) was added to the reaction mixture, which was then washed with water (3 × 50 ml). The organic phase was dried over $MgSO_4$ and the solvent removed *in vacuo* to yield the product (278.6 mg). The product was columned in 1 % NEt_3/DCM solvent and then recrystallised from DCM Petrol mixed solvent to give a solid (64.5 mg, 19 %).

MP: 120 -121 °C.

IR (υ_{max}/cm^{-1}) 3050 (C-H), 3007 (C-H), 2956 (C-H), 2931 (C-H), 2857 (C-H), 1741 (C=O), 1599 (C=C), 1537 (C=N), 1455 (C=C).

δ_H (400 MHz, $CDCl_3$) 0.94 (6H, t, J=7.0 Hz, H-13), 1.35 - 1.51 (8H, m, H-11 + H-12), 1.88 (4H, quin, J=7.2, H-10), 4.49 (4H, t, J=6.9 Hz, H-9), 8.36 (2H, d, J=8.5 Hz, H-3), 8.42 (2H, d, J=8.5 Hz, H-4).

δ_C (100 MHz, $CDCl_3$) 12.0 (C-13), 20.5 (C-12), 26.1 (C-11), 26.5 (C-10), 64.8 (C-9), 121.5 (C-3), 123.4 (C-5), 136.3 (C-4), 150.7 (C-2), 152.5 (C-6), 163.2 (C-7).

M/S (ESI) m/z 357 (100 %, $[M+H]^+$).

HR-M/S: Found 359.1977, Expected 359.1965 ($C_{20}H_{27}N_2O_4$)

7.3.8 Dibenzyl-1,8-naphthyridine-2,7-dicarboxylate (47h)

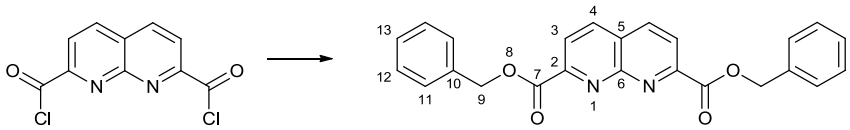

1,8-Naphthyridine-2,7-dicarbonyl dichloride (500.2 mg, 1.96 mmol) was dissolved in DCM (50 mL), benzyl alcohol (0.45 ml, 4.31 mmol) was then added followed by triethylamine (0.60 mL, 4.31 mmol) which gave a blue solution. The reaction mixture was left to stir overnight. The following day the reaction mixture was washed with water (3 x 50 mL) followed by brine (50 mL). The remaining organic residue was dried with magnesium carbonate and then reduced *in vacuo* yielding a grey solid (518 mg). This was recrystallised using a mixed solvent system of DCM:diethyl ether to yield a grey crystalline material (252.4 mg, 32 %)

MP: 214-216 °C.

ν/cm^{-1} 3050 (C-H), 3035 (C-H), 3006 (C-H), 2943 (C-H), 2888 (C-H), 1748 (C=O), 1598 (aromatic C-C), 1536 (aromatic C-N), 1496 (aromatic C-C).

δ_H (300 MHz, $CDCl_3$) 5.53 (4H, s, H-7), 7.32 – 7.43 (6H, m, H-10 & H-11), 7.53 (4H, d, *J*=6.6 Hz, H-9), 8.35 (2H, d, *J*=8.4 Hz, H-3), 8.41 (2H, d, *J*=8.4 Hz, H-4).

δ_C (75 MHz, $CDCl_3$) 68.0 (C-9), 123.5 (C-3), 125.4 (C-5), 128.3 (C-13), 128.5 (C-11), 128.6 (C-12), 128.7 (C-13), 135.3 (C-10) 138.2 (C-4), 152.3 (C-2), 164.8 (C-7).

M/S (ESI (MeCN)) m/z 399 (8 %, [M+H]), 417 (21, $[M+NH_4]^+$), 463 (26, $[M+Na+MeCN]^+$), 501 (43, $[M+NH_4+2MeCN]^+$), 815 (20, $[2M+NH_4]^+$), 820 (26, $[2M+Na]^+$).

HR-M/S: Found 421.1165, Expected 421.1159 ($C_{24}H_{18}N_2O_4Na$)

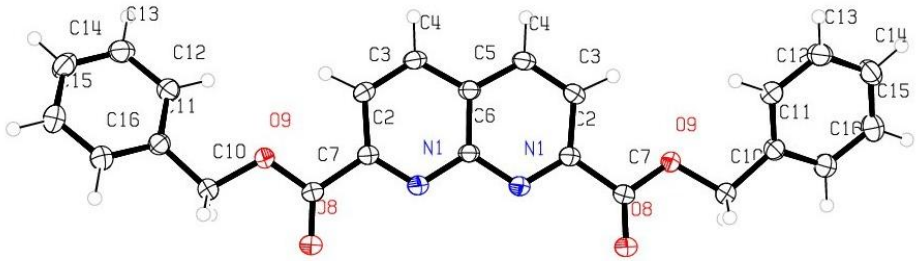

$C_{24}H_{18}N_2O_4$	a = 35.50 (4) Å	T = 120 K
C 2/c	b = 6.307 (8) Å	λ = 0.69390 Å
V = 1872 (4) Å	c = 8.381 (10) Å	D_c = 1.413 g cm^{-3}
Z = 4	α = 90 (0) °	μ = 0.098 mm^{-1}
R_1 = 4.86 %	β = 93.849 (13) °	0.1 x 0.02 x 0.01 mm^3
$wR_2(F^2)$ = 13.28 %	γ = 90 (0) °	Colourless lath

Crystallisation by vapour diffusion of diethyl ether into DCM

7.3.9 *bis*-(2-Methylbenzyl) 1,8-naphthyridine-2,7-dicarboxylate (47i)

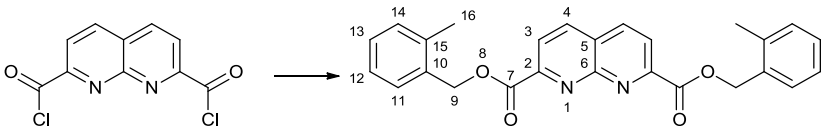

1,8-Naphthyridine-2,7-dicarbonyl dichloride (250 mg, 0.98 mmol) was dissolved in DCM (30 mL), 2-methylbenzyl alcohol (268 mg, 2.16 mmol) was then added, followed by triethylamine (0.30 ml, 2.16 mmol). The blue/grey reaction mixture was left to stir overnight. The following day the reaction mixture was washed with water (3 x 50 mL) followed by brine (50 mL). The remaining organic residue was dried with magnesium sulphate and then reduced *in vacuo* (293 mg). This was recrystallised

using a mixed solvent system of DCM:petrol 40-60 °C to yield a white powder (114.2 mg, 28 %).

MP: 228 – 230 °C.

IR (υ_{max}/cm^{-1}) 3049 (C-H aromatic), 3007 (C-H aliphatic), 1743 (C=O), 1540 (C=C aromatic).

δ_H (300 MHz, $CDCl_3$) 2.46 (6H, s, H-16), 5.54 (4H, s, H-9), 7.16-7.32 (6H, m, H-11 to H-13), 7.51 (2H, dd, *J*=7.1, 2.0 Hz, H-14), 8.34 (2H, d, *J*=8.4 Hz, H-3), 8.41 (2H, d, *J*=8.4 Hz, H-4).

δ_C (75 MHz, $CDCl_3$) 19.1 (C-16), 66.4 (C-9), 123.5 (C-3), 125.3 (C-5), 126.0 (C-11), 128.7 (C-13), 129.6 (C-12), 130.4 (C-14), 133.3 (C-10), 137.1 (C-15), 138.3 (C-4), 152.3 (C-2), 154.5 (C-6), 164.7 (C-7).

M/S (ESI (MeCN)) m/z: 449 (8 %, $[M+Na]^+$), 491 (62, $[M+Na+MeCN]^+$), 876 (100, $[2M+Na]^+$).

HR-M/S: Found 427.1661, Expected 427.1666 ($C_{26}H_{23}N_2O_4$)

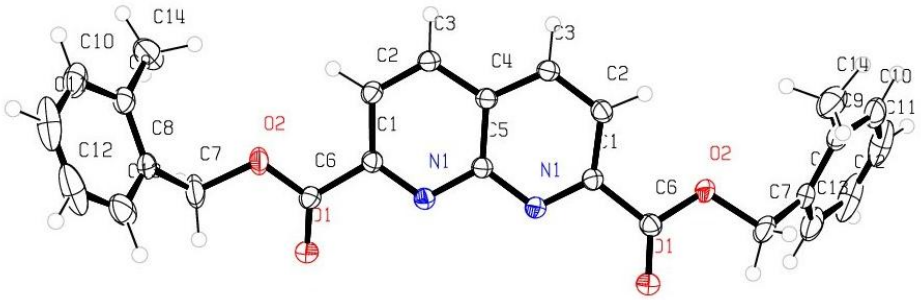

$C_{26}H_{22}N_2O_4$	a = 26.7283 (11) Å	T = 120 K
C2/c	b = 6.3052 (2) Å	λ = 0.71073 Å
V = 2069.93 (14) Å	c = 14.6133 (6) Å	D_c = 1.368 g cm^{-3}
Z = 4	α = 90 (0) °	μ = 0.093 mm^{-1}
R_1 = 5.21 %	β = 122.807 (2) °	0.42 x 0.18 x 0.06 mm^3
$wR_2(F^2)$ = 15.93 %	γ = 90 (0) °	Colourless cut blade

Crystallised from Acetonitrile

7.3.10 *bis*-(3-Methylbenzyl) 1,8-naphthyridine-2,7-dicarboxylate (47j)

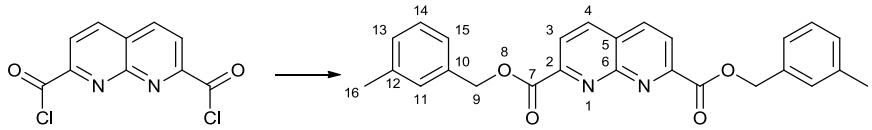

1,8-Naphthyridine-2,7-dicarbonyl dichloride (259 mg, 0.98 mmol) was dissolved in DCM (30 mL), 3-methylbenzyl alcohol (267 mg, 2.16 mmol) was then added, followed by triethylamine (0.30 ml, 2.16 mmol). The reaction mixture was left to stir overnight. The following day the reaction mixture was washed with water (3 x 50 mL) followed by brine (50 mL). The remaining organic residue was dried with magnesium sulphate and then reduced *in vacuo* (341.8 mg, 80 %). This was recrystallised using a mixed solvent system of DCM:petrol 40-60 °C to yield a white powder (114.2 mg, 26 %).

MP: 162 – 164 °C.

IR (υ_{max}, cm^{-1}) 3051 (C-H aromatic), 2932 (C-H aliphatic), 1736 (C=O), 1597 (C=C aromatic).

δ_H (300 MHz, $CDCl_3$) 2.38 (6H, s, H-16), 5.50 (4H, s, H-9), 7.17 (2H, d, *J*=6 Hz, H-15) 7.26 – 7.43 (6H, m, H-11 – H-13), 8.36 (2H, d, *J*=8.4 Hz, H-3), 8.42 (2H, d, *J*=8.4 Hz, H-4).

δ_C (75 MHz, $CDCl_3$) 21.3 (C-16), 68.1 (C-9), 123.5 (C-3), 125.4 (C-5), 125.8 (C-11), 128.5 (C-15), 129.2 (C-13), 129.5 (C-12), 135.2 (C-14), 138.2 (C-4), 152.3 (C-2), 154.4 (C-6), 164.7 (C-7).

M/S (ESI (MeCN)) m/z: 491 (47 %, $[M+Na+MeCN]^+$), 876 (100, $[2M+Na]^+$).

HR-M/S: Found 427.1634, Expected 427.1652 ($C_{26}H_{32}N_2O_4$)

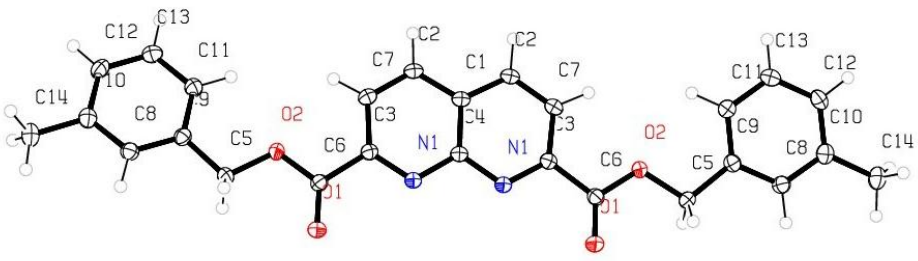

$C_{26}H_{22}N_2O_4$	a = 25.2253 (6) Å	T = 120 K
C2/c	b = 6.5222 (1) Å	λ = 0.71073Å

V =2026.39 (7) Å	c = 14.4903 (3) Å	D_c =1.398 g cm^{-3}
Z = 4	α = 90 (0) °	μ = 0.095mm^{-1}
R_1 = 4.75 %	β = 121.789 (1)°	0.3 × 0.06 × 0.02 mm
$wR_2(F^2)$ = 12.15 %	γ = 90 (0) °	Colourless Needle

Crystallised from acetonitrile

7.3.11 *bis*-(4-Methylbenzyl) 1,8-naphthyridine-2,7-dicarboxylate (47k)

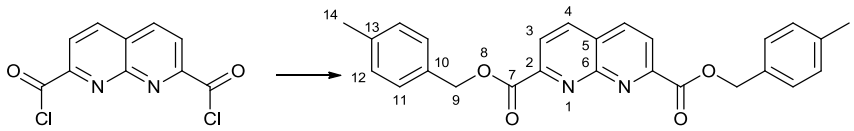

1,8-Naphthyridine-2,7-dicarbonyl dichloride (248.9 mg, 0.98 mmol) was dissolved in DCM (30 mL), 4-methylbenzyl alcohol (270.2 mg, 2.16 mmol) was then added, followed by triethylamine (0.30 ml, 2.16 mmol). The reaction mixture was left to stir overnight. The following day the reaction mixture was washed with water (3 x 50 mL) followed by brine (50 mL). The remaining organic residue was dried with magnesium sulphate and then reduced *in vacuo* to give a solid (309.8 mg, 76 %). This was recrystallised using a mixed solvent system of DCM:petrol 40-60 °C to yield a white powder (94.1 mg, 23 %).

MP: > 212 °C decomp.

IR (υ_{max}/cm^{-1}) 3048 (C-H), 3006 (C-H), 2970 (C-H), 1746 (C=O), 1595 (C=C aromatic), 1537 (C=N aromatic), 1518 (C=C aromatic).

δ_H (400 MHz, $CDCl_3$) 2.33 (6 H, s, H-14), 5.76 (4 H, s, H-9), 7.24 (4 H, d, *J*=8.1Hz, H-11), 7.43 (2 H, d, *J*=7.7 Hz, H-12), 8.32 (2 H, d, *J*=8.4 Hz, H-3), 8.80 (2 H, d, *J*=8.0 Hz, H-4).

HR-M/S: Found 427.1661, Expected 427.1652 ($C_{26}H_{23}N_2O_4$)

Characterisation of this solid proved extremely difficult given its lack of solubility in most solvents tested.

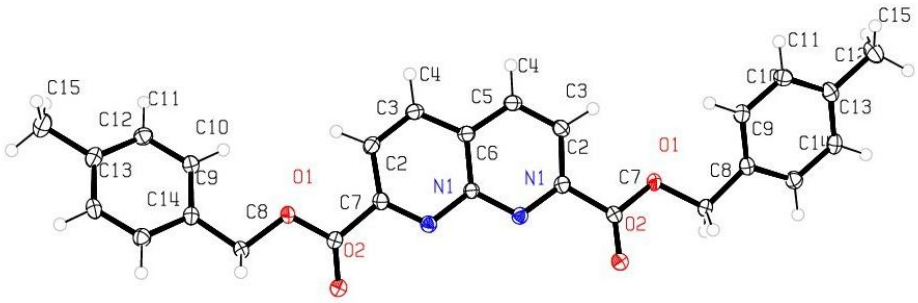

$C_{26}H_{22}N_2O_4$	*a* = 37.4288 (11) Å	T = 120
C2/c	*b* = 6.3295 (2) Å	λ = 0.71073 Å
V = 2040.67 (10) Å3	*c* = 8.6909 (2) Å	D_c = 1.388 g cm^{-3}
Z = 4	α = 90 (0) °	μ = 0.094mm^{-1}
R_1 = 5.79 %	β = 97.635 (2)°	0.36 x 0.1 x 0.02 x mm^3
$wR_2(F^2)$ = 12.76 %	γ = 90 (0) °	Colourless Lath

Crystallised from acetonitrile

7.3.12 *bis*-(2,4,6-Trimethylbenzyl) 1,8-naphthyridine-2,7-dicarboxylate (47l)

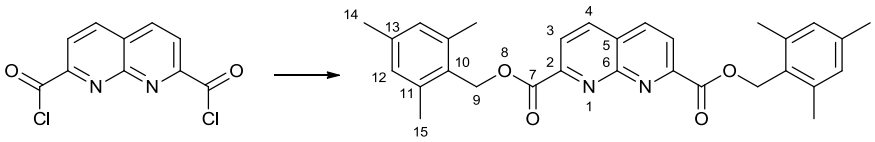

1,8-Naphthyridine-2,7-dicarbonyl dichloride (255.7 mg, 0.98 mmol) was dissolved in DCM (50 mL), 2,4,6-trimethylbenzyl alcohol (332 mg, 2.16 mmol) was then added, followed by triethylamine (0.30 ml, 2.16 mmol). The reaction mixture was left to stir overnight. The following day the reaction mixture was washed with water (3 x 50 mL) followed by brine (50 mL). The remaining organic residue was dried with magnesium sulphate and then reduced *in vacuo* (326.3 mg, 69 %). This was recrystallised using a mixed solvent system of DCM:petrol 40-60 °C to yield a white powder (72.9 mg, 15 %).

MP: approx. ≈ 200 °C (decomp)

IR (υ_{max}/cm^{-1}) 3052, 3008 (C-H aromatic), 2969 (C-H aliphatic), 1739 (C=O), 1603 (C=C aromatic).

δ_H (300 MHz, $CDCl_3$) 2.30 (6H, s, H-14), 2.45 (12H, s, H-15), 5.57 (4H, s, H-9), 6.89 (4H, s, H-12), 8.27 (2H, d, *J*=8.4 Hz, H-3), 8.37 (2H, d, *J*=8.4 Hz, H-4).

δ_C (75 MHz, $CDCl_3$) 19.8 (C-15), 21.0 (C-14), 63.0 (C-9), 123.4 (C-3), 125.1 (C-5), 128.5 (C-10), 129.0 (C-12), 138.1 (C-4), 138.5 (C-11), 138.6 (C-13), 152.4 (C-2), 154.5 (C-6), 164.7 (C-7).

HR-M/S: Found 505.2096, Expected 505.2098 ($C_{30}H_{30}N_2O_4Na$)

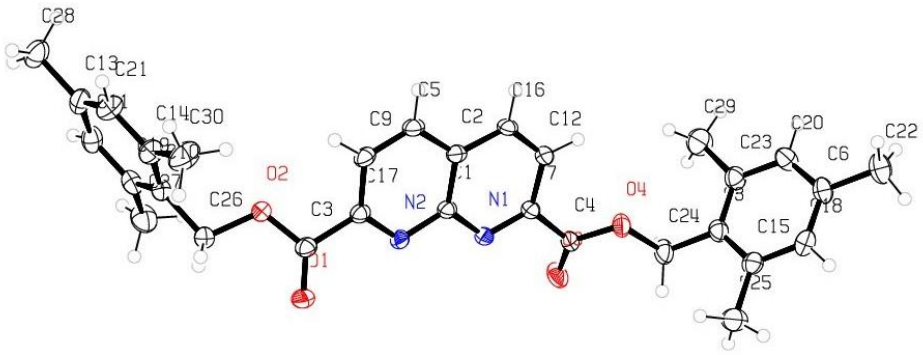

$C_{30}H_{30}N_2O_4$	*a* = 18.5271 (4) Å	T = 120
P21/c	*b* = 6.2749 (1) Å	λ = 0.71073 Å
V = 2500.43 (8) Å	*c* = 22.1145 (4) Å	D_c = 1.282 g cm^{-3}
Z = 4	α = 90 (0) °	μ = 0.085 mm^{-1}
R_1 = 6.87 %	β = 103.449 (1) °	0.14 x 0.06 x 0.01 mm^3
$wR_2(F^2)$ = 16.32 %	γ = 90 (0) °	Colourless cut plate

Recrystallisation by vapour diffusion of diethyl ether into DCM

7.3.13 *bis*-(2,3,5,6-Tetramethylbenzyl) 1,8-naphthyridine-2,7-dicarboxylate (47m)

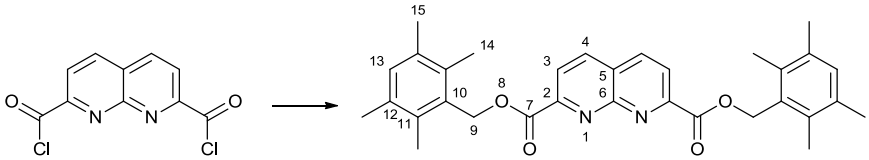

1,8-Naphthyridine-2,7-dicarbonyl dichloride (251.6 mg, 0.98 mmol) was stirred in DCM (30 ml). 2,3,5,6-tetramethylbenzyl alcohol (354.4 mg, 2.16 mmol, 2.2 equiv) was added followed by triethylamine (0.3 ml, 2.16 mmol). DCM (15 ml) was added to the reaction mixture, which was then washed with water (3 × 50 ml). The organic phase was dried over $MgSO_4$ and the solvent removed *in vacuo* to yield the product (505 mg). The product was recrystallised using DCM and petrol 40-60˚C (185.1 mg, 37 %).

MP: > 280 °C

IR (υ_{max}/cm^{-1}) 3044 (C-H), 3004 (C-H), 2961 (C-H), 2920 (C-H), 2863 (C-H), 1740 (C=O) 1597 (C=C aromatic), 1537 (C=N), 1474 (C=C).

δ_H (400 MHz, $CDCl_3$) 2.27 (12H, s, H-14), 2.36 (12H, s, H-15), 5.65 (4H, s, H-9), 7.02 (2H, s, H-13), 8.28 (2H, d, J=8.5, H-3), 8.36 (2H, d, J=8.5, H-4).

δ_C (100 MHz, $CDCl_3$) 15.6 (C-14), 20.4 (C-15), 63.7 (C-9), 123.4 (C-3), 125.2 (C-5), 131.2 (C-10), 132.5 (C-13), 134.0 (C-11), 134.6 (C-12), 138.1 (C-4), 152.5 (C-2), 164.8 (C-6).

HR-M/S: Found 511.2579, Expected 511.2591 ($C_{32}H_{35}N_2O_4$)

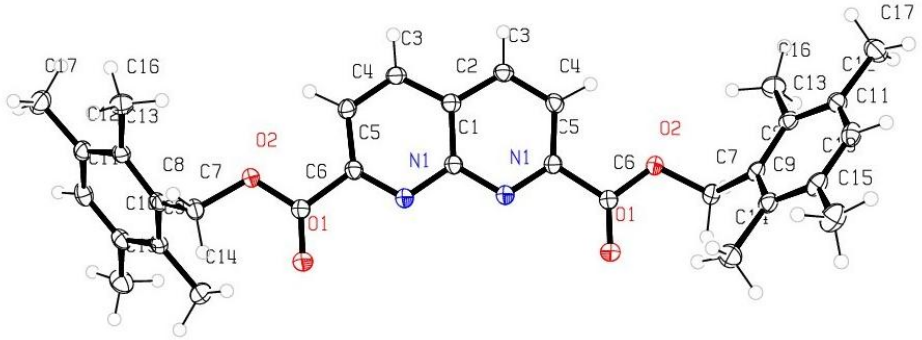

$C_{32}H_{34}N_2O_4$	a =40.2736 (9) Å	T = 120 K
C2/c	b = 6.3180 (1) Å	λ = 0.71073 Å
V = 2575.52 (9) Å	c = 10.3963 (2) Å	D_c = 1.317 g cm^{-3}
Z = 4	α = 90 (0) °	μ = 0.087 mm^{-1}
R_1 = 5.60 %	β = 103.192 (1) °	0.2 x 0.18 x 0.06 mm^3
$wR_2(F^2)$ = 12.17 %	γ = 90 (0) °	Colourless block

Crystallised from acetonitrile

7.3.14 *bis*-(2,3,4,5,6-Pentamethylbenzyl) 1,8-naphthyridine-2,7-dicarboxylate (47n)

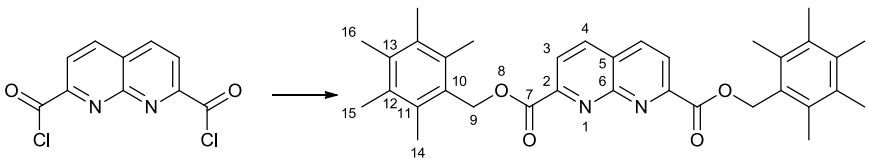

1,8-Naphthyridine-2,7-dicarbonyl dichloride (251.6 mg, 0.98 mmol) was stirred in DCM (30 ml). 2,3,4,5,6-pentamethylbenzyl alcohol (393.8 mg, 2.21 mmol, 2.2 equiv) was added followed by triethylamine (0.3 ml, 2.16 mmol) The reaction was left to stir for 12 h. DCM (15 ml) was added to the reaction mixture, which was then washed with water (3 × 50 ml). The organic phase was dried over $MgSO_4$ and the

solvent removed *in vacuo* to yield the product (524.3 mg, 88 %). The product was recrystallised using DCM and petrol 40-60˚C (124.9 mg, 23 %).

MP: > 210 °C

IR (υ_{max}/cm^{-1}) 3051 (C-H), 3007 (C-H), 2913 (C-H), 1740 (C=O) 1601 (C=C aromatic), 1539 (C=N), 1423 (C=C).

HR-M/S: Found 561.2710, Expected 561.2724 ($C_{34}H_{38}N_2O_4Na$)

Further characterisation of this solid proved extremely difficult given its complete insolubility in all solvents tested.

7.3.15 *bis*-(2-Fluorobenzyl) 1,8-naphthyridine-2,7-dicarboxylate (47o)

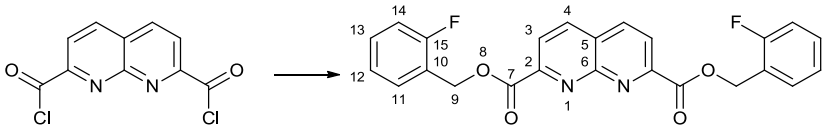

1,8-Naphthyridine-2,7-dicarbonyl dichloride (249.6 mg, 0.98 mmol) was stirred in DCM (30 ml). 2-Fluorobenzyl alcohol (272 mg, 2.16 mmol, 2.2 equiv) was added followed by triethylamine (0.3 ml, 2.16 mmol). The reaction was left stirring overnight. DCM (15 ml) was added to the reaction mixture, which was then washed with water (3 × 50 ml). The organic phase was dried over $MgSO_4$ and the solvent removed *in vacuo* to yield the product (457.6 mg). The product was recrystallised using DCM and petrol 40-60˚C (326.5 mg, 76 %).

MP: 148-151 °C

δ_H (400 MHz, $CDCl_3$) 5.59 (4 H, s, H-9), 7.09 (2 H, td, *J*=9.1, 1.0 Hz, H-12), 7.16 (2 H, td, *J*=7.6, 1.0 Hz, H-14), 7.34 (2 H, tdd, *J*=7.8, 7.8, 5.4, 1.8 Hz, H-13), 7.57 (2 H, td, *J*=7.5, 1.8 Hz, H-11), 8.35 (2 H, d, *J*=8.6 Hz, H-3), 8.42 (2 H, d, *J*=8.6 Hz, H-4)

δ_C (100 MHz, $CDCl_3$) 61.8 (d, *J*=4.4 Hz, C-9), 115.5 (d, *J*=20.5 Hz, C-14), 122.5 (d, *J*=13.2 Hz,), 123.6 (C-3, 124.2 (d, *J*=2.9 Hz, C-12), 125.5 (C-5), 130.5 (d, *J*=7.3 Hz, C-11), 131.0 (d, *J*=2.9 Hz, C-13), 138.3 (C-4), 152.2 (C-2), 154.4 (C-6), 161.0 (d, J= 248.8, C-15), 164.6 (C-7)

δ_F (282 MHz, $CDCl_3$) 117.7

HR-M/S: Found 435.1145, Expected 435.1151 ($C_{24}H_{17}F_2N_2O_4$)

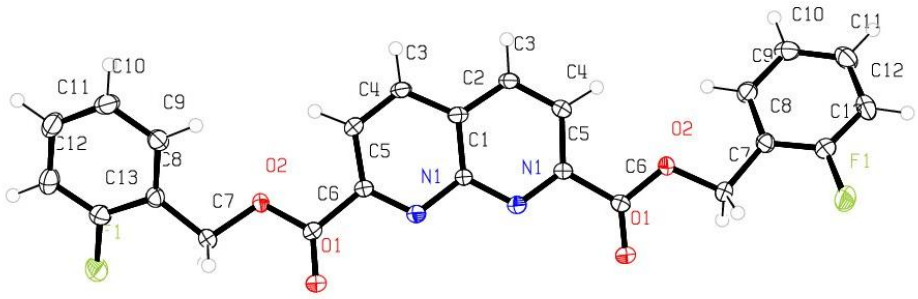

$C_{24}H_{16}F_2N_2O_4$	*a* = 36.128 (2) Å	T = 120 K
C2/c	*b* = 6.3539 (4) Å	λ = 0.71073 Å
V =1937.23 (19) Å	*c* = 8.4870 (4) Å	D_c = 1.489 g cm^{-3}
Z = 4	α = 90 (0) °	μ = 0.115 mm^{-1}
R_1 = 5.75 %	β = 96.089 (3) °	0.48 x 0.2 x 0.02 mm^3
wR2(F2) = 15.05 %	γ = 90 (0) °	Colourless Lath

Crystallisation by vapour diffusion of diethyl ether into DCM

7.3.16 *bis*-(2-Chlorobenzyl) 1,8-naphthyridine-2,7-dicarboxylate (47r)

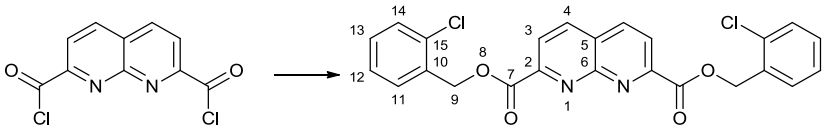

1,8-Naphthyridine-2,7-dicarbonyl dichloride (252.7 mg, 0.98 mmol) was stirred in DCM (30 ml). 2-chlorobenzyl alcohol (299.3 mg, 2.16 mmol, 2.2 equiv) was added followed by triethylamine (0.3 ml, 2.16 mmol). The reaction was left stirring overnight during which time the colour had changed to orange/brown. DCM (15 ml) was added to the reaction mixture, which was then washed with water (3 × 50 ml). The organic phase was dried over $MgSO_4$ and the solvent removed *in vacuo* to yield the product (439.1 mg, 95 %). The product was recrystallised using DCM and petrol 40-60˚C (249.1 mg, 54 %).

MP: 212-215 °C

IR (υ_{max}/cm^{-1}) 3047 (C-H), 3005 (C-H), 1738 (C=O), 1595(C=C aromatic), 1573 (C=N aromatic), 1537 (C=C), 1477 (C=C).

δ_H (400 MHz, $CDCl_3$) 5.57 (4H, s, H-9), 7.22 (4H, dt, J=9.3, 3.7 Hz, H-13 & H-12), 7.34 (2H, dt, J=9.0, 3.8 Hz, H-11), 7.56 (2H, dt, J=9.3, 3.8 Hz, H-14), 8.31 (2H, d, J=8.5 Hz, H-3), 8.37 (2H, d, J=8.5 Hz, H-4).

δ_C (100 MHz, $CDCl_3$) 65.2 (C-9), 123.6 (C-3), 125.5 (C-5), 127.0 (C-12), 129.5 (C-11), 129.7 (C-13), 130.1 (C-14), 133.6 (C-10), 138.4 (C-4), 152.2 (C-2), 154.5 (C-6), 162.5 (C-7).

M/S (ESI (MeCN)) m/z: 467 (10 %, $[M+H]^+$), 489 (77, $[M+Na]^+$), 505 (22, $[M+K]^+$), 530 (23, $[M+Na+MeCN]^+$), 955 (57, $[2M+Na]^+$), 957 (100, $[2M+Na]^+$).

HR-M/S: Found 467.0563, Expected 467.0560 ($C_{24}H_{17}Cl_2N_2O_4$)

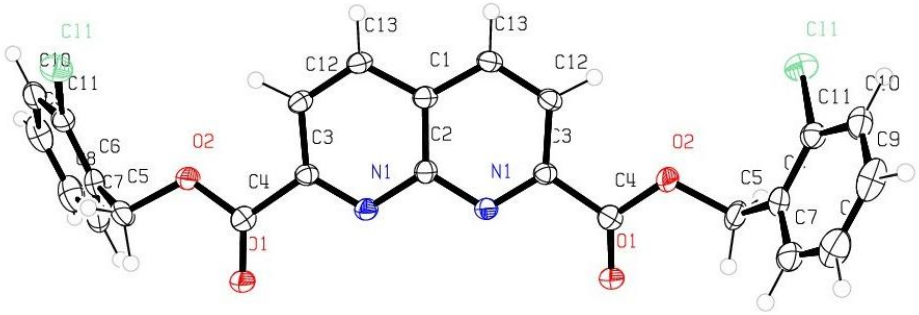

$C_{24}H_{16}Cl_2N_2O_4$	a = 26.2968 (14) Å	T = 120 K
C2/c	b = 6.3268 (2) Å	λ = 0.71073 Å
V = 2036.64 (16) Å	c = 14.3802 (7) Å	D_c = 1.524 g cm^{-3}
Z = 4	α = 90 (0) °	μ = 0.356 mm^{-1}
R_1 = 6.25 %	β = 121.651 (2) °	0.8 x 0.08 x 0.04 mm^3
$wR_2(F^2)$ = 17.31 %	γ = 90 (0) °	Colourless Needle

Crystallised from acetonitrile

7.3.17 *bis*-(2-Bromobenzyl) 1,8-naphthyridine-2,7-dicarboxylate (47u)

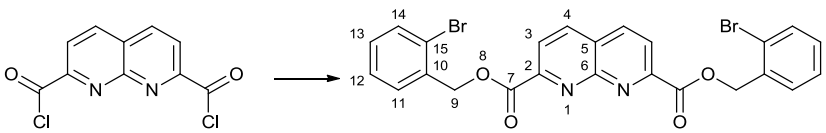

1,8-Naphthyridine-2,7-dicarbonyl dichloride (250 mg, 0.98 mmol) was dissolved in DCM (30 mL), 2-bromobenzyl alcohol (416.4 mg, 2.16 mmol) was then added, followed by triethylamine (0.30 ml, 2.16 mmol), the solution was seen to turn pale orange. The reaction mixture was left to stir overnight. The following day the

reaction mixture was washed with water (3 x 50 mL) followed by brine (50 mL). The remaining organic residue was dried with magnesium sulphate and then reduced *in vacuo* (434 mg, 80 %). This was recrystallised using a mixed solvent system of DCM:petrol 40-60 °C to yield a orange/brown powder (120.5 mg, 22 %)

MP 182 - 185 °C

IR (υ_{max}/cm^{-1}) 3045 (C-H aromatic), 1737 (C=O), 1593 (C=C aromatic), 1568 (C=N aromatic), 1539, (C=C aromatic), 748 (C-Br).

δ_H (400 MHz, $CDCl_3$) 5.62 (4 H, s, H-9), 7.22 (2 H, t, *J*=7.5 Hz, H-2), 7.34 (2 H, t, *J*=7.5 Hz, H-14), 7.53 (4 H, t, *J*=8.3 Hz, H-11 an d H-13), 8.39 (2 H, d, *J*=8.3 Hz, H-3), 8.46 (2 H, d, *J*=8.3 Hz, H-4).

δ_C (100 MHz, $CDCl_3$) 67.4 (C-9), 123.2 (C-15), 123.6 (C-3), 125.5 (C-5), 127.6 (C-12), 129.9 (C-11), 130.0 (C-13), 132.8 (C-14), 134.7 (C-10), 138.4 (C-4), 152.2 (C-2), 154.5 (C-6), 164.4 (C-7).

M/S (ESI (MeCN)) m/z: 377 (100 %, $[2M+2H+Na]^{3+}$).

HR-M/S: Found 554.9549, Expected 554.9550 ($C_{24}H_{17}Br2N_2O_4$)

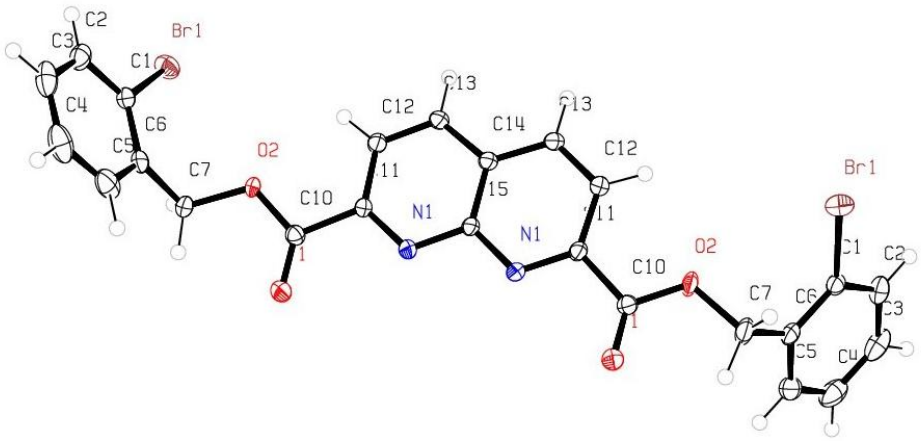

$C_{24}H_{16}Br_2N_2O_4$	a = 26.6641 (7) Å	T = 120 K
C2/c	b = 6.3600 (2) Å	λ = 0.71073 Å
V =2078.05 (10) Å	c = 14.4289 (4) Å	D_c = 1.778 g cm^{-3}
Z = 4	α = 90 (0) °	μ = 3.937 mm^{-1}
R_1 = 2.98 %	β = 121.869 (2) °	0.3 x 0.06 x 0.02 mm^3
$wR_2(F^2)$ = 7.52 %	γ = 90 (0) °	Clear colourless lath

Crystallisation by vapour diffusion of petroleum ether into DCM

7.3.18 *bis*-(3-Fluorobenzyl) 1,8-naphthyridine-2,7-dicarboxylate (47p)

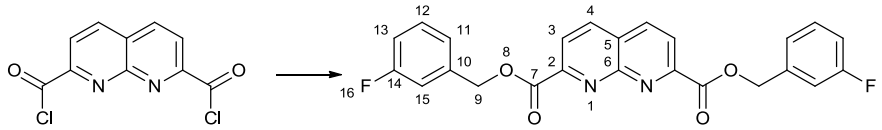

1,8-Naphthyridine-2,7-dicarbonyl dichloride (250.3 mg, 0.98 mmol) was stirred in DCM (30 ml). 3-Fluorobenzyl alcohol (272 mg, 0.23 ml, 2.16 mmol, 2.2 equiv) was added followed by triethylamine (0.3 ml, 2.16 mmol). The solution went a green/brown colour upon the addition of NEt_3. The reaction was left stirring overnight during which time the colour had changed to orange/brown. DCM (15 ml) was added to the reaction mixture, which was then washed with water (3 × 50 ml). The organic phase was dried over $MgSO_4$ and the solvent removed *in vacuo* to yield the product (535.8 mg). The product was recrystallised using DCM and petrol 40-60˚C (49.5 mg, 13 %). A further recrystallisation was then attempted using diethyl ether and petrol, to try to yield a second crop (25.1 mg, 6 %).

MP: decomposed ~145 ˚C

IR (υ_{max}/cm^{-1}) 3051 (C-H aromatic), 3008 (C-H aliphatic), 1745 (C=O), 1618(C=C aromatic), 1590 (C=C aromatic), 1267 (C-Br).

δ_H (400 MHz, $CDCl_3$) 5.43 (4H, s, H-9), 6.96 (2H, tt, J=7.5, 1.3 Hz, H-13), 7.15 (2H, dt, H-15), 8.29 (2H, d, J=8.5Hz, H-3), 8.36 (2H, d, J=8.5Hz, H-4).

δ_C (100 MHz, $CDCl_3$) 67.6 (C-9), 115.8 (C-13, d, J=21.4Hz), 115.9 (C-15, d, J=21.4Hz), 124.0 (C3), 124.5 (C-11, d, J=2.9Hz), 126.0 (C-5), 130.6 (C-12, d, J=7.8Hz), 138.2 (C-10, d, J=6.8Hz), 138.8 (C-4), 152.6 (C-2), 154.8 (C-6), 163.3 (C-14, d, J=246.9Hz), 165.1 (C-7).

M/S (ESI (MeCN)) m/z: 435.4 (37 %, $[M+H]^+$),452.4 (45, $[M+NH_4]^+$), 498.4 (51, $[M+Na+MeCN]^+$), 886.5 (100, $[2M+NH_4]^+$), 891.5 (33, $[2M+Na]^+$).

HR-M/S: Found 435.1151, Expected 435.1151 ($C_{24}H_{17}F_2N_2O_4$)

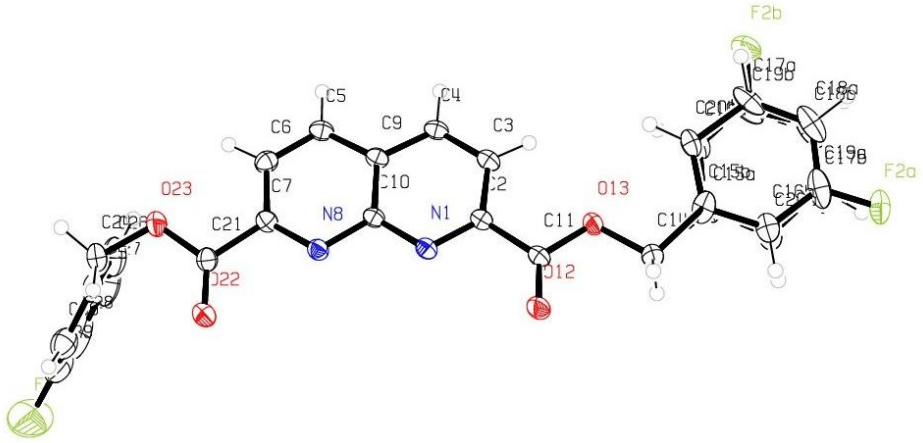

$C_{24}H_{16}F_2N_2O_4$	a = 6.3789 (2) Å	T = 120 K
P1	b = 8.0728 (3) Å	λ = 0.71073 Å
V = 973.21 (6) Å	c = 19.7896 (7) Å	D_c = 1.482 g cm^{-3}
Z = 2	α = 79.869 (2) °	μ = 0.115 mm^{-1}
R_1 = 6.32 %	β = 85.293 (2) °	0.28 x 0.26 x 0.1 mm^3
$wR_2(F^2)$ = 17.05 %	γ = 76.159 (2) °	Pale yellow block

Recrystallisation by vapour diffusion of diethyl ether into DCM

7.3.19 *bis*-(3-Chlorobenzyl) 1,8-naphthyridine-2,7-dicarboxylate (47s)

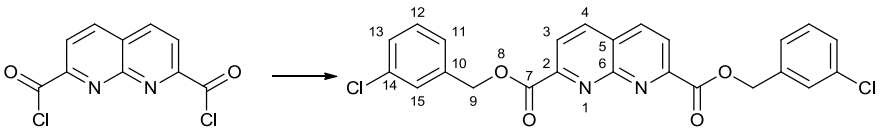

1,8-Naphthyridine-2,7-dicarbonyl dichloride (248.2 mg, 0.98mmol) was stirred in DCM (30 ml). 3-Chlorobenzyl alcohol (308.5 mg, 2.16 mmol, 2.2 equiv) was added followed by triethylamine (0.30 ml, 2.16 mmol). The reaction immediately went green/brown colour, which when left overnight turned orange/brown. DCM (15 ml) was added to the reaction mixture, which was then washed with water (3 × 50 ml). The organic phase dried over $MgSO_4$ and the solvent was then removed *in vacuo* to yield an orange brown oil (403.6 mg, 89 %). This product was recrystallised using DCM and petrol 40-60 ˚C (57 mg, 12 %).

MP: 162-165 ˚C

IR (υ_{max}, cm^{-1}) 3006 (C-H aromatic), 2934 (C-H aliphatic), 1741 (C=O), 1598 (C=C aromatic), 1578 (C=C aromatic).

δ_H (400 MHz, $CDCl_3$) 5.49 (4H, s, H-9), 7.30-7.33 (4H, m, H-11+13), 7.39-7.44 (2H, m, H-12), 7.52 (2H, broad s, H-15), 8.37 (2H, d, J=8.5Hz, H-3), 8.44 (2H, d, J=8.3Hz, H-4).

δ_C (100 MHz, $CDCl_3$) 67.55 (C-9) 124.1 (C-3) 126.0 (C-5) 127.2 (C-11) 129.1 (C-13+15) 130.4 (C12), 134.9 (C14), 137.7 (C10), 138.8 (C4), 152.6 (C6), 165.1 (C7).

M/S (ESI (MeCN)) m/z: 484.4 (55 %, $[M+NH_4]^+$), 489.4 (35), 491.2 (27), 493 (5, $[M+Na]^+$), 530.3 (44), 532.5 (37), 534.5 (8, $[M+Na+MeCN]^+$).

HR-M/S: Found 489.0373, Expected 489.0379 ($C_{24}H_{16}Cl_2N_2O_4Na$)

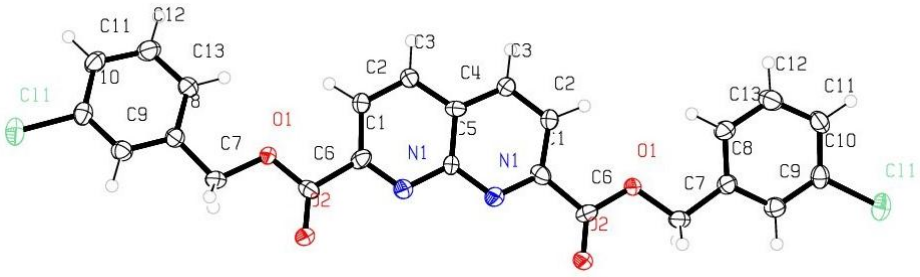

$C_{24}H_{16}Cl_2N_2O_4$	a = 26.159 (4) Å	T = 120 K
C2/c	b = 6.488 (1) Å	λ = 0.71073 Å
V = 2011.2 (5) Å	c = 14.0470 (15) Å	D_c = 1.543 g cm^{-3}
Z = 4	α = 90 (0) °	μ = 0.360 mm^{-1}
R_1 = 12.74 %	β = 122.48 () °	0.1 x 0.1 x 0.01 mm^3
$wR_2(F^2)$ = 29.25 %	γ = 90 (0) °	Colourless plate

Crystallised from acetonitrile

7.3.20 *bis*-(3-Bromobenzyl) 1,8-naphthyridine-2,7-dicarboxylate (47v)

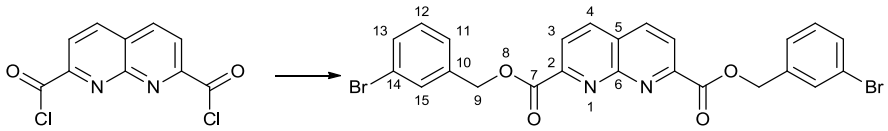

1,8-Naphthyridine-2,7-dicarbonyl dichloride (255.1 mg, 0.98mmol) was stirred in DCM (30 ml). 3-Bromobenzyl alcohol (397.7 mg, 2.16 mmol, 2.2 equiv) was added followed by triethylamine (0.3 ml, 2.16 mmol). A green/brown colour resulted. The reaction was stirred overnight during which time the colour had changed to orange. DCM (15 ml) was added and the reaction was washed with water (3 × 50 ml). The organic phase was dried over $MgSO_4$ and the solvent was removed *in vacuo* to yield

the product (364.8 mg). The product was recrystallised using DCM and petrol 40-60˚C (58 mg, 11 %).

Melting point ~150˚C (decomposed).

IR (υ_{max}/ cm^{-1}) 3050 (C-H aromatic), 2939 (C-H aliphatic), 1739 (C=O stretch), 1597 (C=C aromatic) 1571 (C=C aromatic), 1538 (C=C aromatic), 670 (C-Br).

δ_H (400 MHz, $CDCl_3$) 5.48 (4H, s, H-9), 7.26 (2H, t, J=7.8Hz, H-12), 7.43-7.52 (4H, m, H-11+13), 7.67 (2H, s, H-15), 8.36 (2H, d, J=8.3Hz, H-3), 8.44 (2H, d, J=8.5Hz, H-4).

δ_C (100 MHz, $CDCl_3$) 67.5 (C-9), 123.0 (C-14), 124.0 (C-3), 126.0 (C-5), 127.7 (C-11), 130.6 (C-12), 132.1 (C-15), 132.1 (C-13), 138.0 (C-10), 138.8 (C-4), 152.6 (C-2), 154.8 (C-6).

M/S (ESI (MeCN)) m/z: 555.2 (49 %), 557.2 (65), 559.4 (20, $[M+H]^+$), 618.5 (40) 620.1 (91) 622.1 (48, $[M+Na+MeCN]^+$).

HR-M/S: Found 554.9556, Expected 554.9550 ($C_{24}H_{17}Br_2N_2O_4$)

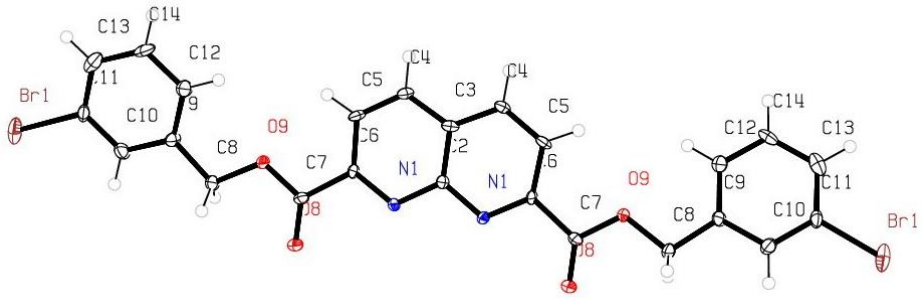

$C_{24}H_{16}Br_2N_2O_4$	a = 26.5361 (11) Å	T = 120 K
C2/c	b = 6.4335 (2) Å	λ = 0.71073 Å
V = 2085.06 (13) Å	c = 13.8345 (5) Å	D_c = 1.772 g cm^{-3}
Z = 4	α = 90 (0) °	μ = 3.924 mm^{-1}
R_1 = 6.23 %	β = 118.016 (2) °	0.6 x 0.5 x 0.06 mm^3
$wR_2(F^2)$ = 19.44 %	γ = 90 (0) °	Colourless slab

Crystallised from acetonitrile

7.3.21 *bis*-(4-Fluorobenzyl) 1,8-naphthyridine-2,7-dicarboxylate (47q)

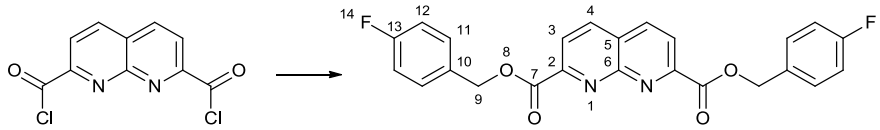

1,8-Naphthyridine-2,7-dicarbonyl dichloride (199.0 mg, 0.768 mmol) was dissolved in DCM (50 mL), 4-fluorobenzyl alcohol (216.4 mg, 1.68 mmol) was then added, followed by triethylamine (0.30 ml, 2.16 mmol), a gas was seen to be evolved and the solution was seen to turn turquoise. The reaction mixture was left to stir overnight during which the colour was seen to turn grey. The following day the reaction mixture was washed with water (3 x 50 mL) followed by brine (50 mL). The remaining organic residue was dried with magnesium sulphate and then reduced *in vacuo* to yield a solid (201.7 mg). This was recrystallised using a mixed solvent system of DCM:petrol 40-60 °C to yield a white powder (48.2 mg, 14 %)

MP: 200-202˚C

IR (υ_{max}/cm^{-1}) 3048 (C-H aromatic), 3005 (C-H aliphatic), 1736 (C=O), 1512 (C=C aromatic).

δ_H (400 MHz, $CDCl_3$) 5.49 (4 H, s, H-9), 7.08 (4 H, t, J=8.7 Hz, H-12), 7.52 (4 H, dd, J=8.2, 5.6 Hz, H-11), 8.36 (2 H, d, J=8.3 Hz, H-3), 8.42 (2 H, d, J=8.5 Hz, H-4).

δ_C (100 MHz, $CDCl_3$) 67.3 (C-9), 115.5 (d, *J*=21.4 Hz, C-12), 123.5 (C-3), 125.5 (C-5), 130.8 (d, *J*=8.7 Hz, C-11), 131.1 (d, *J*=2.9 Hz, C-10), 138.3 (C-4), 152.2 (C-2), 154.3 (C-6), 162.8 (d, *J*=247.8 Hz, C-13), 164.7 (C-7).

M/S (ESI (MeCN)) m/z: 498 (100 %, $[M+Na+MeCN]^+$), 891 (56, $[2M+Na]^+$).

HR-M/S: Found 435.1158, Expected 435.1151 ($C_{24}H_{17}F_2N_2O_4$)

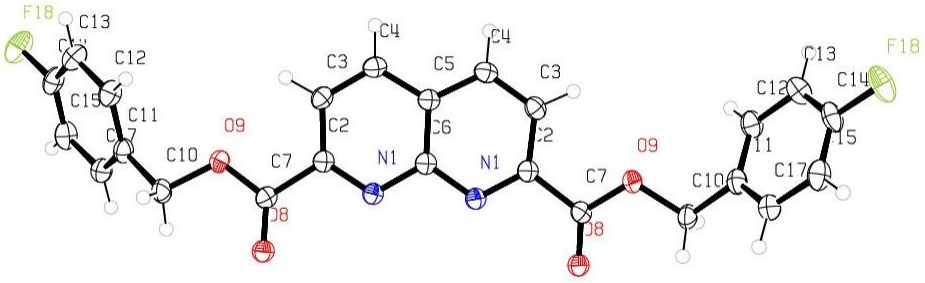

$C_{24}H_{16}F_2N_2O_4$	a = 24.2646 (11) Å	T = 120 K
C2/c	b = 6.3658 (4) Å	λ = 0.71073 Å

V = 1972.92 (18) Å	c = 14.1859 (7) Å	D_c = 1.462 g cm^{-3}
Z = 4	α = 90 (0) °	μ = 0.115 mm^{-1}
R_1 = 5.86 %	β = 115.792 (3) °	0.14 x 0.06 x 0.04 mm^3
$wR_2(F^2)$ = 15.78 %	γ = 90 (0) °	Clear colourless plate

Crystallisation by vapour diffusion of petroleum ether into DCM

7.3.22 *bis*-(4-Chlorobenzyl) 1,8-naphthyridine-2,7-dicarboxylate (47t)

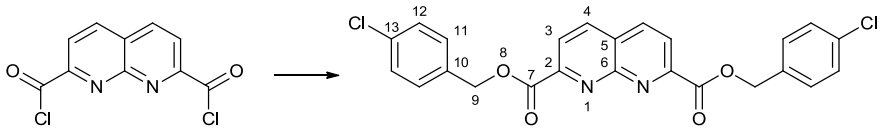

1,8-Naphthyridine-2,7-dicarbonyl dichloride (252.1 mg, 0.98 mmol) was dissolved in DCM (50 mL), 4-chlorobenzyl alcohol (314.7 mg, 2.160 mmol) was then added followed by triethylamine (0.30 mL, 2.16 mmol). The reaction mixture was left to stir overnight during which time a blue precipitate was formed. The following day the reaction mixture was filtered to yield a blue solid (238.2 mg, 52 %).

MP: decomp. 210 °C

ν/cm^{-1} 3051 (C-H), 3007 (C-H), 2928 (C-H), 1736 (C=O), 1596 (aromatic C-C), 1538 (aromatic C-N), 1490 (aromatic C-C), 1458 (aromatic C-C).

δ_H (400 MHz, TFA-d_1) 5.75 (4H, s, H-9), 7.48 (4H, d, J = 8.1 Hz, H-11), 7.57 (4H, d, J = 7.9, H-12), 8.95 (2H, d, J = 8.5, H-3), 9.45 (2H, d, J = 8.5 Hz).

HR-M/S: Found 467.0566, Expected 467.0560 ($C_{24}H_{17}Cl_2N_2O_4$)

While a proton NMR was obtained the complexity of the carbon NMR would tend to suggest that the compound was not entirely stable in the TFA NMR solvent and has decomposed during the data acquisition.

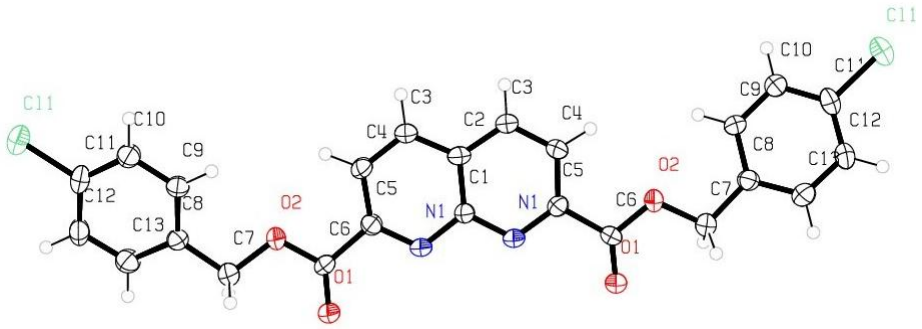

$C_{24}H_{16}Cl_2N_2O_4$	a = 25.107 (5) Å	T = 120 K

C2/c	b = 6.4739 (10) Å	λ = 0.71073 Å
V = 2012.1 (6) Å	c = 14.472 (3) Å	D_c = 1.543 g cm^{-3}
Z = 4	α = 90 (0) °	μ = 0.360 mm^{-1}
R_1 = 8.04 %	β = 121.198 (17) °	0.3 x 0.3 x 0.02 mm^3
$wR_2(F^2)$ = 28.60 %	γ = 90 (0) °	Colourless plate

Crystallised from slowly cooled DMSO

7.3.23 *bis*-(4-Bromobenzyl) 1,8-naphthyridine-2,7-dicarboxylate (47w)

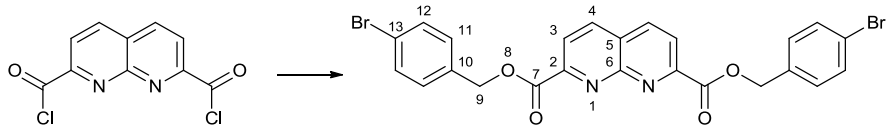

1,8-Naphthyridine-2,7-dicarbonyl dichloride (254 mg, 0.98 mmol) was dissolved in DCM (50 mL), 4-bromobenzyl alcohol (478 mg, 2.160 mmol) was then added followed by triethylamine (0.30 mL, 2.16 mmol) which gave an orange solution. The reaction mixture was left to stir overnight during which time a blue precipitate was formed. The following day the reaction mixture was filtered to yield a blue solid (332 mg, 64 %).

MP: decomp. 210 °C

ν/cm^{-1} 3052 (C-H), 1735 (C=O), 1595 (aromatic C-C), 1538 (aromatic C-N), 1488 (aromatic C-C), 1457 (aromatic C-C).

δ_H (400 MHz, TFA-d_1) 5.70 (4H, s,H-9), 7.47 (4H, d, *J*=8.3 Hz, H-11), 7.61 (4H, d, *J=8.2* Hz, H-12), 8.92 (2H, d, *J*=8.4 Hz, H-3), 9.43 (2H, d, *J*=8.4 Hz, H-4).

δ_C (100 MHz, TFA-d_1) 54.4, 73.0 (C-9), 126.2 (C-), 128.1 (C-3), 130.6 (C-5), 133.0 (C-11), 134.0 (C-10), 134.3 (C-12), 147.9 (C-2), 149.6 (C-4), 153.0 (C-13), 162.7 (C-7)

HR-M/S: Found 576.9369, Expected 576.9369 ($C_{24}H_{16}Br_2N_2O_4Na$)

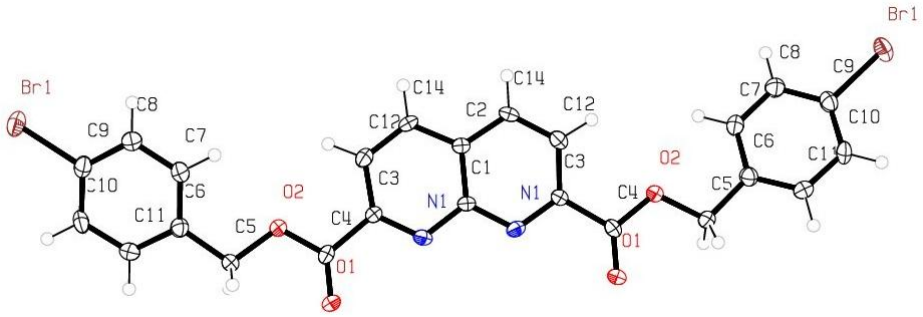

$C_{24}H_{16}Br_2N_2O_4$	a = 24.9220 (7) Å	T = 120 K
C2/c	b = 6.4590 (2) Å	λ = 0.71073 Å
V = 2065.56 (10) Å	c = 14.9105 (4) Å	D_c = 1.789 g cm^{-3}
Z = 4	α = 90 (0) °	μ = 3.961 mm^{-1}
R_1 = 5.11 %	β = 120.617 (10) °	0.6 x 0.04 x 0.02 mm^3
$wR_2(F^2)$ = 10.34 %	γ = 90 (0) °	Colourless needle

Crystallised from slowly cooled DMSO

7.3.24 *bis*-(4-Methoxybenzyl) 1,8-naphthyridine-2,7-dicarboxylate (47x)

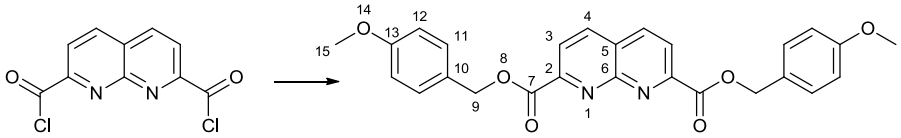

1,8-Naphthyridine-2,7-dicarbonyl dichloride (259 mg, 0.98 mmol) was dissolved in DCM (50 mL), 4-methoxybenzyl alcohol (0.27 ml, 2.16 mmol) was then added followed by triethylamine (0.30 mL, 2.16 mmol) which gave an orange solution. The reaction mixture was left to stir overnight during which time the reaction mixture turned dark brown. The following day the reaction mixture was washed with water (3 x 50 mL) followed by brine (50 mL). The remaining organic residue was dried with magnesium carbonate and then reduced *in vacuo.* This yielded a brown solid (306 mg, 71 %). This was recrystallised using a mixed solvent system of DCM: petroleum ether to yield a light brown solid (167 mg, 39 %)

MP: 165 – 170 °C

ν/cm^{-1} 3051 (C-H), 3007 (C-H), 2959 (C-H), 2836 (C-H), 1739 (C=O), 1612 (aromatic C-C), 1597 (aromatic C-H), 1539 (aromatic C-N), 1513 (aromatic C-C), 1464 (aromatic C-C).

δ_H (400 MHz, $CDCl_3$) 3.81 (6H, s, H-15), 5.46 (4H, s, H-9), 6.90 (4H, d, *J*=8.5 Hz, H-12), 7.46 (4H, d, *J*=8.5, H-11), 8.32 (2H, d, *J*=8.0 Hz, H-3), 8.38 (2H, d, *J*=8.5 Hz, H-4).

δ_C (100 MHz, $CDCl_3$) 55.3 (C-15), 67.8 (C-9), 113.9 (C-12), 123.4 (C-3), 125.3 (C-5), 127.5 (C-10), 130.7 (C-11), 138.2 (C-4), 152.4 (C-13), 154.4 (C-6), 159.8 (C-2), 164.8 (C-7).

M/S (ESI) m/z 268 97, $[M+MeOH+2K]^{2+}$).

HR-M/S: Found 481.1368, Expected 481.1370 ($C_{26}H_{22}N_2O_6Na$)

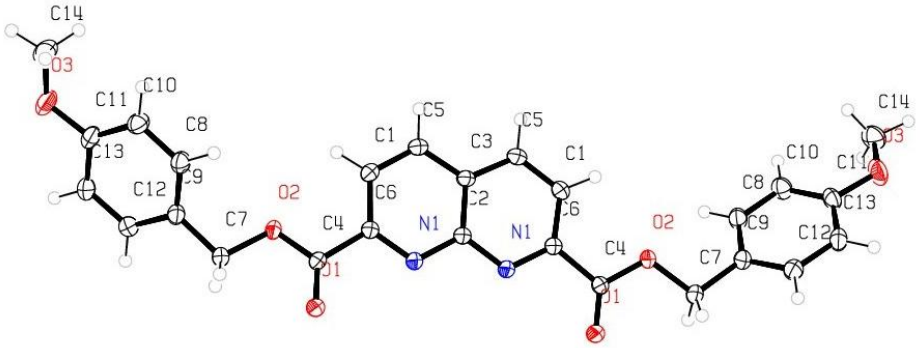

$C_{26}H_{22}N_2O_6$	a = 30.3042 (12) Å	T = 120 K
C2/c	b = 6.3458 (2) Å	λ = 0.71073 Å
V = 2177.04 (13) Å	c = 11.3232 (4) Å	D_c = 1.399 g cm^{-3}
Z = 4	α = 90 (0) °	μ = 0.100 mm^{-1}
R_1 = 5.16 %	β = 91.174 (2) °	0.2 x 0.2 x 0.03 mm^3
$wR_2(F^2)$ = 15.67 %	γ = 90 (0) °	Clear colourless plate

Crystallised from diffusion of petroleum ether into chloroform

7.3.25 *bis*-(4-Nitrobenzyl) 1,8-naphthyridine-2,7-dicarboxylate (47y)

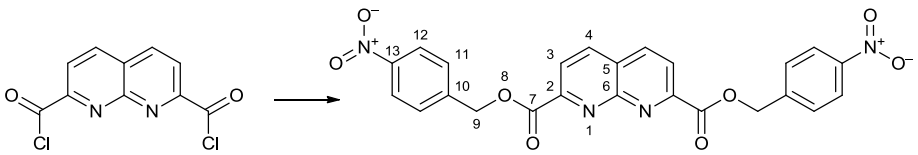

1,8-Naphthyridine-2,7-dicarbonyl dichloride (252.6 mg, 0.98 mmol) was dissolved in DCM (50 mL), 4-bromobenzyl alcohol (340 mg, 2.160 mmol) was then added followed by triethylamine (0.30 mL, 2.16 mmol) . The reaction mixture was left to stir overnight during which time a precipitate was formed. The following day the reaction mixture was filtered to yield a solid (294.2 mg, 62 %).

MP: 257-259 °C (decomp.)

ν/cm^{-1} 3083 (C-H), 3049 (C-H), 3004 (C-H), 1733 (C=O), 1608 (aromatic C-C), 1536 (aromatic C-C), 1495 (aromatic C-C), 1449 (aromatic C-C).

δ_H (300 MHz, TFA-d_1) 6.00 (4H, s, H-9), 7.99 (4H, d, J = 8.3 Hz), 8.54 (4H, d, J = 8.3 Hz), 9.11 (2H, d, J = 8.3), 9.60 (2H, d, J = 8.3 Hz).

HR-M/S: Found 511.0857, Expected 511.0860 ($C_{24}H_{16}N_4O_8Na$)

Characterisation of this solid proved extremely difficult given its complete insolubility in all solvents tested.

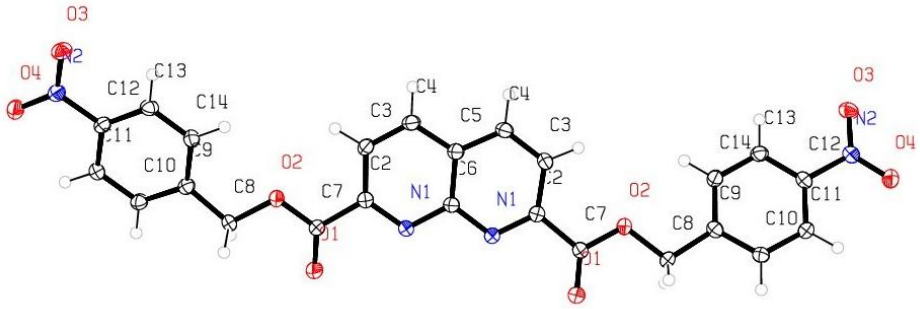

$C_{24}H_{16}N_4O_8$	a = 33.131 (12) Å	T = 120 K
P21212	b = 4.9080 (17) Å	λ = 0.6889 Å
V = 1029.8 (6) Å	c = 6.333 (2) Å	D_c = 1.575 g cm^{-3}
Z = 2	α = 90 (0) °	μ = 0.121 mm^{-1}
R_1 = 3.88 %	β = 90 (0) °	0.10 x 0.01 x 0.01 mm^3
$wR_2(F^2)$ = 10.14 %	γ = 90 (0) °	Colourless needle

Crystallised from slowly cooled DMSO

7.3.26 *bis*-(Pyridin-2-ylmethyl)-1,8-naphthyridine-2,7-dicarboxylate (47z)

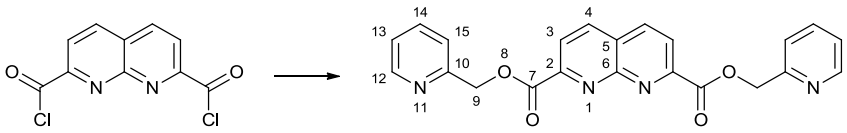

1,8-Naphthyridine-2,7-dicarbonyl dichloride (500.4 mg, 1.96 mmol) was dissolved in DCM (50 mL), 2-(hydroxymethyl)pyridine (0.42 ml, 4.31 mmol) was then added, turning the solution green and a white precipitate formed, followed by triethylamine (0.60 mL, 4.31 mmol) which dissolved the precipitate. The reaction mixture was left to stir overnight. The following day the reaction mixture was washed with water (3 x 50 mL) followed by brine (50 mL). The remaining organic

residue was dried with magnesium carbonate and then reduced *in vacuo.* This yielded a grey solid. This was recrystallised using a mixed solvent system of DCM:diethyl ether to yield a slightly blue tinged white powder (388.6 mg, 49 %).

MP: 208 – 211 °C

ν/cm^{-1} 3050 (N-H), 3007 (C-H), 2931 (C-H), 1749 (C=O), 1592 (aromatic C-C), 1571 (aromatic C-C), 1558 (aromatic C-N), 1537 (aromatic C-N), 1478 (aromatic C-C).

δ_H (400 Mhz, $CDCl_3$) 5.64 (4H, s, H-9), 7.24 (2H, dd, *J*=7.0, 5.0Hz, H-13), 7.57 (2H, d, *J*=8.0 Hz, H-15), 7.71 (2H, td, *J*=7.7, 1.8 Hz, H-14), 8.40 (2H, d, *J*=8.5 Hz, H-3), 8.46 (2H, d, *J*=8.5 Hz, H-4), 8.61 (2H, d, *J*=4.5 Hz, H-12).

δ_C (100 Mhz, $CDCl_3$) 68.3 (C-9), 122.0 (C-13), 123.0 (C-15), 123.7 (C-3), 125.6 (C-5), 136.8 (C-14), 138.4 (C-4), 149.4 (C-12), 152.1 (C-10), 154.4 (C-6), 155.3 (C-2), 164.6 (C-7).

M/S (ESI (MeCN)) m/z 402 (29 %, $[M+H]^+$), 465 (20, $[M+H]^+$), 802 (11, $[2M+H]^+$), 824 (11, $[2M+Na]^+$).

HR-M/S: Found 401.1237, Expected 401.1244 ($C_{22}H_{16}N_4O_4$)

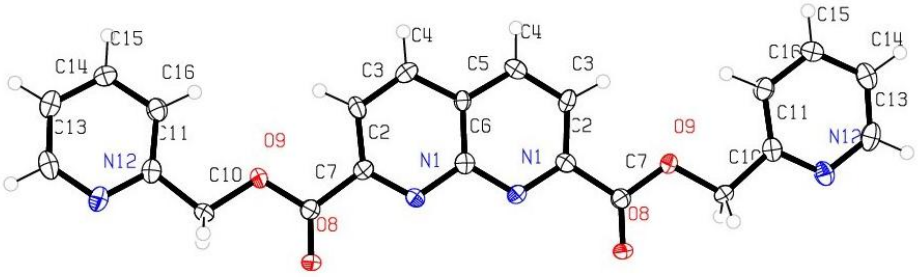

$C_{24}H_{16}N_4O_4$	a = 5.0497 (3) Å	T = 120
P21212	b = 28.8108 (15) Å	λ = 0.71073 Å
V = 920.08 (9) Å	c = 6.3242 (4) Å	D_c = 1.445 g cm^{-3}
Z = 2	α = 90 (0) °	μ = 0.102 mm^{-1}
R_1 = 8.54 %	β = 90 (0) °	0.12 x 0.04 x 0.04 mm^3
$wR_2(F^2)$ = 12.96 %	γ = 90 (0) °	Colourless Needle

Crystallised from diffusion of diethyl ether into chloroform

7.3.27 *bis*-(Pyridin-3-ylmethyl)-1,8-naphthyridine-2,7-dicarboxylate (47aa)

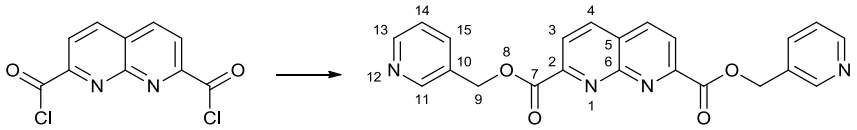

1,8-Naphthyridine-2,7-dicarbonyl dichloride (502.1 mg, 1.96 mmol) was dissolved in DCM (50 mL), 3-(hydroxymethyl)pyridine (0.42 ml, 4.31 mmol) was then added, turning the solution blue and a white precipitate formed, followed by triethylamine (0.60 mL, 4.31 mmol) which dissolved the precipitate. The reaction mixture was left to stir overnight. The following day the reaction mixture was washed with water (3 x 50 mL) followed by brine (50 mL). The remaining organic residue was dried with magnesium carbonate and then reduced *in vacuo* yielding a grey solid. This was recrystallised using a mixed solvent system of DCM:diethyl ether to yield a slightly blue tinged white powder (288 mg, 36 %).

MP: 220 °C (decomposes)

ν/cm^{-1} 3052 (N-H), 3010 (C-H), 1742 (C=O), 1601 (C=O), 1574 (aromatic C-C), 1558 (aromatic C-N), 1539 (aromatic C-N), 1480 (aromatic C-C).

δ_H (400 Mhz, $CDCl_3$) 5.47 (4H, s, H-9), 7.32 (2H, dd, *J*=7.8, 4.8 Hz, H-14), 7.89 (2H, d, *J*=8.0 Hz, H-15), 8.30 (2H, d, *J*=8.0 Hz, H-3), 8.43 (2H, d, *J*=8.5 Hz, H-4), 8.49 (2H, dd, *J*=5.0, 1.5 Hz, H-13), 8.66 (2H, d, *J*=2.0 Hz, H-11).

δ_C (100 Mhz, $CDCl_3$) 65.2 (C-9), 123.5 (C-3), 123.8 (C-14), 125.6 (C-5), 131.22 (C-10), 137.1 (C-15), 138.7 (C-4), 149.3 (C-13), 149.4 (C-11), 151.7 (C-2), 154.0 (C-6), 164.3 (C-7).

M/S (ESI (MeCN)) m/z 402 (35 %, $[M+H]^+$), 424 (68, $[M+Na]^+$), 824 (100, $[2M+Na]^+$).

HR-M/S: Found 401.1247, Expected 401.1244 ($C_{22}H_{17}N_4O_4$)

7.3.28 *bis*-(Pyridin-4-ylmethyl)-1,8-naphthyridine-2,7-dicarboxylate (47bb)

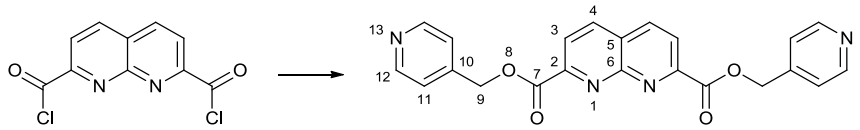

1,8-Naphthyridine-2,7-dicarbonyl dichloride (499.7 mg, 1.96 mmol) was dissolved in DCM (50 mL), 4-(hydroxymethyl)pyridine (0.42 ml, 4.31 mmol) was then added, forming a white precipitate, followed by triethylamine (0.60 mL, 4.31 mmol) which dissolved the precipitate. The reaction mixture was left to stir overnight. The following day the reaction mixture was washed with water (3 x 50 mL) followed by brine (50 mL). The remaining organic residue was dried with magnesium carbonate and then reduced *in vacuo.* This yielded a grey solid. This was recrystallised using a mixed solvent system of DCM:diethyl ether to yield a slightly blue tinged white powder (331.7 mg, 42 %).

MP: 230 °C (decomposes)

ν/cm^{-1} 3050 (C-H), 3008 (C-H), 2945 (C-H), 1742 (C=O), 1600 (aromatic C-C), 1561 (aromatic C-N), 1536 (aromatic C-N), 1497 (aromatic C-C).

δ_H (400 Mhz, $CDCl_3$) 5.53 (4H, s, H-9), 7.42 (4H, d, *J*=6.0 Hz, H-11), 8.39 (2H, d, *J*=8.5 Hz, H-3), 8.48 (2H, d, *J*=8.5 Hz, H-4), 8.63 (4H, d, *J*=6.0 Hz, H-12).

δ_C (100 Mhz, $CDCl_3$) 66.0 (C-9), 122.2 (C-11), 123.7 (C-3), 125.7 (C-5), 138.6 (C-4), 144.1 (C-10), 150.1 (C-12), 151.8 (C-2), 154.4 (C-6), 164.5 (C-7).

M/S (ESI) m/z 402 (64 %, $[M+H]^+$), 424 (81, $[M+Na]^+$), 802 (41, $[2M+H]^+$), 824 (100, $[2M+Na]^+$), 1203 (5, $[3M+H]^+$), 1225(13, $[3M+H]^+$).

HR-M/S: Found 401.1239, Expected 401.1244 ($C_{22}H_{17}N_4O_4$)

7.3.29 *bis*-(2-Thiophenylmethyl) 1,8-naphthyridine-2,7-dicarboxylate (47cc)

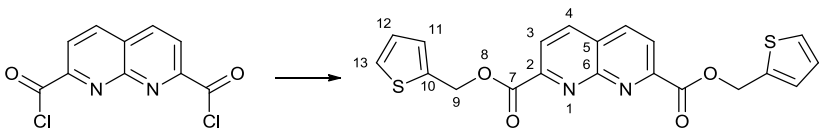

1,8-Naphthyridine-2,7-dicarbonyl dichloride (244.2 mg, 0.98 mmol) was dissolved in DCM (50 mL), 2-thiophenylmethanol (0.2 ml, 2.16 mmol) was then added, forming a

white precipitate, followed by triethylamine (0.3 mL, 2.2 mmol) which dissolved the precipitate. The reaction mixture was left to stir overnight. The following day the reaction mixture was washed with water (3 x 50 mL) followed by brine (50 mL). The remaining organic residue was dried with magnesium carbonate and then reduced *in vacuo.* This yielded a brown solid (442.1 mg). This was then columned using 2 % triethylamine:DCM eluent system to afford a lighter brown solid (141.6 mg, 35 %).

MP: 161 - 164 °C

ν/cm^{-1} 3104 (C-H), 3051 (C-H), 2916 (C-H), 1730 (C=O), 1650 (aromatic C-C), 1596 (aromatic C-C), 1538 (aromatic C-N), 1446 (aromatic C-C), 1422 (aromatic C-C).

δ_H (400 Mhz, $CDCl_3$) 5.67 (4H, s, H-9), 7.01 (2H, dd, *J = 5*.0, 3.5 Hz, H-12), 7.26 (2H, d, *J* = 3.5 Hz, H-11), 7.34 (2H, d, *J* = 5.0 Hz, H-13), 8.35 (2H, d, *J* = 8.0 Hz, H-3), 8.41 (2H, d, *J* = 8.0 Hz, H-4).

δ_C (100 Mhz, $CDCl_3$) 61.9 (C-9), 123.5 (C-3), 125.4 (C-5), 126.9 (C-12), 127.3 (C-11), 129.3 (C-13), 137.0 (C-10), 138.3 (C-4), 152.1 (C-2), 154.3 (C-6), 164.6 (C-7).

M/S (ESI (MeCN)) m/z: 411 (10 %, $[M+H]^+$), 474 (16 %, $[M+Na]^+$), 474 (100 , $[M+Na+MeCN]^+$), 843 (94, $[2M+Na]^+$).

HR-M/S: Found 433.0279, Expected 433.0287 ($C_{20}H_{14}N_2O_4S_2Na$)

7.3.30 *bis*-(3-Thiophenylmethyl) 1,8-naphthyridine-2,7-dicarboxylate (47dd)

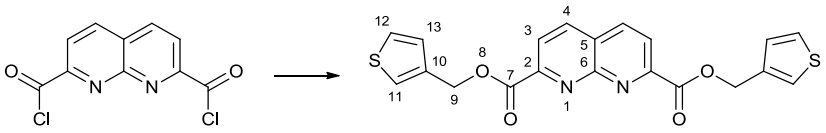

1,8-Naphthyridine-2,7-dicarbonyl dichloride (252.9 mg, 0.98 mmol) was dissolved in DCM (50 mL), 3-thiophenylmethanol (0.2 ml, 2.16 mmol) was then added, forming a white precipitate, followed by triethylamine (0.3 mL, 2.2 mmol) which dissolved the precipitate. The reaction mixture was left to stir overnight. The following day the reaction mixture was washed with water (3 x 50 mL) followed by brine (50 mL). The remaining organic residue was dried with magnesium carbonate and then reduced *in vacuo.* This yielded a brown solid (384.8 mg). This was then columned using 2 % triethylamine:DCM eluent system to afford a lighter brown solid (309 mg, 76 %).

MP: 172 - 175 °C

ν/cm^{-1} 3104 (C-H), 3051 (C-H), 2916 (C-H), 1737 (C=O), 1624 (aromatic C-C), 1600 (aromatic C-C), 1536 (aromatic C-N), 1460 (aromatic C-C), 1422 (aromatic C-C).

δ_H (400 Mhz, $CDCl_3$) 5.44 (4H, s, H-9), 7.00 (2H, dd, *J* = 4.8, 1.3 Hz, H-13), 7.23 (2H, d, *J* = 3.5 Hz, H-11), 7.39 (2H, d, *J* = 2,5 Hz, H-11), 8.26 (2H, d, *J* = 8.0 Hz, H-3), 8.32 (2H, d, *J* = 8.0 Hz, H-4).

HR-M/S: Found 411.0461, Expected 411.0468 ($C_{20}H_{15}N_2O_4S_2$)

This material appears to be contaminated with 3-thiophenylmethanol and required further purification before full characterisation.

7.3.31 *bis*-(Cyclopentylmethyl) 1,8-naphthyridine-2,7-dicarboxylate (47ff)

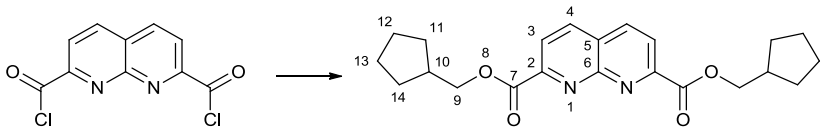

1,8-Naphthyridine-2,7-dicarbonyl dichloride (255.6 mg, 0.98 mmol) was dissolved in DCM (50 mL), cyclopentylmethanol (0.23 ml, 2.16 mmol) was then added, forming a white precipitate, followed by triethylamine (0.3 mL, 2.2 mmol) which dissolved the precipitate. The reaction mixture was left to stir overnight. The following day the reaction mixture was washed with water (3 x 50 mL) followed by brine (50 mL). The remaining organic residue was dried with magnesium carbonate and then reduced *in vacuo.* This yielded an off white solid (386.1 mg). This was then columned using 2 % triethylamine:DCM eluent system to afford a lighter brown solid (229.3 mg, 61 %).

MP: 216 - 218 °C

ν/cm^{-1} 3048 (C-H), 3005 (C-H), 2950 (C-H), 2917 (C-H), 2864 (C-H), 1732 (C=O), 1600 (aromatic C-C), 1534 (aromatic C-N), 1450 (aromatic C-C), 1419 (aromatic C-C).

δ_H (400 Mhz, $CDCl_3$) 1.39 (4H, m), 1.64 (8H, m), 1.87 (4H, m), 2.48 (2H, spt, J= 7.5 Hz, H-10a), 4.39 (4H, d, J=7.5 Hz, H-9), 8.35 (2H, d, *J* = 8.0 Hz, H-3), 8.42 (2H, d, *J* = 8.0 Hz, H-4).

δ_C (100 Mhz, $CDCl_3$) 22.2 (C-12 and C-13), 29.7 (C-11 and C-14), 38.6 (C-10), 70.4 (C-9), 123.4 (C-3), 125.3 (C-5), 138.2 (C-4), 152.6 (C-2), 154.5 (C-6), 165.0 (C-7).

M/S (ESI (MeCN)) m/z: 383 (24 %, $[M+H]^+$), 421 (14, $[M+K]^+$), 446 (96 , $[M+Na+MeCN]^+$), 787 (100, $[2M+Na]^+$), 1169 (8, $[3M+Na]^+$).

HR-M/S: Found 383.1978, Expected 383.1965 ($C_{22}H_{27}N_2O_4$)

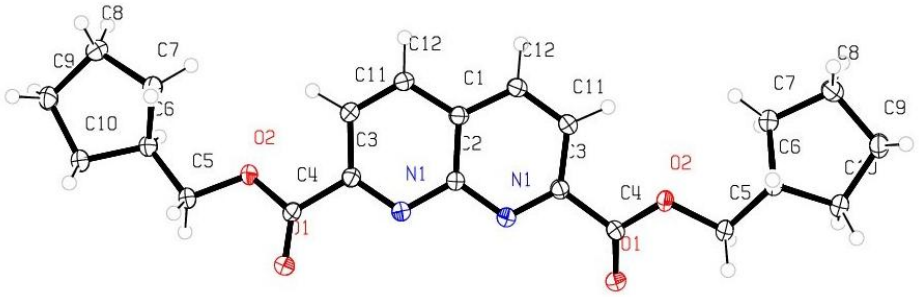

$C_{26}H_{26}N_2O_4$	a = 20.4226 (7) Å	T = 120 K
C2/c	b = 6.2906 (2) Å	λ = 0.71073 Å
V = 1857.02 (10) Å	c = 14.6617 (4) Å	D_c = 1.361 g cm^{-3}
Z = 4	α = 90 (0) °	μ = 0.094 mm^{-1}
R_1 = 5.81 %	β = 99.636 (2) °	0.22 x 0.16 x 0.04 mm^3
$wR_2(F^2)$ = 15.14 %	γ = 90 (0) °	Colourless block

Crystallised from diffusion of petroleum ether into chloroform

7.3.32 *bis*-(Cyclohexylmethyl) 1,8-naphthyridine-2,7-dicarboxylate (47gg)

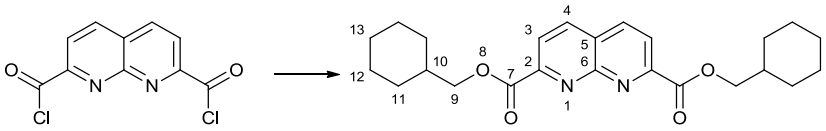

1,8-Naphthyridine-2,7-dicarbonyl dichloride (249.9 mg, 0.98 mmol) was dissolved in DCM (50 mL), cyclohexylmethanol (0.27 ml, 2.16 mmol) was then added, forming a white precipitate, followed by triethylamine (0.3 mL, 2.2 mmol) which dissolved the precipitate. The reaction mixture was left to stir overnight. The following day the reaction mixture was washed with water (3 x 50 mL) followed by brine (50 mL). The remaining organic residue was dried with magnesium carbonate and then reduced *in vacuo.* This yielded an off white solid (443.8 mg). This was then columned using 2 % triethylamine:DCM eluent system to afford a lighter brown solid (330.5 mg, 82 %).

MP: 222 -225 °C

ν/cm^{-1} 3329 (O-H), 3047 (C-H), 3005 (C-H), 2918 (C-H), 2848 (C-H), 1738 (C=O), 1620 (aromatic C-C), 1592 (aromatic C-N), 1522 (aromatic C-C), 1447 (aromatic C-C).

δ_H (400 Mhz, $CDCl_3$) 0.76 – 1.5 (m, unsaturated cyclohexane ring), 4.26 (4H, d, J=7.5 Hz, H-9), 8.35 (2H, d, *J* = 8.0 Hz, H-3), 8.42 (2H, d, *J* = 8.0 Hz, H-4).

M/S (ESI (MeCN)) m/z: 411 (5 %, $[M+H]^+$), 474 (55, $[M+Na+MeCN]^+$), 843 (100 , $[2M+Na]^+$).

HR-M/S: Found 411.2288, Expected 411.2278 ($C_{24}H_{31}N_2O_4$)

This material appears to be contaminated with cyclohexylmethanol and requires further purification.

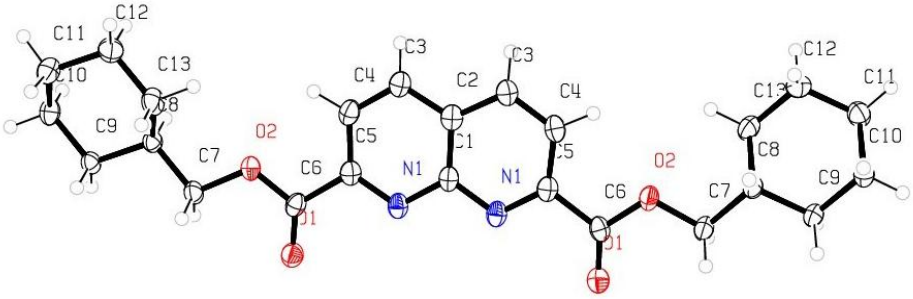

$C_{24}H_{30}N_2O_4$	a = 28.1652 (11) Å	T = 120 K
C2/c	b = 6.4663 (3) Å	λ = 0.71073 Å
V = 2114.95 (16) Å	c = 11.6140 (5) Å	D_c = 1.289 g cm^{-3}
Z = 4	α = 90 (0) °	μ = 0.088 mm^{-1}
R_1 = 7.77 %	β = 90.873 (2) °	0.3 x 0.08 x 0.04 mm^3
$wR_2(F^2)$ = 16.88 %	γ = 90 (0) °	Colourless split rod

Crystallised from diffusion of petroleum ether into chloroform

7.3.33 *bis*-(2-Naphthylmethyl) 1,8-naphthyridine-2,7-dicarboxylate (47hh)

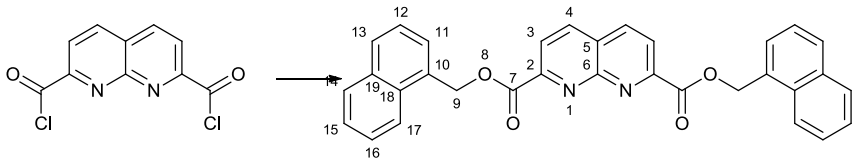

1,8-Naphthyridine-2,7-dicarbonyl dichloride (256.5 mg, 0.98 mmol) was dissolved in DCM (50 mL), 2-naphthylmethanol (341.6 mg, 2.16 mmol) was then added, forming a white precipitate, followed by triethylamine (0.3 mL, 2.2 mmol) which dissolved the precipitate. The reaction mixture was left to stir overnight. The following day a

precipitate had formed; this was filtered off to afford an off white solid (265.2 mg, 54 %).

MP: 248 - 250 °C

ν/cm^{-1} 3050 (C-H), 3009 (C-H), 2156 (aromatic overtone), 2010 (aromatic overtone), 1977 (aromatic overtone), 1750 (C=O), 1597 (aromatic C-C), 1538 (aromatic C-N), 1508 (aromatic C-C), 1424 (aromatic C-C).

HR-M/S: Found 499.1659, Expected 499.1652 ($C_{32}H_{23}N_2O_4$)

Characterisation of this solid proved extremely difficult given its complete insolubility in all solvents tested.

7.3.34 *bis*-(9-Athrylmethyl) 1,8-naphthyridine-2,7-dicarboxylate (47ii)

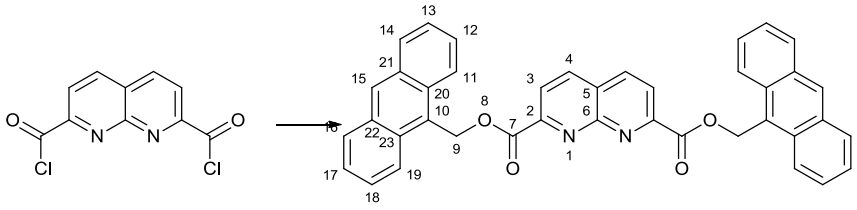

1,8-Naphthyridine-2,7-dicarbonyl dichloride (249.4 mg, 0.98 mmol) was dissolved in DCM (50 mL), 9-anthrylmethanol (450.7 mg, 2.16 mmol) was then added, forming a white precipitate, followed by triethylamine (0.3 mL, 2.2 mmol) which dissolved the precipitate. The reaction mixture was left to stir overnight. The following day a precipitate had formed; this was filtered off to afford an off white solid (238.6 mg, 41 %).

MP: 222 - 224 °C

ν/cm^{-1} 3045 (C-H), 1737 (C=O), 1596 (aromatic C-C), 1557 (aromatic C-C), 1538 (aromatic C-N), 1442 (aromatic C-C).

HR-M/S: Found 621.1774, Expected 621.1785 ($C_{40}H_{26}N_2O_4Na$)

Characterisation of this solid proved extremely difficult given its complete insolubility in all solvents tested.

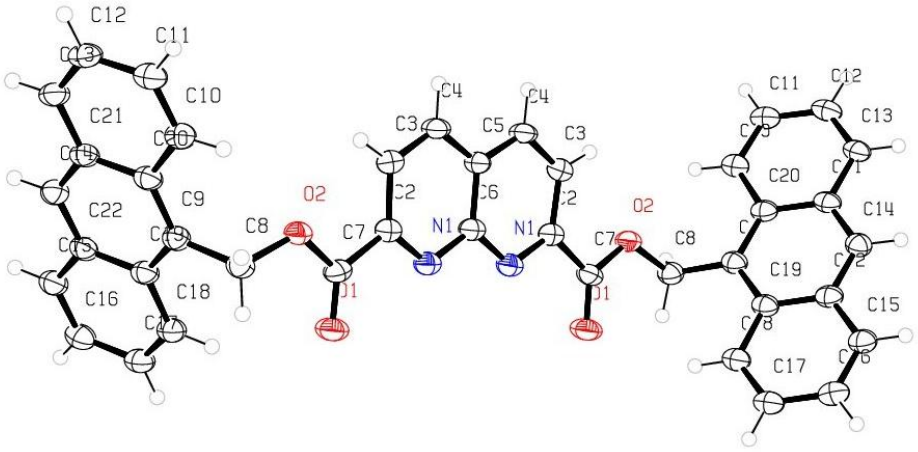

$C_{40}H_{26}N_2O_4$	a = 18.648 (9) Å	T = 120 K
P2/c	b = 6.352 (3) Å	λ = 0.6889 Å
V = 1404.7 (12) Å	c = 12.074 (6) Å	D_c = 1.415 g cm^{-3}
Z = 2	α = 90 (0) °	μ = 0.092 mm^{-1}
R_1 = 6.55 %	β = 100.828 (5) °	0.04 x 0.03 x 0.002 mm^3
$wR_2(F^2)$ = 18.80 %	γ = 90 (0) °	Colourless plate

Crystallised from slow cooled hot DMSO

7.3.35 *bis*-(4-Phenylmethyl) 1,8-naphthyridine-2,7-dicarboxylate (47jj)

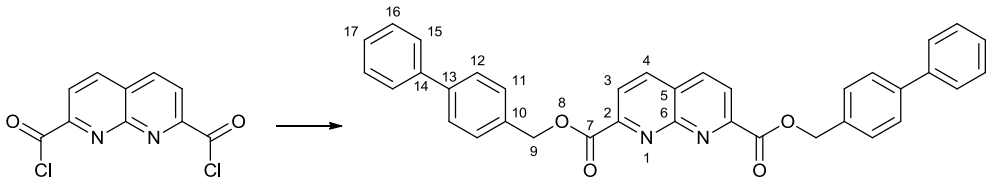

1,8-Naphthyridine-2,7-dicarbonyl dichloride (247.9 mg, 0.98 mmol) was dissolved in DCM (50 mL), 4-biphenylmethanol (400.7 mg, 2.16 mmol) was then added, forming a white precipitate, followed by triethylamine (0.3 mL, 2.2 mmol) which dissolved the precipitate. The reaction mixture was left to stir overnight. The following day a precipitate had formed; this was filtered off to afford an off white solid (421.2 mg, 78 %).

MP: 226 - 228 °C

ν/cm^{-1} 3334 (C-H), 3032 (C-H), 2917 (C-H), 1735 (C=O), 1597 (aromatic C-C), 1538 (aromatic C-N), 1485 (aromatic C-C), 1451(aromatic C-C).

HR-M/S: Found 551.1969, Expected 551.1965 ($C_{36}H_{27}N_2O_4$)

Characterisation of this solid proved extremely difficult given its complete insolubility in all solvents tested.

7.4 1,8-Naphthyridine-2,7-dicarboxamides

7.4.1 *N,N'-bis-B*enzyl-1,8-naphthyridine-2,7-dicarboxamide (48a)

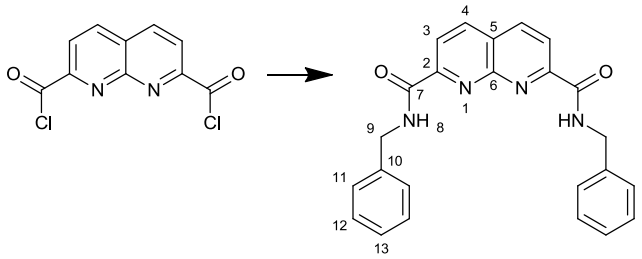

1,8-naphthyridine-2,7-dicarbonyl dichloride (200.4 mg, 0.78 mmol) was dissolved in DCM (10 mL) to this benzyl amine (0.17 mL, 1.64 mmol) was added turning the solution grey. Following this triethylamine (0.23 ml, 1.64 mmol) was added, which turned the reaction solution red. The reaction was left stirring at room temperature for 24 hours. After this time the solution was reduced *in vacuo* to give a crude yellow solid (260 mg). Recrystallisation was attempted from many solvent combinations before a vapour diffusion of diethyl ether into DCM yielded crystals of X-ray crystallography quality (98.7 mg, 32 %).

MP: 136 - 137 °C

ν/cm^{-1} 3380 (m, N-H), 3367 (m, N-H), 3057 (w, C-H), 3025 (w, C-H), 2914 (w, C-H), 2877 (w, C-H), 1683 (s, C=O), 1594 (w, aromatic C-C), 1513 (m, aromatic C-N, 1485 (m, aromatic C-C).

δ_H (300 MHz; $CDCl_3$) 4.73 (4H, d, *J* = 6.2 Hz, H-9), 7.25 – 7.43 (10H, m, H-11 H-12 H-13 H-14 H-15), 8.45 (2H, d, *J* = 8.4 Hz, H-3), 8.53 (2H, d, *J* = 8.4Hz, H-4), 8.56 (2H, t, *J* = 5.7 Hz, H-8).

δ_c (75 MHz; $CDCl_3$) 43.8 (C-9), 121.3 (C-3), 125.4 (C-5), 127.6 (C-13), 128.0 (C-12 + C-14), 128.7 (C-11 + C-15), 137.7 (C-10), 138.9 (C-4), 153.7 (C-6), 153.8 (C-2), 163.4 (C-7).

MS (ES $^+$): *m/z* 397 (52 %, $[M+H]^+$), 419 (72 %, $[M+Na]^+$), 460 (23 %, $[M+Na+MeCN]^+$), 793 (23 %, $[2M+H]^+$), 815 (100 %, $[2M+Na]^+$).

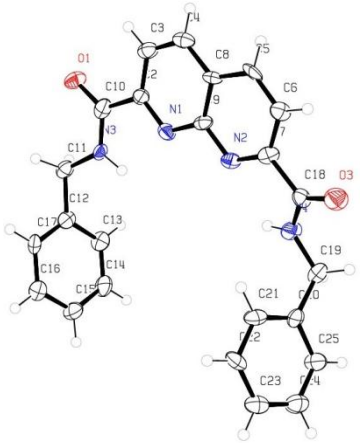

$C_{24}H_{20}N_4O_2$	a = 26.679 (3) Å	T = 120 K
Pna21	b = 5.5098 (6) Å	λ = 0.71073 Å
V = 1961.8 (4) Å	c = 13.3460 (15) Å	D_c = 1.342 g cm^{-3}
Z = 4	α = 90 (0) °	μ = 0.088 mm^{-1}
R_1 = 12.13 %	β = 90 (0) °	0.12 x 0.08 x 0.04 mm^3
$wR_2(F^2)$ = 19.31 %	γ = 90 (0) °	Translucent cut plate

Crystallised from diffusion of diethyl ether into chloroform

7.4.2 *N,N'-bis*-(4-Methylbenzyl)-1,8-naphthyridine-2,7-dicarboxamide (48b)

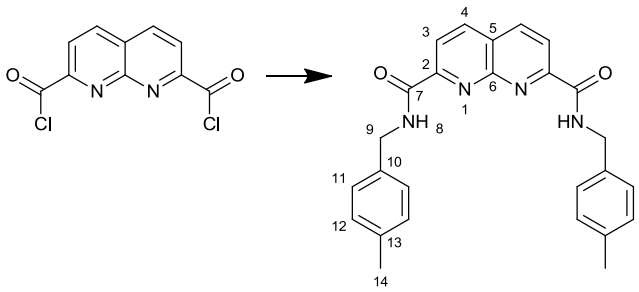

1,8-Naphthyridine-2,7-dicarbonyl dichloride (272.4 mg, 0.98 mmol) was dissolved in DCM (50 mL), 4-methylbenzylamine (0.24 ml, 2.16 mmol) was then added, giving an orange solution, followed by triethylamine (0.30 mL, 2.16 mmol) which gave an green solution. The reaction mixture was left to stir overnight during which time it turned dark red. The following day the reaction mixture was washed with water (3 x 50 mL) followed by brine (50 mL). The remaining organic residue was dried with magnesium carbonate and then reduced *in vacuo.* This yielded a crude brown oil (598.8 mg). This was recrystallised using a mixed solvent system of DCM: petroleum ether to yield a brown solid (183.3 mg, 44 %).

MP: 108 - 113°C

ν/cm^{-1} 3419 (N-H), 3291 (C-H), 3024 (C-H), 2920 (C-H), 1667 (C=O), 1643 (C=O), 1599 (aromatic C-C), 1519 (aromatic C-N), 1495 (aromatic C-C), 1456 (aromatic C-C).

δ_H (400 MHz, $CDCl_3$) 2.34 (6H, s, H-14), 4.68 (4H, d, *J*=6.0, H-9), 7.16 (4H, d, *J=7.5* Hz, H-12), 7.29 (4H, d, *J*=8.0 Hz, H-11), 8.44 (2H, d, *J*=8.5 Hz, H-3), 8.52 (2H, d, *J*=8.5 Hz, H-4), 8.52 (2H,br. S., H-8).

δ_C **(**100 MHz, $CDCl_3$) 21.1 (C-14), 43.6 (C-9), 121.3 (C-3), 125.3 (C-5), 128.0 (C-12), 129.4 (C-11), 134.7 (C-13), 137.3 (C-10), 138.8 (C-4), 152.7 (C-6), 153.8 (C-2), 163.3 (C-7).

M/S (ESI) m/z 425 (32 %, $[M+H]^+$), 447 (50, $[M+Na]^+$), 488 (32, $[M+Na]^+$), 871 (100, $[2M+Na]^+$).

HR-M/S: Found 425.1974, Expected 425.1972 ($C_{26}H_{25}N_4O_2$)

7.4.3 N,N'-*bis*-(2-Methoxybenzyl)-1,8-naphthyridine-2,7-dicarboxamide (48)

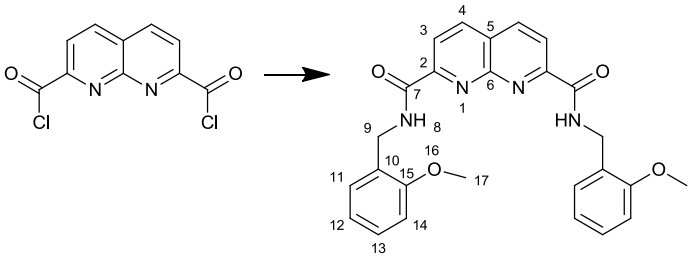

1,8-Naphthyridine-2,7-dicarbonyl dichloride (223.1 mg, 0.85 mmol) was dissolved in DCM (30 mL), 2-methoxybenzyl amine (256 mg, 1.87 mmol) was then added, turning the solution pale blue, followed by triethylamine (0.30 ml, 2.16 mmol), which turned the solution deep red. The reaction mixture was left to stir overnight. The following day the reaction mixture was washed with water (3 x 50 mL) followed by brine (50 mL). The remaining organic residue was dried with magnesium sulphate and then reduced *in vacuo* (293.7g). This was recrystallised using a mixed solvent system of DCM:petrol 40-60 °C to yield a white powder (225.4 mg, 58 %).

MP 153 - 155˚C

IR (υ_{max}/ cm^{-1}) 3423, 3367 (N-H), 3003 (C-H aromatic), 2929 (C-H aliphatic), 1674 (C=O), 1525 (C=C aromatic).

δ_H (400 MHz, $CDCl_3$) 3.89 (6 H, s, H-17), 4.75 (4 H, d, *J*=6.3 Hz, H-9), 6.90 (2 H, d, *J*=8.5 Hz, H-12), 6.94 (2 H, d, *J*=7.3 Hz H-11), 7.28 (2 H, t, *J*=8.0 Hz, H-13), 7.39 (2 H, d, *J*=7.3 Hz, H-14), 8.42 (2 H, d, *J*=8.5 Hz, H-3), 8.51 (2 H, d, *J*=8.5 Hz, H-4), 8.58 (2 H, t, *J*=5.5 Hz, H-8).

δ_C (100 MHz, $CDCl_3$) 39.2 (C-9), 55.4 (C-17), 110.4 (C-14), 120.6 (C-3), 121.3 (C-12), 125.2 (C-5), 125.8 (C-10), 128.9 (C-13), 129.6 (C-11), 138.7 (C-4), 152.8 (C-6), 154.1 (C-2), 157.5 (15), 163.4 (C-7)

M/S (ESI (MeCN)) m/z: 457.0 (7 %, $[M+H]^+$),479.1 (15, $[M+Na]^+$), 935.4 (22, $[2M+Na]^+$).

7.4.4 N,N'-*bis*-(4-Methoxybenzyl)-1,8-naphthyridine-2,7-dicarboxamide

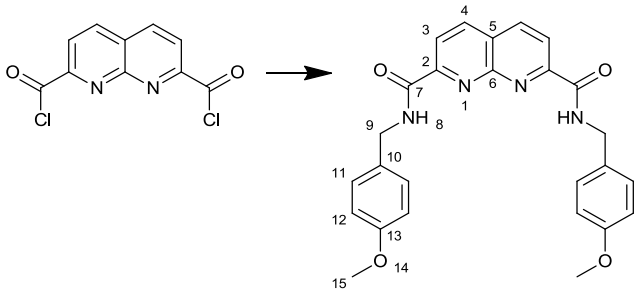

1,8-Naphthyridine-2,7-dicarbonyl dichloride (225 mg, 0.85 mmol) was dissolved in DCM (30 mL), 4-methoxybenzyl amine (264.6 mg, 1.87 mmol) was then added, turning the solution pale blue, followed by triethylamine (0.30 ml, 2.16 mmol), which turned the solution deep red. The reaction mixture was left to stir overnight. The following day the reaction mixture was washed with water (3 x 50 mL) followed by brine (50 mL). The remaining organic residue was dried with magnesium sulphate and then reduced *in vacuo.* This was recrystallised using a mixed solvent system of DCM:petrol 40-60 °C to yield a powder (192.1g, 48 %).

MP: 149-152˚C

IR (υ_{max}, cm^{-1}) 3375 (N-H), 3274 (N-H), 2929 (C-H aromatic), 2837 (C-H aliphatic), 1681 (C=O), 1528 (C=C aromatic), 1510 (C=C aromatic).

δ_H (400 MHz, $CDCl_3$) 3.80 (6 H, s, H-17), 4.66 (4 H, d, *J*=6.0 Hz, H-7), 6.88 (2 H, d, *J*=8.5 Hz, H-11), 7.32 (2 H, d, *J*=8.3 Hz H-12), 8.44 (2 H, d, *J*=8.3 Hz, H-3), 8.49 (2 H, t, *J*=5.8, H-8), 8.52 (2 H, d, *J*=8.5 Hz, H-4).

δ_C (100 MHz, $CDCl_3$) 43.3 (C-9), 55.3 (C-15), 114.1 (C-12), 121.3 (C-3), 125.3 (C-5), 129.4 (C-11), 129.8 (C-10), 138.8 (C-4), 152.7 (C-6), 153.8 (C-2), 159.1 (C-13), 163.3 (C-7).

M/S (ESI (MeCN)) m/z: 457.1 (36 %, $[M+H]^+$), 479.1 (64, $[M+Na]^+$), 520.0 (22, $[M+Na+MeCN]^+$), 935.4 (100, $[2M+Na]^+$).

HR-M/S: 457.1874 Found, 457.1870 Expected ($C_{26}H_{25}N_4O_4$)

7.4.5 N,N'-*bis*-(2-Pyridylmethyl)-1,8-naphthyridine-2,7-dicarboxamide (48c)

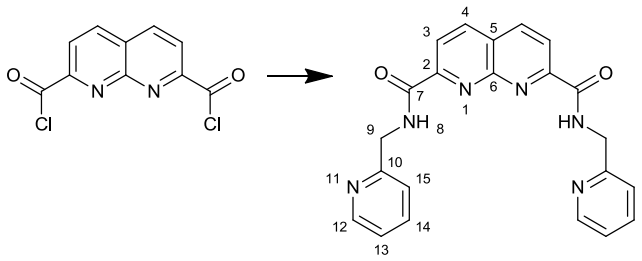

1,8-Naphthyridine-2,7-dicarbonyl dichloride (499.3 mg, 1.96 mmol) was dissolved in DCM (50 mL), 2-(aminomethyl)pyridine (0.45 ml, 4.31 mmol) was then added followed by triethylamine (0.60 mL, 4.31 mmol) which gave a blue solution. The reaction mixture was left to stir overnight. The following day the reaction mixture was washed with water (3 x 50 mL) followed by brine (50 mL). The remaining organic residue was dried with magnesium carbonate and then reduced *in vacuo.* This yielded a grey solid (559 mg). This was recrystallised using a mixed solvent system of DCM:diethyl ether to yield a grey crystalline material (363.8 mg, 46 %).

MP: 168 – 173 °C

ν/cm^{-1} 3404 (N-H), 3164 (C-H), 3164 (C-H), 3049 (C-H), 3014 (C-H), 1666 (C=O), 1663 (C=O), 1595 (aromatic C-C), 1568 (aromatic C-N), 1508 (aromatic C-C), 1483 (aromatic C-C).

δ_H (300 Mhz, $CDCl_3$) 4.88 (4H, d, *J*=5.9 Hz, H-9), 7.20 (2H, dd, *J*=6.8, 5.3 Hz, H-13), 7.37 (2H, d, *J*=8.1 Hz, H-15), 7.66 (2H, td, *J*=7.7, 1.5 Hz, H-14), 8.44 (2H, d, *J*=8.4 Hz, H-3), 8.51 (2H, d, *J*=8.4 Hz, H-4), 8.60 (2H, d, *J*=4.0 Hz, H-12), 9.11 (2H, t, *J*=5.5 Hz, H-9).

δ_C (75 Mhz, $CDCl_3$) 45.1 (C-9), 121.2 (C-3), 121.9 (C-15), 122.4 (C-13), 125.4 (C-5), 136.8 (C-14), 138.8 (C-4), 149.4 (C-12), 152.8 (C-6), 153.8 (C-10), 156.7 (C-2), 163.8 (C-7).

M/S (ESI) m/z 399 (26 %, $[M+H]^+$), 421 (42, $[M+Na]^+$ + $[2M+2Na]^{2+}$), 819 (100, $[2M+H]^+$), 797 (26, [2M+H]).

HR-M/S: Found 399.1559, Expected 399.1551 ($C_{22}H_{19}N_6O_2$)

7.4.5.1 N,N'-*bis*-(2-Pyridylmethyl)-1,8-naphthyridine-2,7-dicarboxamide hydrochloride

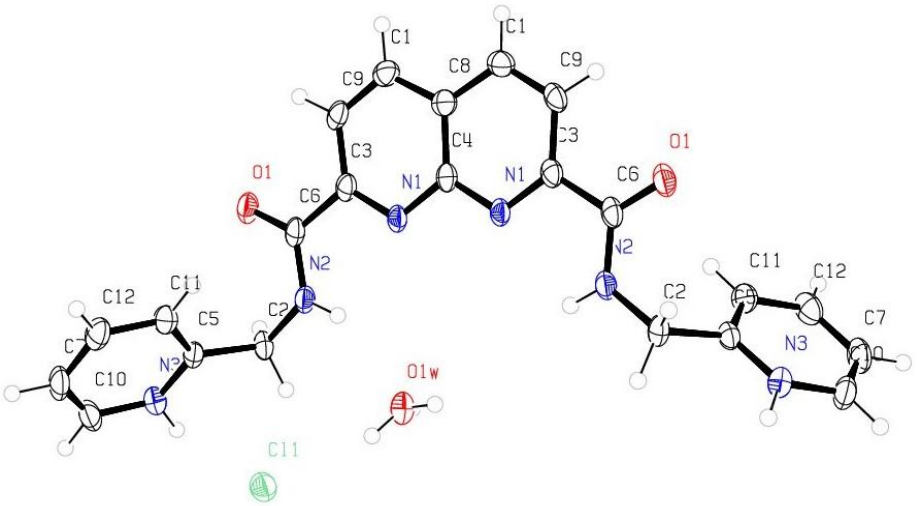

$C_{22}H_{24}Cl_2N_6O_4$	a = 24.382 (1) Å	T = 120 K
Pccn	b = 4.7900 (2) Å	λ = 0.71073 Å
V = 2284.76 (16) Å	c = 19.5630 (8) Å	D_c = 1.475 g cm^{-3}
Z = 4	α = 90 (0) °	μ = 0.328 mm^{-1}
R_1 = 5.14 %	β = 90 (0) °	0.3 x 0.14 x 0.05 mm^3
$wR_2(F^2)$ = 11.96 %	γ = 90 (0) °	Colourless spilt plate

Crystallised from diffusion of petroleum ether into chloroform

7.4.5.2 Metal complex of N,N'-*bis*-(Pyridin-2-ylmethyl)-1,8-naphthyridine-2,7-dicarboxamide

Although it was not possible to successfully determine the structure for N,N'-*bis*-(Pyridin-2-ylmethyl)-1,8-naphthyridine-2,7-dicarboxamide alone, a data collection was obtained which yielded a structure of the hydrochloride salt.

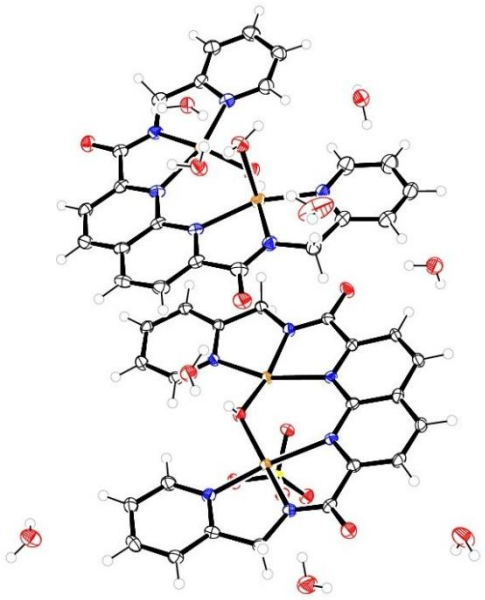

Copper sulphate (347.6 mg, 1.38 mmol) was dissolved in 10 mL of methanol giving a blue solution, potassium hydroxide (104 mg) was added causing the solution to turn turquoise. Finally N,N'-*bis*-(Pyridin-2-ylmethyl)-1,8-naphthyridine-2,7-dicarboxamide (250 mg, 0.63 mmol) added to the mixture in a DCM solvent (5 mL). This caused the solution to turn dark green. After stirring for 24 hours the solvent was removed *in vacuo* to yield a dark green solid (543.2 mg). Small portions of this solid were recrystallised from water to yield small crystalline fragments which yielded the X-ray crystal structure detailed below.

$C_{44}H_{54}Cu_4N_{12}O_{20}S$	a = 13.3695 (4) Å	T = 120 K
P1	b = 13.8078 (3) Å	λ = 0.71073 Å
V = 2519.91 (11) Å	c = 15.4057 (4) Å	D_c = 1.789 g cm^{-3}
Z = 2	α = 99.734 (2) °	μ = 1.800 mm^{-1}
R_1 = 5.29 %	β = 108.570 (1) °	0.2 x 0.2 x 0.02 mm^3
$wR_2(F^2)$ = 10.23 %	γ = 104.031 (1) °	Green plate

Crystallised from slow evaporation of water

7.4.6 N,N'-*bis*-(3-Pyridylmethyl)-1,8-naphthyridine-2,7-dicarboxamide (48d)

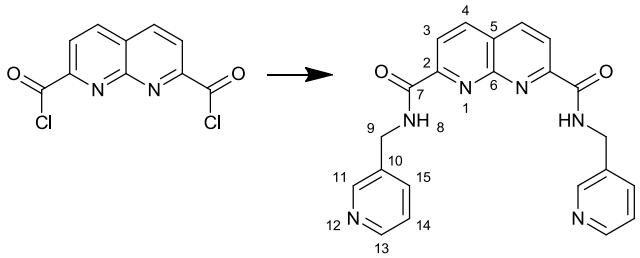

1,8-Naphthyridine-2,7-dicarbonyl dichloride (502.1 mg, 1.96 mmol) was dissolved in DCM (50 mL), 3-(aminomethyl)pyridine (0.45 ml, 4.31 mmol) was then added followed by triethylamine (0.60 mL, 4.31 mmol) which gave a blue solution. The reaction mixture was left to stir overnight. The following day the reaction mixture was washed with water (3 x 50 mL) followed by brine (50 mL). The remaining organic residue was dried with magnesium carbonate and then reduced *in vacuo.* This yielded a grey solid (501 mg). This was recrystallised using a mixed solvent system of DCM:diethyl ether to yield a grey crystalline material (328.2 mg, 41 %).

MP: 161 – 165 °C

ν/cm^{-1} 3389 (N-H), 3285 (C-H), 3066 (C-H), 2916 (C-H), 1680 (C=O), 1649 (C=O), 1595 (aromatic C-C), 1581 (aromatic C-N), 1519 (aromatic C-N), 1496 (aromatic C-C), 1477 (aromatic C-C).

δ_H (400 Mhz, $CDCl_3$) 4.75 (4H, d, *J*=6.5 Hz, H-9), 7.28 (2H, t, *J*=6.5 Hz, H-14), 7.74 (2H, d, *J*=7.5 Hz, H-15), 8.48 (2H, d, *J*=8.5 Hz, H-3), 8.53 (2H, d, *J*=8.5 Hz, H-4), 8.55 (2H, dd, *J*=5.0, 1.5 Hz, H-13), 8.61 (2H, t, *J*=6.0 Hz, H-8), 8.67 (2H, d, *J*=2.0 Hz, H-11).

δ_C (100 Mhz, $CDCl_3$) 41.3 (C-9), 121.4 (C-3), 123.6 (C-15), 125.6 (C-6), 133.4 (C-10), 135.7 (C-15), 139.1 (C-4), 149.1 (C-13), 149.4 (C-11), 152.7 (C-6), 153.5 (C-2), 163.6 (C-7).

M/S (ESI) m/z 399 (100 %, $[M+H]^+$), 421 (47, $[M+Na]^+$), 819 (30, $[2M+Na]^+$).

HR-M/S: Found 399.1560, Expected 399.1564 ($C_{22}H_{19}N_6O_2$)

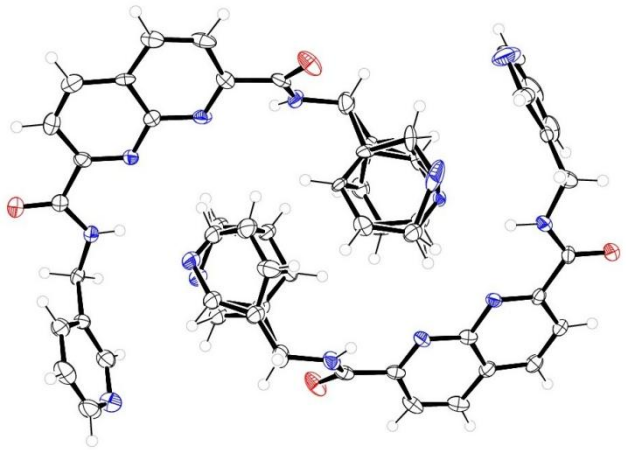

$C_{22}H_{18}N_6O_2$	a = 4.9940 (2) Å	T = 120 K
P21	b = 33.0330 (11) Å	λ = 0.71073 Å
V = 1881.78 (12) Å	c = 11.4450 (4) Å	D_c = 1.406 g cm^{-3}
Z = 4	α = 90 (0) °	μ = 0.095 mm^{-1}
R_1 = 8.67 %	β = 94.668 (2) °	0.2 x 0.02 x 0.02 mm^3
$wR_2(F^2)$ = 17.29 %	γ = 90 (0) °	Colourless cut needle

Crystallised from diffusion of diethyl ether into chloroform

7.4.7 N,N'-*bis*-(4-Pyridylmethyl)-1,8-naphthyridine-2,7-dicarboxamide (48e)

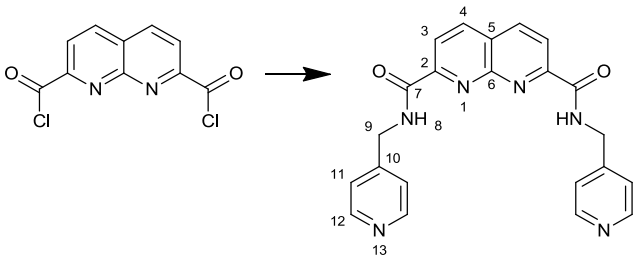

1,8-Naphthyridine-2,7-dicarbonyl dichloride (502.9 mg, 1.96 mmol) was dissolved in DCM (50 mL), 4-(aminomethyl)pyridine (0.45 ml, 4.31 mmol) was then added followed by triethylamine (0.60 mL, 4.31 mmol) which gave a blue solution. The reaction mixture was left to stir overnight. The following day the reaction mixture was washed with water (3 x 50 mL) followed by brine (50 mL). The remaining organic residue was dried with magnesium carbonate and then reduced *in vacuo.* This yielded a grey solid (442 mg). This was recrystallised using a mixed solvent system of DCM:diethyl ether to yield a yellow crystalline material (184.5 mg, 24 %) and a second crop of yellow powder (273.2 mg, 34 %).

MP: 204 – 206 °C

ν/cm^{-1} 3391 (N-H), 3376 (N-H), 3318 (C-H), 3069 (C-H), 1674 (C=O), 1664 (C=O), 1597 (aromatic C-C), 1561 (aromatic C-N), 1519 (aromatic C-N), 1494 (aromatic C-C).

δ_H (400 MHz, $CDCl_3$) 4.75 (4 H, d, *J*=6.0 Hz, H-9), 7.31 (4 H, d, *J*=5.5 Hz, H-11), 8.51 (2 H, d, *J*=8.5 Hz, H-3), 8.56 (2 H, d, *J*=8.5 Hz, H-4), 8.59 (4 H, d, *J*=5.5 Hz, H-12), 8.66 (2 H, t, *J*=6.0 Hz, H-8)

δ_C (75 Mhz, $CDCl_3$) 42.6 (C-9), 121.5 (C-3), 122.4 (C-11), 125.7 (C-5), 139.2 (C-4), 146.8 (C-10), 150.2 (C-12), 152.7 (C-6), 153.5 (C-2), 163.7 (C-7).

M/S (ESI) m/z 200 (17 %, $[M+2H]^{2+}$), 399 (100, $[M+H]^+$), 421 (33 %, $[M+Na]^+$), 798 (9 %, $[2M+H]^+$), 819 (28 %, $[2M+Na]^+$).

HR-M/S: Found 399.1555, Expected 399.1564 ($C_{22}H_{19}N_6O_2$)

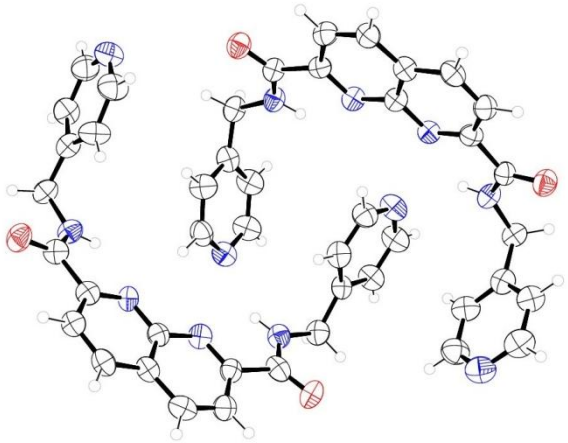

$C_{22}H_{18}N_6O_2$	a = 5.465 (7) Å	T = 120 K
P21	b = 17.15 (2) Å	λ = 0.6939 Å
V = 1923 (4) Å	c = 20.52 (3) Å	D_c = 1.376 g cm^{-3}
Z = 4	α = 90 (0) °	μ = 0.093mm^{-1}
R_1 = 7.23 %	β = 91.160 (13) °	0.06 x 0.04 x 0.03 mm^3
$wR_2(F^2)$ = 19.75 %	γ = 90 (0) °	Colourless block

Crystallised from diffusion of petroleum ether into chloroform

7.4.8 *N,N'-bis*-(2-Fluorobenzyl)-1,8-naphthyridine-2,7-dicarboxamide (48g)

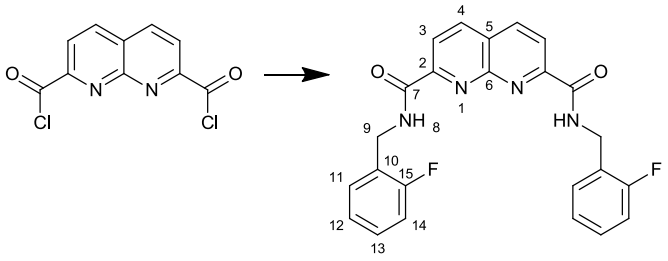

1,8-Naphthyridine-2,7-dicarbonyl dichloride (250.2 mg, 0.98 mmol) was dissolved in DCM (50 mL), 2-fluorobenzylamine (270 mg, 2.16 mmol) was then added followed by triethylamine (0.30 mL, 2.16 mmol). The reaction mixture was left to stir overnight. The following day the reaction mixture was washed with water (3 x 50 mL) followed by brine (50 mL). The remaining organic residue was dried with magnesium carbonate and then reduced *in vacuo.* This yielded an off-white solid (389.8 g). This was columned using a gradiented ethyl acetate: petrol solvent system with the starting composition of 10 % EA in petrol slowly being increased to neat EA over the course of the column. This afforded two main products with the desired product being a white solid (198.2 mg, 47 %).

MP: 119 - 121 °C

ν/cm^{-1} 3364 (N-H), 3055 (C-H), 1682 (C=O), 1590 (aromatic C-C), 1519 (aromatic C-C), 1485 (aromatic C-C).

δ_H (400 MHz, $CDCl_3$) (4 H, d, *J*=6.1 Hz, H-9), 7.03 - 7.15 (4 H, m, H-12 and H-14), 7.23 - 7.32 (2 H, m, 13), 7.46 (2 H, td, *J*=7.5, 1.8 Hz, H-11), 8.45 (2 H, d, *J*=8.6 Hz, H-3), 8.52 (2 H, d, *J*=8.6 Hz, H-4), 8.57 (2 H, t, *J*=6.1 Hz, H-8)

δ_C (100 Mhz, $CDCl_3$) 37.6 (d, *J*=4.4 Hz, C-9), 115.5 (d, *J*=22.0 Hz, C-14), 121.4 (C-3), 124.3 (d, *J*=4.4 Hz, C-12), 124.8 (d, *J*=14.6 Hz, C-10), 125.4 (C-5), 129.5 (d, *J*=8.8 Hz, C-13), 130.4 (d, *J*=2.9 Hz, C-11), 138.9 (C-4), 152.8 (C-6), 153.8 (C-2), 161.0 (d, *J*=247.4 Hz, C-16), 163.5 (C-7)

M/S (ESI) m/z 433 (32 %, $[M+H]^+$), 496 (88, $[M+Na+MeCN]^+$), 887 (100, $[2M+H]^+$).

HR-M/S: Found 433.1470, Expected 433.1471 ($C_{24}H_{19}F_2N_4O_2$)

7.4.9 *N,N'-bis*-(3-Fluorobenzyl)-1,8-naphthyridine-2,7-dicarboxamide (48j)

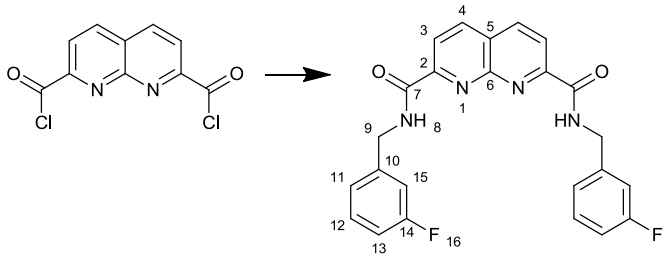

1,8-Naphthyridine-2,7-dicarbonyl dichloride (250.2 mg, 0.98 mmol) was dissolved in DCM (50 mL), 2-fluorobenzylamine (270 mg, 2.16 mmol) was then added followed by triethylamine (0.30 mL, 2.16 mmol). The reaction mixture was left to stir overnight. The following day the reaction mixture was washed with water (3 x 50 mL) followed by brine (50 mL). The remaining organic residue was dried with magnesium carbonate and then reduced *in vacuo.* This yielded an off-white solid (389.8 mg). This was columned using a gradiented ethyl acetate: petrol solvent system with the starting composition of 10 % EA in petrol slowly being increased to neat EA over the course of the column. This afforded two main products with the desired product being a white solid (198.2 mg, 47 %).

MP: 111 - 113 °C

ν/cm^{-1} 3405 (N-H), 3381 (N-H), 3323 (N-H), 3016 (C-H), 2970 (C-H), 1739 (C=O), 1677 (C=O), 1654 (C=O), 1590 (aromatic C-C), 1523 (aromatic C-C), 1486 (aromatic C-C).

δ_H (400 MHz, $CDCl_3$) 4.64 (4 H, d, *J*=6.1 Hz, H-9), 6.89 (2 H, td, *J*=8.2, 2.3 Hz, H-13), 7.01 (2 H, dt, *J*=9.6, 2.0 Hz, H-11), 7.08 (2 H, d, *J*=7.6 Hz, H-15), 7.18 - 7.26 (2 H, m, H-12), 8.39 (2 H, d, *J*=8.6 Hz, H-3), 8.46 (2 H, d, *J*=8.6 Hz, H-4), 8.52 (2 H, t, *J*=5.8 Hz, H-8)

δ_C (75 Mhz, $CDCl_3$) 43.2 (C-9), 114.5 (d, *J*=22.0 Hz, C-15), 114.7 (d, *J*=23.4 Hz, C-13), 121.4 (C-3), 123.4 (C-11), 125.5 (C-5), 130.2 (d, *J*=7.3 Hz, C-12), 139.0 (C-4), 140.3 (d, *J*=7.3 Hz, C-10), 152.7 (C-6), 153.7 (C-2), 163.5 (C-7), 163.0 (d, *J*=231.3 Hz, C-14)

δ_F (282 MHz, $CDCl_3$) -118.6

HR-M/S: Found 433.1479, Expected 433.1471 ($C_{24}H_{19}F_2N_4O_2$)

7.4.10 *N,N'-bis*-(3-Chlorobenzyl)-1,8-naphthyridine-2,7-dicarboxamide (48k)

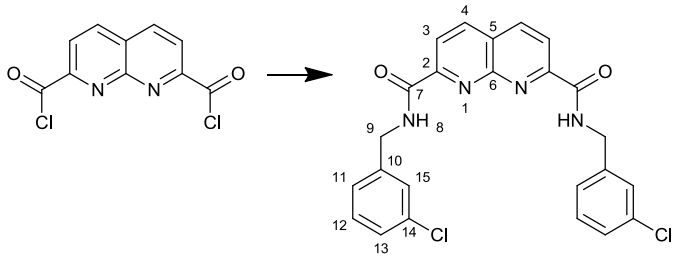

1,8-Naphthyridine-2,7-dicarbonyl dichloride (253.0 mg, 0.98 mmol) was dissolved in DCM (50 mL), 3-chlorobenzylamine (305.8 mg, 2.16 mmol) was then added followed by triethylamine (0.30 mL, 2.16 mmol). The reaction mixture was left to stir overnight. The following day the reaction mixture was washed with water (3 x 50 mL) followed by brine (50 mL). The remaining organic residue was dried with magnesium carbonate and then reduced *in vacuo.* This yielded an off-white solid (469.6 mg). This was columned using a gradiented DCM:methanol solvent system with the starting composition of neat DCM with the addition of 2 % methanol towards the end of the column. This afforded the desired product (227.9 mg, 50 %).

MP: 55 - 57 °C

ν/cm^{-1} 3379 (N-H), 3062 (C-H), 2927 (C-H), 1739 (C=O), 1667 (C=O), 1597 (aromatic C-C), 1573 (aromatic C-N), 1519 (aromatic C-C), 1492 (aromatic C-C).

δ_H (400 MHz, $CDCl_3$) ^{1}H 4.72 (4 H, d, *J*=6.1 Hz, H-9), 7.24 - 7.31 (6 H, m, H-11 H-12 H-13), 7.39 (2 H, s, H-15), 8.48 (2 H, d, *J*=8.6 Hz, H-3), 8.55 (2 H, d, *J*=8.6 Hz, H-4), 8.59 (2 H, t, *J*=6.1 Hz, H-8)

δ_C (100 Mhz, $CDCl_3$) 43.2 (C-9), 121.4 (C-5), 125.5 (C-11), 126.1 (C-12), 127.8 (C-13), 128.0 (C-15), 130.0 (C-15), 134.6 (C-14), 139.0 (C-4), 139.8 (C-10), 152.7 (C-6), 153.7 (C-2), 163.5 (C-7)

M/S (ESI) m/z 528 (15 %, $[M+Na+MeCN]^+$), 953 (25, $[2M+Na]^+$).

HR-M/S: Found 487.0705, Expected 487.0699 ($C_{24}H_{18}Cl_2N_4O_2Na$)

7.4.11 *N,N'-bis*-(4-Chlorobenzyl)-1,8-naphthyridine-2,7-dicarboxamide (48n)

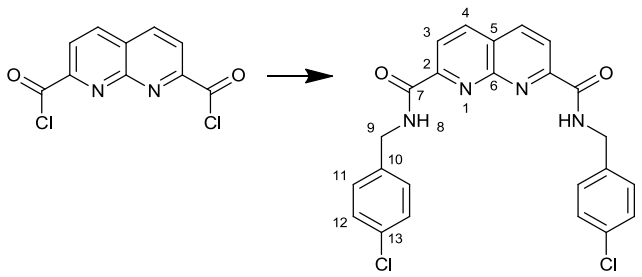

1,8-Naphthyridine-2,7-dicarbonyl dichloride (249.9 mg, 0.98 mmol) was dissolved in DCM (50 mL), 4-chlorobenzylamine (304.8 mg, 2.16 mmol) was then added followed by triethylamine (0.30 mL, 2.16 mmol). The reaction mixture was left to stir overnight. The following day the reaction mixture was washed with water (3 x 50 mL) followed by brine (50 mL). The remaining organic residue was dried with magnesium carbonate and then reduced *in vacuo.* This yielded an off-white solid (415.6 mg). This was columned using a gradiented ethyl acetate: petrol solvent system with the starting composition of 10 % EA in petrol slowly being increased to neat EA over the course of the column. This afforded three fractions with the desired product being a white solid (134.6 mg, 30 %).

MP: 195 - 198 °C

ν/cm^{-1} 3376 (N-H), 3360 (N-H), 3086 (C-H), 3069 (C-H), 1675 (C=O), 1599 (aromatic C-C), 1518 (aromatic C-N), 1488 (aromatic C-C).

δ_H (400 MHz, *DMSO-d*$_6$) 4.57 (4 H, d, *J*=6.1 Hz, H-9), 7.28 - 7.53 (8 H, H-11 and H-12), 8.34 (2 H, d, *J*=8.1 Hz, H-3), 8.80 (2 H, d, *J*=8.1 Hz, H-4), 9.43 (2 H, t, *J*=5.8 Hz, H-8).

δ_C (100 Mhz, *DMSO-d*$_{6)}$ 42.1 (C-9), 120.8 (C-3), 124.4 - 125.5 (m), 128.3 (C-11), 129.4 (C-12), 131.5 (C-13), 138.2 (C-10), 139.8 (C-4), 152.5 (C-6), 153.9 (C-2), 163.7 (C-7).

M/S (ESI) m/z 528 (21 %, $[M+Na+MeCN]^+$), 953 (32, $[2M+Na]^+$).

HR-M/S: Found 465.0880, Expected 465.0880 ($C_{24}H_{19}Cl_2N_4O_2$)

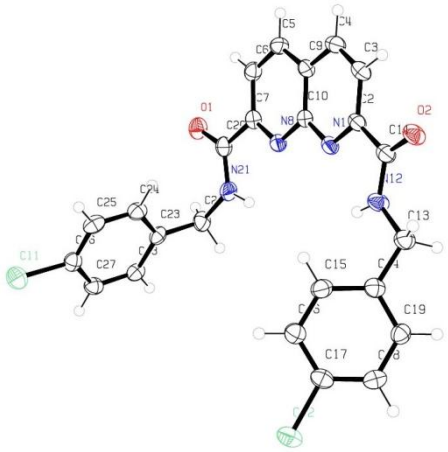

$C_{24}H_{18}Cl_2N_4O_2$	a = 12.5757 (3) Å	T = 120 K
P21/n	b = 5.7350 (1) Å	λ = 0.71073 Å
V = 2146.35 (8) Å	c = 29.7517 (6) Å	D_c = 1.441 g cm^{-3}
Z = 4	α = 90 (0) °	μ = 0.333 mm^{-1}
R_1 = 5.75 %	β = 91.101 (1) °	0.66 x 0.08 x 0.04 mm^3
$wR_2(F^2)$ = 14.44 %	γ = 90 (0) °	Colourless needle

Crystallised from acetonitrile

7.4.12 *N,N'-bis*-(2-Bromobenzyl)-1,8-naphthyridine-2,7-dicarboxamide (48i)

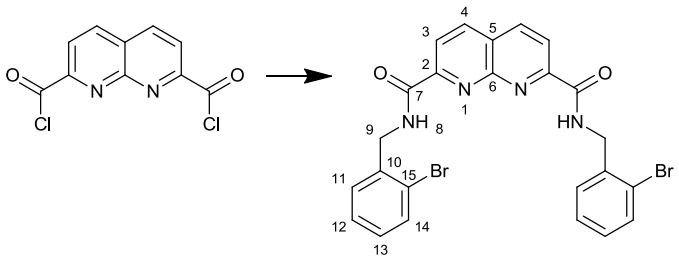

1,8-Naphthyridine-2,7-dicarbonyl dichloride (250.1 mg, 0.98 mmol) was dissolved in DCM (50 mL), 2-bromobenzylamine hydrochloride (409.5 mg, 2.16 mmol) was then added followed by triethylamine (0.6 mL, 4.32 mmol). The reaction mixture was left to stir overnight. The following day the reaction mixture was washed with water (3 x 50 mL) followed by brine (50 mL). The remaining organic residue was dried with magnesium carbonate and then reduced *in vacuo.* This yielded an off-white solid (714.7 mg). This was columned using a gradiented DCM:methanol solvent system with the starting composition of neat DCM with the addition of 2 % methanol towards the end of the column. This afforded the desired product (248.2 mg, 46 %).

MP: 174 - 176 °C

ν/cm^{-1} 3407 (N-H), 3366 (N-H), 3069 (C-H), 1679 (C=O), 1599 (aromatic C-C), 1519 (aromatic C-N), 1491 (aromatic C-C).

δ_H (400 MHz, $CDCl_3$) 4.84 (4 H, d, *J*=6.2 Hz, H-9), 7.17 (2 H, td, *J*=7.7, 1.5 Hz, H-14), 7.30 (2 H, td, *J*=7.7, 1.1 Hz, H-12), 7.49 (2 H, d, *J*=7.7 Hz, H-13), 7.59 (2 H, d, *J*=7.7 Hz, H-11), 8.46 (2 H, d, *J*=8.4 Hz, H-3), 8.53 (2 H, d, *J*=8.8 Hz, H-4), 8.66 (2 H, t, *J*=6.0 Hz, H-8)

δ_C (100 MHz, $CDCl_3$) 44.0 (C-9), 121.4 (C-3), 123.8 (C-15), 125.5 (C-5), 127.7 (C-12), 129.3 (C-13), 130.1 (C-11), 132.9 (C-14), 136.9 (C-10), 138.9 (C-4), 152.8 (C-6), 153.8 (C-2), 163.5 (C-7)

M/S (ESI) m/z 393 (100 %, $[2M+3Na]^{3+}$), 555 (12 %, $[M+H]^+$), 577 (20, $[M+Na]^+$), 618 (83, $[M+Na+MeCN]^+$), 1131 (75, $[2M+Na]^+$).

HR-M/S: Found 552.9860, Expected 552.9869 ($C_{24}H_{19}Br_2N_4O_2$)

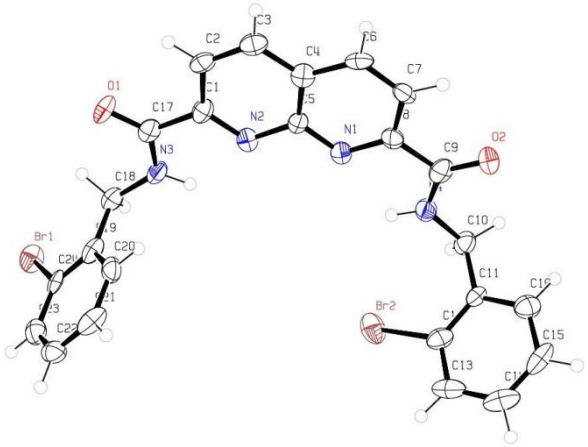

$C_{24}H_{18}Br_2N_4O_2$	a = 27.35.76 (8) Å	T = 120 K
Fdd2	b = 68.327 (2) Å	λ = 0.71073 Å
V = 8690.8 (4) Å	c = 4.6493 (1) Å	D_c = 1.694 g cm^{-3}
Z = 16	α = 90 (0) °	μ = 3.761 mm^{-1}
R_1 = 7.99 %	β = 90 (0) °	0.5 x 0.05 x 0.04 mm^3
$wR_2(F^2)$ = 17.07 %	γ = 90 (0) °	Colourless needle

Crystallised from slow evaporation of chloroform

7.4.13 *N,N'-bis*-(3-Bromobenzyl)-1,8-naphthyridine-2,7-dicarboxamide (48l)

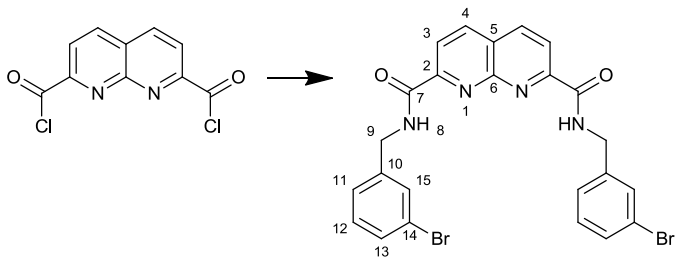

1,8-Naphthyridine-2,7-dicarbonyl dichloride (252.5 mg, 0.98 mmol) was dissolved in DCM (50 mL), 3-bromobenzylamine hydrochloride (401.8 mg, 2.16 mmol) was then added followed by triethylamine (0.60 mL, 4.32 mmol). The reaction mixture was left to stir overnight. The following day the reaction mixture was washed with water (3 x 50 mL) followed by brine (50 mL). The remaining organic residue was dried with magnesium carbonate and then reduced *in vacuo.* This yielded an off-white solid (494.4 g). This was columned using a gradiented ethyl acetate: petrol solvent system with the starting composition of 10 % EA in petrol slowly being increased to neat EA over the course of the column. This afforded three fractions with the desired product being a white solid (286.0 mg, 53 %).

MP: 134 - 136 °C

ν/cm^{-1} 3382 (N-H), 3363 (N-H), 3051 (C-H), 2926 (C-H), 1673 (C=O), 1595 (aromatic C-C), 1569 (aromatic C-C), 1522 (aromatic C-C), 1491 (aromatic C-C).

δ_H (400 MHz, $CDCl_3$) 4.71 (15 H, d, *J*=6.6 Hz, H-9), 7.22 (4 H, t, *J*=8.1 Hz, H-12), 7.33 (2 H, d, *J*=8.1 Hz, H-13), 7.43 (2 H, d, *J*=7.6 Hz, H-11), 7.55 (2 H, s, H-15), 8.48 (2 H, d, *J*=8.6 Hz, H-3), 8.55 (2 H, d, *J*=8.6 Hz, H-4), 8.59 (2 H, t, *J*=5.8 Hz, H-8).

δ_C (100 MHz, $CDCl_3$) 43.2 (C-9), 121.4 (C-3), 122.8 (C-14), 125.6 (C-5), 126.6 (C-11), 130.3 (C-13), 130.8 (C-12), 130.9 (C-15), 139.0 (C-4), 140.1 (C-10), 152.7 (C-6), 153.7 (C-2), 163.5 (C-7).

M/S (ESI) m/z 393 (100 %, $[2M+3Na]^{3+}$), 555 (4 %, $[M+H]^+$), 577 (8, $[M+Na]^+$), 618 (18, $[M+Na+MeCN]^+$), 1131 (75, $[2M+Na]^+$).

HR-M/S: Found 554.9867, Expected 552.9869 ($C_{24}H_{19}Br_2N_4O_2$)

7.4.14 *N,N'-bis*-(4-Nitrobenzyl)-1,8-naphthyridine-2,7-dicarboxamide (48f)

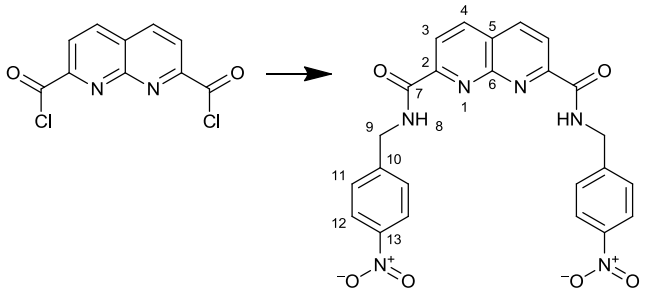

1,8-Naphthyridine-2,7-dicarbonyl dichloride (250.5 mg, 0.98 mmol) was dissolved in DCM (50 mL), 4-nitrobenzylamine hydrochlorde (408.1 mg, 2.16 mmol) was then added followed by triethylamine (0.60 mL, 4.32 mmol). The reaction mixture was left to stir overnight. The following day the reaction mixture contained a precipitate which was removed by filtration (107.9 mg, 23 %), a second crop was collected (131.7g, 28 %).

MP: 245 - 248 °C

ν/cm^{-1} 3380 (N-H), 3014 (C-H), 2969 (C-H), 1739 (C=O), 1686 (C=O), 1599 (aromatic C-C), 1510 (aromatic C-C), 1491 (aromatic C-C), 1447 (aromatic C-C).

δ_H (400 MHz, $CDCl_3$) 4.76 (4 H, d, *J*=6.6 Hz, H-9), 7.48 (4 H, d, *J*=8.6 Hz, H-11), 8.12 (4 H, d, *J*=8.6 Hz, H-12), 8.44 (2 H, d, *J*=8.1 Hz, H-3), 8.48 (2 H, d, *J*=8.6 Hz, H-4), 8.61 (2 H, t, *J*=6.1 Hz, H-8)

δ_C (100 MHz, $CDCl_3$) 43.1 (C-9), 121.5 (C-3), 124.0 (C-12), 125.8 (C-5), 128.4 (C-11), 139.3 (C-4), 145.3 (C-10), 147.5 (C-13), 152.8 (C-6), 153.5 (C-2), 163.7 (C-7).

M/S (ESI) m/z 550 (46 %, $[M+Na+MeCN]^+$), 995 (46 %, $[2M+H]^+$).

HR-M/S: 509.1178 Found, 509.1180 Expected ($C_{24}H_{18}N_6O_6Na$)

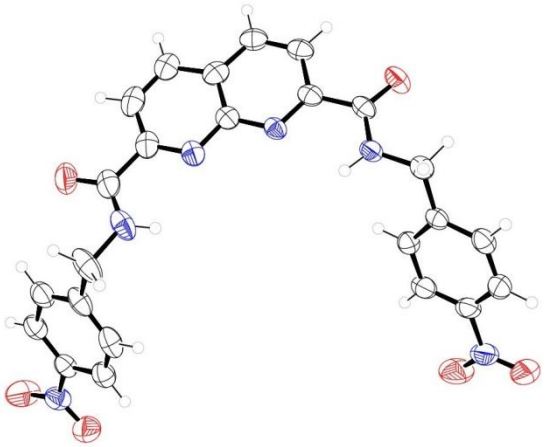

$C_{24}H_{18}N_6O_6$	a = 25.6431 (5) Å	T = 120 K
P21/c	b = 3.9774 (1) Å	λ = 0.71073 Å
V = 2483.92 (10) Å	c = 26.0561 (6) Å	D_c = 1.301 g cm^{-3}
Z = 4	α = 90 (0) °	μ = 0.097 mm^{-1}
R_1 = 9.08 %	β = 110.825 (1) °	0.52 x 0.24 x 0.12 mm^3
$wR_2(F^2)$ = 29.27 %	γ = 90 (0) °	Colourless cut needle

Crystallised from acetonitrile

7.5 Synthesis of Amine Materials as Potential Side Arms

7.5.1 4-Biphenylboronic Acid (110)

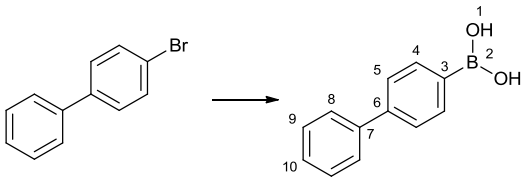

4-Bromobiphenyl (2.0260 g) was mixed with magnesium turnings (0.234 g) in tetrahydrofuran (11 mL). The reaction mixture was then stirred for 30 minutes, with occasional gentle heating until all the magnesium turnings had been consumed. The reaction mixture became a turbid grey during this time. This Grignard solution was then added in a drop-wise manner to a stirred solution of trimethylborate (1.161 g) in dry ether (10 mL) at -78 °C (ensuring that the temperature did not rise above -70 °C. Following the complete addition the reaction was allowed to warm slowly to room temperature. The following day the reaction mixture was added to a stirred solution of ice (20 mL) and sulphuric acid (1 mL, concentrated). This mixture was left to stir for 30 mins before being extracted with diethyl ether (5 x 50 mL). The solvent

was removed *in vacuo* to give a white solid (2.1939 g). This was then recrystallised from aqueous ethanol to give two crops (0.8838 g, 51 % and 0.2369 g, 14 %).

MP: 230 – 234 °C

IR (υ_{max}/cm^{-1}) 3342 (O-H br), 3057 (C-H), 3035 (C-H), 1606 (C=C), 1552 (C=C), 1523 (C=C).

δ_H (400 MHz, Acetone) 7.23 (2H, s, H-1), 7.36 (1H, tt, J=7.53, 2.01 Hz, H-10), 7.46 (2H, t, J=7.5, H-9), 7.65 (2H, d, J=8.5 Hz, H-5), 7.68 (2H, dd, J= 8.3, 1.3 Hz, H-8), 7.97 (2H, d, J=8.0 Hz, H-4).

δ_C (100 MHz, Acetone) 126.9 (C-5), 127.8 (C-8), 128.4 (C-10), 129.8 (C-9), 135.7 (C-4), 141.9 (C-7), 143.6 (C-6).

M/S (ESI -ve (MeOH)) m/z: 211 (100 %, $[M-H]^+$), 423 (14 %, $[2M-H]^+$).

In this case the Mass Spectrometry sample appears to have undergone some form of reaction in the spectrometer to give B(OMe)(OH) species.

7.5.2 4-Amino-*p*-terphenyl (112)

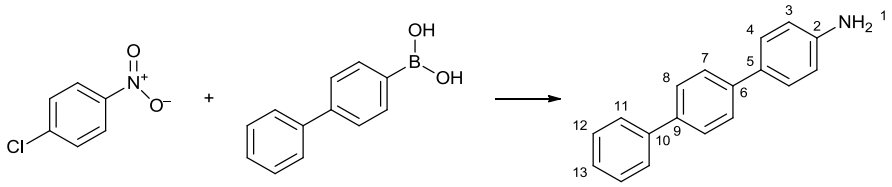

Palladium chloride (13.4 mg, 3 mol %) was stirred with 1,4-diazobicyclo[2.2.2]octane (DABCO) (16.9 mg, 6 mol %) in dimethylformamide/water mixture (5:1, 6 mL) for 10 mins. This was then added to a flask containing 4-biphenylboronic acid (503.2 mg, 2.5 mmol) and 4-chloronitrobenzene (393 mg, 2.5 mmol). The reaction mixture was then heated at 150 °C for 12 hours during which time the reaction went brown. After 12 hours the reaction mixture was filtered to give a red solution. The solvent was removed to give a crude material (986.7 mg). The crude material was then columned with a DCM eluent. This yielded the desired product (175.4 mg, 29 %) as well as the unreduced nitro compound (52.7 mg, 8 %).

MP: 186 -190 °C

IR (υ_{max}/cm^{-1}) 3302 (N-H), 3207 (C-H), 3030 (C-H), 1622 (C=C), 1614 (C=), 1597 (C=C), 1506 (C=C), 1483 (C=C).

δ_H (400 MHz, $CDCl_3$) 3.76 (2H, br. s, H-1), 6.79 (2H, dt, J=8.5, 2.5 Hz, H-3), 7.37 (1H, tt, 7.3, 1.0 Hz, H-13), 7.44 – 7.52 (4H, m, H-7 & H-11), 7.60 – 7.70 (6H, m, H-4 & H-8 & H-12).

δ_C (100 MHz, $CDCl_3$) 115.4 (C-3), 126.7 (C-7), 126.9 (C-11), 127.1 (C-13), 127.4 (C-8), 127.9 (C-4), 128.7 (C-8), 131.0 (C-3), 139.0 (C-9), 140.1 (C-6), 140.9 (C-10), 145.9 (C-2).

7.5.3 *tert*-Butyl (4-aminobenzyl)carbamate (103)

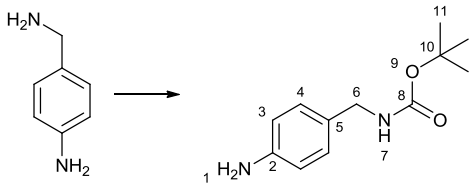

Di-(*tert*-butyl) dicarbonate (4.72 g, 21.61 mmol) was dissolved in THF (16 mL) before being added to a stirred solution of 4-aminobenzylamine (2.22 mL, 19.64 mmol) in THF (32 mL). The reaction mixture was stirred for 3 hours monitoring by TLC.

The solvent was then removed *in vacuo* to give an oil which was triturated with ether/petrol mixture (50:50) to give a solid which was filtered (3.5221 g, 80 %).

MP: 61 -63 °C

IR (υ_{max}/cm^{-1}) 3426 (N-H), 3343 (N-H), 3023 (C-H), 2996 (C-H), 2977 (C-H), 2931 (C-H), 1687 (C=C), 1611 (C=C), 1525 (C=N), 1513 (C=C).

δ_H (400 MHz, $CDCl_3$) 1.46 (9H, s, H-11), 3.66 (2H, br. S, H-1), 4.19 (2H, d, J=5.0 Hz, H-6), 4.76 (1H, br. S H-7), 6.64 (2H, d, J=8.0 Hz, H-3), 7.07 (2H, d, J=8.0 Hz, H-4).

δ_C (100 MHz, $CDCl_3$) 28.9 (C-11), 44.8 (C-6), 79.7 (C-10), 115.6 (C-3), 129.2 (C-5), 129.3 (C-4), 146.1 (C-2), 156.3 (C-8).

7.5.4 *tert*-Butyl (4-Cbz-aminobenzyl)carbamate (104)

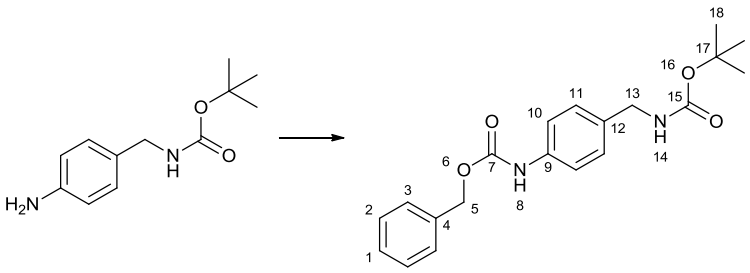

tert-butyl (4-aminobenzyl)carbamate (570 mg, 2.25 mmol) was dissolved in DCM and cooled to 0°C. Benzyl chloroformate (0.42 ml, 3.75 mmol) was added drop-wise followed by NEt_3 (0.414 mL)

before the reaction was allowed to warm to room temperature. Having been left overnight the solvent was removed *in vacuo* to give an oil which was then columned in Ethyl acetate/Petrol (1:1) this yielded the desired product (469.9 mg, 59 %) as well as recovered starting material (211.7 mg, 37 %).

MP: 92 -94 °C

IR (υ_{max}/cm^{-1}) 3394 (N-H), 3352 (N-H), 3010 (C-H), 2981 (C-H), 2932 (C-H), 1714 (C=O), 1683 (C=O), 1651 (C=O), 1615 (C=O), 1600 (C=C), 1521 (C=C), 1498 (C=C).

δ_H (400 MHz, $CDCl_3$) 1.47 (9H, s, H-18), 4.26 (2H, d, J=5.0 Hz, H-13), 4.81 (1H, br.s, H-14), 5.20 (2H, s, H-5), 7.22 (2H, d, J=8.0 Hz, H-11), 7.30 – 7.45 (7H, m, H-1,2,3 & H-10).

δ_C (100 MHz, $CDCl_3$) 28.4 (C-18), 44.2 (C-13), 67.0 (C-5), 79.5 (C-17), 118.9 (C-10), 128.3 (C-1), 128.3 (C-3), 128.4 (C-11), 128.6 (C-2), 134.1 (C-12), 136.0 (C-4), 137.0 (C-9), 153.3 (C-7), 155.9 (C-15).

M/S (ESI (MeOH)) m/z: 379 (100 %, $[M+Na]^+$),736 (16 %, $[2M+Na]^+$).

7.5.5 Benzyl [4-(aminomethyl)phenyl]carbamate trifluoroacetate salt (105.TFA)

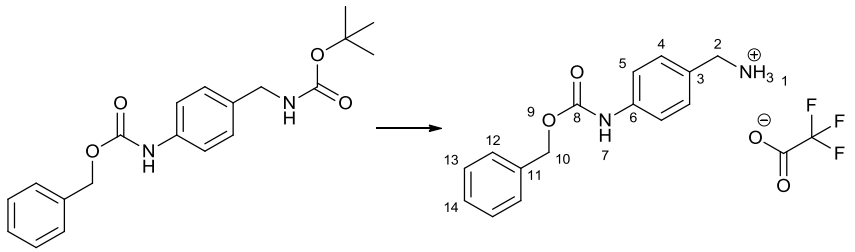

tert-Butyl (4-Cbz-aminobenzyl)carbamate (505 mg, 1.40 mmol) was placed in a flask before a 1:1 TFA/DCM solution was added. The reaction was left to stir overnight. The solvent was then removed *in vacuo* giving a white solid Attempts were made to recrystallise this solid from DCM , however, the material appeared to be insoluble and after drying gave(204 mg, 40 %) It was shown to be the TFA salt of the amine.

MP: 156 – 157 °C

IR (υ_{max}/cm^{-1}) 3291 (N-H), 3104 (O-H br)., 3041 (C-H), 2955 (C-H), 1715 (C=O), 1696 (C=O), 1676 (C=O), 1601 (C=C), 1538 (C=C),1466 (C=C).

δ_H (400 MHz, $CDCl_3$) 3.90 (2H, s, H-2), 5.12 (2H, s, H-10), 7.20 – 7.35 (7H, m, H-5 12, 13 , 14), 7.38 (2H, d, J=8.3 Hz, H-5).

δ_C (100 MHz, $CDCl_3$) 42.7 (C-2), 66.8 (C-10), 119.0 (C-5), 127.0 (C-14), 128.0 (C-4), 128.1 (C-3), 128.4 (C-12), 129.5 (C-13), 135.9 (C-11), 139.1 (C-6), 153.8 (C-8), 181.4 (C=O TFA salt).

δ_F (282 MHz, $CDCl_3$) -72.3 (TFA salt)

7.5.6 2-Amino-7-methyl-1,8-naphthyridine[264] (74)

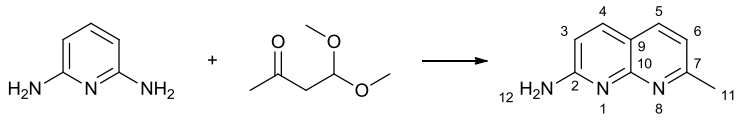

2,6-diaminopyridine (11.0 g, 0.1 mol) was dissolved in *ortho*-phosphoric acid (100 mL) and heated to 90 °C. Acetal acetaldehyde (13.03 g, 0.998 mol) was added drop-wise to the reaction mixture, which was maintained at 90 °C for 3 hours.

Once it had cooled this was neutralised using sodium hydroxide (to pH 6), and the reaction mixture was extracted with chloroform (5 x 150 mL). This yielded a mixed crude material which was then purified using column chromatography (alumina

stationary phase, 10 % methanol in DCM eluent). This yielded a black solid (6.91 g, 47 % yield) it also yielded a mixed fraction (2.17 g, 15 %) and degraded starting material (0.636 g).

δH (300 MHz; CDCl3) 2.60 (3 H, s, H-11), 6.66 (1 H, d, J=8.7 Hz, H-6), 7.01 (1 H, d, J=8.1 Hz, H-3), 7.73 (1 H, d, J=8.7 Hz, H-5), 7.77 (1 H, d, J=8.1 Hz, H-4).

δc (75 MHz; CDCl3) 24.7 (C-11), 111.9 (C-3), 115.1 (C-9), 118.4 (C-6), 136.4 (C-5), 137.7 (C-4), 155.7 (C-7), 160.0 (C-10), 161.3 (C-2)

7.6 Pyridine Starting Materials

7.6.1 Pyridine-2,6-dicarbonyl chloride

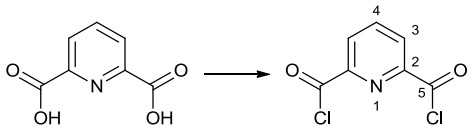

Thionyl chloride (42.1 mL, 0.6 mol) was added to a suspension of pyridine-2,6-dicarboxylic acid (20 g, 0.12 mol) in DCM (200 mL) containing a catalytic amount of DMF (3 drops). The suspension was refluxed at 40 °C for 72 h during which time the suspension went into solution and underwent a colour change from white to orange. Once the solution had been allowed to cool the solvent was removed *in vacuo*. The resulting brown solid was placed in a Soxhlet extraction setup using pentane as the solvent. Over the course of 72 h a white solid was observed to form. The apparatus was allowed to cool before the solid was collected by filtration (37.5g, 82 %).

MP: 54- 56 °C (lit.[184] 56 – 58 °C).

ν/cm^{-1} 3085 (w, C-H), 1748 (s, C=O), 1575 (m, aromatic C-C), 1424 (m, aromatic C-C), 638 (s, C-Cl), 623 (s, C-Cl).

δ_H (300 MHz; $CDCl_3$) 8.21 (1H, t, *J* = 7.6 Hz, 4-H), 8.37 (2H, d, *J* = 7.6 Hz, 3-H).

δc (75 MHz, $CDCl_3$) 129.0 (C-3), 139.4 (C-4), 149.2 (C-2), 169.4 (C-5).

7.6.2 Chelidamic acid (86)

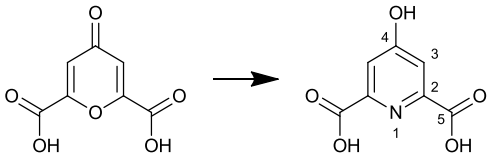

Chelidonic acid (19 g, 0.0942 mol) was placed in a flask and cooled to 0 °C. Ammonium hydroxide solution (200 mL, 30 %) was added drop-wise, and the resulting solution was stirred at RT for 2 days whilst monitoring by TLC. The ammonium hydroxide solution was removed under reduced pressure and the residue was boiled for 5 mins with activated charcoal (4 g) in water (200 mL) to decolourise the solution. After filtering the cooled solution was acidified to pH 1 with hydrochloric acid (concentrated). A white precipitate was formed which was filtered off, and washed with ice cold water. The white precipitate was then re crystallised from boiling water to yield two crops of product (8.558 g, 50 % and 3.0821 g, 17 %).

MP: 255-257 °C (decomposition)

IR (υ_{max}/ cm^{-1}): 3604 (free O-H), 3441 (H bonded O-H), 3121 (C-H), 1614 (C=O), 1590 (C=C), 1469 C=C).

δ_H (300 MHz, DMSO) 7.58 (2H, s, H-3).

δ_H (75 MHz, DMSO) 114.7 (C-3), 149.2 (C-2), 165.2 (C-4), 166.4 (C-5).

7.7 Pyridine-2,6-dicarboxylates (25)

7.7.1 *bis*-(2-Fluorobenzyl) pyridine-2,6-dicarboxylate (25a)

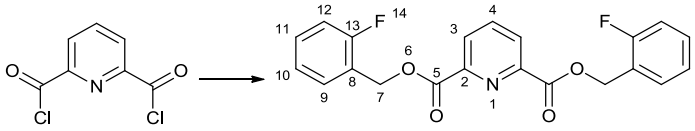

Pyridine-2,6-dicarbonyl dichloride (1.0063 g, 4.9 mmol) was stirred in DCM (50 ml). 2-Fluorobenzyl alcohol (1.362 g, 1.2 ml, 10.78 mmol, 2.2 equiv) was added followed by of triethylamine (1.5 ml) causing the reaction to turn from pink. The reaction was left to stir overnight. The reaction was washed with water (3 × 50 ml) and the organic phase was dried over $MgSO_4$. The solvent was then removed *in vacuo* to

yield an orange yellow solid (1.8683 g). This was then recrystallised using DCM and petrol 40-60˚C (1.0045 g, 53 %).

MP: 78-80˚C

IR (υ_{max}/cm^{-1}) 3062 (C-H aromatic), 2938 (C-H aliphatic), 1736 (C=O), 1574 (C=C aromatic), 1588 (C=C aromatic), 1229 (C-F).

δ_H (400 MHz, $CDCl_3$) 5.54 (4H, s, H-7), 7.09 (2H, ddd, J=9.5, 8.8, 0.8Hz, H-12), 7.15 (2H, td, J=7.5, 1.0Hz, H-10), 7.35 (2H, m, H-11), 7.55 (2H, td, J=7.5,1.6Hz, H-9), 7.99 (1H, t, J=8.0Hz, H-4), 8.28 (2H, d, J=7.8Hz, H-3).

δ_C (100 MHz, $CDCl_3$) 62.3 (C-8), 116.3 (d, J=21.4Hz, C-12), 123.5 (d, J=13.6Hz, C-8), 125.0 (d, J=3.9Hz, C-10), 128.8 (C3), 131.1 (d, J=7.8Hz, C-11), 131.5 (d, J=2.9Hz, C-9), 139.0 (C4), 149.2 (C-2), 161.8 (d, J=248.8Hz, C-13), 165.0 (C-5).

M/S (ESI (MeCN)) m/z: 384.4 (12 %, $[M+H]^+$), 401.4 (5, $[M+NH_4]^+$), 406.3 (24, $[M+Na]^+$), 447.4 (19, $[M+Na+MeCN]^+$), 784.4 (20, $[2M+NH_4]^+$), 789.32 (100, $[2M+Na]^+$).

HR-M/S: Found 406.0864, Expected 406.0861($C_{21}H_{15}F_2N_1O_4Na$)

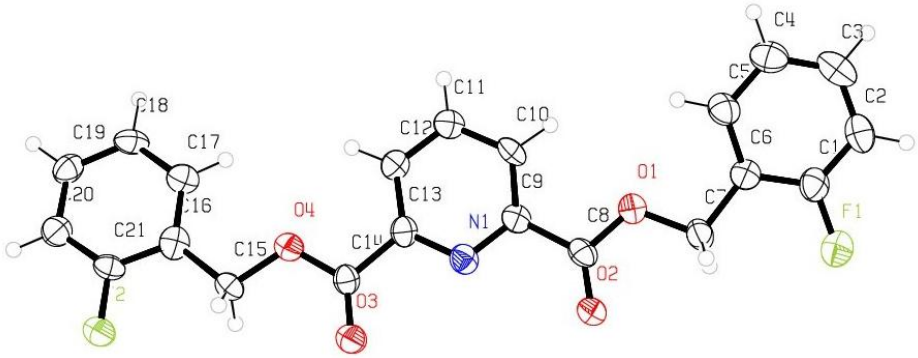

$C_{21}H_{15}F_2NO_4$	a = 10.717 (5) Å	T = 120 K
Pna21	b = 6.773 (5) Å	λ = 0.71069 Å
V = 1703.1 (15) Å	c = 23.463 (5) Å	D_c = 1.495 g cm^{-3}
Z = 4	α = 90 (0) °	μ = 0.118 mm^{-1}
R_1 = 8.44 %	β = 90 (0) °	0.4 x 0.08 x 0.02 mm^3
$wR_2(F^2)$ = 18.91 %	γ = 90 (0) °	Colourless plate

Crystallised by slow diffusion of diethyl ether into DCM

7.7.2 *bis*-(2-Chlorobenzyl) pyridine-2,6-dicarboxylate (25b)

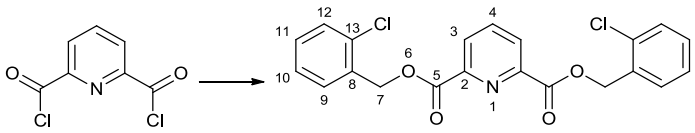

Pyridine-2,6-dicarbonyl dichloride (1.014 g, 4.97 mmol) was dissolved in DCM (30 mL), 2-chlorobenzyl alcohol (1.542 g, 10.93 mmol) was then added, followed by triethylamine (1.5 ml, 10.93 mmol). The reaction mixture was left to stir overnight. The following day the reaction mixture was washed with water (3 x 50 mL) followed by brine (50 mL). The remaining organic residue was dried with magnesium sulphate and then reduced *in vacuo* to yield a solid (2.0632 g). This was recrystallised using a mixed solvent system of DCM:petrol 40-60 °C to yield a powder (1.4257 g, 69 %). A second crop was also gathered (0.224 g, 11 %).

MP 109 – 113 °C

IR (υ_{max}, cm^{-1}) 3054 (C-H aromatic), 1732 (C=O), 1594 (C=C aromatic), 1576(C=C aromatic), 755 (C-Cl).

δ_H (400 MHz, $CDCl_3$) 5.56 (4 H, s, H-7), 7.25 - 7.29 (4 H, m, H-10 & H-11), 7.41 (2 H, dd, *J*=6.8, 2.3 Hz, H-12), 7.60 (2 H, dd, *J*=6.9, 2.4 Hz, H-9), 8.00 (1 H, t, *J*=7.9 Hz, H-4), 8.30 (2 H, d, *J*=7.8 Hz, H-3).

δ_C (100 MHz, $CDCl_3$) 64.8 (C-7), 127.0 (C-10), 128.1 (C-11), 129.5 (C-12), 129.6 (C-9), 129.8 (C-3), 133.2 (C-8), 133.5 (C-12), 138.2 (C-4), 148.3 (C-2), 164.1 (C-5).

M/S (ESI (MeCN)) m/z: 416.0 (28 %), 418.0 (18), 420.0 (4, $[M+H]^+$), 438.0 (47), 440.0 (33),442.0 (6, $[M+Na]^+$), 853.1 (63), 857.1 (31), 461.2 (1, $[2M+Na]^+$), 871.1 (6, $[2M+MeCN]^+$).

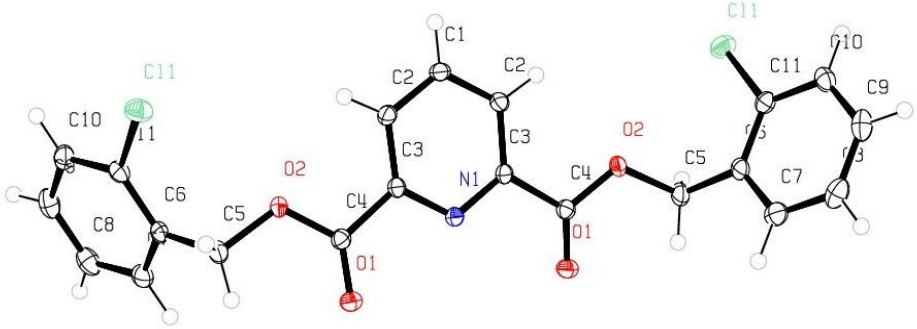

$C_{21}H_{15}Cl_2NO_4$	a = 23.1234 (5) Å	T = 120 K
C2/c	b = 6.2937 (1) Å	λ = 0.71073 Å

V = 1824.14 (6) Å	c = 14.2092 (2) Å	D_c = 1.516 g cm^{-3}
Z = 4	α = 90 (0) °	μ = 0.385 mm^{-1}
R_1 = 3.14 %	β = 118.100 (1) °	0.24 x 0.18 x 0.04 mm^3
$wR_2(F^2)$ = 7.63 %	γ = 90 (0) °	Colourless block

Crystallised from chloroform

7.7.3 *bis*-(2-Bromobenzyl) pyridine-2,6-dicarboxylate (25c)

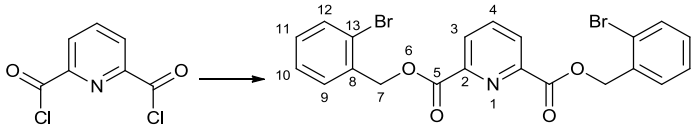

Pyridine-2,6-dicarbonyl dichloride (1.001 g, 4.9 mmol) was stirred in DCM (45 ml). 2-Bromobenzyl alcohol (2.0274 g, 10.8 mmol, 2.2 equiv) was added followed by triethylamine (1.5 ml, 10.8 mmol). On addition of NEt_3, the reaction went yellow, then after a few minutes turned to orange/brown. Having been left overnight the reaction mixture was washed with water (3 × 50 ml) and the organic phase dried over $MgSO_4$. The solvent was removed *in vacuo* to yield a solid (2.6882 g). This product was then recrystallised using DCM and petrol yielding two crops (1.465 g, 59 % and 0.3729 g, 15 %).

MP: 116-118 ˚C

IR (υ_{max}/cm^{-1}) 3053 (C-H aromatic), 2995 (C-H aliphatic), 1731 (C=O), 1474 (C=C aromatic), 1222 (C-Br).

δ_H (400 MHz, $CDCl_3$) 5.55 (4H, s, H-7), 7.22 (2H, td, J=7.8,1.5Hz, H-11), 7.32 (2H, td, J=7.5, 10.Hz, H-10), 7.60 (2H, s, H-9), 7.62 (2H, s, H-12), 8.02 (1H, t, J=7.8Hz, H-4), 8.33 (2H, d, J=7.8Hz, H-3).

δ_C (100 MHz, $CDCl_3$) 67.5 (C-7), 123.7 (C-13), 128.0 (C-10), 128.6 (C-3), 130.2 (C-11), 130.4 (C-9), 133.3 (C-12), 135.4 (C-8), 138.7 (C-4), 148.8 (C-2), 164.6 (C-5).

M/S (ESI (MeCN)) m/z: 504.2 (20 %), 506.3 (37), 508.2 (15, $[M+H]^+$), 526.8 (31) 528.2 (69) 530.0 (32, $[M+Na]^+$), 567.0 (21), 569.2 (43), 571.2 (20, $[M+Na+MeCN]^+$).

HR-M/S: Found 505.9451, Expected 505.9441($C_{21}H_{16}Br_2N_1O_4$)

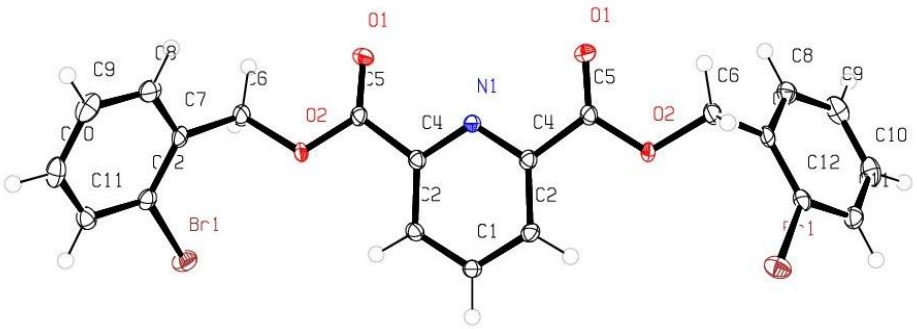

$C_{21}H_{15}Br_2NO_4$	a = 23.3531 (6) Å	T = 120 K
C2/c	b = 6.3509 (1) Å	λ = 0.71073 Å
V = 1889.79 (7) Å	c = 14.3845 (3) Å	D_c = 1.776 g cm^{-3}
Z = 4	α = 90 (0) °	μ = 4.318 mm^{-1}
R_1 = 3.03 %	β = 117.649 (1) °	0.7 x 0.08 x 0.04 mm^3
$wR_2(F^2)$ = 7.64 %	γ = 90 (0) °	Colourless rod

Crystallised from chloroform

7.7.4 *bis*-(3-Fluorobenzyl) pyridine-2,6-dicarboxylate (25d)

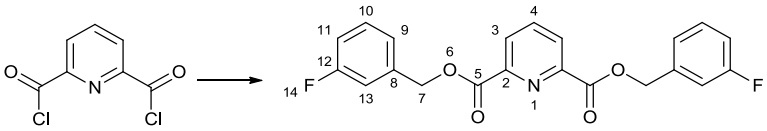

Pyridine-2,6-dicarbonyl dichloride (0.508 g, 2.45 mmol) was dissolved in DCM (30 mL), 3-fluorobenzyl alcohol (0.683 g, 5.39 mmol) was then added, followed by triethylamine (0.75 ml, 5.39 mmol). The reaction mixture was left to stir overnight. The following day the reaction mixture was washed with water (3 x 50 mL) followed by brine (50 mL). The remaining organic residue was dried with magnesium sulphate and then reduced *in vacuo* (1.080 g). This was recrystallised using a mixed solvent system of DCM:petrol 40-60 °C to yield the desired product as a white powder (0.575 g, 60 %).

MP 96-98˚C

IR (υ_{max}/cm^{-1}) 3050 (C-H), 2995 (C-H), 1734 (C=O), 1594 (C=C aromatic), 1537 (C=C aromatic), 1487 (C=C aromatic).

δ_H (400 MHz, $CDCl_3$) 5.46 (4 H, s, H-7), 7.04 (2 H, td, *J*=8.4, 2.5 Hz, H-11), 7.21 (2 H, dt, *J*=9.3, 2.3 Hz, H-13), 7.26 (2 H, d, *J*=7.0 Hz, H-9), 7.35 (2 H, td, *J*=7.8, 6.0 Hz, H-10), 8.01 (1 H, t, *J*=7.9 Hz, H-4), 8.30 (2 H, d, *J*=7.8 Hz, H-3).

δ_C (100 MHz, $CDCl_3$) 66.8 (C-7), 115.1 (d, *J*=15.5 Hz, C-11), 115.3 (d, *J*=13.6 Hz, C-13), 123.8 (d, *J*=2.9 Hz, C-9), 128.1 (C-3), 130.2 (d, *J*=8.7 Hz, C-10), 137.8 (d, *J*=7.8 Hz, C-8), 138.3 (C-4), 148.3 (C-2), 162.8 (d, *J*=246.9 Hz, C-12), 164.2 (C-5).

HR-M/S: Found 384.1034, Expected 384.1042 ($C_{21}H_{16}F_2N_1O_4$)

7.7.5 *bis*-(3-Chlorobenzyl) pyridine-2,6-dicarboxylate (25e)

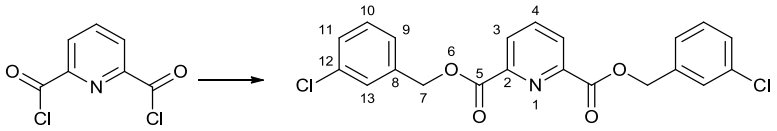

Pyridine-2,6-dicarbonyl dichloride (1.047 g, 4.97 mmol) was dissolved in DCM (30 mL), 3-chlorobenzyl alcohol (1.562 g, 10.93 mmol) was then added, followed by triethylamine (1.5 ml, 10.93 mmol). The reaction mixture was left to stir overnight. The following day the reaction mixture was washed with water (3 x 50 mL) followed by brine (50 mL). The remaining organic residue was dried with magnesium sulphate and then reduced *in vacuo* to yield a solid (2.144 g). This was recrystallised using a mixed solvent system of DCM:petrol 40-60 °C to yield a white powder (1.572 g, 77 %).

MP 72 -74 °C

IR (υ_{max},cm^{-1}) 3064 (C-H aromatic), 2966 (C-H aliphatic), 1707 (C=C), 1575 (C=C aromatic), 750 (C-Cl).

δ_H (400 MHz, $CDCl_3$) 5.44 (4 H, s, H-7), 7.30 - 7.40 (6 H, m, H-9 – H-11), 7.49 (2 H, s, H-13), 8.02 (1 H, t, *J*=7.8 Hz, H-4), 8.30 (2 H, d, *J*=7.8 Hz, H-3).

δ_C (100 MHz, $CDCl_3$) 66.7 (C-7), 126.5 (C-9), 128.1 (C-11), 128.4 (C-13), 128.6 (C-3), 129.9 (C-10), 134.5 (C-12), 137.4 (C-8), 138.3 (C-4), 148.3 (C-2), 164.2 (C-5).

M/S (ESI (MeCN)) m/z: 416.0 (25 %), 417.9 (18), 419.0 (4, $[M+H]^+$), 438.0 (43), 439.9 (28 %) 441.9 (4.6 %) [M+Na] 479.1 (18 %), 481.0 (14), 483.0 (2, $[M+Na+MeCN]^+$), 853.0 (68), 857.1 (45), 861.0 (1, $[2M+Na]^+$).

HR-M/S: Found 416.0447, Expected 416.0451 ($C_{21}H_{15}Cl_2N_1O_4$)

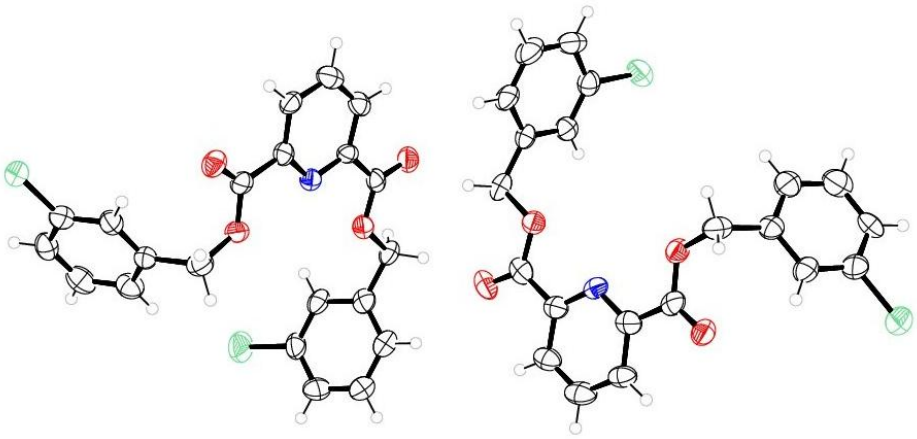

$C_{21}H_{15}Cl_2NO_4$	a = 28.210 (14) Å	T = 120 K
Pca21	b = 4.354 (2) Å	λ = 0.6889 Å
V = 3765 (3) Å	c = 30.657 (15) Å	D_c = 1.468 g cm^{-3}
Z = 8	α = 90 (0) °	μ = 0.373 mm^{-1}
R_1 = 4.53 %	β = 90 (0) °	0.08 x 0.001 x 0.001 mm^3
$wR_2(F^2)$ = 9.49 %	γ = 90 (0) °	Colourless needle

Crystallised from acetonitrile

7.7.6 *bis*-(3-Bromobenzyl) pyridine-2,6-dicarboxylate (25e)

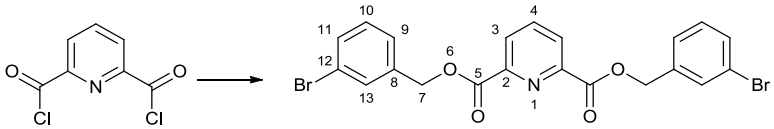

Pyridine-2,6-dicarbonyl dichloride (0.508 g, 2.45 mmol) was dissolved in DCM (30 mL), 3-bromobenzyl alcohol (1.003 g, 5.39 mmol) was then added, followed by triethylamine (0.75 ml, 5.39 mmol). The reaction mixture was left to stir overnight. The following day the reaction mixture was washed with water (3 x 50 mL) followed by brine (50 mL). The remaining organic residue was dried with magnesium sulphate and then reduced *in vacuo* to yield a solid (1.4311 g). This was recrystallised using a mixed solvent system of DCM:petrol 40-60 °C to yield a white powder (0.997 g, 81 %).

MP: 114-116˚C.

IR (υ_{max},cm^{-1}) 3067 (C-H aromatic), 1716 (C=O), 1571 (C=C aromatic), 668 (C-Br).

δ_H (400 MHz, $CDCl_3$) 5.47 (4 H, s, H-7), 7.30 (2 H, d, *J*=8.3 Hz, H-8), 7.47 (2 H, d, *J*=7.5 Hz, H-11), 7.52 (2 H, d, *J*=8.0 Hz, H-9), 7.69 (2 H, s, H-13), 8.06 (1 H, t, *J*=7.5 Hz, H-4), 8.34 (2 H, d, *J*=8.0 Hz, H-3).

δ_C (100 MHz, $CDCl_3$) 66.7 (C-7), 122.6 (C-12), 127.0 (C-9), 128.2 (C-3), 130.2 (C-10), 131.4 (C-13), 131.5 (C-11), 137.6 (C-8), 138.3 (C-4), 148.3 (C-2), 164.2 (C-5).

M/S (ESI (MeCN)) m/z: 526 (10 %), 528.2 (22), 530 (9, $[M+Na]^+$),567.3 (28), 569.3 (60), 571.4 (24, $[M+Na+MeCN]^+$), 1031.3 (70), 1033.4 (98), 1035.5 (60, $[2M+Na]^+$).

HR-M/S: Found 505.9436, Expected 505.9441($C_{21}H_{16}Br_2N_1O_4$)

7.8 Pyridine-2,6-dicarboxamides

7.8.1 N,N'-*bis*[7-Methyl-1,8-napthyridine] pyridine-2,6-dicarboxamide (101)

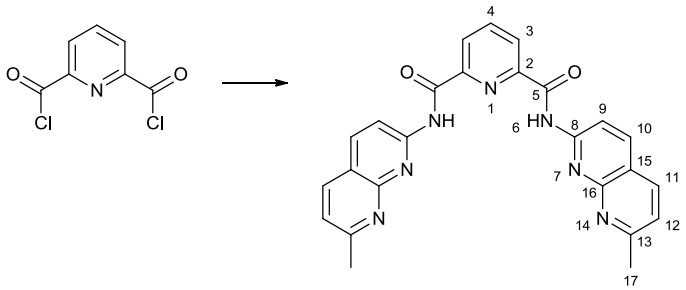

Pyridine dicarbonyl dichloride (353.7 mg, 1.7 mmol) was dissolved in DCM (20 mL). 2-amino-7-methyl-1,8-naphthyridine (500 mg, 3.4 mmol) was added to the reaction mixture followed by triethylamine (0.5 mL). The reaction mixture was left to stir for 18 hours. At this point water was added which formed a brown precipitate which was collected (750 mg), and the remaining reaction mixture was extracted with DCM (3 x 50 mL). The organic phase was dried and the solvent removed *in vacuo* to yield a dark brown solid (255 mg).

By crude NMR the precipitate contained the desired product although seemingly mixed with 2-amino-7-methyl-1,8-naphthyridine and a lot of water, while the organic phase appeared to contain only unreacted material.

After drying the precipitate for 12 hours in a vacuum desiccator, a small sample (100 mg of 400 mg) was taken and trial purification was attempted. The solid was suspended in methanol, and sonicated, the mixture was then centrifuged and the mother liquor removed. This was repeated 3 times and yielded a light brown solid (60 mg) which appeared to be the desired product.

δ_H (400 MHz; DMSO-d6) 2.72 (6 H, s, H-17), 7.46 (2 H, d, J=8.0 Hz, H-12), 8.31 (2 H, d, J=8.3 Hz, H-11), 8.34 (1 H, d, J=7.3 Hz, H-4), 8.47 (2 H, d, J=7.5 Hz, H-3), 8.48 (2 H, d, J=8.8 Hz, H-9), 8.60 (2 H, d, J=8.8 Hz, H-10),12.42 (2 H, br. s., H-6).

δ_c (100 MHz; DMSO-d_6) 25.4 (C-17),114.8 (C-9), 118.5 (C-15), 121.8 (C-12), 126.4 (C-3), 137.0 (C-10), 139.5 (C-11), 139.9 (C-4), 149.1 (C-13), 153.7 (C-8), 154.7 (C-2), 162.9 (C-16), 163.6 (C-5).

MS (ES $^-$): *m/z* 233.1 ($[M+NH_4]^{2+}$, 100 %), 281 ($[M+TFA]^{2+}$, 37 %), 450 ($[M+H]^+$, 33 %), 482 ($[M+H+MeOH]^+$, 12 %).

7.8.2 *N,N'-bis*-(4-Carboxylbenzyl) pyridine-2,7dicarboxamide

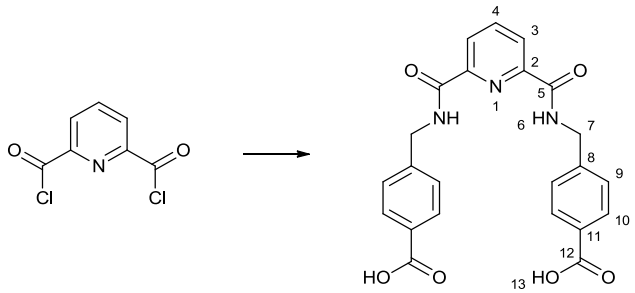

Pyridine-2,6-dicarbonyl dichloride (0.61g, 3 mmol) was dissolved in DCM. 4-aminomethyl benzoic acid (0.911 g, 6 mmol) was then added. This was left for 48 hours. After this time a white solid precipitate was filtered off (1.15 g) this was not the desired product). The filtrate then had the solvent removed *in vacuo* yielding a white solid (0.7 g).

Attempts were made to recrystallise this from methanol, which yielded a small amount of material (35 mg) which was used for X-ray crystallography and other characterisation. Despite the apparent success of the crystallisation, which afforded crystals of sufficient quality for X-ray structural study, the bulk material is not clean by NMR (containing 4-aminomethyl benzoic acid) and the melting point is raised from that seen previously.

MP: >250 °C (lit.[182] 240 - 244 °C)

ν/cm^{-1} 3358 (m, N-H), 3340 (m, N-H), 2917 (br. s, H-Bonded O-H), 1709 (s, C=O), 1681 (s, C=O), 1643 (m, aromatic C=O), 1611 (w, aromatic C-C), 1531 (m, aromatic C-C).

δ_H (300 MHz; DMSO) 4.68 (4H, d, *J* = 6.2 Hz, H-6), 7.44 (4H, d, *J* = 8.2 Hz, H-8), 7.91 (4H, d, *J* = 8.2 Hz, H-9), 8.17 – 8.30 (3H, m, H-1 + H-2), 10.00 (2H, t, *J* = 6.3 Hz).

δ_c (75 MHz; DMSO) 42.1 (C-6), 124.6 (C-2), 127.0 (C-8), 128.9 (C-1), 129.5 (C-9), 139.7 (C-7), 144.4 (C-10), 148.5 (C-3), 163.5 (C-4), 167.1 (C-11).

MS (ES $^-$): *m/z* 432 (100 %, $[M-H]^-$).

MS (ES $^+$): *m/z* 152 (%, $[M+Na]^{3+}$), 158 (16 %, $[M+MeCN]^{3+}$), 255 (12 %, $[M+2K]^+$), 434 (94 %, $[M+H]^+$), 451 (13 %, $[M+NH_4]^+$), 456 (100 %, $[M+Na]^+$), 889 (%, $[2M+Na]^+$).

7.8.3 N,N'-*bis*-(4-(Benzylcarbamate)benzyl)-pyridine-2,6-dicarboxamide (107)

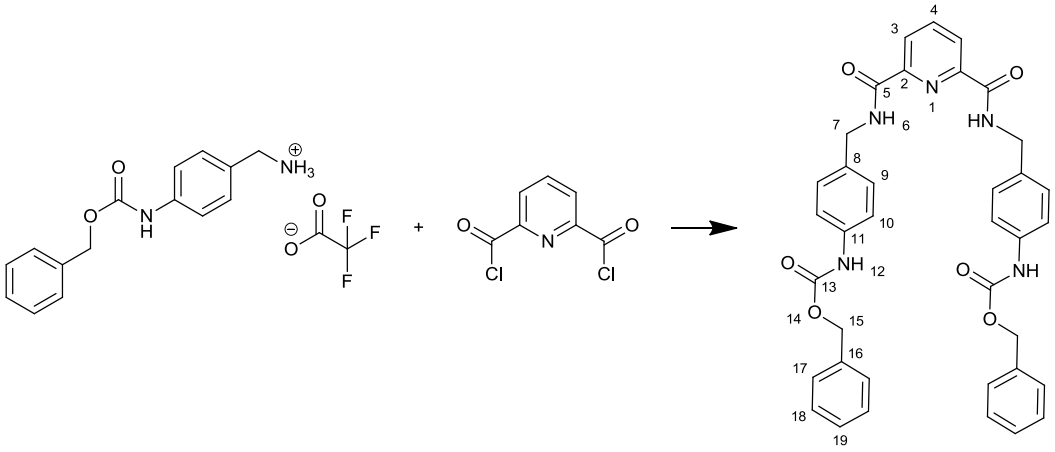

Pyridine-2,6-dicarbonyl dichloride (53.3 mg, 0.27 mmol) was dissolved in DCM (15 mL). benzyl [4-(aminomethyl)phenyl]carbamate trifluoroacetate salt (200 mg, 0.54 mmol) was then added followed by triethylamine (0.3 mL, 1.08 mmol). A white precipitate formed overnight, which was filtered (44.6 mg). The reaction was washed with water (3 x 30 mL) and then dried with magnesium sulphate. The solvent was removed *in vacuo* the give an off white solid (58.6 mg). This was recrystallised from DCM/Petrol to give a white solid (30 mg, 17 %). A further white solid was also recovered (44.6 mg) which appears to be recovered benzyl [4-(aminomethyl)phenyl]carbamate.

MP: 104 – 109 °C (phase transition) & 184 -185 °C

IR (υ_{max}/cm^{-1}) 3289 (N-H), 3032 (C-H), 1703 (C=O), 1655 (C=O), 1600 (C=C), 1522 (C=C).

δ_H (400 MHz, $CDCl_3$) 4.56 (4 H, d, *J*=5.8 Hz, H-7), 5.15 (4 H, s, H-15), 7.13 (2 H, br. s. H-12), 7.17 (4 H, d, *J*=8.5 Hz, H-9), 7.28 - 7.41 (14 H, m, H-2 & H-17 to 19), 8.03 (1 H, t, *J*=7.8 Hz, H-4), 8.09 (2 H, t, *J*=5.7 Hz, H-6), 8.39 (2 H, d, *J*=7.8 Hz, H-3).

δ_C (100 MHz, $CDCl_3$) 43.0 (C-7), 67.1 (C-15), 119.3 (C-10), 125.2 (C-3), 128.2 (C-18), 128.3 (C-19), 128.4 (C-9), 128.6 (C-17), 132.8 (C-8), 135.9 (C-16), 137.2 (C-11), 139.1 (C-4), 148.8 (C-2), 153.6 (C-13), 163.4 (C-5).

HR-M/S: Found 666.2313, Expected 666.2323 ($C_{33}H_{33}N_5O_6Na$)

7.8.4 Diethyl 4-hydroxypyridine-2,6-carboxylate[302] (87)

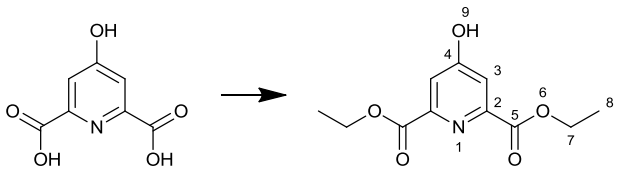

Chelidamic acid (2.0070 g, 10.9mmol) was mixed with ethanol (100 mL), followed by the addition of sulphuric acid (5 drops, concentrated). The reaction mixture was then heated to reflux for 5 h. The reaction was allowed to cool and the solvent was removed *in vacuo*. The white solid was taken up in water (50 mL) however this left a white ppt. This was filtered off and retained (0.1015 g, 5 % recovered starting material). The filtrate was then extracted with ethyl acetate (3 x 50 mL) and DCM (3 x 50 mL) and the combined organic extracts were dried with magnesium sulphate and reduced *in vacuo* to yield a white solid (1.7760 g, 68 %).

MP: 105 – 110 °C (lit 110-112 °C)[302]

ν/cm^{-1} 2983 (C-H), 2905 (C-H), 2681 (C-H), 1738 (C=O), 1722 (C=O), 1602 (aromatic C-C), 1568 (aromatic C-N), 1457 (aromatic C-C).

δ_H (300 Mhz, $CDCl_3$) 1.34 (6H, br t, H-8), 4.38 (4H, d, *J*=5.7 Hz, H-7), 7.48 (2H, br s, H-3), 9.24 (1H, br s, H-9).

δ_C (75 Mhz, $CDCl_3$) 14.1 (C-8), 63.1 (C-7), 114.4 (C-3), 118.6 (C-4), 150.1 (C-2), 162.7 (C-5).

7.8.5 Tetraethyl-4,4`-[butane-1,4-diyl-*bis*-(oxy)]dipyridine-2,6-dicarboxylate[275] (89a)

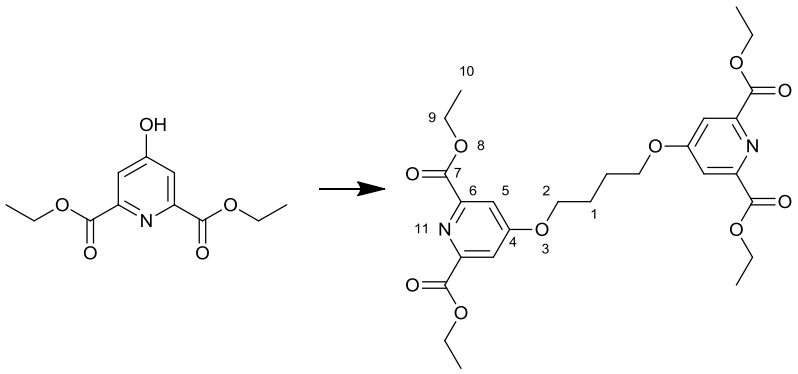

Diethyl 4-hydroxypyridine-2,6-carboxylate (509.3 g, 2.09 mmol) was added to N,N'-dimethylformamide (5 mL) followed by potassium carbonate (295.9 mg, 2.14 mmol). This mixture was left to stir for 1 h with nitrogen bubbling through it. 1,4-Dibromobutane (0.124 mL, 1.04 mmol) was then added drop-wise before the reaction mixture was heated to 80 °C. After 18h further potassium carbonate (295.9 g, 2.14 mmol) was added. After a further 24 h the reaction was reduced to dryness *in vacuo* and was then taken up in water (50 mL) and DCM (100 mL). The aqueous was then washed with additional water (3 x 50 mL). The combined organics were then washed with acetic acid solution (100 ml, 1 % solution). The organic was then dried with sodium sulphate and reduced *in vacuo* to give a slightly yellow oil (0.790 g). Crude NMR showed this to still contain a large proportion of N,N'-dimethylformamide which was removed using a drying pistol *in vacuo* to give a slightly off white solid (497 mg, 93 %).

MP: 125 – 130 °C

ν/cm^{-1} 2986 (C-H), 2954 (C-H), 2903 (C-H), 1707 (C=O), 1596 (aromatic C-C), 1567 (aromatic C-N), 1472 (aromatic C-C).

δ_H (300 MHz, $CDCl_3$) 1.45 (12H, t, *J*=7.1 Hz, H-10), 2.08 (4H, br s, H-1), 4.10 – 4.33 (4H, m, H-2), 4.47 (8H, q, *J*=7.0 Hz, H-9), 7.78 (4H, s, H-5).

δ_C (75 MHz, $CDCl_3$) 14.2 (C-10), 25.4 (C-1), 62.4 (C-9), 68.2 (C-2), 114.2 (C-5),150.2 (C-6), 164.7 (C-4), 166.7 (C-7).

M/S (ESI) m/z 362 (29 %, $[2M+Na+2H]^{3+}$), 533 (33, $[M+H]^+$), 555 (100, $[M+Na]^+$), 1087 (5, $[2M+Na]^+$).

7.8.6 4-Hydroxy-N,N'-*bis*-(2-pyridylmethyl)-2,6-pyridine dicarboxamide (96)

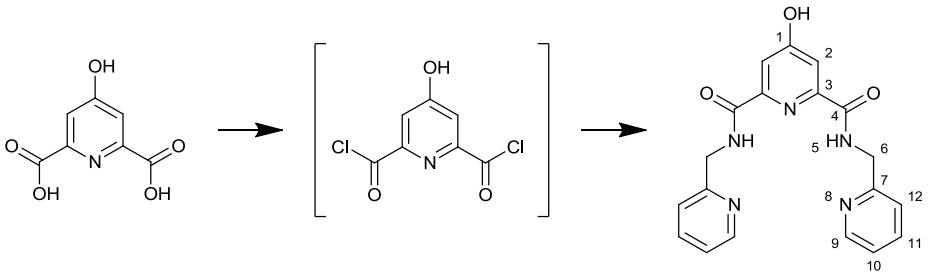

Chelidamic acid (1.00 g, 5.46 mmol) was suspended in DCM (150 mL). Oxalyl chloride was added drop-wise followed by dimethylformamide (3 drops). The reaction was left to stir until gas evolution had ceased. At this point the residual solid was filtered off (recovered starting material) and the solvent was removed from the filtrate *in vacuo.* The resulting solid was then placed on the high vacuum drying line for an hour before being redissovled in DCM. 2-(Aminomethyl)pyridine (1.139 g, 1.194 mL, 10.5 mmol) was then added to the solution colourless solution causing it to turn yellow, followed by triethylamine (1.73 mL). The yellow reaction mixture was then left overnight by which time a white precipitate had formed. The white precipitate was filtered and proved to be the desired product (0.7258 g, 37 %). The filtrate had the solvent removed in vacuo and was shown to be a mixture of 4-chloro-N,N'-*bis*-(2-pyridylmethyl)-2,6-pyridine dicarboxamides and N,N'-*bis*-(2-pyridylmethyl)ethane diamide.

MP 177 – 178 °C

IR (υ_{max}/ cm^{-1}): 3371 (O-H), 2915 (C-H), 1680 (C=O), 1668 (C=O), 1597 (aromatic C=C), 1567 (aromatic C=N), 1521 (aromatic C=C), 1481 (aromatic C=C).

δ_H (300 MHz, $CDCl_3$) 4.70 (4H, s, H-6), 7.18 (2H, ddd, *J*=7.5, 5.3, 1.1 Hz, H-10), 7.37 (2H, d, *J*=7.5 Hz, H-12), 7.62 (2H, s, H-2), 7.66 (2H, td, *J*=7.5, 1.9 Hz, H-11), 8.43 (2H, dd, *J*=4.9, 1.1 Hz, H-9).

δ_C (100 MHz, $CDCl_3$) 44.4 (C-6), 112.3 (C-2), 122.2 (C-10), 122.5 (C-12), 137.3 (C-11), 148.6 (C-9), 157.3 (C-3), 164.6 (C-7), 164.7 (C-1), 166.9 (C-4).

M/S (ESI (MeCN)) m/z: 364 (18 %, $[M+H]^+$), 386 (100, $[M+Na]^+$), 749 (54, $[2M+Na]^+$).

7.8.7 4,4'-[1,4-Butanediyl-*bis*-(oxy)]-*bis*-(N,N'-*bis*-(2-pyridylmethyl)-2,6-pyridine dicarboxamide) (95a)

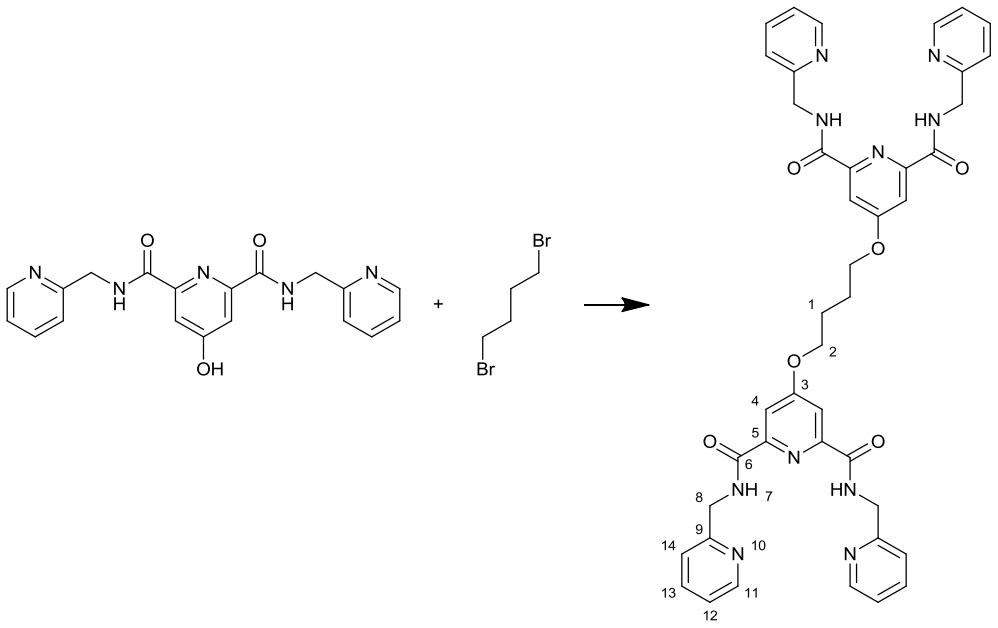

4-hydroxy-N,N'-*bis*-(2-pyridylmethyl)-2,6-pyridine dicarboxamide (250 mg , 0.688 mmol) was dissolved in DMF (5 mL). Potassium carbonate (142 mg, 1.028 mmol) was added and then the reaction mixture was left stirring with nitrogen bubbling through it for 30 min. 1,4-Dibromobutane (74.3 mg, was then added and the reaction mixture was heated to 75 °C and was left stirring overnight. The DMF was then removed *in vacuo* to give a white solid which was then taken up in DCM (100 mL) and then washed with water (3 x 50 mL). The organic mixture was then reduced to dryness *in vacuo* to give a white solid (286.3 mg, 53 %).

MP 205 – 208 °C

IR (υ_{max}/ cm^{-1}): 3382 (N-H), 1671 (C=O), 1599 (aromatic C=C), 1568 (aromatic C=N), 1531 (aromatic C=C), 1500 (aromatic C=C).

δ_H (400 MHz, $CDCl_3$) 1.99 (4H, br. s., H-1), 4.17 (4H, br. s., H-2), 4.70 (8H, s, H-8), 7.18 (4H, dd, *J*=7.5, 5.0 Hz, H-12), 7.38 (4H, d, *J*=7.8 Hz, H-14), 7.65 (4H, td, *J*=7.7, 1.6 Hz, H-13), 7.75 (4H, s, H-4), 8.43 (4H, dd, *J*=4.8, 0.8 Hz, H-11), 9.56 (4H, t, *J*=6.1 Hz, H-7).

δ_C (100 MHz, $CDCl_3$) 25.8 (C-1), 45.1 (C-8), 68.6 (C-2), 111.5 (C-4), 122.9 (C-12), 123.0 (C-14), 137.9 (C-13), 149.2 (C-11), 150.9 (C-9), 157.9 (C-3), 164.7 (C-2), 168.1 (C-6).

M/S (ESI (MeCN)) m/z:781 (15 %, $[M+H]^+$), 803 (100, $[M+Na]^+$).

HR-M/S: Found 781.3222, Expected 781.3205 ($C_{42}H_{41}N_{10}O_6$)

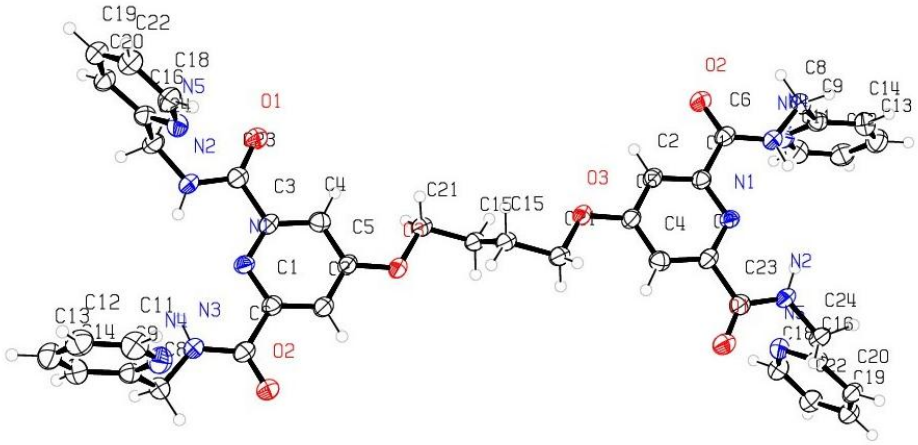

$C_{42}H_{40}N_{10}O_6$	a = 4.864 (2) Å	T = 120 K
P21/n	b = 33.927 (17) Å	λ = 0.6889 Å
V = 1825.6 (15) Å	c = 11.083 (6) Å	D_c = 1.420 g cm^{-3}
Z = 2	α = 90 (0) °	μ = 0.098 mm^{-1}
R_1 = 6.01 %	β = 93.442 (6) °	0.20 x 0.01 x 0.01 mm^3
$wR_2(F^2)$ = 14.37 %	γ = 90 (0) °	Colourless needle
	Crystallised from methanol	

7.8.8 4,4'-[1,4-Phenylene-*bis*-(methyleneoxy)]-*bis*-[N,N'-*bis*-(2-pyridylmethyl)-2,6-pyridine dicarboxamide]) (95b)

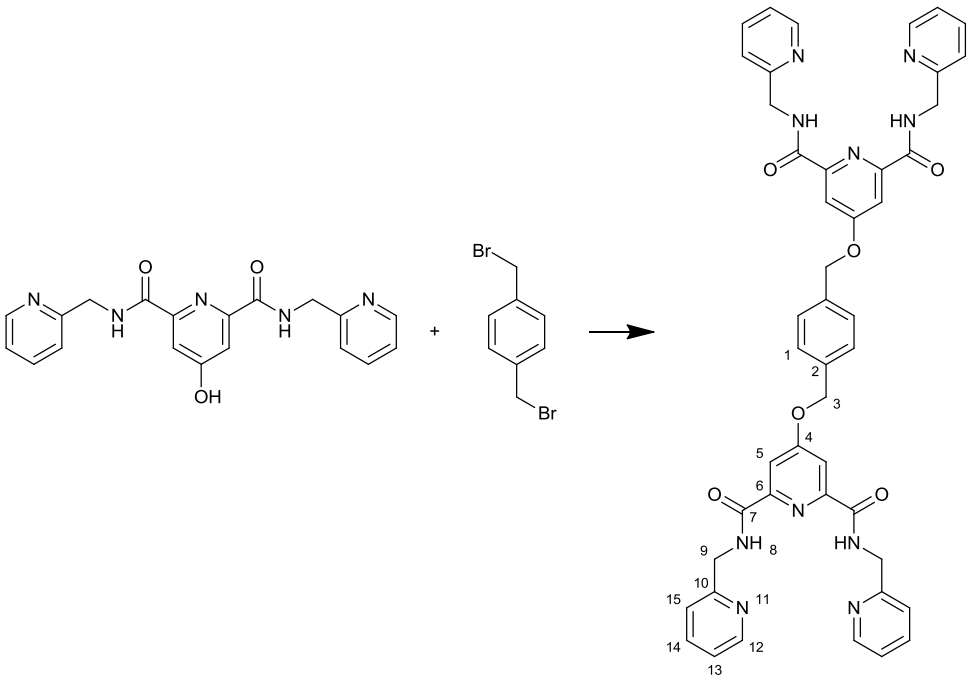

4-hydroxy-N,N'-*bis*-(2-pyridylmethyl)-2,6-pyridine dicarboxamide (250 mg , 0.688 mmol) was dissolved in DMF (5 mL). Potassium carbonate (142 mg, 1.028 mmol) was added and then the reaction mixture was left stirring with nitrogen bubbling through it for 30 min. α,α'-Dibromo-p-xylene (90.5 mg, 0.343 mmol) was then added and the reaction mixture was heated to 75 °C and was left stirring overnight. The DMF was then removed *in vacuo* to give a white solid which was then taken up in DCM (100 mL) and then washed with water (3 x 50 mL). The organic mixture was then reduced to dryness *in vacuo* to give a white solid (312.2 mg, 55 %).

MP 255 – 260 °C

IR (υ_{max}/ cm^{-1}): 3381 (N-H), 3270 (C-H), 1663 (C=O), 1568 (aromatic C=N), 1519 (aromatic C=C), 1479 (aromatic C=C).

δ_H (400 MHz, $CDCl_3$) 4.66 (8H, s, H-9), 5.35 (4H, s, H-3), 7.22 (4H, dd ,J=6.8, 5.3 Hz, H-13), 7.32 (4H, d, J=7.8 Hz, H-15), 7.51 (4H, s, H-1), 7.70 (4H, td, J=7.7, 1.8 Hz, H-14), 7.80 (4H, s, H-5), 8.48 (3H, d, J=4.5 Hz, H-12), 9.93 (1H, t, J=6.3 Hz, H-8).

δ_C (100 MHz, $CDCl_3$) 44.2 (C-9), 69.5 (C-3), 110.6 (C-5), 120.9 (C-12), 121.9 (C-15), 127.6 (C-1), 135.4 (C-2), 136.5 (C-14), 148.6 (C-12), 150.5 (C-6), 158.2 (C-4), 163.1 (C-10), 166.8 (C-7).

M/S (ESI (MeCN)) m/z: 829 (14 %, $[M+H]^+$), 851(83, $[M+Na]^+$).

HR-M/S: Found 829.3176, Expected 829.3205 ($C_{46}H_{41}N_{10}O_6$)

7.8.9 Diethyl-4'[-(8-bromooctyl)biphenyl-4-carbonitrile] pyridine-2,6-dicarboxylate (99)

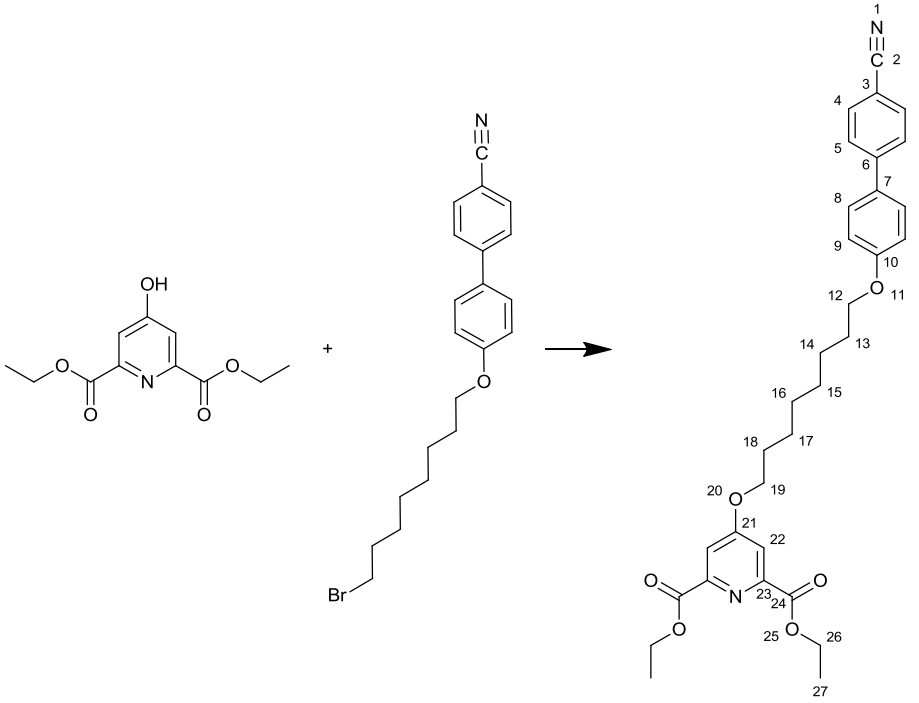

Diethyl 4-hydroxypyridine-2,6-carboxylate (205 mg, 0.836 mmol) was added to N,N'-dimethylformamide (5 mL) followed by potassium carbonate (0.230 g, 1.67 mmol). This mixture was left to stir for 1 h with nitrogen bubbling through it. 4'-(8-bromooctyl)biphenyl-4-carbonitrile[278] (304.6 mg, 0.836 mmol) was then added in portions before the reaction mixture was heated to 80 °C. After 24 h the reaction was cooled and reduced to dryness *in vacuo* and was then taken up in water (50 mL) and DCM (100 mL). The aqueous was then washed with additional water (3 x 50 mL). The combined organics were then washed with acetic acid solution (100 ml, 1 % solution). The organic was then dried with sodium sulphate and reduced *in vacuo* to give an orange oil (491.7 mg). Crude NMR showed this to still contain a large proportion of N,N'-dimethylformamide which was removed using a drying pistol *in vacuo* to give an oil which appears to solidify when left at room temperature for 3 weeks (367 mg, 80 %).

δ_H (300 MHz, $CDCl_3$) 1.37 - 1.57 (14H, m, , H-14,15,16,17,27), 1.84 (4H, q, *J*=6.9 Hz, H-13,18), 4.02 (2H, t, *J*=6.4 Hz, H-12), 4.14 (2H, t, *J*=6.4 Hz, H-19), 4.47 (4H, q, *J*=7.3

Hz, H-26), 6.99 (2H, d, *J*=8.8 Hz, H-9), 7.53 (2H, d, *J*=8.8 Hz, H-8), 7.60 - 7.66 (2H, m, *J*=8.4 Hz, H-5), 7.69 (2H, d, *J*=8.8 Hz, H-4), 7.77 (2 H, s, H-16)

M/S (ESI) m/z 545 (3 %, $[M+H]^+$), 567 (38, $[M+H]^+$),1112 (8, $[2M+Na]^+$)

HR-M/S: Found 545.2628, Expected 545.2646 ($C_{32}H_{37}N_2O_6$)

8 References

1. D. J. Cram, *Angew. Chem., Int. Ed.*, 1988, **27**, 1009-1020.
2. J.-M. Lehn, *Angew. Chem., Int. Ed.*, 1988, **27**, 89-112.
3. C. J. Pedersen, *Angew. Chem., Int. Ed.*, 1988, **27**, 1021-1027.
4. C. J. Pedersen, *J. Am. Chem. Soc.*, 1967, **89**, 7017-7036.
5. B. Dietrich, J.-M. Lehn and J. P. Sauvage, *Tetrahedron Lett.*, 1969, **10**, 2885-2888.
6. D. J. Cram, S. Karbach, Y. H. Kim, L. Baczynskyj and G. W. Kallemeyn, *J. Am. Chem. Soc.*, 1985, **107**, 2575-2576.
7. D. Philp and J. F. Stoddart, *Angew. Chem., Int. Ed.*, 1996, **35**, 1154-1196.
8. J. F. Stoddart, K. C. F. Leung, M. Liong, C. D. Pentecost and J. I. Zink, *Org. Lett.*, 2006, **8**, 3363-3366.
9. J. D. Badjic, C. M. Ronconi, J. F. Stoddart, V. Balzani, S. Silvi and A. Credi, *J. Am. Chem. Soc.*, 2006, **128**, 1489-1499.
10. J. D. Badjic, V. Balzani, A. Credi, S. Silvi and J. F. Stoddart, *Science*, 2004, **303**, 1845-1849.
11. J. Kofoed and J. L. Reymond, *Curr. Opin. Chem. Biol.*, 2005, **9**, 656-664.
12. L. Liu and R. Breslow, *J. Am. Chem. Soc.*, 2003, **125**, 12110-12111.
13. J. M. Yan and R. Breslow, *Tetrahedron Lett.*, 2000, **41**, 2059-2062.
14. S. D. Dong and R. Breslow, *Tetrahedron Lett.*, 1998, **39**, 9343-9346.
15. G. W. Bates, P. A. Gale and M. E. Light, *Chem. Commun.*, 2007, 2121-2123.
16. W. Dehaen, P. A. Gale, S. E. Garcia-Garrido, M. Kostermans and M. E. Light, *New J. Chem.*, 2007, **31**, 691-696.
17. P. A. Gale and R. Quesada, *Coord. Chem. Rev.*, 2006, **250**, 3219-3244.
18. P. A. Gale, *Chem. Commun.*, 2005, 3761-3772.
19. G. R. Desiraju, *Acc. Chem. Res.*, 2002, **35**, 565-573.
20. S. J. Cantrill, A. R. Pease and J. F. Stoddart, *Dalton Trans.*, 2000, 3715-3734.
21. D. Braga, F. Grepioni and G. R. Desiraju, *Chem. Rev.*, 1998, **98**, 1375-1405.
22. G. R. Desiraju, *Angew. Chem., Int. Ed.*, 1995, **34**, 2311-2327.
23. T. Park, E. M. Todd, S. Nakashima and S. C. Zimmerman, *J. Am. Chem. Soc.*, 2005, **127**, 18133-18142.
24. J.-M. Lehn, M. Mascal, A. Decian and J. Fischer, *J. Chem. Soc., Chem. Commun.*, 1990, 479-481.
25. J. D. Dunitz and A. Gavezzotti, *Angew. Chem., Int. Ed.*, 2005, **44**, 1766-1787.
26. S. C. Zimmerman and P. S. Corbin, in *Structure & Bonding*, ed. D. M. P. Mingos, Springer, Heidelberg, 2000, vol. 96, pp. 63-94.
27. S. Goswami, K. Ghosh and R. Mukherjee, *Tetrahedron*, 2001, **57**, 4987-4993.
28. A. Robertson, A. J. Sinclair and D. Philp, *Chem. Soc. Rev.*, 2000, **29**, 141-152.
29. S. J. Howell, N. Spencer and D. Philp, *Tetrahedron*, 2001, **57**, 4945-4954.
30. T. Tjivikua, P. Ballester and J. Rebek, *J. Am. Chem. Soc.*, 1990, **112**, 1249-1250.
31. J. D. Watson and F. H. C. Crick, *Nature*, 1953, **171**, 737-738.
32. M. F. Perutz, M. G. Rossmann, A. F. Cullis, H. Muirhead, G. Will and A. C. T. North, *Nature*, 1960, **185**, 416-422.
33. J. C. Skou, *Biochim. Biophys. Acta.*, 1957, **23**, 394-401.

34. H. Noji, R. Yasuda, M. Yoshida and K. Kinosita, *Nature*, 1997, **386**, 299-302.
35. R. D. Vale and R. A. Milligan, *Science*, 2000, **288**, 88-95.
36. W. O. Hancock, *Curr. Biol.*, 2008, **18**, R715-R717.
37. K. H. Wong, K. Yagi and J. Smid, *J. Membr. Biol.*, 1974, **18**, 379-397.
38. S. Shinkai, T. Nakaji, T. Ogawa, K. Shigematsu and O. Manabe, *J. Am. Chem. Soc.*, 1981, **103**, 111-115.
39. A. G. Gaikwad, H. Noguchi and M. Yoshio, *Sep. Sci. Technol.*, 1991, **26**, 853 - 867.
40. J. Berna, D. A. Leigh, M. Lubomska, S. M. Mendoza, E. M. Perez, P. Rudolf, G. Teobaldi and F. Zerbetto, *Nat. Mater.*, 2005, **4**, 704-710.
41. J. V. Hernandez, E. R. Kay and D. A. Leigh, *Science*, 2004, **306**, 1532-1537.
42. M. von Delius, E. M. Geertsema and D. A. Leigh, *Nat. Chem.*, 2010, **2**, 96-101.
43. P. L. Anelli, M. Asakawa, P. R. Ashton, R. A. Bissell, G. Clavier, R. Gorski, A. E. Kaifer, S. J. Langford, G. Mattersteig, S. Menzer, D. Philp, A. M. Z. Slawin, N. Spencer, J. F. Stoddart, M. S. Tolley and D. J. Williams, *Chem. Eur. J.*, 1997, **3**, 1113-1135.
44. R. Ballardini, V. Balzani, M. T. Gandolfi, L. Prodi, M. Venturi, D. Philp, H. G. Ricketts and J. F. Stoddart, *Angew. Chem., Int. Ed.*, 1993, **32**, 1301-1303.
45. A. de la Escosura, R. J. M. Nolte and J. J. L. M. Cornelissen, *J. Mater. Chem.*, 2009, **19**, 2274-2278.
46. E. Fischer, *Ber. Dtsch. Chem. Ges.*, 1894, **27**, 2985-2993.
47. P. D. Beer, P. A. Gale and D. K. Smith, *Supramolecular Chemistry*, Oxford University Press, Oxford, 1999.
48. G. R. Desiraju, *Angew. Chem., Int. Ed.*, 2007, **46**, 8342-8356.
49. A. Gavezzotti, *Acc. Chem. Res.*, 1994, **27**, 309-314.
50. J. Maddox, *Nature*, 1988, **335**, 201-201.
51. J. D. Dunitz, *Chem. Commun.*, 2003, 545-548.
52. G. R. Desiraju, *Nat. Mater.*, 2002, **1**, 77-79.
53. K. Sanderson, *Nature*, 2007, **450**, 771.
54. M. A. Neumann, F. J. J. Leusen and J. Kendrick, *Angew. Chem., Int. Ed.*, 2008, **47**, 2427-2430.
55. S. M. Woodley and R. Catlow, *Nat. Mater.*, 2008, **7**, 937-946.
56. G. P. Stahly, *Cryst. Growth Des.*, 2007, **7**, 1007-1026.
57. S. S. L. Price, *Acc. Chem. Res.*, 2009, **42**, 117-126.
58. H. G. Brittain, *J. Pharm. Sci.*, 2008, **97**, 3611-3636.
59. H. G. Brittain, *J. Pharm. Sci.*, 2009, **98**, 1617-1642.
60. H. G. Brittain, *J. Pharm. Sci.*, 2009, **99**, 3648 - 3664.
61. H. G. Brittain, *J. Pharm. Sci.*, 2007, **96**, 705-728.
62. J. Bauer, S. Spanton, R. Henry, J. Quick, W. Dziki, W. Porter and J. Morris, *Pharm. Res.*, 2001, **18**, 859-866.
63. W. Cabri, P. Ghetti, G. Pozzi, M. Alpegiani, A. S. A and S. Rivoltana, *Org. Process Res. Dev.*, 2007, **11**, 64-72.
64. P. Vishweshwar, J. A. McMahon, M. Oliveira, M. L. Peterson and M. J. Zaworotko, *J. Am. Chem. Soc.*, 2005, **127**, 16802-16803.
65. A. D. Bond, R. Boese and G. R. Desiraju, *Angew. Chem., Int. Ed.*, 2007, **46**, 615-617.

66. A. D. Bond, R. Boese and G. R. O. Desiraju, *Angew. Chem., Int. Ed.*, 2007, **46**, 618-622.
67. L. Yu, G. A. Stephenson, C. A. Mitchell, C. A. Bunnell, S. V. Snorek, J. J. Bowyer, T. B. Borchardt, J. G. Stowell and S. R. Byrn, *J. Am. Chem. Soc.*, 2000, **122**, 585-591.
68. S. Chen, I. a. Guzei and L. Yu, *J. Am. Chem. Soc.*, 2005, **127**, 9881-9885.
69. K. M. Lutker, Z. P. Tolstyka and A. J. Matzger, *Cryst. Growth Des.*, 2008, **8**, 136-139.
70. T. L. Cottrell, *The Strengths of Chemical Bonds*, Butterworths, London, 1958.
71. S. W. Benson, *J. Chem. Educ.*, 1965, **42**, 502-518.
72. G. N. Lewis, *J. Am. Chem. Soc.*, 1916, **38**, 762-785.
73. L. Pauling, *J. Am. Chem. Soc.*, 1931, **53**, 1367-1400.
74. L. Pauling, *The Nature of the Chemical Bond and the Structure of Molecules and Crystals : An Introduction to Modern Structural Chemistry* Cornell University Press, Ithaca, New York, USA, 1960.
75. M. G. Fisher, P. A. Gale, J. R. Hiscock, M. B. Hursthouse, M. E. Light, F. P. Schmidtchen and C. C. Tong, *Chem. Commun.*, 2009, 3017-3019.
76. L. A. Baumes, M. Buaki Sogo, P. Montes-Navajas, A. Corma and H. Garcia, *Chem. Eur. J.*, 2010, **16**, 4489-4495.
77. L. A. Baumes, M. Buaki Sogo, P. Montes-Navajas, A. Corma and H. Garcia, *Tetrahedron Lett.*, 2009, **50**, 7001-7004.
78. T. Steiner and G. R. Desiraju, *Chem. Commun.*, 1998, 891-892.
79. K. Autumn, M. Sitti, Y. A. Liang, A. M. Peattie, W. R. Hansen, S. Sponberg, T. W. Kenny, R. Fearing, J. N. Israelachvili and R. J. Full, *Proc. Natl. Acad. Sci. U. S. A.*, 2002, **99**, 12252-12256.
80. G. A. Jeffrey, *An Introduction to Hydrogen Bonding*, Oxford Univ. Press, New York, 1997.
81. T. Steiner, *Angew. Chem., Int. Ed.*, 2002, **41**, 48-76.
82. M. L. Huggins, *Angew. Chem., Int. Ed.*, 1971, **10**, 147-152.
83. M. L. Huggins, *J. Org. Chem.*, 1936, **1**, 407-456.
84. M. L. Huggins, *J. Phys. Chem.*, 1936, **40**, 723-731.
85. G. C. Pimental and A. L. McClellan, *The Hydrogen Bond*, University of California, Berkley, and California Research Corporation, Richmond, California, 1960.
86. S. N. Vinogradov, *Hydrogen Bonding*, Van Nostrand Reinhold, New York, 1971.
87. E. Arunan, G. R. Desiraju, R. A. Klein, J. Sadlej, S. Scheiner, I. Alkorta, D. C. Clary, R. H. Crabtree, J. J. Dannenberg, P. Hobza, H. G. Kjaergaard, A. C. Legon, B. Mennucci and D. J. Nesbitt, unpublished work.
88. W. C. Hamilton and J. A. Ibers, *Hydrogen Bonding in Solids*, Benjamin, New York, 1968.
89. G. R. Desiraju, *Acc. Chem. Res.*, 1991, **24**, 290-296.
90. J.-A. van den Berg and K. R. Seddon, *Cryst. Growth Des.*, 2003, **3**, 643-661.
91. J. Kroon and J. A. Kanters, *Nature*, 1974, **248**, 667-669.
92. J. Sartorius and H.-J. Schneider, *Chem. Eur. J.*, 1996, **2**, 1446-1452.
93. J. Pranata, S. G. Wierschke and W. L. Jorgensen, *J. Am. Chem. Soc.*, 1991, **113**, 2810-2819.

94. W. L. Jorgensen and J. Pranata, *J. Am. Chem. Soc.*, 1990, **112**, 2008-2010.
95. S. I. Troyanov, I. V. Morozov and E. Kemnitz, *Z. Anorg. Allg. Chem.*, 2005, **631**, 1651-1654.
96. E. Bartoszak, M. Jaskolski, E. Grech, T. Gustafsson and I. Olovsson, *Acta Crystallogr., Sect. B: Struct. Sci.*, 1994, **50**, 358-363.
97. P. V. Hobbs, *Ice Physics*, Clarendon, Oxford, 1974.
98. C. Lobban, J. L. Finney and W. F. Kuhs, *Nature*, 1998, **391**, 268-270.
99. R. D. Green, *Hydrogen Bonding by C---H Groups*, Wiley, New York, 1974.
100. A. C. Legon and D. J. Millen, *J. Am. Chem. Soc.*, 1987, **109**, 356-358.
101. J. E. Del Bene and H. D. Mettee, *J. Phys. Chem.*, 1993, **97**, 9650-9656.
102. R. D. Hunt and L. Andrews, *J. Phys. Chem.*, 1992, **96**, 6945-6949.
103. D. J. Sutor, *Nature*, 1962, **195**, 68-69.
104. D. J. Sutor, *J. Chem. Soc.*, 1963, **1963**, 1105-1110.
105. J. Donohue, in *Structural Chemistry and Molecular Biology*, eds. A. Rich and N. Davidson, Freeman, San Francisco, California, 1968, pp. 443-465.
106. J. D. Watson, *The Double Helix*, The New American Library Inc., New York, 1968.
107. T. Steiner and W. Saenger, *J. Am. Chem. Soc.*, 1992, **114**, 10146-10154.
108. G. Desiraju, *The Crystal as a Supramolecular Entity*, Wiley, Chichester; New York, 1996.
109. F. A. Cotton, L. M. Daniels, G. T. Jordan and C. A. Murillo, *Chem. Commun.*, 1997, 1673-1674.
110. S. Grimme, *Angew. Chem., Int. Ed.*, 2008, **47**, 3430-3434.
111. S. Burley and G. Petsko, *Science*, 1985, **229**, 23-28.
112. M. Brandl, M. S. Weiss, A. Jabs, J. Sühnel and R. Hilgenfeld, *J. Mol. Biol.*, 2001, **307**, 357-377.
113. M. Nishio, M. Hirota and Y. Umezawa, *The CH-[pi] Interaction : Evidence, Nature, and Consequences*, Wiley, New York, 1998.
114. G. R. Desiraju and T. Steiner, *The Weak Hydrogen Bond in Structural Chemistry and Biology*, Oxford Univ. Press, Oxford, United Kingdom, 1999.
115. Y. Umezawa, S. Tsuboyama, K. Honda, J. Uzawa and M. Nishio, *Bull. Chem. Soc. Jpn.*, 1998, **71**, 1207-1213.
116. O. Takahashi, Y. Kohno and M. Nishio, *Chem. Rev.*, 2010, **110**, 6049-6076.
117. M. Nishio, Y. Umezawa, M. Hirota and Y. Takeuchi, *Tetrahedron*, 1995, **51**, 8665-8701.
118. M. Nishio, *Tetrahedron*, 1989, **45**, 7201-7245.
119. H. S. Rzepa, M. L. Webb, A. M. Z. Slawin and D. J. Williams, *J. Chem. Soc., Chem. Commun.*, 1991, 765-768.
120. M. Tamres, *J. Am. Chem. Soc.*, 1952, **74**, 3375-3378.
121. M. Nishio, Y. Umezawa, K. Honda, S. Tsuboyama and H. Suezawa, *CrystEngComm*, 2009, **11**, 1757-1788.
122. M. Nishio, *CrystEngComm*, 2004, **6**, 130-158.
123. J. Beintema, *Acta Crystallogr.*, 1965, **18**, 647-654.
124. G. Ferraris, K. D. Bartle, J. Yerkess and D. W. Jones, *J. Chem. Soc., Perkin Trans. 2*, 1972, 1628-1632.
125. C. C. Wilson, *Chem. Commun.*, 1997, 1281-1282.
126. T. Dahl, *Acta. Chem. Scand.*, 1975, 170.

127. P. Mignon, S. Loverix, J. Steyaert and P. Geerlings, *Nucleic Acids Res.*, 2005, **33**, 1779-1789.
128. C. A. Hunter and J. K. M. Sanders, *J. Am. Chem. Soc.*, 1990, **112**, 5525-5534.
129. C. A. Hunter, *Chem. Soc. Rev.*, 1994, **23**, 101–109.
130. C. A. Hunter, K. R. Lawson, J. Perkins and C. J. Urch, *J. Chem. Soc., Perkin Trans. 2*, 2001, 651-669.
131. C. A. Hunter, *Angew. Chem., Int. Ed.*, 2004, **43**, 5310-5324.
132. W. B. Motherwell, J. Moïse, A. E. Aliev, M. Nic, S. J. Coles, P. N. Horton, M. B. Hursthouse, G. Chessari, C. A. Hunter and J. G. Vinter, *Angew. Chem., Int. Ed.*, 2007, **46**, 7823-7826.
133. S. L. Cockroft, J. Perkins, C. Zonta, H. Adams, S. E. Spey, C. M. R. Low, J. G. Vinter, K. R. Lawson, C. J. Urch and C. A. Hunter, *Org. Biomol. Chem.*, 2007, **5**, 1062-1080.
134. R. Cabot, C. A. Hunter and L. M. Varley, *Org. Biomol. Chem.*, 2010, **8**, 1455-1462.
135. S. L. Cockroft and C. A. Hunter, *Chem. Commun.*, 2006, 3806-3808.
136. J. L. Cook, C. a. Hunter, C. M. R. Low, A. Perez-Velasco and J. G. Vinter, *Angew. Chem., Int. Ed.*, 2007, **46**, 3706-3709.
137. H. L. Anderson, C. A. Hunter and J. K. M. Sanders, *J. Chem. Soc., Chem. Commun.*, 1989, 226.
138. C. W. Chen and H. W. Whitlock, *J. Am. Chem. Soc.*, 1978, **100**, 4921-4922.
139. S. C. Zimmerman, C. M. VanZyl and G. S. Hamilton, *J. Am. Chem. Soc.*, 1989, **111**, 1373-1381.
140. D. Philp and J. F. Stoddart, *J. Phys. Org. Chem.*, 1997, **10**, 254-272.
141. G. Whitesides, J. Mathias and C. Seto, *Science*, 1991, **254**, 1312-1319.
142. G. M. Whitesides and B. Grzybowski, *Science*, 2002, **295**, 2418-2421.
143. C. T. Seto and G. M. Whitesides, *J. Am. Chem. Soc.*, 1990, **112**, 6409-6411.
144. C. T. Seto and G. M. Whitesides, *J. Am. Chem. Soc.*, 1993, **115**, 905-916.
145. A. Ranganathan, V. R. Pedireddi and C. N. R. Rao, *J. Am. Chem. Soc.*, 1999, **121**, 1752-1753.
146. J. A. Zerkowski, C. T. Seto, D. A. Wierda and G. M. Whitesides, *J. Am. Chem. Soc.*, 1990, **112**, 9025-9026.
147. J. A. Zerkowski, C. T. Seto and G. M. Whitesides, *J. Am. Chem. Soc.*, 1992, **114**, 5473-5475.
148. J.-M. Lehn, M. Mascal, A. DeCian and J. Fischer, *J. Chem. Soc., Perkin Trans. 2*, 1992, 461-467.
149. S. H. Gellman, *Acc. Chem. Res.*, 1998, **31**, 173-180.
150. D. J. Hill, M. J. Mio, R. B. Prince, T. S. Hughes and J. S. Moore, *Chem. Rev.*, 2001, **101**, 3893-4012.
151. L. A. Cuccia, J.-M. Lehn, J.-C. Homo and M. Schmutz, *Chem. Eur. J.*, 2002, **8**, 3448-3457.
152. J.-L. Schmitt, A.-M. Stadler, N. Kyritsakas and J.-M. Lehn, *Helv. Chim. Acta*, 2003, **86**, 1598-1624.
153. A. Petitjean, L. A. Cuccia, M. Schmutz and J.-M. Lehn, *J. Org. Chem.*, 2008, **73**, 2481-2495.
154. V. Berl, I. Huc, R. G. Khoury and J.-M. Lehn, *Chem. Eur. J.*, 2001, **7**, 2798-2809.

155. V. Berl, I. Huc, R. G. Khoury and J.-M. Lehn, *Chem. Eur. J.*, 2001, **7**, 2810-2820.
156. V. Berl, I. Huc, R. G. Khoury, M. J. Krische and J.-M. Lehn, *Nature*, 2000, **407**, 720-723.
157. J.-M. Lehn and A. Rigault, *Angew. Chem., Int. Ed.*, 1988, **27**, 1095-1097.
158. F. H. Beijer, R. P. Sijbesma, H. Kooijman, A. L. Spek and E. W. Meijer, *J. Am. Chem. Soc.*, 1998, **120**, 6761-6769.
159. R. P. Sijbesma, F. H. Beijer, L. Brunsveld, B. J. B. Folmer, J. Hirschberg, R. F. M. Lange, J. K. L. Lowe and E. W. Meijer, *Science*, 1997, **278**, 1601-1604.
160. T. F. A. de Greef, G. B. W. L. Ligthart, M. Lutz, A. L. Spek, E. W. Meijer and R. P. Sijbesma, *J. Am. Chem. Soc.*, 2008, **130**, 5479-5486.
161. J. H. Hirschberg, L. Brunsveld, A. Ramzi, J. A. Vekemans, R. P. Sijbesma and E. W. Meijer, *Nature*, 2000, **407**, 167-170.
162. S. H. M. Söntjens, R. P. Sijbesma, M. H. P. van Genderen and E. W. Meijer, *J. Am. Chem. Soc.*, 2000, **122**, 7487-7493.
163. L. Brunsveld, B. J. Folmer, E. W. Meijer and R. P. Sijbesma, *Chem. Rev.*, 2001, **101**, 4071-4098.
164. F. J. M. Hoeben, P. Jonkheijm, E. W. Meijer and A. P. H. J. Schenning, *Chem. Rev.*, 2005, **105**, 1491-1546.
165. G. B. W. L. Ligthart, H. Ohkawa, R. P. Sijbesma and E. W. Meijer, *J. Am. Chem. Soc.*, 2005, **127**, 810-811.
166. T. F. A. de Greef, M. M. J. Smulders, M. Wolffs, A. P. H. J. Schenning, R. P. Sijbesma and E. W. Meijer, *Chem. Rev.*, 2009, **109**, 5687-5754.
167. T. F. A. de Greef and E. W. Meijer, *Aust. J. Chem.*, 2010, **63**, 596-598.
168. K. E. Feldman, M. J. Kade, E. W. Meijer, C. J. Hawker and E. J. Kramer, *Macromolecules*, 2010, **43**, 5121-5127.
169. J. J. van Gorp, J. A. J. M. Vekemans and E. W. Meijer, *Chem. Commun.*, 2004, **2**, 60-61.
170. R. W. Sinkeldam, F. J. M. Hoeben, M. J. Pouderoijen, I. De Cat, J. Zhang, S. Furukawa, S. De Feyter, J. A. J. M. Vekemans and E. W. Meijer, *J. Am. Chem. Soc.*, 2006, **128**, 16113-16121.
171. R. W. Sinkeldam, M. H. C. J. van Houtem, K. Pieterse, J. a. J. M. Vekemans and E. W. Meijer, *Chem. Eur. J.*, 2006, **12**, 6129-6137.
172. R. A. Parker, Doctor of PhD Thesis, University of Southampton, 1999.
173. C. A. Hunter and D. H. Purvis, *Angew. Chem., Int. Ed.*, 1992, **31**, 792-795.
174. F. J. Carver, C. A. Hunter and R. J. Shannon, *J. Chem. Soc., Chem. Commun.*, 1994, 1277-1280.
175. R. Jäger and F. Vögtle, *Angew. Chem., Int. Ed.*, 1997, **36**, 930-944.
176. F. Vögtle, S. Meier and R. Hoss, *Angew. Chem., Int. Ed.*, 1992, **31**, 1619-1622.
177. F. Vögtle, T. Dünnwald and T. Schmidt, *Acc. Chem. Res.*, 1996, **29**, 451-460.
178. A.-M. L. Fuller, D. A. Leigh and P. J. Lusby, *J. Am. Chem. Soc.*, 2010, **132**, 4954-4959.
179. A. G. Johnston, D. A. Leigh, L. Nezhat, J. P. Smart and M. D. Deegan, *Angew. Chem., Int. Ed.*, 1995, **34**, 1212-1216.
180. A. G. Johnston, D. A. Leigh, R. J. Pritchard and M. D. Deegan, *Angew. Chem., Int. Ed.*, 1995, **34**, 1209-1212.
181. C. A. Golden, PhD Thesis, University of Southampton, 2005.

182. J. R. Gomm, PhD Thesis, University of Southampton, 2002.
183. A. N. Dwyer, M. C. Grossel and P. N. Horton, *Supramol. Chem.*, 2004, **16**, 405-410.
184. A. N. Dwyer, PhD Thesis, University of Southampton, 2004.
185. F. A. Chavez, M. M. Olmstead and P. K. Mascharak, *Inorg. Chem.*, 1996, **35**, 1410-1412.
186. F. A. Chavez, M. M. Olmstead and P. K. Mascharak, *Inorg. Chem.*, 1997, **36**, 6323-6327.
187. F. A. Chavez, M. M. Olmstead and P. K. Mascharak, *Inorg. Chim. Acta*, 1998, **269**, 269-273.
188. D. S. Marlin, M. M. Olmstead and P. K. Mascharak, *Inorg. Chim. Acta*, 2000, **297**, 106-114.
189. D. S. Marlin, M. M. Olmstead and P. K. Mascharak, *Inorg. Chim. Acta*, 2001, **323**, 1-4.
190. D. S. Marlin, M. M. Olmstead and P. K. Mascharak, *Inorg. Chem.*, 2001, **40**, 7003-7008.
191. A. K. Patra, M. J. Rose, M. M. Olmstead and P. K. Mascharak, *J. Am. Chem. Soc.*, 2004, **126**, 4780-4781.
192. L. A. Tyler, M. M. Olmstead and P. K. Mascharak, *Inorg. Chim. Acta*, 2001, **321**, 135-141.
193. M. C. Grossel, unpublished work.
194. M. Oszer, MPhil Thesis, University of Southampton, 1998.
195. J. B. Orton, PhD Thesis, University of Southampton, 2006.
196. J. E. Cheesewright, PhD Thesis, University of Southampton, 2010.
197. M. C. Grossel, C. A. Golden, J. R. Gomm, P. N. Horton, D. A. S. Merckel, M. E. Oszer and R. A. Parker, *CrystEngComm*, 2001, **3**, 170.
198. J. K. Bera, N. Sadhukhan and M. Majumdar, *Eur. J. Inorg. Chem.*, 2009, 4023-4038.
199. P. L. Ferrarini, C. Mori, M. Badawneh, V. Calderone, L. Calzolari, T. Loffredo, E. Martinotti and G. Saccomanni, *Eur. J. Med. Chem.*, 1998, **33**, 383-397.
200. M. Badawneh, C. Manera, C. Mori, G. Saccomanni and P. L. Ferrarini, *Farmaco*, 2002, **57**, 631-639.
201. P. L. Ferrarini, L. Betti, T. Cavallini, G. Giannaccini, A. Lucacchini, C. Manera, A. Martinelli, G. Ortore, G. Saccomanni and T. Tuccinardi, *J. Med. Chem.*, 2004, **47**, 3019-3031.
202. P. L. Ferrarini, C. Mori, V. Calderone, L. Calzolari, P. Nieri, G. Saccomanni and E. Martinotti, *Eur. J. Med. Chem.*, 1999, **34**, 505-513.
203. M. Macchia, S. Bertini, V. Di Bussolo, C. Manera, C. Martini, F. Minutolo, C. Mori, G. Saccomanni, D. Tuscano and P. L. Ferrarini, *Farmaco*, 2002, **57**, 783-786.
204. C. Manera, L. Betti, T. Cavallini, G. Giannaccini, A. Martinelli, G. Ortore, G. Saccomanni, L. Trincavelli, T. Tuccinardi and P. L. Ferrarini, *Bioorg. Med. Chem. Lett*, 2005, **15**, 4604-4610.
205. A. M. Emmerson and A. M. Jones, *J. Antimicrob. Chemother.*, 2003, **51**, 13-20.

206. T. D. Gootz, R. Zaniewski, S. Haskell, B. Schmieder, J. Tankovic, D. Girard, P. Courvalin and R. J. Polzer, *Antimicrob. Agents Chemother.*, 1996, **40**, 2691-2697.
207. A. G. Fraser and A. D. Harrower, *BMJ*, 1977, **2**, 1518.
208. H. K. Pannu, L. Gottlieb and E. K. Fishman, *Emerg. Radiol.*, 2001, **8**, 108-110.
209. J. Kuzelka, J. R. Farrell and S. J. Lippard, *Inorg. Chem.*, 2003, **42**, 8652-8662.
210. T. Tanase, T. Igoshi, K. Kobayashi and Y. Yamamoto, *J. Chem. Res.*, 1998, 538-539.
211. W. R. Tikkanen, C. Kruger, K. D. Bomben, W. L. Jolly, W. C. Kaska and P. C. Ford, *Inorg. Chem.*, 1984, **23**, 3633-3638.
212. C. Mealli and L. Sacconi, *Acta Crystallogr., Sect. B: Struct. Sci.*, 1977, **33**, 710-713.
213. C. He and S. J. Lippard, *Tetrahedron*, 2000, **56**, 8245-8252.
214. C. He and S. J. Lippard, *J. Am. Chem. Soc.*, 2000, **122**, 184-185.
215. C. J. Chandler, L. W. Deady, J. A. Reiss and V. Tzimos, *J. Heterocycl. Chem.*, 1982, **19**, 1017-1019.
216. G. R. Newkome, S. J. Garbis, V. K. Majestic, F. R. Fronczek and G. Chiari, *J. Org. Chem.*, 1981, **46**, 833-839.
217. G. R. Newkome, K. J. Theriot, V. K. Majestic, P. A. Spruell and G. R. Baker, *J. Org. Chem.*, 1990, **55**, 2838-2842.
218. R. Ziessel, A. Harriman, A. El-ghayoury, L. Douce, E. Leize, H. Nierengarten and A. Van Dorsselaer, *New J. Chem.*, 2000, **24**, 729-732.
219. A. E. M. Boelrijk, T. X. Neenan and J. Reedijk, *Dalton Trans.*, 1997, 4561-4570.
220. A. E. M. Boelrijk, M. M. Vanvelzen, T. X. Neenan, J. Reedijk, H. Kooijman and A. L. Spek, *Chem. Commun.*, 1995, 2465-2467.
221. H. Hasan, U.-K. Tan, G.-H. Lee and S.-M. Peng, *Inorg. Chem. Commun.*, 2007, **10**, 983-988.
222. I. P.-C. Liu, M. Bénard, H. Hasanov, I.-W. P. Chen, W.-H. Tseng, M.-D. Fu, M.-M. Rohmer, C.-H. Chen, G.-H. Lee and S.-M. Peng, *Chem. Eur. J.*, 2007, **13**, 8667-8677.
223. I. P.-C. Liu, W.-Z. Wang and S.-M. Peng, *Chem. Commun.*, 2009, 4323-4331.
224. T.-B. Tsao, S.-S. Lo, C.-Y. Yeh, G.-H. Lee and S.-M. Peng, *Polyhedron*, 2007, **26**, 3833-3841.
225. P. S. Corbin and S. C. Zimmerman, *J. Am. Chem. Soc.*, 1998, **120**, 9710-9711.
226. L. Xing, U. Ziener, T. C. Sutherland and L. a. Cuccia, *Chem. Commun.*, 2005, 5751-5753.
227. F. Böhme, M. Rillich and H. Komber, *Macromol. Chem. Phys.*, 1995, **196**, 3209-3216.
228. F. Böhme, C. Kunert, H. Komber, D. Voigt, P. Friedel, M. Khodja and H. Wilde, *Macromolecules*, 2002, **35**, 4233-4237.
229. J. L. Katz, B. J. Geller and P. D. Foster, *Chem. Commun.*, 2007, 1026-1028.
230. C. C. Cheng and S. J. Yan, *The Friedländer Synthesis of Quinolines*, John Wiley & Sons, Inc., 2004.
231. M. A. Spackman, *J. Chem. Phys.*, 1986, **85**, 6587.
232. J. J. McKinnon, A. S. Mitchell and M. A. Spackman, *Chem. Commun.*, 1998, 2071-2072.

233. J. J. McKinnon, A. S. Mitchell and M. A. Spackman, *Chem. Eur. J.*, 1998, **4**, 2136-2141.
234. M. A. Spackman and J. J. McKinnon, *CrystEngComm*, 2002, **4**, 378.
235. D. C. Whitley, *J. Math. Chem.*, 1998, **23**, 377-397.
236. M. Petitjean, *J. Comput. Chem.*, 1994, **15**, 507-523.
237. M. Connolly, *J. Appl. Crystallogr.*, 1983, **16**, 548-558.
238. M. L. Connolly, *J. Mol. Graphics Modell.*, 1993, **11**, 139-141.
239. J. J. McKinnon, F. P. A. Fabbiani and M. A. Spackman, *Cryst. Growth Des.*, 2007, **7**, 755-769.
240. J. J. McKinnon, M. A. Spackman and A. S. Mitchell, *Acta Crystallogr., Sect. B: Struct. Sci.*, 2004, **60**, 627-668.
241. J. J. McKinnon, D. Jayatilaka and M. A. Spackman, *Chem. Commun.*, 2007, 3814.
242. J. J. Li, in *Name Reactions*, Springer Berlin Heidelberg, 2006, pp. 545-548.
243. R. H. Manske, *Chem. Rev.*, 1942, **30**, 113-144.
244. W. P. Utermohlen Jr, *J. Org. Chem.*, 1943, **8**, 544–549.
245. W. W. Paudler and T. J. Kress, *J. Org. Chem.*, 1967, **32**, 832-833.
246. Y. Hamada, I. Takeuchi and M. Hirota, *Chem. Pharm. Bull.*, 1971, **19**, 1751-1755.
247. Y. Hamada and I. Takeuchi, *Chem. Pharm. Bull.*, 1971, **19**, 1857-1862.
248. M. R. Nimlos, S. J. Blanksby, X. Qian, M. E. Himmel and D. K. Johnson, *J. Phys. Chem. A*, 2006, **110**, 6145-6156.
249. Sigma-Aldrich UK PH000472-100MG £144 (on demand synthesis)
250. C. F. Koelsch and A. G. Whitney, *J. Org. Chem.*, 1941, **6**, 795-803.
251. M. K. Anwer and A. F. Spatola, *Tetrahedron Lett.*, 1985, **26**, 1381-1384.
252. H.-K. Fun, C. S. Yeap, N. K. Das, A. K. Mahapatra and S. Goswami, *Acta Crystallogr., Sect. E: Struct. Rep. Online*, 2009, **65**, o1747.
253. A. D. Bond, J. E. Davies and A. J. Kirby, *Acta Crystallogr., Sect. E: Struct. Rep. Online*, 2001, **57**, O1242-O1244.
254. H.-K. Fun, S. Chantrapromma, A. C. Maity and S. Goswami, *Acta Crystallogr., Sect. E: Struct. Rep. Online*, 2010, **66**, o622.
255. S. C. Zimmerman and T. J. Murray, *J. Am. Chem. Soc.*, 1992, **114**, 4010–4011.
256. B. A. Blight, A. Camara-Campos, S. Djurdjevic, M. Kaller, D. A. Leigh, F. M. McMillan, H. McNab and A. M. Z. Slawin, *J. Am. Chem. Soc.*, 2009, **131**, 14116-14122.
257. S. Djurdjevic, D. A. Leigh, H. McNab, S. Parsons, G. Teobaldi and F. Zerbetto, *J. Am. Chem. Soc.*, 2007, **129**, 476-477.
258. P. Caluwe and T. G. Majewicz, *J. Org. Chem.*, 1977, **42**, 3410-3413.
259. G. Evens and P. Caluwe, *Macromolecules*, 1979, **12**, 803-808.
260. J. F. Harper and D. G. Wibberley, *J. Chem. Soc. C*, 1971, 2991.
261. S. Carboni, A. Da Settimo and I. Tonetti, *J. Heterocycl. Chem.*, 1970, **7**, 875-878.
262. C. R. Hauser and M. J. Weiss, *J. Org. Chem.*, 1949, 453-459.
263. C. R. Hauser and G. A. Reynolds, *J. Org. Chem.*, 1950, **15**, 1224-1232.
264. E. V. Brown, *J. Org. Chem.*, 1965, **30**, 1607–1610.
265. T. J. Murray, S. C. Zimmerman and S. V. Kolotuchin, *Tetrahedron*, 1995, **51**, 635-648.

266. M. R. Edwards, W. Jones, W. D. S. Motherwell and G. P. Shields, *Mol. Cryst. Liq. Cryst.*, 2001, **356**, 337-353.
267. G. Desiraju and J. Sarma, *J. Chem. Sci.*, 1986, **96**, 599-605.
268. M. Prasanna, *J. Mol. Struct.*, 2001, **562**, 55-61.
269. P. Restorp, O. B. Berryman, A. C. Sather, D. Ajami and J. Rebek Jr, *Chem. Commun.*, 2009, 5692-5694.
270. V. R. Thalladi, H.-C. Weiss, D. Bläser, R. Boese, A. Nangia and G. R. Desiraju, *J. Am. Chem. Soc.*, 1998, **120**, 8702-8710.
271. E. Carosati, S. Sciabola and G. Cruciani, *J. Med. Chem.*, 2004, **47**, 5114-5125.
272. J. Howard, V. Hoy, D. Hagan and G. Smith, *Tetrahedron*, 1996, **52**, 12613-12622.
273. J. D. Dunitz and R. Taylor, *Chem. Eur. J.*, 1997, **3**, 89-98.
274. P. N. Horton, PhD Thesis, University of Southampton, 2001.
275. X. H. Yin and M. Y. Tan, *Synthetic Communications*, 2003, **33**, 1113-1119.
276. Z. R. Guo, E. D. Dowdy, W. S. Li, R. Polniaszek and E. Delaney, *Tetrahedron Lett.*, 2001, **42**, 1843-1845.
277. F. H. Allen, J. E. Davies, J. J. Galloy, O. Johnson, O. Kennard, C. F. Macrae, E. M. Mitchell, G. F. Mitchell, J. M. Smith and D. G. Watson, *J. Chem. Inform. Comput. Sci.*, 1991, **31**, 187–204.
278. D. J. Jackson, PhD Thesis, University of Southampton, 2007.
279. R. M. Claramunt, F. Herranz, M. D. Santa Maria, C. Jaime, M. de Federico and J. Elguero, *Biosens. Bioelectron.*, 2004, **20**, 1242-1249.
280. F. Herranz, M. D. Santa Maria and R. M. Claramunt, *J. Org. Chem.*, 2006, **71**, 2944-2951.
281. S. Goswami and R. Mukherjee, *Tetrahedron Lett.*, 1997, **38**, 1619-1622.
282. K. Katagiri, T. Tohaya, H. Masu, M. Tominaga and I. Azumaya, *J. Org. Chem.*, 2009, **74**, 2804-2810.
283. R. A. Bowie and O. C. Musgrave, *J. Chem. Soc. C*, 1966, 566-571.
284. H.-S. Wang, Y.-C. Wang, Y.-M. Pan, S.-L. Zhao and Z.-F. Chen, *Tetrahedron Lett.*, 2008, **49**, 2634-2637.
285. R. W. W. Hooft, Collect" data collection software, B. V. Nonius 1998
286. Z. Otwinowski and W. Minor, in *Macromolecular Crystallography*, eds. C. W. J. Carter and R. M. Sweet, Academic Press Inc, San Diego, 1997, vol. 276, pp. 307-326.
287. A. J. M. Duisenberg, *J. Appl. Crystallogr.*, 1992, **25**, 92-96.
288. A. J. M. Duisenberg, R. W. W. Hooft, A. M. M. Schreurs and J. Kroon, *J. Appl. Crystallogr.*, 2000, **33**, 893-898.
289. G. M. Sheldrick, *SADABS*, Bruker AXS Inc, Madison, Wisconsin, 2007.
290. G. M. Sheldrick, *SADABS*, Brucker AXS Inc, Madison, Wisconsin, 2003.
291. *XPREP - Data Preparation & Reciprocal Space Exploration*, Brucker AXS Inc., Madison, Wisconsin, 1997.
292. Bruker, *APEX2*, Bruker AXS Inc, Madison, Wisconsin, USA, 2007.
293. Bruker, *SAINT*, Bruker AXS Inc, Madison, Wisconsin, USA, 2007.
294. G. M. Sheldrick, *SHELX-97 - Programs for Crystal Structure Analysis*, Institit für Anorganische Chemie der Universikit, Gottingen, Germany, 1998.
295. G. M. Sheldrick, *Acta Crystallogr., Sect. A: Found. Crystallogr.*, 2008, **64**, 112-122.

296. L. J. Farrugia, *J. Appl. Crystallogr.*, 1999, **32**, 837-838.
297. A. L. Spek, *J. Appl. Crystallogr.*, 2003, **36**, 7-13.
298. F. H. Allen, O. Johnson, G. P. Shields, B. R. Smith and M. Towler, *J. Appl. Crystallogr.*, 2004, **37**, 335-338.
299. *Mercury*, CCDC, Cambridge, England, 2009.
300. C. F. Macrae, I. J. Bruno, J. A. Chisholm, P. R. Edgington, P. McCabe, E. Pidcock, L. Rodriguez-Monge, R. Taylor, J. van de Streek and P. A. Wood, *J. Appl. Crystallogr.*, 2008, **41**, 466-470.
301. S. K. Wolff, D. J. Grimwood, J. J. McKinnon, D. Jayatilaka and M. A. Spackman, *CrystalExplorer*, University of Western Australia, 2007.
302. J. B. Lamture, Z. H. Zhou, A. S. Kumar and T. G. Wensel, *Inorg. Chem.*, 1995, **34**, 864-869.